INFORMATION TO USERS

This manuscript has been reproduced from the microfilm master. UMI films the text directly from the original or copy submitted. Thus, some thesis and dissertation copies are in typewriter face, while others may be from any type of computer printer.

The quality of this reproduction is dependent upon the quality of the copy submitted. Broken or indistinct print, colored or poor quality illustrations and photographs, print bleedthrough, substandard margins, and improper alignment can adversely affect reproduction.

In the unlikely event that the author did not send UMI a complete manuscript and there are missing pages, these will be noted. Also, if unauthorized copyright material had to be removed, a note will indicate the deletion.

Oversize materials (e.g., maps, drawings, charts) are reproduced by sectioning the original, beginning at the upper left-hand corner and continuing from left to right in equal sections with small overlaps.

Photographs included in the original manuscript have been reproduced xerographically in this copy. Higher quality 6" x 9" black and white photographic prints are available for any photographs or illustrations appearing in this copy for an additional charge. Contact UMI directly to order.

ProQuest Information and Learning
300 North Zeeb Road, Ann Arbor, MI 48106-1346 USA
800-521-0600

UMI®

Hydrothermal Alteration in a Modern Suprasubduction Zone: the Tonga Forearc Crust

by

Neil Raoul Banerjee

B.Sc., University of Toronto, 1993
M.Sc., Dalhousie University, 1996

A Dissertation Submitted in Partial Fulfillment of the
Requirements for the Degree of

DOCTOR OF PHILOSOPHY

In the School of Earth and Ocean Sciences

We accept this dissertation as conforming to the
required standard

Dr. K.M. Gillis, Supervisor (School of Earth and Ocean Sciences)

Dr. D. Canil, Departmental Member (School of Earth and Ocean Sciences)

Dr. R. Hyndman, Outside Member (Centre for Earth and Ocean Research)

Dr. S.T. Johnston, Departmental Member (School of Earth and Ocean Sciences)

Dr. M. Whiticar, Departmental Member (School of Earth and Ocean Sciences)

Dr. S. Bloomer, External Examiner (Department of Geosciences, Oregon State University)

University of Victoria

Supervisor: Dr. Kathryn M. Gillis

ABSTRACT

An extensive suite of hydrothermally altered basalts, gabbros, and plagiogranites, was recovered from the trench-facing slope of the Tonga forearc. The tectonic setting, lithology, and geochemistry of these samples make them a unique collection for comparison with suprasubduction zone (SSZ) ophiolites. Petrography, mineral chemistry, and geothermometry are used to constrain the metamorphic evolution of ocean crust formed in a modern SSZ setting. We report the discovery of the first suite of oceanic epidosites. Tongan epidosites metasomatically replaced basaltic and plagiogranite protoliths and formed under similar conditions to epidosites hosted in many SSZ ophiolites. The range of alteration temperatures and mineral assemblages in basalts and gabbros are similar to those described from both SSZ ophiolites and mid-ocean ridges (MORs). However, the degree of alteration in basalts and the presence of epidosites in the Tonga collection are most similar to alteration characteristics in SSZ ophiolites. We show that the trace element chemistry of epidote may be linked to the composition of fluids circulating deep in hydrothermal systems. This is possible due to the subordinate role crystal chemistry may play in controlling the trace element chemistry of hydrothermal minerals. Whole rock oxygen isotope ratios of the Tonga samples are generally similar to values determined from MOR and SSZ ophiolite samples; however, enriched values in plagiogranites and gabbros may indicate a late, low temperature metamorphic overprint associated with tectonic unroofing during trench rollback. Basalts show an interesting northward decrease in oxygen isotope ratios that remains unresolved.

Examiners:

Dr. K.M. Gillis, Supervisor (School of Earth and Ocean Sciences)

Dr. D. Canil, Departmental Member (School of Earth and Ocean Sciences)

Dr. R. Hyndman, Outside Member (Centre for Earth and Ocean Research)

Dr. S.T. Johnston, Departmental Member (School of Earth and Ocean Sciences)

Dr. M. Whiticar, Departmental Member (School of Earth and Ocean Sciences)

Dr. S. Bloomer, External Examiner (Department of Geosciences, Oregon State University)

TABLE OF CONTENTS

LIST OF TABLES

LIST OF FIGURES

ACKNOWLEDGMENTS

I wish to thank Kathryn Gillis for her constant help, guidance, and support while supervising this thesis. Sherm Bloomer is thanked for agreeing on short notice to act as External Examiner. Comments by Jeffrey Alt, Wolfgang Bach, Sherm Bloomer, Dante Canil, Kathryn Gillis, Robert Gregory, Roy Hyndman, Steve Johnston, Karlis Muehlenbachs, William Seyfried Jr., Peter Schiffman, and Michael Whittaker greatly improved the final draft. Technical assistance by Jianzhong Fan, Olga Levner, Roger Nielsen, Michael Roberts, Lang Shi, and Todd Wood is greatly appreciated. The thesis benefited from discussions with William Blackburn, Sherman Bloomer, James Brenan, Johnson Cann, Laurence Coogan, Gregory Hirth, Melanie Kelman, Dirk Lanwehr, Craig Manning, and Wim van Westrenen. Special thanks to Stephanie Laurence for drafting many of the figures and without whom I would not have been able to complete this thesis on time.

Thank you to my friends and fellow students, graduate and undergraduate, who made my stay at the University of Victoria most enjoyable. Special thanks to Kendrick Brown, Brent Carbno, Jason Mackenzie, and Leanne Pyle for their friendship and support. I could not have completed this thesis without the constant love and encouragement of Stephanie Laurence, my parents, and brother, to whom I am grateful.

This study was financially supported by NSERC grants to Kathryn Gillis.

Chapter 1

INTRODUCTION

Hydrothermal circulation is a ubiquitous process operating in areas of active oceanic crustal accretion such as slow-, intermediate-, and fast-spreading mid-ocean ridges (MORs), and back-arc and forearc basins of island arc systems [*Humphris*, 1995; *Rona and Scott*, 1993]. A number of physical parameters vary between these tectonic settings that affect hydrothermal systems. These include the spreading rate, depth of penetration of normal faulting, rate and volume of magmatic activity, composition of erupted magmas, and volatile contents of magmas [*Mével and Cannat*, 1991; *Olive et al.*, 1997; *Purdy et al.*, 1992; *Smith et al.*, 1997; *Stern and Bloomer*, 1992].

Ophiolites are commonly used as analogues to study modern mid-ocean ridge processes although it is now thought that many ophiolites formed in a suprasubduction zone (SSZ) setting [*Miyashiro*, 1973; *Pearce et al.*, 1984]. Several studies have shown that important differences exist between patterns of hydrothermal alteration in MORs and SSZ ophiolites [*Alt*, 1995; *Gillis and Banerjee*, in press; *Schiffman et al.*, 1990]. Recent studies by Alt et al. [1998] and Kelman [1998] have documented hydrothermal alteration patterns in the shallow crust of modern SSZ environments – the Izu-Bonin and Tonga forearcs, respectively. These studies have shown that the degree of alteration in the volcanic sequences of forearcs is more extensive and occurs at higher water-rock ratios than at MORs, and is comparable to that observed in SSZ ophiolites. It has been suggested that forearcs represent the remnants of early arc volcanism and are one of the best modern analogues for the tectonic setting in which SSZ ophiolites formed [*Bloomer et al.*, 1995]. Two recent studies have focused on hydrothermal alteration of volcanic and dike sequences from modern forearc settings [*Alt et al.*, 1998; *Kelman et al.*, 1997]. This thesis builds upon these studies and extends our knowledge of alteration to the deep crust including the sheeted dikes and gabbros.

In broad terms, this study provides a basis for comparison of high temperature hydrothermal alteration of ocean crust formed in various tectonic environments. The key to this problem lies in the lower portions of the ocean crust in which high temperature chemical exchange between hydrothermal fluids and the surrounding rocks occurs. Here the interaction between tectonic and magmatic processes, which influence hydrothermal alteration, can be best observed and related to differences in tectonic setting. This study provides detailed information on high temperature alteration in one tectonic environment – a SSZ non-accretionary convergent margin. Comparison of the results from this study with similar studies of other tectonic settings, such as slow-, intermediate-, and fast-spreading mid-ocean ridges, provides insight into how oceanic hydrothermal systems within ocean crust are influenced by styles of crustal accretion.

THESIS OBJECTIVES

Most previous hydrothermal studies of forearcs and back-arcs have focused on the upper 100-200m of volcanic basement recovered by the Ocean Drilling Program [*Natland and Hekinian*, 1981; *Natland and Mahoney*, 1981; *Schöps and Herzig*, 1994; *Taylor et al.*, 1992]. More recent studies in the Izu-Bonin and Tonga forearcs have also included samples of altered diabases, which may be fragments of sheeted dikes. These studies have extended our knowledge of high temperature (> 200°C) alteration in a forearc setting [*Alt et al.*, 1998; *Kelman et al.*, 1997]. This study focuses on lower crustal samples, including sheeted dikes and plutonic rocks, recovered by dredging from the trench-facing slope of the Tonga forearc. The Tonga forearc is a non-accretionary convergent margin that represents a possible analogue for the tectonic setting in which SSZ ophiolites may form. This study makes use of one of the most complete suites of rocks ever recovered from a forearc environment.

The purpose of this thesis is to provide the first comprehensive study of the metamorphic evolution of a section of modern forearc crust. The Tonga collection is used as a case study to evaluate the conditions present (e.g., temperature, fluid chemistry, secondary minerals) during the evolution of hydrothermal alteration in ocean crust formed in a modern SSZ setting. The results are then compared with studies of hydrothermal alteration in SSZ ophiolites and MORs to determine the role tectonic setting plays in the development of hydrothermal alteration in the oceanic crust. The detailed objectives of this study are:

1. To document the evolution of hydrothermal processes in the Tonga forearc crust in order to provide the first comprehensive study of high temperature alteration and metamorphism of lower crustal rocks formed in a forearc setting.
2. To document the discovery of rare, highly altered rocks called epidosites, which have been previously described from ophiolites but are absent in collections from modern oceanic crust.
3. To document the trace element content of epidote in epidosites in order to assess the controls on trace element partitioning in hydrothermal epidote.
4. To compare alteration in the Tonga forearc with ophiolites and MORs in order to evaluate if, and how hydrothermal processes are influenced by tectonic setting.

Together, these objectives will provide a picture of how circulating fluids transformed the crust of the Tonga forearc from the original igneous protolith into the hydrothermally altered equivalents presently observed.

METHODS

Several petrological and geochemical tools have been used in order to address these objectives. Standard petrographic techniques are used to determine the igneous and metamorphic mineralogy. Through petrographic analysis of metamorphic textures and cross cutting relationships the relative timing of metamorphic events and evolution of hydrothermal processes are determined, as well as the relationship between metamorphism and deformation. Mineral chemistry, including primary and secondary mineral compositions determined by electron microprobe, is used to help characterize the evolution of alteration conditions during progressive fluid-rock interaction. By specifically analyzing certain coexisting mineral pairs and applying appropriate geothermometers, it is possible to infer the temperatures at which the minerals formed and constrain the relationship between temperature and alteration style. Whole rock major and trace element data from volcanic samples, performed by colleagues at the University of Tasmania, are used to place the Tonga suite in a geochemical framework of other oceanic rocks. These data indicate the Tonga suite represents a complex mix of primitive and evolved rocks including, boninites, arc-tholeiites, N-MORB, dacites, and rhyolites.

One early discovery has been the identification of samples showing evidence of extreme epidotization, including a total loss of igneous texture in the most advanced examples. These samples, called epidosites, were recovered in association with the entire spectrum of rock types from five dredges in the northern half of the fore-arc. Epidosites are well documented in ophiolites. However, the Tonga samples represent one of very few, and perhaps the largest, suite of epidosites recovered from the modern oceans. The prevalence of epidosites in SSZ ophiolites and the Tonga fore-arc suggests that the conditions necessary for their formation, such as high water/rock ratio, are similar in both tectonic settings. The Tonga epidosites are compared with epidosite samples from ophiolites in order to determine if they are the same or not.

A fluid inclusion study was conducted on the five epidotized Tonga samples for comparison with data from epidosites found in ophiolites. Fluid inclusions provide a particularly powerful tool for studying hydrothermal processes because they represent small capsules of the once circulating hydrothermal fluid. Standard microthermometric analysis of fluid inclusions is used to elucidate the temperature, pressure, and composition of fluids present during formation of the epidosites [see *Roedder*, 1984]. This technique relies on the recognition of vapour-, liquid-, and solid-phase changes (depending on the inclusion), which take place during heating, or cooling of a fluid inclusion [*Roedder*, 1984]. The information gained from the microthermometric analysis is further used to determine the temperature and composition of fluids responsible for alteration, the possible role of phase separation, if there is a magmatic component to the fluids, and if fluid properties vary between samples. Substantial data has been collected for epidosites in ophiolites, and in particular, Troodos, which are compared to the data collected for the Tonga samples [e.g. *Cowan and Cann*, 1988; *Kelley and Robinson*, 1990; *Kelley et al.*, 1992].

Many hydrothermal studies have used trace-element concentrations in whole rock samples to document geochemical changes resulting from alteration; however, few have looked at these changes in individual minerals. By looking at the trace-element concentrations in certain secondary minerals, it may be possible to learn something about the chemistry of the fluids from which they precipitate. One such secondary mineral present in the epidosites is epidote. Trace-element concentrations in epidote from the Tonga epidosites were determined using the laser-ablation microprobe inductively coupled mass spectrometry (LAM-ICP-MS) facility at the University of Victoria. Of particular interest are the rare earth elements (REEs), because they are generally believed to be immobile during hydrothermal alteration under greenschist to amphibolite facies conditions [*Thompson*, 1983b]. Gillis [1996] used the ion microprobe to analyze REEs in amphibole in order to resolve the origin of amphibole in oceanic gabbros. Major element data from amphibole indicated a metamorphic origin whereas textural criteria and REE concentrations suggested both magmatic and metamorphic origins [*Gillis*, 1996]. As a result, REE geochemistry was able to unravel the complex origin of magmatic amphibole grains, which may have had their major-element chemistry reset by subsequent interaction with hydrothermal fluids [*Gillis*, 1996]. In this thesis, the controls on the trace element chemistry of hydrothermal epidote are investigated and used to help determine the chemistry of the fluids from which the epidote formed.

The oxygen isotope composition of whole rock samples and mineral separates are also investigated. Whole rock data on basalts, gabbro, plagiogranite, and peridotite are used to provide information on the conditions present during alteration including temperature and degree of alteration. These data are then compared with studies of MORs and ophiolites. The oxygen isotope compositions of quartz and epidote mineral separates from epidosites are used to speculate on the water-rock ratio and oxygen isotope composition of the hydrothermal fluids during formation of the epidosites. In this way, oxygen isotopes are used to evaluate if the conditions of alteration responsible for the formation of the Tonga epidosite samples were similar to those determined for epidosites from ophiolites.

Chapter 2

BACKGROUND

HYDROTHERMAL SYSTEMS

The formation and evolution of ocean crust is a complex process involving magmatism, tectonism, and hydrothermal activity. It is now known that hydrothermal circulation is a ubiquitous process operating in areas of active oceanic crustal accretion. Interaction between circulating hydrothermal fluids and the oceanic crust dissipates large amounts of thermal energy, which accounts for almost 25% of the total heat flux from the oceanic lithosphere [*Sclater et al.*, 1981; *Stein and Stein*, 1994]. As seawater circulates through the crust, a number of chemical and physical reactions occur which result in the formation of volcanic hosted massive sulphide deposits [*Hannington et al.*, 1995], support unique biological communities [*Tunnicliffe*, 1992], and affect seawater chemistry [*Thompson*, 1983a]. Alteration of the crust results in changes to its chemical composition which, when subducted, can contribute to chemical and isotopic heterogeneities in the upper mantle [*Zindler and Hart*, 1986] and may influence the composition of igneous rocks erupted in island arcs [*Olive et al.*, 1997; *Perfit et al.*, 1980; *Tatsumi*, 1989]. In addition, mineral precipitation from hydrothermal fluids has profound affects on crustal porosity and permeability [*Gillis and Sapp*, 1997; *Pezard*, 1990], and seismic structure of the crust [*Jacobson*, 1992].

Hydrothermal systems have been discovered along slow-, intermediate-, and fast-spreading mid-ocean ridges (MORs), at intra-plate volcanic centres, and in back-arc and forearc basins of island arc systems (Figure 2.1) [*Humphris*, 1995; *Rona and Scott*, 1993]. Fluids venting in each of these environments have been sampled [see review in *Von Damm*, 1995]. Although the chemistry of the venting fluids does seem to change as a function of temperature and processes such as phase separation, there is still insufficient data to link their chemistry to physical parameters such as spreading rate [*Von Damm*, 1995]. A number of physical parameters vary between tectonic settings and affect hydrothermal processes.

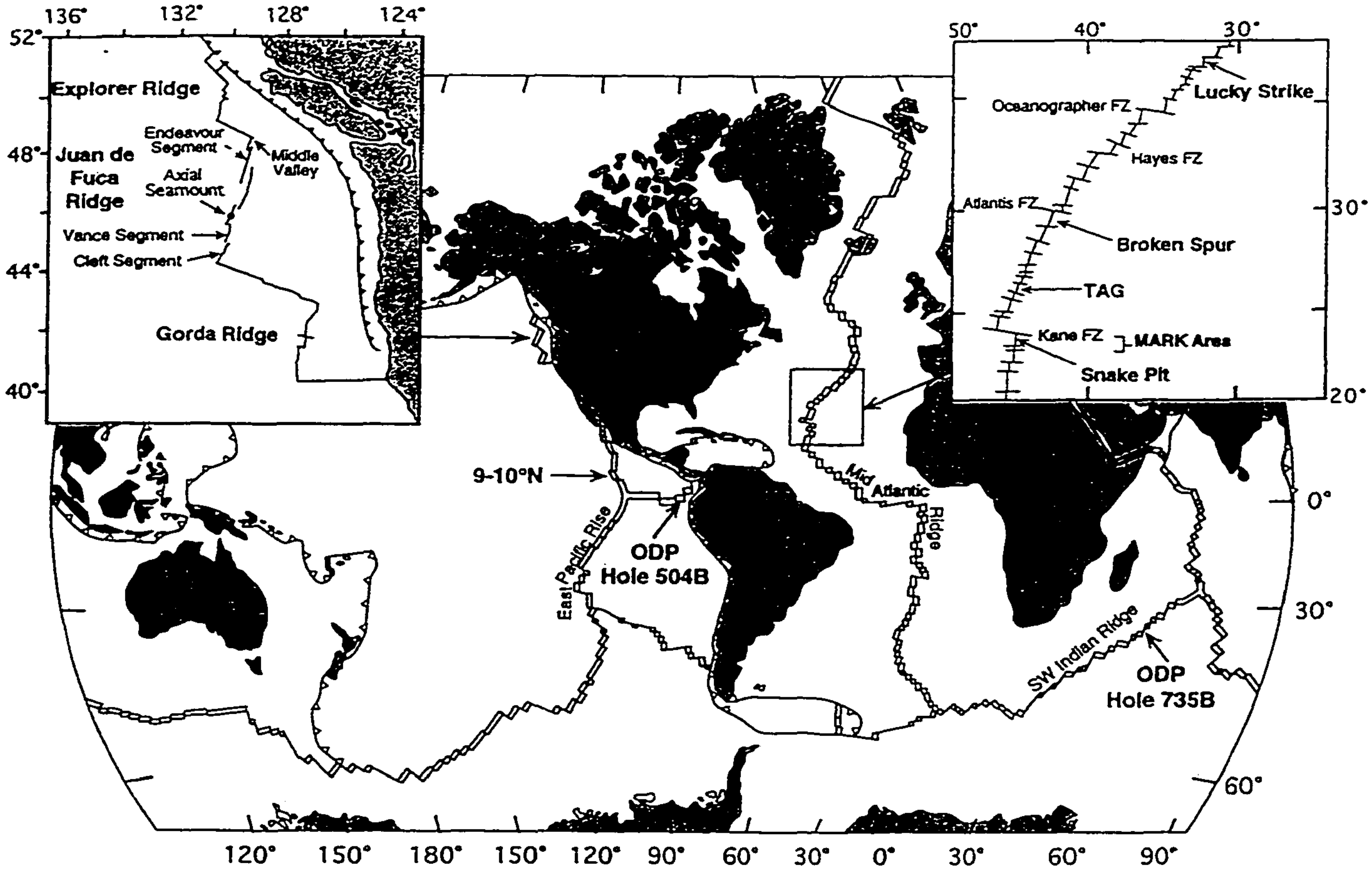

Figure 2.1 Diagram of the global mid-ocean ridge system and the location of some known hydrothermal systems and relevant ODP sites [from *Humphris*, 1995].

These include the depth of penetration of normal faulting, the rate and volume of magmatic activity, the composition of erupted magmas, and the volatile contents of magmas, to name a few [*Mével and Cannat*, 1991; *Olive et al.*, 1997; *Purdy et al.*, 1992; *Smith et al.*, 1997; *Stern and Bloomer*, 1992].

The presence of axial melt lenses imaged at the fast-spreading East Pacific Rise suggests long lived, steady state magma input occurs below the ridge crest [*Carbotte et al.*, 1996; *Detrick et al.*, 1987; *Sinton and Detrick*, 1992]. The lack of geophysical evidence for magma chambers at slow-spreading MORs suggests the crust is formed from short lived, episodic injections of magma [*Sinton and Detrick*, 1992; *Solomon and Toomey*, 1992]. The current understanding of crust formed at incipient forearcs suggests that they form in extensional environments, dominated by normal faulting, above subduction zones where adiabatic decompression and dehydration of the down-going slab result in huge outpourings of magma over relatively short periods of time (1-5 my) [*Bloomer et al.*, 1995; *Stern and Bloomer*, 1992]. The interplay of tectonic and magmatic processes in each of these tectonic settings affects the permeability and thermal structure of the ocean crust and, therefore, hydrothermal circulation. The distribution and characteristics of hydrothermal flow are controlled by permeability, thermal structure, and seafloor topography [*Fisher*, 1998]. Chemical exchange between hydrothermal fluids and the surrounding rocks is controlled by temperature, redox conditions, and water/rock ratio [see review in *Humphris*, 1995]. As a result, crustal accretion processes in different tectonic environments are expected to produce different styles of hydrothermal alteration. The key to this possibility lies in the lower portions of the ocean crust where high-temperature hydrothermal alteration is preserved.

The lower ocean crust is particularly important because it is here that hydrothermal and magmatic processes are linked. Therefore, it is necessary to analyze samples of lower ocean crust in order to determine how high temperature axial hydrothermal alteration varies with tectonic setting. Towards this end, a number of factors need to be considered such as the thermal structure of the ocean crust imposed by crustal accretion processes, the starting compositions of rocks from a variety of tectonic settings, and the chemical modification of hydrothermal fluids and surrounding rocks resulting from fluid-rock interaction.

Hydrothermal Alteration of Ocean Crust

Early studies of altered oceanic rocks recognized that metamorphic grade gradually increased with depth in the crust, from zeolite and greenschist facies in the volcanics to amphibolite facies in the plutonics [*Miyashiro*, 1973; *Quon and Ehlers*, 1963]. However, it wasn't until later that the importance of circulating seawater-salinity fluids was recognised [*Jehl et al.*, 1977]. In the late 70's, discovery of hot springs and black smoker vents on the seafloor began the study of active hydrothermal systems [e.g., *Edmond et al.*, 1979; *Weiss et al.*, 1977].

Current models suggest that axial hydrothermal systems can be divided into three zones: recharge, reaction, and discharge (Figure 2.2) [*Alt*, 1995 and references therein]. The recharge zone represents a widespread area in which seawater penetrates down into the crust, is heated, and reacts with the surrounding rocks at temperatures from ambient seawater to those found in the reaction zone. The reaction zone is characterized by high-temperature (375-450°C), low pressure (<1 kbar), and low water/rock ratios (<5) [*Alt*, 1995; *Saccocia*, 1994]. This is where venting hydrothermal fluids are believed to acquire their chemical signature through fluid-rock interaction. Finally, hydrothermal fluids rise through the discharge zone until they vent on the seafloor.

Recharge Zone

Chemical reactions in the recharge zone are characterized by Mg fixation, anhydrite precipitation, and alkali loss from the crust [*Thompson* , 1983; *Mottl*, 1983]. Mg is removed from seawater by the precipitation of hydrous Mg phases such as smectite, chlorite, and amphibole [*Mottl and Holland*, 1978; *Seyfried and Bischoff*, 1979]. This reaction involves hydration of the crust and the generation of acidity in fluids [*Seyfried*, 1987]. Under high seawater/rock ratios (>50) acidic conditions lead to the leaching of base metals, such as Fe, Cu, and Zn [*Seyfried*, 1987; *Saccocia et al.*, 1994]. The seawater/rock ratio quickly decreases and temperature increases with depth as fluids travel down through the volcanic pile and into the sheeted dikes, which can result in metal loss from the surrounding rocks. As the fluids become heated to 150° - 200°C, precipitation of anhydrite removes almost all of the Ca and two-thirds of the sulphate from seawater [*Bischoff and Seyfried*, 1978]. At temperatures greater than about 150°C alkalis (e.g., Li, K, Rb and Cs) and B can be lost from basaltic rocks, and in particular basaltic glass, during seawater interaction leading to the observed

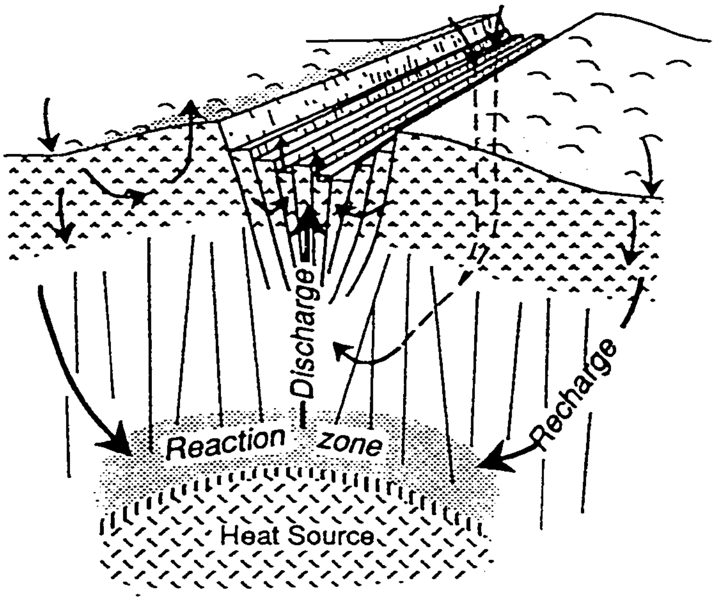

Figure 2.2 Schematic drawing illustrating the portions of submarine hydrothermal systems discussed in the text [from *Alt*, 1995]. Arrows represent traces of fluid flow.

enrichment of these elements in high temperature hydrothermal fluids venting on the seafloor [*Von Damm*, 1995].

Reaction Zone

Actively venting hydrothermal fluids are believed to acquire their chemical signature in the deep portions of the hydrothermal cell (Figure 2.3). In particular, many components of axial hydrothermal fluids (e.g., Cu, Fe, Zn, H_2S, SiO_2, Ca, Na, K) are believed to be fixed in the reaction zone at low pressure (< 1 kbar), high temperature (375-450°C), and low water/rock ratio (<5) [*Alt*, 1995; *Saccocia*, 1994]. Experimental studies have shown that small changes in these physical parameters can substantially influence vent fluid chemistry [*Seewald and Seyfried*, 1990; *Seyfried et al.*, 1991; *Ding and Seyfried*, 1992]. The reaction zone is believed to be located at or near the sheeted dike - gabbro boundary, although some studies indicate that the reaction zone may extend down into the uppermost gabbros at slow-spreading ridges [e.g., *Mével and Cannat*, 1991]. Experimental studies performed at 400°C and < 1 kbar suggest that interaction of hydrothermal fluids with fresh rock in the reaction zone results in equilibrium mineral assemblages which contain Ca-plagioclase and epidote [*Berndt et al.*, 1989; *Seyfried et al.*, 1991]. Unfortunately, experimental studies do not explain all of the possibilities. For example, metabasalts recovered from the Mid-Atlantic Ridge at the Kane Fracture Zone (MARK), which are interpreted to have formed in a reaction zone, exhibit mineral assemblages that contain Na-plagioclase and lack epidote [*Gillis and Thompson*, 1993]. This apparent discrepancy may be the result of non-equilibrium conditions, possible interaction with magmatic fluids, or the MARK metabasalts may not be representative of conditions in the reaction zone [see *Humphris*, 1995].

Studies of hydrothermal processes in oceanic crust have benefited from oceanic drilling. Ocean Drilling Program (ODP) Holes 504B, which penetrated through the volcanic section into the sheeted dikes in 5.9 Ma crust, and Hole 735B, which drilled directly into lower crustal gabbros, are two of the best sections of crust to study the deep portions (> 2 km) of hydrothermal systems [*Alt et al.*, 1993; *Stakes et al.*, 1991]. Below about 1250 m into basement , sheeted dike rocks in Hole 504B show an increase in the abundance of amphibole as well as a change in amphibole compositions from actinolite to Mg hornblende and corresponding increases in Al and Ti [*Alt et al.*, 1994; *Laverne et al.*, 1994]. In addition,

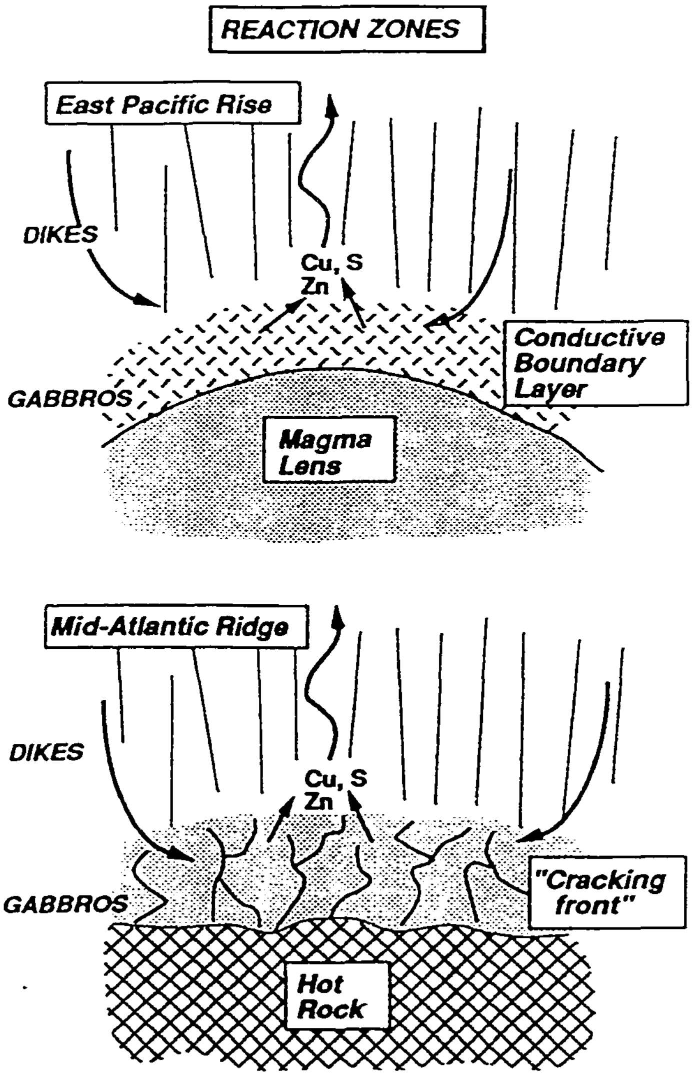

Figure 2.3 Schematic drawing illustrating differing types of heat sources and reaction zones for systems with or without a magma chamber [from *Alt*, 1995].

secondary plagioclase compositions are calcic in contrast to the predominant albitization that occurs further up section [*Alt et al.*, 1994]. Along with oxygen isotopic depletions relative to fresh MORB and an increase in the extent of recrystallization of the rocks, these observations point toward alteration at higher temperatures reflecting reaction zone conditions. Similar mineralogical and chemical effects are observed in dike rocks from the Mid-Atlantic Ridge (MAR) and ophiolites [*Gillis and Thompson*, 1993; *Harper et al.*, 1988; *Nehlig et al.*, 1994]. Hydrothermal alteration of gabbros in Hole 735B indicate that similar conditions extend downward into the plutonic sequence [*Dick et al.*, 1991; *Mevel and Cannat*, 1991]. Gabbros from Hole 735B exhibit evidence of plastic deformation in the form of foliated amphibolites that allowed early penetration of hydrothermal fluids below the brittle-ductile transition [*Dick et al.*, 1991; *Mevel and Cannat*, 1991; *Stakes et al.*, 1991; *Vanko and Stakes*, 1991]. Interestingly, gabbros from the fast-spreading East Pacific Rise at Hess Deep contain similar high temperature mineral assemblages as Hole 735B but do not display any evidence of ductile deformation [*Gillis*, 1995]. Instead, gabbros from Hess Deep and the Semail ophiolite contain tiny amphibole veinlets filled with Mg hornblende interpreted to have formed from penetration of hydrothermal fluids at high temperatures during semibrittle microfracturing [*Manning et al.*, in press]. The reaction zone, therefore, is an area of dynamic, high temperature fluid-rock interaction.

Important information about the temperature and composition of fluids circulating in the reaction zone has been gained from fluid inclusion and vent fluid studies. For example, fluid inclusions hosted in rocks interpreted to have been altered in the reaction zone indicate that phase separation and inputs of magmatic volatiles may play important roles in shaping the chemistry of hydrothermal fluids [*Kelley*, 1996; *Kelley*, 1997]. For example, vent fluids commonly display elevated He^3, CO_2, SO_2 and methane values [*Alt et al.*, 1989;*Craig and Lupton*, 1981; *Craig et al.*, 1981; *Kelley et al.*, 1993]. Isotopic analyses of He and CO_2 in vent fluids commonly exhibit mantle values [*Craig and Lupton*, 1981; *Craig et al.*, 1981]. Unfortunately, quantification of the magmatic contribution to hydrothermal fluids remains difficult. While magmatic inputs may not affect alteration of the host rocks, they likely contribute to salinity and compositional variations of hydrothermal fluids [*Kelley et al.*, 1992].

Discharge Zone

Temperature-pressure conditions inferred for the reaction zone (340-465°C and 350-550 bars) are generally close to the critical point of seawater (407°C and 298 bars) [*Campbell et al.*, 1988; *Von Damm and Bischoff*, 1987]. At these conditions, the density and viscosity of the hydrothermal fluid decrease rapidly resulting in upflow of the fluid due to buoyancy forces (Figure 2.4) [*Norton*, 1984]. Estimates of flow rates in the subsurface from clast sizes in hydrothermal breccias and flow rates observed at active vents are high (0.5-5 m/s) [e.g., *Converse et al.*, 1984; *Delaney et al.*, 1987]. However, these values may be higher than subsurface flow rates. For example, slow, broadly distributed, subsurface flow in the discharge zone may be locally focused along faults and narrow vent orifices resulting in exaggerated flow rates measured at the seafloor [*Haymon et al.*, 1989]. In general, discharge of hydrothermal fluids occurs either by focused, high temperature (200-400°C) or diffuse, low temperature (< 200°C) flow. Estimates of heat flow from hydrothermal systems indicate the diffuse component of hydrothermal discharge transports an order of magnitude more heat than focused flow, suggesting diffuse upflow has significant effects on heat transport, chemical processes, and consequently hydrothermal alteration of the oceanic crust [*Alt*, 1995; *Stein and Stein*, 1994].

For example, core from Hole 504B contains a mineralized zone at the volcanic-dike transition [*Alt et al.*, 1993]. Not all fluids that exit on the seafloor form massive sulphides. Some fluids mix with cold seawater in the subsurface, thereby loosing their sulphide-forming metals, and exit as diffuse, cool (< 50°C), hydrothermal fluid-seawater mixtures [*Alt*, 1995]. Unfortunately, these drill cores do not provide spatial relationships that would be useful for studies of hydrothermal processes. As a result, much our knowledge of the lower portion of hydrothermal systems is based on studies of ophiolites.

Epidosites

Upflow zones in ophiolites are characterized by a special rock type: epidosite[*Bettison-Varga et al.*, 1992; *Haymon et al.*, 1989; *Nehlig et al.*, 1994; *Richardson et al.*, 1987; *Schiffman and Smith*, 1988; *Schiffman et al.*, 1987]. Epidosites are characterized by the replacement of primary

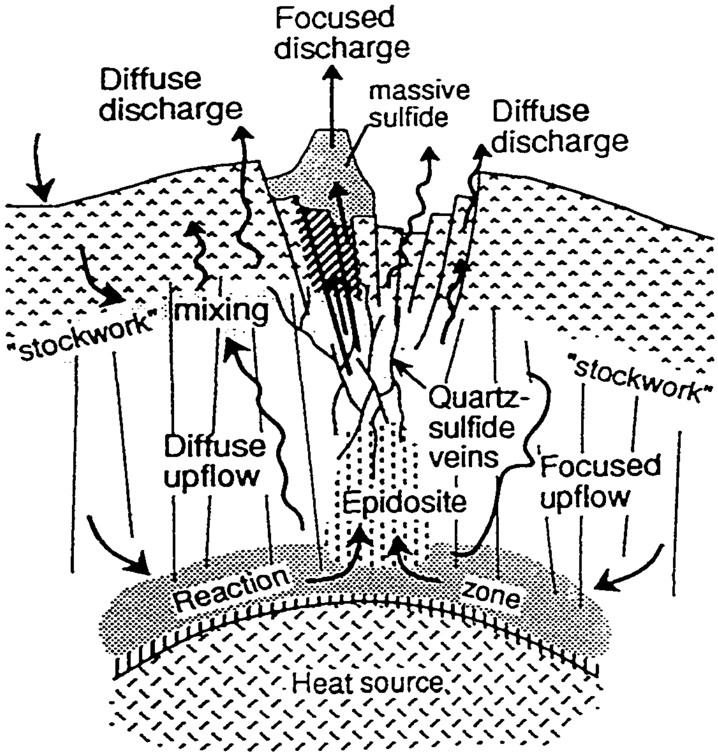

Figure 2.4 Sketch illustrating inferred relationships among different portions of hydrothermal upflow zones. Epidosites are believed to represent the root zones for focused upflow. As fluids reach the surface, they may exit either by focused or diffuse discharge. See text for discussion [from *Alt*, 1995].

igneous minerals in mafic to intermediate rocks by granular assemblages of quartz + epidote, ± chlorite, ± actinolite, ± magnetite ± ilmenite ± sulphides. This replacement is commonly accompanied by a complete loss of igneous texture. Epidosites are chemically distinct and are enriched in Ca, Sr, ^{34}S, Fe^{3+}/Fe^{T}, and $^{87}Sr/^{86}Sr$, and are depleted in Mg, Na, Zr, K, Cu, S, and ^{18}O relative to unaltered diabase [*Bettison-Varga et al.*, 1992; *Harper et al.*, 1988; *Haymon et al.*, 1989; *Nehlig et al.*, 1994; *Richardson et al.*, 1987; *Schiffman and Smith*, 1988]. Epidosites typically occur at the base of the sheeted dike section in zones 100's of metres wide, parallel to the axis of spreading [*Richardson et al.*, 1987; *Schiffman and Smith*, 1988]. Studies of epidosites in some ophiolites (e.g., Troodos and Samail) suggest they may represent root zones, below seafloor massive sulphides [*Bettison-Varga et al.*, 1992; *Haymon et al.*, 1989; *Nehlig et al.*, 1994; *Richardson et al.*, 1987; *Schiffman and Smith*, 1988; *Schiffman et al.*, 1987]. In the Samail ophiolite of Oman, there is evidence for fluid flow along a partially epidotized pathway to a massive sulphide deposit which formed by mixing between hydrothermal fluids and cold seawater [*Haymon et al.*, 1989]. Recent field studies on epidosites suggest the epidotization process occurs early, possibly soon after a dike is injected [*Varga et al.*, 1999].

Ophiolites are now generally thought to represent fossil sections of some type of ocean crust emplaced on land; studies over the last twenty five years suggest that many ophiolites were formed in a suprasubduction zone (SSZ) setting [*Miyashiro*, 1973; *Pearce et al.*, 1984 and others; *Rautenschlein et al.*, 1985; *Robinson et al.*, 1983]. As a result, ophiolites may not be representative of crust formed at MORs, and hydrothermal processes may also differ. The granular texture and complete replacement of primary mafic minerals in epidosites are part of the highly altered nature of ophiolitic rocks in general. Isotopic studies of epidosites suggest they form at high water/rock ratios [e.g., *Bickle and Teagle*, 1992; *Harper et al.*, 1988], whereas, conditions inferred for the reaction zone at MORs from experimental data suggest low water/rock ratios [*Campbell et al.*, 1988; *Von Damm and Bischoff*, 1987]. This is an important difference which has led to the suggestion that epidosites represent areas of focused upflow [*Bettison-Varga et al.*, 1992; *Haymon et al.*, 1989; *Nehlig et al.*, 1994; *Richardson et al.*, 1987; *Schiffman and Smith*, 1988; *Schiffman et al.*, 1987]. To date, very few samples of epidosite have been recovered from the modern oceans [*Fox et al.*, 1976; *Quon and Ehlers*, 1963]. The scarcity of epidosites at MORs may simply be due to the relatively limited sampling of the oceanic crust resulting in a failure to recover any that might exist. Alternatively, their scarcity may reflect a sampling bias, which has focused on active hydrothermal systems at MORs rather than other areas of oceanic accretion such as forearcs in which epidosites may be more common. These possibilities need to be tested by studying hydrothermal alteration from a variety of tectonic environments.

The Troodos Ophiolite

The Troodos ophiolite in Cyprus is one of the world's best-studied ophiolites, which makes it appropriate for comparison with the Tonga forearc. With acceptance of the theory of plate tectonics, Gass [1968] proposed that the Troodos ophiolite represented a fragment of oceanic crust formed by seafloor spreading at a MOR. However, early geochemical studies cast some doubt on the formation of Troodos at a MOR, suggesting that the Troodos extrusives were geochemically similar to rocks formed above subduction zones [*Miyashiro*, 1973; *Pearce*, 1975; *Pearce and Cann*, 1973]. In addition to the geochemical evidence, structural and sedimentological observations on the island of Cyprus also suggest formation of Troodos in a SSZ setting [*Robertson*, 1990]. This view has continued to be favoured with Troodos being formed above a northward-dipping subduction zone within an oceanic basin [*Pearce et al.*, 1984].

Recent work on the tectonic setting of SSZ ophiolites suggests they may have formed during the earliest stages of subduction at intra-oceanic arcs [*Bloomer et al.*, 1995; *Bloomer et al.*, 1996; *Stern and Bloomer*, 1992]. In particular, this model suggests that SW Pacific arcs represent an analogous tectonic setting to that for the formation of the Troodos ophiolite. Although the lack of volcaniclastic sediments blanketing basement rocks in the Troodos ophiolite precludes the possibility of a nearby mature arc [*Robertson*, 1990], rocks collected from the Izu-Bonin and Tonga trenches in the SW Pacific have many similarities to those found in Troodos. Although concrete evidence is lacking, the crustal formation of Troodos and other SSZ ophiolites during the incipient stages of subduction remains one of the best hypotheses.

The earliest studies of hydrothermal alteration in the Troodos ophiolite described pervasive regional metamorphic zones which increased in grade and intensity with depth [e.g., *Gass and Smewing*, 1973]. Specifically, low-grade, zeolite facies metamorphism was observed in the upper volcanics above higher-grade zeolite and greenschist facies metamorphism in the lower volcanics and uppermost sheeted dikes [*Gass and Smewing*, 1973]. This change in alteration was attributed to eruption of lavas in different tectonic settings

[*Gass and Smewing*, 1973]. However, geochemical evidence suggested the entire volcanic suite was co-magmatic [*Smewing et al.*, 1975]. Later work by Gillis and Robinson [1985; 1988; 1990] demonstrated that alteration was not as pervasive as previously described and that there was no systematic change with depth. Gillis and Robinson [1988; 1990] identified five alteration zones in the volcanic and upper-dike sections of the Troodos ophiolite: 1) a Seafloor Weathering Zone (SWZ); 2) a Low-Temperature Zone (LTZ); 3) a Transition Zone (TZ); 4) an Upper Dike Zone (UDZ); and 5) a Mineralized Zone (MZ). In this classification, the SWZ, LTZ, and TZ formed in the off-axis environment within 5-15 m.y. of crustal formation [*Gillis and Robinson*, 1988]. The location of the TZ between low- (LTZ) and high-temperature alteration (UDZ) is controlled by permeability contrast at the sheeted dike-lava transition [*Gillis and Robinson*, 1990]. Further work by Staudigel and Gillis [1990] focused on the timing of hydrothermal alteration which indicates alteration continues for tens of millions of years after the crust is created. Identification of fresh glass preserved at the base of the extrusive sequence provided a useful tool for determining the original chemical composition of volcanic rocks to compare with altered rocks [*Bednarz and Schmincke*, 1987; *Bednarz and Schmincke*, 1989; *Rautenschlein et al.*, 1985].

Of particular significance to this study, the Troodos ophiolite has provided much of our understanding of the lower portion of hydrothermal circulation. Several studies have documented the occurrence of epidosites in the Troodos ophiolite and much of our understanding of these rare rocks has come from Troodos [*Bettison-Varga et al.*, 1995; *Bettison-Varga et al.*, 1992; *Richardson et al.*, 1987; *Schiffman and Smith*, 1988; *Schiffman et al.*, 1987]. Hydrothermal processes in the plutonic section have been investigated using fluid inclusions. These studies showed that brine-rich (36-61 wt% NaCl equivalent) fluid inclusions were trapped during the earliest fracturing events at temperatures > 450-600°C [*Kelley and Robinson*, 1990; *Kelley et al.*, 1992]. These temperatures were much higher than those observed in the volcanics and upper sheeted dikes. Finally, recent work by [*Gillis and Roberts*, 1999] has identified the presence of a contact aureole at the base of the sheeted dikes separating the magmatic system below from the hydrothermal system above.

THE TONGA FOREARC

The Tonga forearc is part of an intra-oceanic convergent margin system which was initiated in the middle Eocene [*Bloomer et al.*, 1995]. The Tonga Trench marks the site of almost perpendicular westward subduction of the Pacific Plate beneath the Indo-Australian Plate at rates which increase northwards to a maximum of 240 ±11 mm/yr. (Figure 2.5) [*Bevis et al.*, 1995]. The system evolved in an extensional environment that resulted in the replacement of the overriding plate by rocks erupted during the natal stages of subduction initiation. Substantial subduction erosion and trench roll back have exposed basement rocks along the entire length of the forearc [*Bloomer et al.*, 1995; *Clift et al.*, 1998]. Preliminary Ar-Ar dating of volcanic samples has revealed two primary age ranges, 47-39 Ma and 15-9 Ma, which are penecontemporaneous with subduction initiation and arc magmatism, respectively [*Bloomer et al.*, 1998]. No rocks with ages older than Eocene have been recovered from the forearc, which is consistent with the overriding plate being replaced after the initiation of subduction [*Bloomer et al.*, 1998; *Bloomer et al.*, 1995].

Basement lithologies in the Tonga forearc include depleted island-arc-tholeiitic basalts, MOR basalts, boninites, andesites, dacites, their plutonic equivalents, and a variety of ultramafic rocks [*Bloomer et al.*, 1995; *Bloomer et al.*, 1996; *Falloon et al.*, 1987; *Kelman et al.*, 1997]. Similar lithologies are observed in the Izu-Bonin-Mariana (IBM) forearc. Recent studies of the earliest stages of intra-oceanic forearc development have drawn heavily from information gathered in the IBM forearc, which is one of the best-studied western Pacific forearcs [e.g., *Fryer et al.*, 1990; *Stern and Bloomer*, 1992]. The IBM system was also initiated in the middle Eocene and is believed to be analogous, with respect to origin and evolution, to the Tonga forearc [*Bloomer et al.*, 1995]. Studies in the IBM forearc have, therefore, been used to explain mechanisms of subduction initiation, related magmatism, and volcanism for the Tonga forearc [e.g., *Bloomer et al.*, 1995; *Stern and Bloomer*, 1992].

Recent studies of the earliest stages of forearc development have tried to explain a number of features which are not addressed by previous models of forearc evolution [*Stern and Bloomer*, 1992]. These features include: "1) an unusually broad zone of volcanism, 2) high magma production and eruption rates, 3) a strongly extensional tectonic environment, and 4) progressive migration and focusing of the magmatic front away from the trench" [*Stern and*

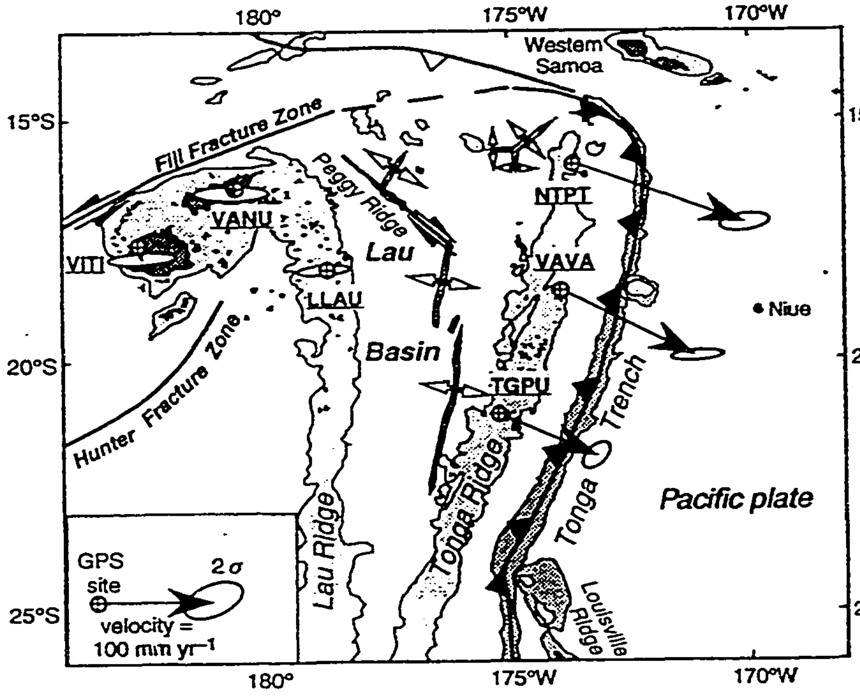

Figure 2.5 Location of the Tonga Trench and crustal velocities derived from GPS measurements based on a fixed Pacific Plate reference. Arrows represent velocity vectors with values at Niuatoputapu (NTPT) reaching a maximum of 240±11 mm/yr. [from *Bevis et al.*, 1995].

Bloomer, 1992 pg. 1621]. These features are also believed to be typical of the tectonic setting in which SSZ ophiolites form [*Bloomer et al.*, 1995; *Bloomer et al.*, 1996].

Although other models exist [e.g., *Seno and Maruyama*, 1984], subduction initiation in the IBM system is widely believed to have occurred at an oceanic transform fault largely due to the gravitational instability between young (0-20 Ma) oceanic lithosphere to the west and old (> 65 Ma) oceanic lithosphere to the east (Figure 2.6). Initially, vertical movement of the subducted lithosphere would begin to displace the underlying asthenosphere, resulting in the transfer of lower-density asthenosphere above the down-going lithosphere [*Stern and Bloomer*, 1992]. This displacement of the asthenosphere also results in extension within the young lithosphere to the west (Figure 2.6) [*Stern and Bloomer*, 1992]. Adiabatic decompression of the rising asthenosphere coupled with dehydration of the down-going slab would lead to extensive melting [*Stern and Bloomer*, 1992 and references therein]. The generation of large volumes of melt beneath the extensional environment of the overriding plate has been suggested to result in the initiation of seafloor spreading [*Stern and Bloomer*, 1992].

Stern and Bloomer [1992] point out two important differences between seafloor spreading in incipient-arc and MOR settings. First, seafloor spreading in the incipient-arc is likely to be poorly organised, characterised by many discrete ridge segments and asymmetric spreading. Second, the compositions of lavas formed in the incipient-arc are likely to be more depleted (i.e., boninites) resulting from partial melting of harzburgite [*Stern and Bloomer*, 1992]. Crust created during poorly organized seafloor spreading is inferred to have formed in a broad zone, approximately 200 km wide, which extends the length of the IBM forearc [*Fryer et al.*, 1990]. If it is assumed that broadly distributed magmatism occurred in the incipient-arc over a 10 m.y. period, crustal production rates would be 120 to 180 km^3 km^{-1} Ma^{-1} - on the order of slow-spreading ridges [*Stern and Bloomer*, 1992]. These rates of magmatism are unseen in mature island arcs which have mean eruption rates of 13 km^3 km^{-1} Ma^{-1} [*Gill*, 1981; *Sample and Karig*, 1982; *Wadge*, 1984]. The final stage of incipient-arc formation is marked by the stabilisation of the locus of volcanism somewhere near the present magmatic front [*Stern and Bloomer*, 1992]. Stern and Bloomer's model has been proposed as a possible tectonic environment for the formation of SSZ ophiolites. Samples dredged from the Tonga forearc represent some of the best plutonic rocks available for comparison with ophiolites. Similarities between rocks from the Tonga forearc and

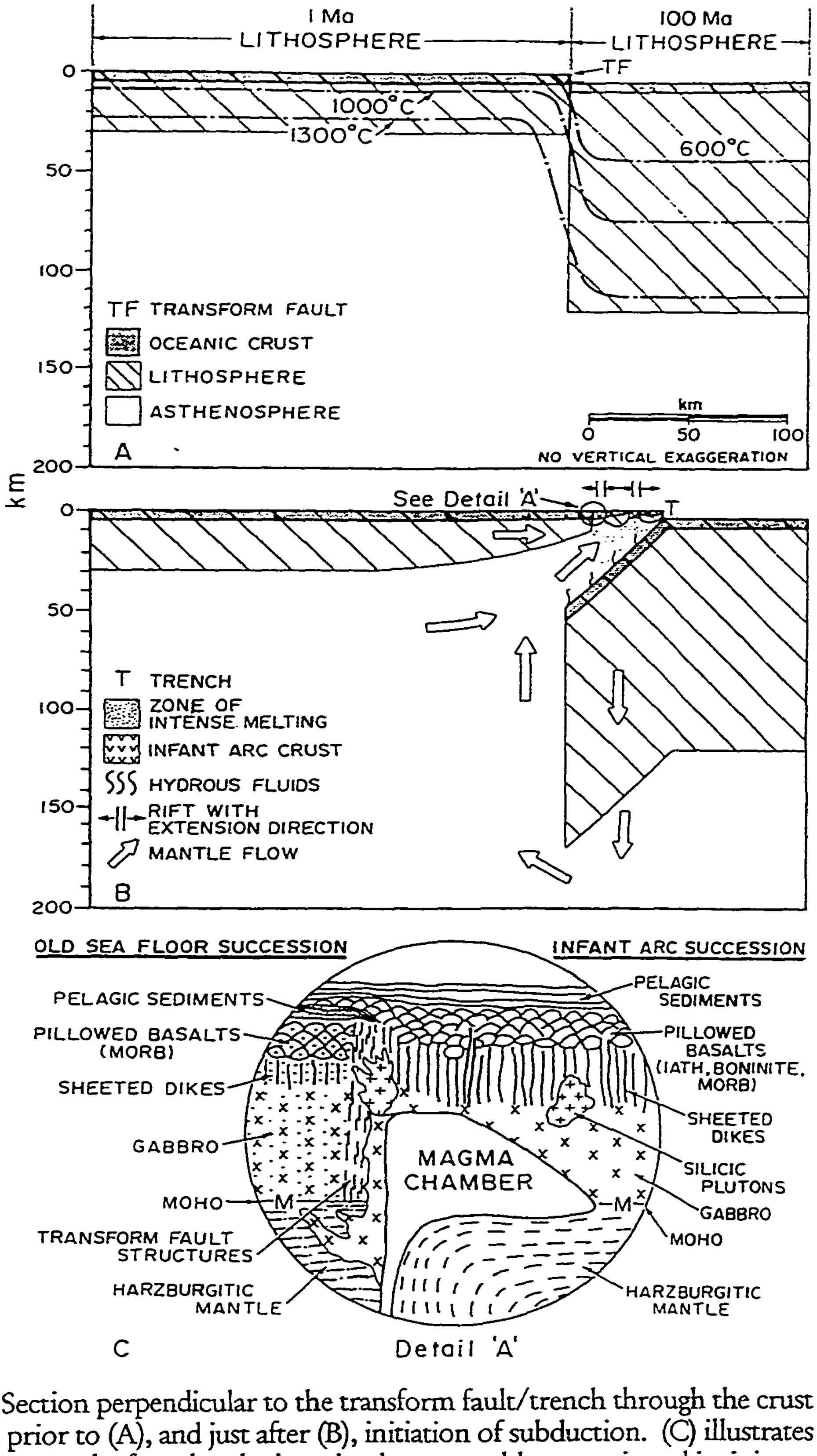

Figure 2.6 Section perpendicular to the transform fault/trench through the crust and upper mantle just prior to (A), and just after (B), initiation of subduction. (C) illustrates geologic relations that may be found at the junction between older oceanic and incipient-arc crust and lithosphere [from *Stern and Bloomer*, 1992].

ophiolites include the presence of boninites, high-Ca plagioclase, and the formation of early cumulus orthopyroxene [*Bloomer et al.*, 1995].

Tonga Forearc Samples

Samples for this study were collected during the 1996 Boomerang Leg 8 cruise on the Scripps Institute of Oceanography R/V *Melville*. Several varieties of rocks were dredged from 39 sites between 26° and 14°S along the trench-facing slope of the Tonga forearc (Figure 2.7). These rocks are similar to those found in many ophiolites, including depleted island-arc-tholeiitic basalts, mid-ocean ridge basalts, boninites, andesites, dacites, their plutonic equivalents, and a variety of ultramafic rocks [*Bloomer et al.*, 1998]. The distribution of lithologies is crudely layered; ultramafic rocks were recovered from the deepest dredges (8000-7000 m), gabbro and diabase are more common above, and volcanic rocks predominate above 5000 m (Figure 2.8) [*Bloomer et al.*, 1996]. A representative suite of samples collected from each dredge haul makes up the working collection for this study; however, the collection is biased toward altered samples. Additional sample material is stored at Oregon State University. These samples represent the most complete collection of lower crustal rocks ever recovered from a forearc setting.

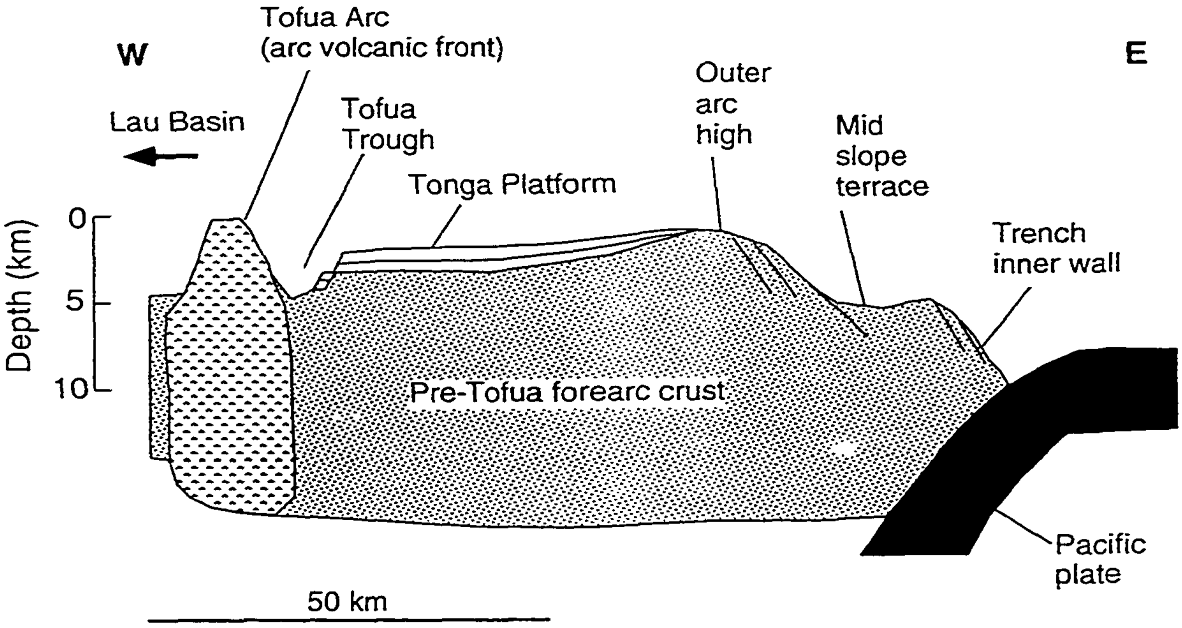

Figure 2.7 Simplified cross-section of the Tonga arc and forearc, showing principal structural and topographic features [*Clift et al.*, 1998]. The trench inner wall is equivalent to the trench-facing slope and is where the samples were recovered by dredging.

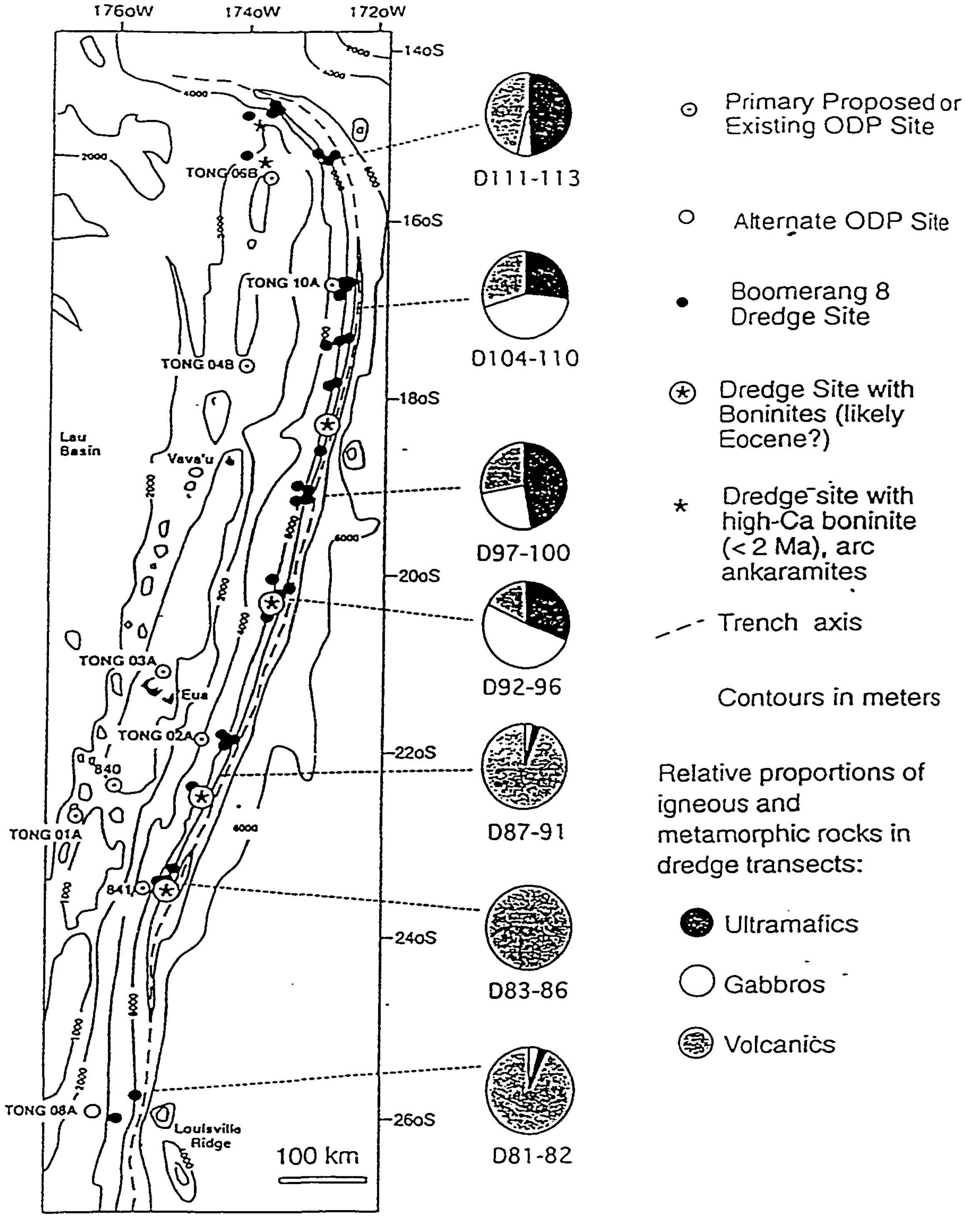

Figure 2.8 Relative proportions of igneous rock types and dredge locations from the 1996 Boomerang Leg 8 cruise [from Boomerang Leg 8 shipboard data].

Chapter 3

METAMORPHIC EVOLUTION

Hydrothermal circulation is a ubiquitous process operating in areas of active oceanic crustal accretion such as slow-, intermediate-, and fast-spreading mid-ocean ridges (MORs), intra-plate volcanic centres, and back-arc and forearc basins of island arc systems [*Humphris*, 1995; *Rona and Scott*, 1993]. There are a number of physical parameters that vary between these tectonic settings and affect hydrothermal systems. These include the spreading rate, depth of penetration of normal faulting, rate and volume of magmatic activity, composition of erupted magmas, and volatile contents of magmas [*Mével and Cannat*, 1991; *Olive et al.*, 1997; *Purdy et al.*, 1992; *Smith et al.*, 1997; *Stern and Bloomer*, 1992].

Ophiolites are commonly used as ancient analogues to study modern mid-ocean ridge processes although it is generally accepted that most ophiolites formed in a suprasubduction zone (SSZ) setting [*Miyashiro*, 1973; *Pearce et al.*, 1984]. Several studies have shown that important differences exist between patterns of hydrothermal alteration in MORs and SSZ ophiolites [*Alt*, 1995; *Gillis and Banerjee*, in press; *Schiffman et al.*, 1990]. Recent studies by Alt et al. [1998] and Kelman [1998] have documented hydrothermal alteration patterns in the shallow crust of modern SSZ environments – the Izu-Bonin and Tonga forearcs, respectively. These studies have shown that the degree of alteration in the volcanic sequences of forearcs is more extensive and occurs at higher water-rock ratios than at MORs, and is comparable to that observed in SSZ ophiolites.

The purpose of this chapter is to document the metamorphic evolution of a section of modern forearc crust using one of the most complete collections of basaltic, gabbroic, and felsic plutonic samples available, dredged from the Tonga forearc. I use the Tonga collection as a case study to evaluate the evolution of hydrothermal alteration in ocean crust formed in a modern SSZ setting. Mineral compositions and textures, and geothermometric calculations are used to constrain the evolution of alteration conditions (e.g., temperature, hydrothermal fluid composition, water-rock ratio) during progressive fluid-rock interaction. I compare the results with studies of hydrothermal alteration in SSZ ophiolites and MORs to assess the role tectonic setting plays in the development of hydrothermal circulation.

IGNEOUS ROCK TYPES

Over 1900 samples, comprising a wide variety of rock types, were dredged from 39 sites between 26° and 14°S along the trench-facing slope of the Tonga forearc during the 1996 Boomerang Leg 8 cruise aboard the *R/V Melville* (Figure 3.1). My study focuses on gabbros, plagiogranites, and basalts that display evidence of high-temperature (>200°C) alteration. The distribution of lithologies on the trench-facing slope is crudely layered with ultramafic rocks common in the deepest dredges (8000-7000 m), gabbros become more common above, and basalts are the prominent rock type at depths <5000 m [*Bloomer et al.*, 1996].

Gabbroic Rocks

Gabbroic samples range from medium- to coarse-grained, poikilitic to equigranular gabbro, olivine gabbro, oxide gabbro, and gabbronorite, all of which are referred to as gabbros. There is no evidence of modal layering, however, a few samples display a magmatic foliation defined by alignment of plagioclase crystals. Several samples contain brown, titaniferous amphibole that occurs as rims on or blebs in clinopyroxene, or as intergranular grains between plagioclase laths (Figure 3.2A).

Felsic Plutonic Rocks

A variety of felsic plutonic rocks, including diorite, quartz diorite, and tonalite, were recovered in association with the entire spectrum of lithologies. These plagiogranites are fine- to medium-grained rocks with subhedral granular and intergranular textures that contain quartz + plagioclase with minor amphibole ± magnetite ± ilmenite. In a few cases, plagiogranites contain >5% Fe-Ti oxides. Quartz and plagioclase commonly exhibit graphic intergrowth. Minor apatite, titanite, and rare zircon are commonly associated with quartz.

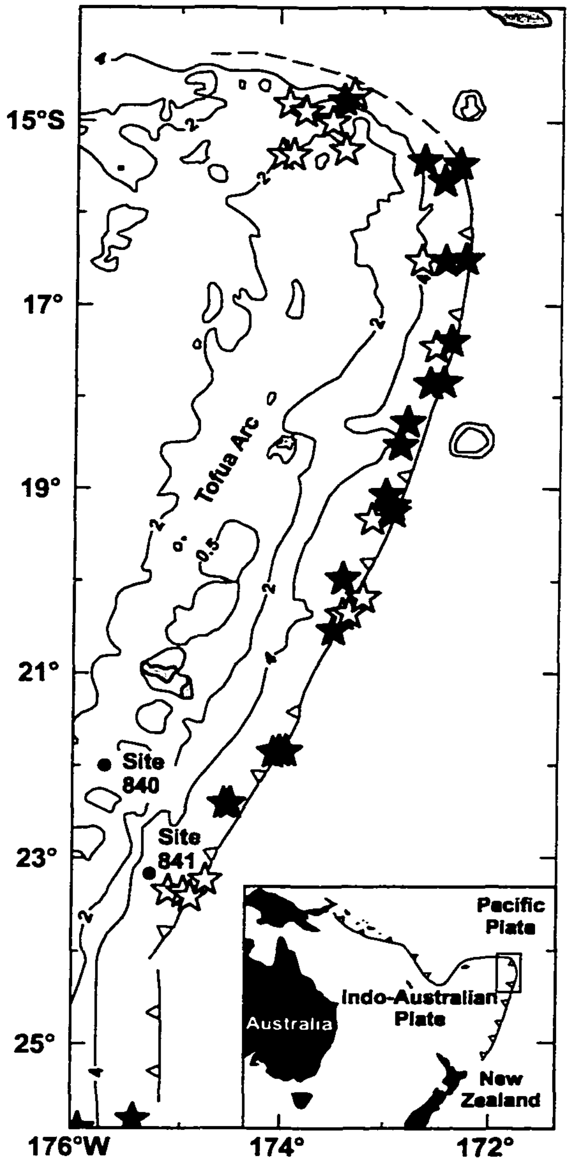

Figure 3.1 Bathymetric map showing dredge sites (stars) along the Tonga forearc. Filled stars indicate dredge locations of samples used in this study. Contour labels are gives in kilometers. Location of Ocean Drilling Program sites 840 and 841 are also shown. Inset map shows the location of the study area in the southwest Pacific. Modifed from Shipboard Scientific Party [1992].

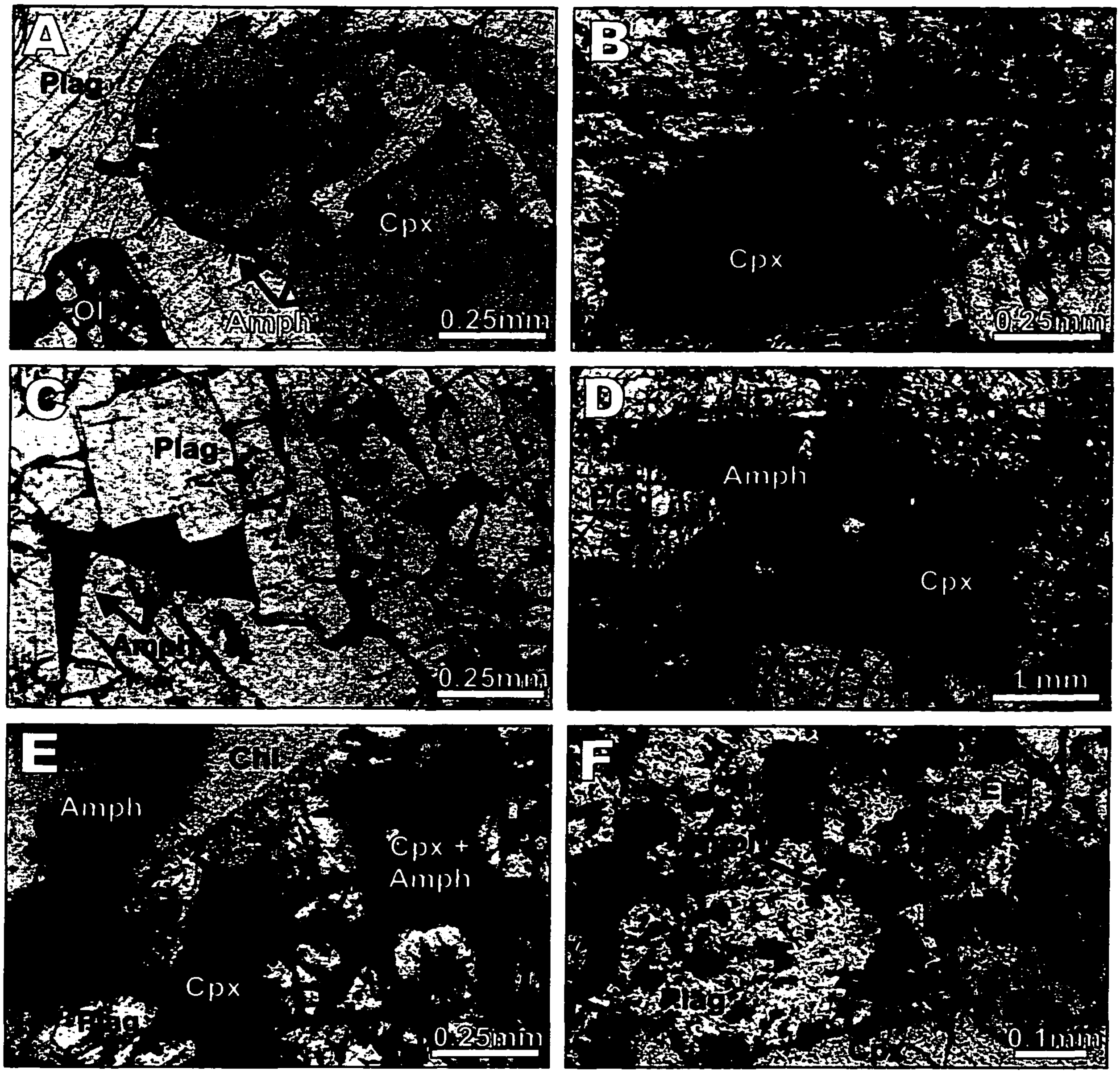

Figure 3.2 Photomicrographs showing typical mineral assemblages and textures: A) Brown (possibly magmatic) amphibole rimming clinopyroxene in olivine gabbro (sample 105-1-6). B) Amphibole veinlets cutting plagioclase and clinopyroxene in gabbro. Amphibole also occurs as rims on clinopyroxene (sample 105-1-25). C) Intergranular amphibole between plagioclase grains in olivine gabbro (sample 94-1-2). D) Replacement of clinopyroxene by amphibole in oxide gabbro. The sample is cut by numerous chlorite veinlets (sample 106-2-5). E) Acicular amphibole with chlorite in alteration patch in olivine gabbro (sample 113-2-11). F) Amphibole associated with patchy alteration in basalt (sample 105-3-6). All photos in plane polarized light. Abbreviations: Amph = amphibole, Cpx = clinopyroxene, Plag = plagioclase, Ol = olivine, Chl = chlorite, Ep = epidote.

Basaltic Rocks

Basaltic rocks are either aphyric to sparsely phyric (plagioclase ± clinopyroxene ± olivine) with a glassy or cryptocrystalline groundmass, or fine to medium grained with intergranular assemblages of plagioclase + clinopyroxene ± olivine ± magnetite ± ilmenite. These rocks may have been emplaced as either volcanic or intrusive units. However, without field relations it is generally not possible to speculate on their origin. Compositions include arc-tholeiites, depleted tholeiites, and magnesium-rich boninites [*Bloomer et al.*, 1998]. Fine to medium grained samples are distinguished from fine-grained gabbroic samples by the presence of vesicles. A few basaltic samples from dredge 96 display chilled margins against plagiogranite.

ALTERATION CHARACTERISTICS

The Tonga suite records the initial high-temperature penetration of hydrothermal fluids into the crust through to pervasive replacement of primary phases at low-temperature and high water-rock ratios. Gabbroic samples contain the broadest range of metamorphic mineral assemblages and preserve the best evidence of initial high-temperature hydrothermal alteration. Basalt and felsic plutonic samples are commonly altered to greenschist facies and lower temperature mineral assemblages. In all cases, pervasively altered samples that preserve high-temperature mineral assemblages have been subsequently overprinted during lower temperature events.

Gabbros

Gabbroic samples are variably altered to amphibolite to sub-zeolite facies assemblages [*Liou et al.*, 1974; *Spear*, 1981]. High-temperature alteration is preserved as green amphibole rims on pyroxene, microscopic green amphibole veinlets, and green amphibole grains interstitial to plagioclase (Figure 3.2B and 3.2C). The freshest samples exhibit limited (<20%) replacement of primary minerals with the most pervasive alteration proximal to amphibole veinlets. Clinopyroxene is variably altered (<20%) to green, blocky to acicular amphibole and chlorite at grain boundaries and proximal to crosscutting amphibole veinlets (Figure 3.2B). Olivine and orthopyroxene are altered (up to 30%) to assemblages of amphibole, chlorite, talc, iddingsite, serpentine, and magnetite. Samples not containing olivine or orthopyroxene are generally less altered. Plagioclase remains fresh or has a slight dusty appearance resulting from the presence of minute opaque inclusions or minor alteration to chlorite.

Samples which show more pervasive alteration (20 to > 50%) typically have higher temperature assemblages overprinted by minerals such as epidote, chlorite, prehnite, zeolites, carbonate, and clay minerals. Alteration near amphibole ± chlorite veins is most pervasive with haloes that extend 1 to 10 mm into the groundmass. Isolated patches of intensely altered primary minerals are also observed which contain chlorite ± epidote ± amphibole. Clinopyroxene is altered to amphibole ± chlorite ± magnetite and plagioclase is cloudy from replacement by sodic plagioclase, chlorite, epidote, and rare amphibole (Figure 3.2D). Olivine and orthopyroxene are rarely preserved.

The most pervasively and uniformly altered (> 50 %) samples contain assemblages of amphibole, chlorite, epidote, prehnite, zeolites, carbonate and clay minerals. Some relict clinopyroxene is present, however, most is replaced by amphibole + chlorite + magnetite (Figure 3.2E). Plagioclase is pervasively (> 30%) altered to sodic plagioclase, epidote, chlorite, and quartz. Pseudomorphs of olivine and orthopyroxene contain assemblages of amphibole, chlorite, talc, iddingsite, serpentine, and secondary magnetite. Brittle fractures and cataclastic zones are common. Veins commonly crosscut primary minerals and in a few cases, veins contain sequentially deposited minerals, which document changing metamorphic conditions. For example, some veins contain chlorite in the core and amphibole at the margins suggesting continued fluid flow at progressively lower temperatures. There is no evidence of ductile deformation in the Tonga collection.

Felsic Plutonic Rocks

Plagiogranites are variably altered to greenschist facies mineral assemblages. Blocky to acicular, dark to grass green, strongly pleochroic amphibole is the most common mafic phase. Brown, Ti-rich amphibole is locally rimmed by green, less Ti-rich amphibole and is locally further altered to chlorite. Fine-grained magnetite is associated with amphibole and chlorite in alteration patches. Plagioclase is typically sodic and varies from slightly dusty, resulting from very fine-grained opaque inclusions, to brown and cloudy, resulting from pervasive replacement by fine-grained chlorite ± epidote ± sericite ± clay minerals. Blocky, prismatic, and needlelike grains of epidote and patches of chlorite are common in more pervasively altered samples. Veins are rare, however, shear zones filled with fine-grained epidote + quartz ± chlorite ± carbonate are observed. Primary ilmenite is partially replaced by titanite. In the most pervasively altered samples, original igneous textures are replaced by granoblastic assemblages of epidote + quartz ± chlorite ± amphibole. These samples are transitional between plagiogranite protoliths and epidosites (see below).

Basalts

Basaltic samples included in this study were restricted to those displaying evidence of high-temperature (greenschist facies and above) alteration. The majority of the basaltic samples in the Tonga suite were altered to low temperature assemblages typical of MOR volcanic sequences [see *Kelman*, 1998]. Basalts are variably altered to mineral assemblages typical of the zeolite, greenschist, and amphibolite facies. In samples that preserve amphibolite facies mineral assemblages, clinopyroxene is pervasively (> 50%) replaced by amphibole. In samples that lack amphibolite facies assemblages, clinopyroxene is typically less altered (<30%) and replaced by amphibole + chlorite along fractures and grain boundaries. Plagioclase alteration in all samples varies from slightly dusty, resulting from very fine-grained opaque inclusions, to brown and cloudy, resulting from alteration to sodic plagioclase + chlorite ± epidote. Within alteration haloes adjacent to veins, plagioclase is altered to more sodic compositions and clinopyroxene is altered to amphibole ± chlorite. Pervasive (> 60%) alteration occurs in brecciated samples where patches of chlorite ± amphibole ± epidote replace groundmass phases (Figure 3.2F). A few samples with diabasic textures display pervasive (>70%) epidotization of plagioclase and replacement of clinopyroxene by chlorite ± amphibole. These samples are transitional to epidosites (see below). Zeolites, clay minerals, quartz, and carbonate commonly fill late veins that crosscut all other alteration features.

Epidosites

Epidosites are characterized by the complete replacement of primary igneous textures by granoblastic assemblages of epidote + quartz ± chlorite. Epidosites metasomatically replace several basalt and plagiogranite samples and represent extremely pervasive alteration resulting from high-temperature fluid-rock interaction at high water-rock ratios [*Richardson et* *al.*, 1987; *Schiffman and Smith*, 1988]. A previous study has shown that the Tongan epidosites are analogous to those described from SSZ ophiolites [*Banerjee et al.*, 2000].

MINERAL COMPOSITIONS

Major element compositions were determined using Camebax SX50 and JEOL JXA-8900R electron microprobes at Oregon State University and the University of Alberta, respectively. Operating conditions were similar for both microprobes in order to minimize inter-lab variation and instrument calibration was performed on natural standards. Overall, primary and secondary mineral compositions from the Tonga samples are similar to those from studies of MOR and ophiolites [e.g., *Alt et al.*, 1996; *Gillis*, 1995; *Gillis et al.*, 1993; *Manning et al.*, 1996; *Mével*, 1988; *Nehlig et al.*, 1994; *Stakes et al.*, 1991].

Amphibole

Amphibole occurs as intergranular grains between plagioclase laths, lines microfractures cutting plagioclase and clinopyroxene, fills veins, and occurs in groundmass alteration patches associated with chlorite. Most amphibole is calcic, however, minor Mg-Fe-Mn amphiboles are also observed. Brown, Ti-rich (Ti > 0.15 cations) amphibole occurs as rims on or blebs in clinopyroxene (Figure 3.2A), as well as interstitial grains between plagioclase in evolved lithologies (i.e., plagiogranite). Green to colorless, low-Ti (< 0.15 cations) fibrous amphibole fills monomineralic veins, occurs as alteration patches, and replaces pyroxene, olivine, and less commonly plagioclase. In a few cases, brown amphibole is rimmed by green, Ti-poor amphibole adjacent to veinlets. The combination of mineral chemistry (high vs. low Ti), geothermometry (see below), and textures suggest brown and green amphiboles are magmatic and hydrothermal in origin, respectively.

Amphibole has a wide range in composition, both within and between samples, from actinolite to magnesio-hornblende to pargasite (Table 3.1). Amphibole compositions correlate with the composition of the host lithology such that the most Mg-rich amphiboles occur in gabbros and basalts whereas Fe-rich amphiboles occur in plagiogranites (Figure 3.3). Site A occupancy systematically increases with increasing Al^{IV} (Figure 3.4A). Amphibole in veins contains < 0.15 Ti cations which is consistent with a hydrothermal origin [e.g., *Ito and Anderson*, 1983; *Mével*, 1988] (Figure 3.4B). MnO is typically low (< 0.5 wt%), but a few analyses contain up to 0.93 wt%. Amphibole contains up to 0.58 wt% F and 0.64 wt% Cl, however, most grains contain less than 0.10 and 0.30 wt%, respectively. Elevated F (>0.1 wt%) is most common in plagiogranites; however, a few gabbroic samples also contain high F values. Elevated (>0.1 wt%) Cl values are found in all rock types.

Chlorite

Chlorite and mixed-layer chlorite/smectite replace pyroxene, olivine, plagioclase, and amphibole, line veinlets cutting plagioclase, fill fractures, and occur in alteration patches associated with amphibole. Chlorites range in composition from chamosite to clinochlore [*Bailey*, 1988]. Several analyses contain >6.25 Si cations suggesting the presence of smectite interlayers (Table 3.2) [*Bettison and Schiffman*, 1988]. This mixed-layer chlorite/smectite is associated with chlorite and amphibole in alteration patches in pervasively altered samples.

Chlorite shows a wide range in $Mg/(Mg+Fe^{2+})$ that, like amphibole, correlates with the composition of the host lithology (Figure 3.5). Chlorite $Mg/(Mg+Fe^{2+})$ is relatively uniform within individual samples and is generally slightly less Mg-rich than coexisting clinopyroxene. Chlorite contains up to 0.70 wt% F and 0.16 wt% Cl; most grains contain <0.10 and <0.05 wt%, respectively. Mixed-layer chlorite/smectite typically has $Mg/(Mg+Fe^{2+})$ values similar to chlorite in the same sample. CaO, Na_2O and K_2O contents in chlorite and mixed-layer chlorite/smectite are <0.5 wt%.

Epidote

Epidote fills veins and vesicles where it occurs as blocky and radiating grains associated with quartz and chlorite, and replaces primary plagioclase. Epidote in all rock types has pistacite (Ps) contents ($Fe^{3+}/Fe^{3+}+Al^{VI}$) that range from Ps_{11} to Ps_{36}. There is no systematic variation in pistacite content with mode of occurrence. Pistacite contents in individual samples generally vary by <0.05 to 0.1, however, variations of 0.15 are recorded in some samples. Grains commonly display zoning with Fe-rich cores and Al-rich rims.

TABLE 3.1 Representative Amphibole Analyses

Sample	105-3-6	99-2-1	108-3-16	105-1-21	105-1-25	111-4-3	94-1-2	96-1-5	96-2-13	106-2-11
Occurrence	patchy	rim	patchy	mag	vein	rep	IG	rep	patchy	IG
Rock Type	basalt	basalt	BE	ol gabbro	gabbro	gabbro	GN	PG	PG	PG
Recalculation	15NK	15NK	15NK	ave	ave	15NK	ave	15NK	15NK	ave
SiO_2	49.46	49.54	51.27	42.97	47.47	52.93	46.02	47.55	52.57	44.53
TiO_2	0.19	0.21	0.83	2.61	0.43	0.06	0.50	0.37	0.48	2.50
Al_2O_3	3.87	7.04	2.70	12.07	7.92	3.97	6.96	2.53	3.65	10.40
FeO^T	22.83	11.47	17.05	9.24	15.40	9.09	18.87	33.48	11.97	14.05
Cr_2O_3	0.01	0.04	0.00	0.40	0.02	0.02	0.00	0.00	0.02	0.02
MnO	0.32	0.25	0.28	0.11	0.24	0.28	0.19	0.40	0.55	0.27
MgO	10.27	15.66	14.25	15.36	12.94	20.50	10.82	3.20	16.39	13.94
CaO	11.32	11.84	8.78	11.67	12.46	9.85	11.63	9.34	12.05	11.10
Na_2O	0.32	0.61	2.45	2.78	1.01	0.32	1.15	0.36	0.60	1.94
K_2O	0.08	0.03	0.39	0.12	0.05	0.05	0.05	0.15	0.02	0.10
F	0.05	0.00	1.21	0.00	0.05	0.04	0.06	0.00	0.00	0.09
Cl	0.03	0.02	0.03	0.03	0.13	0.03	0.31	0.32	0.01	0.06
Total	98.66	96.69	99.24	97.33	98.11	97.08	96.18	97.38	98.32	98.86
Si	7.35	7.16	7.67	6.24	6.91	7.45	6.93	7.59	7.51	6.40
Al^{iv}	0.65	0.85	0.33	1.76	1.09	0.55	1.07	0.41	0.50	1.60
Al^{vi}	0.03	0.35	0.15	0.30	0.27	0.10	0.17	0.07	0.12	0.16
Fe^{3+}	0.48	0.27	0.00	0.27	0.50	0.34	0.57	0.11	0.10	0.65
Fe^{2+}	2.36	1.12	2.14	0.85	1.38	0.73	1.81	4.37	1.33	1.04
Mg	2.28	3.37	3.18	3.32	2.81	4.30	2.43	0.76	3.49	2.99
Mn	0.04	0.03	0.04	0.01	0.03	0.03	0.02	0.05	0.07	0.03
Ti	0.02	0.02	0.09	0.29	0.05	0.01	0.06	0.04	0.05	0.27
Cr	0.00	0.01	0.00	0.05	0.00	0.00	0.00	0.00	0.00	0.00
Ca	1.80	1.83	1.41	1.81	1.94	1.49	1.88	1.60	1.84	1.71
Na	0.09	0.17	0.71	0.78	0.28	0.09	0.34	0.11	0.17	0.54
K	0.02	0.01	0.07	0.02	0.01	0.01	0.01	0.03	0.00	0.02
Cl	0.01	0.01	0.01	0.01	0.03	0.01	0.08	0.09	0.00	0.01
F	0.02	0.00	0.57	0.00	0.02	0.02	0.03	0.00	0.00	0.04
Cations	15.11	15.18	15.79	15.71	15.26	15.10	15.28	15.14	15.17	15.41

FeO^T = Total Fe as FeO; ave = average method; BE = basaltic epidosite; ol gabbro = olivine gabbro; GN = gabbronorite; PG = plagiogranite; rim = rim on clinopyroxene; mag = magmatic; rep = replacive; IG = intergranular; See text for description of amphibole mode of occurrence; Amphibole analyses were recalculated on the basis of 23 anhydrous oxygens according to the 15NK and average methods outlined in *Robinson et al.* [1982] in order to satisfy crystal-chemical limits.

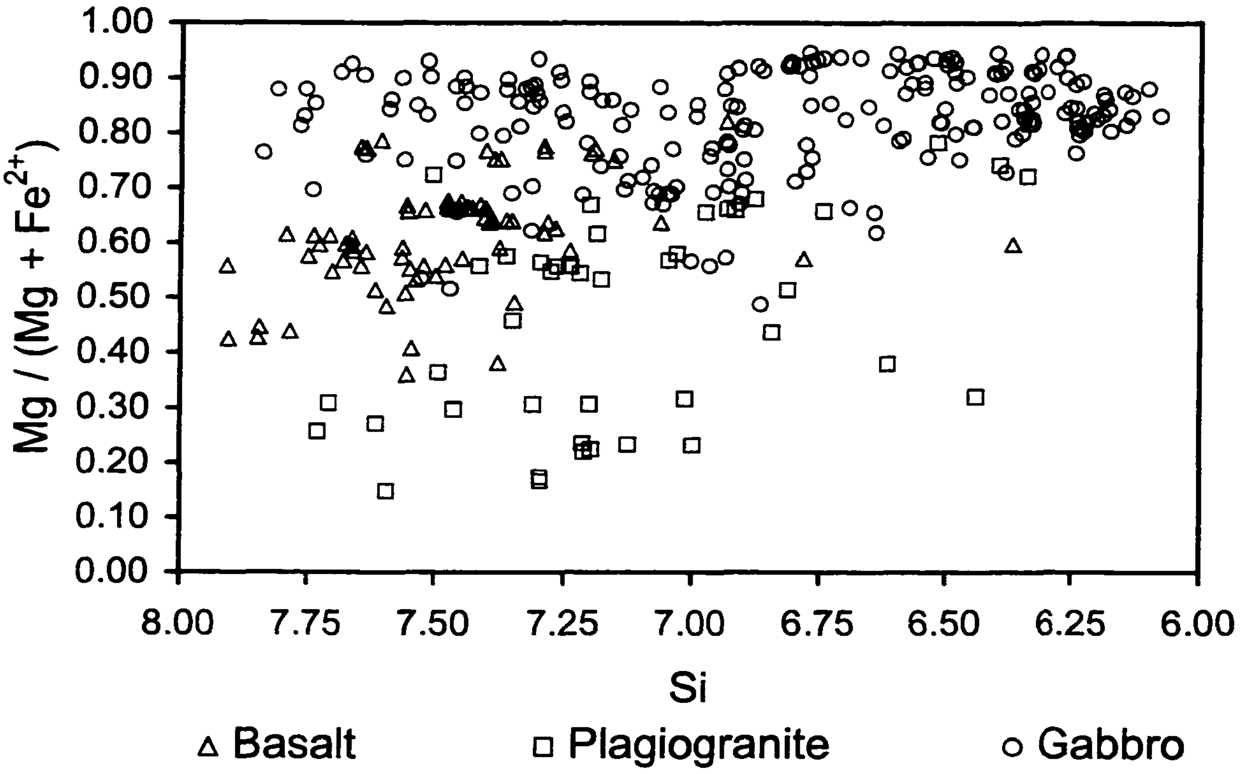

Figure 3.3 Mg / (Mg+Fe^{2+}) versus Si for calcic amphiboles showing correlation with host-rock composition. Fe-rich amphiboles commonly occur in plagiogranites while Mg-rich amphiboles occur in basalts and gabbros.

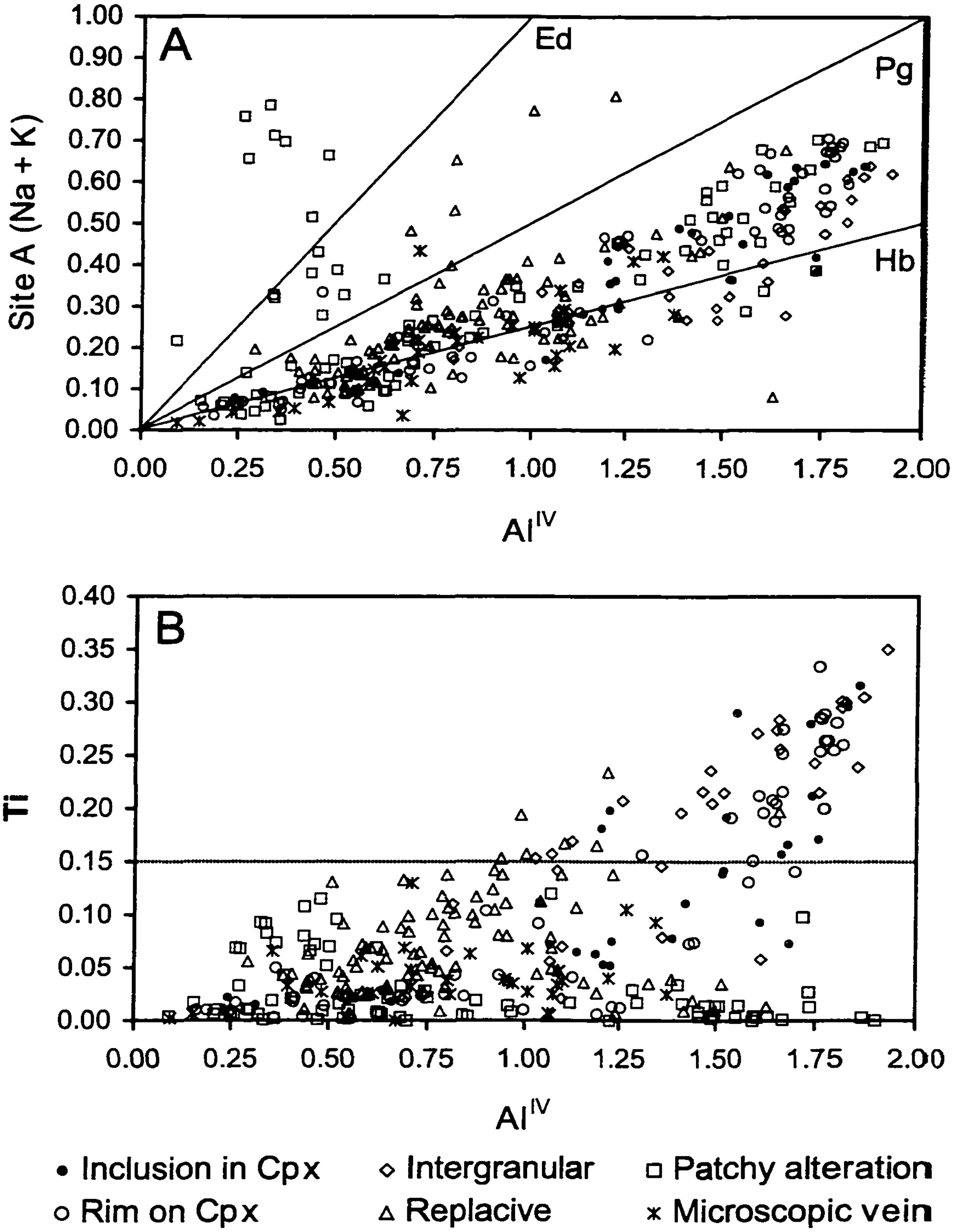

Figure 3.4 Compositions of calcic amphiboles. (A) site A occupancy versus Al^{IV} and (B) Ti versus Al^{IV}. Ed, Pg, and Hb indicate edenite, pargasite, and hornblende substitution trends, respectively. Vein amphibole of clearly hydrothermal origin contain <0.15 Ti cations (dashed line). Amphiboles which contain Ti > 0.15 are believed to be magmatic.

Table 3.2 Representative Chlorite Analyses

Sample	101-1-2	105-3-6	113-1-10	108-2-12	96-1-16	96-1-27	99-1-30	106-2-5	112-2-1	105-1-14
Rock Type	basalt	basalt	basalt	PG	PG	PG	GN	gabbro	gabbro	gabbro
Mineral	sm/chl	chl	chl	chl	chl	chl	chl	chl	sm/chl	chl
SiO_2	31.07	25.62	29.02	23.83	26.18	25.91	30.41	26.12	31.89	24.94
TiO_2	0.03	0.02	0.03	0.00	0.00	0.00	0.00	0.04	0.12	0.08
Al_2O_3	15.50	19.32	17.87	20.52	20.97	20.91	18.99	20.35	15.14	19.98
Cr_2O_3	0.01	nd	nd	0.02	0.00	0.01	0.00	nd	0.43	nd
FeO^T	23.10	30.74	20.98	38.60	30.38	25.75	12.50	26.71	10.47	26.84
MnO	0.25	0.39	0.26	0.32	0.18	0.29	0.14	0.33	0.20	0.24
MgO	17.11	11.78	20.51	4.48	10.98	15.47	25.49	14.87	28.14	14.67
CaO	0.31	0.21	0.06	0.09	0.10	0.02	0.14	0.09	0.15	0.15
Na_2O	0.04	0.05	0.03	0.02	0.03	0.00	0.02	0.02	0.00	0.07
K_2O	0.19	nd	nd	0.01	0.05	0.03	0.01	nd	0.01	nd
F	0.00	0.01	0.02	0.00	0.05	0.00	0.00	0.02	0.00	0.08
Cl	0.01	0.12	0.03	0.00	0.03	0.01	0.01	0.05	0.00	0.08
Total	87.62	88.26	88.81	87.89	88.95	88.40	87.71	88.60	86.55	87.13
Si	6.44	5.55	5.88	5.41	5.57	5.43	5.95	5.49	6.28	5.37
Al^{iv}	1.56	2.45	2.12	2.59	2.43	2.57	2.05	2.51	1.72	2.63
Al^{vi}	2.22	2.48	2.15	2.90	2.83	2.58	2.32	2.53	1.79	2.43
Ti	0.01	0.00	0.01	0.00	0.00	0.00	0.00	0.01	0.02	0.01
Fe^{3+}	0.00	0.00	0.00	0.00	0.00	0.00	0.00	0.00	0.00	0.00
Fe^{2+}	4.00	5.57	3.56	7.33	5.41	4.51	2.05	4.70	1.72	4.83
Cr	0.00	0.00	0.00	0.00	0.00	0.00	0.00	0.00	0.07	0.00
Mn	0.04	0.07	0.05	0.06	0.03	0.05	0.02	0.06	0.03	0.04
Mg	5.29	3.80	6.20	1.52	3.48	4.83	7.43	4.66	8.26	4.71
Ca	0.07	0.05	0.01	0.02	0.02	0.00	0.03	0.02	0.03	0.04
Na	0.02	0.02	0.01	0.01	0.01	0.00	0.01	0.01	0.00	0.03
K	0.05	0.00	0.00	0.00	0.01	0.01	0.00	0.00	0.00	0.00
F	0.00	0.01	0.03	0.00	0.07	0.00	0.00	0.03	0.00	0.11
Cl	0.01	0.09	0.02	0.00	0.02	0.01	0.01	0.04	0.00	0.06
Cations	19.69	19.99	19.98	19.84	19.80	19.99	19.86	19.98	19.92	20.09

FeO^T = total Fe as FeO; chl = chlorite; sm/chl = interlayered smectite/chlorite; nd = not determined; PG = plagiogranite; GN = gabbronorite; Analyses were recalculated on the basis of 28 anhydrous oxygens.

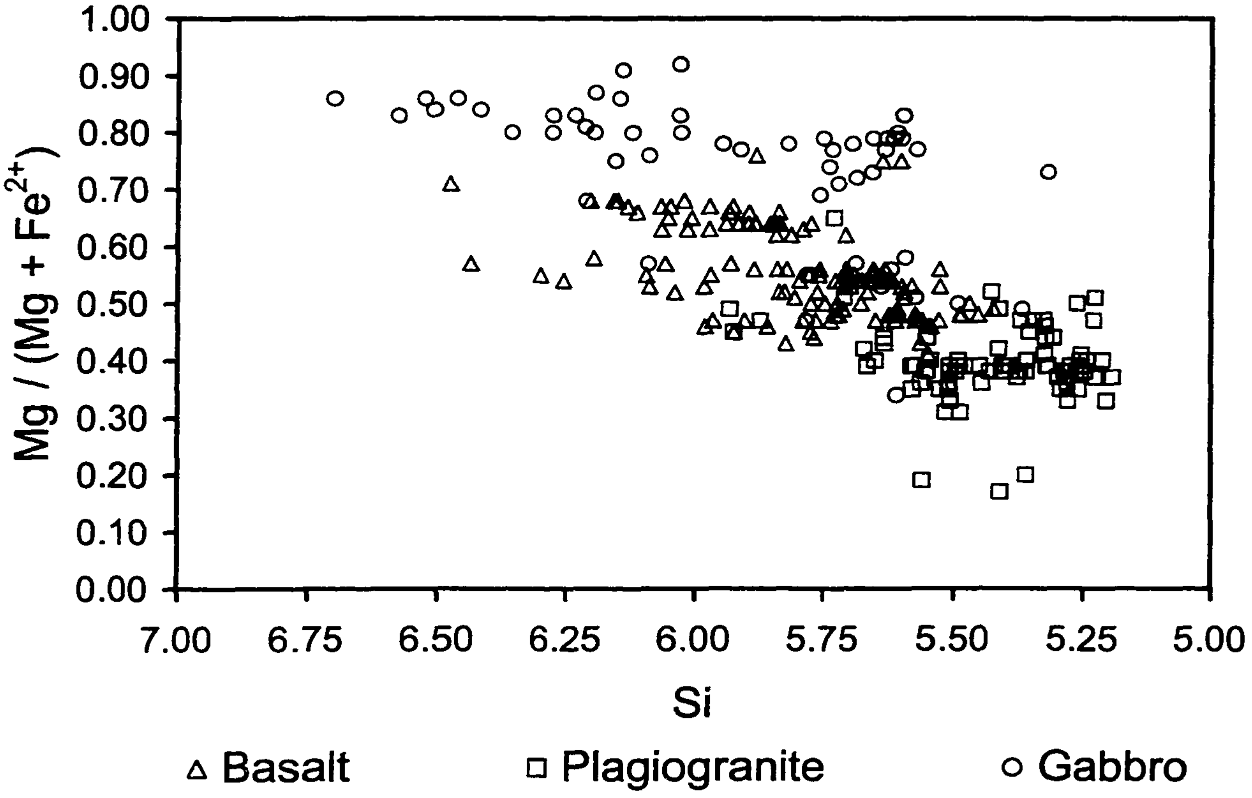

Figure 3.5 Mg / (Mg+Fe^{2+}) versus Si for chlorite showing correlation with host-rock composition. Chlorite in plagiogranites is relatively Fe-rich whereas chlorite in basalts and gabbros is relatively Mg-rich.

Plagioclase

In basaltic and gabbroic samples, primary plagioclase is replaced by secondary plagioclase, chlorite, sericite, and, less commonly, epidote or amphibole. In plagiogranite samples, plagioclase displays graphic intergrowth with quartz and is replaced by secondary plagioclase, epidote, chlorite and sericite.

Anorthite contents (An) display a wide range of values (0-97) due largely to variations in primary plagioclase compositions between lithologies. Anorthite contents in gabbroic samples form three populations. I interpret calcic ($>An_{70}$) and intermediate plagioclase (An_{40}-An_{63}) as primary except where it occurs in patches or as rims on primary grains next to veins, in which case I interpret it to be secondary. Sodic plagioclase (An_{10}-An_{30}) commonly occurs as rims on or patches in primary plagioclase and is hydrothermal in origin. Plagioclase in plagiogranites ranges from pure albite to An_{53}. Individual samples show a narrower range in anorthite contents; however, albite coexists with more calcic plagioclase in a number of samples. Primary plagioclase compositions in basalt range from An_{65} to An_{96}; secondary plagioclase is less than An_{21}.

In all rock types, secondary plagioclase spans a wide range in composition from pure albite to An_{90}, similar to secondary plagioclase in hydrothermally altered MORBs [*Alt et al.*, 1996; *Manning and MacLeod*, 1996; *Vanko and Laverne*, 1998]. The highest secondary anorthite contents are found in gabbros that preserve high-temperature alteration, typically as rims on primary grains adjacent to veins. The shift in the anorthite content of narrow secondary plagioclase rims relative to igneous values is generally less than 10%, and can be both greater and less than the igneous value, similar to what has been observed in oceanic gabbros [e.g., *Manning and MacLeod*, 1996]. Backscattered electron images confirmed the presence of secondary plagioclase and show that secondary plagioclase forms adjacent to veinlets and fractures in all rock types (see section below).

Pyroxene

Clinopyroxene $Mg/(Mg+Fe^{2+})$ ranges from 0.92 to 0.52 and does not show a marked variation between gabbroic lithologies. Cores (0.68 - 0.92) are generally more Mg-rich than rims (0.52 - 0.88). Rims display a wider range in composition than cores, however, it is uncertain if rims represent igneous zoning or hydrothermal overgrowths. Clinopyroxene of clearly hydrothermal origin was not identified, although clear unexsolved grains with low Al and Ti may be hydrothermal [cf., *Manning and Bird*, 1986]. TiO_2 decreases and Cr_2O_3 increases with increasing $Mg/(Mg+Fe^{2+})$. Al_2O_3 and Na_2O show no consistent trend with increasing $Mg/(Mg+Fe^{2+})$.

Fresh orthopyroxene is rare in the Tonga collection and occurs as large anhedral oikocrysts that enclose plagioclase. Orthopyroxene $Mg/(Mg+Fe^{2+})$ ranges from 0.63 to 0.73 and is similar (± 0.05) to those for clinopyroxene from the same sample.

Oxides and Sulphides

Magnetite and ilmenite occur in minor amounts in most samples (< 1 to 5%) but is present in modal proportions between 5 and 10% in a few gabbroic samples. Magnetite occurs as fine euhedral grains in the groundmass or as very fine, disseminated grains in alteration patches after olivine and pyroxene. Ilmenite shows skeletal textures and is commonly partially replaced by titanite. Minor pyrite occurs as very fine, disseminated grains in the groundmass of fine- to medium-grained basaltic samples. Pyrite and trace chalcopyrite occur in quartz ± epidote ± chlorite veins cutting basalt and plagiogranite samples. Sulphides are commonly rimmed by reddish brown Fe-oxyhydroxides.

Zeolites, Analcite, and Prehnite

Zeolites and analcite occur as blocky or radiating grains filling late-stage veins where they are associated with quartz and rarely carbonate. Thomsonite, mesolite, phillipsite, chabazite, laumontite, and analcite were tentatively identified on the basis of Si:Al ratios and Ca, Na, and K contents from electron microprobe analyses. Individual samples commonly contain only one variety of zeolite. Fine-grained, blocky prehnite occurs in late-stage veins in two gabbroic samples. Prehnite is associated with epidote in one sample and zeolites in the other. Prehnite is Fe-poor with $Fe^{3+}/(Fe^{3+}+Al^{VI})$ contents <0.06; MnO contents are <0.09 wt%.

TEMPERATURE CONSTRAINTS

Geothermometry

Metamorphic temperatures were calculated from amphibole-plagioclase pairs using the geothermometers of Holland and Blundy [1994]. The edenite-tremolite exchange thermometer was used for samples that contain quartz and the edenite-richterite thermometer was used for samples that do not. Forty-two pairs failed one or more of the compositional criteria imposed by Holland and Blundy's [1994] data set. Temperatures calculated for the remaining 131 amphibole-plagioclase pairs span a wide range, from 521° to >900°C. The stated uncertainty in the thermometers is ±40°C in the range 400° to 900°C (edenite-tremolite) and 500° to 900°C (edentite-richterite) [*Holland and Blundy*, 1994].

Several factors need to be addressed when considering the accuracy of the calculated temperature data. Foremost is the underlying assumption in Holland and Blundy's [1994] thermometers that exchange equilibrium between amphibole and coexisting plagioclase was achieved during fluid-rock interaction and that there has been little subsequent exchange. I believe this assumption holds for the Tonga collection for a number of reasons. Back-scattered electron images were used to ensure that secondary plagioclase was in contact with amphibole grains considered for thermometric calculations. In partially altered samples, narrow (5 to >20 microns) rims of secondary plagioclase are evident whose An contents are shifted relative to igneous values. Compositionally homogeneous secondary plagioclase adjacent to amphibole is consistent with local scale equilibrium. Since fluids that have penetrated over a kilometer into the lower oceanic crust are expected to be strongly rock-buffered, it is also likely that less exchange between fluid and rock is required to achieve equilibrium. In addition, reaction rates in the amphibolite facies have been shown to occur rapidly, which makes exchange equilibrium more probable [*Spear*, 1981; *Wood and Walther*, 1983]. Diffusive re-equilibration is unlikely in these samples due to the slow diffusion rates in plagioclase and amphibole [e.g., *Brabander and Giletti*, 1995; *Liu and Yund*, 1992].

The upper limit given by Holland and Blundy [1994] for both the edenite-richterite and edenite-tremolite thermometers is 900°C, therefore, temperatures >900°C may be inaccurate. Further limits on the plagioclase-amphibole thermometers are imposed by the compositions of amphibole and plagioclase in the calibrant dataset [*Holland and Blundy*, 1994]. The thermometers ignore Fe and Mg substitution into the M4 site because estimation of Fe and Mg M4 content is difficult and shows no significant effect on the thermometer [*Holland and Blundy*, 1994]. This is likely not a problem for the Tonga samples because their cummingtonite component is low (Table 3.1). The thermometers also ignore Mn and Ti. Mn contents in Tongan amphiboles are low (Table 3.1). Holland and Blundy [1994] caution against the use of their thermometers for kaersutites or Ti-rich richterites, however, these compositions do not occur in the Tonga suite. Similarly, the thermometers ignore substitution of F and Cl in amphibole. Most of the amphiboles used for calculating temperatures have low Cl and F contents (<0.2 and <0.1 wt% respectively). A few grains have elevated values (up to 0.64 wt% Cl and 0.58 wt% F), however, they do not show any systematic errors in calculated temperatures. I also investigated the dependence of amphibole chemistry on bulk-rock composition and found no correlation with calculated temperature. As a result, I believe systematic errors in calculated temperatures due to compositional variation are not likely for the Tonga suite.

Calculated temperatures for amphibole - secondary plagioclase pairs are summarized in Figure 3.6. Temperatures calculated for amphibole hosted in gabbro are typically higher than those for basalt and plagiogranite (Figure 3.6). The highest temperatures (802° to 995°C) in all rock types were calculated for brown amphibole that occurs as intergranular grains or rims on clinopyroxene. These grains commonly have elevated Ti contents (>0.15 cations) and are likely magmatic in origin. In gabbroic samples, amphibole that fills microfractures cutting plagioclase has low Ti contents (<0.15 cations) and records very high temperatures (723° to 917°C). Similar temperatures are recorded from green amphibole that rims or replaces clinopyroxene (721° to 874°C). These high temperatures are likely related to the early penetration of hydrothermal fluids into the lower crust.

Temperatures for plagiogranite and basalt are considerably lower than those from gabbros, with the exception of brown, high-Ti (0.25 cations average), intergranular amphibole grains in an oxide-rich plagiogranite that record an average temperature of 961°C.

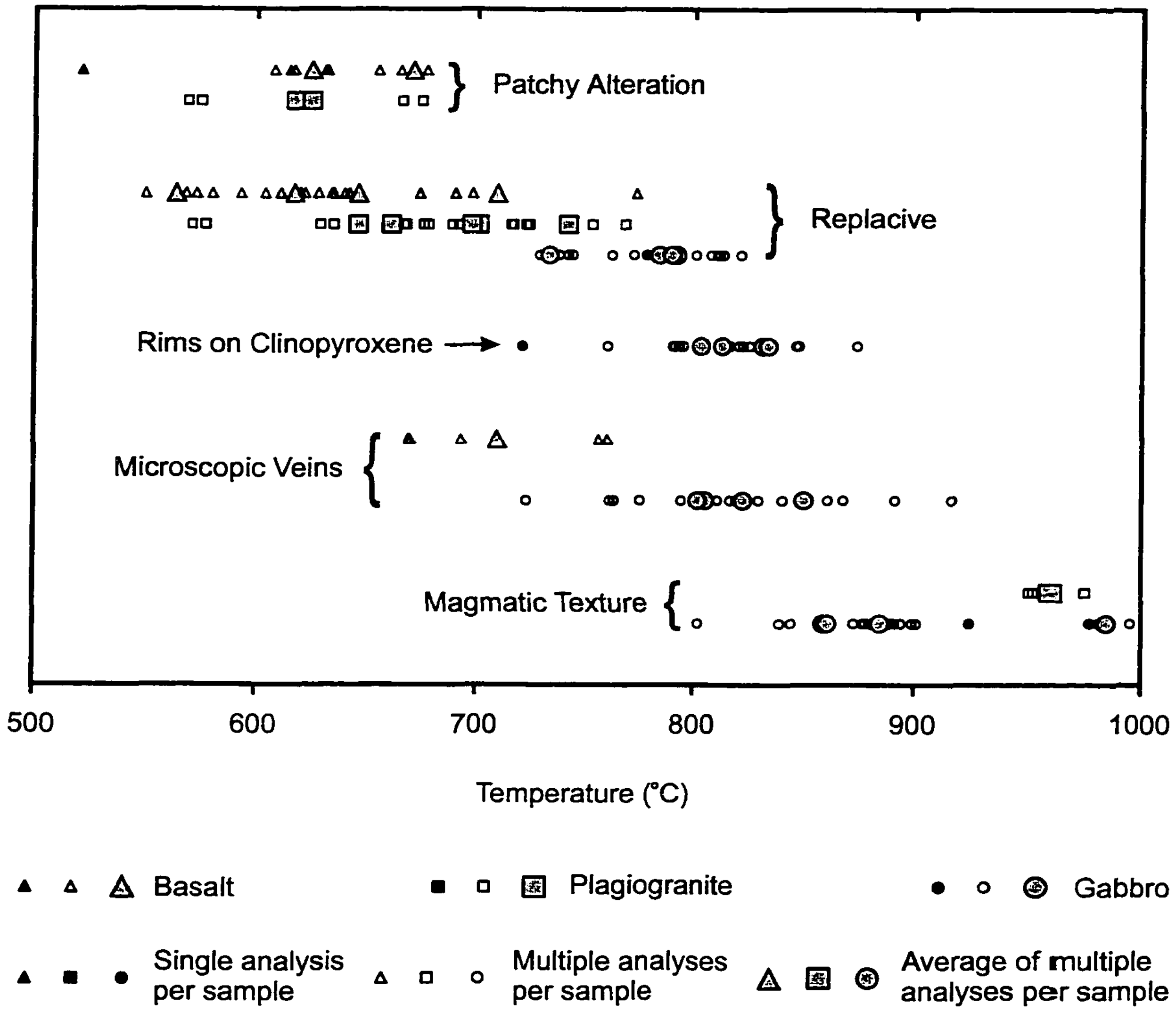

Figure 3.6 Temperatures calculated from plagioclase-amphibole pairs using the geothermometer of Holland and Blundy [1994]. Temperature ranges are grouped by amphibole mode of occurrence and rock type. Small open symbols indicate individual temperature measurements from samples in which multiple temperatures were calculated; small black symbols indicate individual analyses from samples in which only a single temperature for that mode of occurrence was calculated; large symbols represent average values calculated from multiple temperatures in the same sample. Number of calculated temperatures used for averages range from 2 to 8 per sample. Magmatic origin is defined as brown amphibole occurring as intergranular grains or rims on clinopyroxene. See text and Figure 3.2 for additional descriptions of amphibole textures.

Temperatures from secondary amphibole replacing primary amphibole and coexisting secondary plagioclase in plagiogranites span a wide range (571° to 768°C). Amphibole in microscopic veinlets cutting plagioclase in basalt record temperatures between 669° and 760°C. Temperatures from amphibole replacing primary clinopyroxene and coexisting secondary plagioclase in basalts range from 550° to 773°C. Secondary amphibole and plagioclase occurring in alteration patches after groundmass minerals in basalts and plagiogranites exhibit the lowest range in temperatures (521° to 677°C).

Experimental Studies

Several samples in the Tonga collection altered to greenschist facies mineral assemblages do not contain coexisting amphibole and plagioclase in textural equilibrium. For these samples it is necessary to compare mineral assemblages and compositions with experimental studies to constrain temperature. Experimental studies indicate that at low pressures greenschist assemblages include chlorite ± actinolite ± epidote + albite + titanite; transition to the amphibolite facies assemblages are characterized by oligoclase + titanite ± epidote, a decrease in the abundance of chlorite, and an increase in amphibole (actinolite to hornblende); and amphibolite facies assemblages include andesine + hornblende in the absence of chlorite [*Liou et al.*, 1974; *Moody et al.*, 1983; *Spear*, 1980]. Several samples from the Tonga collection contain mineral assemblages that are characteristic of more than one facies. For example, many samples contain chlorite ± epidote in association with calcic plagioclase ($X_{An} > 0.40$) + amphibole of variable composition. Experimental studies would place these samples in the transition to the amphibolite facies, which has peak temperatures near 550°C, assuming the quartz-magnetite-fayalite redox buffer [*Liou et al.*, 1974; *Moody et al.*, 1983; *Spear*, 1980]. These temperatures, in combination with thermometric calculations, indicate that metamorphism spanned several metamorphic facies.

Active Geothermal Systems

Constraints on temperatures of alteration for samples displaying pervasive alteration associated with the development of greenschist facies mineral assemblages can also be estimated by comparison with studies of geothermal systems. These studies have shown that mixed-layer chlorite/smectite first appears at temperatures between 150° and 180°C and discrete chlorite appears from >230° to 275°C [*Kristmannsdottir*, 1975; *Schiffman and Fridleifsson*, 1991]. Epidote, prehnite, and actinolite become stable at somewhat higher temperatures (> ~250°C) [*Bird et al.*, 1984; *Kristmannsdottir*, 1975]. Sub-greenschist facies temperatures (<150°C) are recorded by the presence of analcite and zeolites, which are found in late fractures. The presence of late carbonate and smectite in the most pervasively altered and fractured samples indicate temperatures eventually dropped below 100°C.

DISCUSSION

The metamorphic evolution of the Tonga suite reflects the time-integrated effects of fluid-rock interaction during the natal stages of subduction initiation. In the following sections I propose a sequence of events, including fracturing, fluid penetration, and tectonic exhumation that resulted in the metamorphic evolution of the Tonga suite. Although the Tonga samples lack stratigraphic control, comparison of alteration characteristics in the Tonga samples with MORs and SSZ ophiolites, as well as thermodynamic and experimental studies, allows us to place them in a conceptual framework. This also enables us to speculate on the relative timing of events and how they fit into a general crustal evolution model for the Tonga forearc.

Metamorphic Evolution

Plutonic Sequence

The transition from magmatic to hydrothermal-dominated conditions is marked by the penetration of seawater-derived fluids along grain boundaries and microfractures, at high temperatures (near 850°C). Microscopic (<1 mm), monomineralic amphibole veinlets in the Tonga gabbros penetrate relatively short distances but commonly intersect other microfractures, on a thin section scale, suggesting they represent a network with significant connectivity. This is consistent with recent thermodynamic models of water-rock interaction that suggest fluid flow is initiated at high temperatures in the lower ocean crust (700° to 900°C) [*McCollom and Shock*, 1998] and studies of gabbros from the fast-spreading EPR at Hess Deep [*Gillis*, 1995; *Manning et al.*, 1996; *Weston*, 1998] and Troodos ophiolite [*Gillis and Roberts*, 1999]. Limited replacement of primary minerals in the groundmass adjacent to microfractures and vein mineral chemistry suggest that incipient alteration occurred at low water-rock ratios. Thermodynamic modelling of gabbro alteration, however, suggests that petrographic features may not be useful in deriving information on fluid flow, and higher water-rock ratios may have existed [*McCollom and Shock*, 1998].

As temperature decreased below ~850°C, amphibole formed rims on and pervasively replaced clinopyroxene (Figure 3.6). Samples that preserve these high temperature alteration features commonly exhibit limited (<20%) replacement of primary phases. Replacement of primary amphibole by secondary amphibole in plagiogranites extended from 773° down to 550°C. In addition, more pervasively altered plagiogranites preserve acicular amphibole, associated with patchy chlorite and epidote, which formed at temperatures below 675°C. Below about 550°C, primary minerals are replaced by epidote and chlorite in addition to amphibole. Replacement of secondary amphibole and other high-temperature minerals (20-50%) is observed in more pervasively altered gabbro and plagiogranite samples. These samples commonly contain multiple generations of veins whose mineralogy follows the same progression as groundmass alteration and indicates fracturing continued from amphibolite to zeolite facies conditions. As discussed previously, secondary minerals such as chlorite and amphibole in the groundmass and veins mimic bulk rock chemistry, which suggests the primary mineralogy of the host rock is the controlling factor on vein mineral chemistry. This is similar to the results of several MOR studies [*Früh-Green et al.*, 1996; *Gillis et al.*, 1993; *Manning et al.*, 1996; *Stakes et al.*, 1991; *Vanko and Stakes*, 1991]. These studies attribute the influence of bulk-rock composition on vein mineral chemistry to low water-rock ratios and rapid reaction rates. However, in light of recent thermodynamic models [*McCollom and Shock*, 1998] I believe this may not always be the case.

The most pervasively altered (>50% replacement) gabbros display evidence of cataclastic deformation and/or veins filled with zeolites and other lower temperature (<350°C) minerals. It is clear from geothermometric data and petrographic evidence that the early metamorphism of gabbros occurred as high temperature fluids migrated along microfracture networks and grain boundaries. However, it is less clear whether later macroscopic veins and cataclastic deformation were part of an axial hydrothermal system or if they occurred at some later time. In MOR systems, low-temperature alteration in plutonic rocks is commonly associated with zones of enhanced flow due to processes of tectonic unroofing. For example, re-orientation of metamorphic veins to their original position along with isotopic evidence in samples from Hess Deep, suggest that macroscopic chlorite ± calc-silicate veins represent a later stage of fracturing resulting from off-axis tectonism [*Früh-Green et al.*, 1996; *MacLeod and Manning*, 1996; *Manning et al.*, 1996]. By analogy, late-stage, low-temperature veins in the Tonga gabbros could be related to faulting in the forearc, possibly resulting from trench rollback.

Basalts

Alteration in the basalts spanned a wide range of temperatures, resulting in the formation of overlapping metamorphic mineral assemblages. Although incipient alteration occurred at lower temperatures (<760°C) than in the gabbros (Figure 3.6), these temperatures are higher than have been inferred from previous studies of oceanic basalts. For example, the sheeted dikes in Hole 504B are generally characterized by greenschist facies mineral assemblages, although temperatures >400°C were likely reached in the basal section [*Alt et al.*, 1996]. As in the gabbros, increased fracturing and circulation of hydrothermal fluids resulted in more pervasive replacement at somewhat lower temperatures. The association of acicular amphibole with patchy chlorite marks the waning stages of high-temperature (>500°C) alteration and a change from low to moderate or high water-rock conditions. This transition is particularly evident in samples displaying cataclastic deformation in which the degree of replacement of primary phases is high. In the most pervasively altered samples (>50%), late stage veins and vesicles filled with zeolites, carbonate, and clay minerals indicate that alteration continued to <150°C and high water-rock ratios. However, it is not known if this low-temperature alteration represents a progression from alteration processes initiated at high temperatures or resulted from unrelated processes associated with tectonic unroofing.

Comparison with SSZ Ophiolites and MORs

The basic components of hydrothermal systems include a heat source (i.e., magma or cooling dike) that drives convection, extensional processes (i.e., dike injection, fracturing, and faulting), and circulating seawater, which promotes chemical exchange and recrystallization of the oceanic crust. These components are independent of tectonic setting. As a result, the alteration characteristics documented for the Tonga forearc are generally similar to those described for SSZ ophiolites [see review in *Gillis and Banerjee*, in press] and MOR crust [see review in *Alt*, 1995]. In the following section, I make several comparisons between SSZ ophiolites and MORs that are relevant to my interpretation of the metamorphic evolution of the Tonga forearc crust and place the Tonga collection into this context.

Basalt Alteration Characteristics

Alteration in volcanic sequences of SSZ ophiolites and MORs are highly variable in style, degree, and grade of alteration. Away from zones of hydrothermal discharge, alteration in MOR volcanic sequences is characterized by low temperature (<50°C) assemblages, whereas in ophiolites they commonly preserve higher temperature mineral assemblages (zeolite or prehnite-pumpellyite to greenschist facies) [see review in *Gillis and Banerjee*, in press]. Recent studies of metamorphism in the volcanic sequences of the Tonga and Izu-Bonin forearcs document low temperature mineral assemblages [*Alt et al.*, 1998; *Kelman*, 1998]. Basalts from the Tonga forearc that record high temperature alteration could have occurred either in the volcanic sequence or sheeted dikes, since their stratigraphic position is not known. If alteration of these basalts occurred in the volcanic sequence, their peak temperatures (up to 773°C) are considerably higher than estimates from the volcanic sequences of both MORs and SSZ ophiolites. However, if alteration took place in the sheeted dikes, the temperatures are closer to those observed in MOR and SSZ ophiolite settings [see review in *Gillis and Banerjee*, in press]. For example, high temperature alteration (>700°C) is locally observed in sheeted dikes from Hess Deep [*Gillis et al.*, 1999].

An increase in the degree of replacement of igneous phases, such as clinopyroxene, with depth is commonly attributed to a concomitant increase in alteration temperature and is observed in the sheeted dike sections of both SSZ ophiolites and MORs [*Gillis and Banerjee*, in press]. In the Troodos ophiolite, clinopyroxene is fresh or partially altered and chlorite ± quartz are common groundmass phases in the shallow dikes [*Gillis and Robinson*, 1990]. However, clinopyroxene is commonly completely replaced by amphibole at the base of the sheeted dike sequence [*Gillis and Roberts*, 1999]. Replacement of clinopyroxene by amphibole in Hole 504B follows a similar trend with depth, however, the degree of replacement in the deepest portions of Hole 504B is generally much less than 100% and commonly <50% [*Alt* *et al.*, 1996]. This is also true of the sheeted dikes at Hess Deep, which commonly preserve fresh clinopyroxene [*Gillis*, 1995]. Basalts from the Tonga forearc that record high temperatures are characterized by pervasive (> 50%) replacement of clinopyroxene by amphibole whereas those that preserve fresh clinopyroxene are dominated by chlorite and epidote. These characteristics suggest the high peak alteration temperatures observed in Tonga basalts are similar to those observed in the basal sheeted dikes of both SSZ ophiolites and MORs. The lack of stratigraphy in Tonga makes comparisons of degree of replacement of clinopyroxene with depth somewhat equivocal. However, other studies of metamorphism in forearcs have suggested the degree of alteration in the volcanic sequence is more similar to SSZ ophiolites than MORs [*Alt et al.*, 1998; *Kelman*, 1998].

Presence of Epidosites and Plagiogranites

Epidosites, from both plagiogranite and basalt protoliths, occur in the Tonga collection and provide a link between ancient SSZ ophiolites and crust formed in a modern SSZ setting [*Banerjee et al.*, 2000]. Epidosites are well documented in SSZ ophiolites yet they are conspicuously rare in rock collections from modern oceanic settings [*Gillis and Banerjee*, in press]. Fluid inclusion data indicate that the Tonga epidosites interacted with seawater-derived and possibly magmatic fluids at high temperatures (250° to >450°C) [*Banerjee et al.*, 2000]. Field and petrological data suggest that epidosites form in upflow zones at the base of ore-forming hydrothermal systems [*Bettison-Varga et al.*, 1992; *Nehlig et al.*, 1994; *Richardson et al.*, 1987; *Schiffman et al.*, 1987].

Similarly, plagiogranites are rare in collections from MORs but are commonly observed in SSZ ophiolites. Fluid inclusion studies of plagiogranites in SSZ ophiolites have identified highly saline, three phase (liquid + vapor + halite) inclusions that likely represent brines exsolved directly from late-stage melts [e.g., *Kelley et al.*, 1992; *Nehlig et al.*, 1994]. Fluid inclusions with similar properties are found in Tonga plagiogranites, several of which are partially epidotized. Magmatic volatile contributions from evolved, late-stage melts (plagiogranites) to hydrothermal systems may help explain the presence of epidosites in SSZ ophiolites and the Tonga forearc as well as their absence at mid-ocean ridges.

Brittle–Ductile Deformation

An important characteristic of the Tonga forearc gabbros is the presence of well-developed brittle deformation in the absence of ductile deformation. Brittle fractures range in scale from microscopic (<1 mm) to macroscopic (1 to 5 mm) and also include centimeter-scale zones of cataclastic deformation. The microscopic veinlets are very similar to those described from Hess Deep and Oman [*Manning et al.*, in press]. In all cases, these microfractures are associated with crystal-plastic features such as twinning and undulatory extinction [present study; *Manning et al.*, in press]. I therefore interpret the microscopic amphibole veinlets as evidence that the initial penetration of hydrothermal fluids into the plutonic sequence occurred during semibrittle microfracturing as the gabbros cooled below the brittle-plastic transition [e.g., *Evans et al.*, 1990].

In a recent study, Hirth et al. [1998] modeled the depth to the brittle-plastic transition in the oceanic crust using the dry diabase flow laws of Mackwell et al. [1994]. Their results indicate that the strength of the lower oceanic crust is considerably greater than previously determined using "wet" diabase flow laws [see discussion in *Hirth et al.*, 1998]. Application of a more recent flow law for dry diabase [*Mackwell et al.*, 1998] results in a further increase in strength for the lower crust. The greater strength of the lower oceanic crust, predicted from dry diabase experiments, allows deformation by brittle failure to occur at higher temperatures than expected in weaker crust models based on "wet" diabase flow laws [*Hirth et al.*, 1998]. This is consistent with the high temperatures associated with the development of microfractures in Tonga (present study), Hess Deep, and Oman [*Manning et al.*, in press]. Temperatures recorded from gabbros in the Tonga suite, however, are slightly higher than those reported in the literature [e.g., *Gillis and Roberts*, 1999; *Manning et al.*, 1996] and fall in the ductile regime predicted by Hirth et al. [1998], regardless of which diabase flow law is used. Temperatures of initial fracturing in the Oman ophiolite show an increasing trend with depth and approach those observed in Tonga (829°C ± 38) in the lower gabbros near the crust-mantle boundary [*Manning et al.*, in press]. Although it is possible that the samples with the highest temperatures come from the base of the plutonic sequence, these samples are not restricted to one lithology (e.g., olivine gabbro). I believe that rheological variations with depth such as changes in modal mineralogy, increasing extent of hydrolytic weakening, increasing strain rate, or high pore fluid pressures [such as magmatic volatile buildup, *Gillis and Roberts*, 1999] more likely resulted in the observed high temperatures of microfracturing.

The presence or absence of melt beneath MORs has important implications for hydrothermal systems. Geophysical studies have shown that magma supply at mid-ocean ridges is spreading rate dependent and that magmatism is ephemeral at slow spreading ridges [e.g., *Sinton and Detrick*, 1992]. Models of high-temperature hydrothermal circulation in the lower oceanic crust formed at slow-spreading ridges suggest that the initial penetration of hydrothermal fluids occurs penecontemporaneously with the onset of ductile shearing at temperatures near 750°C [*Cannat et al.*, 1991; *Dick et al.*, 1991; *Gillis et al.*, 1993; *Mével and Cannat*, 1991; *Stakes et al.*, 1991]. In contrast, geophysical investigations of fast-spreading ridges indicate that melt lenses can exist for extended periods of time [e.g., *Sinton and Detrick*, 1992]. Lower crustal rocks formed at fast-spreading MORs show no evidence of sub-solidus ductile deformation and initial metamorphism occurs at temperatures as high as 750°C [*MacLeod et al.*, 1996]. These differences in initial fracture propagation indicate that the presence or absence of ductile deformation in gabbroic rocks is related to the rate of magma supply. This suggests that the mechanism of crustal construction in the Tonga forearc likely involved a magma-rich environment, similar to that of a fast-spreading ridge, although the geometry of crustal construction in forearcs is still poorly understood.

CONCLUSIONS

The extensive suite of hydrothermally altered rocks dredged from the Tonga forearc are a unique collection and provide an opportunity to study the metamorphic evolution of ocean crust formed in a modern SSZ setting. Basalt, plagiogranite, and gabbro samples record a complex history of hydrothermal alteration resulting from interaction with seawater and possibly magmatic fluids. The initial penetration of seawater into the lower crust occurred along grain boundaries and microscopic fractures at temperatures > 800°C. As the plutonic sequence cooled, increased fracturing led to the pervasive replacement of clinopyroxene by amphibole and later chlorite. Late fractures and zones of cataclastic deformation that crosscut all other features may have occurred long after initial emplacement of the crust in the forearc and could be related to faulting associated with trench rollback. These high temperatures may be related to distinctive tectonic and magmatic conditions during crustal construction in forearcs. However, initiation of high temperature brittle deformation in the absence of ductile deformation suggests the Tonga forearc crust was constructed in a magma-rich environment, similar to fast-spreading mid-ocean ridges.

High temperature alteration in basalts is consistent with that observed in the basal sheeted dike sections of SSZ ophiolites and some MORs. Alteration in the gabbros is also similar to both SSZ ophiolites and MORs. However, the degree of alteration in basalts and the presence of epidosites in the Tonga collection are most similar to alteration characteristics in SSZ ophiolites.

Chapter 4

EPIDOSITES

Epidosites are characterized by metasomatic replacement of primary igneous minerals by granoblastic assemblages of quartz + epidote ± chlorite ± actinolite ± ilmenite ± magnetite ± sulfides. Field and petrological data suggest that they form in upflow zones at the base of ore-forming hydrothermal systems [*Bettison-Varga et al.*, 1992; *Nehlig et al.*, 1994; *Richardson et al.*, 1987; *Schiffman et al.*, 1987]. As a result, identification of epidosites can be a useful exploration tool for the location of massive sulfide deposits.

Epidosites are well documented in suprasubduction zone (SSZ) ophiolites [*Gillis and Banerjee*, in press] yet they are conspicuously rare in rock collections from modern oceanic settings, having only been reported from two mid-ocean ridge locations [*Fox et al.*, 1976; *Quon and Ehlers*, 1963]. The sample reported by Fox et al. [1976] is not a true epidosite and is simply a rock with abundant epidote fracture fill. Whether this is also true for the sample reported by Quon and Ehlers [1963] is unknown, because the sample cannot be located.

This chapter reports the discovery of epidosites from the Tonga forearc that represent the first documented suite recovered from a modern oceanic setting. Petrological, mineralogical, and geochemical data are used to demonstrate that the metamorphic conditions necessary for their formation were similar to conditions inferred for SSZ ophiolite-hosted epidosites. As a result, forearcs may represent a modern analogue for the tectonic setting in which SSZ ophiolites formed.

EPIDOSITE TYPES

Epidosites in ophiolites typically occur within basaltic sheeted dikes (type A) and plagiogranites (type B; including tonalite, trondhjemite, and quartz diorite). Within sheeted dike complexes, epidosites either form as patches in single dikes or dike outcrops [e.g., Semail, *Nehlig et al.*, 1994] or compose large zones up to hundreds of meters wide, parallel to the axis of spreading [e.g., Troodos, *Richardson et al.*, 1987; *Schiffman et al.*, 1987].

Plagiogranite-hosted epidosites occur as irregular patches (centimeters to meters wide) in the Troodos [*Cowan and Cann*, 1988; *Kelley et al.*, 1992; *Richardson et al.*, 1987] and Samail [*Stakes and Taylor*, 1992], ophiolites.

SAMPLE DESCRIPTIONS AND PETROGRAPHY

Epidosites

Five epidosites and ten samples displaying various stages of epidotization were recovered from five dredges between 20° and 14°S (Figure 4.1). Both types of epidosites reported from ophiolites are present in the Tonga collection. Type A epidosites from basaltic protoliths are fine grained and contain vesicles filled with quartz + epidote ± chlorite. Type B epidosites from plagiogranite protoliths are fine to medium grained and either completely replace the plagiogranite (sample 96-1-14) or are developed in brittle shears (samples 102-4-1 and 113-1-26). All of the Tongan epidosites have a distinctive pistachio green color and are characterized by the replacement of igneous minerals and textures (Figure 4.2A) by granoblastic assemblages of quartz + epidote ± chlorite (Figure 4.2B). Accessory minerals include acicular amphibole, titanite, apatite, ilmenite, and magnetite.

Epidosites contain only secondary minerals that have replaced either primary minerals or filled voids. For example, clear, euhedral to prismatic grains of epidote and quartz appear to have grown in pore spaces. Turbid, fluid inclusion-rich, anhedral grains are typical of groundmass replacement. Chlorite replaces groundmass plagioclase and clinopyroxene, and fills interstitial spaces between quartz and epidote grains, suggesting growth after quartz and epidote. The modal abundance of epidote generally increases as chlorite decreases (Table 4.1). Ilmenite and magnetite show skeletal textures and are commonly partially replaced by titanite. Amphibole and apatite, where present, occur as fine needles in quartz and chlorite. These textures and assemblages are similar to those found in epidosites described from the Troodos [*Richardson et al.*, 1987; *Schiffman and Smith*, 1988], Josephine [*Harper et al.*, 1988], and Semail [*Nehlig et al.*, 1994] ophiolites.

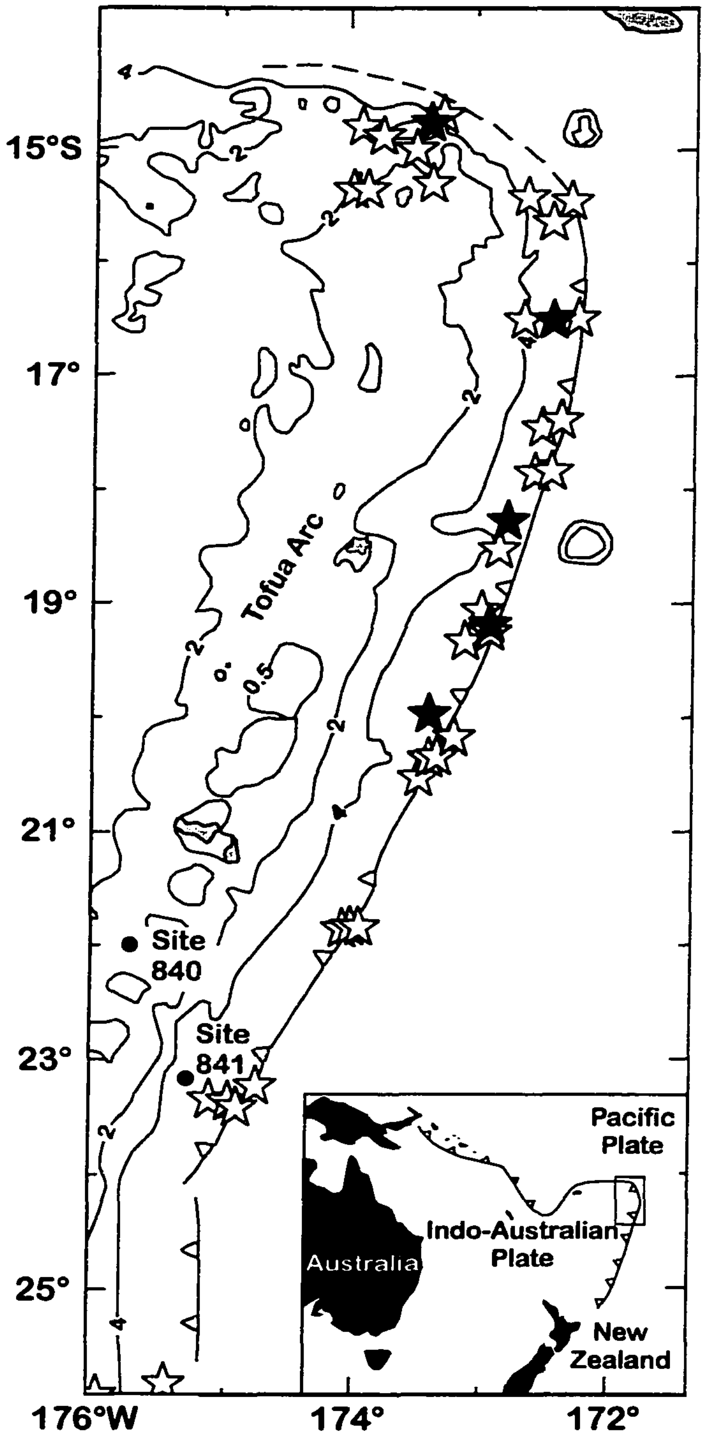

Figure 4.1 Bathymetric map showing locations of dredge sites (stars) along Tonga forearc. Contour labels are given in kilometers. Black stars indicate dredges from which epidosites were recovered. Locations of Ocean Drilling Program Sites 840 and 841 are also shown. Modified from Shipboard Scientific Party [1992].

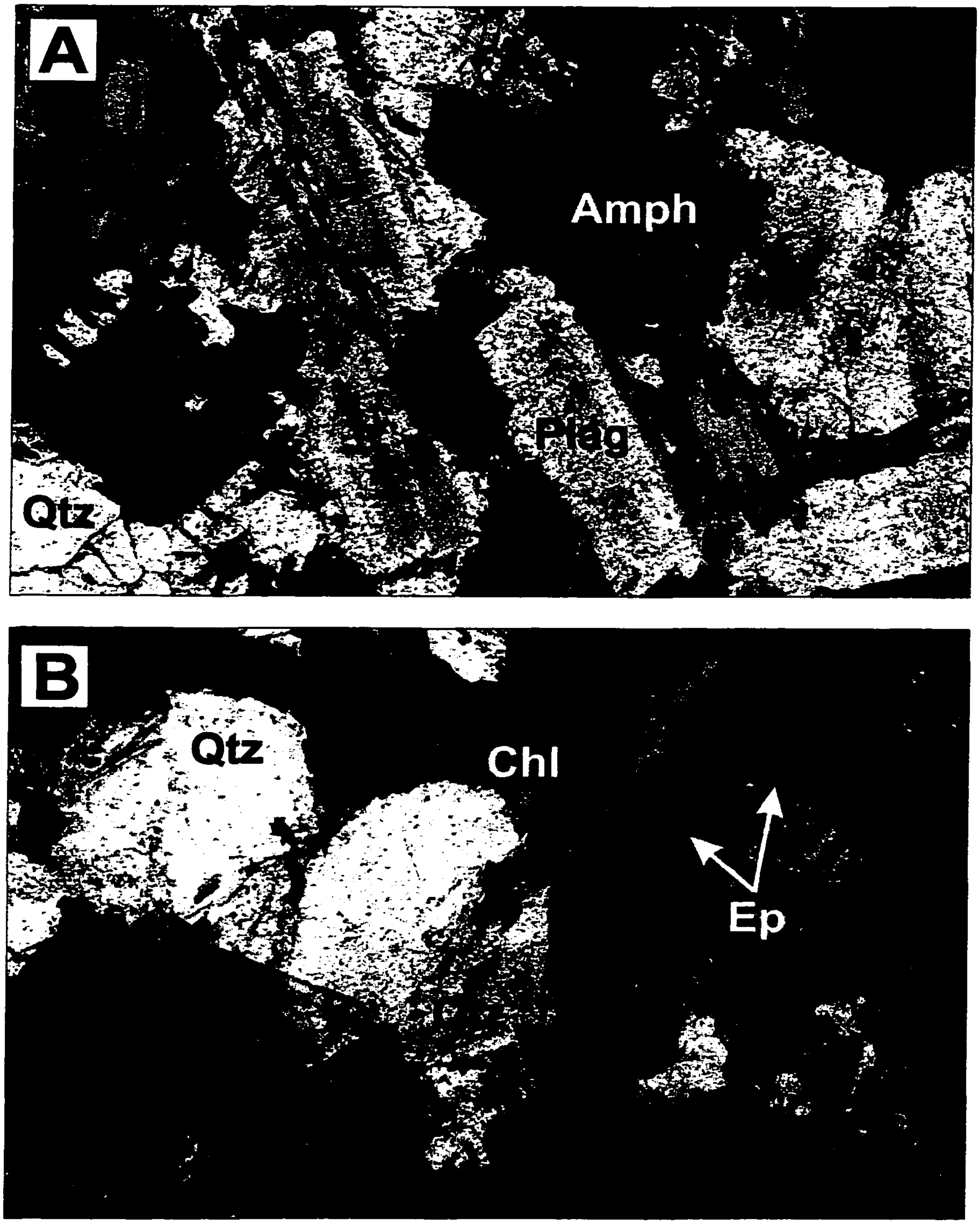

Figure 4.2 Photomicrographs of epidotized samples from Tonga forearc. A) Partially epidotized basalt with cloudy plagioclase (Plag) laths, clear interstitial quartz (Qtz), darker acicular amphibole (Amph), and magnetite-ilmenite. Diabase texture is preserved (sample 108-3-15). B) Epidosite with epidote (Ep), clear and turbid quartz (Qtz), chlorite (Chl), and magnetite-ilmenite. Note absence of igneous texture (sample 108-3-16). Field of view is 1.5mm for both photos.

Table 4.1 Epidosite Modal Mineralogy

Sample	Protolith	Epidote	Quartz	Chlorite	Plagioclase	Opaques + Titanite
96-1-14	Plagiogranite	33	47	11	6	3
99-2-8	Diabase	58	27	8	0	7
102-4-1	Plagiogranite	28	41	2	28	1
108-3-16	Diabase	49	25	19	2	5
113-1-26	Plagiogranite	46	49	3	0	2

Notes: Modal data determined by counting 1200-1600 points per sample. Plagioclase in all samples is relict, and is almost pure albite. Plagioclase in sample 102-4-1 is mostly in the host rock of a shear hosted epidosite. Values in percent.

Protoliths

Because outcrop relations are lacking, protoliths were determined by comparison with the least altered samples from the same dredge. The protoliths can be divided into two groups on the basis of texture and modal abundance of mafic minerals. Basaltic protoliths contain 50% mafic minerals whereas plagiogranite protoliths contain < 10%. Basaltic protoliths are greenish-gray, fine-grained rocks that have diabasic intergranular textures (Figure 4.2A). Primary plagioclase is replaced by albite ± epidote ± chlorite, and primary clinopyroxene is replaced by hornblende ± actinolite ± chlorite. Groundmass assemblages include chlorite, epidote, quartz, magnetite, ilmenite, titanite, and pyrite. Vesicles containing quartz + epidote ± chlorite are common. Based on these textures and mineral assemblages, we believe that these rocks are analogous to those from the sheeted dike complexes of ophiolites, rather than the volcanic section. Indeed, sheeted dikes which host epidosites in SSZ ophiolites are altered to greenschist facies mineral assemblages [*Gillis and Banerjee*, in press]. The plagiogranite protoliths are buff to tan, fine- to medium-grained rocks with subhedral granular and intergranular textures. Quartz and plagioclase make up more than 90% of the rocks and commonly exhibit graphic intergrowth. Minor amounts of amphibole, chlorite, epidote, magnetite, ilmenite, titanite, apatite, and pyrite are also present.

GEOCHEMISTRY

MINERAL CHEMISTRY

Epidote pistacite (Ps) contents range from Ps_{13} to Ps_{33} with an average composition of Ps_{25} (Table 4.2). Zoned grains with Fe-rich cores and Al-rich rims are common. Chlorite is present in four epidosite samples and has Mg#s from 36 to 81 (Table 4.2). Minor, albitic plagioclase is present in three of the epidosite samples. Minor amphibole is present in only one epidosite (sample 108-3-16). Epidote, chlorite, amphibole and plagioclase from Tongan epidosites (Table 4.3) have a similar range in composition to ophiolite-hosted epidosites [*Nehlig et al.*, 1994; *Schiffman and Smith*, 1988].

Table 4.2 Mineralogical, Oxygen Isotope and Fluid Inclusion Data from Tongan Epidosites

Sample Number	Protolith	Epidote Ps[*]	Chlorite Mg#[†]	$\delta^{18}O$[§] Whole-rock	Epidote	Quartz	Mean T_h[#] (°C)
96-1-14	Plagiogranite	19-33 (6)	36-41 (8)	6.8	-0.8	6.0	326 (19)
99-2-8	Diabase	18-33 (24)	NP	2.7	ND	ND	289 (25)
102-4-1	Plagiogranite	13-29 (17)	69-81 (8)	8.5	0.4	7.7	326 (43)
108-3-16	Diabase	20-30 (14)	55-65 (9)	4.7	ND	ND	296 (22)
113-1-26	Plagiogranite	18-26 (10)	67-68 (2)	4.8 (E); 7.2 (F)[**]	ND	ND	314 (18)

Notes: Mineral analyses were performed on a Camebax SX50 microprobe at Oregon State University and a JEOL JXA-8900R microprobe at the University of Alberta with the same operating conditions. Oxygen isotope values were determined using the BrF_5 method of Clayton and Mayeda (1963), at the University of Alberta, except that reaction temperatures were between 600 and 650°C. Numbers in parentheses indicate the number of analyses. Abbreviations: NP = not present; ND = not determined.

[*] Octahedral (Fe^{3+} / Fe^{3+} + Al^{VI}) x 100.

[†] (Mg / Mg + Fe) x 100.

[§] Values are reported in ‰ relative to the SMOW standard.

[#] T_h = homogenization temperature.

[**] E = epidotized; F = fresh.

Table 4.3 Representative Mineral Analyses

Sample	96-1-14	102-4-1	108-3-16	113-1-26	96-1-14	99-2-8	102-4-1	108-3-16	113-1-26	108-3-16	108-3-16	108-3-16	108-3-16
Analysis	B3	D2	C3	A1	B5	B4	D4	A4	A1	A2	A5	D6	D7
Mineral	chlorite	chlorite	chlorite	chlorite	epidote	epidote	epidote	epidote	epidote	amphibole	amphibole	amphibole	amphibole
SiO_2	25.58	28.60	29.79	29.92	38.09	37.91	37.32	37.41	38.26	51.07	50.51	51.07	51.99
TiO_2	0.14	BD	BD	0.04	0.22	0.16	0.09	0.09	0.04	0.72	0.63	0.97	0.62
Al_2O_3	19.96	20.66	17.75	16.31	24.82	26.28	23.12	25.50	26.83	3.36	3.37	3.20	2.35
Cr_2O_3	—	BD	BD	—	0.01	BD	0.01	0.02	0.04	BD	BD	BD	0.01
FeO^*	31.70	14.74	20.00	18.64	—	—	—	—	—	18.11	20.08	17.15	16.86
$Fe_2O_3^\#$	—	—	—	—	12.00	10.99	14.37	11.65	9.43	—	—	—	—
MnO	0.23	0.12	0.32	0.27	0.08	0.46	0.19	0.21	0.04	0.31	0.32	0.27	0.33
MgO	11.71	24.44	21.00	21.80	0.03	0.04	0.05	0.02	0.03	13.68	13.22	13.94	14.99
CaO	0.12	BD	0.07	0.11	23.68	22.99	23.14	23.22	23.88	9.25	8.70	9.68	8.24
Na_2O	0.03	BD	0.01	BD	0.01	BD	0.01	0.02	BD	1.14	1.17	1.57	2.39
K_2O	—	0.02	0.01	—	0.01	0.01	0.01	0.01	BD	0.28	0.27	0.34	0.36
Cl	0.03	0.02	BD	0.03	BD	BD	0.01	BD	BD	0.15	0.22	0.06	0.07
F	0.05	0.19	BD	0.08	0.04	BD	0.02	BD	BD	0.16	0.13	0.48	1.24
Total	89.55	88.79	88.95	87.20	98.98	98.83	98.32	98.15	98.54	98.12	98.50	98.51	98.90
Si	5.47	5.62	5.99	6.11	2.99	2.96	2.97	2.95	2.98	7.56	7.50	7.56	7.74
Al^{IV}	2.53	2.39	2.02	1.89	0.01	0.04	0.03	0.05	0.02	0.44	0.50	0.44	0.26
Al^{VI}	2.49	2.39	2.19	2.03	2.28	2.38	2.15	2.33	2.45	0.15	0.09	0.12	0.15
Cr	—	0.00	0.00	—	0.00	0.00	0.00	0.00	0.00	0.00	0.00	0.00	0.00
Ti	0.02	0.00	0.00	0.01	0.01	0.01	0.01	0.01	0.00	0.08	0.07	0.11	0.07
Mg	3.73	7.15	6.29	6.63	0.00	0.00	0.01	0.00	0.00	3.02	2.93	3.08	3.33
Fe^{2+}	5.67	2.42	3.36	3.18	—	—	—	—	—	2.24	2.49	2.12	2.10
Fe^{3+}	—	—	—	—	0.71	0.65	0.86	0.69	0.55	0.00	0.00	0.00	0.00
Mn	0.04	0.02	0.05	0.05	0.01	0.03	0.01	0.01	0.00	0.04	0.04	0.03	0.04
Ca	0.03	0.00	0.02	0.02	1.99	1.92	1.98	1.96	1.99	1.47	1.38	1.54	1.31
Na	0.01	0.00	0.00	0.00	0.00	0.00	0.00	0.00	0.00	0.33	0.34	0.45	0.69
K	—	0.01	0.00	—	0.00	0.00	0.00	0.00	0.00	0.05	0.05	0.06	0.07
Cl	0.02	0.01	0.00	0.02	0.00	0.00	0.00	0.00	0.00	0.04	0.06	0.02	0.02
F	0.07	0.24	0.00	0.10	0.00	0.00	0.00	0.00	0.00	0.08	0.06	0.23	0.58
Total Cations	20.00	19.99	19.91	19.92	8.01	8.00	8.01	8.01	8.01	15.38	15.39	15.52	15.76
O	28	28	28	28	12.5	12.5	12.5	12.5	12.5	23	23	23	23

Notes: BD = below detection; — = not determined. Amphibole analyses recalculated using the 15 NK method outlined in Robinson [1982] in order to satisfy crystal-chemical limits. *Total iron calculated as ferrous iron. #Total iron calculated as ferric iron.

Cu and Zn Contents

Ophiolite-hosted epidosites [*Harper et al.*, 1988; *Nehlig et al.*, 1994; *Richardson et al.*, 1987; *Schiffman and Smith*, 1988] have markedly lower Cu abundances, and generally lower Zn contents, than their protoliths, which have been hydrothermally altered (Table 4.4; Figure 4.3). Tonga forearc epidosites have similarly low Cu and Zn concentrations; however, Zn values from type A epidosites are slightly higher than those of type B (Figure 4.3).

Oxygen Isotopes

Type A Tongan epidosites have whole-rock $\delta^{18}O$ values of 2.7‰ and 4.7‰ (Table 4.2), which agree well with type A epidosites from the Troodos and Josephine ophiolites, which range from 2.8‰ to 5.0‰ [although values as high as 7.8‰ have been reported from Troodos, *Schiffman et al.*, 1987]. Type B Tongan epidosites have slightly higher whole-rock $\delta^{18}O$ values, ranging from 4.8‰ to 8.5‰ (Table 4.2). Two analyses of sample 113-1-26 from a relatively fresh portion and a completely epidotized section show that the fresh portion has a higher $\delta^{18}O$ value (7.2‰) than the epidotized portion (4.8‰). The decrease in $\delta^{18}O$ is related to the higher modal epidote content of the epidotized portion resulting from high-temperature exchange at high water-rock ratios. This interpretation is consistent with observations from the Josephine [*Harper et al.*, 1988] and Troodos [*Schiffman et al.*, 1987] ophiolites.

Temperatures were calculated using the quartz-epidote oxygen isotope geothermometer of Matthews and Schliestedt [1984] and $\delta^{18}O$ values from quartz and epidote mineral separates. Samples 96-1-14 and 102-4-1 gave temperatures of 276°C and 252°C, respectively. These temperatures are lower than those determined from fluid inclusions (see following) and are believed to reflect continued fluid-rock oxygen isotope exchange at temperatures below peak metamorphic conditions. By combining the quartz $\delta^{18}O$ data with mean fluid-inclusion homogenization temperatures, the $\delta^{18}O$ values of the epidosite-forming fluids can be calculated [*Matsuhisa et al.*, 1979]. The fluids have $\delta^{18}O$ values of 0.1‰ (96-1-14) and 1.7‰ (102-4-1), which are close to those of fluids exiting at black smokers [*Von Damm*, 1995]. These fluid isotope values correspond to minimum

Table 4.4 Epidosite Major and Trace-Element Analyses

Sample	96-1-14	102-4-1	108-3-16	113-1-26
SiO_2	66.00	76.65	50.04	50.31
TiO_2	0.70	0.28	1.38	0.37
Al_2O_3	13.77	12.22	15.63	18.32
Fe_2O_3*	7.19	1.12	10.98	9.05
MnO	0.05	0.01	0.14	0.10
MgO	1.28	0.62	6.71	1.16
CaO	4.65	1.82	8.86	17.68
Na_2O	4.36	5.28	1.91	0.10
K_2O	0.01	0.40	0.01	0.01
P_2O_5	0.20	0.02	0.11	0.05
LOI	1.61	1.17	4.01	2.74
Total	99.83	99.60	99.79	99.90
Sr	125	122	122	360
Y	47	22	25	12
Pb	2	2	2	4
Nb	1	2	1	1
V	13	24	321	400
Cr	1	3	36	11
Co	27	29	36	29
Zn	44	8	87	10
Cu	2	2	4	57
La	5	8	2	1
Ce	15	19	8	3
Nd	16	11	8	3
Sm	5	3	3	1
Eu	2	1	1	1
Tb	1	BD	1	BD
Dy	8	3	4	2
Ho	2	1	1	BD
Er	5	2	3	1
Tm	1	BD	BD	BD
Yb	4	2	3	1
Lu	1	BD	BD	BD

Notes: Major-element data was collected by X-ray fluorescence spectrometry at Cominco Ltd. Exploration Research Laboratory. Trace-element data was collected by inductively coupled plasma mass spectrometry at the University of Victoria using an HF-HNO_3 technique, except for Cu and Zn, which were analysed by atomic absorption spectrometry at Cominco Ltd. Research Labratory using an HF-$HClO_4$ total decomposition technique. Major-element values are in wt%; trace-element values are in ppm. LOI = loss on ignition; BD = below detection.

*Total iron calculated as ferric iron.

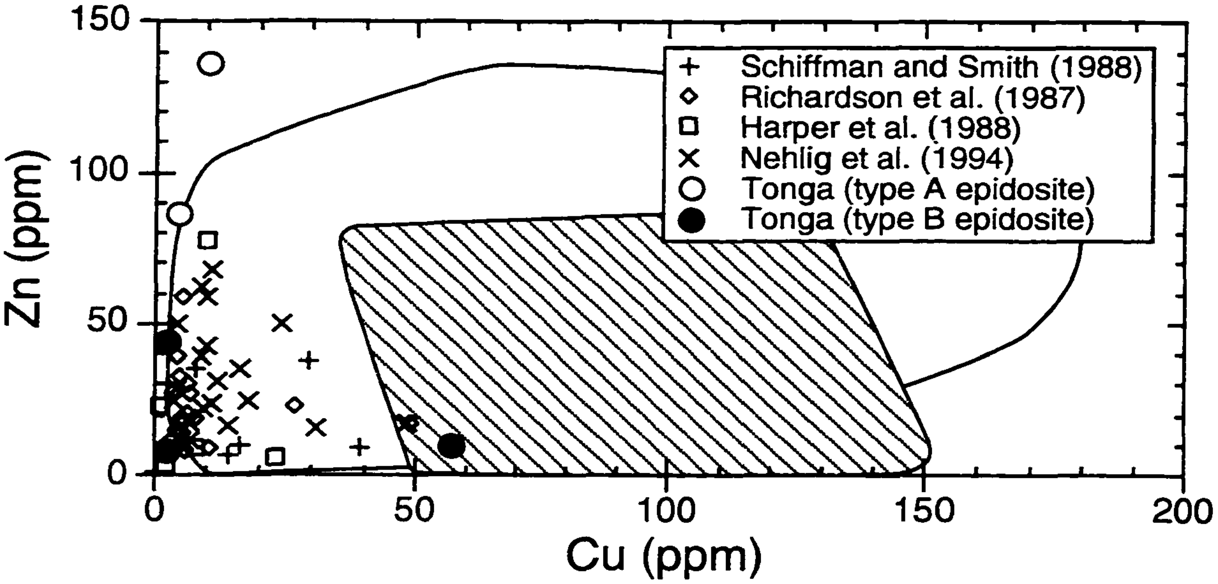

Figure 4.3 Zn vs. Cu concentration for epidosites from Tonga and Troodos, Josephine, and Samail ophiolites. White field encloses analyses of hydrothermally altered volcanic and dike rocks from ophiolite studies (listed in key). Diagonal hatched field enclosed typical values for plagiogranites from Karmoy ophiolite [*Pedersen and Malpas*, 1984]. Both fields incorporate >90% of published data.

integrated water-rock ratios of 0.2 to 1.2, assuming a -1‰ shift in the rock value and an original seawater value of 0‰.

FLUID INCLUSIONS

Fluid inclusions hosted in quartz and epidote was studied in order to characterize the composition, temperature, and origin of hydrothermal fluids that formed the epidosites. Three types of inclusions have been identified based on the number and ratio of phases present at room temperature (Table 4.5). Type 1 low-salinity, liquid-dominated inclusions that homogenize to the liquid phase are the most abundant and are found in both quartz and epidote in all epidosites. Type 2 low-salinity, vapor-dominated inclusions hosted in quartz contain a vapor to liquid ratio > 50%. Type 2a inclusions homogenize to the liquid and type 2b inclusions homogenize to the vapor or display critical behavior. Type 2 inclusions are rare but are observed in all samples. Type 3 high-salinity, liquid-dominated inclusions hosted in quartz contain one (or more) cubic daughter mineral that is probably halite. Type 3a inclusions homogenize into the liquid phase by vapor bubble disappearance and type 3b inclusions homogenize to the liquid by halite dissolution. Type 3 inclusions are also rare and are observed in all samples except 99-2-8. Although type 2 and 3 inclusions are found in the same samples, it could not be determined if they are co-genetic due to the large number of inclusions. In addition, an accurate estimate of pressure cannot be made because of the lack of stratigraphic control. The range of fluid-inclusion homogenization temperatures and salinities in the Tonga epidosites are similar to those described from the Troodos [*Cowan and Cann*, 1988; *Richardson et al.*, 1987; *Schiffman and Smith*, 1988] and Semail [*Nehlig et al.*, 1994] ophiolites (Figure 4.4).

Fluid-inclusion data provide constraints on the possible sources of fluids responsible for epidotization. High-salinity (> 29 wt% NaCl) fluids may have formed by phase separation of seawater or magmatically derived fluids at supercritical conditions. This requires that the brines were physically separated from co-genetic, low-salinity vapors prior to their entrapment [e.g., *Kelley et al.*, 1992]. An alternative mechanism is that brines were exsolved directly from late-stage, evolved melts in the absence of a vapor phase [*Cline and*

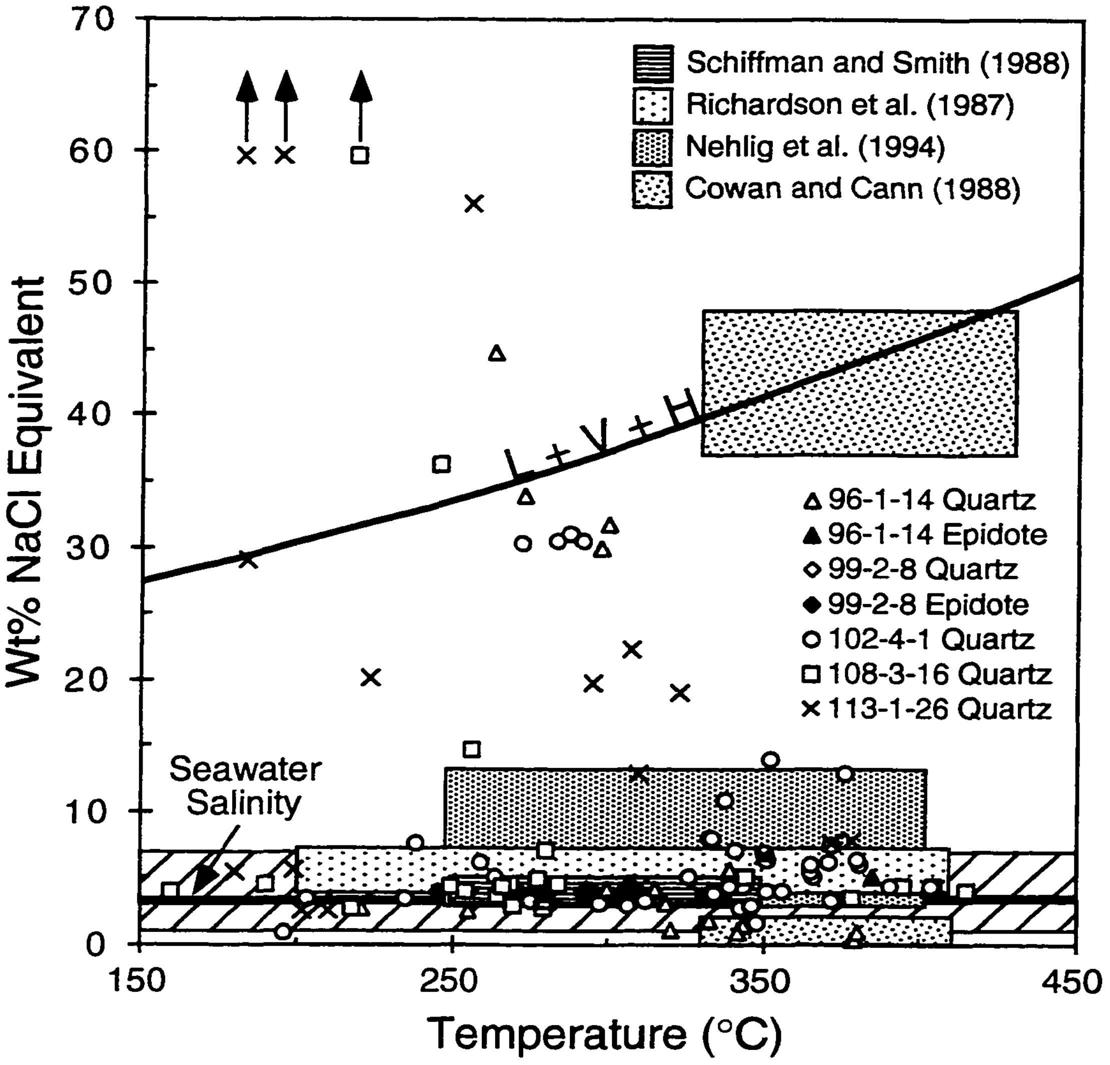

Figure 4.4 Temperatures of vapor bubble disappearance and NaCl equivalent fluid salinites for type 1, 2, and 3 fluid inclusions. Most type 1 and 2 inclusions have salinities that span range oberved at black smokers [diagonal hatch; *Von Damm*, 1995], although some have salinities >22 wt%. Type 3 inclusions have salinities >29 wt%. Type 3b inclusions plot above three phase curve (L + V + H). Arrows indicate that salinity values are minimum estimates (see Table 4.5). Rectangular fields enclose data from studies listed in key. Microthermometric data were collected using Fliud Inc. adapted U.S. Geological Survey heating-freezing stage following procedures outlined in Roedder [1984]. Inclusion salinities were calculated using MacFinCor software package [*Brown and Haegemann*, 1995] and equations of Brown and Lamb [1989] for H_2O-NaCl-(KCl) system.

Table 4.5 Fluid-Inclusion Homogenization Temperatures and Salinities from Tongan Epidosites

Inclusion type*	n	T_h (°C)†			Salinity (wt% NaCl)		
		Min.	Max.	Ave.	Min.	Max.	Ave.
1 (All data)	95	160	391	297	1.0	22.3	5.6
1 (Quartz)	77	160	391	299	1.0	22.3	6.0
1 (Epidote)	18	245	385	287	3.8	5.0	4.1
2a	14	305	404	347	0.8	7.4	3.5
2b§	4	380	415	398	0.3	4.4	3.4
3a	8	184	300	274	29.1	33.9	30.8
3b	6	275	>500#	437	36.3	>59.8#	52.7
All data	127	160	>500#	316	1.0	>59.8#	10.3

Notes: Abbreviations: Min. = minimum; Max. = maximum; Ave. = average.

*See text for explanation.

† T_h = homogenization temperature.

§ Homogenization temperatures represent minimum values due to difficulties in observing phase transitions.

#Three inclusions were still unhomogenized at 500 °C, therefore, salinity values are minimum estimates. See also Figure 4.4.

Bodnar, 1991]. At low pressures (<2 kbar), fluids with salinities up to 80 to 90 wt% may be exsolved from highly evolved, water-rich magmas [*Cline and Bodnar*, 1991]. This is consistent with the lack of co-genetic vapor-rich inclusions and the presence of plagiogranites in the Tongan collection. Indeed, Kelley et al. [1992] proposed that magmatic brines caused localized epidotization of plagiogranites in the Troodos ophiolite. Low-salinity inclusions span the range of fluids exiting active hydrothermal vents (1-7 wt% NaCl) and likely formed from evolved seawater (Figure 4.4). Several fluid inclusions from the Tongan epidosites plot between the low- and high-salinity fields (Figure 4.4) and probably represent mixing of fluids prior to trapping.

CONCLUSONS

Petrologically, type A and type B Tongan epidosites are equivalent to epidosites hosted in basaltic sheeted dikes and plagiogranites, respectively, from SSZ ophiolites. Key characteristics of the Tongan epidosites include a reduction of phases present, loss of metals, and a decrease in $\delta^{18}O$ values. These characteristics point toward their formation in upflow zones beneath ancient hydrothermal systems. Fluid-inclusion data show that the Tongan epidosites interacted with seawater-derived and possibly magmatic fluids at high temperatures (250 to >400°C). Moreover, calculated $\delta^{18}O$ values of the fluids in equilibrium with these epidosites are similar to black-smoker fluids [*Von Damm*, 1995].

It is striking that the first suite of epidosites from a modern oceanic setting was recovered from a forearc setting and apparently formed under similar conditions to epidosites from SSZ ophiolites. Recent studies of the volcanic sequences from the Izu-Bonin and Tonga forearcs have shown that the degree of alteration in forearcs is more extensive and occurs at higher water-rock ratios than at mid-ocean ridges, and is comparable to that observed in SSZ ophiolites [*Alt et al.*, 1998; *Kelman et al.*, 1998]. Theoretical studies suggest that epidosites should exist at mid-ocean ridges [*Rose*, 1995; *Seyfried et al.*, 1988]. Explanations for the lack of epidosites in mid-ocean ridge collections include: (1) they do not exist, (2) they are rare or small, or (3) they have not been recovered due to sampling biases. With ever-increasing sampling in the oceans, we believe that sampling bias is unlikely. The presence of epidosites in the Tonga forearc and SSZ ophiolites, their striking similarities, and their absence in mid-ocean ridge collections lead us to conclude that tectonic setting is an important factor in controlling hydrothermal processes.

Chapter 5

EPIDOTE TRACE ELEMENT CHEMISTRY

Epidote is an important rock-forming mineral that exhibits diverse chemistry and varied paragenesis and one of several minerals that make up the epidote group [*Deer et al.*, 1992]. It is a common constituent in felsic plutonic and volcanic rocks, greenschist and amphibolite facies regionally metamorphosed rocks, and in continental geothermal and oceanic hydrothermal systems. Epidote is not abundant in the oceanic crust as a whole but occurs sporadically in sheeted dike complexes, plutonic sequences (especially felsic lithologies), and in stockwork and upflow zones affected by high-temperature hydrothermal fluids. Epidote is stable at high pressures in eclogites [*Enami and Banno*, 1999], and may be important as a carrier of water and trace elements into the earth's mantle at subduction zones [e.g., *Hickmott et al.*, 1992; *Tribuzio et al.*, 1996]. A great deal is known about the crystal structure and major element crystal chemistry of epidote; however, relatively little is known about its trace-element composition.

In oceanic crustal rocks, epidote is almost exclusively a secondary mineral that forms from interactions with high-temperature hydrothermal fluids. Its crystal structure allows for the favorable substitution of trace elements, such as the rare earth elements (REEs), into the relatively large A sites normally occupied by Ca [e.g., *Bonazzi and Menchetti*, 1995; *Deer et al.*, 1992; *Dollase*, 1971] resulting in commonly elevated REE and trace element concentrations [*Carcangiu et al.*, 1997; *Sakai et al.*, 1984; *Yanev et al.*, 1998].

This chapter documents the trace element chemistry of epidote, determined by laser ablation inductively coupled plasma mass spectrometry (LA-ICP-MS), in samples from the Tonga forearc and Troodos ophiolite. These samples come from rare zones of extreme metasomatism called epidosites, which have been described in suprasubduction zone (SSZ) ophiolites [*Bettison-Varga et al.*, 1992; *Nehlig et al.*, 1994; *Richardson et al.*, 1987; *Schiffman et al.*, 1987] and modern forearc crust [*Banerjee et al.*, 2000]. Epidosites are characterized by the replacement of primary igneous minerals by secondary granoblastic assemblages of quartz + epidote ± chlorite ± actinolite ± ilmenite ± magnetite ± sulphides. Field and petrological data from SSZ ophiolites suggest that epidosites form in upflow zones at the base of ore-forming hydrothermal systems [*Bettison-Varga et al.*, 1992; *Nehlig et al.*, 1994; *Richardson et al.*, 1987; *Schiffman et al.*, 1987].

Epidosites from SSZ ophiolites [*Bettison-Varga et al.*, 1992; *Nehlig et al.*, 1994; *Richardson et al.*, 1987; *Schiffman et al.*, 1987] and modern forearc crust [*Banerjee et al.*, 2000] typically replace basaltic sheeted dikes and plagiogranite (tonalite, trondhjemite, and quartz diorite) bodies. Within the sheeted dike complexes of SSZ ophiolites, epidosites either form as patches in single dikes or dike outcrops [e.g., *Semail, Nehlig et al.*, 1994], or comprise large zones up to hundreds of meters wide, parallel to the axis of spreading [e.g., Troodos, *Richardson et al.*, 1987]. Plagiogranite-hosted epidosites occur as irregular patches (centimeters to meters wide) or are developed in shear zones in the Troodos [*Kelley et al.*, 1992; *Richardson et al.*, 1987] and Samail [*Stakes and Taylor*, 1992] ophiolites.

I have chosen to study epidote from epidosites to investigate the chemistry of high temperature fluids deep within seafloor hydrothermal systems. I demonstrate that crystal chemistry is not the dominant control on the incorporation of trace elements in hydrothermal epidote and that epidote composition can be used as a proxy to deduce the fluid composition. I show that epidote trace element chemistry can be linked to its petrographic characteristics and that epidote with different modes of occurrence likely formed from different fluids as a hydrothermal system evolves.

SAMPLE DESCRIPTIONS

Four Tonga epidosite samples were selected for trace element analyses. Basaltic epidosites formed from metasomatic replacement of primary phases in basaltic protoliths (samples 99-2-8 and 108-3-16); epidotization within plagiogranite protoliths either completely replaces primary phases (sample 96-1-14) or is localized in brittle shears (sample 102-4-1) [*Banerjee et al.*, 2000]. Three epidosite samples were collected from the Troodos ophiolite for comparison with the Tonga epidosites. The Troodos ophiolite formed in a SSZ setting similar to that of the Tonga forearc [*Miyashiro*, 1973; *Pearce et al.*, 1984]. The Troodos samples come from the western Solea graben near the village of Yerakies where epidosites exposed over hundreds of meters in the sheeted dikes have been extensively studied [e.g., *Bettison-Varga et al.*, 1992; *Schiffman and Smith*, 1988].

Careful petrographic examination of the epidosites from both Tonga and Troodos has identified two general modes of occurrence for epidote: clear, euhedral to prismatic grains that have grown in pore spaces (hereafter referred to as void filling) and turbid, fluid inclusion-rich, anhedral grains typical of replacement of primary groundmass phases (hereafter referred to as replacive) (Figure 5.1). These textures are not always easily discernable and intermediate textures are common; however, grains that fit these criteria as closely as possible were selected for chemical analysis. Similar textures have also been described in epidosites from the Troodos [*J. Cann*, pers. com., 2000], Josephine [*Harper et al.*, 1988] and Semail [*Nehlig et al.*, 1994] ophiolites.

ANALYTICAL METHODS

Polished thick sections (~ 100 µm) were prepared from the epidosite samples for analysis of major and trace elements. Individual epidote grains that are representative of replacive and void-filling textures were identified by normal petrographic observation under transmitted light. Digital backscattered electron images of the selected epidote grains were then taken in conjunction with major element compositions using a JEOL JXA-8900R electron microprobe at the University of Alberta. Instrument calibration was performed on natural standards and ZAF corrections were applied to all analyses. Individual mineral analyses were performed using an accelerating voltage of 15 kV and beam current of 20 nA.

A subset of the same epidote grains was analyzed for 22 trace elements at the University of Victoria by LA-ICP-MS. The Merchantek™ Nd:YAG EO UV laser output is frequency quadrupled to 266 nm and is operated in a gated Q-switched mode for optimum stability. The pulse rate was set at 5 Hz and the laser aperture (spot size) was set at 50%. The power setting was set at 40% which results in a power output of ~70±10 mJ. The pits produced were cylindrical with sharp edges that ranged from 50 to 75 µm in diameter (Figure 5.1). The ablated material was transported in a flow of argon to a high sensitivity VG™ PQ II S ICP-MS. Data were acquired in peak-jumping mode over a period of 120 seconds. Background levels of all elements were determined by collecting a 60s gas blank after which the laser was fired and data were acquired for the remaining 60s. Sample

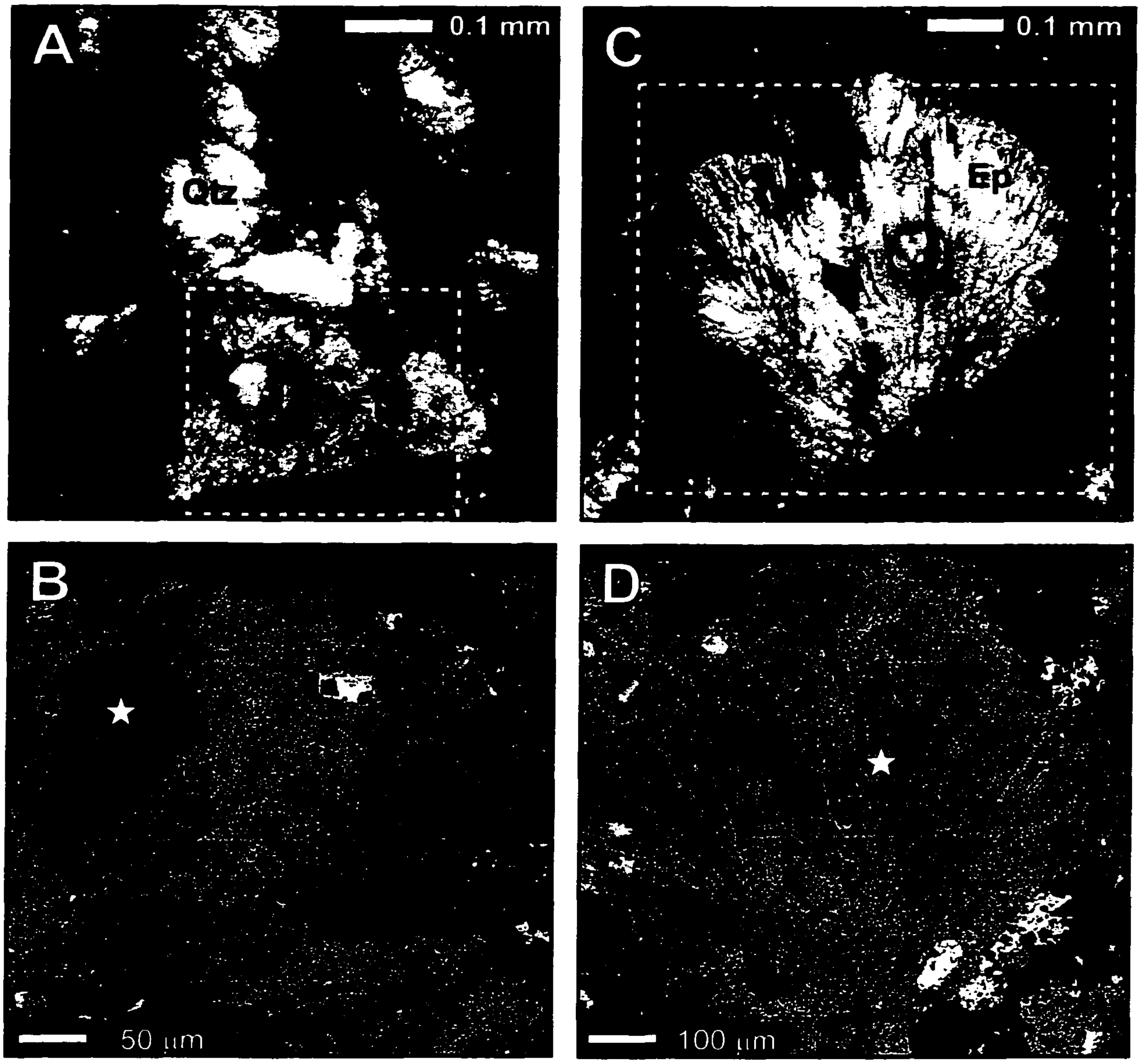

Figure 5.1 Photomicrographs and backscattered electron (BSE) images of replacive (A and B) and void filling (C and D) epidote from basaltic sample 99-2-8. White dotted line in photomicrographs (A and C) approximates area shown in BSE images (B and D). Black circles on BSE images approximate location of laser ablation pits seen in photomicrographs. Stars indicate location of microprobe analyses. Qtz=quartz; Ep=epidote.

concentrations were calibrated against duplicate analyses of National Institute of Standards and Technology (NIST) 613 synthetic silicate standard reference material (SRM) at the beginning and end of each run. Ca from microprobe analyses was used as an internal standard. A glass standard, prepared from the United States Geological Survey reference material BCR-2 (basalt) according to the method outlined in Chen [1999], was also analyzed at the beginning of each run. Relative standard deviations (RSD), calculated from BCR-2 glass repetitions, are less than 8% for all elements. Accuracy expressed as the relative difference between LA-ICP-MS analyses and accepted literature values is better than 5% for all elements except Ce, Y, Zr, and Hf, which are better than 10%. Ce, Y, and Zr showed consistently low values and Hf showed consistently high values during analysis. For this reason slight negative and positive anomalies, respectively, in these elements are analytical rather than natural. Typical LA operating conditions are listed in Table 5.1. In most cases microprobe and laser analyses were taken at the same spot within individual grains (Figure 5.1).

Whole rock trace element analyses of the epidosite samples were collected by solution ICP-MS at the University of Victoria. Epidosite samples were digested using a modified sodium-peroxide sinter technique [*Longerich et al.*, 1990], in which 0.5 ml of 30% H_2O_2 was added before final dilution with water to 90g to aid in the dissolution of the sinter cake. Plagiogranite analyses were performed on samples digested using an HF-HNO_3 technique [*Jenner et al.*, 1990].

RESULTS

Major and Minor Element Compositions

Epidote pistacite contents (Ps; $Fe^{3+}/Fe^{3+} + {}^{VI}Al$) range from Ps_{13} to Ps_{34} with an average composition of Ps_{25}. Pistacite contents in individual grains vary by < 0.15 and zoned grains with Fe-rich cores and Al-rich rims are common. Fe^{3+} varies systematically with ${}^{VI}Al$ (Figure 5.2). There is no systematic variation in Ps with mode of occurrence. CaO contents form a small range from 22.28 wt% to 23.88 wt% (ave. 23.24 wt%). MnO contents range from 0 to 0.76 wt% (ave. 0.16 wt%); TiO_2 contents have a similar range (0 to 0.70 wt%; ave. 0.14 wt%). Halogen contents are generally low (F < 0.05 wt% and Cl < 0.03 wt%) and Cr_2O_3

Table 5.1 LA-ICP-MS Operating Conditions [modified from *Chen*, 1999].

LASER	
Type	UV 266nm frequency quadrupled Nd:YAG
Mode	Q-Switched
Flash Lamp Frequency	20 Hz
Laser Output Frequency	5 Hz
Spot Size	5
Laser Output Power	70 ± 10 mJ
ICP-MS	
Plasma	
Plasma Gas	Argon
RF Power	1.53 kW forward, <5 W reflection
Gas Flow	
Plasma Gas Flow Rate	14 L min $^{-1}$
Auxiliary Gas Flow Rate	0.94 L min $^{-1}$
Inner Gas Flow Rate	~1.20 L min $^{-1}$
Interface	
Sampling Distance	16 mm
Sampling Aperture	Ni, 1.0 mm diameter
Skimmer Aperture	Ni, 0.7 mm diameter
Ion Lens Settings	
Extraction Lens	-320 V
Collector Lens	-78.3 V
L1 Lens	+0.44V
L2 Lens	-24.55
L3 Lens	+6.5
L4 Lens	-42.85
Pole Bias	-4.31 V
Acquisition Parameters	
Ion Detection	pulse counting
Scanning Mode	peak jumping, 1 point/peak
Dwell Time	10.24 ms
Data Acquisition Time	120 s (maximum)

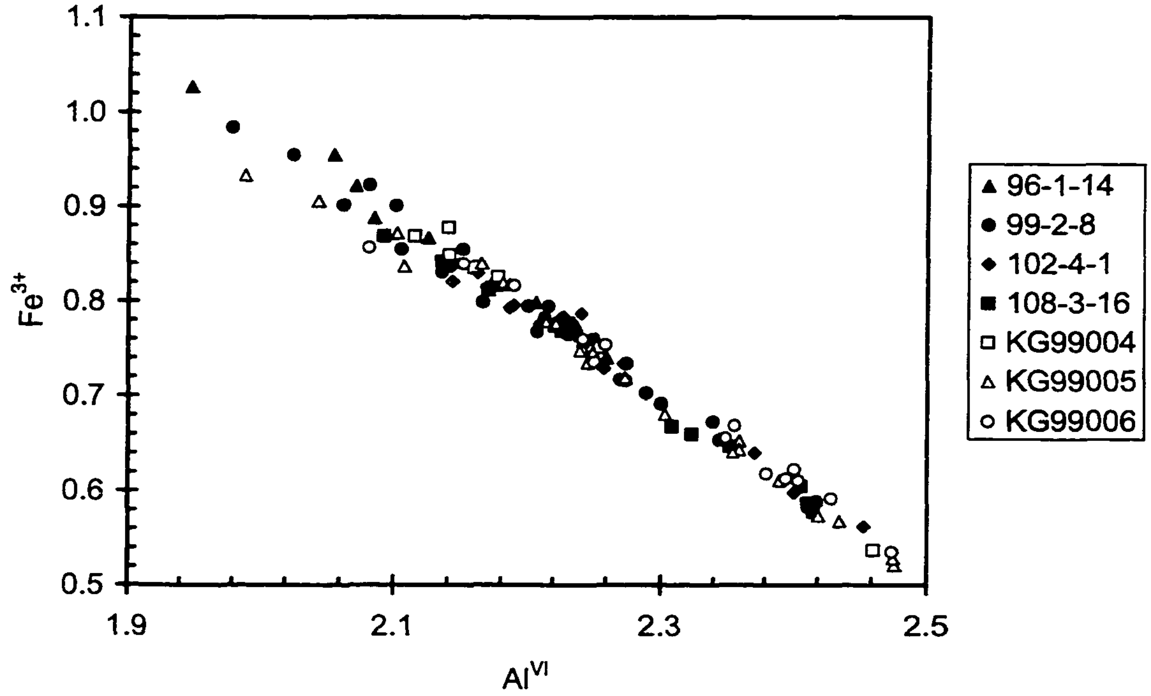

Figure 5.2 Fe^{3+} - Al^{VI} substitution in epidote. Compositions were calculated on the basis of 12.5 anhydrous oxygens and assuming total Fe as Fe_2O_3.

contents are negligible (< 0.01 wt%). My epidote analyses from Tonga and Troodos fall within the range determined from other studies of epidosites from the Troodos ophiolite [e.g., *Schiffman and Smith*, 1988] and other SSZ ophiolites [e.g., *Nehlig et al.*, 1994]. No systematic variations in major or minor element chemistry are observed for epidote from the Tonga or Troodos samples. Representative electron microprobe analyses are given in Table 5.2.

Trace Element Compositions

Forty-nine LA-ICP-MS determinations of individual epidote grains were collected for the rare earth elements (REEs), Ba, Sr, Th, Zr, Hf, Y, and Ga, (Table 5.3). Epidote shows a wide range of trace element concentrations and variations within and between samples. The most abundant trace element is Sr (67-902 ppm). Epidote also contains 1.1-11 ppm Ba, 1-94 ppm Zr, 3-166 ppm Y, and 15-41 ppm Ga. Epidote has relatively low abundances of Th (< 1 ppm) and Hf (< 3 ppm). Two analyses from plagiogranite-hosted epidosites (96-1-14 and 102-4-1) from the Tonga forearc have extremely high trace element concentrations, which fall outside of the range listed above.

Epidote is generally characterized by chondrite-normalized trace element values that are enriched by up to 100 times chondrite (Figure 5.3). A few analyses show chondrite-normalized Ba, Th, Zr, and Hf values below one. Epidote has variable positive Sr anomalies (relative to Pr and Nd), minor negative Zr and Hf anomalies (relative to Nd and Sm), and negative Ga anomalies (relative to Lu) on chondrite-normalized trace element plots. Trace element patterns of basalt and plagiogranite epidote are distinctive; epidote from basaltic protoliths from both Tonga and Troodos show similar patterns. Hf and Zr show a good correlation, which mimics fresh rock values [*T. Falloon*, pers. com., 2000; *Bednarz and Schmincke*, 1994] (Figure 5.4).

Trace element fractionation in igneous systems is controlled by CHARAC (CHarge-and-RAdius-Controlled) behaviour whereas in aqueous solutions it is characterized by non-CHARAC behaviour because other controls dominate [*Bau*, 1996]. Examples of this behaviour include hydrothermal vein fluorite, hydrogenetic Fe-Mn crusts, and seawater, which plot outside the CHARAC field (Figure 5.5). Epidote plots for the most part in the CHARAC field [*Bau*, 1996], suggesting that their trace element compositions either are controlled by CHARAC behaviour or are inherited from a parent that displayed CHARAC

Table 5.2 Representative Epidote Microprobe Analyses

	Tonga Forearc												Troodos Ophiolite								
Sample	102-4-1			108-3-16			96-1-14			99-2-8			KG99004			KG99005			KG99006		
Rock Type	Plagiogranite			Basalt			Plagiogranite			Basalt			Basalt			Basalt			Basalt		
SiO_2	37.27	37.72	37.51	37.65	38.05	37.88	37.51	37.64	37.30	37.63	37.19	37.80	37.08	37.14	37.51	37.75	38.03	37.08	37.94	38.14	37.49
TiO_2	0.28	b.d.	0.26	0.09	0.10	0.01	0.07	0.08	0.37	0.11	0.40	0.04	0.07	0.09	0.11	0.10	0.05	0.30	0.12	0.02	0.20
Al_2O_3	23.24	25.86	23.84	24.92	26.37	23.28	24.15	24.07	23.00	24.61	20.96	25.41	24.51	22.84	26.94	25.88	27.30	22.44	24.54	27.20	25.77
$Fe_2O_3{}^T$	13.99	10.81	13.00	11.21	9.82	13.68	12.98	12.70	14.49	12.03	16.27	11.36	12.53	14.47	9.06	11.06	8.88	14.44	12.75	9.12	11.26
Cr_2O_3	b.d.	0.04	0.04	0.01	0.01	b.d.	b.d.	b.d.	b.d.	0.01	b.d.	0.01	b.d.	0.03	0.03	0.04	b.d.	b.d.	b.d.	b.d.	0.02
MnO	0.06	0.21	0.12	0.14	0.10	0.07	0.01	0.01	0.04	0.16	0.06	0.16	0.27	0.16	0.26	0.33	0.17	0.17	0.30	0.04	0.70
MgO	0.07	0.07	0.03	0.05	0.04	0.03	0.02	b.d.	0.02	0.05	0.04	0.13	0.04	0.02	0.04	0.05	0.07	0.09	0.12	0.01	0.06
CaO	23.44	23.24	23.28	23.69	23.66	23.30	23.33	23.32	23.12	23.46	23.12	23.15	23.15	23.44	23.42	23.15	23.76	23.06	22.96	23.76	22.43
Na_2O	b.d.	0.03	b.d.	0.03	0.01	0.01	b.d.	0.03	0.01	b.d.	0.02	b.d.	b.d.	0.06	0.01	0.01	0.02	0.01	0.01	b.d.	0.02
K_2O	b.d.	0.04	0.01	0.04	0.02	0.02	0.02	0.03	0.02	0.02	0.02	0.01	0.02	0.02	0.02	0.03	0.03	0.01	b.d.	b.d.	0.02
F	b.d.	b.d.	b.d.	b.d.	b.d.	b.d.	b.d.	0.04	b.d.	0.03	b.d.	b.d.	b.d.	b.d.	b.d.	b.d.	b.d.	b.d.	b.d.	b.d.	b.d.
Cl	b.d.	0.02	b.d.	0.03	0.01	0.01	b.d.	0.01	b.d.	0.01	b.d.	0.02	b.d.	0.03	b.d.	b.d.	b.d.	0.01	0.03	b.d.	0.02
Total	98.36	98.03	98.08	97.85	98.19	98.30	98.08	97.93	98.37	98.12	98.08	98.09	97.67	98.29	97.39	98.39	98.30	97.61	98.77	98.30	97.98
Si	2.97	2.97	2.98	2.98	2.98	3.01	2.98	2.99	2.97	2.98	2.99	2.98	2.96	2.97	2.96	2.97	2.97	2.98	2.99	2.98	2.96
Al^{IV}	0.04	0.03	0.02	0.02	0.02	0.00	0.02	0.01	0.03	0.02	0.01	0.02	0.05	0.03	0.04	0.03	0.03	0.02	0.02	0.02	0.04
Al^{VI}	2.14	2.37	2.21	2.31	2.42	2.18	2.23	2.24	2.13	2.27	1.98	2.34	2.26	2.12	2.46	2.36	2.48	2.10	2.26	2.48	2.36
Ti	0.02	-	0.02	0.01	0.01	0.00	0.00	0.01	0.02	0.01	0.02	0.00	0.00	0.01	0.01	0.01	0.00	0.02	0.01	0.00	0.01
Cr	-	0.00	0.00	0.00	0.00	-	-	-	-	0.00		0.00	-	0.00	0.00	0.00	-	-	-	-	0.00
Fe^{3+}	0.84	0.64	0.78	0.67	0.58	0.82	0.77	0.76	0.87	0.72	0.98	0.67	0.75	0.87	0.54	0.65	0.52	0.87	0.75	0.54	0.67
Mn	0.00	0.01	0.01	0.01	0.01	0.01	0.00	0.00	0.00	0.01	0.00	0.01	0.02	0.01	0.02	0.02	0.01	0.01	0.02	0.00	0.05
Mg	0.01	0.01	0.00	0.01	0.00	0.00	0.00	-	0.00	0.01	0.01	0.02	0.00	0.00	0.01	0.01	0.01	0.01	0.01	0.00	0.01
Ca	2.00	1.96	1.98	2.01	1.99	1.98	1.98	1.99	1.97	1.99	1.99	1.96	1.98	2.01	1.98	1.95	1.99	1.99	1.94	1.99	1.90
Na	-	0.00	-	0.01	0.00	0.00	-	0.01	0.00	-	0.00	-	-	0.01	0.00	0.00	0.00	0.00	0.00	-	0.00
K	-	0.00	0.00	0.00	0.00	0.00	0.00	0.00	0.00	0.00	0.00	0.00	0.00	0.00	0.00	0.00	0.00	0.00	-	-	0.00
F	-	-	-	-	-	-	-	0.02	-	0.02	-	-	-	-	-	-	-	-	-	-	-
Cl	-	0.00	-	0.01	0.00	0.00	-	0.00	-	0.00	-	0.01	-	0.01	-	-	-	0.00	0.01	-	0.01
Ps	0.28	0.21	0.26	0.22	0.19	0.27	0.26	0.25	0.29	0.24	0.33	0.22	0.25	0.29	0.18	0.22	0.17	0.29	0.25	0.18	0.22

Note: Epidote analyses were recalculated on the basis of 12.5 anhydrous O. All Fe as Fe_2O_3. b.d. = below detection.

Table 5.3 Trace element compositions of epidote determined by LA-ICP-MS.

Element (ppm)	DL (ppm)	96-1-14 (Tonga - Plagiogranite)							99-2-8 (Tonga - Basalt)						
		void	rep	void	void	void	rep	rep	void	void	trans	void	void	rep	rep
CaO (wt %)		22.89	23.33	23.16	22.86	23.10	23.35	23.35	23.16	23.41	22.81	22.81	23.05	23.15	23.15
Ba	0.6	1.2	2.2	b.d.	b.d.	3.2	1.1	1.6	4.5	7.0	4.9	4.6	6.5	4.7	3.7
Th	0.02	0.32	3.59	0.73	0.04	0.02	0.19	0.27	b.d.	b.d.	0.09	0.02	0.01	0.03	0.13
La	0.05	2.4	145.2	8.4	1.3	1.5	5.2	9.7	1.4	1.3	4.9	0.7	1.5	3.4	3.7
Ce	0.04	5.8	357.1	22.3	4.2	3.2	18.1	21.6	3.7	3.2	11.2	1.5	3.9	9.6	11.8
Pr	0.03	1.2	64.0	4.8	0.9	0.6	3.4	4.1	0.7	0.6	2.1	0.3	0.8	2.0	2.5
Sr	0.6	447	791	479	194	536	593	569	479	602	510	480	455	500	567
Nd	0.1	7.1	324.4	28.1	6.6	3.0	21.5	21.6	3.4	3.3	11.9	1.4	4.2	11.6	15.0
Zr	0.8	31.6	188.5	13.5	29.8	3.5	15.2	27.0	18.7	15.9	53.1	3.6	21.9	94.2	88.0
Hf	0.09	1.35	6.15	0.80	0.93	b.d.	0.92	1.10	0.34	0.29	1.33	0.06	0.50	1.89	2.83
Sm	0.3	2.5	75.1	12.6	3.9	1.2	8.5	6.4	1.0	1.1	3.7	0.5	1.5	4.6	6.3
Eu	0.08	3.0	24.8	15.5	2.5	2.6	4.6	4.1	2.5	2.1	3.5	1.4	4.5	1.9	1.9
Gd	0.2	5.1	74.3	18.8	7.0	1.5	12.0	9.4	1.6	1.7	4.8	0.5	2.0	6.9	8.1
Tb	0.03	1.1	11.9	3.6	1.7	0.3	2.1	1.7	0.4	0.3	1.0	0.1	0.4	1.5	1.6
Dy	0.1	9.0	80.3	21.4	15.8	2.3	14.0	11.7	2.9	2.3	7.3	0.7	2.6	11.6	11.6
Y	0.3	47.4	475.9	109.1	124.1	16.2	74.2	67.2	23.4	16.9	56.0	5.6	18.1	85.0	64.4
Ho	0.04	2.0	17.2	4.1	4.3	0.6	2.8	2.5	0.6	0.5	1.6	0.1	0.7	2.9	2.5
Er	0.1	6.7	49.6	11.6	18.4	2.1	7.8	7.3	2.3	2.1	5.3	0.5	2.0	9.2	7.6
Tm	0.03	0.9	6.0	1.4	3.4	0.3	1.1	0.9	0.4	0.3	0.8	0.1	0.3	1.5	1.2
Yb	0.1	5.3	32.5	8.2	26.5	2.1	7.2	5.5	3.0	2.8	5.0	0.5	2.3	11.4	8.5
Lu	0.04	0.7	4.0	1.1	4.3	0.3	1.0	0.7	0.5	0.4	0.7	0.1	0.3	1.6	1.2
Ga	1	27	35	33	31	26	31	31	41	36	32	33	41	37	32
V	2	3	b.d.	2	b.d.	b.d.	1	b.d.	440	460	367	309	337	485	234

Note: All values are in ppm except CaO which is in wt %. Detection limits are average values from all analyses. DL = Detection Limit; b.d. = below detection; void = void filling; rep = replacive; trans = transitional.

Table 5.3 Trace element compositions of epidote determined by LA-ICP-MS (continued).

Element	DL	99-2-8 (continued)					102-4-1 (Tonga - Plagiogranite)					108-3-16 (Tonga - Basalt)		
(ppm)	(ppm)	void	rep	rep	rep	rep	rep	rep	rep	void	rep	rep	rep	void
CaO (wt %)		23.27	23.15	22.79	23.15	23.15	23.56	22.66	23.32	23.66	23.27	23.08	23.69	23.47
Ba	0.6	5.9	4.8	4.0	4.6	5.0	2.4	7.6	3.6	4.2	9.0	5.2	5.5	9.5
Th	0.02	b.d.	0.18	0.04	0.08	0.14	0.03	0.18	0.07	0.04	3.69	b.d.	0.02	b.d.
La	0.05	1.3	5.2	6.8	7.1	12.3	2.7	2.5	8.8	2.2	166.9	1.3	1.4	3.2
Ce	0.04	2.8	15.5	19.3	19.5	33.7	4.5	3.4	13.5	3.3	311.5	3.3	3.4	7.6
Pr	0.03	0.6	3.5	3.8	4.6	6.6	0.6	0.5	2.0	0.5	46.0	0.7	0.6	1.4
Sr	0.6	633	716	771	769	600	761	902	654	675	908	378	287	285
Nd	0.1	2.9	21.1	22.9	28.4	38.2	3.0	1.9	8.7	2.1	209.4	3.9	3.9	9.0
Zr	0.8	9.7	62.9	52.7	81.1	73.3	5.0	3.4	1.4	8.3	1.8	12.1	21.1	20.6
Hf	0.09	0.25	2.05	1.05	2.87	1.50	0.15	0.14	b.d.	0.33	0.11	0.32	0.57	0.40
Sm	0.3	1.2	9.1	7.7	11.8	13.5	0.9	0.4	2.1	0.6	62.4	1.4	1.3	3.0
Eu	0.08	2.8	3.1	3.8	5.9	4.5	1.1	0.8	1.7	0.6	20.5	2.5	3.0	3.8
Gd	0.2	1.6	12.1	9.9	16.1	17.9	0.8	0.4	2.4	0.9	75.8	1.8	1.8	3.9
Tb	0.03	0.3	2.4	1.8	3.1	3.3	0.2	0.1	0.4	0.2	14.8	0.3	0.3	0.6
Dy	0.1	2.2	16.2	12.9	20.3	24.4	1.3	0.7	2.7	1.4	98.2	2.4	2.3	5.0
Y	0.3	18.5	95.2	75.8	119.4	165.5	9.0	4.0	19.1	9.8	536.7	18.9	13.9	36.5
Ho	0.04	0.5	3.5	2.6	4.4	5.5	0.3	0.2	0.6	0.4	18.6	0.6	0.5	1.0
Er	0.1	1.7	10.8	8.4	12.9	17.7	0.9	0.5	1.9	1.1	51.4	1.9	1.5	3.1
Tm	0.03	0.3	1.6	1.2	1.8	2.5	0.2	0.1	0.3	0.2	6.6	0.3	0.2	0.5
Yb	0.1	2.1	10.9	9.3	12.2	16.0	1.3	0.7	2.3	1.7	40.6	2.3	1.7	3.9
Lu	0.04	0.3	1.6	1.4	1.9	2.0	0.2	0.1	0.4	0.3	6.4	0.3	0.3	0.6
Ga	1	35	32	41	35	38	29	23	30	32	42	21	23	20
V	2	338	266	390	388	333	60	66	87	206	169	332	445	565

Table 5.3 Trace element compositions of epidote determined by LA-ICP-MS (continued).

Element (ppm)	DL (ppm)	108-3-16 (continued)		KG99004 (Troodos - Basalt)						KG99005 (Troodos - Basalt)				
		rep	rep	void	void	void	void	rep	rep	void	void	void	void	void
CaO (wt %)		23.30	23.13	23.31	23.04	23.44	23.24	23.42	23.24	23.22	23.04	23.54	23.14	22.93
Ba	0.6	3.7	6.2	4.9	4.9	4.5	9.8	10.8	9.5	6.1	4.5	7.0	8.5	5.7
Th	0.02	0.04	0.02	b.d.	b.d.	b.d.	b.d.	0.09	0.05	b.d.	0.03	b.d.	0.02	0.05
La	0.05	2.0	1.1	1.5	1.9	0.6	1.5	2.2	2.5	0.9	1.5	1.1	3.1	2.9
Ce	0.04	5.2	2.7	3.4	5.1	1.5	2.9	5.3	5.2	2.2	3.7	2.6	7.4	8.0
Pr	0.03	0.9	0.5	0.6	1.0	0.3	0.6	0.9	1.0	0.4	0.7	0.5	1.5	1.5
Sr	0.6	316	351	242	263	258	343	323	298	142	140	93	229	72
Nd	0.1	5.7	2.7	3.3	5.9	1.6	3.0	4.9	5.3	2.2	3.7	2.9	8.9	8.5
Zr	0.8	23.5	5.8	52.2	43.8	16.8	23.0	57.4	64.0	4.6	23.1	46.0	41.2	71.0
Hf	0.09	0.77	b.d.	1.68	1.39	0.46	0.47	2.26	2.64	0.11	0.58	1.24	0.78	1.65
Sm	0.3	1.9	1.4	0.8	2.1	0.8	1.0	1.8	2.2	0.6	1.5	0.9	3.4	3.1
Eu	0.08	2.2	1.9	2.0	2.7	1.3	3.3	2.5	3.8	2.6	2.5	2.7	4.3	2.6
Gd	0.2	2.5	1.2	1.7	2.9	0.7	1.8	2.4	2.9	1.3	1.8	1.6	5.5	4.2
Tb	0.03	0.5	0.2	0.3	0.6	0.1	0.4	0.5	0.5	0.2	0.4	0.3	1.2	0.8
Dy	0.1	3.0	1.4	2.4	4.4	1.0	2.5	3.1	3.7	1.3	2.2	2.3	9.2	5.9
Y	0.3	19.7	9.7	14.6	27.4	5.5	18.8	17.3	21.6	6.5	15.6	16.8	69.5	41.3
Ho	0.04	0.7	0.3	0.5	1.0	0.2	0.6	0.7	0.8	0.2	0.5	0.5	2.1	1.3
Er	0.1	2.0	1.0	1.6	3.2	0.6	2.2	2.0	2.3	0.8	1.7	1.7	7.5	4.0
Tm	0.03	0.3	0.2	0.2	0.4	0.1	0.4	0.3	0.4	0.1	0.3	0.3	1.4	0.8
Yb	0.1	1.9	0.9	2.0	3.3	0.7	2.5	2.7	4.0	0.7	2.1	2.7	12.8	7.1
Lu	0.04	0.4	0.1	0.4	0.5	0.1	0.4	0.5	0.9	0.1	0.3	0.5	2.3	1.1
Ga	1	19	19	23	17	19	22	20	23	39	39	25	27	27
V	2	336	287	392	291	272	323	378	456	370	819	327	502	269

Table 5.3 Trace element compositions of epidote determined by LA-ICP-MS (continued).

Element	DL	KG99005 (continued)		KG99006 (Troodos - Basalt)						
(ppm)	(ppm)	void	void	rep	rep	rep	void	void	void	void
CaO (wt %)		22.74	23.14	23.08	23.08	23.08	23.15	23.15	22.87	22.43
Ba	0.6	7.0	6.7	6.9	6.7	7.3	4.4	4.6	6.2	4.7
Th	0.02	b.d.	0.07	0.04	0.30	0.18	0.05	0.04	b.d.	0.04
La	0.05	0.7	3.0	2.8	5.7	4.5	1.1	1.2	0.5	0.7
Ce	0.04	1.4	6.8	8.6	17.1	11.5	3.3	2.7	1.0	2.3
Pr	0.03	0.2	1.3	1.8	3.4	2.1	0.6	0.5	0.2	0.4
Sr	0.6	68	109	213	230	156	290	190	304	276
Nd	0.1	1.5	6.9	10.0	20.0	12.3	4.0	2.6	1.0	2.5
Zr	0.8	5.4	35.0	57.7	49.7	50.7	23.6	21.4	3.9	3.2
Hf	0.09	b.d.	0.64	2.05	1.47	1.41	0.70	0.56	0.09	0.08
Sm	0.3	0.6	2.3	4.6	7.8	3.8	1.6	0.8	0.5	1.1
Eu	0.08	1.5	3.4	2.4	1.8	1.7	1.4	1.6	1.6	1.8
Gd	0.2	0.7	3.3	7.1	9.4	5.4	2.3	1.3	0.5	1.2
Tb	0.03	0.1	0.7	1.4	1.7	0.9	0.4	0.2	0.1	0.3
Dy	0.1	0.7	4.6	9.9	12.1	6.4	3.2	1.4	0.6	1.3
Y	0.3	6.0	30.3	60.8	67.2	38.4	21.6	11.0	5.7	7.1
Ho	0.04	0.2	0.9	2.2	2.4	1.3	0.7	0.3	0.1	0.2
Er	0.1	0.6	3.4	6.9	7.4	4.0	2.4	1.0	0.5	0.9
Tm	0.03	0.1	0.5	1.0	1.1	0.6	0.4	0.2	0.1	0.1
Yb	0.1	1.0	4.3	6.9	7.6	4.4	2.5	1.1	0.6	0.5
Lu	0.04	0.1	0.6	1.0	1.1	0.7	0.3	0.2	0.1	0.1
Ga	1	25	30	26	23	30	15	23	22	18
V	2	255	302	417	350	418	326	268	355	340

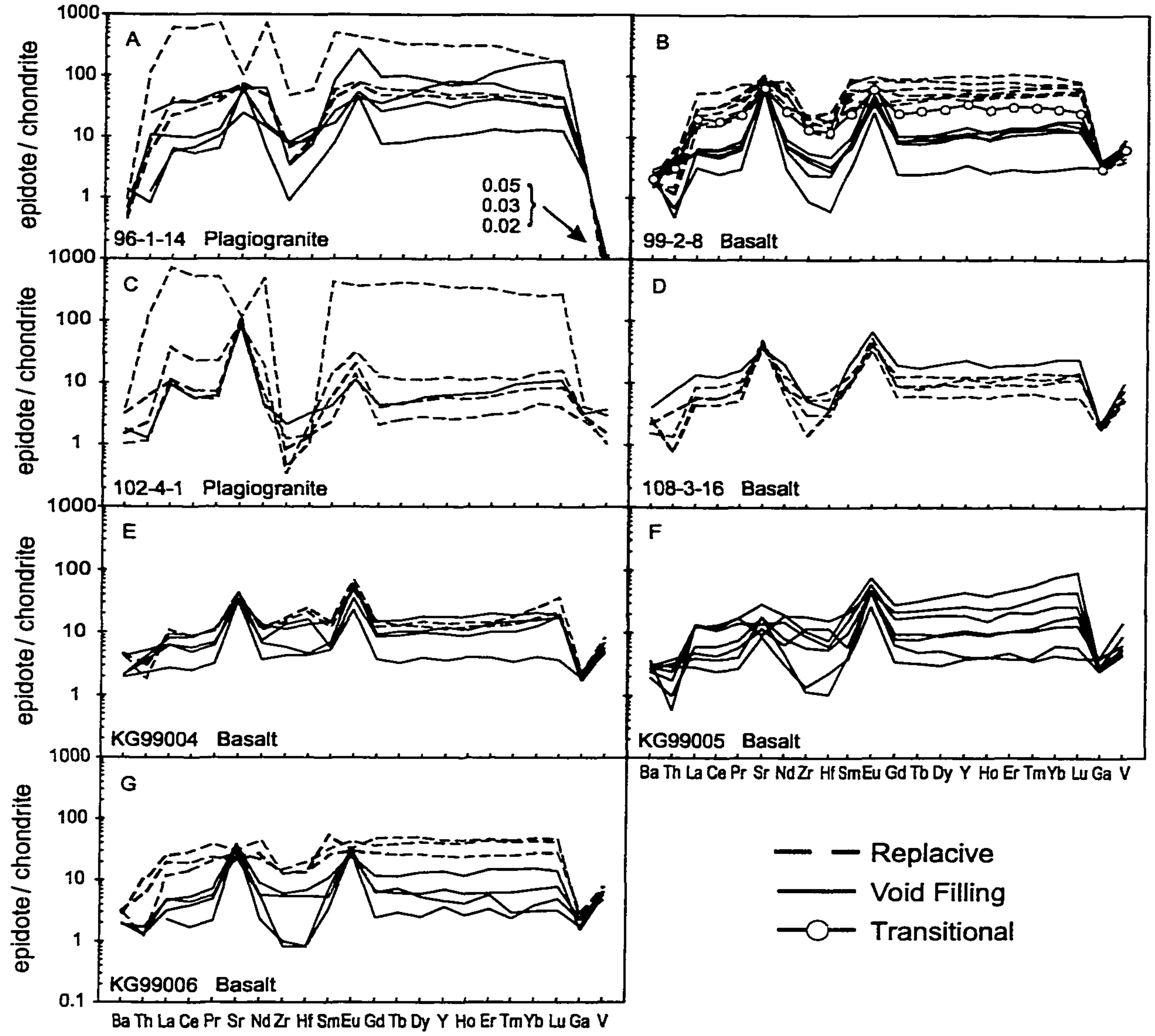

Figure 5.3 Chondrite-normalized multi-element plot showing trace element abundances in epidote separated by sample and mode of occurrence. A - D are from Tonga. E - G are from Troodos. Chondrite values (C1) from Anders and Grevese [1989].

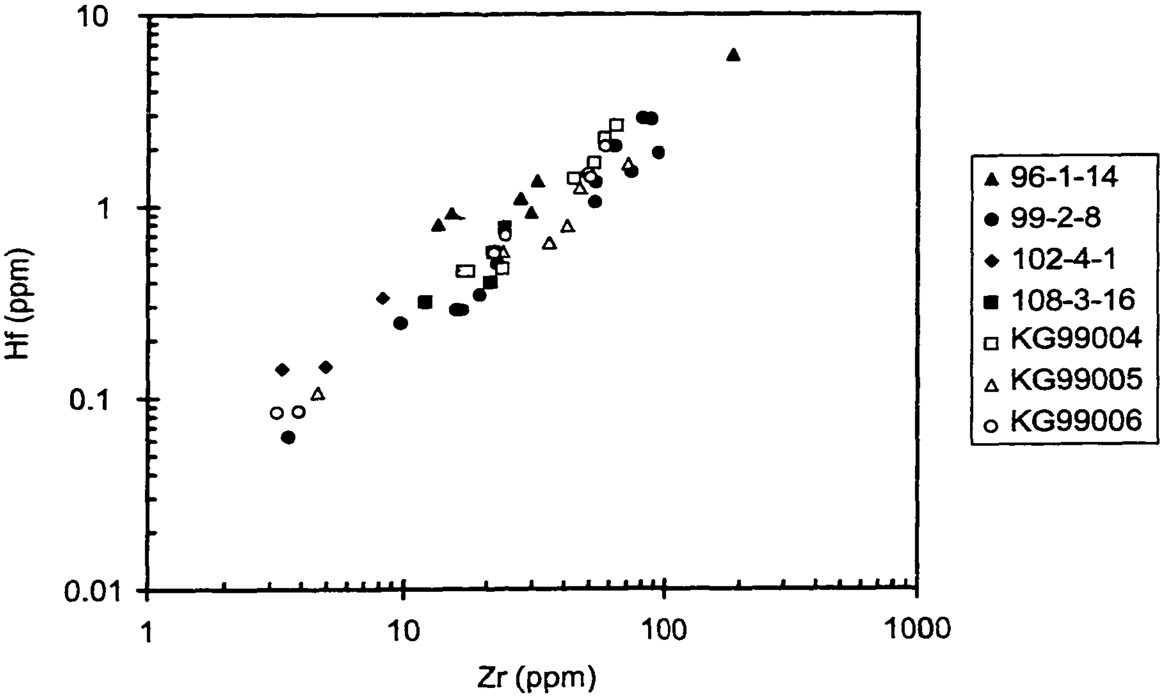

Figure 5.4 Hf vs. Zr in epidote.

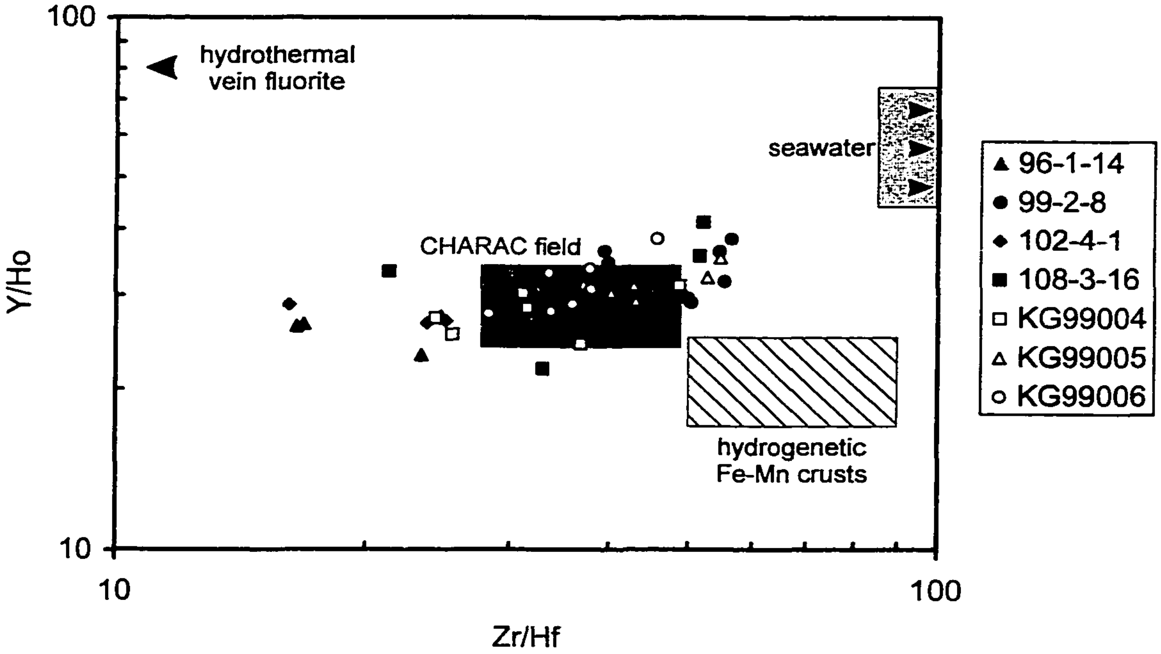

Figure 5.5 Y/Ho vs. Zr/Hf in epidote showing generally CHARAC nature (see text for discussion; after Bau, 1996). A few analyses trend toward seawater and hydrothermal vein fluorite (off diagram).

behaviour. Analyses of the appropriate elements from hydrothermal vent fluids are unavailable for comparison [*K. Von Damm*, pers. com., 2000].

Epidote has variable REE abundances both within and between samples. La varies between 0.5-12 ppm, Gd varies between 0.4-19 ppm, and Lu varies between 0.05 and 4.3 ppm. All patterns have chondrite-normalized (denoted $_N$) La_N/Sm_N values $= 1.1$ except for one plagiogranite epidosite sample (102-4-1) in which all of the analyses are > 1.8 (up to 4.4). Ratios of Gd_N/Lu_N are more variable and range from 0.2 to 2.2; however, most analyses are < 1 (Figure 5.6).

Four REE patterns are evident in the epidote analyses (Figure 5.7). Type I and II REE patterns are characteristic of epidote from basaltic protoliths (Figure 5.8A). Type I patterns show slightly depleted LREE, flat or slightly enriched heavy REE (HREE), and a strong positive europium anomaly. Type II patterns are characterized by higher overall REE concentrations than type I patterns, slightly depleted LREE, generally flat HREE, and only slight Eu anomalies (both positive and negative). Type II patterns are restricted to samples 99-2-8 and KG99006.

Type III and IV REE patterns are characteristic of epidote from plagiogranite protoliths (Figure 5.8B). Type III patterns (sample 96-1-14) are characterized by slightly depleted LREE, slightly depleted, flat or slightly enriched HREE, and a variable positive europium anomaly. Type IV patterns (sample 102-4-1) are characterized by slightly enriched LREE, flat or slightly enriched HREE, and a moderate positive europium anomaly. A few exceptions to these broad classifications are discussed below.

Whole Rock Chemistry

Epidosite whole-rock compositions were determined for comparison with epidote chemistry (Figure 5.9). Chondrite-normalized trace element patterns for the Troodos epidosites display negative Ba, slightly negative Th, and positive Sr anomalies relative to the field for volcanic glass [*Rautenschlein et al.*, 1985]. The Troodos epidosites are characterized by flat to slightly LREE-depleted patterns, with very slight negative Eu anomalies, that plot well within the field of Troodos volcanic glass [*Rautenschlein et al.*, 1985] suggesting only local redistribution of the REE. Basaltic epidosites from Tonga fall within the field defined by least altered Tonga basalts on a chondrite-normalized trace element plot (Figure 5.10).

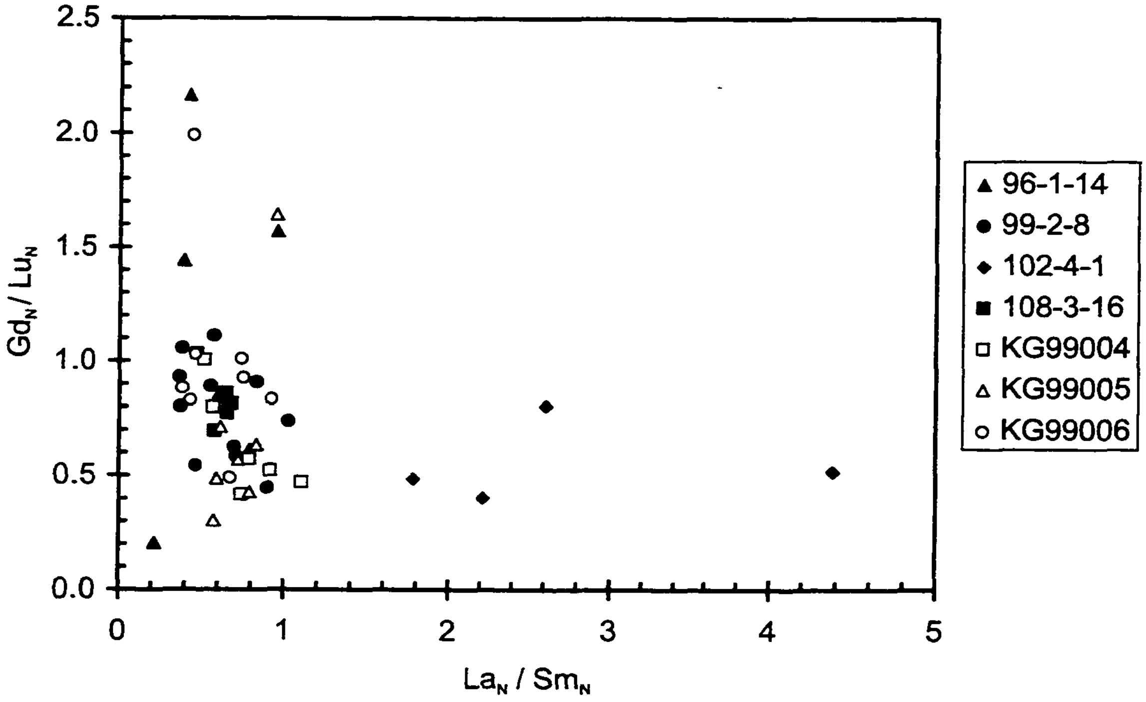

Figure 5.6 Gd_N/Lu_N vs. La_N/Sm_N in epidote showing relative variability in REE abundances. Most analyses have La_N/Sm_N values less than one with variable Gd_N/Lu_N ratios. Sample 102-4-1 is the only sample with consistant La_N/Sm_N values greater than one.

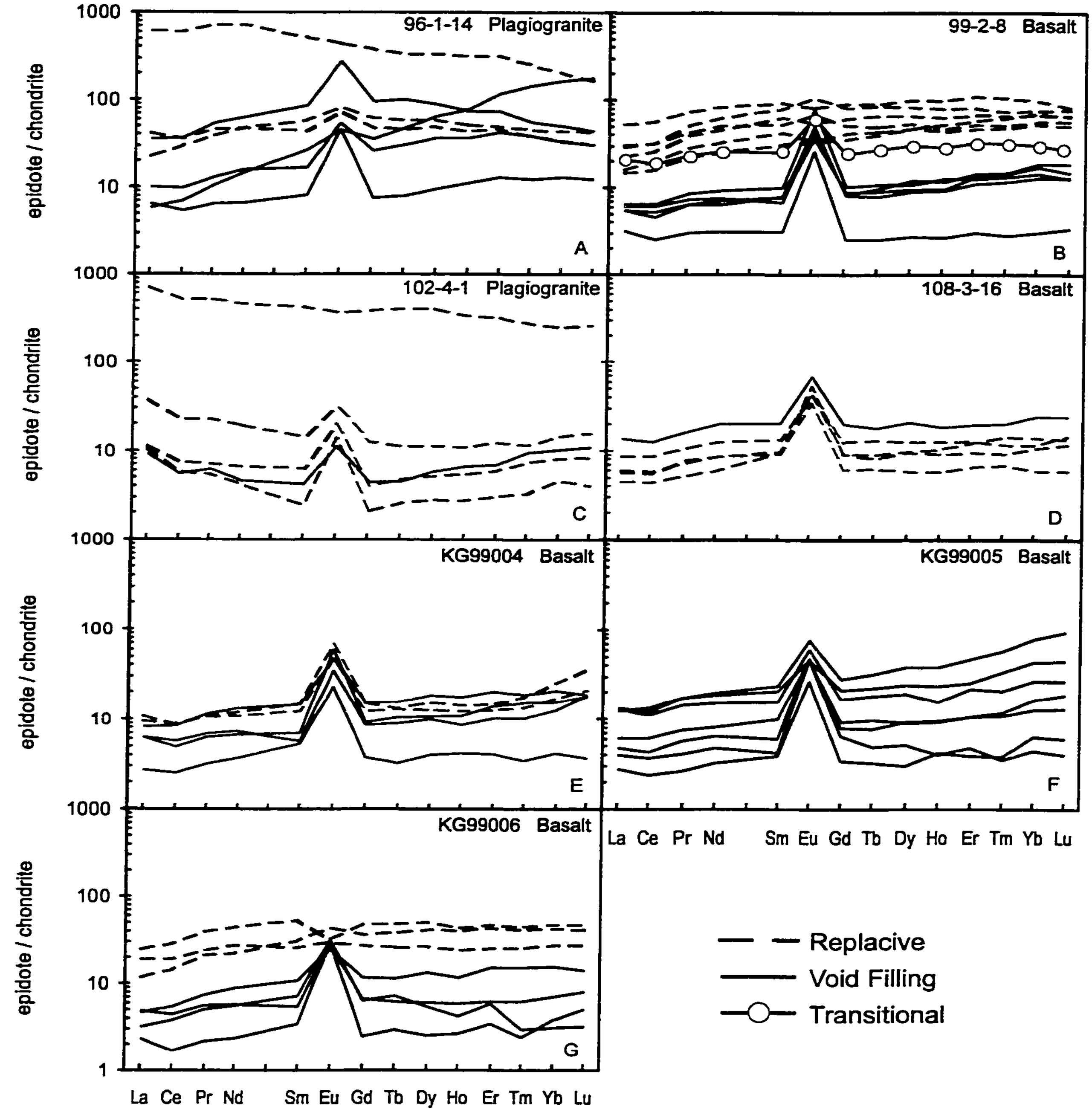

Figure 5.7 Chondrite-normalized REE profiles for epidote separated by sample and mode of occurrence. A - D are from Tonga. E - G are from Troodos.

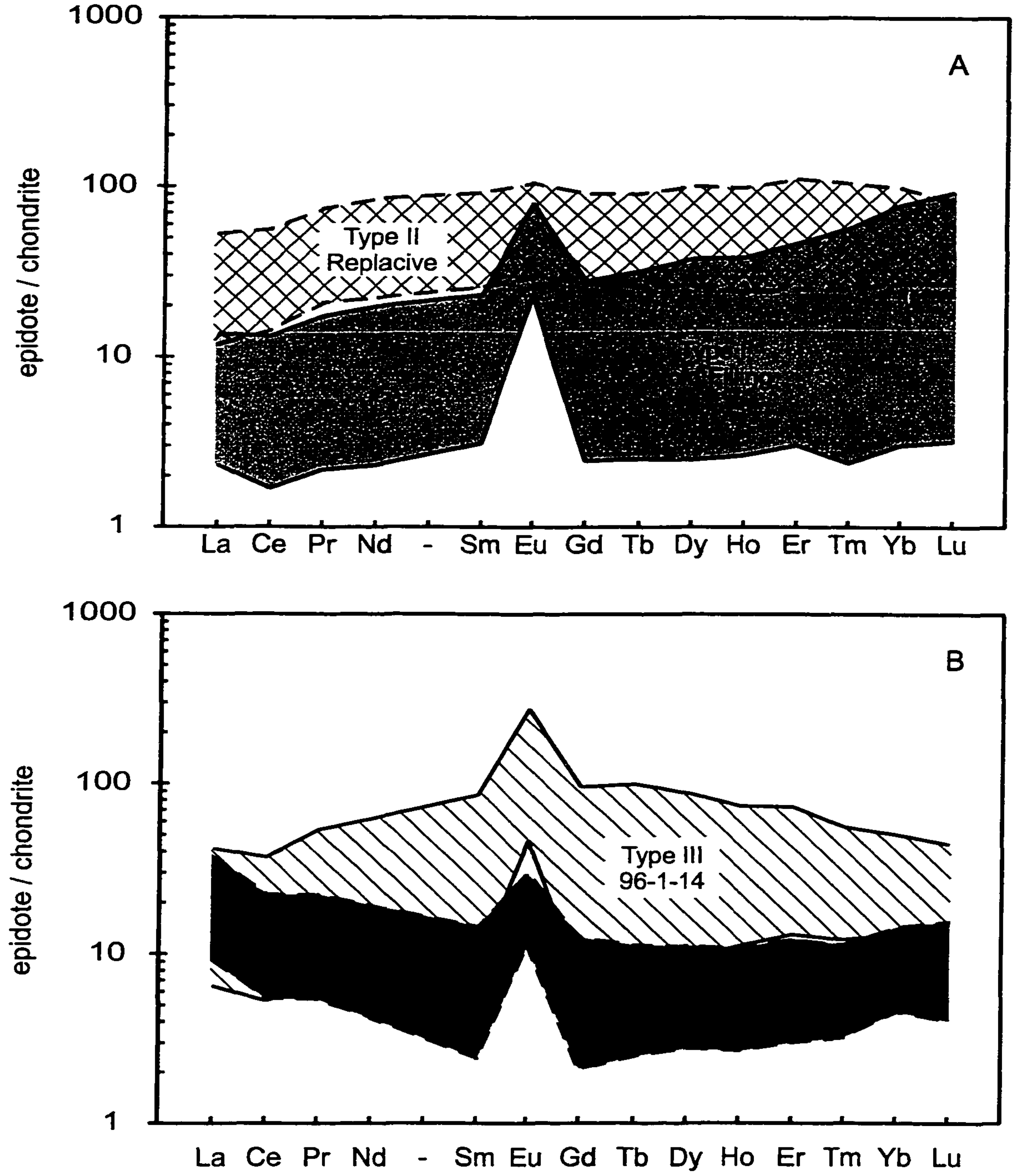

Figure 5.8 Representative chondrite-nomalized REE patterns of epidote from basalt (A) and plagiogranite (B) protoliths. See text for descriptions.

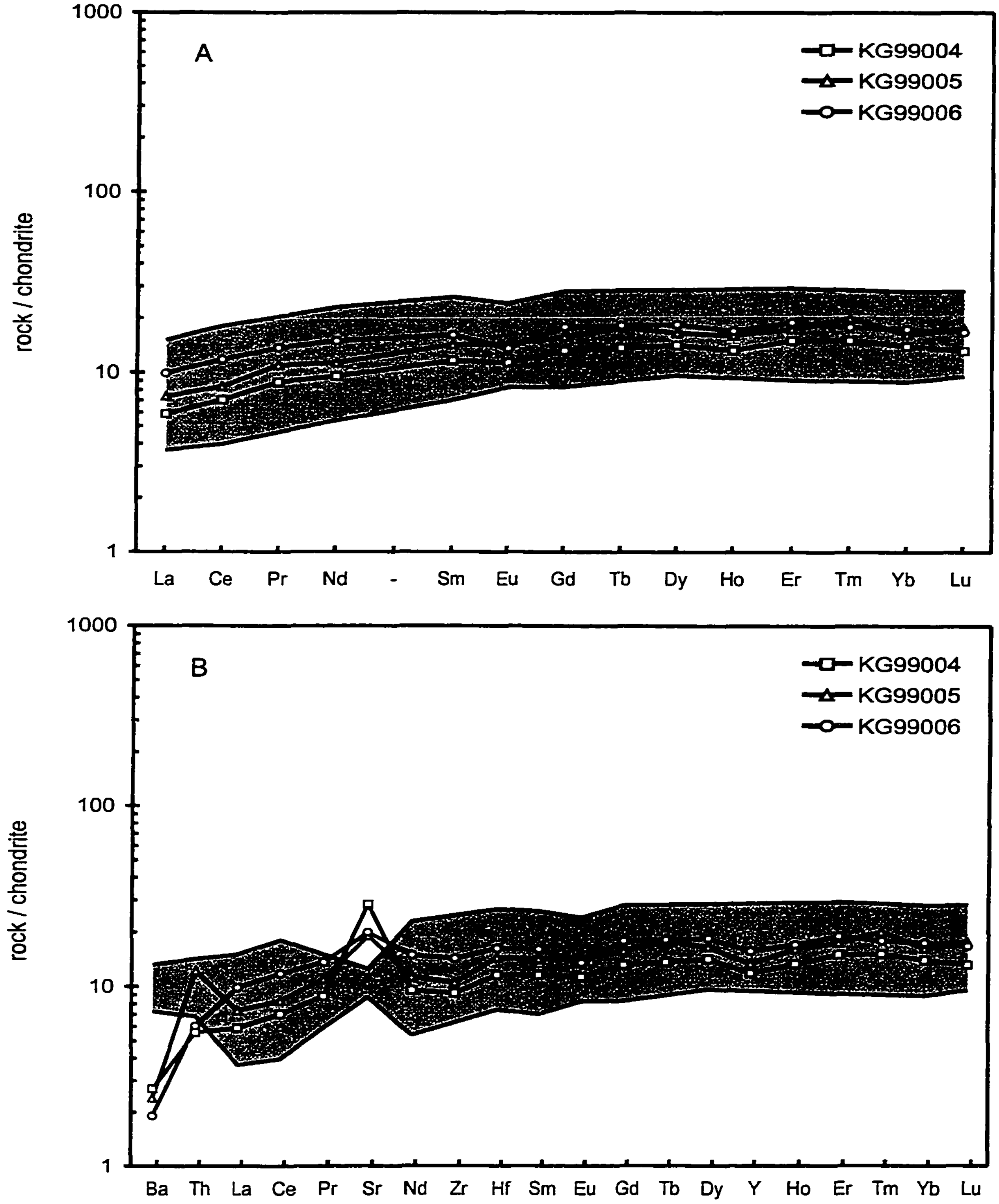

Figure 5.9 Chondrite-normalized whole rock REE (A) and trace element profiles (B) for the Troodos ophiolite. Individual epidosite analyses from this study are indicated by the lines. The shaded fields show the range of values for fresh glass [*Rautenschlein et al.*, 1985].

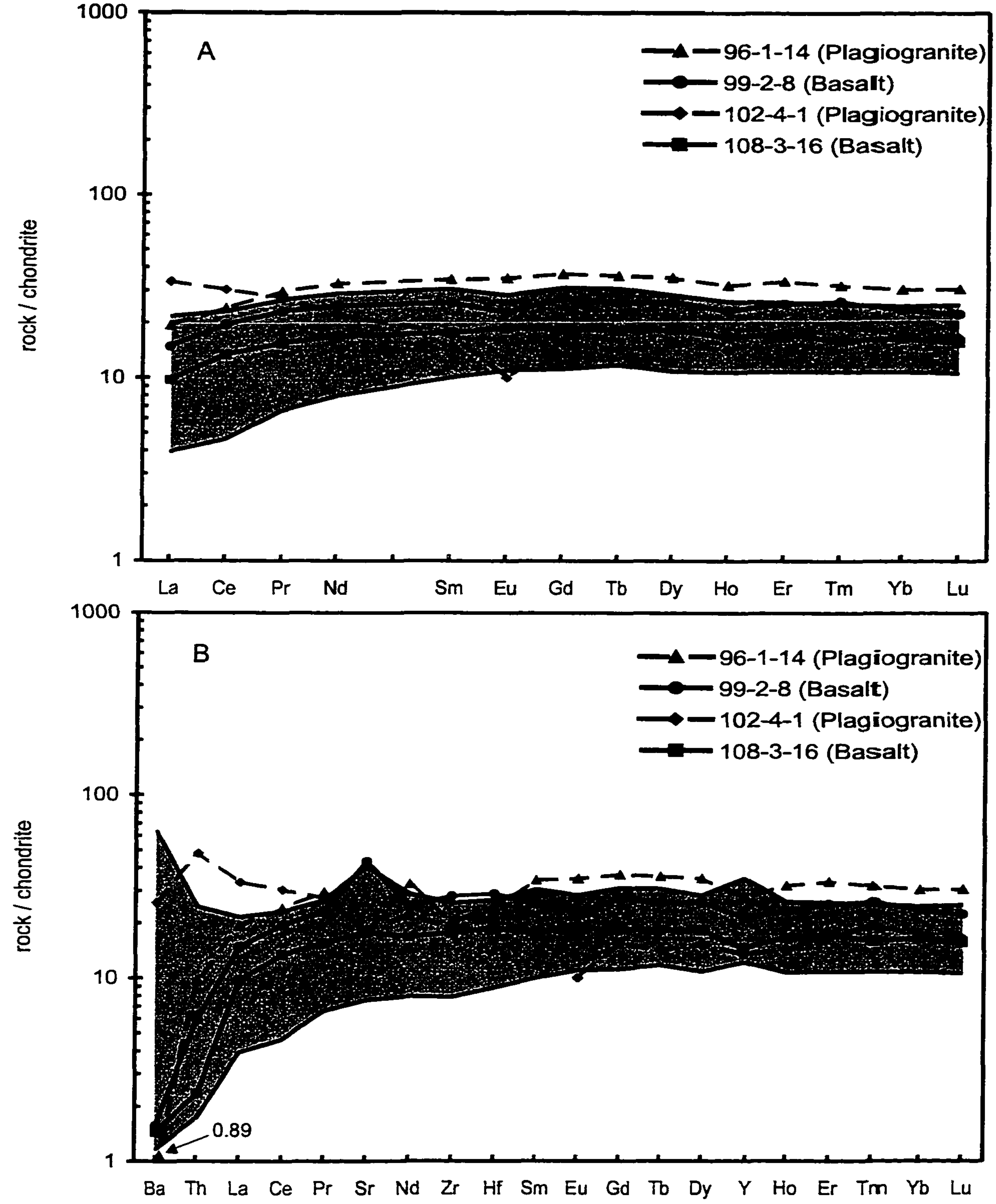

Figure 5.10 Chondrite-normalized whole rock REE (A) and trace element profiles (B) for the Tonga forearc. The shaded fields show the range of values for least altered basalt analyses (Falloon, pers. com.). Dashed lines represent epidosites from plagiogranite protoliths; solid lines represent epidosites from basaltic protoliths.

Sample 99-2-8 exhibits a pronounced positive Sr anomaly similar to the Troodos epidosites and in general, the patterns for basaltic epidosites are extremely similar between Troodos and Tonga. The Tonga basaltic epidosites show a similar LREE depletion as the Troodos samples and fall toward the upper limit of the field defined by the least altered Tonga basalts [*T. Falloon*, pers. com., 2000], again suggesting only local redistribution of the REE.

The two epidosites from plagiogranite protoliths have distinctive patterns (Figure 5.11). Sample 96-1-14 displays a similar REE pattern to the basaltic epidosites from both Tonga and Troodos except that abundances are slightly higher. Chondrite-normalized trace element concentrations are also high and parallel the basaltic epidosites, except for slight negative Sr, Zr, and Hf anomalies. Least altered plagiogranite samples from the same dredge show similar patterns to sample 96-1-14 except for a small negative Eu anomaly. The general REE patterns of these plagiogranites are also similar to plagiogranite analyses from the Troodos ophiolite [*Aldiss*, 1981; *Kay and Senechal*, 1976]. Sample 102-4-1 is characterized by LREE enrichment, a negative Eu anomaly, and elevated Ba_N and Th_N contents. Although distinct from the plagiogranite samples recovered in dredge 96, sample 102-4-1 has a similar REE pattern to plagiogranites dredged from widely spaced localities along the Mid-Atlantic Ridge (MAR) [*Aldiss*, 1981].

DISCUSSION

Trace element substitution in epidote is controlled by a variety of factors, including host rock and fluid compositions, epidote crystal chemistry, pressure, temperature, pH, and oxygen fugacity. In the following sections, the relative importance of these factors is discussed and the findings are used to make predictions on the chemistry of fluids circulating in the deep portions of seafloor hydrothermal systems.

Epidote Mode of Occurrence

Epidote patterns from basaltic protoliths from both Tonga and Troodos are remarkably similar and are generally characterized by type I REE patterns (Figure 5.8). Two basaltic samples (99-2-8 from Tonga and KG99006 from Troodos) show a marked difference between void filling and replacive epidotes not seen in other samples such that void filling epidote is characterized by type I patterns and replacive epidote is characterized by type II

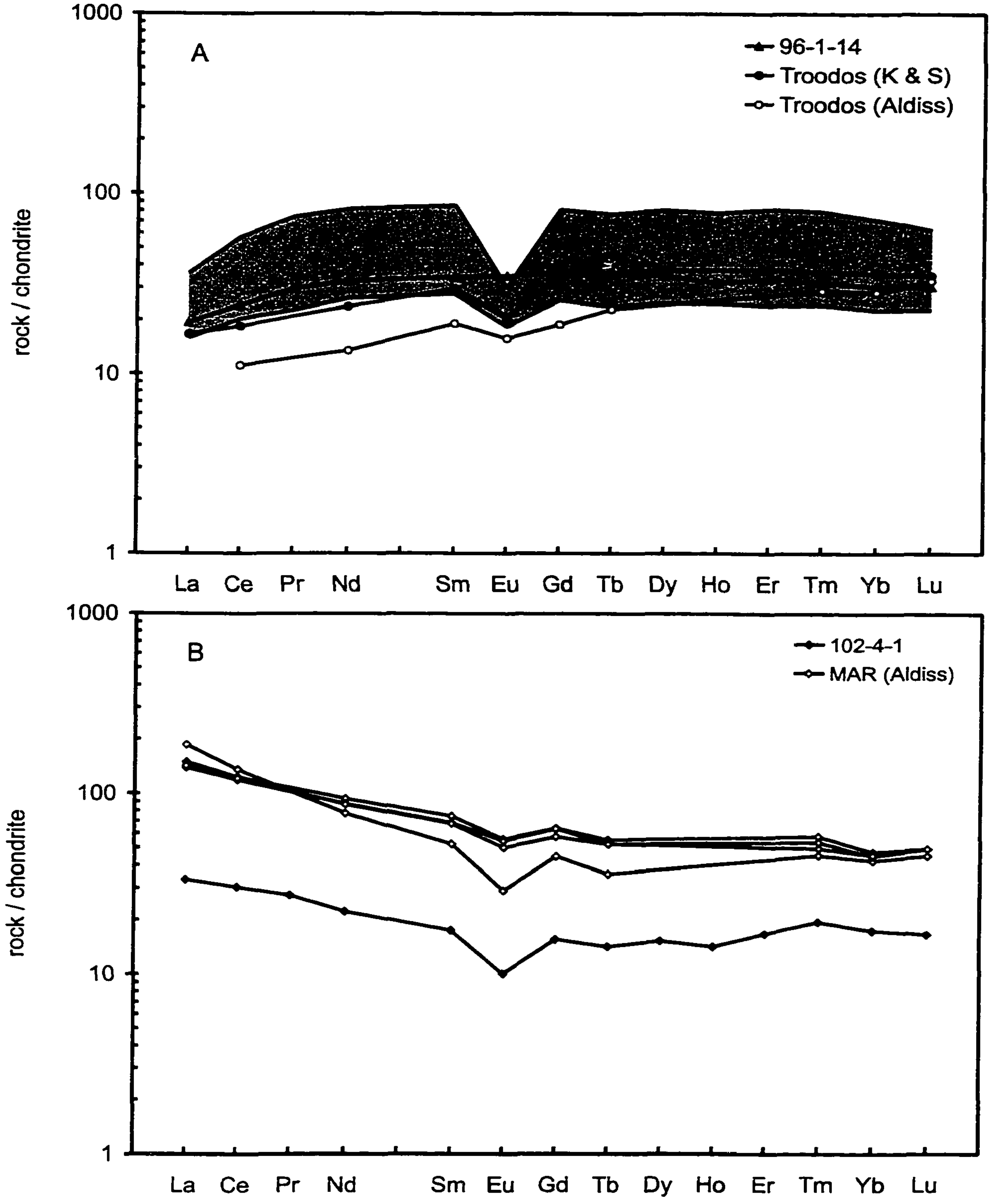

Figure 5.11 Plagiogranite chondrite-normalized whole rock REE profiles. (A) Comparision of pattern for sample 96-1-14 with least altered plagiogranites from Tonga (shaded), and two analyses from Troodos (K & S = Kay and Senechal, 1976; Aldiss = Aldiss, 1981).
(B) Comparision of pattern for sample 102-4-1 with plagiogranites dredged from the Mid-Atlantic Ridge [*Aldiss*, 1981].

patterns. An earlier study on REE in secondary minerals from the Troodos ophiolite shows a similar separation in epidote REE patterns based on mode of occurrence [*Gillis et al.*, 1992]. In their study, replacive epidote displays type I patterns and the void filling epidote displays patterns similar to type IV; however, both of their epidote samples came from basaltic protoliths [*Gillis et al.*, 1992]. One analysis in sample 99-2-8 displays a transitional pattern (between types I and II) that comes from an epidote grain at the edge of a vesicle (Figures 5.3 and 5.7) and displays petrographic features shared by both void filling and replacive epidote. The remaining samples do not show a clear distinction between mode of occurrence and trace element chemistry.

Comparison with Whole-Rock Chemistry

The similarities observed between the fresh rock (or glass), epidosite whole rock, and epidote trace element patterns are striking. It is clear that epidosites inherit the trace element compositions of their protoliths, which suggests that mobilization of trace elements results in only local redistribution. This is further supported by the CHARAC behaviour displayed by the epidote analyses (Figure 5.5). As the dominant REE-bearing phase in epidosites, it is not surprising that epidote mimics the whole-rock patterns, as epidote is the most likely host for the majority of the trace elements in the epidosites. A few differences are observed, however, between the epidote and whole rock patterns. For example, the epidote analyses commonly display negative Ba, Zr, and Hf and positive Sr anomalies relative to the fresh rocks. Sr partitions onto the Ca sites in epidote and is therefore enriched [*Deer et al.*, 1992]. Ba should also partition onto the Ca site but is mobile in hydrothermal fluids and is likely leached from the rock during alteration. Zr and Hf both have high charge and small radii, which makes them less suitable for partitioning into the epidote crystal structure.

Plagiogranites are more chemically evolved than basaltic protoliths and contain minor phases such as apatite and zircon. Epidote in samples with plagiogranite protoliths displays more complex REE patterns than those from basaltic epidosites. Epidote patterns in sample 96-1-14 (type III) are similar to type I patterns except that HREE values converge toward Lu rather than diverge and the positive Eu anomalies are variable. Epidote patterns in sample 102-4-1 (type IV) show LREE enrichment that is distinct from all other samples. These two distinct patterns are remarkably similar to their host rock patterns and patterns from fresh plagiogranites.

Three epidote grains, which are similar in texture and major element chemistry to the other epidotes, display anomalous trace element patterns. One grain in sample 102-4-1 and another in sample 96-1-14 contain extremely high overall trace element concentrations (Figures 5.3 and 5.7). They are characterized by slightly LREE-enriched patterns with no appreciable Eu anomaly and negative Ba, Sr, Zr, and Hf anomalies. Sample 96-1-14 also contains an analysis that is relatively LREE-depleted, HREE-enriched, and whose chondrite-normalized REE concentrations vary over three orders of magnitude. I believe these analyses are accurate because no variation in detection limits is observed and the time resolved LA-ICP-MS spectra do not indicate incorporation of foreign material or inclusions. These grains could represent a different generation of epidote, which formed from a REE-enriched fluid. One source for this fluid could be volatiles exsolved from the plagiogranite melt during crystallization. This possibility is supported by fluid inclusion data, which indicate the epidosites may have interacted with fluids derived from a magmatic source [*Banerjee et al.*, 2000]. Alternatively, these grains may have crystallized from a silicic magma rather than an aqueous fluid since epidote is known to occur as an accessory phase in granitic rocks. Aumento [1969] documents the occurrence of allanite in a sample of diorite dredged from the Mid-Atlantic Ridge. Allanite is the REE-rich member of the epidote group, which is known to occur in felsic volcanic and plutonic rocks [*Deer et al.*, 1992].

The remarkable similarity between the epidosite and fresh rock patterns suggests that only local redistribution of the REE occurs during epidotization. Type II REE patterns in basaltic protoliths are quite similar to their host whole-rock patterns, presumably due to local redistribution during replacement of primary phases. On the other hand, Type I patterns are quite different than host whole-rock patterns and may reflect an external control, possibly fluid composition during precipitation.

Mass Balance Considerations

Mass balance calculations were performed in order to assess the relative contribution of the two epidote textural types and accessory phases (i.e., titanite, apatite) to epidosite whole rock REE patterns. Mass balance models were developed for samples 99-2-8 and KG99006, which show very good separation between epidote textural varieties. It is first assumed that all the REE in the rock are concentrated in the two textural varieties of epidote: void filling and replacive. Quartz and chlorite, which are the other main mineral phases present in the epidosites, contain low REE concentrations and are therefore ignored. Because the epidote textural types show a wide range in REE content, mass balance models were developed using all possible combinations of the minimum, maximum, and average REE contents for both textural varieties (Figure 5.12 and 5.13). The resulting six patterns (minimum void filling, maximum void filling, average void filling, minimum replacive, maximum replacive, and average replacive) were then arranged in five combinations (e.g., minimum void filling plus minimum replacive, minimum void filling plus maximum replacive; maximum void filling plus minimum replacive; etc.). These concentrations were then used to calculate bulk rock compositions, assuming different ratios of void filling to replacive epidote. This approach permits simultaneous evaluation of the whole rock REE patterns against different epidote patterns (in terms of concentration) and in different proportions of textural type (void vs. replacive). The model results are presented in Figures 5.14 and 5.15.

The model that best matches the whole-rock pattern for sample 99-2-8 utilizes the minimum void filling and replacive epidote values, in the proportion of 35:65 (Figure 5.14F). The abundance of void filing epidote used in this model agrees well with their modal proportions determined petrographically. Therefore, if this combination of void filling to replacive epidote at the appropriate concentrations is present in sample 99-2-8 the whole rock pattern could be reflecting REE only in epidote. The same model is appropriate for sample KG99006 (Figure 5.15F), except that it does not produce the slightly negative Eu anomalies of the whole-rock pattern.

Based on this modelling it appears that REE-bearing accessory phases do not contribute significantly to the REE contents of the whole rock. Titanite is common as an accessory phase (<5%) in these samples where it partially to completely replaces ilmenite. Titanite is strongly depleted in Eu [*Green and Pearson*, 1983], which may reconcile Eu in sample KG99006. Overall, the titanite REE pattern is slightly concave down [*Green and Pearson*, 1983]. As a result, titanite would probably not have a large effect on the HREE or LREE of the whole rock pattern but could influence Eu significantly.

Crystal-Chemical Controls

In order to evaluate the influence of crystal-chemical controls on trace element partitioning between hydrothermal fluids and epidote, I have applied the method of Blundy and Wood [1994], which proposes that lattice strain is the dominant control on mineral-melt

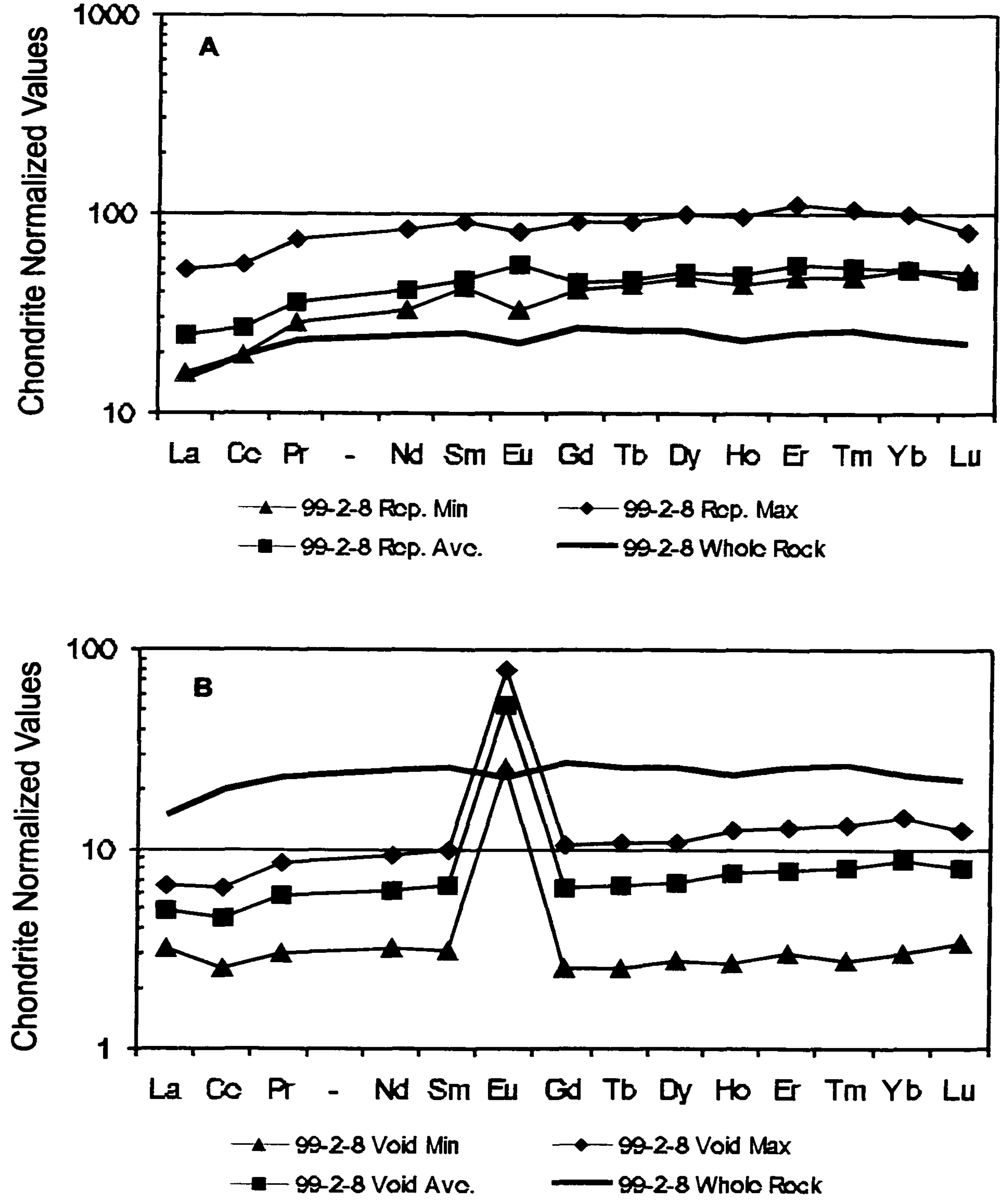

Figure 5.12 Comparison of minimum, maximum, and average epidote REE patterns with whole-rock patterns for (A) replacive and (B) void filling textures in sample 99-2-8. Min = minimum; Max = maximum; Void = void filling; Rep. = replacive; Ave. = average. See text for discussion.

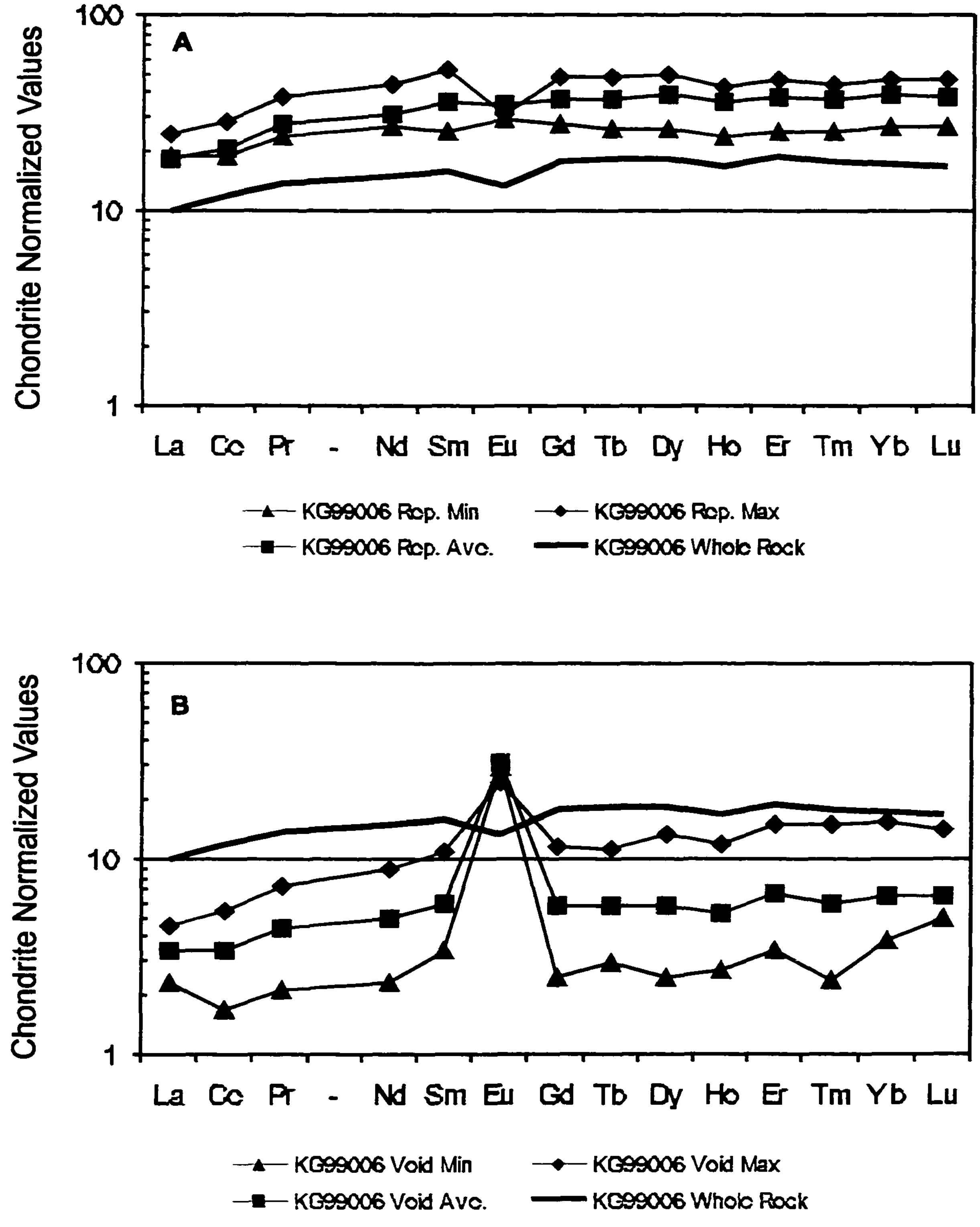

Figure 5.13 Comparison of minimum, maximum, and average epidote REE patterns with whole-rock patterns for (A) replacive and (B) void filling textures in sample KG99006. Min = minimum; Max = maximum; Void = void filling. See text for discussion.

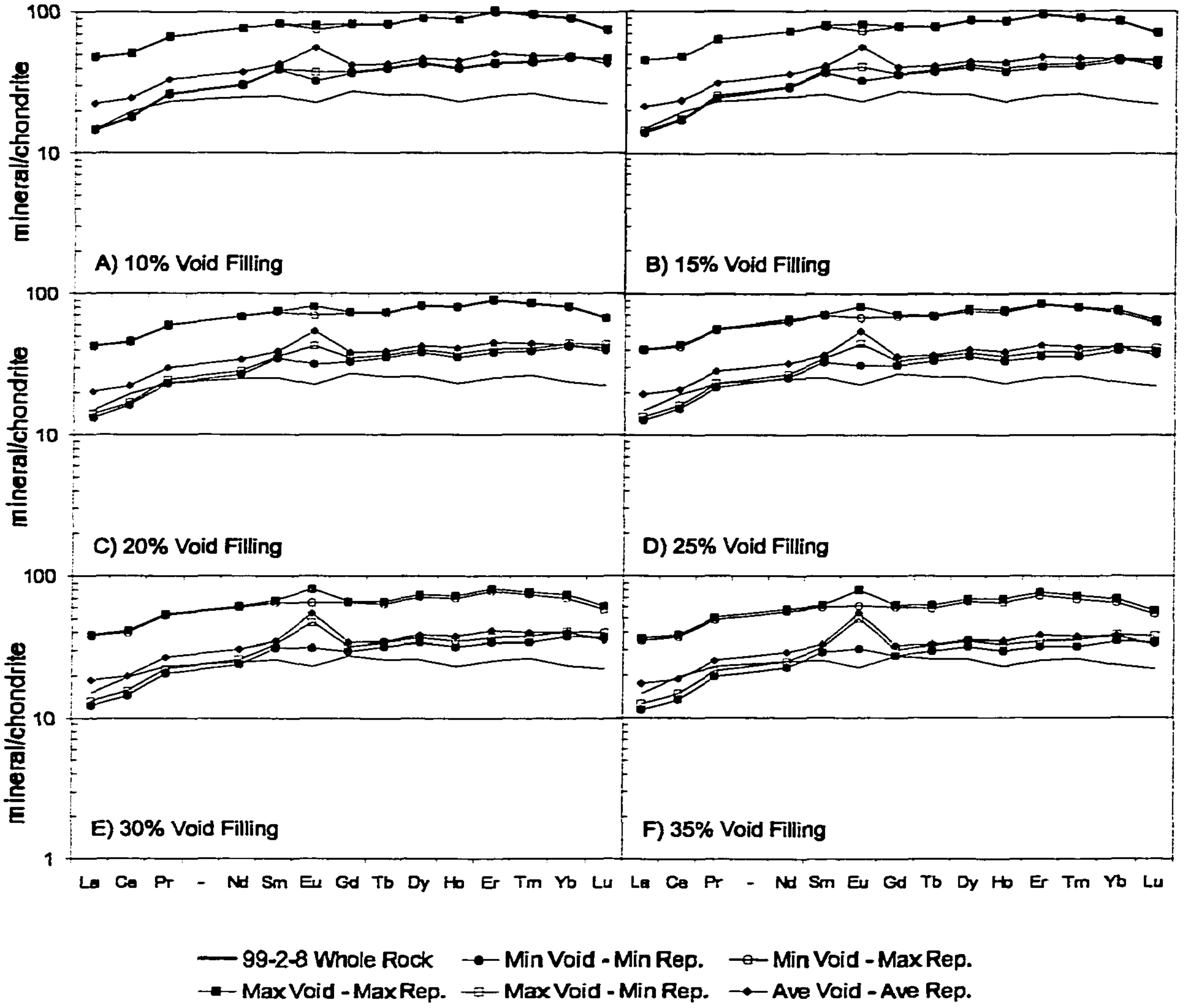

Figure 5.14 Comparison of mass balance calculations using different proportions of void filling to replacive epidote in sample 99-2-8. The whole-rock pattern is shown for comparison. The five different combination patterns were created by adding proportional amounts of the void filling and replacive patterns shown in Figure W. The proportions of void filling to replacive epidote varies from (A) 10% void filling and 90% replacive to (L) 65% void filling and 35% replacive. Min = minimum; Max = maximum; Void = void filling; Rep. = replacive; Ave. = average. See text for discussion.

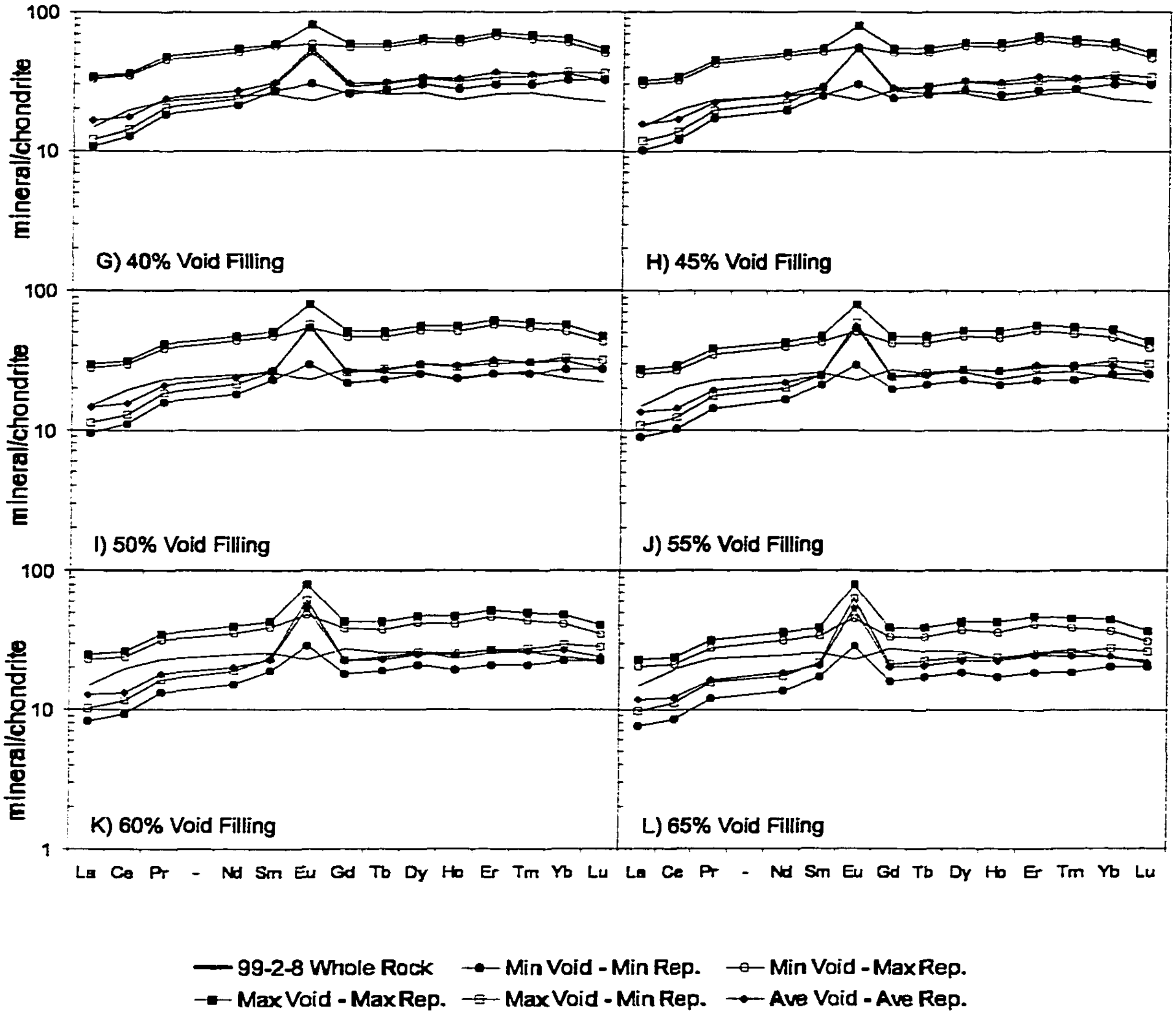

Figure 5.14 Continued.

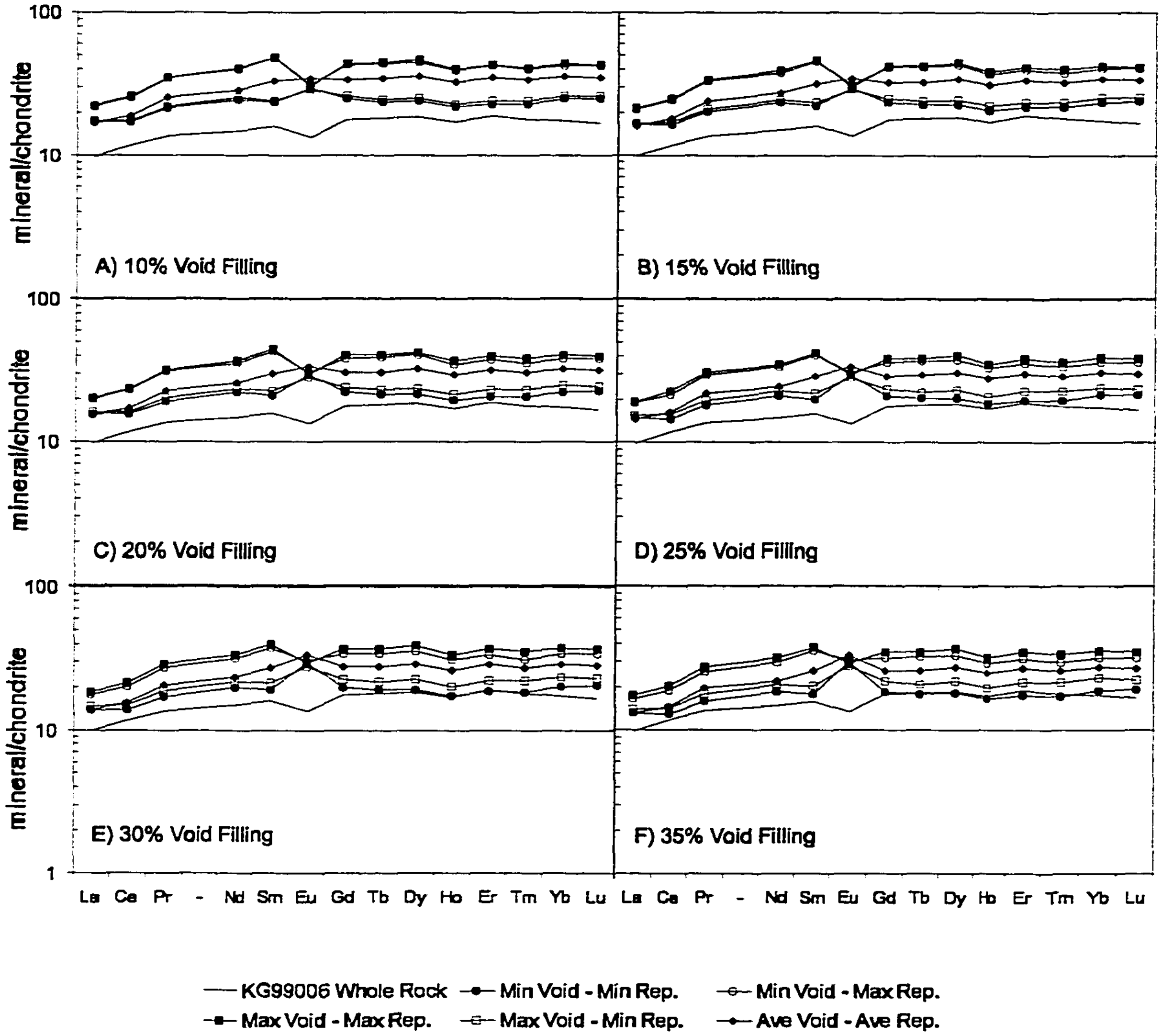

Figure 5.15 Comparison of mass balance calculations using different proportions of void filling to replacive epidote in sample KG99006. The whole-rock pattern is shown for comparison. The five different combination patterns were created by adding proportional amounts of the void filling and replacive patterns shown in Figure Y. The proportions of void filling to replacive epidote varies from (A) 10% void filling and 90% replacive to (L) 65% void filling and 35% replacive. Min = minimum; Max = maximum; Void = void filling; Rep. = replacive; Ave. = average. See text for discussion.

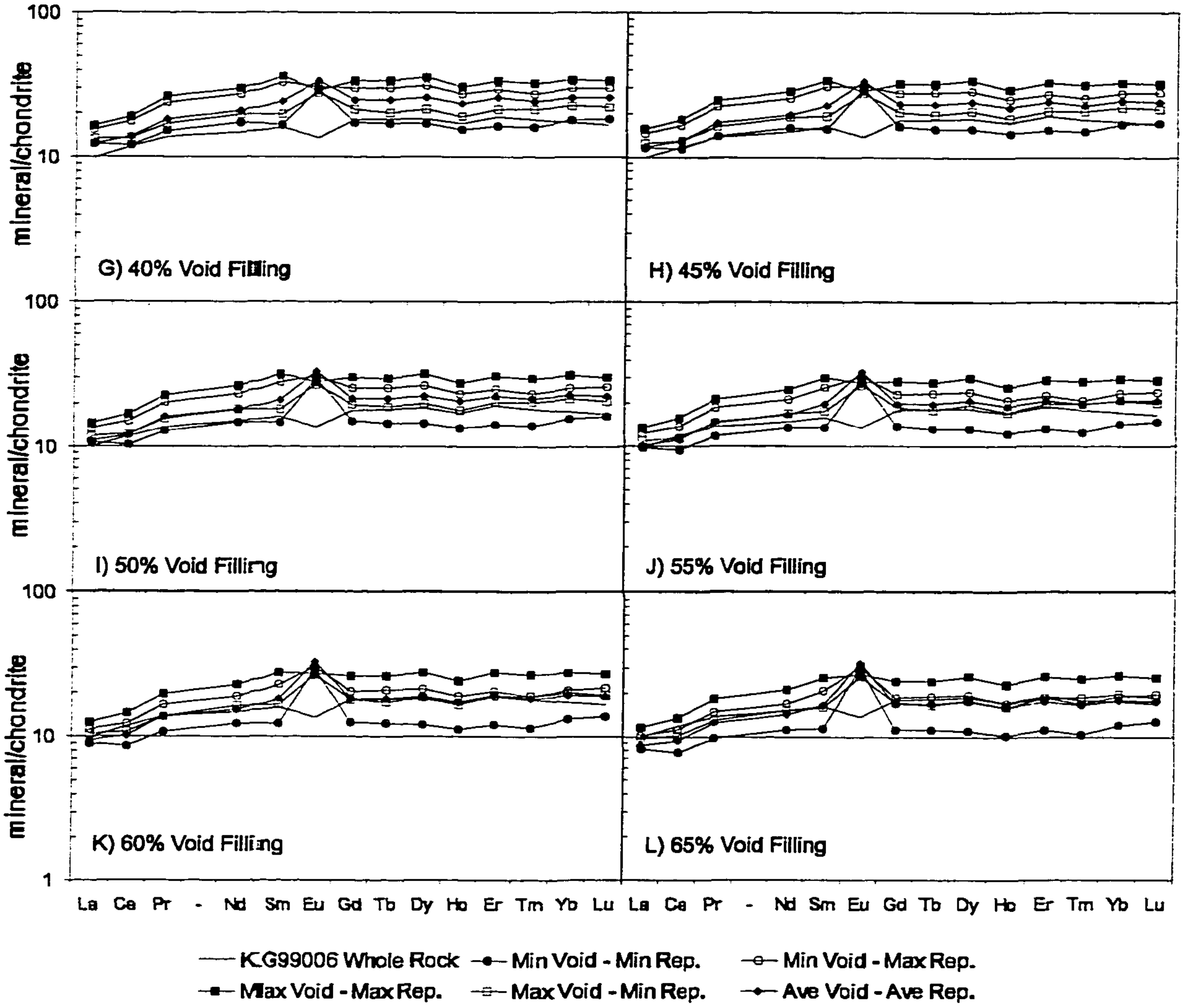

Figure 5.15 Continued.

partitioning of trace elements. In their model, the partitioning (D_i) of trace element (i) with radius (r_i) on a given structural site is described in terms of the optimum site radius (r_0), the site Young's Modulus ($\overline{E}$), and the theoretical strain free partition coefficient (D_0):

$$D_i = D_0 \cdot \exp\left[\frac{-4\pi \overline{E} N_A \left[\frac{r_0}{r_i}(r_i - r_0)^2 + \frac{1}{3}(r_i - r_0)^3\right]}{RT}\right] \qquad (5.1)$$

where N_A is Avogadro's number, R is the gas constant, T is temperature in K, and the bar denotes a site property rather than a bulk crystal property.

The model of Blundy and Wood [1994] can be applied to hydrothermal epidote because most of the variables in equation (5.1) are properties of the crystal and are not affected by the nature of the fluid phase (melt or aqueous solution). I restrict my discussion of crystal-chemical controls to the REEs for two reasons. First, the REE compositions of hydrothermal fluids exiting at black smokers are relatively well known. Second, of the trace elements I have determined, the REE represent the largest group of isovalent cations with which to compare the model data.

The epidote group minerals can be represented by the ideal formula $A_2M_3SiO_{13}H$ in which the A sites are occupied by large, high coordination number (VII to XI) cations such as Ca, Sr, Pb, REE, and the M sites are occupied by octahedrally coordinated, trivalent (sometimes divalent) cations such as Al^{3+}, Fe^{3+}, Mn^{3+}, Fe^{2+}, and Mg^{2+} [*Dollase*, 1971]. The REE partition onto the A sites normally occupied by Ca in epidote, which form large irregular polyhedral cavities. The entry of the REE into the crystal structure of epidote is accommodated by coupled substitution to maintain electrostatic neutrality such as [*Deer et al.*, 1992]:

$$Ca^{2+} + Fe^{3+} = REE^{3+} + Fe^{2+} \qquad (5.2)$$

Of the two A sites (A1 and A2), the REE have been shown to partition primarily onto the A2 site, which is likely due to its much deeper electrostatic potential well despite its larger volume [*Smyth and Bish*, 1988]. For this reason, and in the interest of simplicity, I assume that the REE partition exclusively onto the A2 site.

Since trace element partitioning studies for epidote are unavailable, it is necessary to make several assumptions regarding the parameters required in the model of Blundy and Wood [1994] (Equation 5.1). In the literature, the A sites in epidote have been assigned coordination numbers from VII to XI corresponding to a bond length variation of 2.30 to 3.13 Å [see discussion in *Pan and Fleet*, 1996]. I use a coordination number of VIII for the A2 site and a corresponding mean ‹A2-O› bond length of 2.588 Å as indicated by Smyth and Bish [1988]. Using this value, the value for r_0 was determined as the mean bond length minus the radius of oxygen in 8-fold coordination [1.42 Å - *Shannon*, 1976] which yields a value of r_0=1.168 Å. From single-crystal X-ray diffraction compressibility data, Comodi and Zanazzi [1997] determined the isothermal bulk modulus (K) of clinozoisite to be 130 ± 2 GPa. Using powder X-ray diffraction data, Holland et al. [1996] determined the isothermal bulk modulus of epidote to be 162 ± 4 GPa. I have chosen to use the bulk modulus value from Comodi and Zanazzi [1997] for two reasons. First, the K value for clinozoisite (130 GPa) more closely approximates the A2 lattice site value of $\overline{K}$ obtained by applying the relationship of Hazen and Finger [1979] to my value for mean ‹A2-O› bond length and assuming occupancy by cations with 3^+ charge (129.8 GPa). This is what might be expected if it is assumed that the elastic properties of the crystal are most strongly influenced by the large A cation sites [cf., *Blundy and Wood*, 1994]. Second, the values reported by Holland et al. [1996] for clinozoisite and zoisite are in poor agreement with those of Comodi and Zanazzi [1997], possibly due to discrepancies between the two experimental approaches [cf., *Reynard et al.*, 1996]. I have converted the A2 lattice site bulk modulus ($\overline{K}$) to the A2 lattice site Young's modulus ($\overline{E}$) by applying the identity relating E and K:

$$\overline{E} = 3\overline{K}(1-2\sigma) \qquad (5.3)$$

where σ is Poisson's ratio. I adopt the approach used in Blundy and Wood [1994] that most minerals approximate Poisson solids with a value of σ = 0.25, which results in a value of $\overline{E}$ = 195 GPa for the A2 site in epidote. Unfortunately, I have few constraints on the value of the theoretical strain free partition coefficient (D_0). Measured mineral-melt distribution coefficients for the REE in allanite have been shown to vary from < 10 for Lu to > 800 for La [*Brooks et al.*, 1981; *Mahood and Hildreth*, 1983; *Sawka*, 1988].

The results of applying the above parameters to the model of Blundy and Wood [1994] are presented in Figure 5.16A. The partition coefficient values are only relative since I do not have an appropriate value for D_0. The resulting parabola centered at 1.168 Å, shows a regular progression of the REE along its left limb. This arrangement indicates that La should partition preferentially into epidote followed by the other REE in decreasing atomic radius, which is what has been observed in several other studies of REE in epidote [e.g., *Carcangiu et al.*, 1997; *Sakai et al.*, 1984; *Yanev et al.*, 1998].

It is important to note that my epidote model is restricted in its approach to the trivalent REE. Consequently, Eu and Ce are assumed to be in their trivalent state and behave in a similar manner to their neighbors. This may not be appropriate as Eu can exist in either a 2^+ or 3^+ oxidation state, whereas Ce can exist as either a 3^+ or 4^+ oxidation state depending on redox conditions. Studies of Eu redox in hydrothermal fluids suggest that Eu is most stable in its 2^+ oxidation state at elevated temperature and pressure, regardless of the effects of complexing [*Sverjensky*, 1984]. Calculations by Haas et al. [1995] support this assertion, and indicate little change in complexing behaviour over a range of oxygen fugacities. Therefore, predicted Eu concentrations of my model fluids should be treated with caution.

In order to test my model values, I have used a Levenberg-Marquardt-type, non-linear least squares fitting routine [*Press*, 1992] to derive best-fit values for r_0, D_0, and $\overline{E}$ for partitioning of the REE in allanite based on measured values in natural samples (Figure 5.16B; Table 5.4). The shapes of the parabolas are strikingly similar to my epidote model. The largest difference in fit parameters is in the value of $\overline{E}$, which affects the tightness of the parabolas; values of $\overline{E}$ fitted to the allanite data are consistently higher than my estimated value of 195 GPa, except for the value calculated from the data of Brooks et al. [1981] (Figure 5.16B). Recalculation of my epidote model REE partition coefficients using the average $\overline{E}$ fit value for allanite results in a tighter curve, lower partition coefficients for the HREE, and less similarity to the allanite partitioning data. This may be due, in part, to the temperature value I have chosen in my model (300°C) versus that used for the allanite data (750°C) since increasing the temperature has the effect of increasing the value for $\overline{E}$.

It is significant that my measured REE concentrations in hydrothermal epidote do not support the type of partitioning behaviour predicted by the crystal-chemical model of

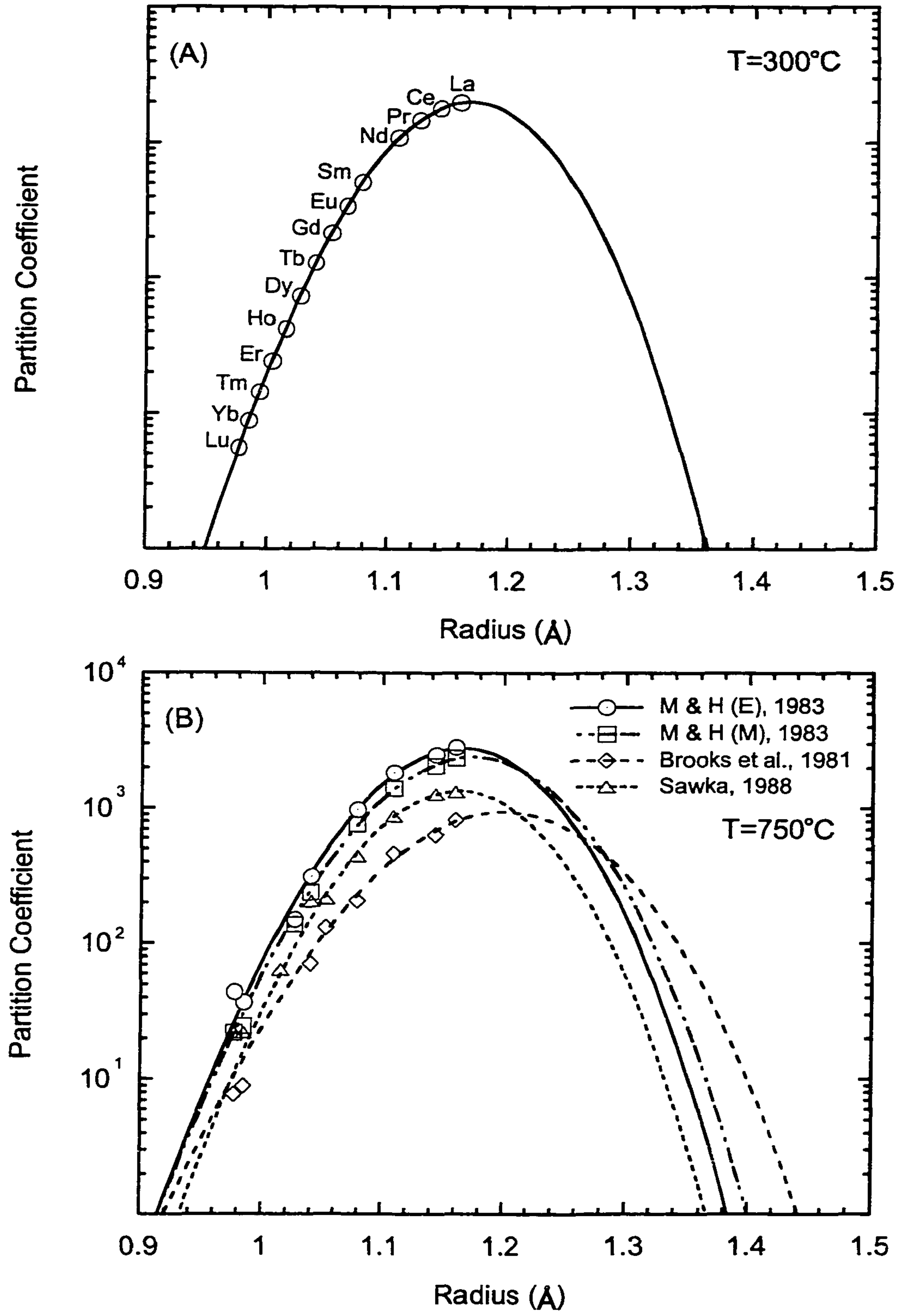

Figure 5.16 Onuma diagram showing partition coefficients for trivalent REE, together with non-linear least squares fits to equation (5.1). (A) Epidote model values are dimensionless due to lack of value for D_0 (see text for discussion). (B) Fits to allanite-melt partition coefficients; fit parameters are given in Table 5.4. M & H, 1983 = Mahood and Hildreth, 1983.

Table 5.4 Fit parameters for allanite-melt partitioning data.

	M&H (E)	M & H (M)	Brooks	Sawka
D_0	2787	2407	941	1643
r_0 (Å)	1.17	1.18	1.20	1.16
$\overline{E}$ (GPa)	284	259	193	301

Note: M&H = Mahood and Hildreth, 1983; Brooks = Brooks et al., 1981; Sawka = Sawka, 1988.

Blundy and Wood [1994]. The epidote model predicts significant fractionation of the LREE over the HREE resulting in a La/Lu value greater than 300. In contrast, my epidote analyses generally have La/Lu values between 1.4 and 36. Although La appears to be preferentially incorporated into the crystal structure of the hydrothermal epidotes, the fractionation is only modest, unlike that predicted by my model. This discrepancy could result from a number of factors: (1) my model may have improperly estimated the values for r_0, D_0, and $\overline{E}$; (2) crystal chemistry may not be the dominant factor controlling partitioning of the REE in hydrothermal epidote; (3) the fluid from which the epidote crystallized may have been extremely HREE-enriched; or (4) the epidote may not be in equilibrium with the fluid from which it precipitated. A final possibility is that the REE may be partitioned into more than one site in the epidote crystal structure; however, this option is not discussed in this thesis. I believe the similarity between my epidote model parabola and the fits to the allanite-melt partitioning data suggest my model is robust and that my estimates for r_0, D_0, and $\overline{E}$ are sound. Below I test possibilities (2), (3), and (4).

Mineral-Fluid Partitioning

I applied the model of Blundy and Wood [1994] to natural and experimental studies that measured mineral-fluid partition coefficients to test if crystal chemistry controls trace element fractionation in aqueous systems. Studies of this type are rare [see review in Gieré, 1996]. For this reason the following discussion is limited to mineral-fluid partitioning in hydrothermal allanite and apatite.

Banks et al. [1994] calculated allanite-fluid partition coefficients for the LREE (La, Ce, Pr, Nd, and Sm) from fluids released from fluid inclusions in naturally occurring allanite and found similar values to mineral-melt data [*Mahood and Hildreth*, 1983; *Sawka*, 1988]. These fluid inclusions are interpreted as primary, representing the original magmatic fluid from which the allanite crystallized [*Banks et al.*, 1994]. I derived best-fit values for the parameters in Blundy and Wood's [1994] model (Equation 5.1) for allanite-fluid partitioning [*Banks et al.*, 1994] (Figure 5.17A). The results converge to form parabolas, however, the fit parameters are unrealistic for several reasons: (1) the LREE partition coefficients cluster together on the extreme left limb of the parabolas; (2) the value for r_0 ranges from 1.51 to 1.72, which would place the optimum ‹A2-O› bond length at the

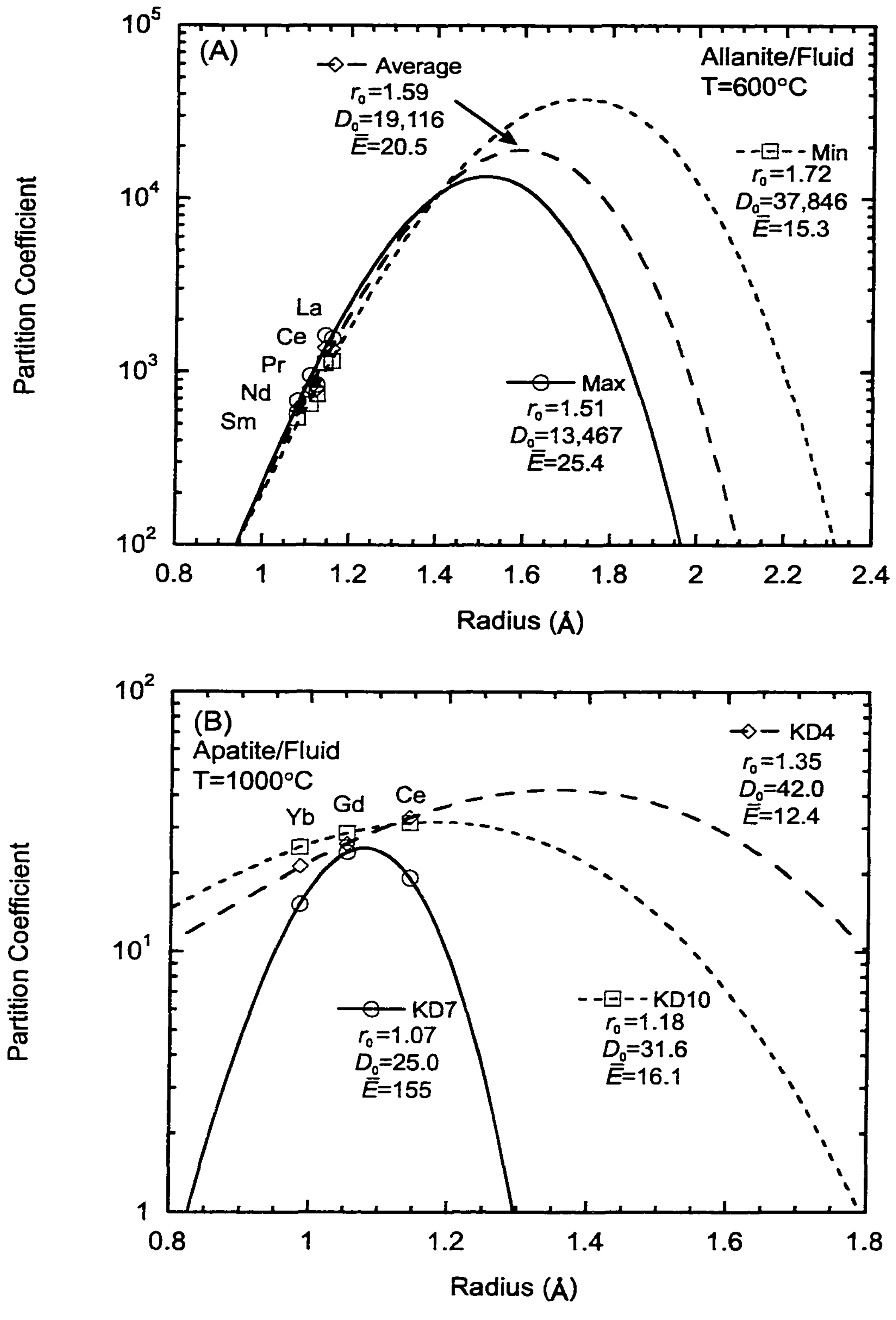

Figure 5.17 Onuma diagram showing partition coefficients for trivalent REE, together with non-linear least squares fits to equation (5.1) for (A) allanite-fluid [*Banks et al.*, 1994] and (B) apatite-fluid [*Ayers and Watson*, 1993].

extreme (> 3 Å) end of those described for the epidote group; and (3) the value for the lattice site Young's Modulus ($\overline{E}$) varies from 15.3 to 25.4 GPa, which is an order of magnitude smaller than what I observed for the fits to the allanite-melt partitioning data.

I further tested the applicability of Blundy and Wood's [1994] model (Equation 5.1) to mineral-fluid partitioning by calculating fit parameters for experimental Ce, Gd, and Yb partition coefficients in hydrothermal apatite at 1 GPa and 1000°C [*Ayers and Watson*, 1993]. One run (KD7 - forward) forms a tight parabola centered at 1.07 Å, with $\overline{E}$ = 155 GPa; these values are reasonable (Figure 5.17B). Two other runs (reversal), however, produce unreasonable fits. Ayers and Watson [1993] state that run KD7 has the lowest errors and thus best approximates the predicted values for REE partitioning, however, they also mention that the agreement between partition coefficients for all experiments suggests equilibrium was reached.

Neither study exhibits partitioning behaviour that can be predicted solely based on crystal-chemical effects. Previous studies of mineral-fluid trace element partitioning at elevated pressures and temperatures appropriate to upper mantle conditions (up to 1200°C and 5.7 GPa) have shown that fractionation is mainly controlled by CHARAC behaviour and the data can be fitted to the model of Blundy and Wood [1994] with acceptable results [*Stalder et al.*, 1998]. However, Stalder et al. [1998] point out that the observed effect of crystal-chemistry may be due to the high pressure-temperature conditions of the experiments. Under these conditions, the physical properties of aqueous fluids approach a critical point where there is little distinction between fluids and melts [see discussion in *Stalder et al.*, 1998]. Such behaviour may explain why only one of the experiments performed by Ayers and Watson [1993] fits reliably to the Blundy and Wood [1994] model – failure to reach equilibrium in is another possibility. Although crystal-chemistry plays an important role in trace element partitioning, based on my attempt to fit mineral-fluid partitioning data to the model of Blundy and Wood [1994], I conclude that other factors likely play an equal or greater role under hydrothermal conditions.

Fluid Modeling

In order to determine if fluid chemistry could produce the observed epidote REE patterns described above, the model REE partition coefficients were used to calculate fluid compositions in equilibrium with the epidote types (Figure 5.18). The relative chondrite-normalized fluid patterns produced are remarkably similar to each other, irrespective of epidote REE pattern type. The patterns are generally characterized by strong HREE enrichment that ranges over four orders of magnitude and variable positive Eu anomalies, except in the case of Type II epidote (replacive), which shows no Eu anomaly. These fluid patterns are distinct from both chondrite-normalized patterns of hydrothermal fluids exiting at black smokers and seawater (Figure 5.18).

Several studies have shown that the REE chemistry of hydrothermal fluids from different locations is generally similar [e.g., *Klinkhammer et al.*, 1994; *Michard*, 1989]. Furthermore, the similarity between the patterns of hydrothermal fluids and those of plagioclase has been used to infer that dissolution of plagioclase may control hydrothermal fluid REE contents [*Klinkhammer et al.*, 1994]. It is clear from Figure 5.18 that plagioclase dissolution alone could not be responsible for the REE of fluids calculated from my epidote model. Because of their REE abundances, I find it hard to reconcile the calculated fluid patterns with simple dissolution of primarily plagioclase and clinopyroxene. Instead, dissolution of HREE-enriched minerals such as olivine or orthopyroxene might be responsible for the equilibrium fluid patterns observed. Olivine and orthopyroxene, however, are commonly observed in modal proportions less than a few percent in oceanic crustal rocks and are relatively REE-poor. Another REE source is interstital glass, which reacts quickly under hydrothermal conditions [e.g., *Bach et al.*, 1996; *Bach and Irber*, 1998]. However, REE released from this material is unlikely to have the strongly HREE-enriched patterns observed for the fluids and should instead have patterns similar to basalt [*Bach et al.*, 1996; *Bach and Irber*, 1998].

Co-precipitation of accessory phases (e.g., titanite) with epidote are probably not responsible for the positive Eu anomalies observed in the void filling epidote, since it probably formed at the same time as the replacive epidote. Replacive epidote does not show a positive Eu anomaly, suggesting co-precipitation of titanite did not affect its REE composition. The positive Eu anomaly displayed by void-filling epidote might be related to dissolution of plagioclase at an advanced stage of alteration. Plagioclase could have provided the Eu and would not have broken down as readily as mafic phases (such as clinopyroxene) during initial alteration. Differences in REE patterns between void filling and replacive

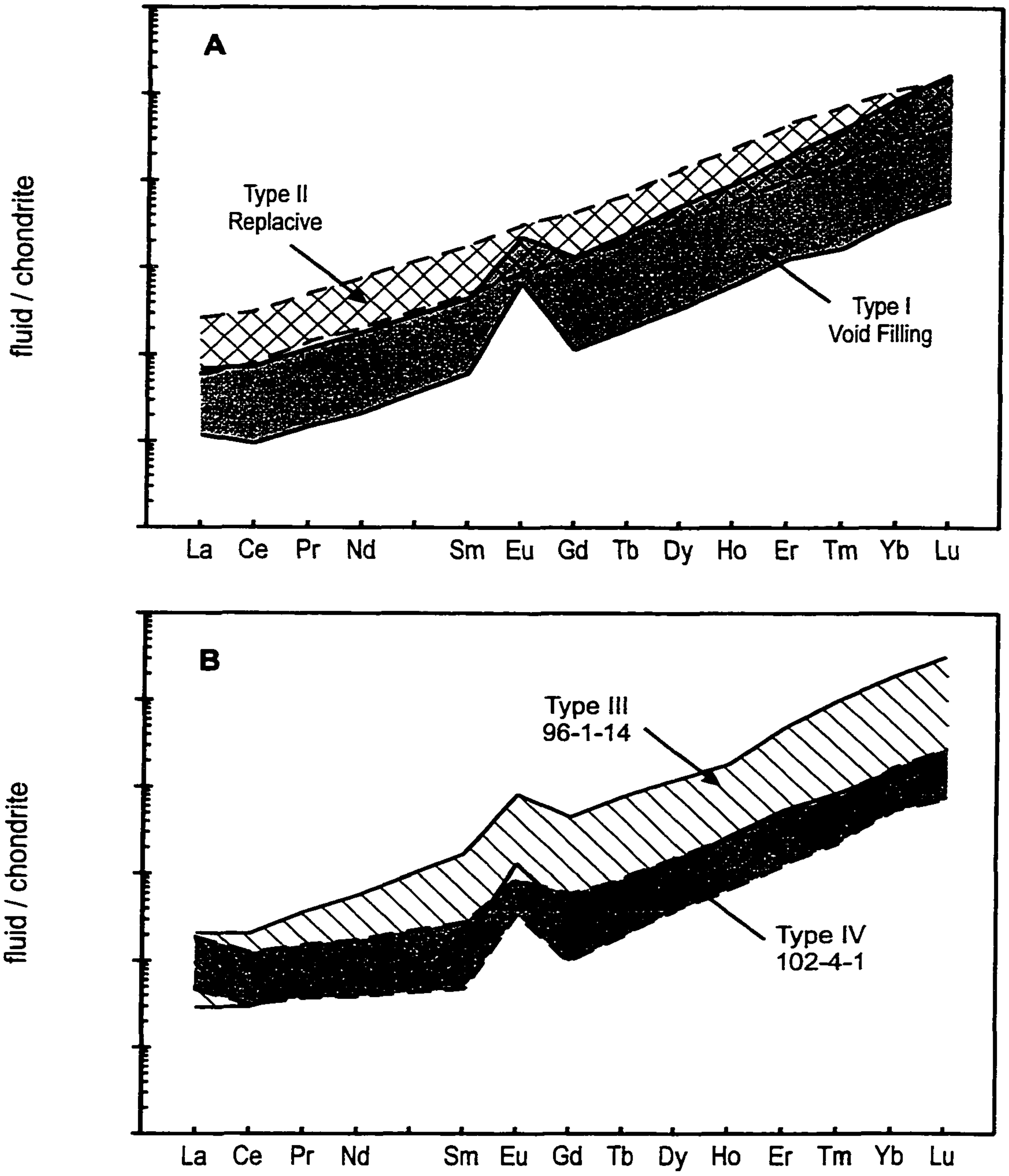

Figure 5.18 Chondrite-normalized REE profiles of fluids predicted to be in equilibrium with (A) epidote from basaltic protoliths and (B) epidote from plagiogranite protoliths, based on partition coefficients from the epidote model. See Figure 5.8 and text for explanation of epidote types.

epidote may therefore be related to dissolution of different primary minerals and/or in different proportions as alteration progressed.

Several studies have commented on the relative abilities of complexing agents (chloride, fluoride, hydroxide, carbonate, sulphate, etc.) to stabilize REE in solution [e.g., *Cantrell and Byrne*, 1987; *Haas et al.*, 1995; *Wood*, 1990]. Calculations for acidic hydrothermal vent fluids from the East Pacific Rise [*Michard et al.*, 1983; *Michard et al.*, 1984] incorporating a Cl/F value of 1000 suggest chloride and fluoride complexes are equally important for the LREE and that fluoride complexes are dominant for the HREE [*Haas et al.*, 1995]. Due to the low concentrations of F in hydrothermal fluids, it is unlikely this type of complexing behaviour could produce the strongly HREE-enriched patterns observed. Some increased stability of the HREE relative to LREE in solution might be expected [cf., *Wood*, 1990] but not on the scale observed in the modeled fluids. Thus it appears that crystal chemistry is not the dominant control on trace element partitioning in seafloor hydrothermal systems and that fluid chemistry may also contribute to epidote trace element abundances.

Composition of Deep Hydrothermal Fluids

Since crystal chemistry does not control trace element abundances in hydrothermal epidote, I can use epidote as a proxy for deep fluid chemistry. I have identified four epidote trace element patterns, based primarily on REE abundances (Figure 5.8). Type I and type II patterns both occur in basaltic protoliths and are separated on the basis of mode of occurrence, which suggest that fluid compositions likely evolve during progressive alteration. Variation between epidote from basaltic and plagiogranite protoliths and comparison with fresh whole rock data demonstrates that fluids interacting with different rock types have different chemistries and that these fluids are rock-dominated. Below I compare my results with direct observations and experimental studies of deep fluids to evaluate the possibility that hydrothermal epidote mimics fluid trace element compositions.

Measured Values

The chemistry of the fluids circulating deep within hydrothermal systems has remained elusive due to difficulties in sampling. One way of looking at fluids deep in the crust is through analysis of fluid inclusions. One study documents the REE and trace element chemistry of fluid inclusions in a sample of metamorphosed gabbro from the Mathematician

Ridge (MR) [*Ghazi et al.*, 1993]. The fluid inclusion microthermometry of this sample [MR sample 7-45; *Vanko*, pers. com., 2000] indicates the presence of several inclusion types. Primary saline inclusions consisting of liquid + vapor + one or more daughter mineral are most abundant [*Vanko*, 1988]. Fluid inclusion homogenization temperatures up to > 700°C and salinities up to >48 wt% NaCl for the primary inclusions provide evidence of formation from high temperatures evolved fluids deep in the plutonic sequence [*Vanko*, 1988]. The REE pattern of these inclusions (Figure 5.19) is flat to slightly HREE-enriched with a slight positive Eu anomaly and displays a surprising similarity to the type II epidotes (Figure 5.8) [*Ghazi et al.*, 1993].

Leaching Experiments

Another technique used to unravel the chemistry of fluids circulating deep within hydrothermal systems involves leaching experiments on altered samples. Bach and Irber [1998] performed leaching experiments on alteration patches in diabase from the lower sheeted dike complex at Ocean Drilling Program (ODP) Hole 504B in order to determine the mobility of REE during high temperature hydrothermal alteration. Oxygen isotope compositions of these rocks indicate only slightly higher water/rock ratios than the surrounding host diabase [*Alt et al.*, 1995], which negates the possibility of REE mobility solely resulting from high water/rock alteration conditions. Bach and Irber [1998] calculated the hypothetical composition of hydrothermal fluids in the reaction zone as the difference between the weakly altered diabase and the highly altered alteration patch (assuming water/rock = 1) (Figure 5.19).

What is interesting about this fluid is that it closely resembles the pattern of the type II epidotes, except that REE abundances are about one order of magnitude lower for the fluid. Bach and Irber [1998] also use a forward modelling approach to calculate the compositions of hypothetical fluids resulting from dissolution of the major rock-forming minerals. The resulting patterns progress from LREE-depleted with only a slight positive Eu anomaly, to flat patterns with a moderate positive Eu anomaly, and finally to strongly HREE-depleted with a large positive Eu anomaly similar to black smoker fluids [*Bach and Irber*, 1998, Fig. 7]. The implication is that as more and more material is leached, the REE pattern of the hydrothermal fluid evolves from a rock-dominated pattern similar to the

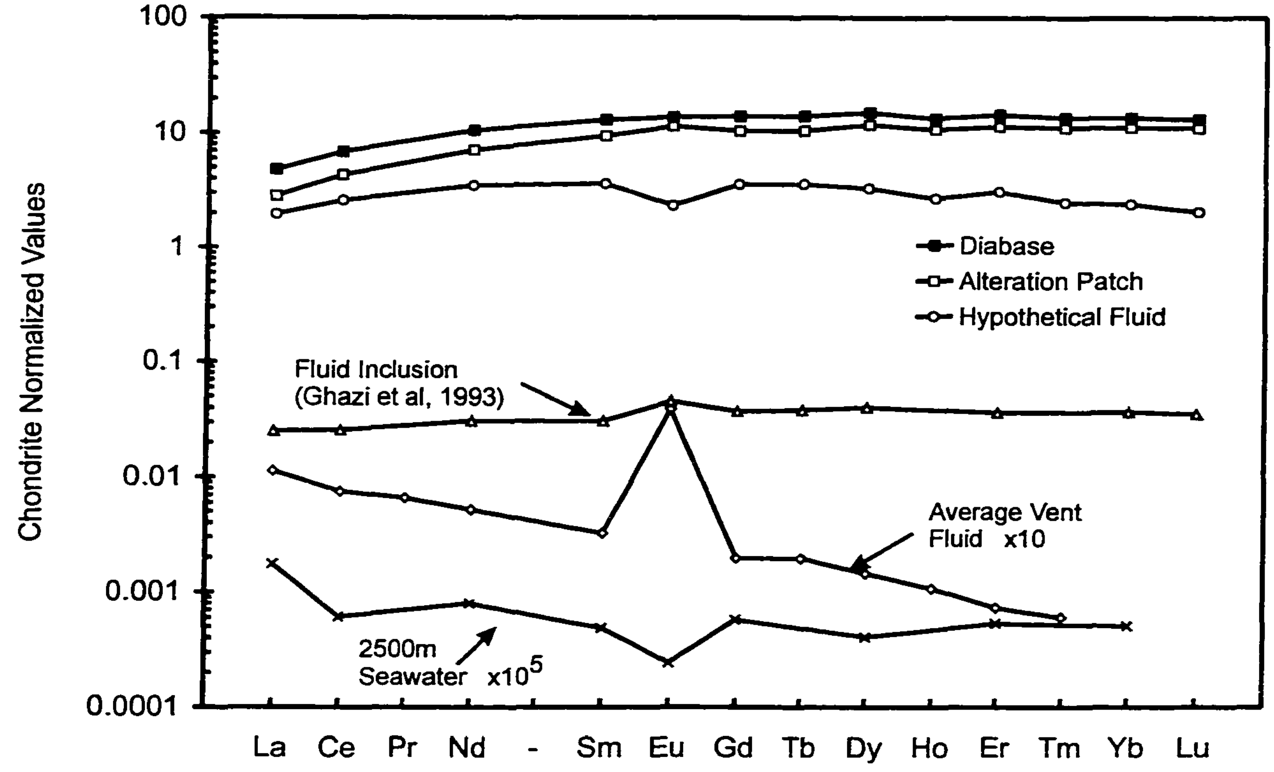

Figure 5.19 Chondrite-normalized REE profiles of Manthematician Ridge sample fluid inclusion [*Ghazi et al.*, 1993], and diabase, alternation patch, and hypothetical fluid from leaching experiments [*Bach et al.*, 1996; *Bach and Irber*, 1998]. Average vent fluid pattern from Klinkhammer et al. [1994]. 2500m seawater pattern from Elderfield and Greaves [1982].

patterns observed for epidote from basaltic protoliths to something more like measured black smoker fluids.

By analogy with these experiments, the observed correlation between mode of occurrence and REE pattern in samples 99-2-8 and KG99006 may represent changing fluid chemistry as alteration progressed. In these samples, replacive epidote is characterized by patterns similar to the LREE-depleted patterns that result from the most limited (1 hour) leaching experiments whereas void filling epidote is similar to patterns calculated for the 2 hour leaching experiments [*Bach and Irber*, 1998]. Petrographically it is not possible to determine the relative timing for the formation of the replacive versus void filling epidote. However, comparison with the patterns calculated by Bach and Irber [1998] suggests the replacive epidote formed early, resulting from local mobilization of elements released by dissolution of primary minerals by hot acidic fluids, followed by precipitation of epidote in voids as alteration progressed. Harper [1988] has suggested that replacement of anorthite by epidote in epidosites results in the creation of secondary porosity during metasomatism. When combined, this evidence suggests the variation in trace element patterns observed in epidote reflect changes in fluid chemistry as alteration progressed.

CONCLUSIONS

Hydrothermal epidote from epidosites is characterized by generally similar major element compositions and variable trace element compositions. Trace element compositions are generally similar to whole rock analyses of the unaltered host. Four general epidote REE patterns are observed that are distinct from those of black smokers and seawater and reflect differences in both protolith and mode of occurrence. My crystal-chemical model for REE partitioning in epidote predicts that significant fractionation of the LREE over the HREE should occur. In contrast, my measured epidote REE concentrations are characterized by La/Lu values that are an order of magnitude lower than those predicted by crystal chemical controls. Calculation of fluids in equilibrium with epidote compositions predicted by crystal chemistry results in unrealistic HREE-enriched fluids. I predict the trace element composition of epidote in seafloor hydrothermal systems approximates the chemistry of the fluid from which it formed. Replacive and void filling epidote show distinct patterns in two basaltic samples suggesting fluids change chemistry as they evolve during progressive alteration. Analysis of hydrothermal epidote trace element chemistry from a variety of locations within hydrothermal systems, therefore, has the potential to help constrain fluid evolution through space and time.

Chapter 6

OXYGEN ISOTOPES

Hydrothermal circulation of seawater through the oceanic crust results in a number of physical and chemical changes. During interaction with circulating fluids, oceanic crust is relatively unstable, resulting in the recrystallization of pre-existing minerals or the precipitation of new ones. It is this process that causes changes to the isotopic composition of both the rock and fluid. In general, cold seawater loses ^{18}O to the rock whereas hot hydrothermal fluids gain ^{18}O from the rock.

Early studies of the isotopic compositions of oceanic rocks showed that mantle derived oceanic rocks (e.g., MORB) have global $\delta^{18}O$ ratios of 5.8 ± 0.3‰ [*Muehlenbachs and Clayton*, 1972a; *Muehlenbachs and Clayton*, 1972b; *Taylor*, 1968]. Muehlenbachs and Clayton [1972a; 1972b] further suggested that the competing processes of interaction between hot and cold hydrothermal fluids along with continental weathering and recycling of subducted fluids buffer the isotopic composition of seawater ($\delta^{18}O_{seawater}$) near 0 ± 2‰. Because of the relatively constant isotopic compositions of both oceanic rocks and seawater, a great deal of information can be gained through analysis of altered oceanic rocks. For example, analysis of oxygen isotopes can help elucidate details such as the temperature of alteration and water-rock ratio. In the following sections, the oxygen isotopic composition of whole rock samples and mineral separates from the Tonga forearc are discussed in the context of previous studies of oceanic rocks and these data are used to make some predictions on the conditions of alteration.

SAMPLING STRATEGY

In order to investigate the isotope geochemistry of the Tonga suite I selected three suites of samples for analysis. The first suite includes the epidosite samples previously described and discussed in Chapter 4. The second suite includes samples representative of the rock types observed in ophiolites (e.g., basalt, diabase, gabbro, peridotite). Finally, the third suite includes a subset of 10 plagiogranites from dredge 96. Together, these samples were chosen to address four goals:

1. to determine if the isotopic composition of the Tonga epidosites was similar to those described from ophiolites;
2. to determine the variation in isotopic abundances between the lithologies commonly observed in ophiolites;
3. to determine the isotopic variation within a rock type along the length of the forearc; and
4. to determine the isotopic composition of the plagiogranites.

These goals were designed to help establish a comparison between the isotopic composition of the Tonga samples with previous studies of oceanic crust and ophiolites. For example, epidosites from ophiolites are characterized by depleted oxygen isotope ratios relative to normal MORB values resulting from high temperature water-rock interaction at high water-rock ratios [*Harper et al.*, 1988; *Schiffman et al.*, 1987]. Similarly, the various lithologies commonly observed in ophiolites (basalt, diabase, and gabbro) typically show a progressive decrease in $\delta^{18}O$ ratios resulting from increasing temperature of water-rock interaction [e.g., *Früh-Green et al.*, 1996; *Gregory and Taylor*, 1981; *Harper et al.*, 1988; *Lécuyer and Reynard*, 1996; *Muehlenbachs and Clayton*, 1972a; *Muehlenbachs and Clayton*, 1972b; *Stakes*, 1991; *Stakes et al.*, 1984]. Because of this temperature effect, any deviations along the length of the forearc could indicate some spatial anomaly in alteration processes possibly related to forearc tectonics. Finally, plagiogranites are relatively rare in oceanic collections and isotopic information provides an additional constraint on their metamorphic evolution and in particular, temperature information derived from quartz and epidote mineral separates.

Transects

This chapter concentrates on the isotope variations in whole rock samples of basalt, diabase, gabbro, and peridotite from three transects along the Tonga forearc, whole rock plagiogranite samples from dredge 96, and quartz and epidote mineral separates from epidotized plagiogranites. The transects are comprised of three to five dredges each in the southern, central, and northern sections of the Tonga forearc. They were chosen to provide a range of depths and latitudes from which samples could be studied in order to explore the isotopic variations both with depth (approximating stratigraphy) and along the length of the forearc. In addition, we also sampled ten plagiogranites from dredge 96. The location of the three transects and dredge 96 are indicated on Figure 6.1.

RESULTS

Whole Rock Analyses

The $\delta^{18}O$ ratios and major element chemistry of the basalts, diabases, gabbros, peridotites, and plagiogranites are given in Appendix E. The $\delta^{18}O$ ratios for basalt range from 5.4 to 13.4‰ (9.8‰ average); diabase $\delta^{18}O$ ratios range from 5.8 to 8.9‰ (7.4‰ average); gabbro $\delta^{18}O$ ratios range from 4.7 to 8.0‰ (6.3‰ average); plagiogranite $\delta^{18}O$ ratios range from 5.5 to 10.6‰ (7.3‰ average); and two peridotites have $\delta^{18}O$ ratios of 5.8 and 4.8‰. The oxygen isotope composition of MORB is well characterized at 5.8 ± 0.3‰ [*Muehlenbachs and Clayton*, 1972a; *Muehlenbachs and Clayton*, 1972b; *Taylor*, 1968].

The oxygen isotope ratios of the mafic Tonga samples generally follow the trend basalt > diabase > gabbro (Figure 6.2). No trends are apparent between $\delta^{18}O$ and MgO, TiO_2, Al_2O_3, or P_2O_5 that might be expected if primary chemistry was controlling the isotope ratios. However, positive correlations between $\delta^{18}O$ ratios and LOI and K_2O are generally observed for all rock types (Figure 6.2). These parameters both increase during alteration at low temperatures (< 250°C) and can be used to estimate the degree of alteration.

Mineral Separates

Quartz and epidote were separated from six epidotized plagiogranites in order to calculate alteration temperatures. Two of these samples are epidosites (samples 96-1-14 and 102-4-1) and have been described previously in Chapter 4. Temperatures were calculated using the quartz-epidote oxygen isotope geothermometer of Matthews and Schliestedt [1984]. This thermometer requires a correction for the pistacite composition of epidote. Since I do not have microprobe data for all of the samples studied, I chose a value of 0.24, which represents the average pistacite composition of epidote from the plagiogranites. The $\delta^{18}O$ ratios of the quartz and epidote separates and the calculated temperatures are presented in Table 6.1.

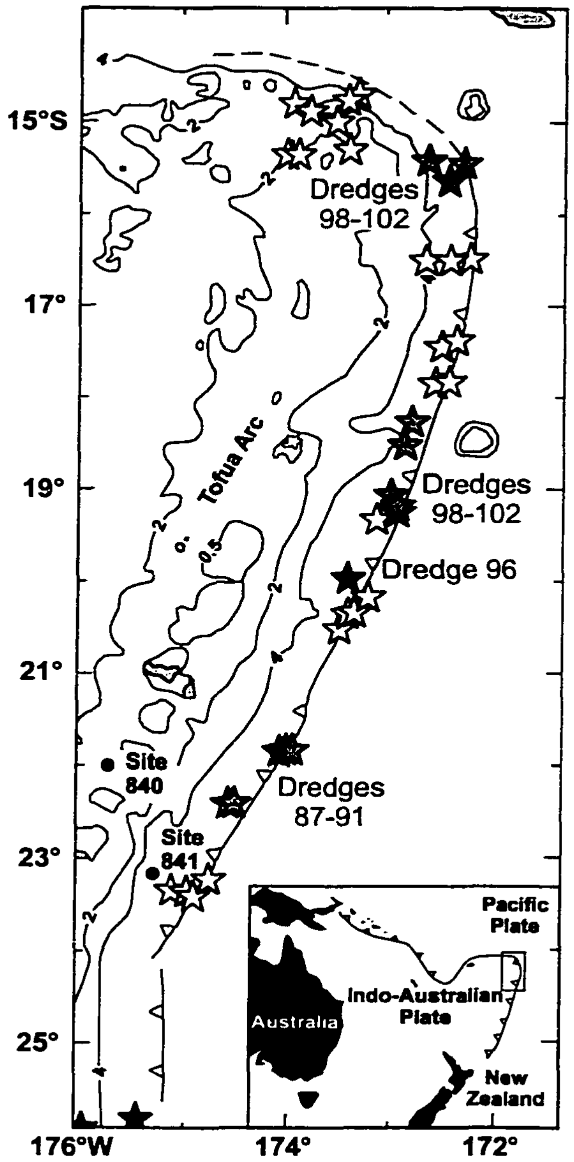

Figure 6.1 Bathymetric map showing locations of dredge sites (stars) along the Tonga forearc. Dredge sites for each of the three transects used in isotope the study are indicated by grey stars. Black star indicates the location of dredge 96. Modified from Shipboard Scientific Party [1992].

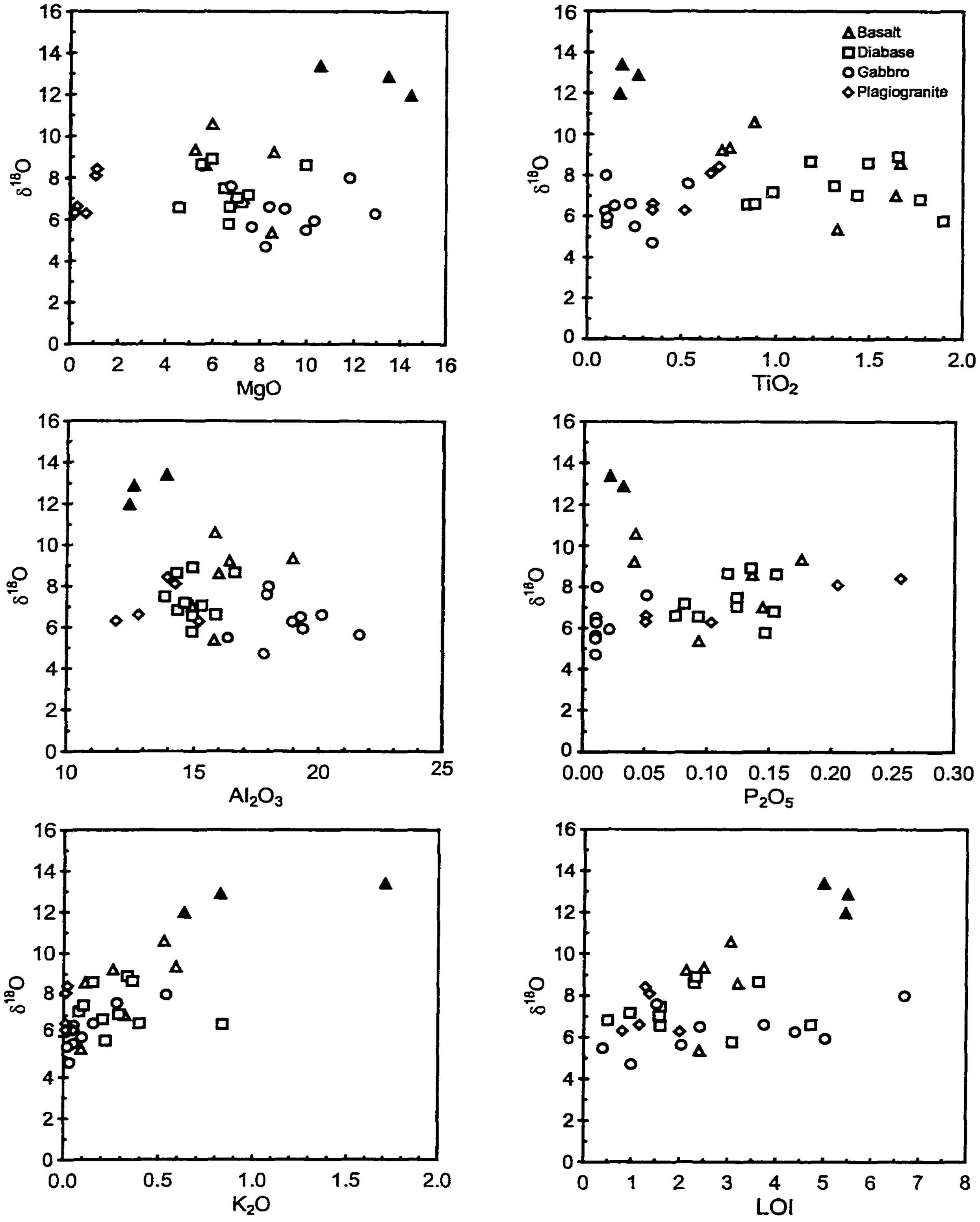

Figure 6.2 Whole rock $\delta^{18}O$ vs. major elements and LOI for Tonga basalts, diabases, gabbros, and plagiogranites. Isotope values are quoted in ‰ relative to the SMOW standard. Boninites are indicated by black triangles.

Table 6.1 Temperatures from epidote and quartz mineral separates.

Sample	$\delta^{18}O$ Quartz	$\delta^{18}O$ Epidote	$\Delta_{Qtz\text{-}Ep}$	Temp (°C)
96-1-10	+6.4	+0.0	6.4	289
96-1-14	+6.0	-0.8	6.8	272
96-1-15	+6.8	+2.0	4.8	376
96-1-30	+7.8	+1.5	6.3	294
96-1-35	+6.3	+0.0	6.3	294
102-4-1	+7.7	+0.4	7.3	253

Note: $\delta^{18}O$ values are reported in ‰ relative to the SMOW standard. Temperatures calculated assuming a mean epidote pistacite content of 0.24.

DISCUSSION

Variation between Rock Types

The variation in whole rock $\delta^{18}O$ ratios are generally typical of those described from studies of ophiolites and oceanic crust [e.g., *Früh-Green et al.*, 1996; *Harper et al.*, 1988; *Lécuyer and Reynard*, 1996; *Muehlenbachs and Clayton*, 1972a; *Muehlenbachs and Clayton*, 1972b; *Stakes*, 1991; *Stakes et al.*, 1984]. In particular, previous studies of whole-rock oxygen isotopic compositions in the Samail ophiolite have shown that pillows commonly have $\delta^{18}O$ ratios $> \sim 8‰$, dyke rocks have values between 4 and 8‰; and gabbros are typically $< \sim 6‰$, relative to fresh MORB values near 5.8‰ [*Gregory and Taylor*, 1981; *Stakes and Taylor*, 1992]. The general trend of basalt > diabase > gabbro reflects the general increase in alteration temperature as fluids are heated during deep penetration into the plutonic sequence. Basalt, diabase, and gabbro have generally similar major element chemistry (Figure 6.2). Most of the basalts are tholeiites or arc tholeiites except for three samples of boninite, which show the highest $\delta^{18}O$ ratios (see below).

The slightly enriched nature of the gabbros (with respect to fresh MORB; 5.8‰) was initially puzzling because gabbros are commonly altered at high temperatures. During water-rock interaction cold seawater loses ^{18}O to the crust, whereas hot hydrothermal fluids extract ^{18}O from the crust. Pillows, dykes, and gabbros that have interacted with high-temperature (>250°C) hydrothermal fluids become depleted in ^{18}O, resulting in $\delta^{18}O$ ratios near 4 or 5‰. Of the nine gabbros analyzed, five show enrichments above typical MORB values (Figure 6.3). As described in Chapter 3, many gabbros from Tonga contain low temperature minerals such as zeolites, carbonate, and clay indicating interaction with low temperature fluids. Plagioclase-amphibole geothermometry in these samples, however, indicate high temperatures during initial alteration. Earlier I speculated that the low temperature mineral assemblages may have formed off axis, and might be associated with tectonic unroofing (see Chapter 3). This suggestion was based on observations that low-temperature alteration in plutonic rocks is commonly associated with zones of enhanced flow due to processes of tectonic unroofing. For example, re-orientation of metamorphic veins to their original position (prior to any tectonic disruption) with enriched isotopic values in samples from Hess Deep, suggest that macroscopic chlorite ± calc-silicate veins represent a later stage of fracturing resulting from off-axis tectonism [*Früh-Green et al.*, 1996; *MacLeod and Manning*, 1996; *Manning et al.*, 1996]. It is possible the Tonga gabbro samples, which have enriched isotopic ratios, contain a low temperature metamorphic overprint. For this reason, the relatively high $\delta^{18}O$ ratios in some of the gabbros analyzed may support a late, low temperature alteration signature associated with faulting in the forearc and subsequent exposure to cold seawater, possibly resulting from trench rollback.

Boninites

Boninites are unusual mafic volcanic rocks common in subduction zone environments that are characterized by high MgO, Ni, Cr, and water contents, low TiO_2, and intermediate SiO_2. Boninites are interpreted to form from partial melting of hydrous peridotite in the mantle wedge. The latter results from interactions with hydrous fluids released from the down going slab [e.g., *Cameron et al.*, 1983; *Hickey and Frey*, 1982]. Boninites are commonly glassy and interaction with seawater results in their hydration beyond normal magmatic ratios of 1-2 wt%. If interaction with seawater occurs at low temperature (< 150°C), it is accompanied by an increase in $\delta^{18}O$ ratios to greater than +10‰ in optically fresh glass [*Kyser et al.*, 1986]. Three boninite samples from Tonga all show large $\delta^{18}O$ enrichments (Figure 6.2).

Variation Along the Forearc

One of our goals was to determine if there is any variation in the $\delta^{18}O$ ratios of individual lithologies along the length of the forearc that could be explained by tectonic variations, the starting compositions of the rocks or spatial variability in hydrothermal processes. To help answer this question we collected samples from three transects along the length of the forearc (Figure 6.1). Little difference is observed in the $\delta^{18}O$ ratios of gabbros and diabases along the length of the forearc; however, there is an apparent decrease in the $\delta^{18}O$ of the basalts from south to north (Figure 6.3). This apparent trend could result from a number of factors: 1) it could result from variation in the primary $\delta^{18}O$ ratios of the basalts from south to north; 2) it could be related to longer exposure to cold seawater in the south relative to the north; or 3) it could simply be a sampling bias. A primary control on the $\delta^{18}O$ ratios of

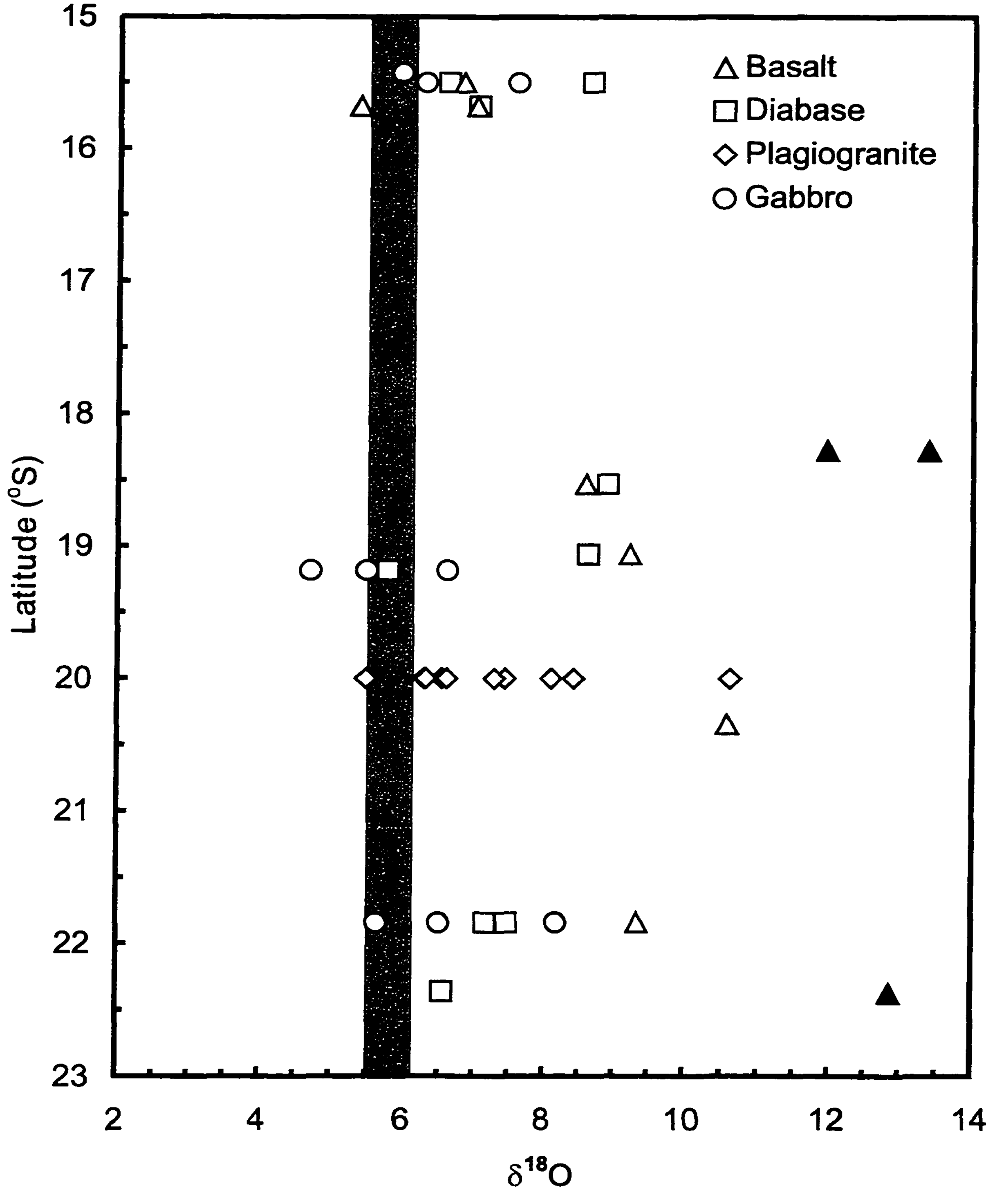

Figure 6.3 Variation of oxygen isotope values along the Tonga forearc. Values of $\delta^{18}O$ are generally similar to the range of values from mid-ocean ridges and ophiolites. The $\delta^{18}O$ values generally follow the trend basalt > diabase > gabbro. Grey field indicates range of fresh MORB $\delta^{18}O$ values (5.8 ± 0.3 ‰). Isotope values are quoted in ‰ relative to the SMOW standard. Boninites are indicated by black triangles.

the basalts does not seem likely when immobile elements are considered. For example, although there appears to be a weak negative correlation between $\delta^{18}O$ and TiO_2 (which is generally considered to be immobile under hydrothermal conditions) there does not seem to be any trend between $\delta^{18}O$ and Al_2O_3 (another immobile element; see Figure 6.2). Varying lengths of time for seawater interaction is more likely but implies a tectonic control, which may be related to the initiation of subduction in the Tonga forearc. This possibility requires an understanding of the paleogeography of the region and geometry of subduction initiation, which is beyond the scope of this thesis. Further analysis of available data on forearc initiation and crustal accretion would be an interesting future project and could potentially validate the use of isotopes to address tectonic problems. However, given the available data, we believe the simplest explanation is that the trend represents a sampling bias.

Plagiogranites

Plagiogranites are rare in collections from MORs but are commonly observed in SSZ ophiolites. The large collection from dredge 96 provides an opportunity to compare plagiogranites formed in a SSZ environment with those from MORs. The $\delta^{18}O$ ratios of the plagiogranites show a wide range of values from 5.5 to 10.6‰. Muehlenbachs and Clayton [1971] report $\delta^{18}O$ ratios for a suite of diorites dredged from the Mid-Atlantic Ridge (MAR). In their study, nine samples ranged in $\delta^{18}O$ from 5.2 to 6.9‰ [*Muehlenbachs and Clayton*, 1971]. Several of our samples contain plagioclase altered to low temperature phases such as sericite and clay. As a result, we interpret the high whole rock $\delta^{18}O$ ratios as resulting from low temperature alteration of the plagiogranites. Like the gabbros in this study, the plagiogranites show enriched $\delta^{18}O$ ratios that may have resulted from late-staged, low temperature interaction with fluids associated with tectonic uplift. Temperatures calculated from quartz and epidote mineral separates from our samples indicate alteration occurred at temperatures between 253 and 376°C, which is in good agreement with the greenschist facies mineral assemblages found in the plagiogranites. Interpretation of $\delta^{18}O$ ratios of mineral separates from the MAR diorites indicated that they had undergone varying degrees of hydrothermal alteration [*Muehlenbachs and Clayton*, 1971].

CONCLUSIONS

Whole rock oxygen isotope analyses of samples from the Tonga forearc show a similar range of values to those from studies of ocean crust and ophiolites. In particular, the $\delta^{18}O$ ratios of the samples follow the general trend basalt > diabase > gabbro that was previously identified in ophiolite studies [*Gregory and Taylor*, 1981; *Stakes and Taylor*, 1992]. In contrast to these studies, however, samples from the Tonga forearc are generally more enriched in ^{18}O. For example, gabbros from the Tonga forearc display enrichment in their $\delta^{18}O$ ratios (6.3‰ average) above normal MORB $\delta^{18}O$ ratios (5.8 ± 0.3‰). The simplest explanation for this enrichment is late interaction with cold seawater after initial high-temperature interaction with hydrothermal fluids during forearc construction. One mechanism capable of exposing the deep crust to cold seawater is normal faulting. Normal faults are quite common along the trench-facing slope of the forearc and likely resulted in tectonic unroofing during trench rollback. In this way, the isotopic signature of the gabbros may be linked to tectonic processes operating in the forearc.

Another example of the ^{18}O-enriched nature of the Tonga samples includes three samples identified as boninites based on major element chemistry. These samples have the highest $\delta^{18}O$ ratios of all samples studied (12-13.4‰). Previous study of these glassy rocks indicates they commonly display elevated $\delta^{18}O$ ratios resulting from interaction with low temperature hydrothermal fluids or seawater, which explains their high values [*Kyser et al.*, 1986].

Basalts from the Tonga forearc show an interesting northward decrease in $\delta^{18}O$ ratios. This trend could be related to the duration of exposure of the basalts to cold seawater. Alternatively it could simply be a sampling bias. If the former possibility is assumed to be true, the northward decrease in $\delta^{18}O$ ratios could be explained by northward propagation of normal faulting, and subsequent exposure to cold seawater, related to rifting in the forearc. However, the exact mechanism for this tectonic control is not known.

Temperatures calculated from epidote and quartz mineral separates from plagiogranites indicate relatively high temperature alteration conditions, however, secondary mineral assemblages and whole rock $\delta^{18}O$ ratios suggest they underwent a low temperature metamorphic overprint. These characteristics are similar to those observed in gabbros and may have resulted from similar alteration events, including late stage interaction with low temperature hydrothermal fluids or seawater during normal faulting.

Chapter 7

CONCLUSIONS

Hydrothermal circulation is a ubiquitous process operating in areas of active oceanic accretion. Hydrothermal processes affect several geological and geochemical aspects of the oceanic lithosphere such as heat flux, crustal porosity and permeability, and crustal geochemistry. Hydrothermal processes also provide a link between the lithosphere and hydrosphere geochemical reservoirs. Most of our knowledge of oceanic hydrothermal processes comes from studies of ophiolites because of their relative ease of accessibility and exposure.

This thesis provides the first comprehensive study of the metamorphic evolution of a section of modern forearc crust. Hydrothermal alteration in forearcs is of particular interest because many ophiolites are now believed to have formed in a similar suprasubduction zone (SSZ) setting. Although the exact mechanism of crustal construction in forearcs remains unresolved, ages of rocks from the Tonga forearc suggest the entire forearc region can be replaced after subduction initiation. Such a magma-rich environment would have high heat flow capable of supporting vigorous hydrothermal circulation. In addition, the volatile-rich nature of magmas in SSZ settings may have contributed fluids to the convecting hydrothermal cell and possibly influenced the extent and nature of crustal alteration.

The extensive suite of fresh and hydrothermally altered rocks dredged from trench-facing slope of the Tonga forearc is a unique collection that is used as a case study to evaluate the evolution of hydrothermal alteration in ocean crust formed in a modern SSZ setting. Recovered basalt, plagiogranite, and gabbro samples record a complex history of hydrothermal alteration resulting from interaction with seawater and possibly magmatic fluids. Geothermometry on the gabbros indicates the initial penetration of seawater into the lower crust occurred along grain boundaries and microscopic fractures at temperatures >800°C. As the plutonic sequence cooled, increased fracturing led to the pervasive replacement of primary minerals by greenschist and lower facies mineral assemblages. Overall, the alteration characteristics observed in the Tonga collection are similar to what has been described from both SSZ ophiolites and MORs. However, the relatively high degree of alteration in basalts and the presence of epidosites in the Tonga collection are most similar to alteration characteristics observed in SSZ ophiolites. Recent studies of the volcanic sequences from the Izu-Bonin and Tonga forearcs have shown that the degree of alteration in forearcs is more extensive and occurs at higher water-rock ratios than at mid-ocean ridges, and is comparable to that observed in SSZ ophiolites [*Alt et al.*, 1998; *Kelman et al.*, 1998]. Similarly, recent study of the incipient alteration of the plutonic sequence of the Semail ophiolite indicates seawater first penetrated along microfractures at high temperatures (>700°C), which is similar to what is observed in Tonga [*Manning et al.*, in press].

The association of high temperature brittle deformation and fluid flow in gabbros from Tonga is also documented for fast-spreading ridges (e.g., Hess Deep). One major difference between slow- and fast-spreading ridges is magma supply, which is higher at fast-spreading ridges. The temperatures recorded in the Tonga gabbros are slightly higher than those at fast-spreading ridges and may be related to distinctive tectonic and magmatic conditions during crustal construction in forearcs. In particular, the volatile-rich nature of forearc magmas resulting from dehydration of the down-going slab in subduction zones may lead to a high magma supply in forearcs, similar to the magma-rich nature of fast-spreading ridges. Volatile-rich magmas may also contribute to observed high water-rock ratios and play a role in the extent and nature of alteration in SSZ settings.

An interesting discovery in the Tonga collection is a suite of pervasively altered samples called epidosites. It is perhaps not surprising that the first suite of epidosites from a modern oceanic setting was recovered from a forearc setting since to date these rocks have only been described from SSZ ophiolites and not MORs. The Tonga epidosites have been shown to have formed under similar conditions to epidosites from SSZ ophiolites, further linking alteration processes in the Tonga forearc and SSZ ophiolites. Although the exact mechanism responsible for epidosite formation is not known one possibility is that the SSZ tectonic setting of forearcs and some ophiolites is an important factor.

An outstanding question in hydrothermal research has been the chemistry of fluids circulating deep within the oceanic crust. This problem has been addressed using a relatively new technique – LA-ICP-MS – that allows *in situ* analysis of trace elements in minerals. Epidote from epidosites was chosen for study because it is a secondary mineral that is believed to precipitate from hydrothermal fluids during alteration. The chemistry of hydrothermal epidote in epidosites from Tonga and the Troodos ophiolite is characterized by generally similar major element compositions but variable trace element compositions. The similarity between patterns in epidote from Tonga and Troodos suggest similar conditions were operating during formation of the epidosites, despite being separated geographically and in time. Mass balance calculations indicate that epidote controls the whole rock trace element compositions of the epidosites (e.g., REE) due to its ability to easily incorporate these elements into its crystal structure.

Replacive epidote rare earth element (REE) patterns mimic those of the whole rock, suggesting only local mobility of elements like the REE. Direct evidence from fluid inclusions as well as leaching experiments indicate fluids deep in hydrothermal systems are similar to those observed for replacive epidote from this study. It is possible that replacive epidote patterns represent an early stage of alteration during which fluid compositions were buffered by mafic phases (e.g., clinopyroxene) and minor plagioclase. Void filling epidote precipitation may have followed as alteration progressed and plagioclase dissolution increased, producing the observed positive Eu anomalies in void filling epidote patterns. Progressive change in fluid compositions related to mineral dissolution may explain the differences between void filling and replacive epidote patterns. This is particularly significant because fluid chemistry in the deep portion of hydrothermal systems is of great interest to those studying MOR hydrothermal processes and yet direct sampling of these fluids is not possible with current technology.

Another important aspect of the epidote study was to assess the relative roles of epidote crystal chemistry versus fluid compositions on epidote REE contents. Application of the model of Blundy and Wood [1994] to REE partitioning in epidote indicates La should partition preferentially into epidote followed by the other REE in order of decreasing atomic radius, resulting in a La/Lu ratio greater than 300. In contrast, our measured epidote REE concentrations are characterized by La/Lu values less than 10. This difference suggests that epidote REE abundances are not solely controlled by crystal chemistry and that fluid compositions may also play a role.

Whole rock oxygen isotope analyses of samples from the Tonga forearc support the generally similar nature of alteration in the Tonga forearc to that observed in ocean crust and ophiolites. Oxygen isotope ratios follow the general trend of basalt > diabase > gabbro, which can be simply attributed to increasing alteration temperature. Gabbros from the Tonga forearc display enrichment in their $\delta^{18}O$ that is likely related to late-stage interaction with low temperature fluids, possibly during faulting associated with tectonic unroofing. Basalts in this study show an interesting northward decrease in $\delta^{18}O$ ratios that could be related to the duration of exposure to cold seawater or may be a sampling bias; however, this remains unresolved. Similarly, temperatures calculated from epidote and quartz mineral separates from plagiogranites indicate relatively high temperature alteration conditions, however, secondary mineral assemblages and whole rock $\delta^{18}O$ ratios suggest low temperature alteration. These contradictory characteristics may also have resulted from late stage interaction with low temperature fluids long after initial high temperature hydrothermal circulation.

This thesis provides a framework with which future studies of alteration in forearcs can be compared. Samples of basalt, plagiogranite, and gabbro from the Tonga forearc record the time integrated effects of hydrothermal fluid flow, including initial penetration of seawater, pervasive replacement of primary phases at high temperatures, gradual cooling and sealing of fractures, and late overprinting by low temperature fluids. Overall, alteration in the Tonga forearc is generally similar to that observed at MORs and SSZ ophiolites. However, the presence of high temperature brittle deformation is more similar to fast-spreading ridges and SSZ ophiolites. Differences between alteration in the Tonga forearc and MORs include the high degree of alteration in volcanic rocks and the presence of epidosites, which may be related to the volatile-rich nature of magmas produced in SSZ tectonic settings. High volatile contents in magmas could increase the water-rock ratio during alteration, resulting in more pervasive alteration, and possibly the generation of epidosites. For these reasons I believe alteration in forearcs is more similar to SSZ ophiolites than MORs and that tectonic setting plays a role in some hydrothermal processes. Finally, development of the use of the trace element chemistry of a variety of secondary minerals will contribute to a better understanding of how fluid compositions evolve deep within hydrothermal systems.

REFERENCES CITED

Aldiss, D.T., Plagiogranites from the ocean crust and ophiolites, *Nature*, *289*, 577-578, 1981.

Alt, J.C., Subseafloor processes in mid-ocean ridge hydrothermal systems, in *Seafloor hydrothermal systems: physical, chemical, biological, and geological interactions*, edited by S.E. Humphris, R.A. Zierenberg, L.S. Mullineaux, and R.E. Thomson, pp. 85-114, American Geophysical Union, Washington, 1995.

Alt, J.C., T.F. Anderson, and L. Bonnell, The geochemistry of sulfur in a 1.3 km section of hydrothermally altered oceanic crust, DSDP Hole 504B, *Geochim. Cosmochim. Acta*, 53, 1011-1023, 1989.

Alt, J.C., H. Kinoshita, L.B. Stokking, and others, *Proc. ODP, Initial Reports*, Ocean Drilling Program, College Station, TX, 1993.

Alt, J.C., E. Zuleger, and J. Erzinger, Mineralogy, chemistry and stable isotope compositions of hydrothermally altered altered sheeted dikes: ODP Hole 504B, in *Proc. ODP, Sci. Results*, edited by J. Erzinger, K. Becker, H.J.B. Dick, and L.B. Stokking, pp. 155-166, Ocean Drilling Program, College Station, TX, 1995.

Alt, J.C., C. Laverne, D.A. Vanko, P. Tartarotti, D.A.H. Teagle, W. Bach, E. Zuleger, J. Erzinger, J. Honnorez, P.A. Pezard, K. Becker, M.H. Salisbury, and R.H. Wilkens, Hydrothermal alteration of a section of upper oceanic crust in the eastern equatorial Pacific: a synthesis of resutls from Site 504 (DSDP Legs 69, 70, and 83, and ODP Legs 111, 137, 140, and148), in *Proc. ODP, Sci. Results*, edited by J.C. Alt, H. Kinoshita, L.B. Stokking, and P.J. Michael, pp. 417-434, Ocean Drilling Program, College Station, TX, 1996.

Alt, J.C., D.A.H. Teagle, T. Brewer, W.C. Shanks III, and A. Halliday, Alteration and mineralization of an oceanic forearc and the ophiolite-ocean crust analogy, *J. Geophys. Res.*, *103* (B6), 12,365-12,380, 1998.

Anders, E., and N. Grevesse, Abundances of the elements: meteoritic and solar, *Geochim. Cosmochim. Acta*, 53, 197-214, 1989.

Aumento, F., Reports: Diorites from the Mid-Atlantic Ridge at 45°N, *Science*, *165*, 1112-1113, 1969.

Ayers, J.C., and E.B. Watson, Apatite / fluid partitioning of rare-earth elements and strontium: Experimental results at 1.0 GPa and 1000°C and application to models of fluid-rock interaction, *Chem. Geol.*, *110*, 299-314, 1993.

Bach, W., J. Erzinger, J.C. Alt, and D.A.H. Teagle, Chemistry of the lower sheeted dike complex hole 504B (leg 148): influence of magmatic differentiation and hydrothermal alteration, in *Proc. ODP, Sci. Results*, edited by J.C. Alt, H. Kinoshita, L.B. Stokking, and P.J. Michael, pp. 39-55, Ocean Drilling Program, College Station, TX, 1996.

Bach, W., and W. Irber, Rare earth element mobility in the oceanic lower sheeted dyke complex: evidence from geochemical data and leaching experiments, *Chem. Geol.*, *151*, 309-326, 1998.

Bailey, S.W., Chlorites; structures and crystal chemistry, in *Hydrous Phyllosilicates*, edited by S. W. Bailey, pp. 347-403, Min. Soc. Am. Rev. Mineral., 1988.

Banerjee, N.R., K.M. Gillis, and K. Muehlenbachs, Discovery of epidosites in a modern oceanic setting, the Tonga forearc, *Geology*, *28*, 151-154, 2000.

Banks, D.A., B.W.D. Yardley, A.R. Campbell, and K.E. Jarvis, REE composition of an aqueous magmatic fluid: A fluid inclusion study from the Capitan Pluton, New Mexico, U.S.A., *Chem. Geol.*, *113*, 259-272, 1994.

Bau, M., Controls on the fractionation of isovalent trace elements in magmatic and aqueous systems: evidence from Y/Ho, Zr/Hf, and lanthanide tetrad effect, *Contrib. Mineral. Petrol.*, *123*, 323-333, 1996.

Bednarz, U., and H.U. Schmincke, Chemical patterns of seawater and hydrothermal alteration in the northeastern Troodos extrusive series and sheeted dyke complex (Cyprus), in *Ophiolites and Oceanic Lithosphere - Troodos*, edited by J. Malpas, A. Panayiotou, E. Moores, and C. Xenophontos, pp. 639-653, Cyprus Geological Survey, 1987.

Bednarz, U., and H.U. Schmincke, Mass transfer during sub-seafloor alteration of the upper Troodos crust (Cyprus), *Contrib. Mineral. Petrol.*, *102*, 93-101, 1989.

Berndt, M.E., W.E. Seyfried, Jr., and D.R. Janecky, Plagioclase and epidote buffering of cation ratios in mid-ocean ridge hydrothermal fluids: Experimental results in and near the supercritical region, *Geochim. Cosmochim. Acta*, *53*, 2283-2300, 1989.

Bettison, L.A., and P. Schiffman, Composition and structural variations of phyllosilicates from the Point Sal ophiolite, California, *Amer. Mineral.*, *73*, 186-226, 1988.

Bettison-Varga, L., P. Schiffman, and D.R. Janecky, Fluid-rock interaction in the hydrothermal upflow zone of the Solea graben, Troodos ophiolite, Cyprus, in *Low-Grade Metamorphism of Mafic Rocks*, edited by P. Schiffman, and H.W. Day, pp. 101-122, Geological Society of America, Boulder, 1995.

Bettison-Varga, L., R.J. Varga, and P. Schiffman, Relation between ore-forming hydrothermal systems and extensional deformation in the Solea graben spreading center, Troodos ophiolite, Cyprus, *Geology*, *20*, 987-990, 1992.

Bevis, M., F.W. Taylor, B.E. Schutz, J. Recy, B.L. Isacks, H. Saimone, S. Rajendra, E. Kendrick, J. Stowell, B. Taylor, and S. Calmant, Geodetic observations of very rapid convergence and back-arc extension at the Tonga arc, *Nature*, *374*, 249-251, 1995.

Bickle, M.J., and D.A.H. Teagle, Strontium alteration in the Troodos ophiolite: implications for fluid fluxes and geochemical transport in mid-ocean ridge hydrothermal systems, *Earth Planet. Sci. Lett.*, *113*, 219-237, 1992.

Bird, D.K., P. Schiffman, W.A. Elders, A.E. Williams, and S.D. McDowell, Calc-silicate mineralization in active geothermal systems, *Econ. Geol.*, *79*, 671-695, 1984.

Bischoff, J.L., and W.E. Seyfried, Hydrothermal chemistry of seawater from 25° to 350°C, *Am. J. Sci.*, *378*, 838-860, 1978.

Bloomer, S.H., T. Falloon, H. Petcovic, R.L. Nielsen, and R.A. Duncan, Petrology and geochemistry of volcanic and plutonic rocks from the Tonga Forearc, southwest Pacific, in *AGU 1998 fall meeting.*, pp. F420, American Geophysical Union, San Francisco, 1998.

Bloomer, S.H., B. Taylor, C.J. MacLeod, R.J. Stern, P. Fryer, J.W. Hawkins, and L. Johnson, Early arc volcanism and the ophiolite problem: A perspective from drilling in the western Pacific, in *Active Margins and Marginal Basins of the Western Pacific*, edited by B. Taylor, and J.H. Natland, pp. 1-30, American Geophysical Union, Washington, D.C., 1995.

Bloomer, S.H., D. Wright, C.J. MacLeod, D. Tappin, P. Clift, T. Falloon, R.L. Fisher, K. Gillis, T. Ishii, M. Kelman, K. Mafi, H. Sato, and M. Winowitch, Geology of the Tonga Forearc: A supra-subduction zone ophiolite, in *AGU 1996 fall meeting.*, pp. F325, American Geophysical Union, San Francisco, 1996.

Blundy, J., and B. Wood, Prediction of crystal-melt partition coefficients from elastic moduli, *Nature*, *372*, 452-454, 1994.

Bonazzi, P., and S. Menchetti, Monoclinc members of the epidote group: effects of the Al<-->Fe^{3+}<-->Fe^{2+} substitution and of the entry of REE^{3+}, *Mineral. Petrol.*, *53*, 133-153, 1995.

Brabander, D.J., and B.J. Giletti, Strontium diffusion kinetics in amphiboles and significance to thermal history determinations, *Geochim. Cosmochim. Acta*, *59*, 2223-2238, 1995.

Brooks, C.K., P. Henderson, and J.G. Ronsbo, Rare-earth partition between allanite and glass in athe obsidian of Sandy Braes, Northern Ireland, *Min. Mag.*, *44*, 157-160, 1981.

Brown, P.E., and S.G. Haegemann, MacFlinCor and its application to fluids in Archean lode-gold deposits, *Geochim. Cosmochim. Acta*, *59* (19), 3943-3952, 1995.

Brown, P.E., and W.M. Lamb, P-V-T properties of fluids in the system $H_2O \pm CO_2 \pm NaCl$: New graphical presentations and implications for fluid inclusions studies, *Geochim. Cosmochim. Acta*, *53*, 1209-1221, 1989.

Cameron, W.E., M.T. McCulloch, and D.A. Walker, Boninite petrogenesis: chemical and Nd-Sr isotopic constraints, *Earth and Planet. Sci. Lett.*, *65*, 75-89, 1983.

Campbell, A.C., M.R. Palmer, G.P. Klinkhammer, T.S. Bowers, J.M. Edmond, J.R. Lawrence, J.F. Casey, G. Thompson, S. Humphris, P. Rona, and J.A. Karson, Chemistry of hot springs on the Mid-Atlantic Ridge, *Nature*, *335*, 514-519, 1988.

Cannat, M., C. Mével, and D. Stakes, Stretching of the deep crust at the slow-spreading Southwest Indian Ridge, *Tectonophysics*, *190*, 73-94, 1991.

Cantrell, K.J., and R.H. Byrne, Rare earth element complexation by carbonate and oxalate ions, *Geochim. Cosmochim. Acta*, *51*, 587-605, 1987.

Carbotte, S., C. Mutter, J. Mutter, M. Spiegelman, G. Correa, M. McNutt, V. Bhat, and R. Cruz-Orozco, Influence of spreading rate and magma supply on crustal magma bodies: Results from a recent seismic ctudy of the shallow East Pacific Rize north of the Orozco Transform Fault, *RIDGE Events*, *7* (1), 1-4, 1996.

Carcangiu, G., M. Palomba, and M. Tamanini, REE-bearing minerals in the albitites of Central Sardinia, Italy, *Min. Mag.*, *61*, 271-283, 1997.

Chen, Z., Inter-element fractionation and correction in laser ablation inductively coupled plasma mass spectrometry, *J. Anal. At. Spectrom.*, *14*, 1823-1828, 1999.

Clayton, R.N., and T.K. Mayeda, The use of bromine pentafluoride in the extraction of oxygen from oxides and silicates for isotopic analysis, *Geochim. Cosmochim. Acta*, *27*, 43-52, 1963.

Clift, P.D., C.J. MacLeod, D.R. Tappin, D.J. Wright, and S.H. Bloomer, Tectonic controls on sedimentation and diagenesis in the Tonga Trench and forearc, southwest Pacific, *Geol. Soc. Am. Bull.*, *110* (4), 483, 1998.

Cline, J.S., and R.J. Bodnar, Can economic porphyry copper mineralization be generated by a typical calc-alkaline melt?, *J. Geophys. Res.*, *96*, 8113-8126, 1991.

Comodi, P., and P.F. Zanazzi, The pressure behavior of clinozoisite and zoisite: An x-ray diffraction study, *Amer. Mineral.*, *82*, 61-68, 1997.

Converse, D.R., H.D. Holland, and J.M. Edmond, Flow rates in the axial hot springs of the East Pacific Rise (21°N): implications for the heat budget and the formation of massive sulfide deposits, *Earth Planet. Sci. Lett.*, *69*, 159-175, 1984.

Cowan, J., and J. Cann, Supercritical two-phase separation of hydrothermal fluids in the Troodos ophiolite, *Nature*, *333*, 259-261, 1988.

Craig, H. and J.E. Lupton, Helium-3 and mantle volatiles in the ocean and the oceanic crust, in *The Sea, v.7, The Oceanic Lithosphere*, edited by C.E. Emiliani, pp. 391-428, J. Wiley, New York, 1981.

Craig, H., J.A. Welhan, K.R. Kim, R. Poreda, and J.E. Lupton, Geochemical studies of the 21°N EPR hydrothermal fluids, *EOS, Trans. AGU*, 61, 992, 1981.

Deer, W.A., R.A. Howie, and J. Zussman, *An introduction to the rock-forming minerals*, 696 pp., Longman Scientific & Technical, New York, NY, 1992.

Delaney, J.R., D.W. Mogk, and M.J. Mottl, Quartz-cemented breccias from the mid-Atlantic ridge: samples of a high-salinity hydrothermal upflow zone, *J. Geophys. Res.*, *92*, 9174-9192, 1987.

Detrick, R.S., P. Buhl, E. Vera, J. Mutter, J. Orcutt, J. Madsen, and T. Brocher, Multichannel seismic imaging of a crustal magma chamber along the East Pacific Rise, *Nature*, *326*, 35-41, 1987.

Dick, H.J.B., P.S. Meyer, S. Bloomer, S. Kirby, D. Stakes, and C. Mawer, Lithostratigraphic evolution of an in-situ section of oceanic layer 3, in *Proc. ODP, Sci. Results*, pp. 439-471, ODP, 1991.

Dollase, W.A., Refinement of the crystal structures of epidote, allanite and hancockite, *Amer. Mineral.*, *56*, 447-464, 1971.

Edmond, J.M., C. Measures, B. Mangum, B. Grant, F.R. Sclater, R. Collier, and A. Hudson, On the formation of metal-rich deposits at Ridge crests, *Earth Planet. Sci. Lett.*, *46*, 19-30, 1979.

Elderfield, H., and M.J. Greaves, The rare earth elements in seawater, *Nature*, *296*, 214-219, 1982.

Enami, M., and S. Banno, Major rock-forming minerals in UHP metamorphic rocks, *International Geology Review*, *41*, 1058-1066, 1999.

Evans, B., J.T. Frederich, and T.-F. Wong, The brittle-ductile transition in rocks: recent experimental and theoretical progress, in *The Brittle Ductile Transition in Rocks*, edited by A.G. Duba, W.B. Durham, J.W. Handin, and H.F. Wang, pp. 1-20, American Geophysical Union, Washington, 1990.

Falloon, T.J., D.H. Green, and A.J. Crawford, Dredged igneous rocks from the northern termination of the Tofua magmatic arc, Tonga and adjacent Lau Basin, *Aust. J. Earth Sci.*, *34*, 487-506, 1987.

Fisher, A.T., Permeability within Basaltic Oceanic Crust, *Reviews of Geophysics*, *36* (2), 143-182, 1998.

Fox, P.J., E. Schreiber, H. Rowlett, and K. McCamy, The geology of the Oceanographer Fracture Zone: A model for fracture zones, *J. Geophys. Res.*, *81*, 4117-4128, 1976.

Früh-Green, G.L., A. Plas, and L.N. Dell'Angelo, Mineralogic and stable isotope record of polyphase alteration of upper crustal gabbros of the East Pacific Rise (Hess Deep, Site 894), in *Proc. ODP, Sci. Results*, *147*, edited by C. Mével, K.M. Gillis, J. Allen, and P. Meyer, Ocean Drilling Program, College Station, TX, 1996.

Fryer, P., J.A. Pearce, L.B. Stokking, and others, Summary of results from Leg 125, in *Proc. ODP, Initial Reports*, edited by P. Fryer, J.A. Pearce, L.B. Stokking, and a. others, pp. 367-380, Ocean Drilling Project, College Station, 1990.

Gass, I.G., Is the Troodos massif of Cyprus a fragment of Mesozoic ocean floor?, *Nature*, *220*, 39-42, 1968.

Gass, I.G., and J.D. Smewing, Intrusion, extrusion and metamorphism at constructive margins: Evidence from the Troodos Massif, Cyprus, *Nature*, *242*, 26-29, 1973.

Ghazi, A.M., D.A. Vanko, E. Roedder, and R.C. Seeley, Determination of rare earth elements in fluid inclusions by inductively coupled plasma-mass spectrometry (ICP-MS), *Geochim. Cosmochim. Acta*, *57*, 4513-4516, 1993.

Gieré, R., Formation of rare earth mineral in hydrothermal systems, in *Rare Earth Minerals: Chemistry, origin and ore deposits*, edited by F.W. Adrien P. Jones, and C. Terry Williams, pp. 105-150, Chapman & Hall, 1996.

Gill, J., *Orogenic Andesites and Plate Tectonics*, 390 pp., Springer-Verlag, New York, 1981.

Gillis, K., An ancient hydrothermal root-zone exposed along the sheeted dyke-plutonic transition in the Troodos ophiolite, Cyprus, in *Geol. Assoc. Can. Prog. Abstr.*, pp. A-54, Ottawa, 1997.

Gillis, K., J. Karson, E. Klein, S. Hurst, and H.D.S. Party, Hydrothermal alteration patterns in young EPR crust, in *AGU 1999 fall meeting*, pp. F985, American Geophysical Union, San Francisco, 1999.

Gillis, K.M., Controls on hydrothermal alteration in a section of fast-spreading oceanic crust, *Earth Planet. Sci. Lett.*, *134*, 473-489, 1995.

Gillis, K.M., Rare earth element constraints on the origin of amphibole in gabbroic rocks from Site 894, Hess Deep, in *Proc. ODP, Sci. Results*, edited by C. Mével, K.M. Gillis, J. Allen, and P. Meyer, pp. 59-75, Ocean Drilling Program, College Station, TX, 1996.

Gillis, K.M., and N.R. Banerjee, Hydrothermal Alteration Patterns in Supra-Subduction Zone Ophiolites, in *Ophiolites and Ocean Crust: New insights from field studies and the ocean drilling program*, edited by Y. Dilek, and E. Moores, Geological Society of America Special Publication, in press.

Gillis, K.M., J.N. Ludden, and A.D. Smith, Mobilization of REE during crustal aging in the Troodos Ophiolite, *Chem. Geol.*, *98*, 71-86, 1992.

Gillis, K.M., and M. Roberts, Cracking at the magma-hydrothermal transition: evidence from the Troodos ophiolite, *Earth Planet. Sci. Lett.*, *169*, 227-244, 1999.

Gillis, K.M., and P.T. Robinson, Low-temperature alteration of the extrusive sequence, Troodos ophiolite, Cyprus, *Can. Mineral.*, *23*, 431-441, 1985.

Gillis, K.M., and P.T. Robinson, Distribution of alteration zones in the upper oceanic crust, *Geology*, *16*, 262-266, 1988.

Gillis, K.M., and P.T. Robinson, Multistage alteration in the extrusive sequence of the Troodos ophiolite, Cyprus, in *Ophiolites - oceanic crustal analogues*, edited by J. Malpas, E.M. Moores, A. Panayiotou, and C. Xenophontos, pp. 655-664, The Gological Survey Department, Nicosia, 1990.

Gillis, K.M., and K. Sapp, Distribution of porosity in a section of upper oceanic crust exposed in the Troodos Ophiolite, *J. Geophys. Res.*, *102* (B5), 10133-10149, 1997.

Gillis, K.M., and G. Thompson, Metabasalts from the Mid-Atlantic ridge: new insights into hydrothermal systems in slow-spreading crust, *Contrib. Mineral. Petrol.*, *113*, 502-523, 1993.

Gillis, K.M., G. Thompson, and D.S. Kelley, A view of the lower crustal component of hydrothermal systems at the Mid-Atlantic ridge, *J. Geophys. Res.*, *98* (B11), 19597-19619, 1993.

Green, T.H., and N.J. Pearson, Effect of pressure on rare earth element partition coefficients in common magmas, *Nature*, *305*, 414-416, 1983.

Haas, J.R., E.L. Shock, and D.C. Sassani, Rare earth elements in hydrothermal systems: Estimates of standard partial molal thermodynamic properties of aqueous complexes of the rare earth elements at high pressures and temperatures, *Geochim. Cosmochim. Acta*, *59* (21), 4329-4350, 1995.

Hannington, M.D., I.R. Jonasson, P.M. Herzig, and S. Petersen, Physical and chemical processes of seafloor mineralization at mid-ocean ridges, in *Seafloor hydrothermal systems: physical, chemical, biological, and geological interactions*, edited by S.E. Humphris, R.A. Zierenberg, L.S. Mullineaux, and R.E. Thomson, pp. 115-157, American Geophysical Union, Washington, 1995.

Harper, G.D., J.R. Bowman, and R. Kuhns, A field, chemical, and stable isotope study of subseafloor metamorphism of the Josephine ophiolite, California-Oregon, *J. Geophys. Res.*, *93*, 4625-4656, 1988.

Haymon, R.M., R.A. Koski, and M.J. Abrams, Hydrothermal discharge zones beneath massive sulfide deposits mapped in the Oman ophiolite, *Geology*, *17*, 531-535, 1989.

Hazen, R.M., and L.W. Finger, Bulk modulus-volume relationship for cation-anion polyhedra, *J. Geophys. Res.*, *84* (B12), 6723-6728, 1979.

Hickey, R.L., and F.A. Frey, Geochemical characteristics of boninite series volcanics: implications for their source, *Geochim. Cosmochim. Acta*, *46*, 2099-2155, 1982.

Hickmott, D.D., S.S. Sorensen, and P.S.Z. Rogers, Metasomatism in a subduction complex: Constraints from microanalysis for trace elements in minerals from garnet amphibolite from the Catalina Schist, *Geology*, *20*, 347-350, 1992.

Hirth, G., J. Escartin, and J. Lin, The Rheology of the Lower Oceanic Crust: Implications for Lithospheric Deformation at Mid-Ocean Ridges, in *Faulting and Magmatism at Mid-Ocean Ridges*, edited by W.R. Buck, P.T. Delaney, J.A. Karson, and Y. Lagabrielle, pp. 291-303, American Geological Union, Washington, D.C., 1998.

Holland, T., and J. Blundy, Non-ideal interactions in calcic amphiboles and their bearing on amphibole-plagioclase thermometry, *Contrib. Mineral. Petrol.*, *116*, 433-447, 1994.

Holland, T.J.B., S.A.T. Redfern, and A.R. Pawley, Volume behavior of hydrous minerals at high pressure and temperature: II. Compressibilities of lawsonite, zoisite, clinozoisite, and epidote, *Amer. Mineral.*, *81*, 341-348, 1996.

Humphris, S.E., Hydrothermal processes at mid-ocean ridges, *Rev. Geophys.*, *Supplement, July 1995*, 71-80, 1995.

Ito, E., and A.T. Anderson, Jr., Submarine metamorphism of gabbros from the Mid-Cayman Rise: petrographic and mineralogic constraints on hydrothermal processes at slow-speading ridges, *Contrib. Mineral. Petrol.*, *82*, 371-388, 1983.

Jacobson, R.S., Impact of crustal evolution on changes of the seismic properties of the uppermost ocean crust, *Rev. Geophys.*, *30*, 27-46, 1992.

Jehl, V., B. Poty, and A. Weisbrod, Hydrothermal metamorphism of the oceanic crust in the North Atlantic Ocean, *Bull. Geol. Soc. France*, *6*, 1213-1221, 1977.

Jenner, G.A., H.P. Longerich, S.E. Jackson, and B.J. Freyer, ICP-MS - A powerful tool for high-precision trace-element analysis in earth sciences: Evidence from analysis of selected U.S.G.S. reference samples., *Chem. Geol.*, *83*, 133-148, 1990.

Kay, R.W., and R.G. Senechal, The rare earth geochemistry of the Troodos ophiolite complex, *J. Geophys. Res.*, *81* (5), 964-970, 1976.

Kelley, D.S., Methane-rich fluids in the oceanic crust, *J. Geophys. Res.*, *101* (B2), 2943-2962, 1996.

Kelley, D.S., Fluid evolution in slow-spreading environments, in *Proc. ODP, Sci. Results*, edited by J.A. Karson, M. Cannat, D.J. Miller, and D. Elthon, pp. 399-415, Ocean Drilling Program, College Station, TX, 1997.

Kelley, D.S., and P.T. Robinson, Development of a brine-dominated hydrothermal system at temperatures of 400-500°C in the upper level plutonic sequence, Troodos ophiolite, Cyprus, *Geochim. Cosmochim. Acta*, *54* (3), 653-661, 1990.

Kelley, D.S., K.M. Gillis, and G. Thompson, Fluid evolution in submarine magma-hydrothermal systems at the Mid-Atlantic Ridge, *J. Geophys. Res.*, 98, 19,579-15,596, 1993.

Kelley, D.S., P.T. Robinson, and J.G. Malpas, Processes of brine generation and circulation in the oceanic crust: fluid inclusion evidence from the Troodos ophiolite, Cyprus, *J. Geophys. Res.*, *97* (B6), 9307-9322, 1992.

Kelman, M., Hydrothermal alteration of a supra-subduction zone ophiolite analog, Tonga, southwest Pacific, Masters thesis, Oregon State University, Corvallis, 1998.

Kelman, M., S. Bloomer, T. Falloon, and K. Gillis, Hydrothermal alteration of a forearc ophiolite, Tonga, Southwest Pacific, in *AGU 1996 fall meeting*, pp. F807, American Geophysical Union, San Francisco, 1997.

Kelman, M., S. Bloomer, K. Gillis, and T. Falloon, Hydrothermal alteration of a supra-subduction zone ophiolite analog, Tonga, southwest Pacific, in *AGU 1998 fall meeting*, pp. F968, American Geophysical Union, San Francisco, 1998.

Klinkhammer, G.P., H. Elderfield, J.M. Edmond, and A. Mitra, Geochemical implications of rare earth element patterns in hydrothermal fluids from mid-ocean ridges, *Geochim. Cosmochim. Acta*, *58* (23), 5105-5113, 1994.

Kristmannsdottir, H., Hydrothermal alteration of basaltic rocks in Iceland geothermal areas, in *2nd United Nations Symposium on the development and use of geothermal resources May 20-29*, edited by Unknown, pp. 441-445, San Francisco, CA, 1975.

Kyser, T.K., W.E. Cameron, and E.G. Nisbet, Boninite petrogenesis and alteration history: constraints from stable isotope compositions of boninites from Cape Vogel, New Caledonia and Cyprus, *Contrib. Mineral. Petrol.*, *93*, 222-226, 1986.

Laverne, C., D.A. Vanko, P. Tartarotti, and J.C. Alt, Chemistry and geothermometry of secondary minerals from the deep sheeted dike complex, DSDP/ODP Hole 504B, in *Proc. ODP, Sci. Results*, edited by J. Erzinger, K. Becker, H.J.B. Dick, and L.B. Stokking, Ocean Drilling Program, College Station, TX, 1995.

Lécuyer, C., and B. Reynard, High-temperature alteration of oceanic gabbros by seawater (Hess Deep, Ocean Drilling Program Leg 147): evidence from oxygen isotopes and elemental fluxes, *J. Geophys. Res.*, *101* (B7), 15-883-15897, 1996.

Liou, J.G., S. Kuniyoshi, and K. Ito, Experimental studies of the phase relations between greenschist and amphiobolite in a basaltic system, *Am J. Sci.*, *274*, 613-632, 1974.

Liu, M., and R.A. Yund, NaSi-CaAl interdiffusion in plagioclase, *Am. Mineral.*, *77*, 275-283, 1992.

Longerich, H.P., G.A. Jenner, B.J. Freyer, and S.E. Jackson, Inductively coupled plasma-mass spectometric analysis of geological samples: A critical evaluation based on case studies, *Chem. Geol.*, *83*, 105-118, 1990.

Mackwell, S.J., M.E. Zimmerman, and D.L. Kohlstedt, High-temperature deformation of dry diabase with application to tectonics on Venus, *J. Geophys. Res.*, *103* (B1), 975-984, 1998.

Mackwell, S.J., M.E. Zimmerman, D.L. Kohlstedt, and D.S. Scherber, Dry deformation of diabase: implications for the tectonics on Venus, in *Lunar and Planetary Sciences*, pp. 817-818, 1994.

MacLeod, C.J., B. Célérier, G.L. Früh-Green, and C.E. Manning, Tectonics of Hess Deep: A synthesis of drilling results from Leg 147, in *Proc. ODP, Sci. Results*, edited by C. Mével, Gillis, K.M., P. Meyer, and e. al., pp. 461-474, Ocean Drilling Program, College Station, TX, 1996.

MacLeod, C.J., and C.E. Maning, Influence of axial segmentation on hydrothermal circulation at fast-spreading ridges: insights from Hess Deep, in *Tectonic, Magmatic, Hydrothermal and Biological Segmentation of Mid-Ocean Ridges*, pp. 185-198, Geological Society Special Publication, 1996.

Mahood, G., and W. Hildreth, Large partition coefficients for trace elements in high-silica rhyolites, *Geochim. Cosmochim. Acta*, *47*, 11-30, 1983.

Manning, C.E., and D.K. Bird, Hydrothermal clinopyroxenes of the Skaergaard intrusion, *Contrib. Mineral. Petrol.*, *92*, 437-447, 1986.

Manning, C. E., and C. J. MacLeod, Fracture-controlled metamorphism of Hess Deep gabbros, Site 894: constraints on the roots of mid-ocean ridge hydrothermal systems at fast-spreading centers, *Proc. Ocean Drill. Program Sci. Results*, *147*, 189-211, 1996.

Manning, C.E., C.J. MacLeod, and P.E. Weston, Lower-crustal cracking front at fast-spreading ridges: evidence from the East Pacific Rise and Oman ophiolite, in *Ophiolites and Ocean Crust: New insights from field studies and the ocean drilling program*, edited by Y. Dilek, and E. Moores, Geological Society of America Special Publication, in press.

Manning, C.E., P.E. Weston, and K. Mahon, Rapid high-temperature metamorphism of East Pacific Rise gabbros from Hess Deep, *Earth Planet. Sci. Lett.*, *144*, 123-132, 1996.

Matsuhisa, Y., J.R. Goldsmith, and R.N. Clayton, Oxygen isotopic fractionation in the system quartz-albite-anorthite-water, *Geochim. Cosmochim. Acta*, *43*, 1131-1140, 1979.

Matthews, A., and M. Schliestedt, Evolution of the blueschist and greenschist facies rocks of Sifnos, Cyclades, Greece, *Contrib. Mineral. Petrol.*, *88*, 150-163, 1984.

McCollom, T.M., and E.L. Shock, Fluid-rock interactions in the lower ocenic crust: Thermodynamic models of hydrothermal alteration, *J. Geophys. Res.*, *103*, 547-575, 1998.

Mével, C., Metamorphism in oceanic layer 3, Gorringe Bank, Eastern Atlantic, *Contrib. Mineral. Petrol.*, *100*, 496-509, 1988.

Mével, C., and M. Cannat, Lithospheric stretching and hydrothermal processes in oceanic gabbros from slow-spreading ridges, in *Ophiolite genesis and evolution of the oceanic lithosphere*, edited by T. Peters, A. Nicolas, and R.G. Coleman, pp. 293-312, Ministry of Petroleum and Mineral Resources, Sultanate of Oman, Muscat, Oman, 1991.

Michard, A., Rare earth element systematics in hydrothermal fluids, *Geochim. Cosmochim. Acta*, *53*, 745-750, 1989.

Michard, A., F. Albarede, G. Michard, J.F. Minster, and J.L. Charlou, Rare-earth elements and uranium in high-temperature solutions from East Pacific Rise hydrothermal vent field (13°N), *Nature*, *303*, 795-797, 1983.

Michard, G., F. Albarde, A. Michard, J.-F. Minster, J.-L. Charlou, and N. Tan, Chemistry of solutions from the 13°N East Pacific Rise hydrothermal site, *Earth Planet. Sci. Lett.*, *67*, 297-307, 1984.

Miyashiro, A., The Troodos ophiolitic complex was probably formed in an island arc, *Earth Planet. Sci. Lett.*, *19*, 218-224, 1973.

Moody, J.B., D. Meyer, and J.E. Jenkins, Experimental characterization of the greenschist/amphibolite boundary in mafic systems, *Am. J. Sci.*, *283*, 48-92, 1983.

Mottl, M.J., Metabasalts, axial hot springs and the structure of hydrothermal systems at mid-ocean ridges: *Geo. Soc. Am Bull*, 94, 161-180, 1983.

Mottl, M.J., and H.D. Holland, Chemical exchange during hydrothermal alteration of basalt by seawater. I. Experimental results from major and minor components of seawater, *Geochim. Cosmochim. Acta*, 42, 1103-1115, 1978.

Muehlenbachs, K., and R.N. Clayton, Oxygen isotop ratios of submarine diorites and their constituent minerals, *Can. J. Earth Sci.*, *8*, 1591-1595, 1971.

Muehlenbachs, K., and R.N. Clayton, Oxygen isotope geochemistry of submarine greenstones, *Can. J. Earth Sci.*, *9* (5), 471-478, 1972a.

Muehlenbachs, K., and R.N. Clayton, Oxygen isotope studies of fresh and weathered submarine basalts, *Can. J. Earth Sci.*, *9* (2), 172-184, 1972b.

Natland, J.H., and R. Hekinian, Hydrothermal alteration of basalts and sediments at DSDP Site 465, Mariana Trough, in *Initial Reports of the Deep Sea Drilling Project*, edited by D. Hussong, and S. Ueda, pp. 759-769, US Government Printing Office, Washington, 1981.

Natland, J.H., and J.J. Mahoney, Alteration of igneous rocks at DSDP Sites 458 and 459, Mariana forearc region: Relationship to basement structure., in *Initial Reports of the Deep Sea Drilling Project*, edited by D. Hussong, and S. Ueda, pp. 769-788, US Government Printing Office, Washington, 1981.

Nehlig, P., T. Juteau, V. Bendel, and J. Cotten, The root zones of oceanic hydrothermal systems: constraints from the Samail ophiolite (Oman)., *J. Geophys. Res.*, *99* (B3), 4703-4713, 1994.

Norton, D., Theory of hydrothermal systems, *Ann. Rev. Earth Planet. Sci.*, *12*, 155-177, 1984.

Olive, V., R. Hebert, and M. Loubet, Isotopic and trace element constraints on the genesis of a bononitic sequence in the Thetford Mines ophiolitic complex, Quebec, Canada, *Can. J. Earth Sci.*, *34*, 1258-1271, 1997.

O'Neil, J.R., L.H. Adami, and S. Epstein, Revised value for the ^{18}O fractionation between CO_2 and H_2O at 25°C, *Jour. Research U.S. Geol. Survey*, *3* (5), 623-624, 1975.

Pan, Y., and M. Fleet, Intrinsic and external controls on the incorporation of rare-earth elements in calc-silicate minerals, *Can. Mineral.*, *34*, 147-159, 1996.

Pearce, J.A., Basalt geochemistry used to investigate past tectonic environments on Cyprus, *Tectonophysics*, *25*, 41-67, 1975.

Pearce, J.A., and J.R. Cann, Tectonic setting of basic volcanic rocks determined using trace element analyses, *Earth Planet. Sci. Lett.*, *19*, 290-300, 1973.

Pearce, J.A., S.J. Lippard, and S. Roberts, Characteristics and tectonic significance of supra-subduction zone ophiolites, *Geol. Soc. Lond.*, *16*, 77-94, 1984.

Pedersen, R.B., and J. Malpas, The origin of oceanic plagiogranites from the Karmoy ophiolite, Western Norway, *Contrib. Mineral. Petrol.*, *88*, 36-52, 1984.

Perfit, M.R., D.A. Gust, A.E. Bence, R.J. Arculus, and S.R. Taylor, Chemical characteristics of island-arc basalts: Implications for mantle sources, *Chem. Geol.*, *30*, 227-256, 1980.

Pezard, P., Electrical properties of mid-ocean ridge basalt and implications for the structure of the upper oceanic crust in Hole 504B, *J. Geophys. Res.*, *95*, 9237-9264, 1990.

Press, W.H., *Numerical recipes in C: the art of scientific computing*, xxvi, 994 pp., Cambridge University Press, New York, 1992.

Purdy, G.M., L.S.L. Kong, G.L. Christeson, and S.C. Solomon, Relationship between spreading rate and the seismic structure of mid-ocean ridges, *Nature*, *355*, 815-817, 1992.

Quon, S.H., and E.G. Ehlers, Rocks of the northern part of the Mid-Atlantic Ridge, *Geol. Soc. Am. Bull.*, *74*, 1-8, 1963.

Rautenschlein, M., G.A. Jenner, J. Hertogen, A.W. Hofmann, R. Kerrich, H.-U. Schmincke, and W.M. White, Isotopic and trace element composition of volcanic glasses from the Akaki Canyon, Cyprus: implications for the origin of the Troodos ophiolite, *Earth Planet. Sci. Lett.*, *75*, 369-383, 1985.

Reynard, B., G. Fiquet, J.-P. Itie, and D.C. Rubie, High-pressure x-ray diffraction study and equation of state of $MgSiO_3$ ilmenite, *Amer. Mineral.*, *81*, 45-50, 1996.

Richardson, C.J., J.R. Cann, H.G. Richards, and J.G. Cowan, Metal-depleted root zones of the Troodos ore-forming hydrothermal systems, Cyprus, *Earth Planet. Sci. Lett.*, *84*, 243-253, 1987.

Robertson, A.H.F., Tectonic evolution of Cyprus, in *Ophiolites: Oceanic crustal analogues, Proceedings of the symposium "Troodos '87"*, edited by J. Malpas, E.M. Moores, A. Panayiotou, and C. Xenophontos, Geological Survey Department, Nicosia, 1990.

Robinson, P., J. C. Schumacher, and F. S. Spear, Formulation of electron probe analyses, in *Amphiboles: Petrology and Experimental Phase Relations*, edited by D. R. Veblen, and P. H. Ribbe, pp. 6-9, Min. Soc. Am. Rev. Mineral., 1982.

Robinson, P.T., W.G. Melson, T. O'Hearn, and H.-U. Schmincke, Volcanic glass compositions of the Troodos ophiolite, Cyprus, *Geology*, *11*, 400-404, 1983.

Roedder, E., *Fluid Inclusions*, 644 pp., Mineralogical Society of America, Washington, D.C., 1984.

Rona, P.A., and S.D. Scott, A special issue on sea-floor hydrothermal mineralization: new perspectives, *Econ. Geol.*, *88* (8), 1989-2017, 1993.

Rose, N.M., Geochemical consequences of fluid flow in porous basaltic crust containing permeability contrasts, *Geochim. Cosmochim. Acta*, *59* (21), 4381-4392, 1995.

Saccocia, P., K. Ding, M.E. Berndt, J.S. Seewald, and W.E. Seyfried, Experimental and theoretical perspectives on crustal alteration at mid-ocean ridges, in *Alteration and Alteration Processes associated with Ore-forming Systems: Short Course Notes*, edited by D.R. Lentz, pp. 403-431, Geological Association of Canada, Waterloo, 1994.

Sakai, C., T. Higashino, and M. Enami, REE-bearing epidote from Sanbagawa pelitic shcists, central Shikoku, Japan, *Geochem. J.*, *18*, 45-53, 1984.

Sample, J. C., and D. E. Karig, A volcanic production rate for the Mariana Island Arc, *J. Volcanology Geothermal Res.*, *13*, 73-82, 1982.

Sawka, W.N., REE and trace element vatiations in accessory minerals and hornblende from the strongly zoned McMurry Meadows Pluton, California, *Transactions of the Royal Society of Edinburgh: Earth Sciences*, *79*, 157-168, 1988.

Schiffman, P., R.C. Evarts, A.E. Williams, and W.J. Pickthorn, Evidences for Polyphased Oceanic Alteration of the Extrusive Sequence of the Semail Ophiolite from teh Salahi Block (Northern Oman), in *Ophilotile Genesis and Evolution of the Oceanic Lithoshpere: Prodeecings of the Ophiloite Conference, held in Muscat, 7-18 Januaery 1990*, edited by T. Peters, A. Nicolas, and R.G. Coleman, pp. 399-425, Kluwar Academic Publishers, Muscat, 1990.

Schiffman, P., and G.O. Fridleifsson, The smectite-chlorite transition in drillhole NJ-15, Nesjavellir geothermal field, Iceland: XRD. BSE and electron microprobe investigations, *J. Meta. Geol.*, *9*, 679-696, 1991.

Schiffman, P., and B.M. Smith, Petrology and oxygen isotope geochemistry of a fossil seawater hydrothermal system within the Solea Graben, Northern Troodos Ophiolite, Cyprus, *J. Geophys. Res.*, *93*, 4612-4624, 1988.

Schiffman, P., B.M. Smith, R.J. Varga, and E.M. Moores, Geometry, conditions and timing of off-axis hydrothermal metamorphism and ore-deposition in the Solea graben, *Nature*, *325*, 423-425, 1987.

Schöps, D., and P.M. Herzig, Hydrothermally altered felsic rocks of the Tonga forearc, in *Proc. ODP, Sci. Results*, edited by J. Hawkins, L. Parsosn, and J. Allan, pp. 653-666, Ocean Drilling Program, College Station, TX, 1994.

Sclater, J.G., B. Parsons, and C. Jaupart, Oceans and continents: similarities and differences in the mechanisms of heat loss, *J. Geophys. Res.*, *86*, 11,535-11,552, 1981.

Seewald, J.S. and W.E. Seyfried Jr., The effect of temperature on metal mobility in subseafloor hydrothermal systems: Constraints from basalt alteration experiments, *Earth Planet. Sci. Lett.*, 101, 388-403, 1990.

Ding, K. and W.E. Seyfried Jr., Determination of Fe-Cl complexing in the low pressure supercritical region (NaCl fluid): Iron solubility constraints on pH of subseafloor hydrothermal fluids, *Geochim. Cosmochim. Acta*, 56, 3681-3692, 1992.

Seno, T., and S. Maruyama, Paleogeographic reconstruction and origin of the Philippine Sea, *Tectonophysics*, *102*, 53-84, 1984.

Seyfried, W.E., Jr., Experimental and theoretical constraints on hydrothermal alteration processes at mid-ocean ridges, *Ann. Rev. Earth Planet. Sci.*, 15, 317-335, 1987.

Seyfried, W.E., Jr. and J.L. Bischoff, Low temperature basalt interaction with seawater: an experimental study at 70°C and 150°C, *Geochim. Cosmochim. Acta*, 43, 1937-1947, 1979.

Seyfried, W.E., M.E. Berndt, and J.S. Seewald, Hydrothermal alteration processes at mid-ocean ridges: constraints from diabase alteration exteriments, hot-spring fluids and composition of the oceanic crust, *Can. Mineral.*, *26*, 787-804, 1988.

Seyfried, W.E., Jr., K. Ding, and M.E. Berndt, Phase equilibria constraints on the chemistry of hot spring fluids at mid-ocean ridges, *Geochim. Cosmochim. Acta*, *55*, 3559-3580, 1991.

Shannon, R.D., Revised effective ionic radii and systematic studies of interatomic distances in halides and chalcogenides, *Acta Cryst.*, *32*, 751-767, 1976.

Shipboard Scientific Party, Introduction, background, and principal results of Leg 135, Lau Basin, in *Ocean Drilling Program, Initial Reports*, edited by J. Hawkins et. al., pp. 5-47, Ocean Drilling Program, College Station, Texas, 1992.

Sinton, J.M., and R.S. Detrick, Mid-ocean ridge magma chambers, *J. Geophys. Res.*, *97* (B1), 197-216, 1992.

Smewing, J.D., K.O. Simonian, and I.G. Gass, Metabasalts from the Troodos Massif, Cyprus: genetic implication deduced from petrography and trace element geochemistry, *Contrib. Mineral. Petrol.*, *51*, 49-64, 1975.

Smith, I.E.M., T.J. Worthington, R.C. Price, and J.A. Gamble, Primitive magmas in arc-type volcanic associations: Examples from the southwest Pacific, *Can. Mineral.*, *35*, 257-273, 1997.

Smyth, J.R., and D.L. Bish, *Crystal structures and cation sites of the rock-forming minerals*, 332 pp., Allen & Unwin, London, 1988.

Solomon, S.C., and D.R. Toomey, The structure of mid-ocean ridges, *Ann. Rev. Earth Planet. Sci.*, *20*, 329-364, 1992.

Spear, F.S., NaSi-CaAl exchange equilibrium between plagioclase and amphibole, *Contrib. Mineral. Petrol.*, *72*, 33-41, 1980.

Spear, F.S., An experimental study of hornblende stability and compositional variability in amphibolite, *Am. J. Sci.*, *281*, 697-734, 1981.

Stakes, D., C. Mevel, M. Cannat, and T. Chaput, Metamorphic stratigraphy of hole 735B, in *Proc. ODP, Sci. Results*, pp. 153-179, ODP, 1991.

Stakes, D.S., Oxygen and hydrogen isotope compositions of oceanic plutonic rocks: high-temperature deformation and metamorphism of oceanic layer 3, in *Stable Isotope Geochemistry: A Tribute to Samuel Epstein*, edited by H.P. Taylor, J.R. O'Neil, and I.R. Kaplan, pp. 77-90, The Geochemical Society, Special Publication, 1991.

Stakes, D.S., and H.P. Taylor, Jr., The Northern Samail Ophiolite: an oxygen isotope, microprobe and field study, *J. Geophys. Res.*, *97* (5), 7043, 1992.

Stakes, D.S., H.P. Taylor, and R.L. Fisher, Oxygen-isotope and geochemical characterization of hydrothermal alteration in ophiolite complexes and modern oceanic crust, in *Ophiolites and Ocean Lithosphere*, edited by I.G. Gass, S.J. Lippard, and A.W. Shelton, pp. 199-214, Geological Society Special Publications, 1984.

Stalder, R., S.F. Foley, G.P. Brey, and I. Horn, Mineral-aqueous fluid partitioning of trace elements at 900-1200°C and 3.0-5.7 GPa: New experimental data for garnet, clinopyroxene, and rutile, and implications for mantle metasomatism, *Geochim. Cosmochim. Acta*, *62* (10), 1781-1801, 1998.

Staudigel, H., and K.M. Gillis, The timing of hydrothermal alteration in the Troodos Ophiolite, in *Ophiolites: Oceanic crust analogues, Proceeding of the symposium "Troodos 1987"*, edited by J. Malpas, E.M. Moores, A. Panayiotou, and C. Xenophontos, Geological Survey Department, Nicosia, 1990.

Stein, C.A., and S. Stein, Constraints on hydrothermal heat flux through the oceanic lithosphere from global heat flow, *J. Geophys. Res.*, *99*, 3081-3095, 1994.

Stern, R.J., and S.H. Bloomer, Subduction zone infancy: Examples from the Eocene Izu-Bonin-Mariana and Jurassic California arcs, *Geol. Soc. Am. Bull.*, *104*, 1621-1636, 1992.

Sverjensky, D.A., Europium redox equilibria in aqueous solution, *Earth Planet. Sci. Lett.*, *67*, 70-78, 1984.

Tatsuni, Y., Migration of fluid phases and genesis of basalt magmas in subduction zones, *J. Geophys. Res.*, *94*, 4697-4707, 1989.

Taylor, B., K. Fujioka, T.R. Janecek, and C. Langmuir, *Proc. ODP, Sci. Results*, Ocean Drilling Program, College Station, TX, 1992.

Taylor, H.P., Jr., The oxygen isotope geochemistry of igneous rocks, *Contib. Mineral. Petrol.*, *19*, 1-71, 1968.

Thompson, G., Basalt-seawater interaction, in *Hydrothermal Processes at seafloor spreading centers*, edited by P.A. Rona, K. Bostrom, L. Laubieer, and K.L. Smith, pp. 225-278, Plenum Press, New York, 1983a.

Thompson, G., Hydrothermal fluxes in the ocean, in *Chemical Oceanography*, edited by J.P. Riley, and R. Chester, pp. 271-337, Academic Press, London, 1983b.

Tribuzio, R., B. Messiga, R. Vannucci, and P. Bottazzi, Rare earth element redistribution during high pressure low temperature metamorphism in ophiolitic Fe-gabbros (Liguria, northwestern Italy): Implications for light REE mobility in subduction zones, *Geology*, *24* (8), 711-714, 1996.

Tunnicliffe, V., The Nature and Origin of the Modern Hydrothermal Vent Fauna, *Palaios*, *7*, 338-350, 1992.

Vanko, D.A., Temperature, pressure, and composition of hydrothermal fluids, with their bearing on the magnitude of tectonic uplift at mid-ocean ridges, inferred from fluid inclusions in oceanic layer 3 rocks, *J. Geophys. Res.*, *93* (B5), 4595-4611, 1988.

Vanko, D., A., and C. Laverne, Hydrothermal anorthitization of plagioclase within the magmatic/hydrothemal transition at mid-ocean ridges: examples from deep sheeted dykes (Hole 504B, Costa Rica Rift) and a sheeted dike root zone (Oman ophiolite), Earth Planet. Sci. Lett., 162, 27-43, 1998.

Vanko, D.A., and D.S. Stakes, Fluids in oceanic layer 3: evidence from veined rocks, Hole 735B, Southwest Indian Ridge, in *Proc. ODP, Sci. Results*, edited by R.P. Von Herzen, and P.T. Robinson, pp. 181-215, Ocean Drilling Program, College Station, TX, 1991.

Varga, R.J., J.S. Gee, L. Bettison-Varga, R.S. Anderson, and C.L. Johnson, Early formation of seafloor hydrothermal systems during structural extension: paleomagnetic evidence from the Troodos Ophiolite, *Earth Planet. Sci. Lett.*, *171*, 221-235, 1999.

Von Damm, K.L., Controls on the chemistry and temporal variability of seafloor hydrothermal systems, in *Seafloor Hydrothermal Systems: Physical, Chemical, Biological, and Geological Interactions*, edited by S.E. Humphris, Zierenberg, Robert A., Mullineaux, Lauren S., and Thomson, Richard E., pp. 222-247, American Geophysical Union, Washington, 1995.

Von Damm, K.L., and J.L. Bischoff, Chemistry of hydrothermal solutions from the southern Juan de Fuca ridge, *J. Geophys. Res.*, *92*, 11334-11346, 1987.

Wadge, G., Comparison of volcanic production rates and subduction rates in the Lesser Antilles and Central America, *Geology*, *2*, 555-558, 1984.

Weiss, R.F., P. Lonsdale, J.E. Lupton, Bainbridge, and H. Craig, Hydrothermal plumes in the Galapagos rift, *Nature*, *267*, 600-603, 1977.

Weston, P.E., Temperature, timing and fluid composition constraints for high temperature fracturing and hydrous mineral formation in gabbros from Hess Deep, Masters thesis, University of California (Los Angeles), Los Angeles, 1998.

Wood, B.J., and J.V. Walther, Rates of hydrothermal reactions, *Science*, *222*, 413-415, 1983.

Wood, S.A., The aqueous geochemistry of the rare earth elements and yttrium, Part II, Theoretical predictions of speciation in hydrothermal solutions to 350°C at saturation water vapor pressure, *Chem. Geol.*, *88*, 99-125, 1990.

Yanev, Y., J.M. Bradintzeff, K. Rakalov, and G. Jelev, Mn-bearing and REE-rich epidote (epidote-allanite) from the hydrothermally acid volcanics, Eastern Rhodopes (Bulgaria), *N. Jb. Miner. Mh.*, *5*, 221-233, 1998.

Zindler, A., and S. Hart, Chemical geodynamics, *Ann. Rev. Earth Planet. Sci.*, *14*, 493-571, 1986.

Appendix A

SAMPLE PETROGRAPHY

The following pages contain brief descriptions of 121 thin sections used for this study. Sample location, rock type, and form were taken from shipboard descriptions. In several cases, the rock type has been modified from the original deck description to better reflect petrographic observations. Sample numbers are presented in the following format: (dredge number) - (rock type) - (sample number). Rock type numbers were arbitrarily assigned on board once the dredge was recovered and are not consistent between dredges. Sample numbers were assigned in the order in which they were processed. Question marks (?) are used throughout wherever an observation is uncertain. Abbreviations: Qtz = quartz; Chl = chlorite; Ep = epidote; Zeol = zeolite; Plag = plagioclase; Opx = orthopyroxene; Cpx = clinopyroxene; Pyx = pyroxene; Ol = olivine; Amph = amphibole; Serp = serpentine; Ap = apatite; Idd = iddingsite; Ser = sericite; Carb = carbonate; Mag = magnetite; Titan = titanite; Ox = oxides; VFG = very fine grained; FG = fine grained; MG = medium grained; CG = coarse grained; GM = groundmass; TS = thin section; TT = Tonga trench; cont = contains; xl = crystal; incl = inclusion; perv = pervasive; w = with; min = mineral; lt = light; FI = fluid inclusion; PPL = plane polarized light; repl = replace; alt = alteration/altered; biref = birefringence; prim = primary; encl = enclosing.

Sample	Location	Rock Type	Form	Mineralogy & Texture	Alteration	Comments
81-2-8	West facing scarp-TF8 transect	Plag phyric andesite	angular clast	FG Plag microlites in a cryptocrystalline matrix; Plag microlites show evidence of flow; vesicles are filled with epidote; possible relict Cpx?	Sample pervasively altered with a green colour; vesicles filled with epidote; GM Plag altered to yellow brown material + epidote; fractures and GM contain abundant epidote	one part of slide appears brecciated and is altered to Ep + Chl + opaques
81-2-9	West facing scarp-TF8 transect	Plag phyric volcanic	angular clast	F to MG Plag grains in VFG matrix; sample contains vesicles filled with epidote + Qtz + Zeol?	Plag is pervasively altered to epidote; vesicles filled with Ep + Qtz + Zeol?; sample has a green colour; probably some Chl but hard to tell	colourless mid biref min (thick Qtz?); VFG Sulfides
82-3-2	lower onshore slope TT, S of Louisville ridge intersection	gabbronorite (Plag-rich troctolite)	angular clast	MG olivine + Plag with minor Opx; olivine and OPX are highly fractured; Plag is also fractured and all are rounded at grain boundaries	Ol and OPX are pervasively altered to serpentine and chlorite? w minor Idd and Oxides; Plag is altered to sericite? and brown clay; some Plag is re-crystallized at grain boundaries.	abundant colourless amphibole at grain boundaries; FG Amph fills spaces
82-3-8	lower onshore slope TT, S of Louisville ridge intersection	gabbronorite	angular clast?	M to FG Cpx, Plag, minor Ol, OPX and Oxides; xls are broken and fractured; porphyroclasts are set in a FG GM of re-crystallized Plag, brown clay and other secondary minerals; cleavage is bent in CPX and Plag.	Ol is completely replaced by secondary Oxides, Talc? and colourless amphibole?; Plag is pervasively altered to brown clay? and sericite; CPX is cross cut by small veinlets of a brown mineral (clay?); yellow-brown clots may be olivine pseudomorphs	bright blue-green mineral? at CPX grain boundaries; zeolites? in vesicles & veins;
87-1-1	east-facing scarp on a trench-slope break high	diabase	angular clast	F to MG Qtz, Plag, CPX, minor Ol, OPX & opaques (pyrite); yellow-brown amphibole (some green acicular) and clay fills interstices between Plag and Cpx grains; Plag shows wormy text (myrmekite?)	Plag is relatively fresh with minor alteration to sericite and brown clay along fractures; Cpx is rimmed by yellow brown-amphibole; dark red-brown hematite patches may be olivine pseudomorphs	chlorite intermixed with yellow-brown amphibole?; opaques have ophitic text enclosing Plag and Amph.

Sample	Location	Rock Type	Form	Mineralogy & Texture	Alteration	Comments
88-1-7	top of seamount feature dredged on D87	Ol-Plag-Cpx phyric andesite	subangular clast	FG Plag, Qtz, and Cpx set in a VFG GM; GM is highly altered and replaced by colourless & green Amph ± red-brown Oxides; Cpx grains are fractured and sometimes rounded	Plag is altered to secondary Plag sericite and brown clay; GM is pervasively altered to brown clay, chlorite?, and secondary Oxides; narrow zeolite? veins crosscut sample.	bright blue-green mineral?; isotropic mineral; euhedral Oxides; Oxides associated with titanite; celadonite
88-1-8	top of seamount feature dredged on D87	Ol-Plag-Cpx phyric andesite	subangular clast	MG Plag and acicular Cpx in a glassy GM w minor Opx and small equant olivine grains; boninitic type text; some Opx is mantled by Cpx along grain boundaries and cleavages; some Plag grains are zoned.	Small veinlets crosscut the sample and contain zeolites? and calcite; small brown patches may be alteration after Pyx; some Pyx are altered along grain boundaries.	feathery crystal form?; blue-green mineral?
88-1-19	top of seamount feature dredged on D87	Plag and Pyx phyric andesite	subangular clast	glomeroporphyritic Plag, Cpx and Opx phenocrysts in a VFG GM of Pyx, Plag and glass; phenocrysts are euhedral with little sign of alteration some Pyx are fractured; some Plag is zoned; some Opx is zoned.	GM is altered to brown clay?; veinlets of zeolite? mineral crosscut the sample.	fresh; some big fluid inclusions in phenocrysts.
90-2-5	TT mid-slopes	aphyric basalt	subangular clast	VFG Plagioclase and Cpx with skeletal Oxides; small patches of red-brown hematite are observed as well as some chlorite?	The sample is cut by several veinlets filled with quartz ± zeolites with possible epidote along margins?; veins of serpentine?	not pervasively altered; whole TS displays interesting pink discolouration pattern
90-4-1	TT mid-slopes	gabbro norite	angular clast	granular F to MG Cpx and Plag with minor Ol? and Oxides; Opx?; grains are relatively fresh; Cpx poikilitically encloses Plag; olivine is completely replaced by serpentine, brown clay and colourless amphibole ± Talc.	small veinlets crosscut the sample containing FG colourless acicular amphibole?; also zeolite minerals?; patches of FG colourless amphibole? may be olivine pseudomorphs; Cpx altered along grain boundaries.	FG amphibole? and epidote? in veins

Sample	Location	Rock Type	Form	Mineralogy & Texture	Alteration	Comments
90-4-2	TT mid-slopes	gabbro norite	angular clast	granular MG Cpx, Opx, Plag, and minor Ol? and Oxides; Pyx show exsolution along cleavage; Plag is relatively fresh but cut by tiny veinlets of brown clay?; Opx and Cpx oikocrysts enclose Plag.	Oxides are replacing Pyx along cleavage; Ol is completely pseudomorphed by serpentine, Oxides and colourless amphibole; sample is cut by small light brown to colourless veinlets containing acicular mineral; Opx altered to brown mineral ± serpentine	FG colourless amphibole veinlets?
90-4-3	TT mid-slopes	gabbro	angular clast	pervasively altered, MG Cpx, Plag, FG Oxides, and minor Opx?; Plag is altered along fractures and at grain boundaries to clay; Pyx is altered to colourless and green amphibole along grain boundaries and along cleavage	the sample is cut by several veins which contain fibrous and prismatic, green and colourless amphibole, and chlorite; quartz ± zeolite veins are also observed; one side of the sample appears to be more pervasively altered; vein may be faulted	chlorite appears to occupy vein margins with amphibole (granular vs. acicular) cores; **high T?**; some alteration patches have cores of Amph and chlorite rims
90-4-4	TT mid-slopes	gabbro norite	angular clast	MG anhedral Cpx, Opx, and Plag with minor Oxides; Pyx are ophitic and enclose subhedral Plag laths; sample fresher than 90-4-3	the sample is criss-crossed by net veins containing chlorite and brown clay; Opx and Cpx are altered to chlorite at grain boundaries; Plag is altered to brown clay; brown clots containing Serp. with mesh text may be Ol pseudomorphs	
90-4-7	TT mid-slopes	gabbro norite	subangular clast	pervasively altered, MG Cpx, Opx and Plag; Plag is completely recrystallized; Pyx are deformed and broken with bent cleavage; some high relief epidote (anomalous blue)?	almost all grains are pseudomorphed and replaced by chlorite and brown clay; the sample is cut by small veinlets containing quartz ± zeolites	epidote??

Sample	Location	Rock Type	Form	Mineralogy & Texture	Alteration	Comments
94-1-1 A & B	upper slope Tonga trench	Oxide gabbro norite	angular block	MG Cpx, Opx, Plag, and Oxides; Oxides are interstitial and poikilitically enclose Cpx & Plag; large Opx grains poikilitically enclose Cpx, Plag, & Oxides; some sulphide in B.	Opx is altered chlorite and green-colourless Amph; small veinlets cross cut the sample which contain zeolites? & chlorite; green amphibole is present at Cpx grain boundaries and mineral interstices; Plag is altered to brown clay along fractures	green Amph **high T?**
94-1-2	upper slope Tonga trench	olivine gabbro	angular block	MG to FG Cpx, minor Opx, Plag and Ol with minor Oxides; small euhedral zircon; prismatic green amphibole grains fill interstices; epidote + calcite associated with chlorite at Plag grain boundaries; some Oxides fill interstices between prim minerals.	Ol pseudomorphed by secondary magnetite + Chl + Talc ± Amph; green Amph is present as alteration rims on Pyx and in mineral interstices; Pyx has a mottled appearance & is altered to Chl + colourless Amph; small veinlets containing Chl ± Zeol cut sample	modal layering; weak foliation defined by aligned Plag laths; interesting sample!!!; wormy text observed in one area (may be after Ol)
94-1-3	upper slope Tonga trench	Oxide olivine gabbro	angular block	FG to CG Cpx, minor Opx, Ol, Plag and Oxides; Pyx are ophitic and enclose Plag laths; Oxides are interstitial and some contain Plag inclusions; some Oxides display wormy text; some primary Ol; Plag shows evidence of compositional zoning	olivine is pseudomorphed by idd, 2nd magnetite & Talc; Cpx altered to chlorite and Amph; Opx almost completely replaced by chlorite; some small veinlets contain brown clay ± chlorite; Pyx have mottled appearance; some intergranular amphibole	some reaction texts in Pyx (myrmekite); High Ti?
94-1-6	upper slope Tonga trench	Oxide gabbro norite	subangular block	F to CG Plag laths with M. to CG anhedral Cpx and Opx; Pyx is ophitic and encloses Plag laths; minor fresh Ol is present; some FG interstitial Oxides	primary Ol is altered to 2nd magnetite and Talc along grain boundaries; brown pseudo are also present; Cpx and Opx are altered to green-brown amphibole and chlorite; the sample is cut by one 2mm chlorite/zeolite vein and several tiny veinlets	described as sub-ophitic to pegmatitic; Plag is altered to brown clay; sample is relatively fresh; Pyx display mottled text; fibrous and prismatic green Amph is found in interstices

Sample	Location	Rock Type	Form	Mineralogy & Texture	Alteration	Comments
96-1-1	upper slope Tonga trench	Diorite	angular fragment	M to CG Plag/K-spar and quartz with Oxides; no Pyx; FG euhedral epidote grains are associated with Plagioclase; Plag/ K-spar and quartz are intimately intergrown in a wormy (granophyric) text	feldspar is pervasively altered to brown clay; chlorite clots are found in the section possibly replacing Amph; epidote is seen replacing Plag; some chlorite patches contains yellow-brown high biref, mineral possibly Amph.	described as having pegmatitic patches; up to 1cm magnetite xis; large pink mineral in TS (opaque) - Oxide?????; look for apatite
96-1-2 A & B	upper slope Tonga trench	Diorite	angular fragment	F to MG K-spar/Plag, quartz and Oxides; similar to 96-1-1 but finer grained; this sample contains coarse grained epidote; K-spar/Plag and quartz are intimately intergrown in a wormy (granophyric) text; simple twins in feldspars	feldspar is pervasively altered to brown clay, chlorite & epidote; chlorite clots are found in the section possibly replacing Amph; some zeolites	**look for apatite**; saucerite??
96-1-3	upper slope Tonga trench	diorite	angular fragment	F to MG Qtz, Plag, blue-green Amph (primary?) and Oxides ± apatite?; MG epidote associated with Plag; some Plag is comp zoned; most Plag is euhedral-subhedral; Amph fills interstices; Plag and Qtz exhibit granophyric text; some Oxides are euhedral.	pervasively altered; Amph and Plag are altered to FG chlorite and epidote; Plag is almost completely sericitized; epidote is abundant and associated with Plag; some amphibole acicular some prismatic (later may be primary); no Pyx	colourless, acicular, high relief, low biref min may be apatite; quartz contains abundant fluid inclusions; Evolved sample
96-1-5	upper slope Tonga trench	diorite	angular fragment	similar to 96-1-3; MG anhedral Qtz, euhedral Plag, an-subhedral Amph and minor Oxides ± apatite; Oxides seem associated with Amph; both prismatic and acicular Amph; epidote associated w Plag; Qtz and Plag display granophyric text; comp zoning in Plag	pervasively altered; Amph and Plag are altered to FG chlorite and epidote; Plag is almost completely sericitized; epidote is abundant and associated with Plag; some amphibole acicular some prismatic (later may be primary); no Pyx	colourless, acicular, high relief, low biref min (some hexagonal x-section- apatite; quartz contains abundant fluid inclusions; Evolved sample; some brown Amph (primary?)

Sample	Location	Rock Type	Form	Mineralogy & Texture	Alteration	Comments
96-1-11	upper slope Tonga trench	gabbro or gabbro norite	angular fragment	MG Cpx & Opx phenocrysts in a FG GM of Plag, Cpx, Opx & Oxides; Opx displays compositional zoning; Pyx phenocrysts are relatively fresh; some Oxides are euhedral; no evidence of Ol psuedomorphs	sample is pervasively altered; Plag is altered to FG sericite, epidote and chlorite; Pyx are fractured and altered to FG Amph and Chl; GM is pervasively altered to FG Amph, Chl, epidote, and sericite;	some brown-green Amph in GM; GM is pervasively altered; abundant chlorite; some sulphides present
96-1-14	upper slope Tonga trench	Epidosite	angular fragment	FG Qtz, Plag, epidote, chlorite, apatite, Amph? and Oxides; granular Ep in GM; Oxides associated with high biref min - titanite?; sample is cut by hairline fractures filled with low biref min	Plag is almost completely sericitized and altered to assemblages of epidote and chlorite; no Pyx seen although some patches of Chl-Ep-Amph? may be Amph pseudomorphs	**apatite x-sections contain fluid inclusions; Chl suggests low temp.**
96-1-15	upper slope Tonga trench	diorite - epidotized	angular block	similar to 96-1-14; FG Qtz, Plag, epidote, chlorite, apatite, Amph? and Oxides; granular Ep in GM; Oxides and yellow-brown min associated with Pyx pseudomorphs; minor granophyric text	Plag is almost completely sericitized and altered to assemblages of epidote and chlorite; no Pyx seen although some patches of Chl-Ep-Amph? may be Amph pseudomorphs; Oxides altered to red clots	**apatite x-sections contain fluid inclusions; Chl suggests low temp.**
96-1-16	upper slope Tonga trench	diorite	angular blocks	FG Qtz, Plag, Ep, Chl, apatite and Oxides; Ep is minor; Oxides associated with high birefringent mineral - titanite? and Chl; quartz is highly fractured and deformed; minor granophyric text	Plag is almost completely sericitized; no Pyx seen; Oxides altered to red clots; sample is cut by hairline veins filled with Qtz? (low biref); Qtz vein? (3mm) cuts sample	sample mostly consists of Plag and Qtz.
96-1-19	upper slope Tonga trench	diorite - granophyric text	angular block	sample contains mostly F to MG Qtz and Plag w minor Ep, Chl, apatite and Oxides; Plag and Qtz are intimately intergrown in a pronounced granophyric text; sample is cut by a 3mm shear zone containing recrystallized Qtz, Plag & Ep	shear zone is cut by narrow epidote vein containing granular Ep.; Plag is extensively replaced by sericite and Ep; Chl is somewhat secondary but replaces Plag; some high biref / high relief minerals may be Amph?;	Ca metasomatism!; abundant epidote in veins; Oxides are alt to red clots (particularly near Ep. vein)

Sample	Location	Rock Type	Form	Mineralogy & Texture	Alteration	Comments
96-1-27	upper slope Tonga trench	diorite	angular fragment	F to MG Qtz, Plag, Chl, titanite, Ep, minor acicular Amph (green and yellow), apatite and Oxides;	relatively abundant titanite assoc. w Ox and Chl (possibly prim Amph pseudo); Plag is extensively replaced by sericite and Ep; granular Ep in ground mass; minor yellow-brown min may be Amph;	**abundant titanite! associated w Oxides and Chl**
96-1-28	upper slope Tonga trench	diorite	angular fragment	FG Qtz, Plag, Chl, Amph, Ap and disseminated Oxides; primary text is almost gone; sample is cut by a few narrow veinlets containing yellow-brown clay?;	Oxides associated w yellow brown acicular Amph?; Plag is heavily sericitized and altered to Chl and Ep; some evidence of Amph pseudomorphs altered to Chl.	abundant Oxides;
96-1-29	upper slope Tonga trench	FG diorite w chilled margin of basaltic dyke	angular fragment	diorite - FG Qtz, Plag, Ep, Chl, Oxides, titanite and Ap; basalt - Plag/Cpx phyric w Plag/Cpx GM; Plag is sericitized and altered to Ep + Chl; some Oxides are euhedral; diorite GM has granophyric text; abundant granular Ep in diorite;	sample is cut by 3-4 mm vein containing Chl + Ep ± Amph?; titanite is moderately abundant and associated w Oxides and Chl (Amph pseudo?); Cpx phenocrysts in basalt are altered to Chl and Plag phenocrysts are sericitized; narrow late veins cut chilled margin	**Very interesting sample!; yellow - brown mineral associated w Oxides; figure out timing**
96-1-35	upper slope Tonga trench	trondhjemite; epidotized Plagiogranite	angular fragment	FG to MG Qtz, Plag, Ep, Chl, acicular Amph?, titanite; no Oxides; granophyric text; abundant granular Ep;	Plag altered to sericite, Ep, and Chl; lots of epidote; loss of primary igneous text; small euhedral Ap and titanite	**Very evolved; fluid inclusions in Qtz**
96-2-1	upper slope Tonga trench	diabase	angular fragment	FG Plag, Qtz, Amph, Pyx?, Ep, Chl, Oxides ± zircon?; sample is cut by a 1 cm wide zone containing abundant Ep, Chl, Amph; Plag is completely altered in the zone otherwise mineralogy is similar;	Plag is altered to sericite, Ep, Chl; Pyx? altered to Amph & Chl; narrow Ep veinlets cut sample in alt zone; primary text in Ep zone is completely gone; pervasively altered	double check Pyx/Amph; not sure if Pyx (may be colourless Amph); check yellow-brown min in alt zone - phyllosilicate?

Sample	Location	Rock Type	Form	Mineralogy & Texture	Alteration	Comments
96-2-2	upper slope Tonga trench	sparsely Plag and Cpx phyric basalt	angular fragment	few Cpx and Plag phenocrysts in a FG matrix of Plag, Cpx, Chl, Oxides and acicular Amph ± titanite; some comp zoning in Plag; Oxides associated w minor titanite	sample is cut by numerous narrow zeolite? veinlets; Plag is altered to sericite and Chl; Chl patches are abundant - some assoc. w Amph; Cpx altered to Chl ± Amph; sample relatively fresh; Oxides altered to red clots	zeolite ± Qtz? veins suggest low temp
96-2-4	upper slope Tonga trench	FG diorite w basalt chilled margin	angular fragment	Plag-Cpx-Ol phyric basalt w chilled margin on FG Qtz-Plag-Chl-Ep-Ap-Titan diorite; granophyric text; titanite associated w Oxides	Plag altered to sericite ± Ep; no primary Pyx or Amph; sample is cut by early VFG Qtz?-Ep veinlets; early veinlets cut by Ep veins; Ep veins end at chill	**Excellent x-cutting relationships between vein and chilled margin!; fluid inclusions in Qtz**
96-2-5	upper slope Tonga trench	FG diorite-diabase	angular fragment	FG Plag, Qtz, Amph, Chl, and Oxides; abundant FG Oxides	sample is cut by narrow Ep ± ? veinlets; brown Amph is altered to Chl; Plag altered to sericite ± Chl ± minor Ep;	**fluid inclusions in Qtz**
96-2-7	upper slope Tonga trench	Cpx phyric basaltic andesite	subangular fragment	Cpx ± Opx phenocrysts in FG matrix of Plag, Qtz, Chl, Amph, Ep, Ap, and abundant Oxides; some titanite assoc. w Oxides	Cpx is altered to Chl and Amph; Plag is sericitized and altered to Ep + Chl; the sample is cut by several narrow veinlets filled with zeolites ± Qtz; some Oxides Oxidized to red clots; few Ep ± Qtz veinlets	fluid incl in Qtz
96-2-8	upper slope Tonga trench	Cpx ± Opx phyric basalt	subangular clast	matrix consists of Plag, Cpx, Opx?, Chl, Oxides, minor Ap, Ep, & Amph; some Pyx are comp zoned	Plag is altered to sericite, Chl and Ep; Pyx are altered Chl ± Amph; some Oxides altered to red clots	fluid incl in Qtz
96-2-13	upper slope Tonga trench	FG diorite	subangular clast	FG Plag, Qtz, acicular Amph, Chl, Oxides, minor Ep; sample is shows evidence of deformation - Qtz grains fractured;	Plag altered to sericite and minor Ep; amphibole altered to Chl; Amph may be primary; sample is cut by several veinlets which contain zeolites ± Qtz?	fluid incl in Qtz;

Sample	Location	Rock Type	Form	Mineralogy & Texture	Alteration	Comments
96-2-17	upper slope Tonga trench	diabase	angular clast	FG Plag, Qtz, Cpx, Amph, Chl, Ep, and Oxides; few Cpx phenocrysts otherwise FG; primary text hard to distinguish; some Oxides altered to red clots	Plag almost completely altered to sericite, Chl and minor Ep; Cpx altered to Amph + Chl; abundant Chl in TS; possible Oxidation along narrow fractures -> yell-red tinge to Chl	pervasively altered
99-1-3	SE of Vava'u Group, upper part of lower trench slope	olivine gabbronorite	sub angular fragment	MG Plag, Cpx, Opx and minor Ol with some Chl, Amph, and Oxides; sample is relatively fresh;	sample cut by 2-3mm vein containing zeolite minerals?; surrounding area is altered; Plag altered to sericite ± Chl; Cpx and Opx altered to Chl ± Amph ± Oxides; Ol altered to Chl, Mag, Talc, Idd;	relatively fresh
99-1-5	SE of Vava'u Group, upper part of lower trench slope	gabbronorite	subangular fragment	MG Plag, Cpx, Opx, Chl, Amph (some acicular); sample relatively fresh except near veins; some Pyx show exsolution; alteration patches containing 2nd Mag, Amph ± Talc may be Ol pseudo	sample is cut by white fractures/veins; GM proximal to veins is pervasively altered; Plag altered to FG sericite; Pyx altered to Amph and Chl; veins filled with FG equivalent to GM ± zeolites; otherwise sample is fresh	
99-1-6	SE of Vava'u Group, upper part of lower trench slope	gabbro-gabbro norite	sub fragment	CG Cpx, Plag, minor Opx + Chl; sample is pervasively alt; some Pyx have sub ophitic text; minor exsolution in Pyx; some green acicular Amph; most Amph colourless; only minor Oxides	sample pervasively alt; Plag almost completely alt; Plag alt to FG sericite + Chl; Pyx alt to Amph + Chl; sample cut by numerous narrow veins filled w Chl + Amph + minor zeolites; some sections of GM completely alt to Chl + Amph; Opx alt to Serp?	sample pervasively alt; **Amph veins!**

Sample	Location	Rock Type	Form	Mineralogy & Texture	Alteration	Comments
99-1-8	SE of Vava'u Group, upper part of lower trench slope	Ol gabbro norite	sub fragment	M to CG Cpx, Ol, Plag, with minor Opx, Chl, Amph, 2nd Mag + Idd; Pyx have sub ophitic text enclosing Plag; Pyx have minor exsolution; most Ol fresh w fractures containing Serp + Chl ± Amph + Talc + 2nd Mag	alt is patchy containing Amph + Chl; some small veinlets cut sample; Ol alt to Chl + Talc + 2nd Mag + Amph; some patches appear to cont FG Qtz? ± Plag?; possible recrystallization; patches possibly contain zeolites?; Ol alt to red-brown patches - Idd	Pyx alt to Amph ± Chl; Ol altered near Chl patches otherwise fresh; interesting alteration pattern;
99-1-11	SE of Vava'u Group, upper part of lower trench slope	Ol gabbro norite	sub fragment	CG Plag, Cpx, Ol + minor Opx; minor exsollution in Pyx along cleavage; sample is relatively fresh; minor Oxides - mostly sec; sample is ct by numerous veinlets filled with zeolites;	GM proximal to veins is pervasively alt; Plag alt to FG sericite and clays; Pyx alt to Amph ± Chl; all Ol partially alt to Talc + Mag + Idd +Amph; some fresh Ol observed	some Pyx have sub ophitic text; zeolites suggest low temp; possible Amph-Plag geothermometer;
99-1-17	SE of Vava'u Group, upper part of lower trench slope	Ol gabbro	sub round clast	Plag, Cpx, Ol, ±Opx; abundant Oxides; Cpx and Ol phenocrysts in a FG GM of Plag laths + Pyx+ Ol; some Pyx zoned; some Ol fresh;	sample is cut by numerous veinlets filled with Qtz ± zeolites; GM is perv alt w patch of Chl ± Amph; Plag is alt to FG sericite ± clay?; Pyx alt to Chl + Amph; some colourless Amph in veins?; some Ox reddish- brown; phenocrysts relatively un alt	Pyx looks like Ol; double check; sample perv alt; temp unsure; some Ep replacing Plag; Ep occurs as fine granular grains;
99-1-21	SE of Vava'u Group, upper part of lower trench slope	gabbro (minor Ol)	sub round clast	CG Plag, Cpx, w Ol; sample is relatively fresh; cut by narrow Amph ±Plag? veinlet apprOx 1mm; 2nd Oxides;	relatively fresh distal from vein; Ol alt to Talc + Amph + Mag + Idd; some fresh Ol pres; Cpx alt to Amph; Plag alt to FG ser ± clay; proximal to vein GM is perv alt; vein contains acicular colourless to lt green Amph ± Plag?; smaller veinlets extend from single vein;	**may be good for Plag Amph geotherm; some exsolution in Pyx; sample relatively fresh; HIGH T?**

Sample	Location	Rock Type	Form	Mineralogy & Texture	Alteration	Comments
99-1-26	SE of Vava'u Group, upper part of lower trench slope	gabbro	angular clast	Plag + Cpx w minor Ol and Opx; some Pyx have exsollution along cleavage; sample relatively fresh; some second Oxides observed;	sample cut by numerous veins containing zeolite minerals; some veins contain colourless Amph; veins cont fraGMents of GM; sample perv alt proximal to veins; Plag alt to ser and recrystallize proximal veins; Pyx alt to Amph ± Chl; patch of Amph + Talc +Mag + Idd may be Ol pseudo	interesting to probe Amph in veins and zeolite minerals; veins also contain other low relief/relief minerals; sample is relatively fresh
99-1-27	SE of Vava'u Group, upper part of lower trench slope	norite (dominant Pyx is Opx)	angular clast	CG Plag and Opx w minor Cpx enclosing Plag and Opx polkilitically; some Cpx exsollution in Opx; sample is relatively fresh; no primary Oxides;	a few veins cut the sample which contain zeolites?; GM alt proximal to veins; Plag alt to FG ser + minor Ep; Pyx alt to colourless Amph + Chl along fractures and green boundaries; there is minor prismatic Amph in vein	check Amph comp in veins; sample relatively fresh; some minor Oxides
99-1-30	SE of Vava'u Group, upper part of lower trench slope	gabbro norite	and clast	CG Plag, Cpx and minor Opx w some CG colourless Amph; some Pyx sub ophitic; evidence of deformation and possible recrystallization?	sample pervasively alt; Plag alt to FG ser + Chl; Pyx alt to colourless Amph + Chl; sample cut by number veins filled w zeolites? + Amph + Chl; GM proximal to veins cuts across primary minerals;	**GEOTHERMOMETRY?; HIGH T?**
99-1-33	SE of Vava'u Group, upper part of lower trench slope	gabbro norite	angular clast	CG Plag, Cpx and Opx; Opx and some Cpx show exsolution along cleavages; some Pyx sub ophitic encl Plag; grains are usually subhedral;	sample cut by numerous veins filled with zeolites? ± Qtz; GM proximal to veins perv alt; Plag alt to FG ser ± Chl; Pyx alt to colourless Amph ±Chl; some Pyx in GM alt along green bound to Amph;	difficult to tell vein minerals due to FG nature; sample generally fresh; evidence of deformation and fracturing near veins;
99-2-1	SE of Vava'u Group, upper part of lower trench slope	alt diabase or microgabbro	sub rounded clast	F to MG Plag + Cpx + Amph + Chl + zeolites? + Oxides; sample highly deformed; GM minerals highly fracture	sample cut by numerous veins filled with Chl + zeolites ± Amph; GM proximal to veins highly alt; Plag alt to ser ± Chl; Cpx alt to Chl + Amph;	interesting x-cutting relationships; GM distal from veins relatively fresh

Sample	Location	Rock Type	Form	Mineralogy & Texture	Alteration	Comments
99-2-8	SE of Vava'u Group, upper part of lower trench slope	Basaltic Epidosite	sub rounded clast	FG Qtz + Ep + Amph + Chl + Oxides; igneous text gone; epidosite!!!!	complete loss of igneous text; abundant Oxides; amygdule filled w granular Ep ± Amph; GM perv alt to Chl + Amph + Ep;	some apatite; possibly some Plag but difficult to tell;
99-2-12	SE of Vava'u Group, upper part of lower trench slope	basaltic andesite; epidotized basalt	angular block	similar to 99-2-8; FG Qtz-Ep-Chl-Amph w minor apatite; sample contains abundant Oxides; sample contains more Chl than 99-2-8; splays of green Ep ± Amph fill vesicles; epidosite?	primary text gone; epidosite?; some round structures appear to be vesicles filled w green Ep + Amph; no fresh Plag; Oxides somewhat alt; Fl in Qtz;	**pervasively alt;**
99-2-21	SE of Vava'u Group, upper part of lower trench slope	volcanic breccia	angular block	2 sections - one F to MG Plag Cpx w minor Opx which grades into FG basalt sparsely phyric w Cpx; CG section contains sparse opaque minerals; basaltic clast contains zeolites in veins and vesicles	last completely alt to Chl ± zeolites?; zeolites restricted to amygdules and veins; CG section has alt of GM to Chl; Plag is alt to FG ser ± clay ± Chl; Pyx appear fresh; some alt of Pyx to Chl;	grain size gradation is sharp in some places and gradual in others; interesting sample of breccia; some min grains are fractured;
100-1-6	upper portion of lower slope, ESE of vava'u Group	alt microgabbro or diabase	angular clast	FG Plag laths, Cpx + Oxides w minor Opx; sample is Cpx and Plag phyric w phenocrysts up to 3-4 mm; interstices are filled w cryptocrystalline material which has been alt	Plag laths altered to FG ser± clay ± Chl; Pyx relatively fresh; some Pyx alt to Chl ± Amph; GM alt to green-brown material; possibly Chl ± clay;	some evidence of fracturing of grains and deformation; some zoning in Plag;
100-1-40	upper portion of lower slope, ESE of vava'u Group	diabasic basalt	angular block	FG Plag-Cpx-Ox w minor Opx?; interstices are filled w FG material; some Plag grains are zoned	GM alt to green-brown mat - possibly clay ± Chl; Plag alt to ser ± Chl ± clay; Pyx relatively fresh; some Pyx alt along fractures to Chl ± clay	GM perv alt although alt does not affect phenocrysts extensively
101-1-14	mid-slope high, Tonga trench	altered Cpx phyric diabase	angular clast	porphyritic to glom-porphyritic w phenocrysts of Cpx ± Opx; GM contains Plag, Cpx, Chl, Oxides± Opx; sample cut by num veinlets filled w Carb + Zeol; GM may contain Qtz?;	phenocrysts are generally fresh; GM altered w clots of Chl (possibly replacing Pyx); Plag alt to FG ser ± Chl; some evidence of increased alt along veinlets;	sample contains 1-2 mm sulphide grain

Sample	Location	Rock Type	Form	Mineralogy & Texture	Alteration	Comments
101-1-16	mid-slope high, Tonga trench	altered diabase	angular clast	FG Cpx, Plag, Oxides, ±Opx in an alt glassy matrix; grains are fractured; sample contains areas of relatively fresh glass; glassy area contain fragments of Cpx + Plag;	sample contains patches of Chl; interstitial glass is comp alt to Chl ± clay?; Plag is alt to ser ±Chl; Pyx are relatively fresh some alt to Chl along rims and fractures	some evidence of zoning in primary minerals; Oxides partially alt; low temp?;
101-1-20	mid-slope high, Tonga trench	Pyx-Pyx phyric andesite	sub angular clast	FG Plag + Cpx ± Opx in alt glassy matrix; num vesicles filled w Chl± Zeol ± Amph ± Ep; sample contains abundant FG Oxides;	perv alt; GM alt to Chl ± Amph ± clay; some vesicles filled w splays of fibrous high biref Amph?; GM Plag alt to Chl + FG ser; vesicles show sequential min growth from rim to core; Chl and Amph typically at core w Zeol at rims; Cpx relatively fresh in GM - some alt to Chl ± Amph;	sample perv alt; **Amph in vesicle = high T?**
101-1-23	mid-slope high, Tonga trench	alt diabase	angular block	F to MG Plag, Cpx, Oxides ± Opx; many grains fractured; GM cont VFG Chl ± clay;	Plag alt to FG ser ± Chl; Cpx alt to Chl ± Amph; GM perv alt; some Amph in GM;	**possible sample for geotherm; Pyx relatively fresh**
101-1-24	mid-slope high, Tonga trench	alt diabase	angular block	Plag + Cpx + Qtz + Oxides; Qtz contains FI;	Plag alt to FG ser ± Chl ± Ep; GM alt to Chl ± Ep ± Amph ± 2nd Ox ± Carb; sample cut by stringer 1-2 mm w acicular Amph + Carb ± Ep; Amph in veins forms radiating slays; Pyx alt to Chl ± Amph along boundaries;	Amph ± Ep veins suggests **high T**; Carb suggests Ca metasomatism;
102-4-1	mid-slope high; Tonga Trench	Plagiogranite - trondjhemite - epidosite	angular fragment	one side - CG Qtz + Plag w granular Ep + Chl + 2nd Oxides; other side approx 1 cm wide contains abundant granular Qtz and minor Oxides; diff to determine relatively of contact - possibly shear zone	Plag comp seriticized - appears as brown grains in PPL; Ep and Chl are dominant meta minerals; this sample looks like an epidosite	**EPIDOSITE!**

Sample	Location	Rock Type	Form	Mineralogy & Texture	Alteration	Comments
102-1-25	mid-slope high; Tonga Trench	vesicular basalt	angular fragment	VFG w VFG Plag laths unoriented in a cryptocrystalline matrix; few larger Plag phenocrysts; sample contains abundant vesicles filled w Carb minerals? ±Zeol ±Chl; vesicles may contain clay ?; clays line vesicles & carbonate fills	sample cut by several narrow veinlets; some veinlets may contain Ep?; GM appear to be alt to clay + Chl; some small grains of high biref min which may be Ep and or Cpx? in GM; some fractures are filled w Ep; Plag altered w patchy zoning	possible Ep filled veins; possible Ep in vesicles; Carb could be low t overprint
104-2-4	lower slope Tonga Trench	diabase	sub angular fragment	MG Plag Cpx ± Opx? + Oxides; Plag and some Pyx are zoned; larger Plag phenocrysts contain abundant inclusions at core; GM glassy;	sample is relatively fresh; Plag alt to FG ser ± Ep ± clay; Pyx alt Chl ± Amph along rims and fractures; GM is alt to Chl ± clay; no veins;	GM perv alt; phenocrysts relatively fresh; minor Ep;
104-2-6	lower slope Tonga Trench	alt diabase	angular fragment	MG Plag + Cpx + Oxides + green Amph + Chl; minerals are highly fractured and deformed; sample cut by 1 cm wide vein cont Qtz ± Zeol ± Amph ± Chl; fraGMents of GM are found in vein;	sp contains patchy alt w patches cont Chl + acicular Amph; Cpx alt to Amph + Chl; Plag alt to ser + Chl; some Oxide assoc. w Chl ± Amph alt; vein contains VFG Qtz	Qtz vein suggests low T; acicular Amph +Chl suggests greenschist facies conditions
105-1-4	Tonga trench slope	Ol gabbro	angular block	CG Plag + Cpx + Ol pseudo; sample cut by several veinlets with varying alt assemblages; minerals highly fractured and net veins x-cut minerals;	sample is highly alt particularly along veins and fractures; Ol comp pseudo to 2nd Oxide, clay, Talc, Amph + Chl; Cpx alt to Amph ± Chl; some veinlets cont Chl; others cont Zeol; some Qtz in veinlets; sample generally perv alt;	no fresh Ol; minor Oxides; evidence of deformation and recrystallization of Plag; sample particularly alt along veinlets
105-1-6	Tonga trench slope	Ol gabbro	angular block	MG subhedral Plag + Cpx + Ol + Ox; possible Opx; Pyx have sub ophitic text; Pyx have minor exsolution along cleavage; sample cut by a few narrow veinlets filled with splays of fibrous zeolites?;	Pyx alt to Amph ± Chl along margins; Ol alt to Idd; GM altered along margins of veins; sample generally fresh w abundant fresh Ol;	sample has weak foliation; large amount of Ol

Sample	Location	Rock Type	Form	Mineralogy & Texture	Alteration	Comments
105-1-8A	Tonga trench slope	gabbro	angular block	MG Plag + Cpx + colourless Amph + Amph + Chl ± zeolites; sample is cut by num veins interesting x-cutting relatively.; sample highly fractured w net veins cutting primary minerals;	perv alt w Plag alt to ser ± clay ± Chl; Pyx alt to acicular colourless Amph ± green Amph; sample cont; num veins filled w Ep; large vein in sample A contains titanite ± green diopside ?; large vein in sample A zoned from core to edge; some veins monomineralic Qtz?; Fault?; abundant CG Ep in veins; sample B cont abundant acicular colourless Amph; some narrow veinlets may cont zeolites?;	Very interesting!; possibly Plag - Amph geotherm; possibly Amph geochron; possible roddingite?; high t?; veins contain monomineralic granular Amph and acicular Amph;
105-1-10	Tonga trench slope	gabbro w dyke margin (margin not in TS)	angular block	sample cont M-CG Plag + Cpx + colourless Amph + Chl ± Serp?; one side cont abundant VCG Ep; Plag and Pyx are both highly fractured and deformed; sample cut by num net veins; some brown Amph?; minor Opx; some exsolution in Pyx along cleavages	one side of sample and vein cont abundant CG Ep +acicular Amph + Chl + hydro gross? ± Qtz; small veinlets which x-cut sample contain low biref minerals possibly Qtz or Zeol?; some tiny veinlets may contain brown hydro gross?; Plag in GM highly ser?; Cpx alt to Amph ± Chl; zoisite	some patches cont Chl ± acicular Amph; **geothermometry; hydro grossular; high T**
105-1-14	Tonga trench slope	gabbro	angular fragment	sample cont M to CG Plag + Cpx + granular primary? Amph + minor Opx + Oxides; Oxides assoc. w Amph; colourless isotropic min poikilitically encl in Amph (hydro gross? or Amph?) equant grains;	sample contains num fractures; GM alt proximal to fractures; fractures cont Amph ± Chl ± Ep; Oxides pres along cleavage in colourless, isotropic grains; Plag in GM alt to Ep ± Chl; some Plag recrystallized near fractures; some Cpx alt along cleavages & grain boundaries to colourless , acicular Amph;	presence of hydro grossular and primary brown Amph?; possibly high t?; geotherm & geochron; **very interesting**

Sample	Location	Rock Type	Form	Mineralogy & Texture	Alteration	Comments
105-1-19	Tonga trench slope	gabbro	angular fragment	MG Plag + Cpx + Amph + minor Opx; Cpx rimmed by primary Amph?; primary grains highly fractured and deformed; Plag appears to be recrystallized	Cpx alt to colourless, fibrous and granular Amph; GM contains FG acicular Amph + Chl; brown patches may be hydro gross?; small round reddish-brown, high biref clots (minerals?); some areas x-crossed by net veins which cont low biref material (Amph?)	abundant Amph; some primary; geothermometry?; hydrogrossular?; only minor Oxides; minor Ep in GM; some alt patches may contain zeolites
105-1-21	Tonga trench slope	Ol gabbro	angular fragment	MG Plag + Cpx + primary Amph? + Ol; brown Amph rims Cpx; 2nd? Oxides assoc. w Ol;	sample cut by several veinlets filled w Zeol; Plag highly alt proximal to veins; int x-cutting relatively; Ol relatively fresh; GM near veins alt to green-brown patches (Amph?);	some Pyx poikilitically enclose Plag; sample has evidence of layering; primary Amph; Zeol = low t?; Amph Plag geothermometer?; some Plag deformation and recrystallization
105-1-25	Tonga trench slope	gabbro	angular block	MG Plag + Cpx + Amph + Ep + hydro gross? + Oxides; Cpx rimmed by brown Amph; sample cut by numerous veins; Cpx poikilitically enclose Plag;	Cpx alt to Amph along cleavages, along rims, and near veins; several veins x-cutting sample contain monomineralic Amph; other veins cont Ep; interesting olive green small min grains in sample (not abundant); some alt patchy (filled w acicular colourless Amph);	Plag alt to Ep; some patches cont Chl? ± Amph; veins possibly contain zeolites; HIGH T?; geothermometry?; geochron?; very interesting

Sample	Location	Rock Type	Form	Mineralogy & Texture	Alteration	Comments
105-1-29	Tonga trench slope	gabbro (more dioritic)	sub angular block	MG Plag w primary Amph + Ep; Plag is somewhat layered; sample perv alt; some primary Cpx rimmed by Amph?;	sample perv alt; sample cont remnants of Cpx rimmed by Amph; Amph primary?; GM contains abundant colourless acicular Amph; some Amph may be replacing Cpx; GM also cont abundant Chl ± hydro gross?; Plag highly fractured and alt to Ep + ser ± Chl; prim Amph alt to colourless acicular Amph;	evolved sample; Amph and Ep suggest high T; Amph-Plag geotherm; geochron?; no Qtz; some layering;
105-3-2	Tonga trench slope	Plag phyric basalt	sub angular clast	F to MG Plag phenocrysts in crypto GM; sample cont FG Oxide phenocrysts; numerous vesicles Filled w FG Plag?, Zeol, Chl ± Ep; GM glassy; some GM contains FG Plag laths ± Qtz ± Chl ± Ep;	Plag sericitized and alt to Ep; GM cont Chl + Ep; Plag laths generally fresh (some alt as before); most high biref material believed to be Ep;	no Pyx; possible hydro gross; some Oxides alt to reddish-brown mat; GM made up of VFG Qtz ± Plag;
105-3-6	Tonga trench slope	Plag and Cpx phyric basalt	sub angular clast	Plag + Cpx phenocrysts in FG matrix (Plag + Cpx + Chl + Amph ± Qtz); phenocrysts are anhedral to euhedral; sample is cut by tiny Qtz? veinlets; sample cut by 1 large zoned vein w Ep + Qtz at margins and Ep + Qtz + Chl at centre (1-4mm diam);	phenocrysts are relatively fresh; Pyx alt to Amph + Chl at rims; some patches of Chl ± Amph near phenocrysts may be pseudo; GM is part alt; Plag in GM alt to ser + Ep + Chl; Ep vein x-cut by smaller veinlets (X-Cutting relatively);	**HIGH T?; abundant Ep and Amph; Qtz FI; geothermometer; Oxides alt to red-brown clots; Oxides VFG and disseminated;**
106-2-5	thought to be at very base of upper plate	Oxide gabbro	angular clast	CG Plag + Cpx + Opx? + Oxides; Pyx rimmed by Amph; Pyx/Amph grains poikilitically enclose Plag laths; sample cut by num veins	Plag alt to ser ± Ep particularly along veins; Cpx alt to green and fibrous colourless Amph; clots of Amph + 2nd Oxides + Chl may be Ol pseudo?; sample cut by net veins cont Zeol + Chl + Amph; Oxides altered along fractures -> titanite?;	**abundant CG Amph - some Amph may be primary; High T?; look at Oxides; some Chl assoc. w Plag;**

Sample	Location	Rock Type	Form	Mineralogy & Texture	Alteration	Comments
106-2-7	thought to be at very base of upper plate	diorite	angular clast	F to MG Plag + Amph + Qtz + Chl + Ep + Ox; no Pyx observed; numerous veins;	Plag almost comp ser; granular Amph alt to fibrous colourless Amph + Chl; some Oxides alt to red-brown patches; Plag alt to Ep + Chl; sample cut by num veins; some veins cont Qtz + Ep + Chl + Amph; others contain Qtz; GM proximal to veins perv alt;	some late stage veins cont brown mat and x-cut all other features and alter Oxides; highly evolved sample; abundant Amph; geotherm; geochron; abundant Oxides; perv alt; int x-cutting relatively
106-2-10	thought to be at very base of upper plate	gabbronorite	angular clast	CG Plag + poikilitic Cpx and Opx encl Plag; Pyx cont brown Amph incl?; brown Amph may be prim?; some brown high relief min may be tit assoc. w Cpx; brownish min assoc. w Amph may be hydro gross?; sample cont green high relatively isotropic min (Cr-rich hydro gross?)	Opx alt along fractures to Serp ± Idd; Pyx alt to Amph + Chl along edges; Plag alt to Ep ± Chl along fractures; veins cont Amph ± Ep ± Zeol minerals; some veins monomineralic	**some brown Amph primary? and poikilitic encl Plag; brownish and green min may be hydro gross (PROBE!); possibly geotherm + geochron**
106-2-11	thought to be at very base of upper plate	Oxide diorite	angular clast	3-8% interstitial Oxides + prim Amph? + Qtz + titanite + Ep; tit assoc. w Oxides; brown high biref min w high relatively assoc. w Ep (uncertain min); Chl in GM; Fl in Qtz; num veinlets; brown Amph poikilitic encl Plag	brown Amph alt along edges to green and colourless acicular Amph; Plag alt to Ep + Chl ± FG ser; some veins cont Ep ± Chl; Oxides alt to high biref min along cleavages (tit?); 1 green of brown min poikilitic encl in Amph (hydro gross?); some veinlets mono min Chl;	abundant titanite; interesting sample; very evolved; Amph alt suggest higher T; good for Amph geochron and geotherm; some patches of 2nd Amph + 2nd Oxides may have been prim Pyx; no fresh Pyx

Sample	Location	Rock Type	Form	Mineralogy & Texture	Alteration	Comments
106-3-5	thought to be at very base of upper plate	aphyric basalt	angular clast	Plag laths + Cpx + Opx in cryptocrystalline matrix (part devitrified); FG disseminated Oxides; some Pyx show bent cleavages and evidence of def; some zoning in Plag; matrix: brown material -> Amph + Chl + clay?; Plag laths random oriented.	Pyx and Plag relatively fresh; some Plag alt to ser + Ep + Chl; most alt restricted to GM; some Pyx alt to Amph ± Chl along rims;	sample relatively fresh; glassy matrix starting to devitrify; in PPL matrix is green-brown; some evidence of def
107-1-3	lower mid slope Tonga trench	Plag - Cpx phyric basalt	sub rounded fragment	FG Cpx + Plag + Oxides in alt GM; grains highly fractured; GM minerals - Chl + clay ± Qtz;	GM alt to red-brown clots near Oxides and green-brown minerals (Chl + clay?); no veins; some Ox of Oxides to red-brown minerals	predominantly greenschist facies min assemblage; some small narrow veinlets contain Qtz?;
107-1-14	lower mid slope Tonga trench	fractured aphyric basalt breccia	angular cobble	green Amph + Chl + Qtz + Plag + Oxides; green Amph may be prim?; sample cut by num Qtz veins; Qtz and Plag have und extinct; no Pyx; andesitic comp?	Plag is ser and alt to Ep + Chl; some granular Amph is alt to fibrous green and colourless Amph along edges ± Chl; large veins x-cut sample cont Zeol ± Qtz ± Ep; Zeol restrict to core w Qtz on margins; GM perv alt proximal to veins; int x-cutting relationships	**andesitic comp?; abundant Qtz w Fl; Plag-Amph geotherm; evolved sample**
108-1-6	mid slope Tonga trench	gabbroic breccia	unknown?	gabbroic blocks -> Cpx + Opx + Plag in FG muddy matrix w suspended clasts of Pyx + Plag; matrix is chloritic w patchy orange brown alt	Pyx alt to fibrous green Amph at margins of clasts and along fractures; Plag ser and alt to Chl along margins; several clasts rimmed by fib Amph and/or zeolite minerals?; GM is alt and grains within are fractured; GM cont some Qtz;	diff to distinguish Qtz from Zeol; some Pyx have mottled text - exsolution of Opx in Cpx or Amph; cores of Plag in clasts have incl;

Sample	Location	Rock Type	Form	Mineralogy & Texture	Alteration	Comments
108-2-1	mid slope Tonga trench	Ol gabbro	angular clast	CG to VCG Opx poikilitic encl Ol & Cpx + Plag + Ox; possibly Ol gabbronorite;	Pyx have mottled text w incl of Amph (possibly primary)?; some Ol fresh some alt along fractures to Serp + Idd; alt is patchy w FG Chl+Amph+Zeol?; most prim minerals highly fractured; Ol is alt to 2nd Mag; some FG patches may be recrystallized Plag?;	**abundant Serp (show Kathy) and amphibole; some fresh Ol; Amph poikilitic encl in Pyx may be prim; x-fiber text in Serp; interesting sample**
108-2-6	mid slope Tonga trench	Ol gabbro	sub angular clast	M to CG Plag + Ol + Cpx; Ol fresh; num small veinlets; some Pyx have sub ophitic text encl Plag;	Ol fractured and alt to Serp + Idd ± Amph ± Chl; GM cont patches filled w Amph ± Chl; min proximal to veins perv alt; veins cont Zeol?; GM Plag recrystallized near vein margins; Ol + Cpx in GM alt to Amph + Chl; some Plag is ser and alt to Ep + Chl	some Ol poikilitic encl Plag; Plag is relatively fresh
108-2-10	mid slope Tonga trench	lherzolite	sub angular clast	M to CG Cpx + Ol + Opx; ultramafic rock; large (4mm) Opx poikilitic encl Cpx; Ol comp pseudo; small Amph veins cut Opx and other minerals; grain size layering evident in TS	Ol completely altered mostly to Serp but also colourless Amph + 2nd Mag + Talc? + Amph; Opx alt to Talc? + Amph; Cpx alt to Amph + Chl	no Plag; abundant Amph; interesting to look at Amph veins; probe Talc vs. Amph;
108-2-12	mid slope Tonga trench	diorite - granophyric text	sub angular clast	F to MG Plag + Qtz + green Amph + Ep + Chl + Ap? + Ox + sulphides; Amph may be prim hornblende; sample cut by Ep vein and Chl + Ep veinlets; Oxides assoc. w Chl patches	Plag ser and alt to Ep ± Chl; primary green Amph alt to colourless Amph ± Chl; interstitial Ep; one side of sample slightly less alt; primary Amph fresher on one side	**abundant Fl in Qtz; Epidosite?; Plag Amph geotherm?; interesting; Fl have daughter minerals!**
108-3-1	mid slope Tonga trench	aphyric basaltic andesite	angular block	VFG Amph + Plag + Qtz + Oxides + minor Ep; sample cut by narrow Amph + Ep + Chl + sulphide vein; sample relatively fresh	Plag partially altered to sericite + Ep; some Amph alt to Chl; some Oxides alt to brown high biref min (titanite?); sample relatively fresh; no alt along vein margin	Fl in Qtz; interesting; geotherm / geochron?;

Sample	Location	Rock Type	Form	Mineralogy & Texture	Alteration	Comments
108-3-11	mid slope Tonga trench	micro-gabbro norite	sub angular fragment	FG to MG Plag + Cpx + Opx; Pyx have ophitic text encl Plag;	Cpx and Opx alt to Amph ± Chl along green boundaries and cleavages; some Pyx have mottled text; sample alt proximal to Qtz?/Zeol? veins; some veinlets contain Carb + Qtz ± Chl; possible mono min Amph veinlets?;	sample generally fresh; Plag may be recrystallized near some veins; diff to tell Qtz from FG Plag
108-3-15	mid slope Tonga trench	FG diorite - one side has possible fault breccia	sub angular block	FG Plag + Amph + Qtz + Oxides; minor sulphides; possibly some apatite	sample relatively fresh; some Amph alt to Chl ± 2nd Amph; Plag alt to FG ser ± Chl; Plag - Qtz boundaries show wormy text; sample cut by tiny veinlets (uncertain fill); Amph recrystallized near veinlets	abundant Amph; sample relatively fresh; possibly good for Plag Amph geotherm / geochron; Chl is not abundant; hard to determine T
108-3-16	mid slope Tonga trench	Basaltic Epidosite	angular block	FG Plag + Qtz + Ep + Chl + Oxide + Amph + apatite; FI in Qtz!; no veins observed; secondary Plag!	Oxides altered to brown min may be titanite; Plag alt to Ep + Chl; Chl clots in GM; some Chl + Amph clots may represent Amph or Pyx pseudo; GM contains granular Ep; some brown material in GM may be hydro gross?	**EPIDOSITE?; FI in Qtz; minor Amph; Oxides seem completely altered;**
108-3-17	mid slope Tonga trench	FG diorite	and block	FG Plag + Qtz + Amph + Chl + Ep + Oxides + sulphide ± apatite; minor titanite assoc. w Oxides;	Plag alt to Ep + Chl; Chl clots in GM; some Chl + Amph clots Amph pseudo; granular prim Amph alt to acicular Amph; GM contains abundant granular Ep; some brown material in GM may be hydro gross?	**sample epidotized; FI in Qtz; large Qtz grains assoc. w sulphides; Amph geotherm / geochron; very interesting!**

Sample	Location	Rock Type	Form	Mineralogy & Texture	Alteration	Comments
110-1-5	upper slope Tonga trench	aphyric basalt	angular block	VFG Plag + Cpx splays + Chl + Qtz + glass; fibrous mineral in veins may be acicular Amph; brown min may be hydro gross; sample cut by numerous veins; some structures appear to be asymmetric tension gashes - suggesting some shearing;	sample cut by numerous small Qtz veinlets and larger veins filled w Chl + Ep + Qtz; some veins zoned with Chl at margins and Qtz + Ep in centres; GM contains some Chl which is probably alt after Cpx and glassy material; some alt along vein margins	**Qtz has FI's; abundant epidote!; sample is definitely becoming epidotized (some Ep in GM); shear sense indicators; CG Ep + Chl + Qtz veins!**
110-1-7	upper slope Tonga trench	Plag glomero - porphyritic basalt breccia	angular block	MG Plag glomerocrysts in a VFG GM; VFG Cpx observed; sample is brecciated and fraGMents are cemented w Qtz + Ep; some small vesicles filled w Chl ± zeolites; minor Oxides and sulphides	Plag phenocrysts alt to ser ± Ep; GM alt patches of Chl possibly after Cpx; veins contain mostly CG Qtz with minor Ep ± Chl; some fine veins contain Chl + Ep w brown material ? at centres; host rock seems to be alt proximal to veins	**CG Ep + Qtz veins; FI in Qtz; some epidotized Plag in GM; very interesting**
110-1-15	upper slope Tonga trench	alt basalt	sub angular clast	FG Plag + Cpx + Ox + Chl + Amph + Ep; sample contains 5mm wide Ep + Qtz + Chl vein; sample cont some larger grains of Plag and Cpx; large Plag grains cont wormy Cpx incl; GM may cont some Qtz	Plag alt to Chl + Ep; Cpx alt to Amph + Chl; one patch Cpx gone and replaced by granular Amph; Oxides alt to brownish high biref material (Titanite?); Ep vein has slightly increased alt proximal to vein; GM is slightly silicified	**FI in Qtz; good sample for Plag Amph geotherm; one patch of alt is very pervasive and may be epidotization; sample epidotized**
110-1-17	upper slope Tonga trench	alt basalt	angular block	FG Plag + Cpx in a glassy matrix; grains are rounded and broken; GM contains a few grains of sulphide; sample contains several green stringers containing Chl + Ep + Qtz; possibly some acicular Amph assoc. w Qtz in veins; some Carb	GM alt to brown material + Chl; Ep + Chl replaces Plag; Cpx in GM partially alt to Chl ± Amph?; Oxides/sulphide found in vein; sample has patches containing one or more of: Chl ± Ep ± Qtz ± Carb ± brown material; some evidence of alt near stringers	very FG GM; diff to determine alt; Ep + Amph + Chl = relatively high T; Carb + Qtz suggest low T; grains broken up suggests deformation; some FI in large Qtz grains

Sample	Location	Rock Type	Form	Mineralogy & Texture	Alteration	Comments
110-1-25	upper slope Tonga trench	alt basaltic andesite	angular clast	FG Plag + Cpx + Amph + Chl + Ep + Ox ± titanite; sample cut by num veinlets which contain one or more of Chl ± Amph ± Ep ± Qtz ± orange min.	Oxides replaced by brown high biref min (titanite?); some opaques alt to red clots; orange fibrous min may be Amph? (ask Kathy); Plag alt to FG ser + Chl + Ep; Cpx perv alt in places to Amph ± Chl; alt increases near veins	**Qtz has FI; Plag Amph geotherm / geochron; interesting sample; red clots may have been sulphides**
110-1-25	upper slope Tonga trench	alt basaltic andesite	rounded clast	FG Plag + Cpx + Amph + Chl + Ep + Ox; sample cut by num veinlets (Chl ± Ep ± Qtz ± Amph)	Plag alt to FG ser + Chl + Ep; Cpx perv alt in places to Amph ± Chl; alt increases near veins; some opaques alt to brown high biref min (titanite) or red clots; GM appears silicified w interstitial Qtz; Qtz and Plag form wormy intergrowth text	**Qtz has FI; Plag Amph geotherm / geochron; interesting sample; red clots may have been sulphides**
110-1-27	upper slope Tonga trench	alt basalt	angular clast	FG Plag + Cpx + sulphide w minor glassy matrix; one side of sample is heavily veined and epidotized; brown amorphous min may be hydro grossular?	GM alt to Chl + Ep ± Amph?; Cpx alt to Chl ± Amph; Plag alt to FG ser + Ep ± Chl; sample cont 7 mm straight sided Qtz Ep vein w Ep at margins and Qtz in centre; sample heavily epidotized near vein margin;	**sample on its way to an epidosite; CG Qtz has small FI; possibly hydro grossular; abundant sulphide!**
110-1-32	upper slope Tonga trench	alt volcanic glass	sub angular clast	vitrophyre with devitrification spots containing Qtz ± Chl ± Ep ± Amph? ± titanite; sample cont tiny veinlets of Qtz ± Chl ± Ep; possibly a few grains of high biref zircon?	sample originally glassy and now contains VFG Qtz + Chl + Ep ± Amph ± titanite; some areas still glassy; some veinlets w coarser grained Qtz cut the sample	VFG; Qtz veinlets may have been source fro fluids; FG Ep + Qtz; some small FI in Qtz;
111-1-3	lower slope Tonga trench	aphyric basaltic andesite	angular clast	FG Plag + Qtz + Chl + Ep + Carb + Ox + some Cpx ± Amph; sample cut by light coloured vein; vein may be more evolved liquid intruded into basalt; vein has very similar mineralogy	Plag perv alt to ser + Chl + Ep + Carb; only minor Cpx; Chl clots may be after Pyx; "vein" contains more abundant Qtz + Chl; some small FI in Qtz; sample generally perv alt	**late magmatic vein cuts sample containing abundant Qtz + sulphides**; sample perv alt

Sample	Location	Rock Type	Form	Mineralogy & Texture	Alteration	Comments
111-4-3	lower slope Tonga trench	gabbro	angular clast	MG Plag + Cpx ± minor Opx; sample cut by several tiny veinlets; some Pyx sub ophitically enclose Plag	sample alt along fractures; Pyx alt to Chl + Amph; Plag alt to Chl ± clay; Qtz ± Zeol ± Chl ± Amph in veinlets that cut sample; sample perv alt near fractures and veins; late Chl veins cut everything;	pink min in TS off cut; may be hydro grossular; some granular Amph may be primary
112-2-1	upper slope Tonga trench	Ol gabbro	sub rounded fragment	VCG Cpx + Plag + Ol; grains up to 1-2 cm;	Ol grains replaced by Serp ± Talc?; Plag perv alt to sericite ± epidote; sample contains VFG alt material (low and high biref)	very coarse gained; no amphibole veins
112-2-6	upper part of steep fault scarp - upper slope Tonga trench	gabbro	sub rounded fragment	MG to CG Plag + Cpx + Ol; Plag may have encl Pyx?;	sample perv alt; Ol alt to Serp; Plag completely replaced by clay ± ser ± Chl; sample silicified and cont 2nd Qtz; sample cont splays of fibrous Zeol; Pyx relatively fresh; some fractured and have bent cleavages	Qtz + Zeol suggest low temp; Cpx relatively fresh
113-1-3	trench slope ImMiately below TF7	Cpx-Plag glomero-porphyritic basaltic andesite	angular block	MG Plag + Cpx + Opx + Qtz + Ox + Chl + Amph ± Ep; sample contains a few glomerocrysts of Cpx + Plag; some Ol pseudomorphs	sample is perv alt; Opx completely replaces by acicular Amph + Chl; Plag alt to FG ser + clay ± Chl; Ol pseudo by Amph + Chl + hematite; minerals heavily fractured; abundant Chl in GM	TS offcut has pink min; sample perv alt;
113-1-6	trench slope ImMiately below TF7	pervasively alt basalt	angular block	GM completely alt to Qtz + Chl + carbonate + Oxides;	complete loss of igneous text; large Carb & Qtz & Chl clots; GM VFG - may contain some Plag; Qtz / Chl veins x-cut sample	probably low t; **looks like an epidosite** but wrong mineralogy; interesting
113-1-7	trench slope ImMiately below TF7	sparsely Plag phyric basalt	sub rounded clast	VFG Plag + Ox ± Cpx? in glassy matrix; GM contains abundant Chl + Carb ± minor Ep;	sample cut by numerous Carb ± Qtz veins; GM is not necessarily more alt near veins but does cont more abundant Carb proximal to veins; vesicles filled w Chl + Carb	Carb + Qtz suggests low temp;

Sample	Location	Rock Type	Form	Mineralogy & Texture	Alteration	Comments
113-1-8	trench slope imMiately below TF7	brecciated basalt	sub rounded clast	similar to above sample; VFG sparsely Plag and Cpx phyric basalt w glassy GM; Cpx grains pseudo by Chl; Plag alt to Carb ± Ep?;	sample cut by numerous Carb ± Qtz veins; GM is more alt near veins; vesicles filled w Chl + Carb; some purplish alt observed in TS offcut	Carb + Qtz suggests low temp; margins on basalt pieces may be chilled - altered hyaloclastite
113-1-9	trench slope imMiately below TF7	olivine? - Cpx - Plag phyric basalt	sub rounded clast	VFG; primary minerals completely alt; sample cut by two 1-2 mm mono mineralic Chl veins	Ol/Cpx/Plag alt to Carb + Chl; GM contains abundant Carb + Chl + Qtz; sample cut by numerous Carb + Qtz veins	Carb + Qtz suggests low temp;
113-1-10	trench slope imMiately below TF7	epidotized basalt	angular block	FG Plag + Cpx + Qtz + Chl + Ep + Oxides ± Amph ± Carb; sample cut by 5mm Qtz + Ep vein	sample is pervasively alt; Plag alt to Chl + Ep; Cpx alt to Chl ± Amph; GM contains patches of Chl/Qtz/Carb; CG Qtz + Ep veins x-cut sample; some evidence of added alt proximal to vein	**sample epidotized; some loss of igneous text; abundant CG Ep; Qtz grains contain small FI**
113-1-11	trench slope imMiately below TF7	pervasively alt diabase?	angular block	MG Plag + Cpx ± Opx; sample completely alt; VFG "vein" may be late melt; sample cut by narrow carbonate veins	Pyx alt to Amph + Chl; Plag alt to FG ser + Chl + Carb; GM alt to green-brown material (mostly Chl); outlines of phenocrysts still preserved	Carb veins suggest low T
113-1-13	trench slope imMiately below TF7	altered diabase	sub rounded fragment	matrix pervasively alt; difficult to discern primary minerals; interesting opaque text along Pyx? cleavage? traces; GM contains Qtz + cal + Chl + Amph?	sample almost completely altered to Qtz + cal + Chl + Amph + opaques (hematite?); sample cut by 1 cm wide Qtz + Zeol? + Chl/Amph? vein; birefringence may be high	sulphides altered in vein; some Chl/Amph in vein?
113-1-16	trench slope imMiately below TF7	VFG alt basalt	sub rounded cobble	VFG Plag microphenocrysts + Qtz + Chl + Carb + Oxides in a glassy GM; sample cut by two 3-4mm carbonate-carbonate veins; Oxides may be secondary	GM alt to Chl + Carb; Plag alt to Carb + Chl; Chl more abundant near veins; small Qtz veinlets	Carb suggests low T

Sample	Location	Rock Type	Form	Mineralogy & Texture	Alteration	Comments
113-1-19	trench slope ImMiately below TF8	sparsely Plag phyric basalt	sub rounded clast	FG Plag phenocrysts in a glassy-crypto matrix; one side dark brown the other green; perv alt	sample pervasively alt to Chl + cal + Qtz; some veinlets and vesicles filled with Qtz-Chl; green side has slight breccia text; Plag phenocrysts completely replaced by cal ± Qtz ± Chl	
113-1-20	trench slope ImMiately below TF7	alt basalt / diabase	angular cobble	FG Plag + cp + Chl + Carb + Ep + Qtz + Ox; sample cut by narrow Carb veinlets	similar to above; some fresh Cpx; GM alt to Chl + Carb; Plag alt to Carb + Chl; minerals fractured; some brown alt	Carb suggests low T
113-1-22	trench slope ImMiately below TF7	aphyric basalt	sub angular fragment	FG Plag + Qtz + Carb + Chl + Ox; sample cut by narrow Carb veins	Plag alt to Chl + Carb; GM cont abundant Chl; abundant Carb + Qtz proximal to veins; GM brown colour	Low T?
113-1-26	trench slope ImMiately below TF7	Basaltic Epidosite	angular fragment	one side VFG Qtz + Ep + Ox + Chl + Oxides ± titanite other side coarser grained; two sections separated by Ep + Qtz vein	complete loss of igneous text; granular Ep concentrated at vein margin	**epidosite; small FI in Qtz**
113-1-30	trench slope ImMiately below TF7	basalt-basalt contact	angular cobble	FG Plag + phenocrysts pseudo (possibly Ol); very straight contact w 5mm Carb vein; grey half preserves igneous text; green half totally alt;	GM completely alt to Chl + Carb; phenocrysts completely alt to Chl + Carb or Qtz; may be Ol & Plag phenocrysts respectively	Low T ?; vein has interesting text with progressive layers of Carb deposited
113-1-31	trench slope ImMiately below TF9	sparsely Plag ±Cpx phyric basalt	angular cable	FG Plag ± Cpx phenocrysts in glassy-cryptocrystalline GM; Phenocrysts relatively fresh	sample contains vesicles filled with Chl + Qtz; pore space and veins filled with Qtz ± Zeol ±Serp; GM pervasively alt to Chl ± Serp? ± clay	

Appendix B

ELECTRON MICROPROBE DATA

Miroprobe analyses were performed using Camebax SX-50 and JEOL JXA-8900R electron microprobes at Oregon State University (OSU) and the University of Alberta (UofA), respectively. Operating conditions were similar (accelerating voltage 15 kV; beam current 20 nA) for both microprobes in order to minimize inter-lab variation. Instrument calibration was performed on natural standards and ZAF corrections were applied to all analyses.

In this appendix, micropbrobe data for the following primary and secondary minerals are summarized:

B1. Chlorite
B2. Epidote
B3. Prehnite
B4. Olivine
B5. Pyroxene
B6. Plagioclase
B7. Amphibole

Lab locations are listed under the sample number (UofA or OSU). Rock type has been simplified such that basalt, gabbro, and plagiogranite (PG) represent the broad varieties of rock types described in Chapter 3. Occurrence refers to the mode of occurrence determined by petrography. Further particulars are described in the notes at the bottom of the first page for each table.

Appendix B1. Chlorite Analyses (recalculated on the basis of 28 anhydrous O)

Sample	81-2-8A1	81-2-8A2	81-2-8A4	81-2-8B1	81-2-8B2	81-2-8B3	81-2-8B4	81-2-8B5	81-2-8B6	81-2-8B7	81-2-9A1	81-2-9A2	81-2-9B1	81-2-9B2	81-2-9B3	81-2-9C1
Rock Type	basalt	basalt	basalt	basalt	basalt	basalt	basalt	basalt	basalt	basalt	basalt	basalt	basalt	basalt	basalt	basalt
Location	UofA	UofA	UofA	UofA	UofA	UofA	UofA	UofA	UofA	UofA	UofA	UofA	UofA	UofA	UofA	UofA
Occurrence	ves	ves	gm	ves	ves	ves	ves	gm	gm	gm	ves	ves	gm	gm	gm	gm
SiO_2	30.31	29.66	30.15	29.73	28.54	30.07	29.47	30.08	28.59	28.95	28.62	28.12	27.53	28.07	27.89	28.00
TiO_2	b.d.	b.d.	b.d.	b.d.	b.d.	b.d.	b.d.	b.d.	0.04	0.01	0.03	0.04	b.d.	0.02	0.03	0.01
Al_2O_3	17.01	17.63	17.26	17.41	18.27	17.44	17.22	17.09	17.82	18.14	18.44	18.72	19.40	18.51	18.90	18.77
Cr_2O_3	0.02	0.01	0.05	0.01	0.01	0.01	0.01	b.d.	0.02	0.04	0.04	0.04	0.02	0.03	0.01	b.d.
FeO^T	17.43	18.18	17.41	18.01	18.34	17.95	18.13	17.64	18.32	18.13	19.60	19.48	20.33	19.41	19.69	19.99
MnO	0.40	0.40	0.42	0.41	0.41	0.39	0.36	0.40	0.38	0.34	0.48	0.48	0.53	0.46	0.49	0.49
MgO	20.69	20.81	20.89	20.94	20.14	20.59	19.94	20.72	20.21	20.77	19.63	19.20	18.86	19.23	19.49	19.47
CaO	0.24	0.18	0.27	0.27	0.32	0.24	0.35	0.33	0.18	0.21	0.08	0.10	0.07	0.09	0.05	0.01
Na_2O	0.04	0.03	0.04	0.05	0.03	0.05	0.03	0.05	0.08	0.05	0.05	0.02	0.07	0.06	0.01	0.04
K_2O	0.06	0.06	0.04	0.06	0.05	0.06	0.04	0.05	0.10	0.03	0.04	0.03	0.03	0.03	0.04	0.04
F	b.d.	b.d.	b.d.	b.d.	b.d.	b.d.	b.d.	b.d.	b.d.	b.d.	b.d.	b.d.	b.d.	b.d.	b.d.	b.d.
Cl	0.03	0.01	0.01	0.01	0.03	0.03	0.06	0.03	0.03	0.01	0.01	b.d.	0.02	0.04	b.d.	0.01
Total	86.23	86.97	86.54	86.90	86.14	86.83	85.61	86.39	85.77	86.68	87.02	86.23	86.86	85.95	86.60	86.83
Si	6.20	6.05	6.15	6.07	5.90	6.13	6.11	6.16	5.94	5.93	5.89	5.84	5.71	5.85	5.77	5.79
Al^{IV}	1.80	1.95	1.85	1.94	2.10	1.87	1.89	1.84	2.07	2.07	2.12	2.16	2.30	2.15	2.23	2.21
Al^{VI}	2.30	2.28	2.30	2.25	2.34	2.32	2.32	2.28	2.29	2.30	2.35	2.41	2.44	2.39	2.38	2.36
Ti	-	-	-	-	-	-	-	-	0.01	0.00	0.01	0.01	-	0.00	0.01	0.00
Fe^{2+}	2.98	3.10	2.97	3.07	3.17	3.06	3.14	3.02	3.18	3.11	3.37	3.38	3.52	3.38	3.41	3.46
Cr	0.00	0.00	0.01	0.00	0.00	0.00	0.00	-	0.00	0.01	0.01	0.01	0.00	0.01	0.00	-
Mn	0.07	0.07	0.07	0.07	0.07	0.07	0.06	0.07	0.07	0.06	0.08	0.08	0.09	0.08	0.09	0.09
Mg	6.31	6.33	6.35	6.37	6.20	6.26	6.16	6.32	6.25	6.34	6.02	5.94	5.83	5.97	6.01	6.00
Ca	0.05	0.04	0.06	0.06	0.07	0.05	0.08	0.07	0.04	0.05	0.02	0.02	0.02	0.02	0.01	0.00
Na	0.02	0.01	0.02	0.02	0.01	0.02	0.01	0.02	0.03	0.02	0.02	0.01	0.03	0.02	0.00	0.02
K	0.02	0.02	0.01	0.02	0.01	0.02	0.01	0.01	0.03	0.01	0.01	0.01	0.01	0.01	0.01	0.01
F	-	-	-	-	-	-	-	-	-	-	-	-	-	-	-	-
Cl	0.02	0.01	0.01	0.01	0.02	0.02	0.04	0.02	0.02	0.01	0.01	-	0.01	0.03	-	0.01
Cations	19.76	19.84	19.78	19.86	19.89	19.79	19.79	19.79	19.90	19.89	19.88	19.87	19.94	19.88	19.92	19.93

Notes: b.d. = below detection; n.d. = not determined; gm = groundmass; ves = vesicle; vel = vein; pla = in plagioclase; int = interstitial; am = associated with amphibole; inc = inclusion; cor = core; alt = alteration patch.

Appendix B1. Chlorite Analyses (continued)

Sample	81-2-9C2	90-4-3A1	90-4-3A2	90-4-3C1	90-4-3C2	94-1-1A1	94-1-1B1	94-1-1D1	94-1-1D2	94-1-2A2	96-1-10A1	96-1-10A2	96-1-10A3	96-1-10A4	96-1-10B1	96-1-10B2
Rock Type	basalt	gabbro	gabbro	gabbro	gabbro	gabbro	gabbro	gabbro	gabbro	gabbro	PG	PG	PG	PG	PG	PG
Location	UofA	UofA	UofA	UofA	UofA	OSU	OSU	OSU	OSU	OSU	UofA	UofA	UofA	UofA	UofA	UofA
Occurrence	gm	gm	gm	gm	gm	pla	vei	vei	vei	pla	gml	gmd	gm	gm	gm	gm
SiO_2	28.32	28.12	28.21	28.19	28.56	28.18	27.24	27.29	26.60	28.60	25.01	25.03	24.80	24.96	24.27	24.52
TiO_2	0.03	0.01	0.01	b.d.	b.d.	b.d.	0.02	0.02	0.02	0.01	0.02	0.02	0.03	0.03	b.d.	0.02
Al_2O_3	18.58	20.46	20.71	20.31	21.44	17.01	18.59	18.18	19.06	19.36	20.55	20.20	20.73	20.45	20.92	21.11
Cr_2O_3	0.01	0.02	0.01	b.d.	b.d.	n.d.	n.d.	n.d.	n.d.	n.d.	b.d.	0.01	0.01	0.01	b.d.	0.01
FeO^T	19.24	11.80	11.62	11.73	11.89	22.04	24.09	24.35	23.83	17.74	31.54	30.08	30.98	31.62	32.04	31.91
MnO	0.51	0.13	0.13	0.16	0.14	0.17	0.21	0.19	0.19	0.16	0.22	0.27	0.23	0.27	0.25	0.25
MgO	18.97	25.29	25.42	25.01	24.73	16.23	17.61	16.62	17.00	21.71	11.31	12.19	11.48	11.12	10.84	11.31
CaO	0.04	0.07	0.04	0.06	0.09	0.26	0.14	0.16	0.12	0.24	0.01	0.03	b.d.	b.d.	0.02	b.d.
Na_2O	0.03	0.01	0.01	0.02	0.01	0.10	0.03	0.07	0.06	0.06	0.03	0.02	0.03	0.02	0.02	b.d.
K_2O	0.04	0.03	0.01	0.03	0.07	n.d.	n.d.	n.d.	n.d.	n.d.	0.04	0.02	0.04	0.04	0.04	0.03
F	b.d.	b.d.	b.d.	b.d.	b.d.	0.10	0.05	0.04	0.08	b.d.	b.d.	b.d.	b.d.	b.d.	b.d.	b.d.
Cl	0.02	0.02	b.d.	b.d.	0.01	0.07	0.05	0.04	0.04	0.10	0.01	0.01	0.04	0.02	b.d.	0.02
Total	85.79	85.96	86.17	85.51	86.94	84.16	88.03	86.96	87.00	87.98	88.74	87.88	88.37	88.54	88.40	89.18
Si	5.90	5.61	5.61	5.65	5.63	6.09	5.69	5.78	5.62	5.76	5.39	5.41	5.36	5.40	5.28	5.27
Al^{IV}	2.10	2.39	2.39	2.35	2.37	1.91	2.31	2.22	2.38	2.24	2.61	2.59	2.64	2.60	2.72	2.73
Al^{VI}	2.46	2.43	2.46	2.45	2.60	2.42	2.26	2.31	2.36	2.35	2.61	2.56	2.63	2.61	2.64	2.62
Ti	0.01	0.00	0.00	-	-	-	0.00	0.00	0.00	0.00	0.00	0.00	0.01	0.01	-	0.00
Fe^{2+}	3.35	1.97	1.93	1.97	1.96	3.98	4.21	4.31	4.21	2.99	5.69	5.44	5.60	5.72	5.83	5.74
Cr	0.00	0.00	0.00	-	-	-	-	-	-	-	-	0.00	0.00	0.00	-	0.00
Mn	0.09	0.02	0.02	0.03	0.02	0.03	0.04	0.03	0.03	0.03	0.04	0.05	0.04	0.05	0.05	0.05
Mg	5.89	7.53	7.53	7.48	7.26	5.23	5.48	5.24	5.35	6.52	3.64	3.93	3.70	3.59	3.51	3.63
Ca	0.01	0.02	0.01	0.01	0.02	0.06	0.03	0.04	0.03	0.05	0.00	0.01	-	-	0.01	-
Na	0.01	0.00	0.00	0.01	0.00	0.04	0.01	0.03	0.03	0.02	0.01	0.01	0.01	0.01	0.01	-
K	0.01	0.01	0.00	0.01	0.02	-	-	-	-	-	0.01	0.01	0.01	0.01	0.01	0.01
F	-	-	-	-	-	0.14	0.07	0.05	0.11	-	-	-	-	-	-	-
Cl	0.01	0.01	-	-	0.01	0.05	0.04	0.03	0.03	0.07	0.01	0.01	0.03	0.02	-	0.02
Cations	19.82	19.98	19.96	19.95	19.89	19.76	20.02	19.96	20.01	19.95	20.00	20.01	20.00	19.99	20.05	20.05

Appendix B1. Chlorite Analyses (continued)

Sample	96-1-10B5	96-1-10B6	96-1-10C1	96-1-10C2	96-1-10C3	96-1-10C4	96-1-14A1	96-1-14A2	96-1-14A3	96-1-14A4	96-1-14A5	96-1-14B1	96-1-14B2	96-1-14B3	96-1-16A1
Rock Type	PG	PG	PG	PG	PG	PG	epidosite	epidosite	epidosite	epidosite	epidosite	epidosite	epidosite	epidosite	PG
Location	UofA	UofA	UofA	UofA	UofA	UofA	OSU	OSU	OSU	OSU	OSU	OSU	OSU	OSU	UofA
Occurrence	gm	gm	gm	gm	gm	gm	gm	gm	gm	pla	gm	gm	gm	gm	gm
SiO_2	25.14	26.04	24.39	25.34	25.26	24.51	24.87	24.34	23.58	24.38	23.82	24.41	24.99	25.58	25.20
TiO_2	0.01	0.06	0.03	0.02	0.02	0.05	0.08	0.05	0.03	0.01	0.03	0.01	0.01	0.14	0.03
Al_2O_3	20.33	19.09	21.32	19.55	20.08	21.26	20.21	20.13	19.40	19.44	20.77	19.40	19.62	19.96	19.36
Cr_2O_3	0.02	0.02	b.d.	0.01	b.d.	0.02	n.d.	n.d.	n.d.	n.d.	n.d.	n.d.	n.d.	n.d.	0.01
FeO^T	32.45	31.00	31.04	32.04	31.92	31.83	32.58	31.22	32.24	30.75	31.91	32.02	31.13	31.70	32.07
MnO	0.25	0.23	0.23	0.24	0.24	0.25	0.25	0.26	0.18	0.23	0.31	0.24	0.26	0.23	0.17
MgO	11.06	10.89	11.57	11.32	11.25	11.45	11.04	11.65	10.36	10.58	11.03	10.60	11.93	11.71	9.74
CaO	0.03	0.05	0.02	0.03	0.02	0.02	0.04	0.07	0.02	0.05	0.02	0.07	0.04	0.12	0.02
Na_2O	0.03	0.11	b.d.	0.03	b.d.	b.d.	0.07	0.05	0.07	0.24	0.05	0.03	0.03	0.03	0.21
K_2O	0.05	0.44	0.02	0.07	0.06	0.04	n.d.	n.d.	n.d.	n.d.	n.d.	n.d.	n.d.	n.d.	0.10
F	b.d.	b.d.	b.d.	b.d.	b.d.	b.d.	0.10	0.07	b.d.	0.03	b.d.	b.d.	0.08	0.05	0.07
Cl	0.01	0.02	0.01	0.02	0.02	0.02	0.08	0.05	0.02	0.09	0.04	0.05	0.04	0.03	0.02
Total	89.38	87.95	88.63	88.67	88.87	89.45	89.32	87.89	85.90	85.80	87.98	86.83	88.13	89.55	87.00
Si	5.41	5.66	5.26	5.49	5.45	5.25	5.37	5.32	5.32	5.46	5.22	5.42	5.43	5.47	5.58
Al^{IV}	2.59	2.34	2.75	2.51	2.55	2.75	2.63	2.68	2.68	2.54	2.78	2.58	2.57	2.53	2.42
Al^{VI}	2.56	2.55	2.66	2.48	2.55	2.62	2.51	2.50	2.47	2.58	2.57	2.50	2.46	2.49	2.63
Ti	0.00	0.01	0.01	0.00	0.00	0.01	0.01	0.01	0.01	0.00	0.01	0.00	0.00	0.02	0.01
Fe^{2+}	5.84	5.64	5.59	5.80	5.76	5.70	5.89	5.70	6.08	5.76	5.84	5.95	5.66	5.67	5.94
Cr	0.00	0.00	-	0.00	-	0.00	-	-	-	-	-	-	-	-	0.00
Mn	0.05	0.04	0.04	0.04	0.04	0.05	0.05	0.05	0.03	0.04	0.06	0.05	0.05	0.04	0.03
Mg	3.55	3.53	3.72	3.66	3.62	3.66	3.56	3.79	3.48	3.53	3.60	3.51	3.87	3.73	3.22
Ca	0.01	0.01	0.01	0.01	0.01	0.01	0.01	0.02	0.01	0.01	0.01	0.02	0.01	0.03	0.01
Na	0.01	0.05	-	0.01	-	-	0.03	0.02	0.03	0.10	0.02	0.01	0.01	0.01	0.09
K	0.01	0.12	0.01	0.02	0.02	0.01	-	-	-	-	-	-	-	-	0.03
F	-	-	-	-	-	-	0.14	0.10	-	0.04	-	-	0.11	0.07	0.10
Cl	0.01	0.02	0.01	0.02	0.02	0.02	0.06	0.04	0.02	0.07	0.03	0.04	0.03	0.02	0.02
Cations	20.02	19.96	20.03	20.02	20.00	20.05	20.05	20.09	20.11	20.03	20.10	20.04	20.05	20.00	19.94

Appendix B1. Chlorite Analyses (continued)

Sample	96-1-16A2	96-1-16A3	96-1-16A4	96-1-16B1	96-1-16B2	96-1-16B3	96-1-16B4	96-1-16C1	96-1-16C2	96-1-16D2	96-1-19B1	96-1-27A1	96-1-27A2	96-1-27B1	96-1-27B2
Rock Type	PG	PG	PG	PG	PG	PG	PG	PG	PG	PG	PG	PG	PG	PG	PG
Location	UofA	UofA	UofA	UofA	UofA	UofA	UofA	UofA	UofA	UofA	OSU	UofA	UofA	UofA	UofA
Occurrence	gm	gm	gm	vei	vei	vei	vei	gm	gm	gm	gm	gm	gm	gm	gm
SiO_2	25.13	27.29	25.24	26.18	25.76	24.44	26.55	26.27	26.79	25.34	28.16	24.62	25.91	24.84	25.35
TiO_2	0.05	b.d.	0.03	b.d.	b.d.	b.d.	b.d.	0.02	0.02	0.08	0.03	0.03	b.d.	b.d.	b.d.
Al_2O_3	19.62	19.78	19.54	20.97	20.50	21.94	19.70	19.74	20.71	16.59	18.74	21.51	20.91	21.25	21.21
Cr_2O_3	0.01	0.01	b.d.	b.d.	b.d.	b.d.	b.d.	b.d.	b.d.	b.d.	n.d.	b.d.	0.01	0.02	b.d.
FeO^T	32.61	26.01	31.13	30.38	30.06	31.97	29.38	29.13	30.30	33.65	20.11	32.07	25.75	29.24	29.12
MnO	0.16	0.13	0.14	0.18	0.17	0.18	0.16	0.16	0.15	0.11	0.51	0.14	0.29	0.19	0.18
MgO	10.14	14.90	11.36	10.98	11.25	10.04	12.94	12.38	11.31	12.29	20.66	10.83	15.47	12.80	13.28
CaO	0.03	0.18	0.05	0.10	0.10	0.02	0.02	0.09	0.13	0.16	0.06	b.d.	0.02	0.03	b.d.
Na_2O	0.08	b.d.	0.04	0.03	0.04	0.01	0.01	0.02	0.02	0.03	0.05	b.d.	b.d.	b.d.	0.02
K_2O	0.13	0.06	0.07	0.05	0.16	0.02	0.04	0.12	0.14	0.42	n.d.	0.03	0.03	0.03	0.03
F	0.08	0.01	0.03	0.05	0.07	0.05	0.05	0.04	0.02	0.07	0.13	0.03	b.d.	0.01	b.d.
Cl	0.01	0.02	0.03	0.03	0.02	0.02	0.03	0.01	b.d.	0.05	0.09	0.02	0.01	0.01	0.02
Total	88.05	88.39	87.66	88.95	88.13	88.69	88.88	87.98	89.59	88.79	88.54	89.28	88.40	88.42	89.21
Si	5.51	5.71	5.51	5.57	5.55	5.28	5.63	5.63	5.65	5.58	5.73	5.29	5.43	5.31	5.36
Al^{IV}	2.49	2.29	2.49	2.43	2.46	2.72	2.37	2.37	2.35	2.42	2.27	2.71	2.57	2.69	2.65
Al^{VI}	2.57	2.58	2.53	2.83	2.74	2.86	2.55	2.61	2.79	1.88	2.22	2.72	2.58	2.66	2.63
Ti	0.01	-	0.01	-	-	-	-	0.00	0.00	0.01	0.01	0.01	-	-	-
Fe^{2+}	5.98	4.55	5.68	5.41	5.41	5.78	5.21	5.22	5.34	6.20	3.42	5.76	4.51	5.23	5.14
Cr	0.00	0.00	-	-	-	-	-	-	-	-	-	-	0.00	0.00	-
Mn	0.03	0.02	0.03	0.03	0.03	0.03	0.03	0.03	0.03	0.02	0.09	0.03	0.05	0.03	0.03
Mg	3.31	4.65	3.70	3.48	3.61	3.23	4.09	3.96	3.56	4.03	6.26	3.47	4.83	4.08	4.18
Ca	0.01	0.04	0.01	0.02	0.02	0.01	0.01	0.02	0.03	0.04	0.01	-	0.00	0.01	-
Na	0.03	-	0.02	0.01	0.02	0.00	0.00	0.01	0.01	0.01	0.02	-	-	-	0.01
K	0.04	0.02	0.02	0.01	0.04	0.01	0.01	0.03	0.04	0.12	-	0.01	0.01	0.01	0.01
F	0.11	0.01	0.04	0.07	0.10	0.07	0.07	0.05	0.03	0.10	0.17	0.04	-	0.01	-
Cl	0.01	0.01	0.02	0.02	0.02	0.02	0.02	0.01	-	0.04	0.06	0.02	0.01	0.01	0.01
Cations	19.98	19.86	19.99	19.80	19.88	19.92	19.91	19.89	19.79	20.32	20.03	19.99	19.99	20.01	20.01

Appendix B1. Chlorite Analyses (continued)

Sample	96-1-27C1	96-1-27C2	96-1-27C3	96-1-27C4	96-1-27E1	96-1-27E2	96-1-27E3	96-1-27E4	96-1-29A1	96-1-29A2	96-1-29A3	96-1-2A1	96-1-2A2	96-1-2A3	96-1-2B1
Rock Type	PG	PG	PG	PG	PG	PG	PG	PG	PG/basalt	PG/basalt	PG/basalt	PG	PG	PG	PG
Location	UofA	UofA	UofA	UofA	UofA	UofA	UofA	UofA	OSU	OSU	OSU	UofA	UofA	UofA	UofA
Occurrence	gm	gm	gm	gm	gm	gm	gm	gm	gm	gm	gm	gm	gm	gm	gm
SiO_2	25.29	25.28	24.75	25.44	25.58	25.05	24.64	24.67	28.05	27.24	27.21	24.70	24.17	23.84	24.40
TiO_2	0.01	0.01	0.07	0.07	0.02	0.01	b.d.	0.04	0.05	0.06	0.02	0.02	0.05	0.02	0.03
Al_2O_3	21.31	20.62	20.81	21.54	21.08	21.01	21.06	20.97	16.83	17.20	17.35	20.26	21.01	20.71	21.08
Cr_2O_3	0.01	b.d.	0.02	b.d.	0.01	b.d.	b.d.	b.d.	n.d.	n.d.	n.d.	0.02	b.d.	b.d.	0.01
FeO^T	28.41	28.39	30.84	28.91	26.73	27.80	31.32	28.56	28.01	28.11	28.04	32.29	31.03	31.48	32.34
MnO	0.21	0.20	0.18	0.20	0.19	0.16	0.20	0.23	0.24	0.37	0.41	0.24	0.14	0.22	0.27
MgO	13.86	13.93	11.91	13.60	14.31	13.75	11.29	12.78	15.08	13.94	12.94	10.73	11.68	11.58	10.96
CaO	b.d.	0.01	b.d.	0.04	0.01	0.03	b.d.	0.03	0.18	0.17	0.22	0.04	0.02	0.01	0.05
Na_2O	0.01	0.04	b.d.	0.01	b.d.	0.01	b.d.	0.09	0.14	0.08	0.11	b.d.	0.03	0.01	0.01
K_2O	0.04	0.02	0.03	0.03	0.03	0.02	0.04	0.04	n.d.	n.d.	n.d.	0.10	0.04	0.01	0.03
F	0.02	b.d.	0.01	0.02	0.02	b.d.	0.04	b.d.	0.10	0.07	0.38	b.d.	b.d.	b.d.	b.d.
Cl	b.d.	0.01	b.d.	0.02	0.01	0.01	0.01	0.02	0.02	0.02	0.04	0.03	0.03	0.01	b.d.
Total	89.17	88.51	88.62	89.88	87.99	87.85	88.60	87.43	88.70	87.26	86.72	88.43	88.20	87.89	89.18
Si	5.33	5.37	5.33	5.33	5.41	5.35	5.32	5.32	5.93	5.87	5.93	5.38	5.24	5.21	5.26
Al^{IV}	2.67	2.63	2.68	2.68	2.59	2.65	2.68	2.68	2.07	2.13	2.07	2.62	2.76	2.79	2.74
Al^{VI}	2.61	2.53	2.60	2.64	2.66	2.63	2.67	2.65	2.13	2.24	2.38	2.57	2.61	2.54	2.62
Ti	0.00	0.00	0.01	0.01	0.00	0.00	-	0.01	0.01	0.01	0.00	0.00	0.01	0.00	0.01
Fe^{2+}	5.01	5.05	5.55	5.06	4.73	4.96	5.65	5.15	4.96	5.07	5.11	5.88	5.63	5.75	5.83
Cr	0.00	-	0.00	-	0.00	-	-	-	-	-	-	0.00	-	-	0.00
Mn	0.04	0.04	0.03	0.04	0.03	0.03	0.04	0.04	0.04	0.07	0.08	0.04	0.03	0.04	0.05
Mg	4.35	4.41	3.82	4.24	4.51	4.37	3.63	4.11	4.76	4.48	4.20	3.48	3.78	3.77	3.52
Ca	-	0.00	-	0.01	0.00	0.01	-	0.01	0.04	0.04	0.05	0.01	0.01	0.00	0.01
Na	0.00	0.02	-	0.00	-	0.00	-	0.04	0.06	0.03	0.05	-	0.01	0.00	0.00
K	0.01	0.01	0.01	0.01	0.01	0.01	0.01	0.01	-	-	-	0.03	0.01	0.00	0.01
F	0.03	-	0.01	0.03	0.03	-	0.06	-	0.13	0.10	0.52	-	-	-	-
Cl	-	0.01	-	0.01	0.01	0.01	0.01	0.02	0.01	0.02	0.03	0.02	0.02	0.01	-
Cations	20.03	20.05	20.02	20.01	19.96	20.01	20.00	20.02	19.98	19.94	19.86	20.02	20.07	20.12	20.05

Appendix B1. Chlorite Analyses (continued)

Sample	96-1-2B2	96-1-2C1	96-1-2C2	96-1-2C3	96-1-3A1	96-1-3A2	96-1-3B2	96-1-3B3	96-1-3C1	96-1-3C2	96-1-3C3	96-1-3D1	96-1-3D2	96-1-5B2	96-1-5B4	96-2-1A1
Rock Type	PG	PG	PG	PG	PG	PG	PG	PG	PG	PG	PG	PG	PG	PG	PG	basalt
Location	UofA	UofA	UofA	UofA	UofA	UofA	UofA	UofA	UofA	UofA	UofA	UofA	UofA	UofA	UofA	OSU
Occurrence	gm	gm	gm	gm	gm	gm	gm	gm	gm	gm	gm	gm	gm	gm	gm	int
SiO_2	24.70	24.43	24.38	23.78	24.12	24.06	25.04	25.26	23.90	24.73	24.41	24.93	25.49	25.26	25.18	27.30
TiO_2	0.05	0.10	0.06	0.04	0.07	0.05	0.01	0.04	0.08	0.04	0.03	0.08	0.07	0.04	0.01	0.06
Al_2O_3	20.69	21.15	21.12	21.64	21.20	21.32	19.07	19.61	21.08	20.39	20.87	20.84	20.97	19.28	19.61	17.09
Cr_2O_3	b.d.	b.d.	b.d.	b.d.	b.d.	b.d.	b.d.	b.d.	b.d.	b.d.	b.d.	b.d.	b.d.	0.01	b.d.	n.d.
FeO^T	31.52	30.82	31.95	33.52	33.50	31.58	32.05	30.90	31.95	31.85	33.65	31.68	31.31	31.99	31.61	28.72
MnO	0.28	0.21	0.29	0.32	0.24	0.27	0.34	0.30	0.21	0.27	0.25	0.25	0.22	0.23	0.23	0.46
MgO	11.46	11.97	10.42	9.18	9.25	10.65	11.02	11.59	10.73	10.99	10.03	11.12	11.44	11.05	11.13	13.06
CaO	0.20	b.d.	0.02	0.02	0.05	0.03	0.20	0.12	b.d.	0.03	b.d.	0.06	0.36	0.14	0.19	0.14
Na_2O	0.02	0.01	0.08	0.04	0.01	0.01	0.02	0.03	0.01	0.01	b.d.	0.05	0.04	0.09	0.11	0.05
K_2O	0.04	0.02	0.04	0.04	0.01	b.d.	0.03	0.02	0.01	b.d.	b.d.	b.d.	0.01	0.14	0.17	n.d.
F	b.d.	b.d.	b.d.	b.d.	0.09	0.05	0.04	b.d.	0.04	0.04	0.03	0.01	0.04	b.d.	b.d.	0.08
Cl	0.02	b.d.	0.02	0.02	0.01	0.02	0.01	0.01	0.02	b.d.	b.d.	b.d.	0.01	0.03	0.02	0.04
Total	88.98	88.71	88.38	88.60	88.55	88.04	87.83	87.88	88.03	88.35	89.27	89.02	89.96	88.26	88.26	87.00
Si	5.32	5.25	5.30	5.20	5.28	5.25	5.50	5.49	5.22	5.37	5.30	5.36	5.41	5.51	5.48	5.93
Al^{IV}	2.68	2.75	2.70	2.80	2.72	2.76	2.51	2.51	2.78	2.63	2.71	2.64	2.59	2.49	2.52	2.07
Al^{VI}	2.57	2.61	2.71	2.78	2.75	2.72	2.42	2.51	2.65	2.59	2.63	2.64	2.64	2.46	2.50	2.30
Ti	0.01	0.02	0.01	0.01	0.01	0.01	0.00	0.01	0.01	0.01	0.01	0.01	0.01	0.01	0.00	0.01
Fe^{2+}	5.68	5.54	5.81	6.13	6.13	5.76	5.88	5.62	5.84	5.79	6.11	5.70	5.55	5.83	5.75	5.21
Cr	-	-	-	-	-	-	-	-	-	-	-	-	-	0.00	-	-
Mn	0.05	0.04	0.05	0.06	0.04	0.05	0.06	0.06	0.04	0.05	0.05	0.05	0.04	0.04	0.04	0.09
Mg	3.68	3.84	3.38	3.00	3.02	3.46	3.61	3.76	3.50	3.56	3.24	3.56	3.62	3.59	3.61	4.23
Ca	0.05	-	0.01	0.01	0.01	0.01	0.05	0.03	-	0.01	-	0.01	0.08	0.03	0.04	0.03
Na	0.01	0.00	0.03	0.02	0.00	0.00	0.01	0.01	0.00	0.00	-	0.02	0.02	0.04	0.05	0.02
K	0.01	0.01	0.01	0.01	0.00	-	0.01	0.01	0.00	-	-	-	0.00	0.04	0.05	-
F	-	-	-	-	0.13	0.07	0.06	-	0.06	0.06	0.04	0.01	0.05	-	-	0.11
Cl	0.02	-	0.02	0.02	0.01	0.02	0.01	0.01	0.02	-	-	-	0.01	0.02	0.02	0.03
Cations	20.05	20.05	20.00	20.01	19.97	20.01	20.04	19.99	20.05	20.01	20.03	19.99	19.97	20.04	20.05	19.88

Appendix B1. Chlorite Analyses (continued)

Sample	96-2-1B1	96-2-1B2	96-2-1C1	96-2-1C2	96-2-1D2	96-2-1D3	96-2-1E1	96-2-1E2	96-2-7A1	96-2-7A2	96-2-7B1	96-2-7B2	96-2-7C1	96-2-7C2	99-1-30A1	99-1-30A2
Rock Type	basalt	basalt	basalt	basalt	basalt	basalt	basalt	basalt	basalt	basalt	basalt	basalt	basalt	basalt	gabbro	gabbro
Location	OSU	OSU	OSU	OSU	OSU	OSU	OSU	OSU	OSU	OSU	OSU	OSU	OSU	OSU	UofA	UofA
Occurrence	vei	gm	int	int	int	int	int	gm	gm	int	gm	gm	gm	gm	gm	gm
SiO_2	26.39	28.14	27.72	27.63	26.23	27.22	26.02	26.12	25.04	27.12	26.44	26.14	26.14	26.77	30.41	29.65
TiO_2	0.05	0.06	0.06	0.05	0.02	0.02	0.01	0.01	0.03	0.02	0.03	0.04	0.02	0.02	b.d.	b.d.
Al_2O_3	17.06	16.38	16.15	16.94	17.05	16.44	18.92	16.62	19.56	17.00	18.86	18.53	19.07	18.65	18.99	19.56
Cr_2O_3	n.d.	n.d.	n.d.	n.d.	n.d.	n.d.	n.d.	n.d.	n.d.	n.d.	n.d.	n.d.	n.d.	n.d.	b.d.	b.d.
FeO^T	29.24	29.69	28.87	28.31	29.70	29.77	30.57	29.16	26.93	26.26	27.70	25.86	28.06	25.59	12.50	12.57
MnO	0.54	0.56	0.47	0.52	0.47	0.56	0.74	0.59	0.32	0.29	0.35	0.29	0.28	0.24	0.14	0.13
MgO	13.36	14.08	14.29	14.34	12.94	14.12	12.88	12.55	14.58	15.66	14.86	15.63	14.45	14.24	25.49	25.52
CaO	0.06	0.10	0.11	0.13	0.09	0.04	0.03	0.06	0.01	0.10	0.07	0.49	0.03	0.22	0.14	0.07
Na_2O	0.05	0.02	0.08	0.10	0.06	0.03	0.02	0.28	0.04	0.10	0.07	0.04	0.02	0.23	0.02	0.02
K_2O	n.d.	n.d.	n.d.	n.d.	n.d.	n.d.	n.d.	n.d.	n.d.	n.d.	n.d.	n.d.	n.d.	n.d.	0.01	b.d.
F	b.d.	0.01	0.01	0.14	b.d.	b.d.	b.d.	0.12	b.d.	0.03	0.01	0.06	b.d.	0.18	b.d.	b.d.
Cl	0.02	0.02	0.06	0.06	0.04	0.02	0.02	0.03	0.02	0.03	0.04	0.08	0.03	0.05	0.01	0.01
Total	86.77	89.06	87.82	88.22	86.60	88.22	89.21	85.54	86.53	86.61	88.43	87.16	88.10	86.19	87.71	87.53
Si	5.78	5.98	5.97	5.91	5.77	5.86	5.56	5.82	5.42	5.84	5.61	5.59	5.57	5.77	5.95	5.82
Al^{IV}	2.23	2.02	2.04	2.10	2.23	2.14	2.44	2.18	2.58	2.16	2.39	2.41	2.43	2.23	2.05	2.18
Al^{VI}	2.17	2.08	2.06	2.17	2.18	2.03	2.33	2.19	2.41	2.15	2.32	2.26	2.36	2.51	2.32	2.34
Ti	0.01	0.01	0.01	0.01	0.00	0.00	0.00	0.00	0.01	0.00	0.01	0.01	0.00	0.00	-	-
Fe^{2+}	5.35	5.28	5.20	5.06	5.46	5.36	5.47	5.44	4.88	4.73	4.91	4.63	5.00	4.62	2.05	2.06
Cr	-	-	-	-	-	-	-	-	-	-	-	-	-	-	-	-
Mn	0.10	0.10	0.09	0.09	0.09	0.10	0.13	0.11	0.06	0.05	0.06	0.05	0.05	0.04	0.02	0.02
Mg	4.36	4.46	4.58	4.57	4.24	4.53	4.11	4.17	4.71	5.03	4.70	4.99	4.59	4.58	7.43	7.47
Ca	0.01	0.02	0.03	0.03	0.02	0.01	0.01	0.01	0.00	0.02	0.02	0.11	0.01	0.05	0.03	0.02
Na	0.02	0.01	0.03	0.04	0.03	0.01	0.01	0.12	0.02	0.04	0.03	0.02	0.01	0.10	0.01	0.01
K	-	-	-	-	-	-	-	-	-	-	-	-	-	-	0.00	-
F	-	0.01	0.01	0.19	-	-	-	0.17	-	0.04	0.01	0.08	-	0.25	-	-
Cl	0.02	0.01	0.04	0.04	0.03	0.02	0.02	0.02	0.02	0.02	0.03	0.06	0.02	0.04	0.01	0.01
Cations	20.02	19.96	19.99	19.97	20.03	20.05	20.05	20.05	20.08	20.02	20.04	20.07	20.03	19.90	19.86	19.92

Appendix B1. Chlorite Analyses (continued)

Sample	99-1-30A3	99-1-30A4	99-1-30B1	99-1-30B2	99-1-30B3	99-1-30B4	99-2-12A1	99-2-12A2	99-2-12A3	99-2-12B1	99-2-12B2	99-2-12B3	99-2-12B4	99-2-12C1	99-2-12C2
Rock Type	gabbro	gabbro	gabbro	gabbro	gabbro	gabbro	basalt	basalt	basalt	basalt	basalt	basalt	basalt	basalt	basalt
Location	UofA	UofA	UofA	UofA	UofA	UofA	UofA	UofA	UofA	UofA	UofA	UofA	UofA	UofA	UofA
Occurrence	gm	gm	gm	gm	gm	gm	gm	gm	gm	gm	gm	gm	gm	gm	gm
SiO_2	29.08	28.88	30.50	30.61	28.09	28.75	25.25	25.83	26.45	26.09	27.07	26.05	26.64	27.32	25.28
TiO_2	b.d.	b.d.	b.d.	0.01	b.d.	b.d.	0.02	0.02	b.d.	b.d.	b.d.	0.06	0.03	b.d.	b.d.
Al_2O_3	19.63	19.61	17.17	16.91	20.83	20.70	19.09	19.28	18.94	19.86	18.95	18.75	19.24	18.56	19.16
Cr_2O_3	b.d.	b.d.	0.03	b.d.	b.d.	b.d.	b.d.	0.03	b.d.	0.02	0.01	0.01	b.d.	b.d.	b.d.
FeO^T	12.40	13.17	13.82	14.01	12.05	12.13	27.27	28.03	23.69	28.18	24.31	24.85	24.15	25.56	26.25
MnO	0.14	0.16	0.16	0.13	0.09	0.07	0.73	0.73	1.02	0.74	0.69	0.94	1.06	0.83	0.91
MgO	25.59	25.08	24.78	24.10	24.97	24.77	14.18	13.96	16.24	14.43	17.09	15.88	16.05	15.42	14.86
CaO	0.06	0.07	0.20	0.29	0.04	0.06	0.04	0.08	0.11	0.04	0.04	0.10	0.06	0.16	0.02
Na_2O	0.02	0.01	0.02	0.03	0.01	0.10	b.d.	0.01	0.02	b.d.	b.d.	b.d.	0.03	0.06	0.04
K_2O	0.01	0.01	0.03	0.06	b.d.	b.d.	0.02	0.03	0.04	0.05	0.02	0.02	0.04	0.04	0.04
F	b.d.	b.d.	b.d.	b.d.	b.d.	b.d.	b.d.	b.d.	b.d.	b.d.	b.d.	b.d.	b.d.	b.d.	b.d.
Cl	0.02	b.d.	0.01	b.d.	0.01	b.d.	b.d.	0.01	0.01	b.d.	0.01	b.d.	0.02	0.03	b.d.
Total	86.95	86.99	86.72	86.15	86.09	86.58	86.60	88.01	86.52	89.41	88.19	86.66	87.32	87.98	86.56
Si	5.75	5.73	6.09	6.15	5.60	5.69	5.49	5.53	5.64	5.49	5.65	5.58	5.63	5.76	5.47
Al^{IV}	2.25	2.27	1.91	1.85	2.40	2.31	2.52	2.47	2.37	2.51	2.35	2.42	2.37	2.24	2.53
Al^{VI}	2.32	2.32	2.12	2.16	2.49	2.52	2.37	2.39	2.39	2.41	2.31	2.31	2.42	2.37	2.35
Ti	-	-	-	0.00	-	-	-	0.00	-	-	-	0.01	0.01	-	-
Fe^{2+}	2.05	2.19	2.31	2.36	2.01	2.01	4.95	5.02	4.22	4.96	4.25	4.45	4.27	4.51	4.75
Cr	-	-	0.01	-	-	-	-	0.01	-	0.00	0.00	0.00	-	-	-
Mn	0.02	0.03	0.03	0.02	0.02	0.01	0.13	0.13	0.18	0.13	0.12	0.17	0.19	0.15	0.17
Mg	7.54	7.42	7.37	7.22	7.42	7.31	4.59	4.46	5.16	4.53	5.32	5.07	5.06	4.85	4.79
Ca	0.01	0.02	0.04	0.06	0.01	0.01	0.01	0.02	0.03	0.01	0.01	0.02	0.01	0.04	0.01
Na	0.01	0.00	0.01	0.01	0.00	0.04	-	0.00	0.01	-	-	-	0.01	0.03	0.02
K	0.00	0.00	0.01	0.02	-	-	0.01	0.01	0.01	0.01	0.01	0.01	0.01	0.01	0.01
F	-	-	-	-	-	-	-	-	-	-	-	-	-	-	-
Cl	0.01	-	0.01	-	0.01	-	-	0.01	0.01	-	0.01	-	0.01	0.02	-
Cations	19.96	19.97	19.90	19.85	19.95	19.90	20.07	20.03	19.99	20.05	20.01	20.04	19.98	19.95	20.10

Appendix B1. Chlorite Analyses (continued)

Sample	99-2-1B1	99-2-1B3	99-2-1B4	101-1-24B1	101-1-24B4	101-1-2A1	101-1-2A2	101-1-2A3	101-1-2B1	101-1-2B2	102-4-1B2	102-4-1C1	102-4-1C2	102-4-1C3	102-4-1D1
Rock Type	basalt	basalt	basalt	basalt	basalt	basalt	basalt	basalt	basalt	basalt	epidosite	epidosite	epidosite	epidosite	epidosite
Location	UofA	UofA	UofA	UofA	UofA	UofA	UofA	UofA	UofA	UofA	UofA	UofA	UofA	UofA	UofA
Occurrence	am	am	am	gm	gm	gm	gm	gm	gm	gm	gm	gm	gm	gm	gm
SiO_2	28.72	27.75	28.25	29.29	28.56	29.67	29.47	28.98	31.07	28.51	29.92	27.78	27.44	29.31	29.44
TiO_2	0.08	0.06	0.05	0.04	0.02	0.03	0.06	0.04	0.03	0.05	b.d.	0.01	b.d.	b.d.	b.d.
Al_2O_3	18.62	20.75	20.51	15.37	16.87	15.28	15.06	16.42	15.50	17.13	19.47	20.60	20.63	19.89	20.30
Cr_2O_3	0.04	0.02	0.02	0.02	b.d.	0.01	0.01	b.d.	0.01	b.d.	b.d.	b.d.	b.d.	b.d.	b.d.
FeO^T	13.05	13.70	14.06	23.34	22.90	24.41	25.26	24.42	23.10	24.57	11.20	16.29	17.28	12.19	11.71
MnO	0.13	0.14	0.12	0.25	0.25	0.25	0.25	0.25	0.25	0.24	0.19	0.22	0.18	0.16	0.09
MgO	23.40	23.19	23.77	17.72	17.06	16.43	16.57	16.90	17.11	16.98	26.50	22.08	21.58	25.25	26.08
CaO	0.20	0.19	0.15	0.26	0.17	0.17	0.12	0.13	0.31	0.17	0.02	0.03	0.01	0.04	0.03
Na_2O	0.03	0.06	0.04	0.06	0.02	0.05	0.01	0.07	0.04	0.04	b.d.	b.d.	b.d.	0.01	b.d.
K_2O	0.03	0.02	0.02	0.06	0.06	0.15	0.15	0.12	0.19	0.08	0.03	0.01	0.02	0.02	0.01
F	b.d.	b.d.	b.d.	b.d.	b.d.	b.d.	b.d.	b.d.	b.d.	b.d.	0.20	0.15	0.12	0.20	0.21
Cl	0.01	0.03	0.03	b.d.	0.06	0.01	b.d.	0.01	0.01	0.01	b.d.	b.d.	b.d.	b.d.	b.d.
Total	84.31	85.91	87.02	86.41	85.97	86.46	86.96	87.34	87.62	87.78	87.53	87.17	87.26	87.07	87.87
Si	5.88	5.60	5.64	6.20	6.06	6.30	6.25	6.09	6.44	5.97	5.85	5.61	5.56	5.79	5.74
Al^{IV}	2.12	2.40	2.37	1.80	1.94	1.70	1.75	1.91	1.56	2.03	2.16	2.40	2.44	2.21	2.26
Al^{VI}	2.37	2.53	2.45	2.03	2.27	2.12	2.02	2.16	2.22	2.19	2.32	2.50	2.49	2.41	2.41
Ti	0.01	0.01	0.01	0.01	0.00	0.01	0.01	0.01	0.01	0.01	-	0.00	-	-	-
Fe^{2+}	2.24	2.31	2.35	4.13	4.06	4.34	4.48	4.29	4.00	4.30	1.83	2.75	2.93	2.01	1.91
Cr	0.01	0.00	0.00	0.00	-	0.00	0.00	-	0.00	-	-	-	-	-	-
Mn	0.02	0.02	0.02	0.05	0.05	0.05	0.05	0.05	0.04	0.04	0.03	0.04	0.03	0.03	0.02
Mg	7.15	6.98	7.07	5.59	5.39	5.20	5.24	5.30	5.29	5.30	7.72	6.64	6.52	7.43	7.58
Ca	0.04	0.04	0.03	0.06	0.04	0.04	0.03	0.03	0.07	0.04	0.00	0.01	0.00	0.01	0.01
Na	0.01	0.02	0.02	0.03	0.01	0.02	0.00	0.03	0.02	0.02	-	-	-	0.00	-
K	0.01	0.01	0.01	0.02	0.02	0.04	0.04	0.03	0.05	0.02	0.01	0.00	0.01	0.01	0.00
F	-	-	-	-	-	-	-	-	-	-	0.25	0.19	0.15	0.25	0.26
Cl	0.01	0.02	0.02	-	0.04	0.01	-	0.01	0.01	0.01	-	-	-	-	-
Cations	19.86	19.93	19.95	19.90	19.84	19.81	19.87	19.89	19.69	19.92	19.91	19.94	19.97	19.90	19.92

Appendix B1. Chlorite Analyses (continued)

Sample	102-4-1D2	102-4-1D3	102-4-1D4	105-1-14A1	105-1-14A2	105-1-25A1	105-1-6A1	105-1-6D2	105-1-8(b)C1	105-1-8(b)D1	105-3-6a1	105-3-6a2	105-3-6a3	105-3-6a4
Rock Type	epidosite	epidosite	epidosite	gabbro	gabbro	gabbro	gabbro	gabbro	gabbro	gabbro	basalt	basalt	basalt	basalt
Location	UofA	UofA	UofA	OSU	OSU	OSU	OSU	OSU	OSU	OSU	OSU	OSU	OSU	OSU
Occurrence	gm	gm	gm	gm	inc	vei	gm	pla	gm	gm	gm	gm	int	pla
SiO_2	28.60	29.38	28.30	25.78	24.94	28.01	27.50	30.32	28.37	28.48	27.45	27.26	26.84	26.81
TiO_2	b.d.	b.d.	0.02	0.01	0.08	b.d.	0.02	0.02	b.d.	b.d.	0.03	0.05	0.02	0.04
Al_2O_3	20.66	20.21	20.71	22.46	19.98	21.17	18.11	15.03	21.11	20.96	18.18	17.81	18.08	18.04
Cr_2O_3	b.d.	b.d.	b.d.	n.d.	n.d.	n.d.	n.d.	n.d.	n.d.	n.d.	n.d.	n.d.	n.d.	n.d.
FeO^T	14.74	12.56	16.19	14.11	26.84	12.87	28.62	18.77	9.91	9.52	27.73	28.93	27.81	28.28
MnO	0.12	0.18	0.18	0.21	0.24	0.18	0.37	0.25	0.16	0.19	0.38	0.41	0.40	0.37
MgO	24.44	25.79	22.97	21.68	14.67	24.40	14.48	22.35	26.44	27.00	15.38	14.26	14.61	14.22
CaO	b.d.	b.d.	0.01	0.10	0.15	0.01	0.18	0.18	b.d.	0.07	0.17	0.45	0.20	0.11
Na_2O	b.d.	b.d.	b.d.	0.02	0.07	0.02	0.07	0.05	0.01	0.02	0.04	0.05	0.03	0.03
K_2O	0.02	0.01	0.02	n.d.	n.d.	n.d.	n.d.	n.d.	n.d.	n.d.	n.d.	n.d.	n.d.	n.d.
F	0.19	0.25	0.20	0.13	0.08	b.d.	b.d.	b.d.	b.d.	b.d.	0.04	0.07	0.38	b.d.
Cl	0.02	b.d.	b.d.	0.05	0.08	0.02	0.11	0.12	0.02	0.05	0.06	0.06	0.09	0.06
Total	88.79	88.38	88.60	84.55	87.13	86.68	89.46	87.09	86.02	86.29	89.46	89.35	88.46	87.96
Si	5.62	5.73	5.61	5.32	5.37	5.57	5.78	6.21	5.60	5.60	5.75	5.76	5.72	5.74
Al^{IV}	2.39	2.27	2.39	2.68	2.63	2.43	2.22	1.79	2.40	2.40	2.25	2.24	2.28	2.27
Al^{VI}	2.39	2.37	2.45	2.78	2.43	2.53	2.27	1.84	2.50	2.45	2.23	2.20	2.27	2.28
Ti	-	-	0.00	0.00	0.01	-	0.00	0.00	-	-	0.01	0.01	0.00	0.01
Fe^{2+}	2.42	2.05	2.69	2.44	4.83	2.14	5.03	3.22	1.64	1.56	4.86	5.12	4.96	5.06
Cr	-	-	-	-	-	-	-	-	-	-	-	-	-	-
Mn	0.02	0.03	0.03	0.04	0.04	0.03	0.07	0.04	0.03	0.03	0.07	0.07	0.07	0.07
Mg	7.15	7.50	6.79	6.67	4.71	7.24	4.54	6.82	7.78	7.91	4.80	4.50	4.65	4.54
Ca	-	-	0.00	0.02	0.04	0.00	0.04	0.04	-	0.02	0.04	0.10	0.05	0.03
Na	-	-	-	0.01	0.03	0.01	0.03	0.02	0.00	0.01	0.02	0.02	0.01	0.01
K	0.01	0.00	0.01	-	-	-	-	-	-	-	-	-	-	-
F	0.24	0.31	0.25	0.17	0.11	-	-	-	-	-	0.05	0.09	0.51	-
Cl	0.01	-	-	0.04	0.06	0.01	0.08	0.08	0.01	0.03	0.04	0.04	0.07	0.04
Cations	19.99	19.95	19.96	19.95	20.09	19.95	19.98	19.98	19.95	19.97	20.01	20.01	20.00	19.98

Appendix B1. Chlorite Analyses (continued)

Sample	105-3-6a5	105-3-6B1	105-3-6B2	105-3-6C2	105-3-6C3	105-3-6C4	105-3-6D1	106-2-10A2	106-2-11B1	106-2-11C2	106-2-11C3	106-2-11D1	106-2-11D2	106-2-5a1
Rock Type	basalt	basalt	basalt	basalt	basalt	basalt	basalt	gabbro	PG	PG	PG	PG	PG	gabbro
Location	OSU	OSU	OSU	OSU	OSU	OSU	OSU	OSU	OSU	OSU	OSU	OSU	OSU	OSU
Occurrence	gm	gm	gm	gm	gm	int	gm	inc	gm	int	int	gm	gm	gm
SiO_2	25.62	25.88	25.59	26.44	25.70	27.14	26.40	25.42	23.89	23.51	23.01	23.87	24.46	26.50
TiO_2	0.02	0.06	0.04	0.03	0.04	0.03	0.03	0.09	0.03	0.02	0.02	0.04	0.09	0.01
Al_2O_3	19.32	19.02	19.86	19.11	18.96	18.34	18.51	17.82	21.08	20.10	20.06	20.49	20.96	19.73
Cr_2O_3	n.d.	n.d.	n.d.	n.d.	n.d.	n.d.	n.d.	n.d.	n.d.	n.d.	n.d.	n.d.	n.d.	n.d.
FeO^T	30.74	27.90	27.70	28.00	27.81	27.43	28.22	34.62	24.79	32.64	31.86	27.22	26.05	22.43
MnO	0.39	0.42	0.46	0.37	0.37	0.42	0.40	0.23	0.30	0.37	0.35	0.36	0.37	0.26
MgO	11.78	13.83	14.28	14.43	13.74	13.92	14.77	10.18	14.31	9.97	10.37	13.80	14.60	17.09
CaO	0.21	0.16	0.13	0.11	0.15	0.36	0.13	0.06	0.45	0.07	0.11	0.13	0.12	0.20
Na_2O	0.05	0.06	0.06	b.d.	0.06	0.07	0.03	0.05	0.12	0.04	0.09	0.03	0.07	0.10
K_2O	n.d.	n.d.	n.d.	n.d.	n.d.	n.d.	n.d.	n.d.	n.d.	n.d.	n.d.	n.d.	n.d.	n.d.
F	0.01	0.12	b.d.	b.d.	0.35	0.19	b.d.	0.06	0.05	b.d.	0.04	b.d.	0.06	0.09
Cl	0.12	0.09	0.09	0.06	0.06	0.05	0.04	0.04	0.03	0.04	0.06	0.08	0.11	0.06
Total	88.26	87.54	88.21	88.55	87.24	87.95	88.53	88.57	85.05	86.76	85.97	86.02	86.89	86.47
Si	5.55	5.57	5.45	5.61	5.57	5.79	5.61	5.61	5.23	5.26	5.19	5.23	5.26	5.59
Al^{IV}	2.45	2.43	2.55	2.40	2.43	2.21	2.39	2.39	2.78	2.74	2.81	2.77	2.74	2.41
Al^{VI}	2.48	2.40	2.44	2.38	2.40	2.40	2.25	2.24	2.66	2.55	2.52	2.51	2.57	2.50
Ti	0.00	0.01	0.01	0.01	0.01	0.01	0.01	0.02	0.01	0.00	0.00	0.01	0.02	0.00
Fe^{2+}	5.57	5.03	4.94	4.96	5.04	4.89	5.02	6.39	4.53	6.11	6.01	4.99	4.69	3.96
Cr	-	-	-	-	-	-	-	-	-	-	-	-	-	-
Mn	0.07	0.08	0.08	0.07	0.07	0.08	0.07	0.04	0.06	0.07	0.07	0.07	0.07	0.05
Mg	3.80	4.44	4.54	4.56	4.44	4.43	4.68	3.35	4.67	3.33	3.49	4.51	4.68	5.38
Ca	0.05	0.04	0.03	0.03	0.04	0.08	0.03	0.01	0.11	0.02	0.03	0.03	0.03	0.05
Na	0.02	0.03	0.03	-	0.03	0.03	0.01	0.02	0.05	0.02	0.04	0.01	0.03	0.04
K	-	-	-	-	-	-	-	-	-	-	-	-	-	-
F	0.01	0.16	-	-	0.48	0.26	-	0.08	0.07	-	0.06	-	0.08	0.12
Cl	0.09	0.07	0.07	0.04	0.04	0.04	0.03	0.03	0.02	0.03	0.05	0.06	0.08	0.04
Cations	19.99	20.01	20.05	20.00	20.01	19.91	20.06	20.07	20.07	20.09	20.15	20.12	20.08	19.97

Appendix B1. Chlorite Analyses (continued)

Sample	106-2-5a2	106-2-5b1	106-2-5c1	106-2-5c2	108-1-6D1	108-1-6D3	108-2-12A1	108-2-12A2	108-2-12B1	108-2-12B3	108-2-12C1	108-2-12C2	108-2-12C3	108-2-12C4
Rock Type	gabbro	gabbro	gabbro	gabbro	gabbro	gabbro	PG	PG	PG	PG	PG	PG	PG	PG
Location	OSU	OSU	OSU	OSU	UofA	UofA	UofA	UofA	UofA	UofA	UofA	UofA	UofA	UofA
Occurrence	gm	inc	int	int	vei	vei	gm	gm	vei	vei	gm	gm	gm	gm
SiO_2	26.53	26.18	26.12	28.41	31.05	31.09	23.54	23.83	23.55	24.37	24.70	24.46	24.62	25.22
TiO_2	0.02	0.12	0.04	0.02	b.d.	b.d.	0.01	b.d.	b.d.	0.04	b.d.	b.d.	b.d.	b.d.
Al_2O_3	19.22	19.08	20.35	18.78	18.13	18.03	19.94	20.52	18.84	19.81	19.61	19.95	19.74	19.99
Cr_2O_3	n.d.	n.d.	n.d.	n.d.	b.d.	b.d.	b.d.	0.02	b.d.	b.d.	b.d.	b.d.	b.d.	b.d.
FeO^T	24.91	26.11	26.71	24.93	11.92	11.55	38.32	38.60	36.46	32.79	32.00	32.95	32.69	32.38
MnO	0.27	0.29	0.33	0.35	0.16	0.16	0.29	0.32	0.39	0.32	0.28	0.35	0.31	0.30
MgO	15.69	15.35	14.87	17.28	26.70	25.43	5.52	4.48	4.72	8.10	9.58	8.48	8.94	9.72
CaO	0.20	0.14	0.09	0.48	0.12	0.23	0.03	0.09	0.20	0.06	0.07	0.07	0.04	0.08
Na_2O	0.03	0.14	0.02	0.10	0.04	0.18	0.03	0.02	0.11	0.03	0.05	0.02	0.04	0.04
K_2O	n.d.	n.d.	n.d.	n.d.	b.d.	0.04	0.01	0.01	b.d.	0.01	0.03	0.05	0.02	0.03
F	b.d.	b.d.	0.02	0.18	b.d.	b.d.	b.d.	b.d.	b.d.	b.d.	b.d.	b.d.	b.d.	b.d.
Cl	0.03	0.14	0.05	0.16	0.03	0.04	b.d.	b.d.	b.d.	0.01	0.01	0.01	b.d.	0.02
Total	86.90	87.55	88.60	90.69	88.15	86.75	87.69	87.89	84.27	85.54	86.33	86.34	86.40	87.78
Si	5.64	5.57	5.49	5.78	6.03	6.12	5.36	5.41	5.56	5.52	5.51	5.49	5.51	5.53
Al^{IV}	2.36	2.43	2.51	2.22	1.97	1.88	2.64	2.59	2.44	2.48	2.49	2.51	2.49	2.47
Al^{VI}	2.45	2.36	2.53	2.28	2.17	2.30	2.71	2.90	2.80	2.80	2.66	2.76	2.71	2.69
Ti	0.00	0.02	0.01	0.00	-	-	0.00	-	-	0.01	-	-	-	-
Fe^{2+}	4.43	4.65	4.70	4.24	1.94	1.90	7.30	7.33	7.20	6.21	5.97	6.18	6.12	5.94
Cr	-	-	-	-	-	-	-	0.00	-	-	-	-	-	-
Mn	0.05	0.05	0.06	0.06	0.03	0.03	0.06	0.06	0.08	0.06	0.05	0.07	0.06	0.06
Mg	4.97	4.87	4.66	5.24	7.73	7.46	1.87	1.52	1.66	2.73	3.19	2.84	2.98	3.18
Ca	0.05	0.03	0.02	0.11	0.03	0.05	0.01	0.02	0.05	0.02	0.02	0.02	0.01	0.02
Na	0.01	0.06	0.01	0.04	0.02	0.07	0.01	0.01	0.05	0.01	0.02	0.01	0.02	0.02
K	-	-	-	-	-	0.01	0.00	0.00	-	0.00	0.01	0.01	0.01	0.01
F	-	-	0.03	0.23	-	-	-	-	-	-	-	-	-	-
Cl	0.02	0.10	0.04	0.11	0.02	0.03	-	-	-	0.01	0.01	0.01	-	0.02
Cations	19.95	20.04	19.98	19.98	19.90	19.82	19.96	19.84	19.84	19.84	19.92	19.88	19.90	19.90

Appendix B1. Chlorite Analyses (continued)

Sample	108-2-12C5	108-2-12D1	108-2-12D2	108-2-12D3	108-2-12D4	108-3-16A1	108-3-16A2	108-3-16A3	108-3-16A4	108-3-16A5	108-3-16C1	108-3-16C2	108-3-16C3
Rock Type	PG	PG	PG	PG	PG	epidosite	epidosite	epidosite	epidosite	epidosite	epidosite	epidosite	epidosite
Location	UofA	UofA	UofA	UofA	UofA	UofA	UofA	UofA	UofA	UofA	UofA	UofA	UofA
Occurrence	gm	gm	gm	gm	gm	gm	gm	gm	gm	gm	gm	gm	gm
SiO_2	25.17	25.22	24.51	24.77	26.43	27.98	28.91	28.08	29.00	28.63	29.42	28.98	29.79
TiO_2	b.d.	0.03	0.04	b.d.	b.d.	b.d.	b.d.	b.d.	b.d.	b.d.	b.d.	b.d.	b.d.
Al_2O_3	19.56	19.52	18.79	20.00	19.64	17.82	18.26	18.70	18.02	16.67	17.71	16.59	17.75
Cr_2O_3	b.d.	b.d.	b.d.	b.d.	0.01	b.d.	b.d.	b.d.	0.01	b.d.	b.d.	b.d.	b.d.
FeO^T	31.82	30.97	30.14	32.24	29.49	24.99	22.85	23.48	22.23	24.94	22.36	24.05	20.00
MnO	0.29	0.32	0.32	0.36	0.32	0.31	0.36	0.32	0.38	0.33	0.30	0.32	0.32
MgO	9.94	10.66	10.53	10.15	12.01	17.22	19.41	18.11	19.00	17.55	19.55	18.36	21.00
CaO	0.05	0.07	0.11	0.04	0.07	0.02	0.03	0.02	0.09	0.03	0.03	b.d.	0.07
Na_2O	0.03	b.d.	0.01	0.01	0.01	0.02	b.d.	b.d.	0.01	0.01	0.01	b.d.	0.01
K_2O	0.05	0.03	0.04	0.01	0.02	0.01	0.01	0.03	b.d.	0.02	0.04	0.02	0.01
F	b.d.	b.d.	b.d.	b.d.	b.d.	b.d.	0.01	b.d.	0.06	0.05	b.d.	0.03	b.d.
Cl	b.d.	0.02	0.04	0.02	0.02	0.02	0.01	b.d.	0.01	b.d.	0.01	b.d.	b.d.
Total	86.91	86.84	84.53	87.60	88.02	88.39	89.85	88.74	88.81	88.23	89.43	88.35	88.95
Si	5.56	5.55	5.55	5.45	5.67	5.83	5.85	5.77	5.92	5.98	5.96	6.01	5.99
Al^{IV}	2.44	2.45	2.45	2.55	2.33	2.17	2.16	2.23	2.08	2.02	2.05	1.99	2.02
Al^{VI}	2.65	2.62	2.56	2.62	2.63	2.21	2.19	2.30	2.25	2.08	2.18	2.06	2.19
Ti	-	0.01	0.01	-	-	-	-	-	-	-	-	-	-
Fe^{2+}	5.88	5.70	5.71	5.93	5.29	4.36	3.86	4.04	3.79	4.36	3.79	4.17	3.36
Cr	-	-	-	-	0.00	-	-	-	0.00	-	-	-	-
Mn	0.05	0.06	0.06	0.07	0.06	0.06	0.06	0.06	0.07	0.06	0.05	0.06	0.05
Mg	3.27	3.50	3.56	3.33	3.84	5.35	5.85	5.55	5.78	5.46	5.90	5.67	6.29
Ca	0.01	0.02	0.03	0.01	0.02	0.00	0.01	0.00	0.02	0.01	0.01	-	0.02
Na	0.01	-	0.00	0.00	0.00	0.01	-	-	0.00	0.00	0.00	-	0.00
K	0.01	0.01	0.01	0.00	0.01	0.00	0.00	0.01	-	0.01	0.01	0.01	0.00
F	-	-	-	-	-	-	0.01	-	0.08	0.07	-	0.04	-
Cl	-	0.02	0.03	0.02	0.02	0.01	0.01	-	0.01	-	0.01	-	-
Cations	19.90	19.91	19.94	19.96	19.85	19.98	19.98	19.96	19.91	19.97	19.93	19.96	19.91

Appendix B1. Chlorite Analyses (continued)

Sample	108-3-16C4	108-3-17C1	108-3-17E2	110-1-15B1	110-1-15B2	110-1-15D1	110-1-15D2	110-1-15E1	110-1-15E2	110-1-15E3	110-1-15F1	110-1-15F2	110-1-15F3
Rock Type	epidosite	PG	PG	basalt	basalt	basalt	basalt	basalt	basalt	basalt	basalt	basalt	basalt
Location	UofA	UofA	UofA	UofA	UofA	UofA	UofA	UofA	UofA	UofA	UofA	UofA	UofA
Occurrence	gm	gm	gm	vei	vei	gm	gm	gm	gm	gm	gm	gm	gm
SiO_2	29.06	24.17	25.14	25.92	26.95	26.34	27.10	26.01	26.69	27.28	28.76	28.55	28.79
TiO_2	b.d.	b.d.	b.d.	b.d.	b.d.	0.12	0.01	0.01	0.05	0.05	0.02	0.04	0.04
Al_2O_3	18.41	19.79	19.90	19.36	19.55	19.79	18.87	18.12	19.43	18.90	16.23	16.46	16.06
Cr_2O_3	b.d.	b.d.	0.02	b.d.	b.d.	b.d.	b.d.	0.04	0.05	0.06	0.05	0.06	0.06
FeO^T	20.98	30.39	27.22	23.87	23.89	25.61	24.60	24.42	25.57	25.53	26.66	26.58	26.12
MnO	0.34	0.28	0.28	0.25	0.25	0.30	0.27	0.24	0.25	0.28	0.22	0.26	0.25
MgO	19.93	10.40	12.17	16.74	16.93	15.90	16.42	15.24	16.02	16.28	16.40	16.52	16.22
CaO	0.06	0.10	0.09	0.06	0.11	0.17	0.16	0.11	0.07	0.08	0.06	0.12	0.07
Na_2O	b.d.	b.d.	0.06	0.03	0.01	0.03	0.02	0.02	b.d.	b.d.	0.05	0.05	0.01
K_2O	0.01	0.04	0.04	b.d.	b.d.	0.01	0.01	0.05	0.07	0.08	0.03	0.06	0.04
F	0.02	b.d.	b.d.	0.01	0.02	b.d.	b.d.	0.01	0.04	0.01	0.01	b.d.	0.03
Cl	0.01	0.01	0.03	0.01	0.01	0.01	0.01	b.d.	b.d.	b.d.	b.d.	0.02	b.d.
Total	88.82	85.18	84.95	86.25	87.72	88.28	87.47	84.27	88.24	88.55	88.49	88.72	87.69
Si	5.88	5.43	5.55	5.53	5.63	5.53	5.70	5.71	5.60	5.70	6.04	5.98	6.09
Al^{IV}	2.12	2.57	2.45	2.47	2.37	2.47	2.30	2.29	2.40	2.31	1.96	2.02	1.91
Al^{VI}	2.27	2.67	2.73	2.39	2.44	2.42	2.38	2.39	2.40	2.34	2.05	2.04	2.08
Ti	-	-	-	-	-	0.02	0.00	0.00	0.01	0.01	0.00	0.01	0.01
Fe^{2+}	3.55	5.71	5.03	4.26	4.17	4.49	4.33	4.48	4.49	4.46	4.68	4.66	4.62
Cr	-	-	0.00	-	-	-	-	0.01	0.01	0.01	0.01	0.01	0.01
Mn	0.06	0.05	0.05	0.05	0.04	0.05	0.05	0.05	0.04	0.05	0.04	0.05	0.05
Mg	6.02	3.48	4.01	5.32	5.27	4.97	5.15	4.98	5.01	5.07	5.13	5.16	5.11
Ca	0.01	0.02	0.02	0.01	0.03	0.04	0.04	0.03	0.02	0.02	0.01	0.03	0.02
Na	-	-	0.03	0.01	0.00	0.01	0.01	0.01	-	-	0.02	0.02	0.00
K	0.00	0.01	0.01	-	-	0.00	0.00	0.01	0.02	0.02	0.01	0.02	0.01
F	0.03	-	-	0.01	0.03	-	-	0.01	0.05	0.01	0.01	-	0.04
Cl	0.01	0.01	0.02	0.01	0.01	0.01	0.01	-	-	-	-	0.01	-
Cations	19.92	19.95	19.87	20.04	19.96	20.01	19.96	19.95	19.99	19.97	19.96	19.99	19.91

Appendix B1. Chlorite Analyses (continued)

Sample	110-1-25A1	110-1-25A2	110-1-25A3	110-1-25A4	110-1-25A5	110-1-25C1	110-1-25C2	110-1-25C3	110-1-25C4	110-1-25C5	110-1-25C6	110-1-32A1	110-1-32A2
Rock Type	basalt	basalt	basalt	basalt	basalt	basalt	basalt	basalt	basalt	basalt	basalt	basalt	basalt
Location	UofA	UofA	UofA	UofA	UofA	UofA	UofA	UofA	UofA	UofA	UofA	UofA	UofA
Occurrence	gm	gm	gm	gm	gm	vei	vei	vei	vei	gm	gm	gm	gm
SiO_2	26.41	25.81	26.69	25.67	26.15	26.71	25.42	26.55	26.89	26.49	26.37	28.67	28.92
TiO_2	0.09	0.09	0.02	b.d.	0.02	0.02	0.01	b.d.	b.d.	b.d.	0.01	0.01	0.07
Al_2O_3	19.20	18.86	18.69	19.39	19.76	19.67	18.29	19.08	18.77	18.78	18.36	18.07	17.78
Cr_2O_3	0.05	0.05	0.01	0.02	0.01	0.03	0.01	b.d.	b.d.	0.27	0.52	0.04	0.06
FeO^T	27.36	27.42	27.04	28.06	28.04	26.47	26.75	26.22	26.36	25.46	26.32	17.74	17.02
MnO	0.27	0.29	0.24	0.28	0.23	0.30	0.30	0.31	0.34	0.26	0.27	0.22	0.22
MgO	13.75	13.62	13.98	13.51	13.83	15.38	13.89	14.59	14.75	15.20	14.02	20.03	20.32
CaO	0.30	0.11	0.43	0.06	0.08	0.06	0.05	0.17	0.27	0.11	0.15	0.09	0.20
Na_2O	0.02	b.d.	0.05	0.04	0.05	0.04	0.01	0.01	b.d.	0.11	0.05	0.08	0.06
K_2O	0.06	0.05	0.04	0.04	0.02	0.05	0.04	0.03	0.02	0.10	0.21	0.02	0.07
F	b.d.	b.d.	b.d.	b.d.	b.d.	b.d.	b.d.	b.d.	b.d.	b.d.	b.d.	b.d.	b.d.
Cl	0.03	0.02	0.02	0.02	0.04	0.02	0.01	0.01	0.01	0.01	0.01	0.07	0.07
Total	87.54	86.32	87.21	87.09	88.23	88.75	84.78	86.97	87.41	86.79	86.29	85.04	84.79
Si	5.65	5.61	5.72	5.55	5.56	5.59	5.62	5.68	5.72	5.66	5.71	5.97	6.02
Al^{IV}	2.35	2.39	2.28	2.46	2.44	2.41	2.38	2.33	2.28	2.34	2.29	2.03	1.98
Al^{VI}	2.48	2.44	2.44	2.48	2.51	2.44	2.38	2.48	2.43	2.39	2.39	2.41	2.38
Ti	0.01	0.02	0.00	-	0.00	0.00	0.00	-	-	-	0.00	0.00	0.01
Fe^{2+}	4.89	4.99	4.85	5.07	4.99	4.64	4.95	4.69	4.69	4.55	4.77	3.09	2.96
Cr	0.01	0.01	0.00	0.00	0.00	0.01	0.00	-	-	0.05	0.09	0.01	0.01
Mn	0.05	0.05	0.04	0.05	0.04	0.05	0.06	0.06	0.06	0.05	0.05	0.04	0.04
Mg	4.38	4.41	4.47	4.35	4.38	4.80	4.58	4.65	4.68	4.84	4.53	6.22	6.31
Ca	0.07	0.03	0.10	0.01	0.02	0.01	0.01	0.04	0.06	0.03	0.04	0.02	0.05
Na	0.01	-	0.02	0.02	0.02	0.02	0.00	0.00	-	0.05	0.02	0.03	0.02
K	0.02	0.01	0.01	0.01	0.01	0.01	0.01	0.01	0.01	0.03	0.06	0.01	0.02
F	-	-	-	-	-	-	-	-	-	-	-	-	-
Cl	0.02	0.02	0.02	0.02	0.03	0.01	0.01	0.01	0.01	0.01	0.01	0.05	0.05
Cations	19.92	19.96	19.93	19.99	19.97	19.98	20.00	19.92	19.92	19.98	19.94	19.82	19.80

Appendix B1. Chlorite Analyses (continued)

Sample	110-1-32B2	110-1-5AA2	110-1-5AA3	110-1-5AA4	110-1-5AA5	110-1-5AA6	110-1-5AA7	110-1-5AA8	110-1-5AB1	110-1-5AB2	110-1-5AB3	110-1-5AB4	110-1-5AB5
Rock Type	basalt	basalt	basalt	basalt	basalt	basalt	basalt	basalt	basalt	basalt	basalt	basalt	basalt
Location	UofA	UofA	UofA	UofA	UofA	UofA	UofA	UofA	UofA	UofA	UofA	UofA	UofA
Occurrence	gm	cor	rim	rim	rim	rim	cor	cor	vei	vei	vei	gm	gm
SiO_2	27.75	27.15	26.78	27.42	27.50	27.38	26.67	26.65	27.17	27.45	27.50	26.84	26.61
TiO_2	0.49	b.d.	0.02	0.01	0.02	0.02	0.02	b.d.	b.d.	b.d.	b.d.	b.d.	b.d.
Al_2O_3	18.20	18.89	17.74	19.29	18.49	18.73	18.49	18.95	18.82	19.32	19.73	19.08	18.40
Cr_2O_3	0.09	0.03	b.d.	0.01	0.03	0.01	0.02	0.02	0.03	0.03	0.03	0.01	0.02
FeO^T	17.88	24.59	23.85	24.43	24.16	24.38	25.16	25.11	24.74	25.26	25.33	24.62	24.44
MnO	0.24	0.30	0.27	0.27	0.30	0.35	0.33	0.28	0.34	0.31	0.30	0.30	0.29
MgO	19.40	16.33	16.34	16.26	17.06	17.20	16.41	16.59	16.78	16.51	17.00	16.44	16.28
CaO	0.45	0.07	0.25	0.17	0.07	0.08	0.01	0.03	0.05	0.13	0.13	0.04	0.04
Na_2O	b.d.	b.d.	b.d.	0.01	b.d.	0.02	0.01	0.02	0.01	0.04	0.03	0.01	0.07
K_2O	0.03	0.05	0.05	0.03	0.05	0.04	0.03	b.d.	0.02	0.02	0.01	b.d.	0.03
F	b.d.	b.d.	b.d.	b.d.	b.d.	b.d.	b.d.	b.d.	b.d.	b.d.	b.d.	b.d.	b.d.
Cl	0.03	b.d.	b.d.	b.d.	b.d.	0.02	0.01	0.02	0.01	0.02	0.01	0.02	b.d.
Total	84.56	87.41	85.30	87.90	87.68	88.23	87.16	87.67	87.97	89.09	90.07	87.36	86.18
Si	5.84	5.72	5.78	5.73	5.76	5.71	5.66	5.62	5.69	5.68	5.63	5.66	5.69
Al^{IV}	2.16	2.29	2.22	2.27	2.24	2.30	2.34	2.38	2.31	2.32	2.38	2.34	2.31
Al^{VI}	2.35	2.40	2.28	2.47	2.32	2.30	2.28	2.32	2.33	2.39	2.38	2.39	2.33
Ti	0.08	-	0.00	0.00	0.00	0.00	0.00	-	-	-	-	-	-
Fe^{2+}	3.15	4.33	4.30	4.27	4.23	4.25	4.47	4.43	4.33	4.37	4.33	4.34	4.37
Cr	0.02	0.01	-	0.00	0.01	0.00	0.00	0.00	0.01	0.01	0.01	0.00	0.00
Mn	0.04	0.05	0.05	0.05	0.05	0.06	0.06	0.05	0.06	0.05	0.05	0.05	0.05
Mg	6.08	5.13	5.26	5.06	5.32	5.34	5.19	5.21	5.24	5.09	5.18	5.17	5.19
Ca	0.10	0.02	0.06	0.04	0.02	0.02	0.00	0.01	0.01	0.03	0.03	0.01	0.01
Na	-	-	-	0.00	-	0.01	0.00	0.01	0.00	0.02	0.01	0.00	0.03
K	0.01	0.01	0.01	0.01	0.01	0.01	0.01	-	0.01	0.01	0.00	-	0.01
F	-	-	-	-	-	-	-	-	-	-	-	-	-
Cl	0.02	-	-	-	-	0.01	0.01	0.01	0.01	0.01	0.01	0.01	-
Cations	19.82	19.94	19.97	19.90	19.96	20.00	20.02	20.03	19.99	19.97	20.00	19.97	20.00

Appendix B1. Chlorite Analyses (continued)

Sample	110-1-5AB6	110-1-5AC1	110-1-5AC2	110-1-5AC3	110-1-5AD1	110-1-5AD2	110-1-5AD3	110-1-5AD4	110-1-5AD5	110-1-5AD6	111-1-3A2	111-1-3A3	111-1-3B1
Rock Type	basalt	basalt	basalt	basalt	basalt	basalt	basalt	basalt	basalt	basalt	basalt	basalt	basalt
Location	UofA	UofA	UofA	UofA	UofA	UofA	UofA	UofA	UofA	UofA	OSU	OSU	OSU
Occurrence	gm	vei	vei	gm	vei	vei	vei	vei	vei	vei	gm	gm	gm
SiO_2	27.32	27.14	27.83	28.08	27.13	26.55	26.87	27.23	27.39	28.11	26.91	27.36	27.08
TiO_2	b.d.	b.d.	0.01	0.04	b.d.	b.d.	b.d.	b.d.	b.d.	b.d.	0.03	0.03	0.05
Al_2O_3	19.45	18.84	18.07	17.22	18.56	18.35	18.94	18.26	17.80	18.02	17.68	17.81	17.61
Cr_2O_3	0.03	0.01	b.d.	b.d.	0.01	0.01	0.02	b.d.	b.d.	0.01	n.d.	n.d.	n.d.
FeO^T	24.16	24.30	23.78	23.38	24.58	24.88	24.55	24.39	23.93	23.68	25.81	25.74	24.88
MnO	0.34	0.31	0.30	0.28	0.35	0.35	0.32	0.26	0.26	0.26	0.55	0.54	0.43
MgO	16.64	16.73	17.11	17.33	16.98	16.31	16.76	16.73	16.87	17.09	15.08	15.42	16.16
CaO	0.04	0.03	0.07	0.16	0.02	0.02	0.03	0.05	0.05	0.06	0.09	0.23	0.14
Na_2O	0.05	0.08	0.04	0.05	0.01	0.02	0.01	0.03	0.02	0.01	0.03	0.02	0.03
K_2O	0.02	0.03	0.03	0.03	0.01	0.03	0.02	0.03	0.04	0.04	n.d.	n.d.	n.d.
F	b.d.	b.d.	b.d.	b.d.	b.d.	b.d.	b.d.	b.d.	b.d.	b.d.	0.08	0.19	0.18
Cl	b.d.	0.02	0.02	0.01	0.01	b.d.	b.d.	0.01	0.03	b.d.	0.06	0.07	0.07
Total	88.05	87.49	87.26	86.58	87.66	86.52	87.52	86.99	86.39	87.28	86.32	87.41	86.63
Si	5.69	5.70	5.84	5.93	5.70	5.67	5.65	5.76	5.82	5.89	5.81	5.83	5.80
Al^{IV}	2.31	2.30	2.16	2.07	2.30	2.33	2.35	2.24	2.18	2.11	2.19	2.17	2.20
Al^{VI}	2.46	2.37	2.31	2.22	2.29	2.29	2.35	2.31	2.28	2.33	2.30	2.29	2.24
Ti	-	-	0.00	0.01	-	-	-	-	-	-	0.01	0.01	0.01
Fe^{2+}	4.21	4.27	4.17	4.13	4.32	4.45	4.32	4.31	4.25	4.15	4.66	4.58	4.45
Cr	0.01	0.00	-	-	0.00	0.00	0.00	-	-	0.00	-	-	-
Mn	0.06	0.06	0.05	0.05	0.06	0.06	0.06	0.05	0.05	0.05	0.10	0.10	0.08
Mg	5.17	5.24	5.35	5.46	5.32	5.20	5.26	5.27	5.35	5.34	4.85	4.90	5.16
Ca	0.01	0.01	0.02	0.04	0.01	0.01	0.01	0.01	0.01	0.01	0.02	0.05	0.03
Na	0.02	0.03	0.02	0.02	0.00	0.01	0.00	0.01	0.01	0.00	0.01	0.01	0.01
K	0.01	0.01	0.01	0.01	0.00	0.01	0.01	0.01	0.01	0.01	-	-	-
F	-	-	-	-	-	-	-	-	-	-	0.11	0.26	0.24
Cl	-	0.01	0.01	0.01	0.01	-	-	0.01	0.02	-	0.04	0.05	0.05
Cations	19.93	19.98	19.93	19.93	20.00	20.02	20.00	19.97	19.95	19.89	19.95	19.93	19.98

Appendix B1. Chlorite Analyses (continued)

Sample	112-2-1A1	112-2-1A2	112-2-1A3	112-2-1A4	113-1-10a1	113-1-10a2	113-1-10b1	113-1-10b2	113-1-10b3	113-1-10c1	113-1-10d1	113-1-10d2	113-1-10d3	113-1-10d4
Rock Type	gabbro	gabbro	gabbro	gabbro	basalt	basalt	basalt	basalt	basalt	basalt	basalt	basalt	basalt	basalt
Location	UofA	UofA	UofA	UofA	OSU	OSU	OSU	OSU	OSU	OSU	OSU	OSU	OSU	OSU
Occurrence	inc	inc	inc	inc	int	int	gm	gm	gm	gm	gm	gm	gm	gm
SiO_2	31.32	31.13	31.14	31.89	28.58	28.39	28.61	29.00	29.85	29.56	29.77	29.51	28.59	29.02
TiO_2	b.d.	0.02	0.03	0.12	0.01	0.02	0.02	0.01	0.02	0.01	0.03	0.03	0.02	0.03
Al_2O_3	17.30	18.45	17.02	15.14	17.91	17.86	17.40	17.31	17.73	17.35	17.34	17.83	18.20	17.87
Cr_2O_3	0.02	0.07	0.31	0.43	n.d.	n.d.	n.d.	n.d.	n.d.	n.d.	n.d.	n.d.	n.d.	n.d.
FeO^T	5.42	4.83	8.29	10.47	20.36	20.31	19.95	20.53	19.99	19.06	20.51	21.01	21.84	20.98
MnO	0.02	0.05	0.26	0.20	0.28	0.33	0.35	0.32	0.34	0.33	0.31	0.31	0.39	0.26
MgO	29.98	30.30	28.02	28.14	20.44	20.26	20.25	19.93	20.62	20.27	19.64	20.51	19.90	20.51
CaO	0.26	0.25	0.14	0.15	0.07	0.10	0.12	0.11	0.22	0.44	0.46	0.06	0.04	0.06
Na_2O	0.04	0.01	b.d.	b.d.	0.03	0.05	0.08	0.07	0.09	0.07	0.05	0.04	0.02	0.03
K_2O	0.03	0.03	0.05	0.01	n.d.	n.d.	n.d.	n.d.	n.d.	n.d.	n.d.	n.d.	n.d.	n.d.
F	b.d.	b.d.	b.d.	b.d.	0.05	0.14	0.34	b.d.	0.70	0.01	0.07	0.09	b.d.	0.02
Cl	b.d.	b.d.	0.01	b.d.	0.06	0.02	0.12	0.08	0.12	0.07	0.04	0.05	0.03	0.03
Total	84.39	85.14	85.27	86.55	87.79	87.48	87.24	87.36	89.68	87.17	88.22	89.44	89.03	88.81
Si	6.14	6.03	6.15	6.28	5.86	5.84	5.92	5.97	6.01	6.05	6.06	5.94	5.81	5.88
Al^{IV}	1.86	1.97	1.86	1.72	2.15	2.16	2.08	2.03	1.99	1.95	1.94	2.06	2.19	2.12
Al^{VI}	2.13	2.24	2.10	1.79	2.18	2.17	2.16	2.17	2.21	2.23	2.22	2.17	2.17	2.15
Ti	-	0.00	0.00	0.02	0.00	0.00	0.00	0.00	0.00	0.00	0.01	0.01	0.00	0.01
Fe^{2+}	0.89	0.78	1.37	1.72	3.49	3.50	3.45	3.54	3.36	3.26	3.49	3.54	3.71	3.56
Cr	0.00	0.01	0.05	0.07	-	-	-	-	-	-	-	-	-	-
Mn	0.00	0.01	0.04	0.03	0.05	0.06	0.06	0.06	0.06	0.06	0.05	0.05	0.07	0.05
Mg	8.76	8.75	8.24	8.26	6.24	6.22	6.24	6.12	6.19	6.19	5.96	6.15	6.03	6.20
Ca	0.06	0.05	0.03	0.03	0.02	0.02	0.03	0.02	0.05	0.10	0.10	0.01	0.01	0.01
Na	0.02	0.00	-	-	0.01	0.02	0.03	0.03	0.04	0.03	0.02	0.02	0.01	0.01
K	0.01	0.01	0.01	0.00	-	-	-	-	-	-	-	-	-	-
F	-	-	-	-	0.07	0.18	0.45	-	0.89	0.01	0.09	0.12	-	0.03
Cl	-	-	0.01	-	0.04	0.01	0.08	0.06	0.08	0.05	0.03	0.03	0.02	0.02
Cations	19.87	19.86	19.85	19.92	19.98	19.99	19.97	19.94	19.90	19.86	19.86	19.95	20.00	19.98

Appendix B1. Chlorite Analyses (continued)

Sample	113-1-10d5	113-1-10d6	113-1-26a1	113-1-26a2	113-1-3C2	113-2-11A1	113-2-11A2	113-2-11A3	113-2-11A4	113-2-11C1	113-2-11C2	113-2-11C3	113-2-11C4	113-2-11D1
Rock Type	basalt	basalt	epidosite	epidosite	basalt	gabbro	gabbro	gabbro	gabbro	gabbro	gabbro	gabbro	gabbro	gabbro
Location	OSU	OSU	OSU	OSU	OSU	UofA	UofA	UofA	UofA	UofA	UofA	UofA	UofA	UofA
Occurrence	gm	gm	int	int	gm	gm	gm	gm	gm	alt	alt	alt	alt	alt
SiO_2	29.19	27.92	29.92	29.49	32.11	31.80	30.71	31.27	31.52	28.10	28.47	28.34	28.25	29.80
TiO_2	0.02	0.04	0.04	b.d.	0.01	0.02	b.d.	0.01	0.02	b.d.	0.05	0.04	0.03	b.d.
Al_2O_3	17.15	18.00	16.31	17.29	15.59	15.74	17.42	15.71	15.67	19.37	18.92	19.00	19.25	18.43
Cr_2O_3	n.d.	n.d.	n.d.	n.d.	n.d.	0.04	b.d.	0.04	0.03	0.03	b.d.	0.01	0.01	b.d.
FeO^T	20.25	20.49	18.64	17.74	15.90	10.15	10.01	12.05	11.44	15.87	15.12	16.41	16.26	13.50
MnO	0.32	0.33	0.27	0.15	0.16	0.34	0.16	0.61	0.69	0.19	0.14	0.16	0.17	0.17
MgO	19.75	19.09	21.80	20.65	22.27	28.51	28.06	27.02	27.51	23.59	23.92	23.09	23.32	25.04
CaO	0.48	0.13	0.11	0.15	0.26	0.04	0.01	0.03	0.03	0.02	b.d.	0.06	0.03	0.08
Na_2O	0.01	0.05	b.d.	0.04	0.10	0.02	0.01	0.02	0.01	0.01	0.02	0.03	0.02	0.04
K_2O	n.d.	n.d.	n.d.	n.d.	n.d.	0.05	0.02	0.04	0.06	0.05	0.03	0.02	0.02	0.03
F	0.05	0.38	0.08	0.25	0.11	b.d.	b.d.	b.d.	b.d.	b.d.	b.d.	b.d.	b.d.	b.d.
Cl	0.06	0.05	0.03	0.10	0.06	0.03	0.06	0.02	0.03	0.02	0.02	b.d.	b.d.	b.d.
Total	87.28	86.48	87.20	85.86	86.57	86.74	86.46	86.82	87.01	87.25	86.69	87.16	87.36	87.09
Si	6.01	5.84	6.11	6.09	6.48	6.23	6.03	6.20	6.21	5.65	5.74	5.72	5.68	5.91
Al^{IV}	1.99	2.16	1.89	1.91	1.52	1.77	1.97	1.81	1.79	2.35	2.26	2.28	2.32	2.09
Al^{VI}	2.18	2.28	2.03	2.30	2.18	1.86	2.06	1.86	1.85	2.24	2.23	2.24	2.25	2.22
Ti	0.00	0.01	0.01	-	0.00	0.00	-	0.00	0.00	-	0.01	0.01	0.01	-
Fe^{2+}	3.49	3.59	3.18	3.07	2.68	1.66	1.64	2.00	1.89	2.67	2.55	2.77	2.74	2.24
Cr	-	-	-	-	-	0.01	-	0.01	0.01	0.01	-	0.00	0.00	-
Mn	0.06	0.06	0.05	0.03	0.03	0.06	0.03	0.10	0.12	0.03	0.02	0.03	0.03	0.03
Mg	6.07	5.96	6.63	6.36	6.70	8.33	8.21	7.98	8.08	7.08	7.19	6.95	7.00	7.41
Ca	0.11	0.03	0.02	0.03	0.06	0.01	0.00	0.01	0.01	0.00	-	0.01	0.01	0.02
Na	0.00	0.02	-	0.02	0.04	0.01	0.00	0.01	0.00	0.00	0.01	0.01	0.01	0.02
K	-	-	-	-	-	0.01	0.01	0.01	0.02	0.01	0.01	0.01	0.01	0.01
F	0.07	0.50	0.10	0.33	0.14	-	-	-	-	-	-	-	-	-
Cl	0.04	0.04	0.02	0.07	0.04	0.02	0.04	0.01	0.02	0.01	0.01	-	-	-
Cations	19.90	19.93	19.92	19.80	19.68	19.95	19.95	19.97	19.97	20.05	20.01	20.02	20.03	19.94

Appendix B1. Chlorite Analyses (continued)

Sample	113-2-11D2	113-2-11D3	113-2-11D4	113-2-4B1	113-2-4B3	113-2-4B4	113-2-4D1	113-2-4D2	113-2-4D3	113-2-4D4
Rock Type	gabbro	gabbro	gabbro	gabbro	gabbro	gabbro	gabbro	gabbro	gabbro	gabbro
Location	UofA	UofA	UofA	UofA	UofA	UofA	UofA	UofA	UofA	UofA
Occurrence	alt	alt	alt	gm	gm	gm	am	am	am	am
SiO_2	28.42	32.24	31.60	31.80	34.52	33.04	33.33	33.52	32.87	32.55
TiO_2	0.02	0.02	0.03	0.01	0.03	0.05	0.01	0.01	b.d.	0.02
Al_2O_3	20.51	14.97	14.97	16.31	13.00	13.68	13.33	14.12	14.60	14.64
Cr_2O_3	0.01	0.01	0.02	0.01	0.02	b.d.	0.02	0.01	0.01	b.d.
FeO^T	13.14	11.94	12.28	7.89	8.82	9.11	10.41	8.60	9.40	9.41
MnO	0.13	0.15	0.11	0.01	0.06	0.06	0.16	0.09	0.10	0.11
MgO	24.83	27.33	27.31	29.93	29.94	30.23	28.56	29.77	27.97	28.72
CaO	0.05	0.03	0.04	0.03	0.06	0.02	0.15	0.09	0.11	0.07
Na_2O	0.01	0.04	0.06	0.03	0.04	b.d.	0.07	0.06	0.07	0.06
K_2O	0.02	0.08	0.06	0.03	0.04	0.03	0.04	0.05	0.07	0.06
F	b.d.	b.d.	b.d.	b.d.	b.d.	b.d.	b.d.	b.d.	b.d.	b.d.
Cl	0.01	0.03	0.02	0.05	0.04	0.03	b.d.	b.d.	b.d.	b.d.
Total	87.15	86.84	86.50	86.10	86.57	86.25	86.03	86.32	85.20	85.64
Si	5.63	6.36	6.28	6.19	6.70	6.46	6.58	6.52	6.51	6.42
Al^{IV}	2.37	1.64	1.72	1.81	1.30	1.54	1.43	1.48	1.49	1.58
Al^{VI}	2.42	1.84	1.78	1.93	1.67	1.62	1.67	1.76	1.91	1.82
Ti	0.00	0.00	0.00	0.00	0.00	0.01	0.00	0.00	-	0.00
Fe^{2+}	2.18	1.97	2.04	1.29	1.43	1.49	1.72	1.40	1.56	1.55
Cr	0.00	0.00	0.00	0.00	0.00	-	0.00	0.00	0.00	-
Mn	0.02	0.03	0.02	0.00	0.01	0.01	0.03	0.02	0.02	0.02
Mg	7.33	8.04	8.09	8.69	8.66	8.82	8.40	8.64	8.25	8.44
Ca	0.01	0.01	0.01	0.01	0.01	0.00	0.03	0.02	0.02	0.02
Na	0.00	0.02	0.02	0.01	0.02	-	0.03	0.02	0.03	0.02
K	0.01	0.02	0.02	0.01	0.01	0.01	0.01	0.01	0.02	0.02
F	-	-	-	-	-	-	-	-	-	-
Cl	0.01	0.02	0.01	0.03	0.03	0.02	-	-	-	-
Cations	19.97	19.91	19.98	19.94	19.82	19.95	19.89	19.87	19.81	19.89

Appendix B2. Epidote Analyses (recalculated on the basis of 12.5 anhydrous O)

Sample	81-2-8A1	81-2-8A2	81-2-8A3	81-2-8A4	81-2-8A5	81-2-8A6	81-2-8B1	81-2-8B10	81-2-8B11	81-2-8B2	81-2-8B3	81-2-8B4	81-2-8B5	81-2-8B6	81-2-8B7	81-2-8B8
Rock Type	basalt	basalt	basalt	basalt	basalt	basalt	basalt	basalt	basalt	basalt	basalt	basalt	basalt	basalt	basalt	basalt
Location	UofA	UofA	UofA	UofA	UofA	UofA	UofA	UofA	UofA	UofA	UofA	UofA	UofA	UofA	UofA	UofA
Occurrence	gm	gm	gm	gm	gm	gm	ves	gm d	gm	ves	ves	ves	ves	ves	ves	ves
SiO_2	37.80	37.31	37.23	37.46	37.16	36.96	37.16	37.78	37.01	37.47	37.54	37.76	37.16	37.42	37.38	37.58
TiO_2	0.05	0.13	0.23	0.03	0.03	0.12	0.61	0.09	0.09	0.05	0.04	0.05	0.33	0.04	0.46	0.04
Al_2O_3	25.35	23.04	23.38	25.02	23.87	25.93	22.44	27.71	23.70	25.10	25.02	27.43	23.10	25.38	22.97	27.70
$Fe_2O_3^T$	11.32	14.39	13.66	12.31	13.77	11.30	14.05	8.91	13.84	11.69	12.05	9.16	13.92	11.38	14.29	8.83
Cr_2O_3	b.d.	b.d.	b.d.	b.d.	b.d.	b.d.	b.d.	b.d.	0.01	0.01	0.04	b.d.	0.01	0.01	b.d.	b.d.
MnO	0.18	0.10	0.07	0.12	0.05	0.37	0.15	0.19	0.20	0.24	0.19	0.34	0.16	0.30	0.18	0.34
MgO	0.05	0.10	0.09	0.03	0.02	0.07	0.07	0.03	0.07	0.07	0.02	0.02	0.04	0.07	0.08	0.02
CaO	23.23	22.75	23.28	23.15	23.33	22.69	23.56	23.35	22.79	23.64	23.47	23.24	23.24	23.10	23.03	23.36
Na_2O	b.d.	b.d.	0.01	0.01	0.02	b.d.	b.d.	0.01	b.d.	0.01	0.01	b.d.	0.01	b.d.	b.d.	b.d.
K_2O	0.02	0.03	0.03	0.02	0.03	0.02	0.02	0.02	0.02	b.d.	b.d.	0.02	0.01	0.01	0.02	0.02
F	b.d.	b.d.	b.d.	b.d.	b.d.	b.d.	0.02	b.d.	b.d.	b.d.	b.d.	b.d.	b.d.	b.d.	b.d.	b.d.
Cl	0.02	0.01	0.02	0.02	0.01	b.d.	b.d.	0.01	0.03	b.d.	b.d.	0.02	0.01	0.02	0.01	0.02
Total	98.02	97.86	98.00	98.17	98.29	97.46	98.08	98.10	97.76	98.28	98.38	98.04	97.99	97.73	98.42	97.91
Si	2.98	2.98	2.97	2.96	2.95	2.93	2.97	2.95	2.96	2.96	2.96	2.96	2.97	2.97	2.97	2.95
Al^{IV}	0.02	0.02	0.03	0.04	0.05	0.07	0.03	0.05	0.04	0.04	0.04	0.04	0.03	0.04	0.03	0.06
Al^{VI}	2.34	2.15	2.17	2.29	2.19	2.36	2.09	2.50	2.19	2.30	2.29	2.49	2.14	2.33	2.13	2.50
Ti	0.00	0.01	0.01	0.00	0.00	0.01	0.04	0.01	0.01	0.00	0.00	0.00	0.02	0.00	0.03	0.00
Cr	-	-	-	-	-	-	-	-	0.00	0.00	0.00	-	0.00	0.00	-	-
Fe^{3+}	0.67	0.86	0.82	0.73	0.82	0.67	0.85	0.52	0.83	0.69	0.72	0.54	0.84	0.68	0.85	0.52
Mn	0.01	0.01	0.01	0.01	0.00	0.03	0.01	0.01	0.01	0.02	0.01	0.02	0.01	0.02	0.01	0.02
Mg	0.01	0.01	0.01	0.00	0.00	0.01	0.01	0.00	0.01	0.01	0.00	0.00	0.01	0.01	0.01	0.00
Ca	1.96	1.95	1.99	1.96	1.99	1.93	2.02	1.96	1.95	2.00	1.99	1.95	1.99	1.96	1.96	1.96
Na	-	-	0.00	0.00	0.00	-	-	0.00	-	0.00	0.00	-	0.00	-	-	-
K	0.00	0.00	0.00	0.00	0.00	0.00	0.00	0.00	0.00	-	-	0.00	0.00	0.00	0.00	0.00
F	-	-	-	-	-	-	0.01	-	-	-	-	-	-	-	-	-
Cl	0.01	0.00	0.01	0.01	0.00	-	-	0.00	0.01	-	-	0.01	0.00	0.01	0.00	0.01
Ps	0.22	0.28	0.27	0.24	0.27	0.22	0.29	0.17	0.27	0.23	0.24	0.18	0.28	0.22	0.28	0.17

Notes: b.d. = below detection; gm = groundmass; ves = vesicle; cor = core; inc = inclusion; vel = vein; l and d = light and dark in backscattered electron images, respectively.

Appendix B2. Epidote Analyses (continued)

Sample	81-2-8B9	81-2-8C1	81-2-8C10	81-2-8C2	81-2-8C3	81-2-8C4	81-2-8C5	81-2-8C6	81-2-8C7	81-2-8C8	81-2-8C9	81-2-8D1	81-2-8D10	81-2-8D11	81-2-8D12	81-2-8D13
Rock Type	basalt	basalt	basalt	basalt	basalt	basalt	basalt	basalt	basalt	basalt	basalt	basalt	basalt	basalt	basalt	basalt
Location	UofA	UofA	UofA	UofA	UofA	UofA	UofA	UofA	UofA	UofA	UofA	UofA	UofA	UofA	UofA	UofA
Occurrence	ves	gm l	gm	gm d	ves	ves	ves	ves	ves	ves	gm	cor	gm d	gm l	gm d	gm l
SiO_2	37.10	37.57	37.12	38.01	37.19	37.79	37.72	37.81	37.49	38.00	36.94	37.69	37.84	37.17	37.71	37.76
TiO_2	0.01	0.07	0.04	0.11	0.09	0.07	0.02	0.14	0.04	0.05	0.22	0.15	0.11	0.10	0.06	0.21
Al_2O_3	25.14	25.11	24.01	27.01	24.99	25.89	24.22	26.51	24.03	27.75	22.76	25.74	25.79	23.86	25.60	25.72
$Fe_2O_3^T$	12.14	11.71	12.79	9.22	11.28	10.73	12.55	9.99	13.12	8.46	13.76	10.94	11.05	13.33	10.95	11.02
Cr_2O_3	b.d.	b.d.	b.d.	b.d.	b.d.	b.d.	0.02	b.d.	b.d.	0.01	0.01	b.d.	b.d.	b.d.	b.d.	b.d.
MnO	0.53	0.10	0.32	0.13	0.25	0.32	0.18	0.69	0.12	0.33	0.06	0.23	0.26	0.29	0.34	0.27
MgO	0.03	0.08	0.14	0.05	0.09	0.07	0.02	0.03	0.02	0.03	0.06	0.05	0.08	0.06	0.05	0.04
CaO	22.69	23.46	22.44	23.21	23.48	23.61	23.30	22.73	23.30	23.55	23.10	23.11	23.36	23.18	23.16	23.04
Na_2O	0.03	0.01	0.02	0.02	0.01	b.d.	0.01	0.01	0.01	b.d.	b.d.	b.d.	b.d.	0.01	b.d.	b.d.
K_2O	0.01	0.01	0.01	0.01	b.d.	0.02	0.01	b.d.	0.01	0.01	0.01	0.03	0.01	0.01	0.02	0.01
F	b.d.	b.d.	0.02	b.d.	b.d.	b.d.	b.d.	b.d.	b.d.	b.d.	b.d.	b.d.	b.d.	b.d.	b.d.	b.d.
Cl	0.01	b.d.	b.d.	b.d.	b.d.	0.01	b.d.	b.d.	b.d.	b.d.	b.d.	0.01	b.d.	b.d.	b.d.	b.d.
Total	97.69	98.12	96.91	97.77	97.38	98.51	98.05	97.91	98.14	98.19	96.92	97.95	98.50	98.01	97.89	98.07
Si	2.95	2.97	2.98	2.98	2.96	2.97	2.99	2.97	2.98	2.96	2.98	2.97	2.97	2.96	2.98	2.97
Al^{IV}	0.05	0.03	0.02	0.02	0.04	0.03	0.01	0.03	0.02	0.04	0.02	0.03	0.03	0.04	0.02	0.03
Al^{VI}	2.30	2.30	2.25	2.47	2.31	2.36	2.25	2.43	2.22	2.51	2.14	2.36	2.35	2.20	2.36	2.36
Ti	0.00	0.00	0.00	0.01	0.01	0.00	0.00	0.01	0.00	0.00	0.01	0.01	0.01	0.01	0.00	0.01
Cr	-	-	-	-	-	-	0.00	-	-	0.00	0.00	-	-	-	-	-
Fe^{3+}	0.73	0.70	0.77	0.54	0.68	0.63	0.75	0.59	0.78	0.50	0.84	0.65	0.65	0.80	0.65	0.65
Mn	0.04	0.01	0.02	0.01	0.02	0.02	0.01	0.05	0.01	0.02	0.00	0.02	0.02	0.02	0.02	0.02
Mg	0.00	0.01	0.02	0.01	0.01	0.01	0.00	0.00	0.00	0.00	0.01	0.01	0.01	0.01	0.01	0.01
Ca	1.93	1.99	1.93	1.95	2.00	1.99	1.98	1.92	1.98	1.97	2.00	1.95	1.96	1.98	1.96	1.94
Na	0.01	0.00	0.00	0.00	0.00	-	0.00	0.00	0.00	-	-	-	-	0.00	-	-
K	0.00	0.00	0.00	0.00	-	0.00	0.00	-	0.00	0.00	0.00	0.00	0.00	0.00	0.00	0.00
F	-	-	0.01	-	-	-	-	-	-	-	-	-	-	-	-	-
Cl	0.00	-	-	-	-	0.00	-	-	-	-	-	0.00	-	-	-	-
Ps	0.24	0.23	0.25	0.18	0.22	0.21	0.25	0.19	0.26	0.16	0.28	0.21	0.21	0.26	0.21	0.21

Appendix B2. Epidote Analyses (continued)

Sample	81-2-8D14	81-2-8D2	81-2-8D3	81-2-8D4	81-2-8D5	81-2-8D6	81-2-8D7	81-2-8D8	81-2-8D9	81-2-9A1	81-2-9A2	81-2-9A3	81-2-9A4	81-2-9A5	81-2-9A6	81-2-9B1
Rock Type	basalt	basalt	basalt	basalt	basalt	basalt	basalt	basalt	basalt	basalt	basalt	basalt	basalt	basalt	basalt	basalt
Location	UofA	UofA	UofA	UofA	UofA	UofA	UofA	UofA	UofA	UofA	UofA	UofA	UofA	UofA	UofA	UofA
Occurrence	gm d	rim	cor	rim	gm l	gm d	gm l	gm d	gm l	cor	rim	cor	rim	cor	rim	cor
SiO_2	37.47	37.13	37.29	37.32	37.25	38.08	37.38	37.67	37.20	37.15	37.78	37.36	38.05	37.07	37.73	37.20
TiO_2	0.11	0.05	0.19	0.11	b.d.	0.06	0.26	0.18	0.46	0.14	0.07	0.11	0.02	0.26	0.05	0.52
Al_2O_3	26.54	24.05	22.94	25.91	24.36	26.56	22.86	26.57	22.07	22.46	25.50	22.73	26.59	21.64	24.60	22.14
$Fe_2O_3^T$	10.26	13.45	14.55	11.46	13.27	10.07	14.35	9.93	14.61	15.47	11.52	15.18	10.39	16.39	12.88	14.79
Cr_2O_3	0.01	0.01	b.d.	b.d.	0.01	b.d.	0.01	0.02	0.02	b.d.	0.03	0.02	b.d.	b.d.	b.d.	0.02
MnO	0.27	0.06	0.02	0.35	0.03	0.13	0.02	0.20	0.10	0.05	0.16	0.04	0.08	0.03	0.08	0.09
MgO	0.05	0.03	0.04	0.08	0.03	0.05	0.04	0.03	0.06	0.02	0.03	b.d.	0.02	0.05	0.06	0.07
CaO	23.32	23.35	23.35	23.05	23.39	23.71	23.43	23.32	23.17	23.25	23.31	23.29	23.50	23.36	23.37	23.17
Na_2O	0.01	b.d.	b.d.	b.d.	b.d.	b.d.	b.d.	b.d.	0.01	b.d.	b.d.	0.01	b.d.	b.d.	0.01	b.d.
K_2O	0.01	0.01	0.01	0.01	0.01	0.01	0.02	0.01	0.01	0.03	0.02	0.04	0.03	0.03	0.03	0.03
F	b.d.	b.d.	b.d.	b.d.	b.d.	b.d.	b.d.	b.d.	0.01	b.d.	b.d.	b.d.	b.d.	b.d.	b.d.	b.d.
Cl	b.d.	0.01	b.d.	b.d.	0.01	b.d.	0.01	b.d.	b.d.	b.d.	b.d.	b.d.	b.d.	b.d.	b.d.	b.d.
Total	98.05	98.15	98.39	98.29	98.36	98.67	98.38	97.93	97.72	98.57	98.42	98.78	98.68	98.83	98.81	98.03
Si	2.95	2.95	2.97	2.94	2.95	2.97	2.98	2.96	2.99	2.96	2.97	2.97	2.97	2.96	2.97	2.98
Al^{IV}	0.05	0.05	0.03	0.06	0.05	0.03	0.02	0.04	0.01	0.04	0.03	0.03	0.03	0.04	0.03	0.02
Al^{VI}	2.41	2.21	2.12	2.34	2.23	2.41	2.12	2.42	2.08	2.07	2.33	2.10	2.41	2.00	2.25	2.07
Ti	0.01	0.00	0.01	0.01	-	0.00	0.02	0.01	0.03	0.01	0.00	0.01	0.00	0.02	0.00	0.03
Cr	0.00	0.00	-	-	0.00	-	0.00	0.00	0.00	-	0.00	0.00	-	-	-	0.00
Fe^{3+}	0.61	0.80	0.87	0.68	0.79	0.59	0.86	0.59	0.88	0.93	0.68	0.91	0.61	0.98	0.76	0.89
Mn	0.02	0.00	0.00	0.02	0.00	0.01	0.00	0.01	0.01	0.00	0.01	0.00	0.01	0.00	0.01	0.01
Mg	0.01	0.00	0.01	0.01	0.00	0.01	0.01	0.00	0.01	0.00	0.00	-	0.00	0.01	0.01	0.01
Ca	1.97	1.99	1.99	1.95	1.99	1.98	2.00	1.96	1.99	1.99	1.96	1.98	1.97	2.00	1.97	1.99
Na	0.00	-	-	-	-	-	-	-	0.00	-	-	0.00	-	-	0.00	-
K	0.00	0.00	0.00	0.00	0.00	0.00	0.00	0.00	0.00	0.00	0.00	0.00	0.00	0.00	0.00	0.00
F	-	-	-	-	-	-	-	-	0.01	-	-	-	-	-	-	-
Cl	-	0.00	-	-	0.00	-	0.00	-	-	-	-	-	-	-	-	-
Ps	0.20	0.26	0.29	0.22	0.26	0.19	0.29	0.19	0.30	0.31	0.22	0.30	0.20	0.33	0.25	0.30

Appendix B2. Epidote Analyses (continued)

Sample	81-2-9B10	81-2-9B11	81-2-9B12	81-2-9B2	81-2-9B3	81-2-9B4	81-2-9B5	81-2-9B6	81-2-9B7	81-2-9B8	81-2-9B9	81-2-9C1	81-2-9C2	81-2-9C3	81-2-9C4	96-1-2B1
Rock Type	basalt	basalt	basalt	basalt	basalt	basalt	basalt	basalt	basalt	basalt	basalt	basalt	basalt	basalt	basalt	PG
Location	UofA	UofA	UofA	UofA	UofA	UofA	UofA	UofA	UofA	UofA	UofA	UofA	UofA	UofA	UofA	UofA
Occurrence	rim	gm	gm	rim	cor	rim	cor	rim	cor	rim	cor	gm l	gm d	gm l	gm d	gm l
SiO_2	37.32	38.09	37.37	37.69	37.12	37.51	36.89	37.48	37.56	37.33	37.40	36.55	37.18	36.98	37.29	37.85
TiO_2	0.04	0.03	0.01	0.13	0.56	0.05	0.39	0.09	0.16	0.03	0.56	0.45	0.17	0.44	0.08	0.14
Al_2O_3	23.98	28.63	23.68	25.75	22.18	23.84	22.43	24.75	26.10	23.81	22.56	20.28	24.79	23.23	24.81	26.70
$Fe_2O_3^T$	13.31	7.46	13.77	11.12	14.80	13.47	14.54	12.32	10.48	13.26	14.54	17.32	12.44	13.71	12.29	11.29
Cr_2O_3	0.03	b.d.	0.01	0.01	0.01	0.03	0.03	b.d.	b.d.	0.03	b.d.	b.d.	b.d.	0.01	b.d.	0.03
MnO	0.07	0.10	0.06	0.26	0.06	0.10	0.05	0.12	0.28	0.09	0.06	0.07	0.28	0.12	0.25	0.45
MgO	0.02	b.d.	0.03	0.04	0.07	0.02	0.08	0.06	0.03	0.02	0.07	0.04	0.05	0.08	0.05	0.09
CaO	23.25	23.60	23.12	23.08	23.35	23.42	23.15	23.37	22.91	23.17	23.17	23.05	22.88	23.25	23.35	21.97
Na_2O	b.d.	b.d.	b.d.	0.01	b.d.	0.01	b.d.	b.d.	b.d.	b.d.	b.d.	b.d.	0.02	b.d.	b.d.	b.d.
K_2O	0.01	0.03	0.04	0.02	0.03	0.02	0.02	0.03	0.01	0.02	0.02	0.01	0.01	0.02	0.02	0.02
F	b.d.	b.d.	0.01	b.d.	b.d.	b.d.	b.d.	b.d.	b.d.	b.d.	b.d.	0.03	b.d.	b.d.	b.d.	b.d.
Cl	b.d.	b.d.	b.d.	b.d.	b.d.	b.d.	b.d.	b.d.	b.d.	b.d.	b.d.	b.d.	b.d.	b.d.	0.01	b.d.
Total	98.03	97.94	98.10	98.11	98.18	98.47	97.58	98.22	97.53	97.76	98.38	97.80	97.82	97.84	98.15	98.54
Si	2.97	2.96	2.97	2.97	2.97	2.97	2.97	2.97	2.97	2.98	2.98	2.97	2.95	2.96	2.96	2.96
Al^{IV}	0.03	0.04	0.03	0.03	0.03	0.03	0.03	0.04	0.03	0.02	0.02	0.03	0.05	0.04	0.05	0.04
Al^{VI}	2.21	2.59	2.19	2.36	2.06	2.20	2.09	2.27	2.40	2.21	2.10	1.91	2.27	2.14	2.27	2.42
Ti	0.00	0.00	0.00	0.01	0.03	0.00	0.02	0.01	0.01	0.00	0.03	0.03	0.01	0.03	0.01	0.01
Cr	0.00	-	0.00	0.00	0.00	0.00	0.00	-	-	0.00	-	-	-	0.00	-	0.00
Fe^{3+}	0.80	0.44	0.82	0.66	0.89	0.80	0.88	0.73	0.62	0.80	0.87	1.06	0.74	0.82	0.73	0.66
Mn	0.01	0.01	0.00	0.02	0.00	0.01	0.00	0.01	0.02	0.01	0.00	0.01	0.02	0.01	0.02	0.03
Mg	0.00	-	0.00	0.01	0.01	0.00	0.01	0.01	0.00	0.00	0.01	0.01	0.01	0.01	0.01	0.01
Ca	1.98	1.97	1.97	1.95	2.00	1.99	1.99	1.98	1.94	1.98	1.98	2.00	1.95	1.99	1.98	1.84
Na	-	-	-	0.00	-	0.00	-	-	-	-	-	-	0.00	-	-	-
K	0.00	0.00	0.00	0.00	0.00	0.00	0.00	0.00	0.00	0.00	0.00	0.00	0.00	0.00	0.00	0.00
F	-	-	0.01	-	-	-	-	-	-	-	-	0.02	-	-	-	-
Cl	-	-	-	-	-	-	-	-	-	-	-	-	-	-	0.00	-
Ps	0.26	0.14	0.27	0.22	0.30	0.27	0.29	0.24	0.20	0.26	0.29	0.35	0.24	0.27	0.24	0.21

Appendix B2. Epidote Analyses (continued)

Sample	96-1-2B2	96-1-2B3	96-1-2B4	96-1-3B1	96-1-3B2	96-1-3B3	96-1-3D1	96-1-3D2	96-1-3D3	96-1-5A1	96-1-5A2	96-1-5A3	96-1-5A4	96-1-5B1	96-1-5D1	96-1-5D2
Rock Type	PG	PG	PG	PG	PG	PG	PG	PG	PG	PG	PG	PG	PG	PG	PG	PG
Location	UofA	UofA	UofA	UofA	UofA	UofA	UofA	UofA	UofA	UofA	UofA	UofA	UofA	UofA	UofA	UofA
Occurrence	gm d	gm l	gm d	gm	gm	gm	gm l	gm d	gm	gm l	gm l	gm d	gm d	inc	gm l	gm d
SiO_2	37.81	37.64	37.54	37.46	37.78	37.69	37.11	37.20	37.59	37.35	37.32	37.77	38.01	37.71	37.26	37.82
TiO_2	0.12	0.05	0.09	0.13	0.08	0.16	0.04	0.08	0.02	0.05	b.d.	0.03	b.d.	0.16	0.16	b.d.
Al_2O_3	26.43	24.60	25.10	26.79	26.62	26.68	24.55	26.75	26.28	24.38	24.48	27.14	26.65	26.73	22.16	26.73
$Fe_2O_3^T$	11.38	12.49	11.78	9.74	10.04	10.19	12.74	10.59	10.93	12.65	12.54	9.49	9.91	9.27	15.62	9.81
Cr_2O_3	0.01	0.02	0.02	b.d.	b.d.	b.d.	b.d.	b.d.	b.d.	0.02	0.02	0.02	0.03	0.03	b.d.	b.d.
MnO	0.42	0.03	0.06	0.12	0.06	0.11	0.04	0.53	0.30	0.07	0.07	0.25	0.06	0.03	0.04	0.05
MgO	0.06	b.d.	0.01	0.01	0.03	b.d.	b.d.	0.01	0.02	0.01	0.01	0.02	b.d.	b.d.	0.04	0.04
CaO	21.95	23.23	23.17	23.39	23.75	23.16	23.35	22.54	22.88	23.47	23.39	23.04	23.55	23.28	23.35	23.75
Na_2O	0.01	b.d.	b.d.	b.d.	0.02	b.d.	b.d.	b.d.	b.d.	0.01	0.02	0.03	0.04	0.07	b.d.	b.d.
K_2O	0.02	0.02	b.d.	0.03	0.02	0.02	0.04	0.02	0.04	0.02	0.02	0.02	b.d.	0.02	0.02	0.02
F	b.d.	b.d.	b.d.	b.d.	b.d.	b.d.	b.d.	0.03	b.d.	b.d.	b.d.	b.d.	b.d.	b.d.	b.d.	b.d.
Cl	0.01	b.d.	b.d.	b.d.	0.01	b.d.	0.01	b.d.	b.d.	0.01	b.d.	0.02	0.02	b.d.	0.02	b.d.
Total	98.22	98.08	97.77	97.67	98.41	98.01	97.88	97.75	98.06	98.04	97.87	97.83	98.27	97.30	98.67	98.22
Si	2.97	2.98	2.97	2.95	2.96	2.96	2.95	2.94	2.96	2.97	2.97	2.96	2.98	2.97	2.97	2.96
Al^{IV}	0.03	0.02	0.03	0.05	0.04	0.04	0.05	0.06	0.04	0.03	0.03	0.04	0.03	0.03	0.03	0.04
Al^{VI}	2.41	2.27	2.31	2.44	2.41	2.43	2.25	2.42	2.39	2.25	2.26	2.47	2.43	2.46	2.05	2.43
Ti	0.01	0.00	0.01	0.01	0.01	0.01	0.00	0.01	0.00	0.00	-	0.00	-	0.01	0.01	-
Cr	0.00	0.00	0.00	-	-	-	-	-	-	0.00	0.00	0.00	0.00	0.00	-	-
Fe^{3+}	0.67	0.74	0.70	0.58	0.59	0.60	0.76	0.63	0.65	0.76	0.75	0.56	0.58	0.55	0.94	0.58
Mn	0.03	0.00	0.00	0.01	0.00	0.01	0.00	0.04	0.02	0.01	0.01	0.02	0.00	0.00	0.00	0.00
Mg	0.01	-	0.00	0.00	0.00	-	-	0.00	0.00	0.00	0.00	0.00	-	-	0.01	0.01
Ca	1.85	1.97	1.97	1.97	1.99	1.95	1.99	1.91	1.93	2.00	1.99	1.94	1.98	1.97	2.00	1.99
Na	0.00	-	-	-	0.00	-	-	-	-	0.00	0.00	0.01	0.01	0.01	-	-
K	0.00	0.00	-	0.00	0.00	0.00	0.00	0.00	0.00	0.00	0.00	0.00	-	0.00	0.00	0.00
F	-	-	-	-	-	-	-	0.02	-	-	-	-	-	-	-	-
Cl	0.00	-	-	-	0.00	-	0.00	-	-	0.00	-	0.01	0.01	-	0.01	-
Ps	0.22	0.24	0.23	0.19	0.19	0.20	0.25	0.20	0.21	0.25	0.25	0.18	0.19	0.18	0.31	0.19

Appendix B2. Epidote Analyses (continued)

Sample	96-1-5D3	96-1-5D4	96-1-10B1	96-1-10B2	96-1-10B3	96-1-10C1	96-1-10C2	96-1-10C3	96-1-10C4	96-1-10C5	96-1-10C6	96-1-14A1	96-1-14A2	96-1-14B1	96-1-14B2
Rock Type	PG	PG	PG	PG	PG	PG	PG	PG	PG	PG	PG	epidosite	epidosite	epidosite	epidosite
Location	UofA	UofA	UofA	UofA	UofA	UofA	UofA	UofA	UofA	UofA	UofA	OSU	OSU	OSU	OSU
Occurrence	gm l	gm d	gm	gm	gm	gm	gm	gm l	gm d	gm l	gm d	gm	gm	gm	gm
SiO_2	37.05	37.61	36.90	37.46	37.42	37.50	37.53	37.58	37.78	37.36	37.77	39.59	37.02	37.20	37.75
TiO_2	0.25	0.10	0.05	0.03	0.02	0.27	0.05	0.25	0.22	0.44	0.20	0.10	0.26	0.06	0.12
Al_2O_3	22.27	25.61	21.63	22.37	21.90	23.30	24.38	23.27	25.40	22.95	25.84	27.80	23.89	21.26	25.57
$Fe_2O_3^T$	15.26	11.23	15.87	14.92	15.66	13.82	13.65	14.13	11.47	14.21	10.86	8.45	12.99	16.17	11.86
Cr_2O_3	b.d.	b.d.	b.d.	b.d.	0.01	b.d.	b.d.	0.02	0.02	b.d.	b.d.	0.02	b.d.	b.d.	0.02
MnO	0.05	0.15	0.03	0.01	0.02	0.04	0.06	0.01	0.02	0.02	0.02	0.15	0.05	b.d.	0.17
MgO	0.04	0.01	0.02	0.02	0.01	0.03	0.02	0.06	0.02	0.06	0.03	0.01	0.04	0.03	0.02
CaO	23.18	23.15	23.01	23.10	23.02	23.21	23.02	23.32	23.30	23.30	23.55	23.91	23.33	23.34	23.67
Na_2O	b.d.	b.d.	b.d.	b.d.	b.d.	b.d.	b.d.	b.d.	b.d.	b.d.	b.d.	0.04	0.02	b.d.	0.04
K_2O	0.02	0.01	0.03	0.02	0.02	0.02	0.01	0.03	0.03	0.03	0.02	0.01	b.d.	0.01	0.01
F	b.d.	b.d.	b.d.	b.d.	b.d.	b.d.	b.d.	b.d.	b.d.	b.d.	b.d.	b.d.	0.11	0.17	0.04
Cl	b.d.	b.d.	b.d.	0.01	b.d.	b.d.	b.d.	b.d.	0.02	b.d.	b.d.	b.d.	b.d.	0.01	0.01
Total	98.12	97.87	97.54	97.94	98.08	98.19	98.72	98.67	98.28	98.37	98.29	100.08	97.71	98.25	99.28
Si	2.97	2.97	2.98	3.00	3.00	2.98	2.96	2.98	2.97	2.97	2.97	3.02	2.96	2.99	2.95
Al^{IV}	0.03	0.03	0.02	0.00	0.00	0.02	0.04	0.02	0.03	0.03	0.03	0.00	0.04	0.01	0.05
Al^{VI}	2.07	2.35	2.04	2.11	2.07	2.17	2.23	2.15	2.33	2.12	2.36	2.50	2.21	2.01	2.31
Ti	0.02	0.01	0.00	0.00	0.00	0.02	0.00	0.02	0.01	0.03	0.01	0.01	0.02	0.00	0.01
Cr	-	-	-	-	0.00	-	-	0.00	0.00	-	-	0.00	-	-	0.00
Fe^{3+}	0.92	0.67	0.96	0.90	0.94	0.83	0.81	0.84	0.68	0.85	0.64	0.49	0.78	0.98	0.70
Mn	0.00	0.01	0.00	0.00	0.00	0.00	0.00	0.00	0.00	0.00	0.00	0.01	0.00	-	0.01
Mg	0.01	0.00	0.00	0.00	0.00	0.00	0.00	0.01	0.00	0.01	0.00	0.00	0.01	0.00	0.00
Ca	1.99	1.96	1.99	1.98	1.98	1.98	1.95	1.98	1.97	1.99	1.98	1.95	2.00	2.01	1.98
Na	-	-	-	-	-	-	-	-	-	-	-	0.01	0.00	-	0.01
K	0.00	0.00	0.00	0.00	0.00	0.00	0.00	0.00	0.00	0.00	0.00	0.00	-	0.00	0.00
F	-	-	-	-	-	-	-	-	-	-	-	-	0.06	0.09	0.02
Cl	-	-	-	0.00	-	-	-	-	0.01	-	-	-	-	0.00	0.00
Ps	0.30	0.22	0.32	0.30	0.31	0.27	0.26	0.28	0.22	0.28	0.21	0.16	0.26	0.33	0.23

Appendix B2. Epidote Analyses (continued)

Sample	96-1-14B3	96-1-14B4	96-1-14B5	96-1-19A3	96-1-19A4	96-1-19B3	96-1-19C1	96-1-19C2	96-1-19C3	96-1-19C4	96-1-27C1	96-1-29B2	96-1-29C2	96-1-29D2	96-1-29D3
Rock Type	epidosite	epidosite	epidosite	PG	PG	PG	PG	PG	PG	PG	PG	PG/basalt	PG/basalt	PG/basalt	PG/basalt
Location	OSU	OSU	OSU	OSU	OSU	OSU	OSU	OSU	OSU	OSU	UofA	OSU	OSU	OSU	OSU
Occurrence	gm	gm	gm	gm	gm	inc	vei	gm	gm	vei	gm	gm	gm	vei	gm
SiO_2	36.62	38.29	38.09	36.99	36.32	37.41	35.98	35.58	38.63	36.65	37.35	37.80	37.95	39.08	37.73
TiO_2	0.03	0.12	0.22	0.18	0.04	0.13	0.05	0.04	0.09	0.08	0.06	0.10	0.17	0.08	0.05
Al_2O_3	22.25	26.96	24.82	25.10	23.64	27.07	24.40	20.99	27.42	25.12	24.26	27.20	24.82	25.73	23.71
$Fe_2O_3^T$	15.06	9.74	12.00	12.45	13.63	9.16	12.50	16.82	8.79	11.66	13.56	9.12	11.80	10.67	13.84
Cr_2O_3	b.d.	b.d.	0.01	0.01	b.d.	b.d.	0.01	b.d.	0.02	0.02	0.03	b.d.	b.d.	b.d.	0.02
MnO	b.d.	0.12	0.08	1.09	0.44	0.43	0.20	b.d.	0.43	0.53	0.08	0.36	0.70	0.54	0.11
MgO	0.04	0.05	0.03	0.05	0.04	0.03	0.04	b.d.	0.04	0.04	0.02	0.03	0.20	0.02	0.04
CaO	23.01	23.94	23.68	21.74	23.42	23.30	23.50	23.13	23.52	22.89	23.29	22.95	21.70	23.00	23.38
Na_2O	b.d.	0.02	0.01	0.03	b.d.	0.07	0.01	0.02	0.01	0.01	b.d.	b.d.	0.04	0.01	0.01
K_2O	b.d.	0.02	0.01	b.d.	b.d.	b.d.	b.d.	0.01	b.d.	b.d.	0.01	0.01	b.d.	b.d.	b.d.
F	0.07	b.d.	0.04	0.05	b.d.	b.d.	b.d.	b.d.	b.d.	0.03	0.03	b.d.	b.d.	b.d.	b.d.
Cl	0.01	b.d.	b.d.	0.01	0.02	0.02	0.01	0.01	b.d.	0.01	b.d.	0.01	0.02	0.02	0.01
Total	97.09	99.26	98.99	97.70	97.55	97.62	96.70	96.60	98.95	97.04	98.69	97.58	97.40	99.15	98.90
Si	2.97	2.97	2.99	2.95	2.92	2.95	2.91	2.92	2.99	2.94	2.95	2.97	3.01	3.04	2.98
Al^{IV}	0.03	0.03	0.01	0.06	0.08	0.05	0.09	0.08	0.01	0.07	0.05	0.03	0.00	0.00	0.02
Al^{VI}	2.09	2.43	2.28	2.30	2.16	2.46	2.23	1.95	2.49	2.30	2.21	2.49	2.32	2.35	2.18
Ti	0.00	0.01	0.01	0.01	0.00	0.01	0.00	0.00	0.01	0.01	0.00	0.01	0.01	0.01	0.00
Cr	-	-	0.00	0.00	-	-	0.00	-	0.00	0.00	0.00	-	-	-	0.00
Fe^{3+}	0.92	0.57	0.71	0.75	0.82	0.54	0.76	1.04	0.51	0.70	0.81	0.54	0.70	0.62	0.82
Mn	-	0.01	0.01	0.07	0.03	0.03	0.01	-	0.03	0.04	0.01	0.02	0.05	0.04	0.01
Mg	0.01	0.01	0.00	0.01	0.01	0.00	0.01	-	0.01	0.01	0.00	0.00	0.02	0.00	0.01
Ca	2.00	1.99	1.99	1.85	2.02	1.97	2.03	2.04	1.95	1.96	1.97	1.93	1.85	1.91	1.98
Na	-	0.00	0.00	0.01	-	0.01	0.00	0.00	0.00	0.00	-	-	0.01	0.00	0.00
K	-	0.00	0.00	-	-	-	-	0.00	-	-	0.00	0.00	-	-	-
F	0.04	-	0.02	0.03	-	-	-	-	-	0.02	0.02	-	-	-	-
Cl	0.00	-	-	0.00	0.01	0.01	0.00	0.00	-	0.00	-	0.00	0.01	0.01	0.00
Ps	0.30	0.19	0.24	0.24	0.27	0.18	0.25	0.34	0.17	0.23	0.26	0.18	0.23	0.21	0.27

Appendix B2. Epidote Analyses (continued)

Sample	96-2-1A1	96-2-1B1	96-2-1B2	96-2-1C1	96-2-1C2	96-2-1C3	96-2-4A1	96-2-4A2	96-2-4A3	96-2-4A4	96-2-4A5	96-2-4A6	96-2-4B1	96-2-4B2	96-2-4B3
Rock Type	basalt	basalt	basalt	basalt	basalt	basalt	PG/basalt	PG/basalt	PG/basalt	PG/basalt	PG/basalt	PG/basalt	PG/basalt	PG/basalt	PG/basalt
Location	OSU	OSU	OSU	OSU	OSU	OSU	UofA	UofA	UofA	UofA	UofA	UofA	UofA	UofA	UofA
Occurrence	gm	vei	vei	vei	vei	gm	vei	vei	vei	vei	gm l	gm l	gm l	gm d	gm l
SiO_2	35.99	38.93	38.77	37.98	37.95	37.89	37.28	37.80	37.70	37.31	37.16	37.89	37.18	37.90	37.83
TiO_2	0.19	0.04	b.d.	0.16	0.07	0.12	0.10	0.07	0.04	0.03	0.08	0.01	0.06	b.d.	0.09
Al_2O_3	16.95	24.49	23.87	25.40	24.91	23.54	23.67	25.90	25.54	24.89	24.39	26.70	23.27	28.56	26.51
$Fe_2O_3^T$	21.74	12.30	12.65	11.43	12.04	12.82	13.57	10.50	11.24	11.45	13.09	9.77	13.90	7.62	10.18
Cr_2O_3	b.d.	b.d.	0.02	b.d.	b.d.	b.d.	b.d.	b.d.	b.d.	b.d.	b.d.	b.d.	b.d.	b.d.	b.d.
MnO	0.06	0.20	0.13	0.77	0.11	0.47	0.07	0.23	0.20	0.26	0.37	0.15	0.08	0.07	0.15
MgO	0.01	0.02	0.05	0.05	0.02	0.04	0.02	0.04	0.04	0.02	0.04	0.05	0.28	0.01	0.03
CaO	22.6	23.66	23.53	21.56	23.77	22.59	23.21	23.15	23.16	22.97	22.65	23.87	22.74	23.54	23.20
Na_2O	0.01	0.01	0.01	0.02	0.02	0.02	b.d.	0.02	b.d.	b.d.	b.d.	b.d.	0.02	b.d.	0.01
K_2O	0.01	b.d.	b.d.	b.d.	b.d.	0.01	0.04	0.02	0.02	0.02	0.02	0.02	0.02	0.01	0.02
F	b.d.	0.01	0.08	b.d.	b.d.	b.d.	b.d.	b.d.	b.d.	b.d.	b.d.	b.d.	b.d.	b.d.	b.d.
Cl	0.02	b.d.	0.01	0.01	0.01	0.02	0.01	0.01	b.d.	0.01	b.d.	b.d.	0.01	b.d.	0.01
Total	97.58	99.66	99.12	97.38	98.90	97.52	97.97	97.74	97.94	96.96	97.80	98.46	97.56	97.71	98.03
Si	2.978	3.03	3.04	3.01	2.98	3.02	2.97	2.98	2.98	2.98	2.96	2.96	2.98	2.96	2.97
Al^{IV}	0.022	0.00	0.00	0.00	0.02	0.00	0.03	0.02	0.02	0.02	0.04	0.04	0.02	0.04	0.03
Al^{VI}	1.63	2.24	2.20	2.37	2.28	2.21	2.19	2.39	2.35	2.32	2.25	2.42	2.17	2.58	2.42
Ti	0.012	0.00	-	0.01	0.00	0.01	0.01	0.00	0.00	0.00	0.01	0.00	0.00	-	0.01
Cr	-	-	0.00	-	-	-	-	-	-	-	-	-	-	-	-
Fe^{3+}	1.352	0.72	0.75	0.68	0.71	0.77	0.81	0.62	0.67	0.69	0.78	0.57	0.84	0.45	0.60
Mn	0.004	0.01	0.01	0.05	0.01	0.03	0.01	0.02	0.01	0.02	0.03	0.01	0.01	0.01	0.01
Mg	0.001	0.00	0.01	0.01	0.00	0.01	0.00	0.01	0.01	0.00	0.01	0.01	0.03	0.00	0.00
Ca	2.004	1.97	1.98	1.83	2.00	1.93	1.98	1.96	1.96	1.97	1.93	2.00	1.95	1.97	1.95
Na	0.002	0.00	0.00	0.00	0.00	0.00	-	0.00	-	-	-	-	0.00	-	0.00
K	0.001	-	-	-	-	0.00	0.00	0.00	0.00	0.00	0.00	0.00	0.00	0.00	0.00
F	-	0.01	0.04	-	-	-	-	-	-	-	-	-	-	-	-
Cl	0.006	-	0.00	0.00	0.00	0.01	0.00	0.00	-	0.00	-	-	0.00	-	0.00
Ps	0.45	0.24	0.25	0.22	0.24	0.26	0.27	0.21	0.22	0.23	0.26	0.19	0.28	0.15	0.20

Appendix B2. Epidote Analyses (continued)

Sample	96-2-4B4	96-2-4C1	96-2-4C2	96-2-4C4	96-2-7A1	96-2-7C2	99-2-1C1	99-2-1C2	99-2-1C3	99-2-1C4	99-2-1C5	99-2-1C6	99-2-8A1	99-2-8A2	99-2-8A3	99-2-8A4
Rock Type	PG/basalt	PG/basalt	PG/basalt	PG/basalt	basalt	basalt	basalt	basalt	basalt	basalt	basalt	basalt	PG	PG	PG	PG
Location	UofA	UofA	UofA	UofA	OSU	OSU	UofA	UofA	UofA	UofA	UofA	UofA	UofA	UofA	UofA	UofA
Occurrence	gm d	gm	gm	gm d	gm	rim	vei	vei	vei	vei	vei	vei	gm l	gm d	gm l	gm d
SiO_2	37.93	36.99	37.55	38.25	37.26	37.45	37.97	37.99	38.03	37.95	38.02	38.25	37.02	37.74	37.02	37.38
TiO_2	0.01	0.57	0.01	0.05	0.13	0.05	b.d.	0.01	0.06	b.d.	b.d.	0.02	0.15	0.08	0.11	0.08
Al_2O_3	28.45	23.67	27.36	27.78	24.54	24.11	27.72	27.94	27.97	27.89	28.74	28.34	21.99	26.84	21.43	24.21
$Fe_2O_3{}^T$	7.54	13.19	8.88	8.69	12.63	13.02	7.66	6.69	7.49	7.08	5.76	6.76	16.13	9.81	16.22	13.04
Cr_2O_3	b.d.	0.01	b.d.	b.d.	0.03	0.01	0.01	0.02	0.01	0.02	b.d.	b.d.	b.d.	b.d.	b.d.	b.d.
MnO	0.07	0.06	0.07	0.24	0.12	0.16	0.07	0.11	0.04	0.11	0.15	0.17	0.42	0.16	0.09	0.08
MgO	0.01	0.07	0.01	0.01	0.06	0.03	0.06	0.07	0.04	0.05	0.07	0.07	0.27	0.07	0.07	0.06
CaO	23.82	23.37	23.47	23.49	22.46	23.24	23.66	23.23	23.39	23.37	23.70	23.35	22.39	23.28	23.09	23.24
Na_2O	0.01	b.d.	0.01	0.01	b.d.	b.d.	0.01	b.d.	0.01	b.d.	b.d.	b.d.	0.01	b.d.	b.d.	0.02
K_2O	0.02	0.02	0.03	0.03	b.d.	0.01	0.01	0.01	0.01	0.04	0.01	0.01	b.d.	0.01	0.01	0.01
F	b.d.	b.d.	b.d.	b.d.	b.d.	0.01	b.d.	b.d.	b.d.	b.d.	b.d.	b.d.	b.d.	b.d.	0.01	b.d.
Cl	0.01	0.01	b.d.	0.01	0.02	0.01	b.d.	b.d.	0.01	0.01	b.d.	b.d.	b.d.	0.01	0.02	0.01
Total	97.87	97.96	97.39	98.56	97.25	98.10	97.17	96.07	97.06	96.52	96.45	96.97	98.38	98.00	98.07	98.13
Si	2.96	2.95	2.96	2.97	2.97	2.97	2.98	3.00	2.99	2.99	2.99	3.00	2.96	2.96	2.98	2.97
Al^{IV}	0.04	0.05	0.04	0.03	0.03	0.03	0.02	0.00	0.02	0.01	0.01	0.00	0.04	0.04	0.02	0.03
Al^{VI}	2.57	2.17	2.49	2.51	2.28	2.23	2.55	2.60	2.57	2.58	2.65	2.61	2.04	2.44	2.01	2.23
Ti	0.00	0.03	0.00	0.00	0.01	0.00	-	0.00	0.00	-	-	0.00	0.01	0.01	0.01	0.01
Cr	-	0.00	-	-	0.00	0.00	0.00	0.00	0.00	0.00	-	-	-	-	-	-
Fe^{3+}	0.44	0.79	0.53	0.51	0.76	0.78	0.45	0.40	0.44	0.42	0.34	0.40	0.97	0.58	0.98	0.78
Mn	0.01	0.00	0.01	0.02	0.01	0.01	0.01	0.01	0.00	0.01	0.01	0.01	0.03	0.01	0.01	0.01
Mg	0.00	0.01	0.00	0.00	0.01	0.00	0.01	0.01	0.01	0.01	0.01	0.01	0.03	0.01	0.01	0.01
Ca	1.99	2.00	1.98	1.96	1.92	1.98	1.99	1.97	1.97	1.98	2.00	1.96	1.92	1.96	1.99	1.98
Na	0.00	-	0.00	0.00	-	-	0.00	-	0.00	-	-	-	0.00	-	-	0.00
K	0.00	0.00	0.00	0.00	-	0.00	0.00	0.00	0.00	0.00	0.00	0.00	-	0.00	0.00	0.00
F	-	-	-	-	-	0.01	-	-	-	-	-	-	-	-	0.01	-
Cl	0.00	0.00	-	0.00	0.01	0.00	-	-	0.00	0.00	-	-	-	0.00	0.01	0.00
Ps	0.14	0.26	0.17	0.17	0.25	0.26	0.15	0.13	0.15	0.14	0.11	0.13	0.32	0.19	0.33	0.26

Appendix B2. Epidote Analyses (continued)

Sample	99-2-8B1	99-2-8B10	99-2-8B11	99-2-8B12	99-2-8B2	99-2-8B3	99-2-8B4	99-2-8B5	99-2-8B6	99-2-8B7	99-2-8B8	99-2-8B9	99-2-8C1	99-2-8C2	99-2-8C3	99-2-8C4
Rock Type	PG	PG	PG	PG	PG	PG	PG	PG	PG	PG	PG	PG	PG	PG	PG	PG
Location	UofA	UofA	UofA	UofA	UofA	UofA	UofA	UofA	UofA	UofA	UofA	UofA	UofA	UofA	UofA	UofA
Occurrence	ves	vei	vei	vei	ves	ves	ves	vei	vei	vei	vei	vei	ves	ves	ves	ves
SiO_2	37.17	38.19	37.35	37.76	37.44	37.55	37.91	36.91	37.29	36.98	37.51	37.16	37.32	37.89	37.02	37.70
TiO_2	0.32	0.12	0.41	0.16	0.07	0.07	0.16	0.32	0.16	0.06	0.13	0.05	0.26	0.07	0.35	0.13
Al_2O_3	21.57	27.56	23.03	26.74	23.69	24.25	26.28	21.52	25.24	22.55	25.08	21.63	22.97	25.31	22.31	26.43
$Fe_2O_3^T$	15.99	9.40	14.20	10.38	13.34	13.24	10.99	16.25	11.93	15.65	12.28	16.58	14.50	11.66	15.31	10.67
Cr_2O_3	0.03	b.d.	0.03	0.02	b.d.	0.01	b.d.	0.02	0.01	0.04	0.02	0.03	0.03	0.02	0.03	0.02
MnO	0.07	0.18	0.11	0.28	0.13	0.09	0.46	0.10	0.34	0.28	0.55	0.26	0.03	0.14	0.11	0.24
MgO	0.05	b.d.	0.05	0.05	0.04	0.01	0.04	0.03	0.03	0.08	0.05	0.06	0.03	0.07	0.04	0.02
CaO	23.04	23.27	23.04	22.81	23.23	23.41	22.99	23.17	22.73	22.58	22.69	22.80	23.35	23.23	23.17	22.80
Na_2O	0.01	b.d.	b.d.	b.d.	b.d.	0.01	b.d.	0.01	b.d.	b.d.	b.d.	b.d.	b.d.	b.d.	b.d.	b.d.
K_2O	0.02	0.02	0.02	0.02	0.01	0.01	0.01	0.01	0.03	0.02	0.03	0.03	0.02	b.d.	0.02	0.02
F	b.d.	b.d.	b.d.	b.d.	b.d.	b.d.	b.d.	0.03	b.d.	b.d.	b.d.	b.d.	b.d.	b.d.	b.d.	b.d.
Cl	0.01	b.d.	b.d.	b.d.	b.d.	0.01	b.d.	0.01	b.d.	b.d.	b.d.	0.01	0.01	b.d.	b.d.	b.d.
Total	98.28	98.74	98.24	98.22	97.95	98.66	98.84	98.38	97.76	98.24	98.34	98.61	98.52	98.39	98.36	98.03
Si	2.98	2.97	2.97	2.96	2.98	2.97	2.96	2.96	2.96	2.96	2.96	2.98	2.97	2.98	2.96	2.96
Al^{IV}	0.02	0.04	0.03	0.04	0.02	0.03	0.04	0.04	0.04	0.04	0.04	0.03	0.03	0.02	0.04	0.04
Al^{VI}	2.02	2.49	2.13	2.43	2.20	2.22	2.38	2.00	2.31	2.08	2.29	2.01	2.12	2.32	2.06	2.41
Ti	0.02	0.01	0.03	0.01	0.00	0.00	0.01	0.02	0.01	0.00	0.01	0.00	0.02	0.00	0.02	0.01
Cr	0.00	-	0.00	0.00	-	0.00	-	0.00	0.00	0.00	0.00	0.00	0.00	0.00	0.00	0.00
Fe^{3+}	0.96	0.55	0.85	0.61	0.80	0.79	0.65	0.98	0.71	0.94	0.73	1.00	0.87	0.69	0.92	0.63
Mn	0.01	0.01	0.01	0.02	0.01	0.01	0.03	0.01	0.02	0.02	0.04	0.02	0.00	0.01	0.01	0.02
Mg	0.01	-	0.01	0.01	0.01	0.00	0.01	0.00	0.00	0.01	0.01	0.01	0.00	0.01	0.01	0.00
Ca	1.98	1.94	1.97	1.92	1.98	1.98	1.92	1.99	1.93	1.94	1.92	1.96	1.99	1.96	1.99	1.92
Na	0.00	-	-	-	-	0.00	-	0.00	-	-	-	-	-	-	-	-
K	0.00	0.00	0.00	0.00	0.00	0.00	0.00	0.00	0.00	0.00	0.00	0.00	0.00	-	0.00	0.00
F	-	-	-	-	-	-	-	0.02	-	-	-	-	-	-	-	-
Cl	0.00	-	-	-	-	0.00	-	0.00	-	-	-	0.00	0.00	-	-	-
Ps	0.32	0.18	0.28	0.20	0.26	0.26	0.21	0.33	0.23	0.31	0.24	0.33	0.29	0.23	0.30	0.20

Appendix B2. Epidote Analyses (continued)

Sample	99-2-8C5	99-2-8C6	99-2-8C7	99-2-8C8	99-2-12A1	99-2-12A2	99-2-12A3	99-2-12A4	99-2-12A5	99-2-12A6	99-2-12B1	99-2-12B2	99-2-12B3	99-2-12B4	99-2-12C1
Rock Type	PG	PG	PG	PG	basalt	basalt	basalt	basalt	basalt	basalt	basalt	basalt	basalt	basalt	basalt
Location	UofA	UofA	UofA	UofA	UofA	UofA	UofA	UofA	UofA	UofA	UofA	UofA	UofA	UofA	UofA
Occurrence	gm l	gm d	gm l	gm d	ves	ves	ves	ves	ves	ves	ves	ves	ves	ves	gm l
SiO_2	37.04	37.41	37.23	37.39	37.08	37.67	37.57	38.02	37.44	37.61	37.40	37.26	37.43	37.38	37.33
TiO_2	0.09	0.12	0.19	0.09	0.43	0.04	0.33	0.05	0.25	0.08	0.20	0.05	0.10	0.16	0.06
Al_2O_3	21.87	23.68	22.81	24.68	21.98	24.53	23.22	26.43	23.56	24.59	24.27	23.35	23.48	23.28	24.19
$Fe_2O_3^T$	16.46	14.19	15.00	12.52	15.05	12.17	13.35	9.96	13.36	12.38	12.98	13.95	13.88	13.95	13.39
Cr_2O_3	0.04	0.01	0.03	b.d.	0.01	b.d.	0.01	b.d.	b.d.	b.d.	0.01	b.d.	0.01	b.d.	b.d.
MnO	0.33	0.21	0.27	0.75	0.06	0.12	0.06	0.14	0.09	0.14	0.17	0.18	0.18	0.17	0.09
MgO	0.11	0.14	0.04	0.04	0.02	0.03	0.01	0.02	0.02	0.06	0.25	0.03	0.24	0.17	0.03
CaO	22.34	22.73	23.07	22.41	23.01	23.39	23.12	23.35	23.17	23.38	22.76	22.95	22.80	22.82	23.43
Na_2O	b.d.	b.d.	b.d.	b.d.	0.02	b.d.	0.01	0.02	0.01	0.02	0.02	b.d.	0.02	0.01	0.02
K_2O	0.03	0.02	0.03	0.03	0.01	b.d.	0.01	b.d.	0.01	0.01	0.02	0.01	0.02	0.01	0.02
F	0.01	b.d.	b.d.	b.d.	b.d.	b.d.	b.d.	b.d.	b.d.	b.d.	b.d.	b.d.	b.d.	b.d.	b.d.
Cl	b.d.	b.d.	b.d.	b.d.	0.01	0.02	0.01	b.d.	b.d.	b.d.	0.02	b.d.	b.d.	b.d.	b.d.
Total	98.32	98.51	98.67	97.91	97.68	97.97	97.70	97.99	97.91	98.27	98.10	97.78	98.16	97.95	98.56
Si	2.97	2.97	2.96	2.97	2.98	2.99	3.00	2.98	2.98	2.97	2.97	2.98	2.98	2.98	2.96
Al^{IV}	0.03	0.03	0.04	0.03	0.02	0.02	0.00	0.02	0.02	0.03	0.03	0.02	0.02	0.02	0.05
Al^{VI}	2.04	2.18	2.10	2.28	2.06	2.27	2.18	2.43	2.19	2.26	2.23	2.18	2.18	2.17	2.21
Ti	0.01	0.01	0.01	0.01	0.03	0.00	0.02	0.00	0.02	0.01	0.01	0.00	0.01	0.01	0.00
Cr	0.00	0.00	0.00	-	0.00	-	0.00	-	-	-	0.00	-	0.00	-	-
Fe^{3+}	0.99	0.85	0.90	0.75	0.91	0.73	0.80	0.59	0.80	0.74	0.77	0.84	0.83	0.84	0.80
Mn	0.02	0.01	0.02	0.05	0.00	0.01	0.00	0.01	0.01	0.01	0.01	0.01	0.01	0.01	0.01
Mg	0.01	0.02	0.01	0.01	0.00	0.00	0.00	0.00	0.00	0.01	0.03	0.00	0.03	0.02	0.00
Ca	1.92	1.93	1.97	1.91	1.98	1.99	1.98	1.96	1.98	1.98	1.93	1.97	1.94	1.95	1.99
Na	-	-	-	-	0.00	-	0.00	0.00	0.00	0.00	0.00	-	0.00	0.00	0.00
K	0.00	0.00	0.00	0.00	0.00	-	0.00	-	0.00	0.00	0.00	0.00	0.00	0.00	0.00
F	0.01	-	-	-	-	-	-	-	-	-	-	-	-	-	-
Cl	-	-	-	-	0.00	0.01	0.00	-	-	-	0.01	-	-	-	-
Ps	0.32	0.28	0.30	0.24	0.30	0.24	0.27	0.19	0.27	0.24	0.25	0.28	0.27	0.28	0.26

Appendix B2. Epidote Analyses (continued)

Sample	99-2-12C2	99-2-12C3	99-2-12C4	101-1-24A1	101-1-24A2	101-1-24A3	101-1-24A4	101-1-24C1	101-1-24C2	101-1-24C3	101-1-24C4	101-1-24C5	101-1-24C6
Rock Type	basalt	basalt	basalt	basalt	basalt	basalt	basalt	basalt	basalt	basalt	basalt	basalt	basalt
Location	UofA	UofA	UofA	UofA	UofA	UofA	UofA	UofA	UofA	UofA	UofA	UofA	UofA
Occurrence	gm d	gm l	gm d	vei	vei	vei	vei	vei	vei	vei	vei	vei	vei
SiO_2	37.60	37.03	38.00	37.57	37.22	37.22	37.28	36.93	37.40	37.43	37.15	37.47	36.48
TiO_2	0.08	0.54	0.03	0.06	0.01	0.12	0.05	0.07	0.12	0.07	0.11	0.12	0.11
Al_2O_3	25.43	22.39	26.54	24.03	22.69	23.34	23.73	22.69	24.48	24.75	24.87	24.54	19.92
$Fe_2O_3^T$	11.17	14.40	10.08	12.58	13.74	13.00	12.69	14.07	11.58	11.22	11.17	11.77	17.48
Cr_2O_3	0.02	b.d.	b.d.	0.01	0.03	0.03	b.d.	0.01	b.d.	b.d.	0.01	b.d.	b.d.
MnO	0.12	0.06	0.13	0.06	0.01	0.09	0.08	0.07	0.12	0.09	0.07	0.13	0.04
MgO	0.06	0.04	0.06	0.04	0.04	0.04	0.05	0.11	0.03	0.04	0.02	0.05	0.02
CaO	23.63	23.29	23.49	23.27	22.87	23.02	22.91	22.60	22.87	23.19	23.15	22.58	22.80
Na_2O	0.01	0.01	0.02	b.d.	0.01	b.d.	0.02	0.02	b.d.	b.d.	0.01	0.04	b.d.
K_2O	b.d.	0.01	0.01	0.04	0.01	0.05	0.04	0.01	0.03	0.02	0.02	0.01	0.02
F	b.d.	b.d.	b.d.	b.d.	b.d.	b.d.	b.d.	b.d.	b.d.	b.d.	b.d.	b.d.	b.d.
Cl	b.d.	b.d.	b.d.	0.03	b.d.	0.01	b.d.	b.d.	0.01	0.01	0.01	0.02	b.d.
Total	98.12	97.77	98.36	97.69	96.63	96.92	96.85	96.58	96.64	96.82	96.59	96.73	96.87
Si	2.97	2.97	2.97	2.99	3.01	2.99	2.99	2.99	3.00	2.99	2.98	3.00	2.99
Al^{IV}	0.03	0.03	0.03	0.01	0.00	0.01	0.01	0.01	0.00	0.01	0.02	0.00	0.01
Al^{VI}	2.33	2.09	2.42	2.24	2.16	2.20	2.24	2.15	2.31	2.32	2.32	2.31	1.91
Ti	0.01	0.03	0.00	0.00	0.00	0.01	0.00	0.00	0.01	0.00	0.01	0.01	0.01
Cr	0.00	-	-	0.00	0.00	0.00	-	0.00	-	-	0.00	-	-
Fe^{3+}	0.66	0.87	0.59	0.75	0.83	0.79	0.77	0.86	0.70	0.67	0.67	0.71	1.08
Mn	0.01	0.00	0.01	0.00	0.00	0.01	0.01	0.01	0.01	0.01	0.01	0.01	0.00
Mg	0.01	0.01	0.01	0.01	0.01	0.01	0.01	0.01	0.00	0.01	0.00	0.01	0.00
Ca	2.00	2.00	1.97	1.99	1.98	1.98	1.97	1.96	1.96	1.99	1.99	1.94	2.00
Na	0.00	0.00	0.00	-	0.00	-	0.00	0.00	-	-	0.00	0.01	-
K	-	0.00	0.00	0.00	0.00	0.01	0.00	0.00	0.00	0.00	0.00	0.00	0.00
F	-	-	-	-	-	-	-	-	-	-	-	-	-
Cl	-	-	-	0.01	-	0.00	-	-	0.00	0.00	0.00	0.01	-
Ps	0.22	0.29	0.20	0.25	0.28	0.26	0.25	0.28	0.23	0.22	0.22	0.23	0.36

Appendix B2. Epidote Analyses (continued)

Sample	102-4-1A1	102-4-1A2	102-4-1A3	102-4-1A4	102-4-1A5	102-4-1B1	102-4-1B2	102-4-1B3	102-4-1B4	102-4-1C1	102-4-1C2	102-4-1C3	102-4-1C4	102-4-1D1	102-4-1D2
Rock Type	epidosite	epidosite	epidosite	epidosite	epidosite	epidosite	epidosite	epidosite	epidosite	epidosite	epidosite	epidosite	epidosite	epidosite	epidosite
Location	UofA	UofA	UofA	UofA	UofA	UofA	UofA	UofA	UofA	UofA	UofA	UofA	UofA	UofA	UofA
Occurrence	vei	vei	vei	vei	vei	vei	vei	vei	gm	gm l	gm d	gm l	gm d	gm l	gm d
SiO_2	37.59	37.24	37.84	37.43	37.74	37.10	37.35	37.64	37.25	37.31	36.30	37.26	37.64	37.09	37.59
TiO_2	0.19	0.02	0.11	0.11	0.01	0.01	0.11	0.16	0.09	0.42	0.13	0.39	0.04	0.37	0.07
Al_2O_3	25.90	24.87	26.32	26.15	27.54	25.55	23.88	24.91	22.82	22.73	25.95	24.43	28.53	23.45	25.97
$Fe_2O_3^T$	10.57	12.25	10.40	10.74	8.84	11.16	13.76	12.23	14.64	14.15	11.13	12.22	6.49	13.46	10.98
Cr_2O_3	b.d.	0.01	0.02	b.d.	b.d.	b.d.	0.02	0.01	0.03	0.01	0.01	0.01	b.d.	b.d.	0.01
MnO	0.11	b.d.	0.12	0.41	0.10	0.07	0.12	0.07	0.16	0.14	0.41	0.07	0.14	0.35	0.26
MgO	0.08	0.01	0.15	0.13	0.03	0.02	0.02	0.06	0.03	0.05	0.05	0.11	0.02	0.04	0.07
CaO	23.20	23.08	23.16	22.66	23.27	23.12	23.07	23.47	22.81	22.47	22.82	23.59	23.55	23.03	23.28
Na_2O	0.03	0.01	0.02	0.01	b.d.	0.01	0.01	0.01	0.02	0.07	b.d.	0.01	0.01	b.d.	b.d.
K_2O	0.01	b.d.	0.01	0.01	0.01	b.d.	0.01	b.d.	b.d.	b.d.	b.d.	0.01	b.d.	b.d.	b.d.
F	b.d.	b.d.	0.04	0.01	b.d.	0.03	b.d.	b.d.	b.d.	0.02	b.d.	b.d.	b.d.	b.d.	b.d.
Cl	0.01	b.d.	b.d.	b.d.	b.d.	0.01	b.d.	0.01	b.d.	0.01	0.01	b.d.	b.d.	b.d.	0.02
Total	97.69	97.49	98.19	97.66	97.54	97.08	98.35	98.57	97.85	97.38	96.81	98.10	96.42	97.79	98.25
Si	2.97	2.96	2.97	2.96	2.96	2.96	2.96	2.97	2.98	2.99	2.91	2.96	2.97	2.96	2.96
Al^{IV}	0.03	0.04	0.03	0.04	0.04	0.04	0.04	0.04	0.02	0.01	0.09	0.05	0.03	0.04	0.04
Al^{VI}	2.38	2.29	2.40	2.39	2.51	2.35	2.20	2.28	2.13	2.14	2.35	2.24	2.62	2.17	2.36
Ti	0.01	0.00	0.01	0.01	0.00	0.00	0.01	0.01	0.01	0.03	0.01	0.02	0.00	0.02	0.00
Cr	-	0.00	0.00	-	-	-	0.00	0.00	0.00	0.00	0.00	0.00	-	-	0.00
Fe^{3+}	0.63	0.73	0.61	0.64	0.52	0.67	0.82	0.72	0.88	0.85	0.67	0.73	0.39	0.81	0.65
Mn	0.01	-	0.01	0.03	0.01	0.01	0.01	0.01	0.01	0.01	0.03	0.01	0.01	0.02	0.02
Mg	0.01	0.00	0.02	0.02	0.00	0.00	0.00	0.01	0.00	0.01	0.01	0.01	0.00	0.01	0.01
Ca	1.96	1.97	1.95	1.92	1.96	1.97	1.96	1.98	1.96	1.93	1.96	2.00	1.99	1.97	1.96
Na	0.01	0.00	0.00	0.00	-	0.00	0.00	0.00	0.00	0.01	-	0.00	0.00	-	-
K	0.00	-	0.00	0.00	0.00	-	0.00	-	-	-	-	0.00	-	-	-
F	-	-	0.02	0.01	-	0.02	-	-	-	0.01	-	-	-	-	-
Cl	0.00	-	-	-	-	0.00	-	0.00	-	0.00	0.00	-	-	-	0.01
Ps	0.21	0.24	0.20	0.21	0.17	0.22	0.27	0.24	0.29	0.28	0.21	0.24	0.13	0.27	0.21

Appendix B2. Epidote Analyses (continued)

Sample	102-4-1D3	102-4-1D4	105-1-8(b)A5	105-1-8(b)B1	105-1-8(b)C4	105-1-8(b)D1	105-1-8(b)E1	105-1-8(b)E2	105-1-14A1	105-1-25B2	105-1-25B3	105-1-25B5	105-1-25D2
Rock Type	epidosite	epidosite	gabbro	gabbro	gabbro	gabbro	gabbro	gabbro	gabbro	gabbro	gabbro	gabbro	gabbro
Location	UofA	UofA	OSU	OSU	OSU	OSU	OSU	OSU	OSU	OSU	OSU	OSU	OSU
Occurrence	gm l	gm d	gm	gm	gm	gm	vei	vei	gm	vei	gm	vei	vei
SiO_2	37.11	37.32	37.98	38.88	38.69	40.33	39.12	38.74	37.66	38.00	38.31	37.69	37.86
TiO_2	0.06	0.09	0.06	0.01	0.11	0.02	0.02	0.02	0.07	0.09	0.10	0.22	0.01
Al_2O_3	23.21	23.12	25.35	26.10	26.11	23.49	28.48	28.93	24.31	26.06	26.73	27.17	25.97
$Fe_2O_3^T$	14.07	14.37	11.68	10.38	8.98	11.65	6.77	5.96	12.80	10.36	9.16	9.45	10.54
Cr_2O_3	b.d.	0.01	b.d.	0.02	0.01	b.d.	b.d.	0.02	0.10	0.02	b.d.	0.05	b.d.
MnO	0.18	0.19	b.d.	0.14	b.d.	0.08	0.23	0.22	0.11	0.03	0.18	0.60	0.09
MgO	0.03	0.05	0.03	0.09	0.07	0.09	0.32	0.38	b.d.	0.05	0.11	0.23	0.16
CaO	23.12	23.14	23.78	24.23	24.06	24.05	24.03	24.30	23.14	23.79	23.51	22.85	23.56
Na_2O	0.02	0.01	0.02	0.03	0.04	0.03	b.d.	0.01	0.01	0.02	0.01	0.02	b.d.
K_2O	b.d.	0.01	0.01	0.02	0.02	b.d.	b.d.	b.d.	b.d.	b.d.	0.01	b.d.	b.d.
F	0.01	0.02	0.10	0.01	0.08	0.10	0.07	0.06	0.06	0.02	0.13	0.08	b.d.
Cl	0.01	0.01	0.01	0.01	0.03	0.02	0.03	0.01	0.01	0.01	b.d.	0.01	0.01
Total	97.82	98.34	99.02	99.92	98.20	99.86	99.07	98.65	98.27	98.45	98.25	98.37	98.20
Si	2.97	2.97	2.97	3.00	3.03	3.12	3.01	2.99	2.98	2.98	3.00	2.95	2.97
Al^{IV}	0.03	0.03	0.03	0.00	0.00	0.00	0.00	0.02	0.02	0.02	0.01	0.05	0.03
Al^{VI}	2.16	2.14	2.31	2.37	2.41	2.14	2.58	2.61	2.25	2.38	2.46	2.45	2.38
Ti	0.00	0.01	0.00	0.00	0.01	0.00	0.00	0.00	0.00	0.01	0.01	0.01	0.00
Cr	-	0.00	-	0.00	0.00	-	-	0.00	0.01	0.00	-	0.00	-
Fe^{3+}	0.85	0.86	0.69	0.60	0.53	0.68	0.39	0.35	0.76	0.61	0.54	0.56	0.62
Mn	0.01	0.01	-	0.01	-	0.01	0.02	0.01	0.01	0.00	0.01	0.04	0.01
Mg	0.00	0.01	0.00	0.01	0.01	0.01	0.04	0.04	-	0.01	0.01	0.03	0.02
Ca	1.98	1.98	2.00	2.00	2.02	2.00	1.98	2.01	1.96	2.00	1.97	1.92	1.98
Na	0.00	0.00	0.00	0.00	0.01	0.01	-	0.00	0.00	0.00	0.00	0.00	-
K	-	0.00	0.00	0.00	0.00	-	-	-	-	-	0.00	-	-
F	0.01	0.01	0.05	0.01	0.04	0.05	0.03	0.03	0.03	0.01	0.06	0.04	-
Cl	0.00	0.00	0.00	0.00	0.01	0.01	0.01	0.00	0.00	0.00	-	0.00	0.00
Ps	0.28	0.28	0.23	0.20	0.18	0.24	0.13	0.12	0.25	0.20	0.18	0.18	0.21

Appendix B2. Epidote Analyses (continued)

Sample	105-3-6a1	105-3-6B1	105-3-6B2	105-3-6B3	105-3-6B4	105-3-6B5	105-3-6D6	106-2-11A1	106-2-11D2	106-2-11D3	108-2-12A1	108-2-12A2	108-2-12A3	108-2-12A4
Rock Type	basalt	basalt	basalt	basalt	basalt	basalt	basalt	PG	PG	PG	PG	PG	PG	PG
Location	OSU	OSU	OSU	OSU	OSU	OSU	OSU	OSU	OSU	OSU	UofA	UofA	UofA	UofA
Occurrence	gm	vei	vei	cor	inc	inc	gm	vei	gm	gm	gm	gm	gm	gm
SiO_2	38.30	38.13	38.08	39.06	38.22	38.02	37.92	37.62	38.17	37.68	37.58	37.71	38.01	37.72
TiO_2	0.03	0.06	0.13	0.03	0.04	0.09	0.01	0.10	0.10	0.08	0.04	0.06	0.11	0.04
Al_2O_3	23.28	25.36	23.78	29.38	24.45	25.95	23.42	26.18	27.37	27.11	25.89	26.45	27.65	25.57
$Fe_2O_3{}^T$	14.38	11.58	13.09	5.82	12.30	10.49	14.08	9.93	8.34	9.45	11.12	9.74	7.93	10.76
Cr_2O_3	0.01	b.d.	0.06	0.01	0.02	b.d.	b.d.	b.d.	b.d.	0.01	0.01	b.d.	b.d.	0.02
MnO	0.23	0.04	0.09	0.01	0.12	0.13	0.10	0.22	0.11	0.24	0.11	0.15	0.17	0.08
MgO	0.05	0.07	0.02	0.07	0.01	0.03	0.03	b.d.	b.d.	0.03	0.31	0.03	b.d.	0.01
CaO	23.42	23.76	23.67	24.58	23.72	23.58	23.53	22.88	23.34	23.00	22.96	23.35	23.62	23.16
Na_2O	0.01	b.d.	b.d.	0.01	0.01	0.01	0.01	0.03	0.02	0.02	b.d.	b.d.	b.d.	0.01
K_2O	b.d.	b.d.	b.d.	0.03	b.d.	0.01	0.01	0.01	0.02	0.02	0.03	0.01	0.02	0.02
F	0.05	b.d.	0.02	0.17	0.03	0.08	b.d.	0.08	b.d.	b.d.	b.d.	b.d.	b.d.	b.d.
Cl	0.02	0.01	0.02	b.d.	0.02	0.03	0.01	0.01	0.02	0.02	0.02	b.d.	b.d.	0.02
Total	99.78	99.01	98.96	99.17	98.94	98.42	99.12	97.06	97.49	97.66	98.07	97.50	97.51	97.41
Si	3.00	2.98	3.00	2.99	3.00	2.98	2.99	2.98	2.99	2.96	2.96	2.98	2.98	2.99
Al^{IV}	0.00	0.02	0.00	0.01	0.00	0.02	0.01	0.02	0.01	0.04	0.04	0.03	0.02	0.01
Al^{VI}	2.15	2.32	2.21	2.64	2.26	2.38	2.17	2.43	2.52	2.47	2.36	2.43	2.53	2.37
Ti	0.00	0.00	0.01	0.00	0.00	0.01	0.00	0.01	0.01	0.01	0.00	0.00	0.01	0.00
Cr	0.00	-	0.00	0.00	0.00	-	-	-	-	0.00	0.00	-	-	0.00
Fe^{3+}	0.85	0.68	0.78	0.34	0.73	0.62	0.84	0.59	0.49	0.56	0.66	0.58	0.47	0.64
Mn	0.02	0.00	0.01	0.00	0.01	0.01	0.01	0.02	0.01	0.02	0.01	0.01	0.01	0.01
Mg	0.01	0.01	0.00	0.01	0.00	0.00	0.00	-	-	0.00	0.04	0.00	-	0.00
Ca	1.97	1.99	2.00	2.02	2.00	1.98	1.99	1.94	1.96	1.94	1.94	1.97	1.98	1.97
Na	0.00	-	-	0.00	0.00	0.00	0.00	0.01	0.00	0.00	-	-	-	0.00
K	-	-	-	0.00	-	0.00	0.00	0.00	0.00	0.00	0.00	0.00	0.00	0.00
F	0.03	-	0.01	0.08	0.02	0.04	-	0.04	-	-	-	-	-	-
Cl	0.01	0.00	0.01	-	0.01	0.01	0.00	0.00	0.01	0.01	0.01	-	-	0.01
Ps	0.28	0.23	0.26	0.11	0.24	0.21	0.28	0.19	0.16	0.18	0.22	0.19	0.15	0.21

Appendix B2. Epidote Analyses (continued)

Sample	108-2-12B1	108-2-12B2	108-2-12B3	108-2-12B4	108-2-12B5	108-2-12B6	108-2-12C1	108-2-12C2	108-2-12C3	108-2-12C4	108-2-12C5	108-2-12C6	108-3-1A1
Rock Type	PG	PG	PG	PG	PG	PG	PG	PG	PG	PG	PG	PG	basalt
Location	UofA	UofA	UofA	UofA	UofA	UofA	UofA	UofA	UofA	UofA	UofA	UofA	UofA
Occurrence	gm	gm	gm	gm	gm	gm	gm	gm	gm	gm	gm	gm	vei
SiO_2	37.31	37.45	37.01	37.91	37.01	37.00	37.29	37.75	37.30	37.45	37.18	37.54	37.94
TiO_2	0.16	0.17	0.41	0.09	0.32	0.38	0.08	0.10	0.02	0.16	0.29	0.01	0.16
Al_2O_3	24.76	25.19	23.09	26.66	23.19	23.21	23.60	26.85	24.38	26.25	22.62	25.44	26.41
$Fe_2O_3^T$	11.77	11.38	13.43	9.77	13.13	12.76	13.78	9.16	12.10	10.81	14.39	11.36	10.41
Cr_2O_3	b.d.	b.d.	b.d.	b.d.	0.01	0.01	b.d.	b.d.	0.02	0.02	0.02	0.01	b.d.
MnO	0.09	0.13	0.04	0.09	0.04	0.03	0.16	0.26	0.05	0.49	0.02	0.06	0.31
MgO	0.01	0.01	0.01	0.04	0.01	0.03	0.03	0.02	0.01	0.03	0.03	0.01	0.02
CaO	23.33	23.41	23.20	23.21	22.89	22.76	22.87	22.92	23.31	22.36	23.18	23.58	23.06
Na_2O	b.d.	b.d.	b.d.	b.d.	0.04	b.d.	b.d.	b.d.	b.d.	0.01	b.d.	b.d.	b.d.
K_2O	b.d.	0.01	0.02	0.03	0.03	0.02	0.02	0.01	0.02	0.01	0.03	0.03	0.03
F	b.d.	b.d.	b.d.	b.d.	b.d.	b.d.	b.d.	b.d.	b.d.	b.d.	b.d.	b.d.	b.d.
Cl	b.d.	0.01	b.d.	b.d.	b.d.	b.d.	b.d.	b.d.	b.d.	0.02	0.01	0.02	b.d.
Total	97.43	97.76	97.21	97.80	96.67	96.20	97.83	97.07	97.21	97.61	97.77	98.06	98.34
Si	2.97	2.97	2.97	2.98	2.99	2.99	2.98	2.98	2.98	2.96	2.98	2.97	2.97
Al^{IV}	0.03	0.03	0.03	0.02	0.02	0.01	0.03	0.02	0.02	0.04	0.02	0.04	0.03
Al^{VI}	2.29	2.32	2.16	2.44	2.19	2.21	2.19	2.48	2.27	2.40	2.12	2.33	2.41
Ti	0.01	0.01	0.03	0.01	0.02	0.02	0.01	0.01	0.00	0.01	0.02	0.00	0.01
Cr	-	-	-	-	0.00	0.00	-	-	0.00	0.00	0.00	0.00	-
Fe^{3+}	0.70	0.68	0.81	0.58	0.80	0.78	0.83	0.54	0.73	0.64	0.87	0.68	0.61
Mn	0.01	0.01	0.00	0.01	0.00	0.00	0.01	0.02	0.00	0.03	0.00	0.00	0.02
Mg	0.00	0.00	0.00	0.01	0.00	0.00	0.00	0.00	0.00	0.00	0.00	0.00	0.00
Ca	1.99	1.99	2.00	1.95	1.98	1.97	1.96	1.94	2.00	1.89	1.99	2.00	1.94
Na	-	-	-	-	0.01	-	-	-	-	0.00	-	-	-
K	-	0.00	0.00	0.00	0.00	0.00	0.00	0.00	0.00	0.00	0.00	0.00	0.00
F	-	-	-	-	-	-	-	-	-	-	-	-	-
Cl	-	0.00	-	-	-	-	-	-	-	0.01	0.00	0.01	-
Ps	0.23	0.22	0.27	0.19	0.27	0.26	0.27	0.18	0.24	0.21	0.29	0.22	0.20

Appendix B2. Epidote Analyses (continued)

Sample	108-3-1A2	108-3-1A3	108-3-1A4	108-3-1A5	108-3-1D1	108-3-1D2	108-3-1F1	108-3-1F2	108-3-1G3	108-3-16A1	108-3-16A2	108-3-16A3	108-3-16A4
Rock Type	basalt	basalt	basalt	basalt	basalt	basalt	basalt	basalt	basalt	epidosite	epidosite	epidosite	epidosite
Location	UofA	UofA	UofA	UofA	UofA	UofA	UofA	UofA	UofA	UofA	UofA	UofA	UofA
Occurrence	vei	vei	vei	vei	vei	vei	gm l	gm d	gm	gm l	gm d	gm l	gm d
SiO_2	37.12	37.72	36.96	37.73	36.91	37.54	37.16	37.80	37.51	37.38	37.67	37.25	37.41
TiO_2	0.55	0.19	0.41	0.07	0.04	0.08	0.14	b.d.	0.01	0.04	0.18	0.26	0.09
Al_2O_3	23.05	26.87	22.27	25.24	21.51	24.96	22.21	23.76	24.44	24.12	26.50	22.84	25.50
$Fe_2O_3^T$	14.01	10.15	14.63	11.89	16.92	12.22	14.63	12.68	12.69	13.27	10.21	13.94	11.65
Cr_2O_3	b.d.	b.d.	b.d.	b.d.	b.d.	b.d.	0.01	b.d.	b.d.	0.02	b.d.	0.01	0.02
MnO	0.08	0.41	0.07	0.16	0.08	0.18	0.08	0.15	0.22	0.06	0.28	0.06	0.21
MgO	0.03	0.04	0.02	0.04	b.d.	0.02	0.04	0.04	0.01	b.d.	0.03	0.06	0.02
CaO	23.37	22.92	23.13	23.27	22.93	23.35	23.24	23.29	23.33	23.24	23.06	23.19	23.22
Na_2O	b.d.	b.d.	b.d.	b.d.	b.d.	0.02	b.d.	b.d.	b.d.	b.d.	0.02	0.01	0.02
K_2O	0.03	0.03	0.04	0.03	0.03	0.04	0.03	0.03	0.03	0.02	0.02	0.02	0.01
F	b.d.	b.d.	b.d.	b.d.	0.02	0.01	0.01	0.03	b.d.	b.d.	b.d.	0.03	b.d.
Cl	b.d.	b.d.	b.d.	b.d.	b.d.	b.d.	0.01	0.01	b.d.	b.d.	b.d.	0.01	b.d.
Total	98.24	98.33	97.53	98.43	98.44	98.42	97.56	97.79	98.24	98.15	97.97	97.68	98.15
Si	2.96	2.95	2.97	2.97	2.96	2.96	2.99	3.01	2.97	2.97	2.96	2.98	2.95
Al^{IV}	0.04	0.05	0.03	0.03	0.04	0.04	0.01	0.00	0.03	0.03	0.04	0.02	0.05
Al^{VI}	2.12	2.43	2.09	2.31	2.00	2.28	2.09	2.23	2.25	2.22	2.41	2.14	2.32
Ti	0.03	0.01	0.03	0.00	0.00	0.01	0.01	-	0.00	0.00	0.01	0.02	0.01
Cr	-	-	-	-	-	-	0.00	-	-	0.00	-	0.00	0.00
Fe^{3+}	0.84	0.60	0.89	0.70	1.02	0.73	0.89	0.76	0.76	0.79	0.60	0.84	0.69
Mn	0.01	0.03	0.01	0.01	0.01	0.01	0.01	0.01	0.02	0.00	0.02	0.00	0.01
Mg	0.00	0.01	0.00	0.01	-	0.00	0.01	0.01	0.00	-	0.00	0.01	0.00
Ca	2.00	1.92	1.99	1.96	1.97	1.98	2.00	1.99	1.98	1.98	1.94	1.99	1.96
Na	-	-	-	-	-	0.00	-	-	-	-	0.00	0.00	0.00
K	0.00	0.00	0.00	0.00	0.00	0.00	0.00	0.00	0.00	0.00	0.00	0.00	0.00
F	-	-	-	-	0.01	0.01	0.01	0.02	-	-	-	0.02	-
Cl	-	-	-	-	-	-	0.00	0.00	-	-	-	0.00	-
Ps	0.28	0.19	0.30	0.23	0.33	0.24	0.30	0.25	0.25	0.26	0.20	0.28	0.23

Appendix B2. Epidote Analyses (continued)

Sample	108-3-16B1	108-3-16B2	108-3-16C1	108-3-16C2	108-3-16C3	108-3-16C4	108-3-16D1	108-3-16D2	108-3-16D3	108-3-16D4	110-1-5AA1	110-1-5AA2	110-1-5AA3	110-1-5AA4
Rock Type	epidosite	epidosite	epidosite	epidosite	epidosite	epidosite	epidosite	epidosite	epidosite	epidosite	basalt	basalt	basalt	basalt
Location	UofA	UofA	UofA	UofA	UofA	UofA	UofA	UofA	UofA	UofA	UofA	UofA	UofA	UofA
Occurrence	gm l	gm d	gm l	gm d	gm l	gm d	gm l	gm d	gm l	gm d	vei	vei	vei	vei
SiO_2	37.09	37.56	36.65	37.20	37.18	37.37	37.18	37.54	37.09	37.34	37.15	37.06	37.21	37.52
TiO_2	0.18	0.11	0.49	0.09	0.06	0.12	0.28	0.10	0.43	0.11	0.16	0.66	0.43	0.15
Al_2O_3	23.04	26.31	22.18	25.63	25.26	26.37	22.50	26.18	22.91	25.74	22.86	21.87	21.96	24.33
$Fe_2O_3^T$	14.11	10.00	14.37	11.19	12.14	10.05	14.49	10.64	14.02	10.89	13.64	14.62	14.40	12.39
Cr_2O_3	b.d.	b.d.	0.01	0.04	0.05	0.02	0.02	b.d.	0.01	0.01	b.d.	b.d.	0.01	0.01
MnO	b.d.	0.17	0.07	0.56	0.50	0.16	0.05	0.40	0.12	0.32	0.03	0.06	0.08	0.08
MgO	0.04	0.04	0.06	0.05	0.06	0.03	0.04	0.04	0.07	0.04	0.02	0.08	0.03	0.17
CaO	23.06	23.01	23.03	22.19	22.23	23.13	23.16	22.71	23.00	22.77	23.03	23.05	22.76	23.16
Na_2O	0.02	0.02	0.02	0.01	b.d.	0.01	b.d.	b.d.	0.01	0.02	0.01	b.d.	b.d.	b.d.
K_2O	0.02	0.02	0.03	0.02	0.01	0.03	0.01	b.d.	0.01	0.01	0.02	0.02	0.01	0.01
F	0.04	b.d.	0.06	0.01	0.01	b.d.	0.04	0.01	0.03	0.02	b.d.	b.d.	b.d.	b.d.
Cl	b.d.	0.01	0.01	b.d.	0.01	b.d.	b.d.	b.d.	b.d.	0.01	0.03	b.d.	0.01	b.d.
Total	97.60	97.25	96.98	96.99	97.51	97.29	97.77	97.62	97.70	97.28	96.95	97.42	96.90	97.82
Si	2.97	2.97	2.97	2.96	2.96	2.96	2.98	2.97	2.97	2.97	2.99	2.99	3.01	2.98
Al^{IV}	0.03	0.03	0.03	0.04	0.04	0.04	0.02	0.04	0.03	0.04	0.01	0.02	0.00	0.02
Al^{VI}	2.15	2.42	2.08	2.37	2.32	2.42	2.11	2.40	2.13	2.37	2.16	2.06	2.09	2.25
Ti	0.01	0.01	0.03	0.01	0.00	0.01	0.02	0.01	0.03	0.01	0.01	0.04	0.03	0.01
Cr	-	-	0.00	0.00	0.00	0.00	0.00	-	0.00	0.00	-	-	0.00	0.00
Fe^{3+}	0.85	0.60	0.88	0.67	0.73	0.60	0.87	0.63	0.84	0.65	0.83	0.89	0.88	0.74
Mn	-	0.01	0.01	0.04	0.03	0.01	0.00	0.03	0.01	0.02	0.00	0.00	0.01	0.01
Mg	0.01	0.01	0.01	0.01	0.01	0.00	0.01	0.01	0.01	0.01	0.00	0.01	0.00	0.02
Ca	1.98	1.95	2.00	1.89	1.89	1.96	1.99	1.92	1.97	1.94	1.99	1.99	1.97	1.97
Na	0.00	0.00	0.00	0.00	-	0.00	-	-	0.00	0.00	0.00	-	-	-
K	0.00	0.00	0.00	0.00	0.00	0.00	0.00	-	0.00	0.00	0.00	0.00	0.00	0.00
F	0.02	-	0.03	0.01	0.01	-	0.02	0.01	0.02	0.01	-	-	-	-
Cl	-	0.00	0.00	-	0.00	-	-	-	-	0.00	0.01	-	0.00	-
Ps	0.28	0.20	0.29	0.22	0.23	0.20	0.29	0.21	0.28	0.21	0.28	0.30	0.30	0.25

Appendix B2. Epidote Analyses (continued)

Sample	110-1-5AA5	110-1-5AA6	110-1-5AA7	110-1-5AA8	110-1-5AB1	110-1-5AB2	110-1-5AB3	110-1-5AB4	110-1-5AC1	110-1-5AC2	110-1-5AC3	110-1-5AC4	110-1-15A1
Rock Type	basalt	basalt	basalt	basalt	basalt	basalt	basalt	basalt	basalt	basalt	basalt	basalt	basalt
Location	UofA	UofA	UofA	UofA	UofA	UofA	UofA	UofA	UofA	UofA	UofA	UofA	UofA
Occurrence	vei	vei	vei	vei	vei	vei	vei	vei	cor	rim	cor	rim	cor
SiO_2	37.36	36.99	37.20	37.41	37.52	37.77	37.34	37.69	37.34	37.40	38.05	37.55	37.49
TiO_2	0.13	0.14	b.d.	0.01	0.49	0.03	0.09	0.07	0.15	0.13	0.04	0.05	0.10
Al_2O_3	24.10	23.47	22.09	24.69	22.43	24.60	24.13	24.49	24.02	22.33	25.82	23.78	25.35
$Fe_2O_3{}^T$	12.54	13.18	14.95	11.87	13.59	11.85	12.54	11.94	12.42	14.17	9.53	12.35	11.26
Cr_2O_3	b.d.	b.d.	0.01	b.d.	0.03	0.01	0.01	0.01	0.01	b.d.	b.d.	b.d.	b.d.
MnO	0.10	0.07	0.12	0.17	0.04	0.09	0.09	0.05	0.09	0.04	0.07	0.06	0.11
MgO	0.12	0.06	0.07	0.07	0.03	0.05	0.01	0.12	0.03	0.05	b.d.	0.03	0.04
CaO	22.89	23.22	23.06	23.12	23.01	23.31	23.25	23.10	23.30	23.20	23.60	23.08	23.54
Na_2O	b.d.	0.01	b.d.	b.d.	0.01	b.d.	b.d.	b.d.	b.d.	0.02	b.d.	b.d.	b.d.
K_2O	0.04	0.01	0.02	0.04	0.03	0.02	0.01	0.02	0.02	0.02	0.03	0.02	0.03
F	b.d.	b.d.	b.d.	b.d.	b.d.	b.d.	b.d.	b.d.	b.d.	b.d.	b.d.	b.d.	b.d.
Cl	b.d.	b.d.	b.d.	b.d.	b.d.	b.d.	0.01	b.d.	b.d.	b.d.	b.d.	b.d.	0.01
Total	97.28	97.15	97.52	97.38	97.18	97.73	97.48	97.49	97.38	97.36	97.14	96.92	97.93
Si	2.98	2.97	3.00	2.98	3.02	3.00	2.98	3.00	2.98	3.01	3.01	3.01	2.97
Al^{IV}	0.02	0.03	0.01	0.02	0.00	0.00	0.02	0.00	0.02	0.00	0.00	0.00	0.04
Al^{VI}	2.25	2.19	2.09	2.30	2.12	2.29	2.25	2.29	2.24	2.11	2.41	2.24	2.33
Ti	0.01	0.01	-	0.00	0.03	0.00	0.01	0.00	0.01	0.01	0.00	0.00	0.01
Cr	-	-	0.00	-	0.00	0.00	0.00	0.00	0.00	-	-	-	-
Fe^{3+}	0.75	0.80	0.91	0.71	0.82	0.71	0.75	0.71	0.75	0.86	0.57	0.74	0.67
Mn	0.01	0.01	0.01	0.01	0.00	0.01	0.01	0.00	0.01	0.00	0.01	0.00	0.01
Mg	0.01	0.01	0.01	0.01	0.00	0.01	0.00	0.01	0.00	0.01	-	0.00	0.01
Ca	1.96	2.00	1.99	1.97	1.98	1.98	1.99	1.97	1.99	2.00	2.00	1.98	2.00
Na	-	0.00	-	-	0.00	-	-	-	-	0.00	-	-	-
K	0.00	0.00	0.00	0.00	0.00	0.00	0.00	0.00	0.00	0.00	0.00	0.00	0.00
F	-	-	-	-	-	-	-	-	-	-	-	-	-
Cl	-	-	-	-	-	-	0.00	-	-	-	-	-	0.00
Ps	0.25	0.26	0.30	0.23	0.28	0.24	0.25	0.24	0.25	0.29	0.19	0.25	0.22

Appendix B2. Epidote Analyses (continued)

Sample	110-1-15A2	110-1-15A3	110-1-15A4	110-1-15B1	110-1-15B2	110-1-25A1	110-1-25A6	110-1-25A7	110-1-25B1	110-1-25B2	110-1-25B3	110-1-25B4	110-1-25C1
Rock Type	basalt	basalt	basalt	basalt	basalt	basalt	basalt	basalt	basalt	basalt	basalt	basalt	basalt
Location	UofA	UofA	UofA	UofA	UofA	UofA	UofA	UofA	UofA	UofA	UofA	UofA	UofA
Occurrence	rim	cor	rim	cor	rim	gm	vel	vel	vel	vel	vel	vel	vel
SiO_2	37.21	37.31	37.28	37.17	37.73	38.00	38.15	38.22	37.83	37.75	38.08	37.71	37.38
TiO_2	0.35	b.d.	0.08	0.62	0.05	0.09	0.19	0.02	0.03	0.04	0.10	0.03	0.06
Al_2O_3	23.53	23.53	26.06	23.52	25.95	23.81	26.14	24.62	24.74	24.51	25.39	23.20	23.53
$Fe_2O_3{}^T$	13.51	13.88	10.15	13.18	11.08	11.75	9.55	11.13	11.69	11.62	10.23	13.20	12.61
Cr_2O_3	0.02	b.d.	0.01	b.d.	b.d.	b.d.	b.d.	b.d.	0.02	b.d.	b.d.	b.d.	b.d.
MnO	0.04	0.04	0.22	0.07	0.15	0.32	0.25	0.25	0.12	0.13	0.05	0.10	0.12
MgO	0.05	0.01	0.04	0.10	0.03	0.23	0.18	0.37	0.13	0.13	0.15	0.17	0.10
CaO	23.30	23.12	22.83	23.12	23.39	23.21	22.96	23.03	23.42	23.21	23.35	23.06	23.08
Na_2O	b.d.	b.d.	b.d.	b.d.	0.01	b.d.	b.d.	0.01	b.d.	0.01	b.d.	0.03	b.d.
K_2O	0.03	0.03	0.05	0.04	0.02	0.02	b.d.	0.01	0.03	0.02	0.02	b.d.	0.01
F	b.d.	0.01	b.d.	0.02	b.d.	b.d.	b.d.	b.d.	b.d.	b.d.	b.d.	b.d.	b.d.
Cl	b.d.	b.d.	b.d.	b.d.	b.d.	0.01	b.d.	b.d.	0.01	b.d.	0.01	0.02	b.d.
Total	98.04	97.93	96.72	97.84	98.41	97.44	97.42	97.66	98.02	97.42	97.38	97.52	96.89
Si	2.96	2.98	2.97	2.96	2.96	3.03	3.01	3.02	2.99	3.00	3.01	3.01	3.00
Al^{IV}	0.04	0.02	0.03	0.04	0.04	0.00	0.00	0.00	0.01	0.00	0.00	0.00	0.00
Al^{VI}	2.17	2.19	2.41	2.17	2.36	2.23	2.43	2.29	2.30	2.30	2.37	2.18	2.23
Ti	0.02	-	0.01	0.04	0.00	0.01	0.01	0.00	0.00	0.00	0.01	0.00	0.00
Cr	0.00	-	0.00	-	-	-	-	-	0.00	-	-	-	-
Fe^{3+}	0.81	0.83	0.61	0.79	0.65	0.70	0.57	0.66	0.70	0.70	0.61	0.79	0.76
Mn	0.00	0.00	0.02	0.01	0.01	0.02	0.02	0.02	0.01	0.01	0.00	0.01	0.01
Mg	0.01	0.00	0.01	0.01	0.00	0.03	0.02	0.04	0.02	0.02	0.02	0.02	0.01
Ca	1.99	1.98	1.95	1.98	1.97	1.98	1.94	1.95	1.98	1.98	1.98	1.97	1.99
Na	-	-	-	-	0.00	-	-	0.00	-	0.00	-	0.01	-
K	0.00	0.00	0.01	0.00	0.00	0.00	-	0.00	0.00	0.00	0.00	-	0.00
F	-	0.01	-	0.01	-	-	-	-	-	-	-	-	-
Cl	-	-	-	-	-	0.00	-	-	0.00	-	0.00	0.01	-
Ps	0.27	0.27	0.20	0.26	0.21	0.24	0.19	0.22	0.23	0.23	0.20	0.27	0.25

Appendix B2. Epidote Analyses (continued)

Sample	110-1-25C2	110-1-25C3	110-1-25C4	110-1-32A1	110-1-32A2	110-1-32A3	110-1-32A4	110-1-32A5	110-1-32A6	110-1-32C2	110-1-32C3	110-1-32C4	110-1-32C5
Rock Type	basalt	basalt	basalt	basalt	basalt	basalt	basalt	basalt	basalt	basalt	basalt	basalt	basalt
Location	UofA	UofA	UofA	UofA	UofA	UofA	UofA	UofA	UofA	UofA	UofA	UofA	UofA
Occurrence	vei	vel	vei	gm	gm	gm	gm	gm	gm	gm	gm	gm	gm
SiO_2	37.29	36.98	37.27	37.59	37.27	37.09	37.25	37.59	37.07	36.80	37.20	36.71	37.21
TiO_2	b.d.	0.33	0.15	0.15	0.31	0.31	0.74	0.73	0.84	0.98	0.64	1.48	0.50
Al_2O_3	22.08	22.37	23.31	24.56	24.06	24.02	23.10	24.21	22.41	22.90	23.41	22.58	23.49
$Fe_2O_3^T$	14.56	14.33	13.11	11.56	12.57	12.07	13.08	11.61	13.65	12.43	12.55	12.36	12.55
Cr_2O_3	b.d.	b.d.	b.d.	0.01	b.d.	0.02	0.02	0.02	0.02	0.03	0.06	0.03	b.d.
MnO	0.08	0.03	0.06	0.13	0.20	0.13	0.17	0.11	0.09	0.12	0.16	0.07	0.14
MgO	0.14	0.03	0.01	0.12	0.10	0.08	0.21	0.11	0.08	0.16	0.09	0.08	0.09
CaO	23.28	22.95	22.91	23.10	22.87	22.94	23.00	22.93	22.96	23.24	22.99	23.22	22.98
Na_2O	b.d.	b.d.	b.d.	b.d.	0.01	b.d.	0.01	0.02	b.d.	0.01	b.d.	b.d.	b.d.
K_2O	0.02	0.03	0.02	0.03	0.04	0.01	0.04	0.05	0.03	0.03	0.03	0.03	b.d.
F	b.d.	b.d.	b.d.	b.d.	b.d.	b.d.	b.d.	b.d.	b.d.	b.d.	b.d.	b.d.	b.d.
Cl	0.01	b.d.	b.d.	0.01	b.d.	b.d.	b.d.	b.d.	b.d.	0.02	0.02	b.d.	b.d.
Total	97.46	97.05	96.84	97.26	97.43	96.67	97.62	97.38	97.15	96.72	97.15	96.56	96.96
Si	3.00	2.99	3.00	2.99	2.98	2.98	2.98	2.99	2.98	2.97	2.98	2.97	2.99
Al^{IV}	0.00	0.02	0.00	0.01	0.03	0.02	0.02	0.01	0.02	0.03	0.02	0.03	0.01
Al^{VI}	2.09	2.11	2.21	2.30	2.24	2.25	2.15	2.26	2.11	2.15	2.19	2.12	2.21
Ti	-	0.02	0.01	0.01	0.02	0.02	0.04	0.04	0.05	0.06	0.04	0.09	0.03
Cr	-	-	-	0.00	-	0.00	0.00	0.00	0.00	0.00	0.00	0.00	-
Fe^{3+}	0.88	0.87	0.79	0.69	0.75	0.73	0.79	0.69	0.83	0.75	0.76	0.75	0.76
Mn	0.01	0.00	0.00	0.01	0.01	0.01	0.01	0.01	0.01	0.01	0.01	0.01	0.01
Mg	0.02	0.00	0.00	0.01	0.01	0.01	0.03	0.01	0.01	0.02	0.01	0.01	0.01
Ca	2.01	1.99	1.97	1.97	1.96	1.98	1.97	1.96	1.98	2.01	1.98	2.01	1.98
Na	-	-	-	-	0.00	-	0.00	0.00	-	0.00	-	-	-
K	0.00	0.00	0.00	0.00	0.00	0.00	0.00	0.01	0.00	0.00	0.00	0.00	-
F	-	-	-	-	-	-	-	-	-	-	-	-	-
Cl	0.00	-	-	0.00	-	-	-	-	-	0.01	0.01	-	-
Ps	0.30	0.29	0.26	0.23	0.25	0.24	0.27	0.23	0.28	0.26	0.25	0.26	0.25

Appendix B2. Epidote Analyses (continued)

Sample	110-1-32C6	111-1-3A2	111-1-3D1	111-4-3B2	113-1-10b2	113-1-10b3	113-1-10c1	113-1-10c2	113-1-10c3	113-1-10c4	113-1-10c5	113-1-10c6
Rock Type	basalt	basalt	basalt	gabbro	basalt	basalt	basalt	basalt	basalt	basalt	basalt	basalt
Location	UofA	OSU	OSU	OSU	OSU	OSU	OSU	OSU	OSU	OSU	OSU	OSU
Occurrence	gm	gm	gm	vei	cor	rim	rim	cor	cor	rim	cor	rim
SiO_2	37.12	36.78	37.80	39.13	35.68	36.15	38.75	37.85	37.95	38.23	38.30	38.57
TiO_2	1.52	0.18	0.25	0.08	0.06	b.d.	0.01	0.17	0.05	0.03	0.06	0.07
Al_2O_3	23.39	25.30	24.02	28.51	20.52	21.99	24.67	22.16	22.38	22.49	24.35	22.43
$Fe_2O_3^T$	11.83	11.16	12.38	6.54	17.39	15.48	12.34	15.07	15.28	14.98	13.19	15.41
Cr_2O_3	0.04	b.d.	0.02	0.03	b.d.	0.01	b.d.	b.d.	0.01	b.d.	0.01	b.d.
MnO	0.18	0.55	0.46	0.08	b.d.	0.10	0.30	0.11	0.06	0.16	0.26	0.07
MgO	0.13	0.06	0.05	0.13	0.02	b.d.	0.05	0.05	0.02	0.02	0.11	0.01
CaO	23.01	22.49	22.70	22.58	22.96	23.13	23.11	23.24	23.49	23.62	22.96	23.40
Na_2O	b.d.	0.14	0.02	0.09	b.d.	0.02	b.d.	b.d.	0.01	0.01	0.03	b.d.
K_2O	0.01	0.02	0.02	0.01	0.02	0.01	b.d.	0.01	b.d.	0.01	0.01	0.02
F	b.d.	0.10	0.07	b.d.	0.12	0.06	0.09	b.d.	b.d.	b.d.	0.07	b.d.
Cl	b.d.	0.02	0.01	0.02	0.01	0.02	0.02	0.01	0.01	0.01	0.01	0.02
Total	97.23	96.80	97.80	97.20	96.78	96.97	99.34	98.67	99.26	99.56	99.36	100.00
Si	2.97	2.95	3.00	3.04	2.93	2.94	3.02	3.01	3.00	3.01	3.00	3.02
Al^{IV}	0.03	0.05	0.00	0.00	0.07	0.06	0.00	0.00	0.00	0.00	0.00	0.00
Al^{VI}	2.17	2.34	2.25	2.61	1.92	2.05	2.27	2.08	2.08	2.09	2.24	2.07
Ti	0.09	0.01	0.02	0.01	0.00	-	0.00	0.01	0.00	0.00	0.00	0.00
Cr	0.00	-	0.00	0.00	-	0.00	-	-	0.00	-	0.00	-
Fe^{3+}	0.71	0.67	0.74	0.38	1.08	0.95	0.72	0.90	0.91	0.89	0.78	0.91
Mn	0.01	0.04	0.03	0.01	-	0.01	0.02	0.01	0.00	0.01	0.02	0.01
Mg	0.02	0.01	0.01	0.02	0.00	-	0.01	0.01	0.00	0.00	0.01	0.00
Ca	1.97	1.93	1.93	1.88	2.02	2.02	1.93	1.98	1.99	1.99	1.93	1.97
Na	-	0.02	0.00	0.01	-	0.00	-	-	0.00	0.00	0.01	-
K	0.00	0.00	0.00	0.00	0.00	0.00	-	0.00	-	0.00	0.00	0.00
F	-	0.05	0.04	-	0.06	0.03	0.04	-	-	-	0.04	-
Cl	-	0.01	0.00	0.01	0.00	0.01	0.01	0.00	0.00	0.00	0.00	0.01
Ps	0.24	0.22	0.25	0.13	0.35	0.31	0.24	0.30	0.30	0.30	0.26	0.30

Appendix B2. Epidote Analyses (continued)

Sample	13-1-10d4	113-1-10d5	113-1-26a1	113-1-26a2	113-1-26a3	113-1-26b1	113-1-26b2	113-1-26b3	113-1-26b4	113-1-26c1	113-1-26c2	113-1-26c3
Rock Type	basalt	basalt	epidosite	epidosite	epidosite	epidosite	epidosite	epidosite	epidosite	epidosite	epidosite	epidosite
Location	OSU	OSU	OSU	OSU	OSU	OSU	OSU	OSU	OSU	OSU	OSU	OSU
Occurrence	gm	gm	gm	gm	gm	rim	cor	cor	rim	gm	gm	gm
SiO_2	38.23	38.17	38.26	39.59	37.52	37.14	37.56	38.03	36.44	37.46	37.67	38.29
TiO_2	0.32	0.04	0.04	0.17	0.04	0.16	0.04	0.19	0.26	0.05	0.11	0.12
Al_2O_3	21.61	23.78	26.83	24.22	23.98	25.14	26.37	26.59	24.09	24.87	25.24	26.07
$Fe_2O_3^T$	15.95	13.75	9.43	10.87	12.87	11.38	9.68	9.13	12.51	11.63	11.14	9.78
Cr_2O_3	0.01	0.01	0.04	b.d.	b.d.	b.d.	b.d.	b.d.	b.d.	b.d.	0.09	b.d.
MnO	0.04	0.10	0.04	0.01	0.04	0.07	0.12	0.08	0.12	0.16	0.09	0.65
MgO	0.05	0.05	0.03	0.07	0.02	0.02	0.03	0.08	0.07	0.06	0.30	0.06
CaO	23.57	23.51	23.88	22.80	23.50	23.55	23.86	23.63	23.39	23.37	23.29	22.64
Na_2O	0.02	0.01	b.d.	0.01	0.04	b.d.	0.02	0.01	0.01	b.d.	0.02	0.02
K_2O	0.02	0.02	b.d.	0.01	0.01	b.d.	b.d.	b.d.	0.01	b.d.	b.d.	b.d.
F	b.d.	b.d.	b.d.	b.d.	b.d.	0.04	0.07	0.06	0.07	0.07	0.05	0.19
Cl	0.03	0.02	b.d.	0.05	0.02	0.02	0.04	0.03	0.02	0.01	0.01	0.02
Total	99.85	99.46	98.55	97.80	98.04	97.52	97.79	97.83	96.99	97.68	98.01	97.84
Si	3.01	2.99	2.98	3.11	2.98	2.95	2.96	2.99	2.93	2.98	2.97	3.01
Al^{IV}	0.00	0.01	0.02	0.00	0.02	0.05	0.04	0.01	0.07	0.02	0.03	0.00
Al^{VI}	2.01	2.19	2.45	2.24	2.23	2.31	2.41	2.45	2.22	2.30	2.32	2.42
Ti	0.02	0.00	0.00	0.01	0.00	0.01	0.00	0.01	0.02	0.00	0.01	0.01
Cr	0.00	0.00	0.00	-	-	-	-	-	-	-	0.01	-
Fe^{3+}	0.95	0.81	0.55	0.64	0.77	0.68	0.57	0.54	0.76	0.69	0.66	0.58
Mn	0.00	0.01	0.00	0.00	0.00	0.01	0.01	0.01	0.01	0.01	0.01	0.04
Mg	0.01	0.01	0.00	0.01	0.00	0.00	0.00	0.01	0.01	0.01	0.04	0.01
Ca	1.99	1.98	1.99	1.92	2.00	2.01	2.02	1.99	2.02	1.99	1.97	1.91
Na	0.00	0.00	-	0.00	0.01	-	0.00	0.00	0.00	-	0.00	0.00
K	0.00	0.00	-	0.00	0.00	-	-	-	0.00	-	-	-
F	-	-	-	-	-	0.02	0.04	0.03	0.04	0.04	0.03	0.10
Cl	0.01	0.01	-	0.01	0.01	0.01	0.01	0.01	0.01	0.00	0.00	0.01
Ps	0.32	0.27	0.18	0.22	0.26	0.22	0.19	0.18	0.25	0.23	0.22	0.19

Appendix B3. Prehnite Analyses (recalculated on the basis of 22 anhydrous O)

Sample	99-2-1C4	99-2-1C3	99-2-1C2	99-2-1C1	112-2-6C5	112-2-6C4	112-2-6A2
Rock Type	basalt	basalt	basalt	basalt	gabbro	gabbro	gabbro
Location	UofA	UofA	UofA	UofA	UofA	UofA	UofA
SiO_2	43.40	43.39	43.53	43.72	43.20	43.25	43.01
Al_2O_3	24.16	23.64	23.94	24.03	24.49	24.33	24.68
MnO	0.07	0.07	0.09	0.07	0.02	0.02	0.01
MgO	0.03	0.02	b.d.	0.02	0.07	0.03	0.68
CaO	26.44	26.20	26.30	26.37	26.28	25.81	26.15
Na_2O	b.d.	0.01	0.01	0.01	0.14	0.18	0.09
K_2O	b.d.	0.01	0.04	0.02	0.02	0.01	0.01
$Fe_2O_3{}^T$	0.68	1.04	0.72	0.69	0.10	0.12	0.08
Total	94.78	94.38	94.63	94.93	94.32	93.75	94.71
Si	6.02	6.04	6.04	6.05	6.01	6.04	5.96
Al	3.94	3.88	3.91	3.91	4.01	4.00	4.02
Fe^{3+}	0.07	0.11	0.08	0.07	0.01	0.01	0.01
Mn	0.01	0.01	0.01	0.01	0.00	0.00	0.00
Mg	0.01	0.00	-	0.00	0.02	0.01	0.14
Ca	3.93	3.91	3.91	3.91	3.92	3.86	3.88
Na	-	0.00	0.00	0.00	0.04	0.05	0.02
K	-	0.00	0.01	0.00	0.00	0.00	0.00
Cations	13.97	13.96	13.96	13.96	14.00	13.97	14.03

Note: b.d. = below detection.

Appendix B4. Olivine Analyses (recalculated on the basis of 4 O)

Sample	82-3-2A1	82-3-2A2	82-3-2A3	82-3-2B1	82-3-2B2	82-3-2B3	82-3-2C1	82-3-2C2	82-3-2C3	94-1-2E1	94-1-3A1	99-1-21A1	99-1-21A2	99-1-21A3	99-1-21A4	99-1-21C1
Rock Type	troctolite	troctolite	troctolite	troctolite	troctolite	troctolite	troctolite	troctolite	troctolite	gabbro	gabbro	gabbro	gabbro	gabbro	gabbro	gabbro
Location	UofA	UofA	UofA	UofA	UofA	UofA	UofA	UofA	UofA	OSU	OSU	UofA	UofA	UofA	UofA	UofA
Occurrence	gm	gm	gm	gm	gm	gm	gm	gm	gm	gm	gm	gm	gm	gm	gm	cor
SiO_2	40.03	39.98	39.92	39.92	39.74	40.00	40.01	40.08	39.64	37.72	37.77	37.70	37.86	37.47	37.79	37.53
TiO_2	b.d.	b.d.	0.01	0.05	0.04	0.04	0.01	0.07	0.02	0.02	0.01	0.02	b.d.	b.d.	0.03	b.d.
Al_2O_3	b.d.	b.d.	b.d.	0.12	0.01	0.02	0.01	b.d.	0.01	b.d.	b.d.	0.02	0.01	0.01	0.01	0.01
FeO^T	10.56	10.66	10.79	10.66	10.74	10.81	10.91	10.94	11.06	27.72	28.95	21.04	21.17	21.04	21.18	20.96
MnO	0.11	0.13	0.14	0.17	0.15	0.15	0.18	0.14	0.17	0.41	0.37	0.30	0.30	0.31	0.29	0.29
MgO	49.09	48.72	49.09	48.08	49.18	48.75	48.80	49.03	48.84	35.10	35.38	40.64	40.82	40.73	40.62	40.87
CaO	0.01	0.01	0.03	0.46	0.05	0.02	0.02	0.02	0.03	0.07	0.06	0.04	0.04	0.03	0.04	b.d.
Na_2O	b.d.	b.d.	b.d.	0.03	0.01	0.01	0.01	0.01	b.d.	0.03	0.02	0.01	b.d.	b.d.	0.01	b.d.
Total	99.80	99.50	99.98	99.49	99.92	99.80	99.95	100.29	99.77	101.08	102.56	99.77	100.20	99.59	99.97	99.66
Si	0.99	0.99	0.98	0.99	0.98	0.99	0.99	0.99	0.98	1.00	0.99	0.98	0.98	0.98	0.98	0.98
Al	-	-	-	0.00	0.00	0.00	0.00	-	0.00	-	-	0.00	0.00	0.00	0.00	0.00
Ti	-	-	0.00	0.00	0.00	0.00	0.00	0.00	0.00	0.00	0.00	0.00	-	-	0.00	-
Fe^{2+}	0.22	0.22	0.22	0.22	0.22	0.22	0.23	0.23	0.23	0.61	0.63	0.46	0.46	0.46	0.46	0.46
Mn	0.00	0.00	0.00	0.00	0.00	0.00	0.00	0.00	0.00	0.01	0.01	0.01	0.01	0.01	0.01	0.01
Mg	1.81	1.80	1.81	1.78	1.81	1.80	1.80	1.80	1.80	1.38	1.38	1.57	1.58	1.58	1.57	1.59
Ca	0.00	0.00	0.00	0.01	0.00	0.00	0.00	0.00	0.00	0.00	0.00	0.00	0.00	0.00	0.00	-
Na	-	-	-	0.00	0.00	0.00	0.00	0.00	-	0.00	0.00	0.00	-	-	0.00	-
Cations	3.01	3.01	3.02	3.01	3.02	3.01	3.01	3.01	3.02	3.00	3.01	3.02	3.02	3.02	3.02	3.02
Mg#	0.89	0.89	0.89	0.89	0.89	0.89	0.89	0.89	0.89	0.69	0.69	0.77	0.77	0.78	0.77	0.78

Notes: b.d. = below detection; gm = groundmass; cor = core; Mg# = Mg / Mg + Fe^{2+}.

Appendix B4. Olivine Analyses (continued)

Sample	99-1-21C2	99-1-21C3	99-1-21C4	105-1-6A2	105-1-6C1	105-1-6C2	105-1-6C3	105-1-6C4	105-1-21A1	105-1-21A2	105-1-21B1	105-1-21B2	105-1-21D1	105-1-21D2
Rock Type	gabbro	gabbro	gabbro	gabbro	gabbro	gabbro	gabbro	gabbro	gabbro	gabbro	gabbro	gabbro	gabbro	gabbro
Location	UofA	UofA	UofA	OSU	OSU	OSU	OSU	OSU	UofA	UofA	UofA	UofA	UofA	UofA
Occurrence	cor	rim	rim	gm	gm	gm	inc	inc	gm	gm	gm	gm	gm	gm
SiO_2	37.74	37.43	38.04	38.68	38.13	38.94	39.42	39.58	38.42	38.12	38.05	38.34	38.36	38.03
TiO_2	b.d.	b.d.	b.d.	b.d.	0.01	b.d.	0.03	0.03	b.d.	0.01	0.04	b.d.	b.d.	b.d.
Al_2O_3	0.02	0.02	0.01	b.d.	b.d.	b.d.	0.02	b.d.	b.d.	0.01	0.02	b.d.	b.d.	0.01
FeO^T	20.69	21.00	21.21	23.06	22.92	22.57	21.61	19.69	20.02	20.01	19.69	19.97	19.83	19.82
MnO	0.29	0.30	0.26	0.31	0.37	0.38	0.38	0.50	0.29	0.27	0.27	0.28	0.29	0.26
MgO	40.91	40.36	41.05	40.58	40.19	40.95	41.24	43.14	41.63	41.21	41.63	41.46	41.77	41.76
CaO	0.04	0.03	0.05	0.01	0.03	0.03	b.d.	0.04	0.03	0.02	b.d.	0.04	0.02	0.01
Na_2O	b.d.	b.d.	b.d.	b.d.	0.02	0.01	0.02	0.01	0.01	b.d.	b.d.	0.01	b.d.	0.01
Total	99.69	99.14	100.62	102.65	101.69	102.89	102.70	103.00	100.40	99.65	99.70	100.10	100.27	99.90
Si	0.98	0.98	0.98	0.98	0.98	0.99	0.99	0.99	0.99	0.99	0.98	0.99	0.99	0.98
Al	0.00	0.00	0.00	-	-	-	0.00	-	-	0.00	0.00	-	-	0.00
Ti	-	-	-	-	0.00	-	0.00	0.00	-	0.00	0.00	-	-	-
Fe^{2+}	0.45	0.46	0.46	0.49	0.49	0.48	0.46	0.41	0.43	0.43	0.43	0.43	0.43	0.43
Mn	0.01	0.01	0.01	0.01	0.01	0.01	0.01	0.01	0.01	0.01	0.01	0.01	0.01	0.01
Mg	1.58	1.57	1.58	1.54	1.54	1.54	1.55	1.60	1.59	1.59	1.60	1.59	1.60	1.61
Ca	0.00	0.00	0.00	0.00	0.00	0.00	-	0.00	0.00	0.00	-	0.00	0.00	0.00
Na	-	-	-	-	0.00	0.00	0.00	0.00	0.00	-	-	0.00	-	0.00
Cations	3.02	3.02	3.02	3.02	3.02	3.02	3.01	3.01	3.01	3.02	3.02	3.01	3.02	3.02
Mg#	0.78	0.77	0.78	0.76	0.76	0.76	0.77	0.80	0.79	0.79	0.79	0.79	0.79	0.79

Appendix B4. Olivine Analyses (continued)

Sample	106-2-10C1	106-2-10C2	108-2-6A1	108-2-6A2	108-2-6A3	108-2-6A4	108-2-6B1	108-2-6B2	108-2-6C1	108-2-6C2	113-2-11A1	113-2-11A2	113-2-11A3	113-2-11A4
Rock Type	gabbro	gabbro	gabbro	gabbro	gabbro	gabbro	gabbro	gabbro	gabbro	gabbro	gabbro	gabbro	gabbro	gabbro
Location	OSU	OSU	UofA	UofA	UofA	UofA	UofA	UofA	UofA	UofA	UofA	UofA	UofA	UofA
Occurrence	gm	gm	cor	rim	cor	rim	gm	gm	cor	rim	gm	gm	gm	gm
SiO_2	38.17	37.96	38.01	38.13	38.27	38.06	38.10	38.06	38.08	37.96	39.26	39.12	39.09	39.28
TiO_2	b.d.	b.d.	b.d.	0.01	0.02	0.02	0.02	0.05	0.03	0.01	b.d.	0.04	0.01	0.05
Al_2O_3	b.d.	0.02	b.d.	b.d.	0.01	b.d.	0.01	0.02	0.01	0.01	0.01	0.02	0.03	0.01
FeO^T	24.84	24.51	19.00	19.35	19.37	19.21	19.25	19.46	19.50	19.47	17.90	17.75	18.03	18.04
MnO	0.36	0.37	0.23	0.22	0.20	0.23	0.25	0.25	0.20	0.26	0.23	0.25	0.27	0.26
MgO	38.58	38.50	41.98	41.64	41.74	41.58	41.70	41.64	41.82	41.90	42.42	42.50	42.26	42.26
CaO	0.03	0.02	0.06	0.01	0.02	0.02	0.04	0.03	0.03	0.02	0.16	0.16	0.13	0.12
Na_2O	b.d.	b.d.	b.d.	0.01	b.d.	b.d.	0.01	0.01	0.01	b.d.	b.d.	b.d.	b.d.	b.d.
Total	102.00	101.38	99.28	99.37	99.63	99.12	99.38	99.52	99.68	99.63	99.98	99.84	99.82	100.02
Si	0.99	0.99	0.98	0.99	0.99	0.99	0.99	0.98	0.98	0.98	1.00	1.00	1.00	1.00
Al	-	0.00	-	-	0.00	-	0.00	0.00	0.00	0.00	0.00	0.00	0.00	0.00
Ti	-	-	-	0.00	0.00	0.00	0.00	0.00	0.00	0.00	-	0.00	0.00	0.00
Fe^{2+}	0.54	0.53	0.41	0.42	0.42	0.42	0.42	0.42	0.42	0.42	0.38	0.38	0.39	0.38
Mn	0.01	0.01	0.01	0.01	0.00	0.01	0.01	0.01	0.00	0.01	0.01	0.01	0.01	0.01
Mg	1.48	1.49	1.62	1.61	1.60	1.61	1.61	1.60	1.61	1.61	1.61	1.62	1.61	1.60
Ca	0.00	0.00	0.00	0.00	0.00	0.00	0.00	0.00	0.00	0.00	0.00	0.00	0.00	0.00
Na	-	-	-	0.00	-	-	0.00	0.00	0.00	-	-	-	-	-
Cations	3.01	3.02	3.02	3.02	3.01	3.01	3.02	3.02	3.02	3.02	3.00	3.00	3.00	3.00
Mg#	0.73	0.74	0.80	0.79	0.79	0.79	0.79	0.79	0.79	0.79	0.81	0.81	0.81	0.81

Appendix B5. Pyroxene Analyses (recalculated on the basis of 6 O)

Sample	81-2-8C1	81-2-8C2	81-2-8C3	81-2-8C4	81-2-8C5	82-3-8A2	82-3-8A3	82-3-8A4	82-3-8B2	82-3-8B3	82-3-8C1	82-3-8C2	82-3-8D1	82-3-8D3	82-3-8D4	90-4-3C1
Rock Type	basalt	basalt	basalt	basalt	basalt	gabbro	gabbro	gabbro	gabbro	gabbro	gabbro	gabbro	gabbro	gabbro	gabbro	gabbro
Location	UofA	UofA	UofA	UofA	UofA	OSU	OSU	OSU	OSU	OSU	OSU	OSU	OSU	OSU	OSU	UofA
Occurrence	cor	rim	rim	cor	rim	rim	cor	rim	rim	gm	cor	rim	cor	cor	rim	gm
SiO_2	53.05	52.67	52.93	53.24	53.18	52.34	52.43	52.03	52.39	52.52	52.34	52.29	51.78	51.42	50.58	53.16
TiO_2	0.20	0.17	0.20	0.19	0.15	0.55	0.62	0.75	0.88	0.54	0.63	0.59	0.72	0.50	0.79	0.38
Al_2O_3	1.97	2.07	2.19	1.50	1.65	2.08	2.35	2.29	2.60	2.55	3.07	2.50	2.66	2.74	3.34	2.06
FeO^T	6.38	5.61	5.73	6.04	5.38	9.56	7.70	7.72	7.96	6.35	6.75	6.16	8.74	6.97	8.28	5.13
Cr_2O_3	0.11	0.33	0.22	0.18	0.24	0.15	0.12	0.03	0.16	0.44	0.21	0.12	0.46	0.47	0.18	0.28
MnO	0.19	0.15	0.17	0.19	0.14	0.20	0.23	0.21	0.23	0.16	0.17	0.16	0.19	0.17	0.22	0.14
MgO	17.10	17.22	17.46	17.41	17.82	19.39	15.49	15.16	15.21	17.21	16.63	16.09	15.74	15.50	15.07	16.87
CaO	20.44	21.02	20.77	21.04	20.62	16.49	21.99	22.21	21.53	20.90	21.11	22.50	20.54	21.89	21.45	21.95
Na_2O	0.16	0.16	0.18	0.15	0.16	0.23	0.32	0.33	0.34	0.29	0.32	0.32	0.36	0.35	0.33	0.25
Total	99.60	99.40	99.85	99.94	99.34	100.99	101.25	100.73	101.30	100.96	101.23	100.73	101.19	100.01	100.24	100.22
Si	1.95	1.94	1.94	1.95	1.95	1.90	1.91	1.91	1.91	1.90	1.90	1.91	1.89	1.89	1.87	1.94
Al^{IV}	0.05	0.06	0.07	0.05	0.05	0.09	0.09	0.09	0.09	0.10	0.10	0.10	0.11	0.11	0.13	0.06
Al^{VI}	0.04	0.03	0.03	0.01	0.02	0.00	0.01	0.01	0.03	0.01	0.03	0.01	0.01	0.01	0.01	0.03
Fe^{2+}	0.20	0.17	0.18	0.18	0.17	0.29	0.24	0.24	0.24	0.19	0.21	0.19	0.27	0.22	0.26	0.16
Mg	0.94	0.94	0.95	0.95	0.98	1.05	0.84	0.83	0.83	0.93	0.90	0.87	0.86	0.85	0.83	0.92
Ti	0.01	0.01	0.01	0.01	0.00	0.02	0.02	0.02	0.02	0.02	0.02	0.02	0.02	0.01	0.02	0.01
Cr	0.00	0.01	0.01	0.01	0.01	0.00	0.00	0.00	0.01	0.01	0.01	0.00	0.01	0.01	0.01	0.01
Mn	0.01	0.01	0.01	0.01	0.00	0.01	0.01	0.01	0.01	0.01	0.01	0.01	0.01	0.01	0.01	0.00
Ca	0.81	0.83	0.81	0.83	0.81	0.64	0.86	0.87	0.84	0.81	0.82	0.88	0.80	0.86	0.85	0.86
Na	0.01	0.01	0.01	0.01	0.01	0.02	0.02	0.02	0.02	0.02	0.02	0.02	0.03	0.03	0.02	0.02
Sum	4.00	4.00	4.00	4.00	4.00	4.00	4.00	4.00	4.00	4.00	4.00	4.00	4.00	4.00	4.00	4.00
Mg#	0.83	0.85	0.84	0.84	0.86	0.78	0.78	0.78	0.77	0.83	0.81	0.82	0.76	0.80	0.76	0.85

Notes: b.d. = below detection; cor = core; gm = groundmass. Mg# = Mg / Mg + Fe^{2+}.

Appendix B5. Pyroxene Analyses (continued)

Sample	90-4-3C2	90-4-3C3	90-4-3C4	90-4-3D1	90-4-3D2	90-4-3D3	90-4-3D4	94-1-1A1	94-1-1D2	94-1-2B1	94-1-2C1	94-1-2C2	94-1-2E2	96-1-29A1	96-1-29A2	96-2-1E1
Rock Type	gabbro	gabbro	gabbro	gabbro	gabbro	gabbro	gabbro	gabbro	gabbro	gabbro	gabbro	gabbro	gabbro	PG/basalt	PG/basalt	basalt
Location	UofA	UofA	UofA	UofA	UofA	UofA	UofA	OSU	OSU	OSU	OSU	OSU	OSU	OSU	OSU	OSU
Occurrence	gm	gm	gm	gm	gm	gm	gm	gm	gm	gm	gm	gm	gm	gm	gm	gm
SiO_2	52.65	52.90	52.18	52.21	52.44	52.91	53.26	52.32	52.41	51.31	53.30	53.71	52.30	51.67	52.57	51.78
TiO_2	0.35	0.34	0.35	0.34	0.33	0.29	0.34	0.41	0.74	0.62	0.13	0.34	0.58	0.58	0.80	0.48
Al_2O_3	2.00	2.08	2.06	2.48	2.40	2.16	2.15	1.56	1.83	2.02	0.48	0.82	2.04	3.66	4.94	2.14
FeO^T	5.14	5.01	4.88	4.97	5.13	5.80	5.23	9.06	11.23	10.10	8.00	7.56	7.82	9.09	11.97	9.20
Cr_2O_3	0.27	0.26	0.26	0.35	0.43	0.34	0.28	0.03	0.02	0.07	0.02	0.06	0.05	0.05	0.04	0.04
MnO	0.16	0.13	0.17	0.15	0.15	0.15	0.14	0.32	0.24	0.21	0.29	0.21	0.23	0.25	0.29	0.14
MgO	16.24	16.51	16.10	16.11	16.35	17.18	16.52	14.72	15.54	16.22	14.79	15.51	14.98	18.54	15.65	16.27
CaO	22.10	22.52	22.96	22.42	22.33	20.64	22.12	21.15	18.14	18.31	22.76	22.54	22.19	17.16	14.54	20.15
Na_2O	0.28	0.30	0.29	0.30	0.29	0.28	0.28	0.21	0.27	0.21	0.16	0.18	0.29	0.16	0.20	0.21
Total	99.19	100.05	99.25	99.33	99.85	99.75	100.32	99.78	100.42	99.07	99.93	100.93	100.48	101.16	101.00	100.41
Si	1.94	1.93	1.92	1.92	1.92	1.94	1.94	1.95	1.94	1.92	1.98	1.97	1.93	1.87	1.94	1.90
Al^{IV}	0.06	0.07	0.08	0.08	0.08	0.06	0.06	0.05	0.06	0.08	0.02	0.03	0.07	0.13	0.06	0.09
Al^{VI}	0.03	0.02	0.01	0.03	0.03	0.03	0.04	0.02	0.02	0.01	0.00	0.01	0.02	0.03	0.15	0.00
Fe^{2+}	0.16	0.15	0.15	0.15	0.16	0.18	0.16	0.28	0.35	0.32	0.25	0.23	0.24	0.28	0.37	0.28
Mg	0.89	0.90	0.89	0.89	0.89	0.94	0.90	0.82	0.86	0.90	0.82	0.85	0.82	1.00	0.86	0.89
Ti	0.01	0.01	0.01	0.01	0.01	0.01	0.01	0.01	0.02	0.02	0.00	0.01	0.02	0.02	0.02	0.01
Cr	0.01	0.01	0.01	0.01	0.01	0.01	0.01	0.00	0.00	0.00	0.00	0.00	0.00	0.00	0.00	0.00
Mn	0.01	0.00	0.01	0.01	0.01	0.01	0.00	0.01	0.01	0.01	0.01	0.01	0.01	0.01	0.01	0.00
Ca	0.87	0.88	0.91	0.89	0.88	0.81	0.87	0.84	0.72	0.73	0.91	0.89	0.88	0.67	0.57	0.79
Na	0.02	0.02	0.02	0.02	0.02	0.02	0.02	0.02	0.02	0.02	0.01	0.01	0.02	0.01	0.01	0.02
Sum	4.00	4.00	4.00	4.00	4.00	4.00	4.00	4.00	4.00	4.00	4.00	4.00	4.00	4.00	4.00	4.00
Mg#	0.85	0.85	0.85	0.85	0.85	0.84	0.85	0.74	0.71	0.74	0.77	0.79	0.77	0.78	0.70	0.76

Appendix B5. Pyroxene Analyses (continued)

Sample	96-2-1E2	96-2-4B1	96-2-4C1	96-2-4C2	96-2-7A1	96-2-7A2	96-2-7B1	96-2-7B2	96-2-7B3	96-2-7B4	96-2-7C1	99-1-21A1	99-1-21A2	99-1-21A3	99-1-21A4	99-1-21B1
Rock Type	basalt	PG/basalt	PG/basalt	PG/basalt	basalt	basalt	basalt	basalt	basalt	basalt	basalt	gabbro	gabbro	gabbro	gabbro	gabbro
Location	OSU	UofA	UofA	UofA	OSU	OSU	OSU	OSU	OSU	OSU	OSU	UofA	UofA	UofA	UofA	UofA
Occurrence	gm	cor	gm	gm	cor	cor	cor	cor	rim	rim	cor	cor	rim	cor	rim	gm
SiO_2	50.72	51.33	51.64	52.06	51.39	52.65	51.75	52.16	51.14	52.01	51.87	52.57	51.89	51.44	52.25	51.60
TiO_2	0.56	0.46	0.39	0.38	0.73	0.40	0.34	0.36	0.60	0.36	0.57	0.57	0.67	0.69	0.59	0.58
Al_2O_3	2.48	3.38	3.20	3.01	2.96	2.40	2.74	2.42	1.66	2.83	2.84	2.45	2.66	2.53	2.46	2.96
FeO^T	9.56	7.40	7.49	7.73	8.12	6.59	5.34	5.46	12.58	5.30	6.85	7.54	6.23	8.85	6.97	6.25
Cr_2O_3	0.08	0.03	0.10	0.04	0.11	0.18	0.53	0.28	0.02	0.53	0.33	0.15	0.19	0.51	0.11	0.13
MnO	0.21	0.21	0.20	0.21	0.22	0.15	0.11	0.10	0.40	0.12	0.18	0.18	0.13	0.20	0.20	0.16
MgO	16.01	16.97	18.13	18.53	16.62	17.25	17.39	17.09	12.89	17.40	17.16	18.07	15.84	16.87	17.00	16.32
CaO	19.95	20.04	18.32	18.17	20.21	21.06	21.39	21.41	21.20	21.12	20.23	18.28	21.71	19.14	20.26	20.82
Na_2O	0.22	0.18	0.15	0.16	0.23	0.20	0.19	0.17	0.26	0.20	0.26	0.30	0.38	0.34	0.32	0.37
Total	99.79	100.00	99.62	100.29	100.59	100.88	99.78	99.45	100.75	99.87	100.29	100.11	99.70	100.57	100.16	99.19
Si	1.88	1.88	1.89	1.89	1.88	1.91	1.89	1.92	1.91	1.90	1.89	1.92	1.91	1.88	1.91	1.91
Al^{IV}	0.11	0.12	0.11	0.11	0.12	0.09	0.11	0.08	0.07	0.10	0.11	0.08	0.09	0.11	0.09	0.10
Al^{VI}	0.00	0.03	0.03	0.02	0.01	0.01	0.01	0.02	0.00	0.02	0.02	0.03	0.03	0.00	0.02	0.03
Fe^{2+}	0.30	0.23	0.23	0.24	0.25	0.20	0.16	0.17	0.39	0.16	0.21	0.23	0.19	0.27	0.21	0.19
Mg	0.88	0.93	0.99	1.01	0.91	0.93	0.95	0.94	0.72	0.95	0.93	0.98	0.87	0.92	0.93	0.90
Ti	0.02	0.01	0.01	0.01	0.02	0.01	0.01	0.01	0.02	0.01	0.02	0.02	0.02	0.02	0.02	0.02
Cr	0.00	0.00	0.00	0.00	0.00	0.01	0.02	0.01	0.00	0.02	0.01	0.00	0.01	0.02	0.00	0.00
Mn	0.01	0.01	0.01	0.01	0.01	0.01	0.00	0.00	0.01	0.00	0.01	0.01	0.00	0.01	0.01	0.01
Ca	0.79	0.79	0.72	0.71	0.79	0.82	0.84	0.84	0.85	0.83	0.79	0.72	0.86	0.75	0.79	0.82
Na	0.02	0.01	0.01	0.01	0.02	0.01	0.01	0.01	0.02	0.01	0.02	0.02	0.03	0.02	0.02	0.03
Sum	4.00	4.00	4.00	4.00	4.00	4.00	4.00	4.00	4.00	4.00	4.00	4.00	4.00	4.00	4.00	4.00
Mg#	0.75	0.80	0.81	0.81	0.79	0.82	0.85	0.85	0.65	0.85	0.82	0.81	0.82	0.77	0.81	0.82

Appendix B5. Pyroxene Analyses (continued)

Sample	99-1-21B2	99-1-21B3	99-1-21C1	99-1-21C2	99-1-21C3	99-1-21C4	99-1-30A1	99-1-30A2	99-1-30A3	99-1-30A4	99-1-30B1	99-1-30B2	99-1-30B3	99-1-30B4	99-2-1B1
Rock Type	gabbro	gabbro	gabbro	gabbro	gabbro	gabbro	gabbro	gabbro	gabbro	gabbro	gabbro	gabbro	gabbro	gabbro	basalt
Location	UofA	UofA	UofA	UofA	UofA	UofA	UofA	UofA	UofA	UofA	UofA	UofA	UofA	UofA	UofA
Occurrence	gm	gm	cor	cor	rim	rim	cor	cor	rim	rim	cor	cor	rim	rim	gm
SiO_2	51.68	51.89	52.73	52.50	52.15	52.14	52.47	52.02	52.11	51.46	52.25	51.99	52.19	51.70	51.50
TiO_2	0.65	0.66	0.57	0.64	0.67	0.56	0.44	0.42	0.50	0.46	0.52	0.62	0.56	0.69	0.67
Al_2O_3	2.58	2.49	2.31	2.42	2.51	2.32	2.26	2.20	2.21	2.21	2.52	2.40	2.41	2.53	2.38
FeO^T	6.36	6.06	7.06	7.51	6.33	6.14	5.97	5.85	5.73	6.04	5.92	5.85	6.22	6.01	7.13
Cr_2O_3	0.15	0.05	0.07	0.10	0.10	0.08	0.32	0.49	0.25	0.33	0.07	0.11	0.18	0.17	0.02
MnO	0.17	0.18	0.16	0.18	0.16	0.16	0.18	0.18	0.19	0.16	0.14	0.19	0.16	0.14	0.18
MgO	15.96	15.96	17.36	17.99	16.21	16.23	16.35	16.36	16.30	16.42	16.22	16.03	16.45	16.32	15.52
CaO	21.76	21.72	19.63	18.86	21.90	22.16	21.79	21.64	21.84	21.64	21.79	22.00	21.56	21.70	21.67
Na_2O	0.37	0.35	0.29	0.30	0.37	0.27	0.29	0.30	0.31	0.32	0.34	0.34	0.33	0.35	0.35
Total	99.68	99.36	100.18	100.50	100.40	100.06	100.07	99.46	99.44	99.04	99.77	99.53	100.06	99.61	99.42
Si	1.90	1.92	1.93	1.91	1.91	1.91	1.92	1.92	1.92	1.90	1.92	1.92	1.91	1.90	1.91
Al^{IV}	0.10	0.08	0.07	0.09	0.09	0.09	0.08	0.08	0.08	0.10	0.08	0.08	0.09	0.10	0.09
Al^{VI}	0.02	0.02	0.03	0.01	0.01	0.01	0.02	0.01	0.02	0.00	0.03	0.02	0.02	0.01	0.01
Fe^{2+}	0.20	0.19	0.22	0.23	0.19	0.19	0.18	0.18	0.18	0.19	0.18	0.18	0.19	0.19	0.22
Mg	0.88	0.88	0.95	0.98	0.88	0.89	0.89	0.90	0.90	0.91	0.89	0.88	0.90	0.90	0.86
Ti	0.02	0.02	0.02	0.02	0.02	0.02	0.01	0.01	0.01	0.01	0.01	0.02	0.02	0.02	0.02
Cr	0.00	0.00	0.00	0.00	0.00	0.00	0.01	0.01	0.01	0.01	0.00	0.00	0.01	0.01	0.00
Mn	0.01	0.01	0.01	0.01	0.01	0.01	0.01	0.01	0.01	0.01	0.00	0.01	0.01	0.00	0.01
Ca	0.86	0.86	0.77	0.74	0.86	0.87	0.86	0.86	0.86	0.86	0.86	0.87	0.85	0.86	0.86
Na	0.03	0.03	0.02	0.02	0.03	0.02	0.02	0.02	0.02	0.02	0.02	0.02	0.02	0.03	0.03
Sum	4.00	4.00	4.00	4.00	4.00	4.00	4.00	4.00	4.00	4.00	4.00	4.00	4.00	4.00	4.00
Mg#	0.82	0.82	0.81	0.81	0.82	0.83	0.83	0.83	0.84	0.83	0.83	0.83	0.83	0.83	0.79

Appendix B5. Pyroxene Analyses (continued)

Sample	99-2-1B2	99-2-1B3	99-2-1B4	99-2-1C2	100-1-39A1	100-1-39A2	100-1-39A3	100-1-39A4	100-1-39B1	100-1-39B2	100-1-39B3	100-1-39B4	100-1-39C1	100-1-39C2
Rock Type	basalt	basalt	basalt	basalt	basalt	basalt	basalt	basalt	basalt	basalt	basalt	basalt	basalt	basalt
Location	UofA	UofA	UofA	UofA	UofA	UofA	UofA	UofA	UofA	UofA	UofA	UofA	UofA	UofA
Occurrence	gm	gm	gm	gm	gm	gm	gm	gm	gm	gm	gm	gm	gm	gm
SiO_2	51.37	51.97	51.46	52.43	53.22	52.95	51.96	51.74	51.70	53.09	51.50	52.72	52.32	51.07
TiO_2	0.74	0.66	0.66	0.33	0.52	0.49	0.64	0.85	0.73	0.56	0.96	0.70	0.74	1.13
Al_2O_3	2.55	2.42	2.22	1.61	1.69	1.58	2.39	1.65	3.15	1.63	2.01	1.36	2.58	2.47
FeO^T	6.80	7.69	7.44	7.04	8.41	8.74	8.74	14.12	6.60	9.56	13.81	13.76	8.77	11.24
Cr_2O_3	0.04	0.04	0.04	b.d.	0.13	0.07	0.18	b.d.	0.51	0.04	b.d.	b.d.	0.05	0.02
MnO	0.21	0.18	0.22	0.16	0.28	0.22	0.23	0.40	0.15	0.25	0.35	0.34	0.22	0.23
MgO	15.47	15.67	15.96	15.87	18.51	18.51	18.42	16.89	16.92	18.32	16.36	18.11	17.42	15.55
CaO	21.77	21.50	21.18	21.92	17.23	17.31	16.93	14.49	20.03	16.83	15.14	13.39	18.33	18.35
Na_2O	0.28	0.38	0.30	0.20	0.23	0.21	0.26	0.21	0.22	0.20	0.28	0.24	0.22	0.35
Total	99.23	100.51	99.48	99.56	100.22	100.08	99.75	100.35	100.01	100.48	100.41	100.62	100.65	100.41
Si	1.91	1.91	1.91	1.94	1.95	1.94	1.91	1.92	1.90	1.94	1.92	1.94	1.91	1.89
Al^{IV}	0.09	0.09	0.10	0.06	0.06	0.06	0.09	0.07	0.11	0.06	0.09	0.06	0.09	0.11
Al^{VI}	0.02	0.01	0.00	0.01	0.02	0.01	0.01	0.00	0.03	0.01	0.00	0.00	0.02	0.00
Fe^{2+}	0.21	0.24	0.23	0.22	0.26	0.27	0.27	0.44	0.20	0.29	0.43	0.42	0.27	0.35
Mg	0.86	0.86	0.88	0.88	1.01	1.01	1.01	0.94	0.93	1.00	0.91	1.00	0.95	0.86
Ti	0.02	0.02	0.02	0.01	0.01	0.01	0.02	0.02	0.02	0.02	0.03	0.02	0.02	0.03
Cr	0.00	0.00	0.00	-	0.00	0.00	0.01	-	0.02	0.00	-	-	0.00	0.00
Mn	0.01	0.01	0.01	0.01	0.01	0.01	0.01	0.01	0.01	0.01	0.01	0.01	0.01	0.01
Ca	0.87	0.85	0.84	0.87	0.68	0.68	0.67	0.58	0.79	0.66	0.60	0.53	0.72	0.73
Na	0.02	0.03	0.02	0.01	0.02	0.02	0.02	0.02	0.02	0.01	0.02	0.02	0.02	0.03
Sum	4.00	4.00	4.00	4.00	4.00	4.00	4.00	4.00	4.00	4.00	4.00	4.00	4.00	4.00
Mg#	0.80	0.78	0.79	0.80	0.80	0.79	0.79	0.68	0.82	0.77	0.68	0.70	0.78	0.71

Appendix B5. Pyroxene Analyses (continued)

Sample	101-1-2A1	101-1-2A2	101-1-2A3	101-1-2A4	101-1-2A5	101-1-2A6	101-1-2B1	101-1-2B2	101-1-2B3	101-1-2B4	101-1-2B5	101-1-2B6	101-1-24A1	101-1-24A2
Rock Type	basalt	basalt	basalt	basalt	basalt	basalt	basalt	basalt	basalt	basalt	basalt	basalt	basalt	basalt
Location	UofA	UofA	UofA	UofA	UofA	UofA	UofA	UofA	UofA	UofA	UofA	UofA	UofA	UofA
Occurrence	gm	gm	gm	gm	gm	gm	gm	gm	gm	gm	gm	gm	gm	gm
SiO_2	52.63	52.01	52.25	50.80	52.25	52.05	52.09	50.91	50.73	51.29	50.58	50.21	51.81	52.04
TiO_2	0.41	0.57	0.49	0.92	0.61	0.52	0.57	0.82	0.84	0.65	0.91	1.06	0.55	0.59
Al_2O_3	2.39	2.33	2.42	2.52	1.97	2.26	2.32	2.80	3.24	2.58	2.46	2.99	1.95	2.15
FeO^T	6.82	8.23	6.88	11.96	9.49	8.55	8.43	10.24	9.35	8.82	13.36	12.23	8.30	8.59
Cr_2O_3	0.15	0.09	0.14	b.d.	0.01	0.04	0.07	0.03	0.05	0.02	b.d.	b.d.	0.04	0.06
MnO	0.16	0.20	0.17	0.28	0.26	0.19	0.20	0.19	0.18	0.20	0.35	0.34	0.21	0.22
MgO	17.05	16.36	17.02	14.34	16.42	16.52	16.37	15.37	15.80	15.89	15.18	14.70	16.67	16.95
CaO	20.50	19.92	20.10	18.78	18.94	19.57	19.90	19.42	19.20	19.68	16.58	18.45	19.72	18.86
Na_2O	0.20	0.22	0.20	0.29	0.26	0.20	0.27	0.23	0.22	0.23	0.23	0.30	0.22	0.20
Total	100.31	99.93	99.67	99.89	100.21	99.90	100.22	100.01	99.61	99.36	99.65	100.28	99.47	99.66
Si	1.92	1.92	1.92	1.90	1.93	1.92	1.92	1.89	1.88	1.91	1.90	1.87	1.92	1.92
Al^{IV}	0.08	0.08	0.08	0.10	0.07	0.08	0.08	0.11	0.12	0.09	0.10	0.13	0.08	0.08
Al^{VI}	0.03	0.02	0.03	0.02	0.01	0.02	0.02	0.01	0.03	0.02	0.01	0.00	0.00	0.02
Fe^{2+}	0.21	0.25	0.21	0.38	0.29	0.26	0.26	0.32	0.29	0.27	0.42	0.38	0.26	0.27
Mg	0.93	0.90	0.93	0.80	0.90	0.91	0.90	0.85	0.87	0.88	0.85	0.82	0.92	0.93
Ti	0.01	0.02	0.01	0.03	0.02	0.01	0.02	0.02	0.02	0.02	0.03	0.03	0.02	0.02
Cr	0.00	0.00	0.00	-	0.00	0.00	0.00	0.00	0.00	0.00	-	-	0.00	0.00
Mn	0.01	0.01	0.01	0.01	0.01	0.01	0.01	0.01	0.01	0.01	0.01	0.01	0.01	0.01
Ca	0.80	0.79	0.79	0.75	0.75	0.77	0.78	0.77	0.76	0.78	0.67	0.74	0.78	0.75
Na	0.01	0.02	0.01	0.02	0.02	0.01	0.02	0.02	0.02	0.02	0.02	0.02	0.02	0.01
Sum	4.00	4.00	4.00	4.00	4.00	4.00	4.00	4.00	4.00	4.00	4.00	4.00	4.00	4.00
Mg#	0.82	0.78	0.82	0.68	0.76	0.77	0.78	0.73	0.75	0.76	0.67	0.68	0.78	0.78

Appendix B5. Pyroxene Analyses (continued)

Sample	101-1-24A3	101-1-24A4	101-1-24A5	101-1-24A6	101-1-24B1	101-1-24B2	101-1-24B3	101-1-24B4	101-1-24C1	101-1-24C2	101-1-24C3	105-1-6A1	105-1-6A3
Rock Type	basalt	basalt	basalt	basalt	basalt	basalt	basalt	basalt	basalt	basalt	basalt	gabbro	gabbro
Location	UofA	UofA	UofA	UofA	UofA	UofA	UofA	UofA	UofA	UofA	UofA	OSU	OSU
Occurrence	gm	gm	gm	gm	gm	gm	gm	gm	gm	gm	gm	gm	gm
SiO_2	51.64	51.76	52.00	51.22	52.09	51.60	51.27	50.54	51.88	51.26	51.68	51.43	51.84
TiO_2	0.63	0.55	0.59	0.70	0.48	0.68	0.68	0.98	0.60	0.74	0.66	0.58	0.54
Al_2O_3	2.35	2.09	2.29	2.94	2.30	3.01	2.53	2.63	2.42	2.65	2.43	2.96	2.85
FeO^T	8.54	8.23	8.74	8.86	6.53	8.25	8.93	12.71	8.50	9.13	8.70	6.50	6.60
Cr_2O_3	0.07	0.05	0.08	0.14	0.17	0.11	0.01	0.04	0.09	0.05	0.05	0.42	0.37
MnO	0.21	0.20	0.25	0.24	0.19	0.21	0.19	0.34	0.26	0.24	0.19	0.15	0.16
MgO	16.68	16.55	16.80	16.55	17.38	16.74	16.02	14.63	16.97	16.15	16.53	15.66	16.16
CaO	19.48	19.89	18.71	18.95	20.17	19.34	19.54	17.83	19.36	19.29	19.28	22.30	22.35
Na_2O	0.21	0.24	0.26	0.24	0.25	0.26	0.23	0.21	0.20	0.28	0.25	0.44	0.44
Total	99.81	99.56	99.72	99.84	99.56	100.20	99.40	99.91	100.28	99.79	99.77	100.44	101.31
Si	1.91	1.91	1.92	1.89	1.91	1.89	1.91	1.90	1.90	1.90	1.91	1.88	1.88
Al^{IV}	0.09	0.09	0.08	0.11	0.09	0.11	0.10	0.10	0.10	0.10	0.09	0.12	0.12
Al^{VI}	0.01	0.01	0.02	0.02	0.01	0.02	0.02	0.01	0.01	0.01	0.01	0.01	0.00
Fe^{2+}	0.26	0.26	0.27	0.27	0.20	0.25	0.28	0.40	0.26	0.28	0.27	0.20	0.20
Mg	0.92	0.91	0.93	0.91	0.95	0.92	0.89	0.82	0.93	0.89	0.91	0.85	0.87
Ti	0.02	0.02	0.02	0.02	0.01	0.02	0.02	0.03	0.02	0.02	0.02	0.02	0.02
Cr	0.00	0.00	0.00	0.00	0.01	0.00	0.00	0.00	0.00	0.00	0.00	0.01	0.01
Mn	0.01	0.01	0.01	0.01	0.01	0.01	0.01	0.01	0.01	0.01	0.01	0.01	0.01
Ca	0.77	0.79	0.74	0.75	0.79	0.76	0.78	0.72	0.76	0.77	0.76	0.87	0.87
Na	0.02	0.02	0.02	0.02	0.02	0.02	0.02	0.02	0.01	0.02	0.02	0.03	0.03
Sum	4.00	4.00	4.00	4.00	4.00	4.00	4.00	4.00	4.00	4.00	4.00	4.00	4.00
Mg#	0.78	0.78	0.77	0.77	0.83	0.78	0.76	0.67	0.78	0.76	0.77	0.81	0.81

Appendix B5. Pyroxene Analyses (continued)

Sample	105-1-6B2	105-1-6D1	105-1-6D2	105-1-6D3	105-1-8(b)B2	105-1-8(b)B3	105-1-21A1	105-1-21B1	105-1-21B2	105-1-21B3	105-1-21B4	105-1-21C1	105-1-21C2
Rock Type	gabbro	gabbro	gabbro	gabbro	gabbro	gabbro	gabbro	gabbro	gabbro	gabbro	gabbro	gabbro	gabbro
Location	OSU	OSU	OSU	OSU	OSU	OSU	UofA	UofA	UofA	UofA	UofA	UofA	UofA
Occurrence	gm	rim	cor	cor	cor	rim	gm	cor	rim	cor	rim	cor	rim
SiO_2	51.95	51.95	51.61	52.63	51.20	52.75	50.83	51.58	51.72	51.39	51.51	51.04	50.85
TiO_2	0.68	0.48	0.62	0.48	0.63	0.75	0.94	0.57	0.50	0.59	0.48	0.76	0.73
Al_2O_3	2.79	2.48	3.03	2.41	2.68	4.39	3.13	3.20	2.82	2.94	2.84	3.21	2.85
FeO^T	6.79	6.50	6.15	6.49	5.55	5.34	5.73	5.43	5.43	5.56	5.36	5.51	5.42
Cr_2O_3	0.12	0.16	0.32	0.15	0.29	0.25	0.44	0.38	0.34	0.36	0.36	0.56	0.24
MnO	0.17	0.20	0.16	0.17	0.19	0.11	0.17	0.15	0.14	0.15	0.16	0.17	0.14
MgO	16.29	15.75	15.49	16.05	15.76	15.31	15.65	15.62	15.80	15.96	16.03	15.58	15.82
CaO	21.86	22.42	22.67	22.60	22.47	21.03	22.18	22.54	22.32	21.96	22.15	22.10	22.51
Na_2O	0.44	0.43	0.45	0.38	0.32	0.52	0.44	0.41	0.41	0.43	0.38	0.50	0.45
Total	101.09	100.37	100.50	101.36	99.09	100.45	99.51	99.88	99.48	99.34	99.27	99.43	99.01
Si	1.89	1.90	1.89	1.91	1.90	1.93	1.88	1.89	1.91	1.89	1.90	1.88	1.88
Al^{IV}	0.12	0.10	0.11	0.09	0.11	0.08	0.13	0.11	0.10	0.11	0.10	0.12	0.12
Al^{VI}	0.00	0.01	0.02	0.01	0.01	0.11	0.01	0.03	0.03	0.02	0.02	0.02	0.00
Fe^{2+}	0.21	0.20	0.19	0.20	0.17	0.16	0.18	0.17	0.17	0.17	0.17	0.17	0.17
Mg	0.88	0.86	0.84	0.87	0.87	0.83	0.86	0.86	0.87	0.88	0.88	0.86	0.87
Ti	0.02	0.01	0.02	0.01	0.02	0.02	0.03	0.02	0.01	0.02	0.01	0.02	0.02
Cr	0.00	0.01	0.01	0.00	0.01	0.01	0.01	0.01	0.01	0.01	0.01	0.02	0.01
Mn	0.01	0.01	0.01	0.01	0.01	0.00	0.01	0.01	0.00	0.01	0.01	0.01	0.00
Ca	0.85	0.88	0.89	0.88	0.89	0.82	0.88	0.89	0.88	0.87	0.88	0.87	0.89
Na	0.03	0.03	0.03	0.03	0.02	0.04	0.03	0.03	0.03	0.03	0.03	0.04	0.03
Sum	4.00	4.00	4.00	4.00	4.00	4.00	4.00	4.00	4.00	4.00	4.00	4.00	4.00
Mg#	0.81	0.81	0.82	0.81	0.83	0.84	0.83	0.84	0.84	0.84	0.84	0.83	0.84

Appendix B5. Pyroxene Analyses (continued)

Sample	105-1-25A1	105-1-25A2	105-1-25B1	105-1-25B2	105-1-25C1	105-1-25C2	105-1-25D2	105-1-25D3	105-3-6a1	105-3-6a2	105-3-6a3	105-3-6a4	105-3-6a5	105-3-6b1
Rock Type	gabbro	gabbro	gabbro	gabbro	gabbro	gabbro	gabbro	gabbro	basalt	basalt	basalt	basalt	basalt	basalt
Location	OSU	OSU	OSU	OSU	OSU	OSU	OSU	OSU	OSU	OSU	OSU	OSU	OSU	OSU
Occurrence	rim	cor	cor	rim	cor	cor	rim	cor	cor	rim	gm	cor	rim	cor
SiO_2	51.82	51.47	51.07	53.63	51.87	51.86	52.05	51.87	52.47	51.58	52.71	52.80	50.76	52.54
TiO_2	0.55	0.58	0.52	0.03	0.47	0.49	0.50	0.58	0.22	0.44	0.30	0.32	0.56	0.31
Al_2O_3	2.65	2.86	3.32	0.64	2.45	3.12	2.43	2.59	2.83	2.80	2.56	2.00	3.49	2.57
FeO^T	6.65	6.96	6.55	4.71	6.46	6.10	6.53	5.97	5.41	10.83	6.46	7.86	11.65	6.98
Cr_2O_3	0.13	0.16	0.14	0.10	0.11	0.16	0.09	0.12	0.18	b.d.	0.05	0.02	0.01	0.10
MnO	0.19	0.19	0.20	0.20	0.17	0.11	0.17	0.20	0.15	0.25	0.16	0.21	0.24	0.18
MgO	15.91	15.76	16.45	16.67	15.91	16.03	15.93	15.32	16.97	16.10	17.20	16.83	14.75	17.01
CaO	22.64	22.20	20.97	23.41	22.51	22.48	22.49	23.07	22.20	18.90	21.57	20.75	19.60	21.54
Na_2O	0.36	0.42	0.32	0.10	0.33	0.35	0.35	0.35	0.16	0.20	0.17	0.18	0.25	0.17
Total	100.90	100.60	99.54	99.49	100.28	100.70	100.54	100.07	100.59	101.10	101.18	100.97	101.31	101.40
Si	1.89	1.88	1.88	1.97	1.90	1.89	1.90	1.91	1.91	1.89	1.91	1.92	1.87	1.90
Al^{IV}	0.11	0.12	0.12	0.03	0.10	0.11	0.10	0.09	0.10	0.11	0.09	0.08	0.13	0.10
Al^{VI}	0.00	0.00	0.02	0.00	0.01	0.02	0.01	0.02	0.03	0.01	0.02	0.01	0.02	0.01
Fe^{2+}	0.20	0.21	0.20	0.15	0.20	0.19	0.20	0.18	0.16	0.33	0.20	0.24	0.36	0.21
Mg	0.86	0.86	0.90	0.91	0.87	0.87	0.87	0.84	0.92	0.88	0.93	0.91	0.81	0.92
Ti	0.02	0.02	0.01	0.00	0.01	0.01	0.01	0.02	0.01	0.01	0.01	0.01	0.02	0.01
Cr	0.00	0.01	0.00	0.00	0.00	0.01	0.00	0.00	0.01	-	0.00	0.00	0.00	0.00
Mn	0.01	0.01	0.01	0.01	0.01	0.00	0.01	0.01	0.01	0.01	0.01	0.01	0.01	0.01
Ca	0.88	0.87	0.83	0.92	0.88	0.88	0.88	0.91	0.86	0.74	0.84	0.81	0.77	0.83
Na	0.03	0.03	0.02	0.01	0.02	0.03	0.03	0.03	0.01	0.01	0.01	0.01	0.02	0.01
Sum	4.00	4.00	4.00	4.00	4.00	4.00	4.00	4.00	4.00	4.00	4.00	4.00	4.00	4.00
Mg#	0.81	0.80	0.82	0.86	0.81	0.82	0.81	0.82	0.85	0.73	0.83	0.79	0.69	0.81

Appendix B5. Pyroxene Analyses (continued)

Sample	105-3-6b2	105-3-6b3	105-3-6b4	105-3-6C1	105-3-6C2	105-3-6C3	105-3-6C4	105-3-6C5	105-3-6D1	105-3-6D2	106-2-5c1	106-2-5c2	106-2-10A2	106-2-10A3
Rock Type	basalt	basalt	basalt	basalt	basalt	basalt	basalt	basalt	basalt	basalt	gabbro	gabbro	gabbro	gabbro
Location	OSU	OSU	OSU	OSU	OSU	OSU	OSU	OSU	OSU	OSU	OSU	OSU	OSU	OSU
Occurrence	rim	cor	rim	cor	rim	cor	cor	rim	cor	gm	gm	gm	cor	rim
SiO_2	52.49	52.64	52.42	51.76	52.42	52.76	52.88	52.81	51.97	52.14	52.40	52.85	52.70	53.37
TiO_2	0.32	0.29	0.33	0.33	0.34	0.28	0.26	0.32	0.41	0.30	0.05	0.12	0.24	0.16
Al_2O_3	2.49	2.18	2.47	2.68	2.73	2.76	2.10	2.67	2.96	2.94	0.55	0.65	1.53	1.25
FeO^T	7.26	7.51	7.72	7.49	7.00	6.45	7.05	7.09	8.78	6.61	8.39	8.34	5.72	5.71
Cr_2O_3	0.09	0.05	0.06	0.09	0.10	0.09	0.04	0.04	0.03	0.07	0.01	0.02	b.d.	0.02
MnO	0.21	0.20	0.15	0.15	0.16	0.14	0.17	0.14	0.21	0.16	0.37	0.36	0.16	0.17
MgO	16.62	16.64	16.44	16.04	16.82	16.85	16.87	16.66	16.14	16.97	13.51	13.92	15.86	15.98
CaO	21.49	21.04	21.30	21.40	21.24	21.77	21.16	21.28	20.19	21.34	24.05	23.63	23.90	23.81
Na_2O	0.18	0.18	0.22	0.17	0.18	0.18	0.19	0.18	0.19	0.17	0.21	0.10	0.08	0.11
Total	101.15	100.73	101.11	100.11	100.99	101.28	100.72	101.19	100.88	100.70	99.54	99.99	100.19	100.58
Si	1.91	1.92	1.91	1.90	1.90	1.91	1.93	1.92	1.90	1.90	1.96	1.97	1.93	1.95
Al^{IV}	0.09	0.08	0.09	0.10	0.10	0.09	0.07	0.08	0.10	0.11	0.02	0.03	0.07	0.05
Al^{VI}	0.01	0.02	0.01	0.02	0.02	0.03	0.02	0.03	0.03	0.02	0.00	0.00	0.00	0.00
Fe^{2+}	0.22	0.23	0.24	0.23	0.21	0.20	0.21	0.22	0.27	0.20	0.26	0.26	0.18	0.18
Mg	0.90	0.91	0.89	0.88	0.91	0.91	0.92	0.90	0.88	0.92	0.76	0.77	0.87	0.87
Ti	0.01	0.01	0.01	0.01	0.01	0.01	0.01	0.01	0.01	0.01	0.00	0.00	0.01	0.00
Cr	0.00	0.00	0.00	0.00	0.00	0.00	0.00	0.00	0.00	0.00	0.00	0.00	-	0.00
Mn	0.01	0.01	0.01	0.01	0.01	0.00	0.01	0.00	0.01	0.01	0.01	0.01	0.01	0.01
Ca	0.84	0.82	0.83	0.84	0.83	0.84	0.83	0.83	0.79	0.83	0.97	0.94	0.94	0.93
Na	0.01	0.01	0.02	0.01	0.01	0.01	0.01	0.01	0.01	0.01	0.02	0.01	0.01	0.01
Sum	4.00	4.00	4.00	4.00	4.00	4.00	4.00	4.00	4.00	4.00	4.00	4.00	4.00	4.00
Mg#	0.80	0.80	0.79	0.79	0.81	0.82	0.81	0.81	0.77	0.82	0.74	0.75	0.83	0.83

Appendix B5. Pyroxene Analyses (continued)

Sample	106-2-10E1	106-2-10E2	108-1-6A1	108-1-6A2	108-1-6A3	108-1-6A4	108-1-6A5	108-1-6B1	108-1-6B3	108-1-6C1	108-1-6C2	108-2-6A1	108-2-6A2	108-2-6B1
Rock Type	gabbro	gabbro	gabbro	gabbro	gabbro	gabbro	gabbro	gabbro	gabbro	gabbro	gabbro	gabbro	gabbro	gabbro
Location	OSU	OSU	UofA	UofA	UofA	UofA	UofA	UofA	UofA	UofA	UofA	UofA	UofA	UofA
Occurrence	gm	gm	cor	rim	cor	gm	rim	cor	cor	cor	rim	rim	cor	cor
SiO_2	51.73	52.14	53.02	52.37	53.24	52.59	53.04	52.99	52.28	52.55	52.67	52.44	52.10	52.26
TiO_2	0.49	0.32	0.15	0.23	0.30	0.20	0.15	0.26	0.25	0.24	0.27	0.25	0.20	0.31
Al_2O_3	2.13	2.35	1.44	2.55	1.82	2.52	1.38	2.19	2.48	2.20	1.80	2.43	2.60	2.59
FeO^T	8.18	6.64	4.97	5.10	5.05	5.09	4.82	5.37	4.56	5.07	4.79	6.40	5.68	5.55
Cr_2O_3	b.d.	0.02	0.07	0.12	0.13	0.10	0.04	0.08	0.05	0.02	0.06	0.33	0.33	0.31
MnO	0.22	0.17	0.15	0.15	0.11	0.09	0.13	0.13	0.12	0.11	0.11	0.19	0.17	0.16
MgO	15.46	15.58	16.25	16.41	16.68	16.51	16.67	16.76	16.43	16.51	16.25	17.63	16.88	16.39
CaO	21.93	22.99	22.92	22.19	22.53	22.42	22.87	22.04	23.11	22.38	23.24	19.96	21.40	22.08
Na_2O	0.27	0.13	0.07	0.14	0.15	0.16	0.08	0.13	0.11	0.16	0.14	0.20	0.23	0.22
Total	100.41	100.34	99.04	99.26	100.01	99.68	99.18	99.95	99.39	99.24	99.33	99.83	99.59	99.87
Si	1.90	1.91	1.96	1.93	1.95	1.93	1.96	1.94	1.92	1.94	1.94	1.92	1.91	1.92
Al^{IV}	0.09	0.09	0.04	0.07	0.05	0.07	0.04	0.06	0.08	0.06	0.06	0.08	0.09	0.08
Al^{VI}	0.00	0.02	0.03	0.04	0.03	0.04	0.02	0.03	0.03	0.03	0.02	0.02	0.02	0.03
Fe^{2+}	0.25	0.20	0.15	0.16	0.16	0.16	0.15	0.16	0.14	0.16	0.15	0.20	0.17	0.17
Mg	0.85	0.85	0.90	0.90	0.91	0.90	0.92	0.92	0.90	0.91	0.89	0.96	0.92	0.90
Ti	0.01	0.01	0.00	0.01	0.01	0.01	0.00	0.01	0.01	0.01	0.01	0.01	0.01	0.01
Cr	-	0.00	0.00	0.00	0.00	0.00	0.00	0.00	0.00	0.00	0.00	0.01	0.01	0.01
Mn	0.01	0.01	0.01	0.01	0.00	0.00	0.00	0.00	0.00	0.00	0.00	0.01	0.01	0.01
Ca	0.87	0.90	0.91	0.88	0.88	0.88	0.90	0.86	0.91	0.88	0.92	0.78	0.84	0.87
Na	0.02	0.01	0.01	0.01	0.01	0.01	0.01	0.01	0.01	0.01	0.01	0.01	0.02	0.02
Sum	4.00	4.00	4.00	4.00	4.00	4.00	4.00	4.00	4.00	4.00	4.00	4.00	4.00	4.00
Mg#	0.77	0.81	0.85	0.85	0.85	0.85	0.86	0.85	0.87	0.85	0.86	0.83	0.84	0.84

Appendix B5. Pyroxene Analyses (continued)

Sample	108-2-6B2	108-2-6C1	108-2-6C2	110-1-5AB1	110-1-5AB2	110-1-5AB3	110-1-5AB4	110-1-5AB5	110-1-5AB6	110-1-5AB7	110-1-5AC1	110-1-5AC2	110-1-5AC3
Rock Type	gabbro	gabbro	gabbro	basalt	basalt	basalt	basalt	basalt	basalt	basalt	basalt	basalt	basalt
Location	UofA	UofA	UofA	UofA	UofA	UofA	UofA	UofA	UofA	UofA	UofA	UofA	UofA
Occurrence	rim	cor	rim	gm	gm	gm	gm	gm	rim	rim	gm	gm	gm
SiO_2	52.41	52.30	52.33	47.94	48.61	49.05	49.60	48.55	52.13	51.56	48.29	49.83	48.26
TiO_2	0.29	0.29	0.25	1.76	1.55	1.74	1.49	1.62	0.04	0.02	1.89	1.10	1.67
Al_2O_3	2.51	2.67	2.46	5.53	5.12	4.00	3.56	4.93	0.83	1.23	4.87	3.25	5.45
FeO^T	5.34	5.44	5.32	10.56	10.08	11.64	11.79	11.86	15.13	14.69	11.61	13.16	10.91
Cr_2O_3	0.29	0.35	0.33	0.18	0.16	0.23	0.08	0.24	0.04	0.01	0.24	0.10	0.14
MnO	0.15	0.15	0.15	0.21	0.20	0.23	0.28	0.25	0.63	0.52	0.23	0.26	0.21
MgO	16.53	16.79	16.48	13.05	13.26	13.33	14.22	13.41	9.08	9.06	13.03	14.04	13.24
CaO	22.16	21.68	22.26	20.26	20.73	19.43	18.69	19.45	21.92	22.79	19.30	17.96	19.83
Na_2O	0.18	0.23	0.21	0.30	0.30	0.33	0.34	0.34	0.22	0.32	0.38	0.30	0.32
Total	99.86	99.90	99.79	99.79	100.01	99.98	100.05	100.65	100.02	100.20	99.84	100.00	100.03
Si	1.92	1.91	1.92	1.80	1.82	1.84	1.86	1.81	2.01	1.98	1.82	1.87	1.81
Al^{IV}	0.08	0.09	0.08	0.20	0.18	0.16	0.15	0.19	0.00	0.02	0.18	0.13	0.20
Al^{VI}	0.03	0.03	0.03	0.04	0.04	0.02	0.01	0.03	0.04	0.03	0.03	0.01	0.05
Fe^{2+}	0.16	0.17	0.16	0.33	0.32	0.37	0.37	0.37	0.49	0.47	0.37	0.41	0.34
Mg	0.90	0.92	0.90	0.73	0.74	0.75	0.79	0.75	0.52	0.52	0.73	0.79	0.74
Ti	0.01	0.01	0.01	0.05	0.04	0.05	0.04	0.05	0.00	0.00	0.05	0.03	0.05
Cr	0.01	0.01	0.01	0.01	0.01	0.01	0.00	0.01	0.00	0.00	0.01	0.00	0.00
Mn	0.01	0.01	0.01	0.01	0.01	0.01	0.01	0.01	0.02	0.02	0.01	0.01	0.01
Ca	0.87	0.85	0.88	0.81	0.83	0.78	0.75	0.78	0.91	0.94	0.78	0.72	0.80
Na	0.01	0.02	0.02	0.02	0.02	0.02	0.03	0.03	0.02	0.02	0.03	0.02	0.02
Sum	4.00	4.00	4.00	4.00	4.00	4.00	4.00	4.00	4.00	4.00	4.00	4.00	4.00
Mg#	0.85	0.85	0.85	0.69	0.70	0.67	0.68	0.67	0.52	0.52	0.67	0.66	0.68

Appendix B5. Pyroxene Analyses (continued)

Sample	110-1-5AC4	110-1-5AC5	110-1-5AC6	110-1-5AC7	110-1-25D1	110-1-25D2	110-1-25D3	110-1-25D4	111-4-3C3	111-4-6B1	111-4-6B3	111-4-6B4	111-4-6C2	111-4-6C3
Rock Type	basalt	basalt	basalt	basalt	basalt	basalt	basalt	basalt	gabbro	gabbro	gabbro	gabbro	gabbro	gabbro
Location	UofA	UofA	UofA	UofA	UofA	UofA	UofA	UofA	OSU	UofA	UofA	UofA	UofA	UofA
Occurrence	gm	rim	rim	rim	gm	gm	gm	gm	cor	gm	gm	gm	gm	gm
SiO_2	49.29	49.52	49.04	48.98	52.95	52.19	51.57	53.23	52.03	52.95	53.41	52.62	53.20	53.59
TiO_2	1.32	1.35	1.41	1.50	0.34	0.45	0.57	0.35	0.29	0.16	0.12	0.19	0.16	0.05
Al_2O_3	4.48	2.71	2.44	2.79	1.98	2.68	3.41	1.88	2.20	0.70	0.50	0.82	0.67	0.33
FeO^T	10.71	16.83	17.82	17.22	6.38	6.14	6.47	6.61	5.72	8.62	8.77	9.26	9.33	8.42
Cr_2O_3	0.13	0.05	b.d.	b.d.	0.43	0.60	0.68	0.36	0.02	b.d.	0.02	0.03	0.01	0.01
MnO	0.19	0.41	0.48	0.38	0.16	0.14	0.16	0.20	0.17	0.25	0.30	0.31	0.29	0.33
MgO	13.23	11.99	10.68	10.47	18.89	17.47	17.21	18.33	16.07	14.42	14.50	14.31	14.32	13.95
CaO	20.32	16.99	17.78	18.58	18.85	20.16	19.82	18.49	22.77	22.54	22.40	22.21	21.73	23.24
Na_2O	0.33	0.26	0.33	0.28	0.20	0.25	0.24	0.19	0.24	0.15	0.18	0.17	0.27	0.18
Total	100.00	100.11	99.98	100.20	100.18	100.08	100.13	99.64	99.51	99.79	100.20	99.92	99.98	100.10
Si	1.84	1.89	1.89	1.88	1.92	1.91	1.89	1.95	1.92	1.98	1.98	1.96	1.98	2.00
Al^{IV}	0.16	0.11	0.11	0.12	0.08	0.09	0.12	0.05	0.08	0.03	0.02	0.04	0.02	0.00
Al^{VI}	0.04	0.01	0.00	0.01	0.01	0.02	0.03	0.03	0.01	0.01	0.01	0.00	0.01	0.01
Fe^{2+}	0.34	0.54	0.57	0.55	0.19	0.19	0.20	0.20	0.18	0.27	0.27	0.29	0.29	0.26
Mg	0.74	0.68	0.61	0.60	1.02	0.95	0.94	1.00	0.88	0.80	0.80	0.80	0.80	0.78
Ti	0.04	0.04	0.04	0.04	0.01	0.01	0.02	0.01	0.01	0.00	0.00	0.01	0.00	0.00
Cr	0.00	0.00	-	-	0.01	0.02	0.02	0.01	0.00	-	0.00	0.00	0.00	0.00
Mn	0.01	0.01	0.02	0.01	0.01	0.00	0.01	0.01	0.01	0.01	0.01	0.01	0.01	0.01
Ca	0.82	0.70	0.73	0.76	0.73	0.79	0.78	0.73	0.90	0.90	0.89	0.89	0.87	0.93
Na	0.02	0.02	0.03	0.02	0.01	0.02	0.02	0.01	0.02	0.01	0.01	0.01	0.02	0.01
Sum	4.00	4.00	4.00	4.00	4.00	4.00	4.00	4.00	4.00	4.00	4.00	4.00	4.00	4.00
Mg#	0.69	0.56	0.52	0.52	0.84	0.83	0.83	0.83	0.83	0.75	0.75	0.73	0.73	0.75

Appendix B5. Pyroxene Analyses (continued)

Sample	112-2-1A1	112-2-1A2	112-2-1A3	112-2-1A4	112-2-1C1	112-2-1C10	112-2-1C2	112-2-1C3	112-2-1C4	112-2-1C5	112-2-1C6	112-2-1C7	112-2-1C8	112-2-1C9
Rock Type	gabbro	gabbro	gabbro	gabbro	gabbro	gabbro	gabbro	gabbro	gabbro	gabbro	gabbro	gabbro	gabbro	gabbro
Location	UofA	UofA	UofA	UofA	UofA	UofA	UofA	UofA	UofA	UofA	UofA	UofA	UofA	UofA
Occurrence	gm	gm	gm	gm	gm	rim	gm	gm	gm	gm	gm	cor	rim	cor
SiO_2	53.40	53.19	52.87	53.90	52.84	52.94	52.93	52.60	52.27	51.93	52.02	54.28	52.31	55.12
TiO_2	0.22	0.24	0.31	0.14	0.27	b.d.	0.29	0.28	0.34	0.43	0.43	0.04	b.d.	0.03
Al_2O_3	2.40	2.48	2.48	1.33	3.12	0.58	3.09	3.04	3.36	3.72	3.77	0.30	0.66	0.20
FeO^T	3.70	3.71	3.68	3.33	3.60	8.86	3.64	3.61	3.44	3.44	3.43	3.20	11.55	2.73
Cr_2O_3	0.54	0.46	0.46	0.32	0.42	0.18	0.45	0.49	0.42	0.53	0.56	0.11	0.06	0.11
MnO	0.14	0.11	0.13	0.10	0.11	0.58	0.10	0.16	0.09	0.11	0.10	0.13	0.73	0.12
MgO	17.21	17.13	16.96	17.18	17.02	12.53	17.10	17.23	16.82	16.78	16.82	17.05	10.81	17.57
CaO	22.62	22.73	22.68	23.59	22.33	24.07	22.57	22.40	22.92	22.68	22.63	24.96	24.39	24.99
Na_2O	0.29	0.35	0.31	0.16	0.28	0.14	0.31	0.30	0.24	0.24	0.25	0.09	0.11	0.07
Total	100.52	100.40	99.88	100.05	99.99	99.88	100.48	100.11	99.90	99.86	100.01	100.16	100.62	100.94
Si	1.93	1.93	1.93	1.96	1.92	1.99	1.92	1.91	1.90	1.89	1.89	1.98	1.98	1.99
Al^{IV}	0.07	0.07	0.07	0.04	0.08	0.01	0.09	0.09	0.10	0.11	0.11	0.01	0.02	0.01
Al^{VI}	0.04	0.03	0.03	0.02	0.06	0.02	0.05	0.04	0.05	0.05	0.05	0.00	0.01	0.00
Fe^{2+}	0.11	0.11	0.11	0.10	0.11	0.28	0.11	0.11	0.11	0.10	0.10	0.10	0.37	0.08
Mg	0.93	0.93	0.92	0.93	0.92	0.70	0.92	0.93	0.91	0.91	0.91	0.93	0.61	0.94
Ti	0.01	0.01	0.01	0.00	0.01	-	0.01	0.01	0.01	0.01	0.01	0.00	-	0.00
Cr	0.02	0.01	0.01	0.01	0.01	0.01	0.01	0.01	0.01	0.02	0.02	0.00	0.00	0.00
Mn	0.00	0.00	0.00	0.00	0.00	0.02	0.00	0.01	0.00	0.00	0.00	0.00	0.02	0.00
Ca	0.88	0.88	0.89	0.92	0.87	0.97	0.88	0.87	0.89	0.89	0.88	0.97	0.99	0.97
Na	0.02	0.03	0.02	0.01	0.02	0.01	0.02	0.02	0.02	0.02	0.02	0.01	0.01	0.01
Sum	4.00	4.00	4.00	4.00	4.00	4.00	4.00	4.00	4.00	4.00	4.00	4.00	4.00	4.00
Mg#	0.89	0.89	0.89	0.90	0.89	0.72	0.89	0.89	0.90	0.90	0.90	0.91	0.63	0.92

Appendix B5. Pyroxene Analyses (continued)

Sample	112-2-6A1	112-2-6A2	112-2-6B1	112-2-6B2	112-2-6C1	112-2-6C2	113-1-3A4	113-1-3B1	113-1-3B2	113-1-3B3	113-1-3D1	113-1-3D2	113-1-3D3	113-1-10a1
Rock Type	gabbro	gabbro	gabbro	gabbro	gabbro	gabbro	basalt	basalt	basalt	basalt	basalt	basalt	basalt	basalt
Location	UofA	UofA	UofA	UofA	UofA	UofA	OSU	OSU	OSU	OSU	OSU	OSU	OSU	OSU
Occurrence	gm	gm	gm	gm	gm	gm	rim	cor	rim	cor	cor	rim	cor	gm
SiO_2	53.27	53.36	53.90	53.22	53.44	52.92	52.51	52.64	52.56	52.37	53.29	53.84	52.70	51.26
TiO_2	0.36	0.37	0.28	0.40	0.24	0.39	0.13	0.15	0.13	0.19	0.10	0.07	0.11	0.67
Al_2O_3	2.66	2.42	1.99	2.30	1.96	2.67	1.37	2.53	1.99	2.01	2.06	1.38	2.10	3.53
FeO^T	3.78	3.56	3.83	3.97	3.65	4.17	9.76	6.64	6.25	13.69	4.68	4.85	4.58	7.92
Cr_2O_3	0.40	0.45	0.35	0.40	0.39	0.45	b.d.	0.62	0.26	0.01	0.71	0.62	0.86	b.d.
MnO	0.11	0.11	0.11	0.12	0.12	0.11	0.26	0.19	0.15	0.44	0.13	0.16	0.13	0.26
MgO	16.56	16.26	16.68	16.33	16.37	17.09	18.21	18.68	18.25	16.53	18.80	19.57	18.44	16.71
CaO	22.37	22.92	22.90	22.63	23.28	21.17	16.86	18.57	19.93	14.95	20.27	19.71	20.44	20.09
Na_2O	0.26	0.29	0.26	0.24	0.16	0.27	0.06	0.19	0.09	0.09	0.11	0.10	0.11	0.19
Total	99.77	99.74	100.30	99.61	99.61	99.24	99.16	100.21	99.61	100.28	100.15	100.30	99.47	100.63
Si	1.95	1.95	1.96	1.95	1.96	1.94	1.95	1.91	1.92	1.95	1.93	1.95	1.93	1.87
Al^{IV}	0.05	0.05	0.04	0.05	0.04	0.06	0.05	0.09	0.08	0.05	0.07	0.05	0.08	0.13
Al^{VI}	0.06	0.06	0.05	0.05	0.05	0.06	0.01	0.02	0.01	0.04	0.02	0.00	0.02	0.02
Fe^{2+}	0.12	0.11	0.12	0.12	0.11	0.13	0.30	0.20	0.19	0.43	0.14	0.15	0.14	0.24
Mg	0.90	0.89	0.91	0.89	0.90	0.94	1.01	1.01	1.00	0.92	1.02	1.05	1.00	0.91
Ti	0.01	0.01	0.01	0.01	0.01	0.01	0.00	0.00	0.00	0.01	0.00	0.00	0.00	0.02
Cr	0.01	0.01	0.01	0.01	0.01	0.01	-	0.02	0.01	0.00	0.02	0.02	0.03	-
Mn	0.00	0.00	0.00	0.00	0.00	0.00	0.01	0.01	0.01	0.01	0.00	0.01	0.00	0.01
Ca	0.88	0.90	0.89	0.89	0.92	0.83	0.67	0.72	0.78	0.60	0.79	0.76	0.80	0.79
Na	0.02	0.02	0.02	0.02	0.01	0.02	0.00	0.01	0.01	0.01	0.01	0.01	0.01	0.01
Sum	4.00	4.00	4.00	4.00	4.00	4.00	4.00	4.00	4.00	4.00	4.00	4.00	4.00	4.00
Mg#	0.89	0.89	0.89	0.88	0.89	0.88	0.77	0.83	0.84	0.68	0.88	0.88	0.88	0.79

Appendix B5. Pyroxene Analyses (continued)

Sample	113-1-10a2	113-1-10a3	113-1-20A1	113-1-20A2	113-1-20A3	113-1-20A4	113-1-20C1	113-1-20C2	113-2-4C1	113-2-4C2	113-2-4C3	113-2-4C4	113-2-11A1	113-2-11A2
Rock Type	basalt	basalt	basalt	basalt	basalt	basalt	basalt	basalt	gabbro	gabbro	gabbro	gabbro	gabbro	gabbro
Location	OSU	OSU	UofA	UofA	UofA	UofA	UofA	UofA	UofA	UofA	UofA	UofA	UofA	UofA
Occurrence	cor	rim	cor	rim	cor	rim	cor	rim	gm	gm	gm	gm	gm	gm
SiO_2	51.76	51.78	52.68	53.44	52.58	52.41	52.42	52.84	54.55	54.67	54.54	54.29	53.14	53.31
TiO_2	0.49	0.57	0.05	0.03	0.09	0.13	0.09	0.11	0.06	0.08	0.10	0.07	0.26	0.24
Al_2O_3	3.33	3.41	1.83	1.44	2.11	2.45	2.22	1.83	0.77	0.40	0.89	1.08	2.25	2.22
FeO^T	6.47	6.58	5.31	4.86	4.26	6.63	4.68	5.68	3.32	3.44	3.06	2.75	5.46	5.52
Cr_2O_3	0.33	0.30	0.23	0.56	0.97	0.03	0.87	0.17	1.01	0.48	0.71	0.56	0.53	0.50
MnO	0.19	0.16	0.16	0.16	0.15	0.19	0.15	0.18	0.10	0.10	0.10	0.14	0.15	0.19
MgO	17.30	16.25	18.28	19.41	18.39	17.49	18.34	18.54	16.67	16.96	17.03	17.17	17.42	17.43
CaO	20.27	19.86	20.53	19.71	20.80	19.97	20.55	20.04	23.20	23.48	23.42	23.35	20.53	20.42
Na_2O	0.21	0.24	0.07	0.08	0.08	0.06	0.07	0.06	0.37	0.21	0.22	0.16	0.19	0.18
Total	100.35	99.15	99.14	99.69	99.43	99.36	99.39	99.45	100.05	99.82	100.07	99.57	99.93	100.01
Si	1.89	1.92	1.93	1.94	1.92	1.93	1.92	1.93	1.99	2.00	1.99	1.99	1.94	1.95
Al^{IV}	0.11	0.08	0.07	0.06	0.08	0.07	0.08	0.07	0.01	0.00	0.01	0.02	0.06	0.05
Al^{VI}	0.03	0.07	0.01	0.01	0.01	0.04	0.01	0.01	0.02	0.02	0.03	0.03	0.04	0.04
Fe^{2+}	0.20	0.20	0.16	0.15	0.13	0.21	0.14	0.17	0.10	0.11	0.09	0.08	0.17	0.17
Mg	0.94	0.90	1.00	1.05	1.00	0.96	1.00	1.01	0.91	0.93	0.93	0.94	0.95	0.95
Ti	0.01	0.02	0.00	0.00	0.00	0.00	0.00	0.00	0.00	0.00	0.00	0.00	0.01	0.01
Cr	0.01	0.01	0.01	0.02	0.03	0.00	0.03	0.01	0.03	0.01	0.02	0.02	0.02	0.01
Mn	0.01	0.01	0.01	0.01	0.01	0.01	0.01	0.01	0.00	0.00	0.00	0.00	0.01	0.01
Ca	0.79	0.79	0.81	0.77	0.82	0.79	0.81	0.79	0.91	0.92	0.91	0.92	0.80	0.80
Na	0.02	0.02	0.01	0.01	0.01	0.00	0.01	0.00	0.03	0.02	0.02	0.01	0.01	0.01
Sum	4.00	4.00	4.00	4.00	4.00	4.00	4.00	4.00	4.00	4.00	4.00	4.00	4.00	4.00
Mg#	0.83	0.81	0.86	0.88	0.89	0.82	0.88	0.85	0.90	0.90	0.91	0.92	0.85	0.85

Appendix B5. Pyroxene Analyses (continued)

Sample	113-2-11A3	113-2-11A4	113-2-11B1	113-2-11B2	113-2-11B3	113-2-11B4	113-2-11E1	113-2-11E2
Rock Type	gabbro	gabbro	gabbro	gabbro	gabbro	gabbro	gabbro	gabbro
Location	UofA	UofA	UofA	UofA	UofA	UofA	UofA	UofA
Occurrence	gm	rim	gm	gm	gm	gm	gm	gm
SiO_2	53.26	53.26	54.85	53.47	52.94	53.66	53.89	54.50
TiO_2	0.25	0.24	0.06	0.22	0.25	0.24	0.29	0.09
Al_2O_3	2.21	2.33	0.56	2.07	2.32	1.66	1.30	0.52
FeO^T	5.14	5.29	4.07	5.47	5.11	4.19	4.56	3.76
Cr_2O_3	0.67	0.61	0.42	0.47	0.64	0.42	0.35	0.19
MnO	0.16	0.13	0.16	0.14	0.11	0.12	0.10	0.12
MgO	17.62	17.18	16.99	17.58	17.09	16.18	16.55	16.83
CaO	20.34	20.30	22.92	20.47	21.01	22.80	22.41	23.74
Na_2O	0.15	0.16	0.22	0.16	0.16	0.36	0.28	0.13
Total	99.80	99.50	100.25	100.05	99.63	99.63	99.73	99.88
Si	1.95	1.96	2.00	1.95	1.94	1.97	1.98	1.99
Al^{IV}	0.05	0.04	0.00	0.05	0.06	0.03	0.02	0.01
Al^{VI}	0.04	0.06	0.02	0.04	0.04	0.04	0.03	0.02
Fe^{2+}	0.16	0.16	0.12	0.17	0.16	0.13	0.14	0.12
Mg	0.96	0.94	0.92	0.96	0.94	0.89	0.91	0.92
Ti	0.01	0.01	0.00	0.01	0.01	0.01	0.01	0.00
Cr	0.02	0.02	0.01	0.01	0.02	0.01	0.01	0.01
Mn	0.01	0.00	0.01	0.00	0.00	0.00	0.00	0.00
Ca	0.80	0.80	0.90	0.80	0.83	0.90	0.88	0.93
Na	0.01	0.01	0.02	0.01	0.01	0.03	0.02	0.01
Sum	4.00	4.00	4.00	4.00	4.00	4.00	4.00	4.00
Mg#	0.86	0.85	0.88	0.85	0.86	0.87	0.87	0.89

Appendix B6. Plagioclase Analyses (recalculated on the basis of 32 O)

Sample	81-2-8A1	81-2-8A2	81-2-8A3	81-2-8B1	81-2-8B2	81-2-8B3	81-2-8B4	81-2-8B5	81-2-8C1	81-2-8C2	81-2-8C3	81-2-8C4	81-2-9A1	81-2-9A2	81-2-9B1	81-2-9B2
Rock Type	basalt	basalt	basalt	basalt	basalt	basalt	basalt	basalt	basalt	basalt	basalt	basalt	basalt	basalt	basalt	basalt
Location	UofA	UofA	UofA	UofA	UofA	UofA	UofA	UofA	UofA	UofA	UofA	UofA	UofA	UofA	UofA	UofA
Occurrence	gm	gm	gm	gm	gm	gm	gm	gm	gm	gm	gm	gm	gm	gm	gm	gm
SiO_2	66.71	66.94	67.30	66.78	67.43	67.23	66.90	67.09	67.32	67.15	66.88	66.71	65.59	66.42	65.68	67.42
Al_2O_3	20.18	19.99	20.26	20.20	19.81	20.17	20.29	20.31	20.02	19.92	20.14	20.10	21.31	20.71	20.90	20.04
FeO^T	0.33	0.28	0.13	0.30	0.30	0.25	0.27	0.33	0.34	0.29	0.24	0.28	0.26	0.28	0.28	0.06
MnO	n.d.	n.d.	n.d.	n.d.	n.d.	n.d.	n.d.	n.d.	n.d.	n.d.	n.d.	n.d.	n.d.	n.d.	n.d.	n.d.
MgO	b.d.	b.d.	b.d.	b.d.	0.01	0.01	b.d.	0.01	0.01	0.02	b.d.	0.01	0.01	b.d.	0.01	b.d.
CaO	0.74	0.58	0.87	0.75	0.38	0.69	0.80	0.79	0.56	0.58	0.72	0.73	1.99	1.34	1.60	0.59
Na_2O	11.29	11.42	11.46	11.20	11.39	11.31	11.05	11.33	10.96	11.01	11.11	11.32	10.55	10.78	10.53	11.15
K_2O	0.07	0.07	0.05	0.08	0.05	0.04	0.06	0.06	0.06	0.07	0.05	0.05	0.08	0.09	0.10	0.09
Total	99.32	99.28	100.07	99.31	99.37	99.70	99.37	99.92	99.27	99.04	99.14	99.20	99.79	99.62	99.10	99.35
Si	11.78	11.82	11.79	11.79	11.88	11.82	11.79	11.78	11.86	11.86	11.81	11.79	11.56	11.70	11.64	11.87
Al	4.20	4.16	4.18	4.20	4.11	4.18	4.21	4.20	4.15	4.14	4.19	4.19	4.43	4.30	4.36	4.15
Fe^{2+}	0.05	0.04	0.02	0.04	0.04	0.04	0.04	0.05	0.05	0.04	0.04	0.04	0.04	0.04	0.04	0.01
Mn	-	-	-	-	-	-	-	-	-	-	-	-	-	-	-	-
Mg	-	-	-	-	0.00	0.00	-	0.00	0.00	0.01	-	0.00	0.00	-	0.00	-
Ca	0.14	0.11	0.16	0.14	0.07	0.13	0.15	0.15	0.11	0.11	0.14	0.14	0.38	0.25	0.30	0.11
Na	3.87	3.91	3.89	3.83	3.89	3.85	3.78	3.86	3.75	3.77	3.81	3.88	3.61	3.68	3.62	3.81
K	0.02	0.02	0.01	0.02	0.01	0.01	0.01	0.01	0.01	0.02	0.01	0.01	0.02	0.02	0.02	0.02
Cations	20.05	20.06	20.06	20.03	20.01	20.02	19.99	20.05	19.93	19.95	19.99	20.05	20.03	19.99	19.99	19.96
An	3.50	2.70	4.00	3.60	1.80	3.30	3.80	3.70	2.70	2.80	3.40	3.40	9.40	6.40	7.70	2.80

Notes: n.d. = not determined; b.d. = beolw detection; gm = groundmass; vei = vein; cor = core; inc = inclusion; myr = myrmekite; An = mole fraction anorthite.

Appendix B6. Plagioclase Analyses (continued)

Sample	82-3-2A5	82-3-2A6	82-3-2B1	82-3-2B2	82-3-2B3	82-3-2B4	82-3-2C1	82-3-2C2	82-3-2C3	82-3-2C4	82-3-8D3	90-4-3A1	90-4-3A10	90-4-3A12	90-4-3A2	90-4-3A3
Rock Type	troctolite	troctolite	troctolite	troctolite	troctolite	troctolite	troctolite	troctolite	troctolite	troctolite	gabbro	gabbro	gabbro	gabbro	gabbro	gabbro
Location	UofA	UofA	UofA	UofA	UofA	UofA	UofA	UofA	UofA	UofA	OSU	UofA	UofA	UofA	UofA	UofA
Occurrence	gm	gm	gm	gm	gm	gm	gm	gm	gm	gm	gm	gm	vei	vei	gm	gm
SiO_2	45.35	45.62	46.12	45.57	45.85	46.18	45.89	45.74	45.85	45.05	52.83	47.51	65.29	65.43	47.47	47.59
Al_2O_3	34.90	34.69	34.17	34.24	34.40	33.99	34.28	34.58	34.40	34.78	30.12	34.03	22.39	22.52	34.06	34.19
FeO^T	0.05	0.03	b.d.	0.04	0.03	0.08	0.03	0.02	0.07	0.02	0.45	0.24	0.02	0.03	0.24	0.32
MnO	n.d.	n.d.	n.d.	n.d.	n.d.	n.d.	n.d.	n.d.	n.d.	n.d.	n.d.	b.d.	b.d.	b.d.	b.d.	b.d.
MgO	b.d.	0.01	0.01	b.d.	0.10	b.d.	b.d.	0.03	b.d.	b.d.	0.08	0.03	b.d.	b.d.	0.02	b.d.
CaO	18.30	18.50	18.00	17.72	17.75	17.41	17.91	18.09	18.02	18.44	12.92	16.95	3.21	3.26	16.96	17.02
Na_2O	1.26	1.25	1.48	1.46	1.50	1.66	1.52	1.37	1.50	1.22	4.37	1.86	9.78	9.36	1.88	1.90
K_2O	0.02	0.01	0.01	0.01	0.01	b.d.	0.02	b.d.	0.02	0.01	0.02	0.04	0.01	0.03	0.04	0.02
Total	99.88	100.11	99.79	99.04	99.64	99.32	99.65	99.83	99.86	99.52	100.80	100.66	100.70	100.63	100.67	101.04
Si	8.37	8.41	8.51	8.47	8.47	8.55	8.48	8.44	8.46	8.35	9.52	8.67	11.41	11.42	8.66	8.65
Al	7.59	7.53	7.43	7.50	7.49	7.41	7.46	7.52	7.48	7.60	6.39	7.31	4.61	4.63	7.32	7.32
Fe^{2+}	0.01	0.01	0.00	0.01	0.01	0.01	0.01	0.00	0.01	0.00	0.07	0.04	0.00	0.00	0.04	0.05
Mn	-	-	-	-	-	-	-	-	-	-	-	-	-	-	-	-
Mg	-	0.00	0.00	-	0.03	-	-	0.01	-	-	0.02	0.01	-	-	0.01	-
Ca	3.62	3.65	3.56	3.53	3.51	3.45	3.55	3.58	3.56	3.66	2.50	3.31	0.60	0.61	3.32	3.32
Na	0.45	0.45	0.53	0.53	0.54	0.60	0.55	0.49	0.54	0.44	1.53	0.66	3.31	3.17	0.67	0.67
K	0.01	0.00	0.00	0.00	0.00	-	0.01	-	0.01	0.00	0.01	0.01	0.00	0.01	0.01	0.01
Cations	20.05	20.04	20.03	20.03	20.04	20.03	20.05	20.03	20.06	20.06	20.04	20.00	19.94	19.84	20.01	20.01
An	88.80	89.10	87.00	87.00	86.70	85.30	86.60	88.00	86.80	89.30	61.90	83.20	15.30	16.10	83.10	83.10

Appendix B6. Plagioclase Analyses (continued)

Sample	90-4-3A4	90-4-3A5	90-4-3C1	90-4-3C2	90-4-3C3	90-4-3C4	94-1-1C1	94-1-1C2	94-1-1D1	94-1-1D2	94-1-2B1	94-1-2B2	94-1-2B2	94-1-2B3	94-1-2B4	94-1-2B5
Rock Type	gabbro	gabbro	gabbro	gabbro	gabbro	gabbro	gabbro	gabbro	gabbro	gabbro	gabbro	gabbro	gabbro	gabbro	gabbro	gabbro
Location	UofA	UofA	UofA	UofA	UofA	UofA	OSU	OSU	OSU	OSU	UofA	OSU	UofA	UofA	UofA	UofA
Occurrence	gm	gm	gm	gm	gm	gm	gm	gm	inc	gm	gm	inc	gm	gm	gm	gm
SiO_2	66.68	64.48	47.82	47.78	47.87	48.08	53.73	54.82	53.14	54.30	51.53	49.86	49.91	51.10	52.24	49.29
Al_2O_3	21.98	22.56	33.80	33.86	33.67	33.68	28.86	28.78	30.08	28.88	30.91	31.90	31.80	31.00	30.45	32.26
FeO^T	0.10	0.16	0.25	0.29	0.32	0.32	0.40	0.44	0.37	0.37	0.35	0.45	0.44	0.45	0.53	0.63
MnO	b.d.	b.d.	b.d.	b.d.	b.d.	0.03	n.d.	n.d.	n.d.	n.d.	b.d.	n.d.	b.d.	0.04	0.02	b.d.
MgO	0.01	b.d.	0.01	0.03	0.03	0.02	0.02	0.03	0.05	0.02	0.03	0.05	0.01	0.03	0.02	0.02
CaO	2.32	3.30	16.66	16.78	16.58	16.37	11.20	11.13	12.78	11.40	13.65	14.58	14.71	13.97	12.97	15.35
Na_2O	9.98	9.48	1.97	1.89	2.12	2.18	4.95	4.95	4.26	5.03	3.75	3.08	3.34	3.76	4.18	2.98
K_2O	0.03	0.03	0.01	0.02	0.03	0.05	0.09	0.08	0.08	0.08	0.06	0.04	0.05	0.08	0.11	0.07
Total	101.10	100.01	100.52	100.65	100.62	100.73	99.25	100.22	100.75	100.09	100.28	99.95	100.27	100.44	100.52	100.60
Si	11.57	11.35	8.72	8.71	8.73	8.76	9.79	9.87	9.57	9.81	9.35	9.11	9.10	9.28	9.45	8.99
Al	4.49	4.68	7.26	7.27	7.23	7.22	6.19	6.10	6.38	6.14	6.61	6.86	6.83	6.63	6.49	6.92
Fe^{2+}	0.02	0.02	0.04	0.04	0.05	0.05	0.06	0.07	0.06	0.06	0.05	0.07	0.07	0.07	0.08	0.10
Mn	-	-	-	-	-	0.01	-	-	-	-	-	-	-	0.01	0.00	-
Mg	0.00	-	0.00	0.01	0.01	0.01	0.00	0.01	0.01	0.01	0.01	0.01	0.00	0.01	0.00	0.01
Ca	0.43	0.62	3.26	3.28	3.24	3.19	2.19	2.15	2.47	2.21	2.65	2.85	2.88	2.72	2.52	3.00
Na	3.36	3.24	0.70	0.67	0.75	0.77	1.75	1.73	1.49	1.76	1.32	1.09	1.18	1.32	1.47	1.05
K	0.01	0.01	0.00	0.01	0.01	0.01	0.02	0.02	0.02	0.02	0.01	0.01	0.01	0.02	0.03	0.02
Cations	19.87	19.92	19.98	19.98	20.02	20.01	19.99	19.94	19.99	20.00	20.00	20.00	20.07	20.06	20.04	20.08
An	11.40	16.10	82.30	83.00	81.10	80.30	55.20	55.20	62.10	55.40	66.6	72.20	70.7	66.9	62.7	73.8

Appendix B6. Plagioclase Analyses (continued)

Sample	94-1-2C1	94-1-2E1	94-1-3C1	94-1-3D2	94-1-3E2	96-1-2A1	96-1-2A2	96-1-2A3	96-1-2B1	96-1-2B2	96-1-2B3	96-1-2C2	96-1-3A1	96-1-3A3	96-1-3A4	96-1-3B2
Rock Type	gabbro	gabbro	gabbro	gabbro	gabbro	PG	PG	PG	PG	PG	PG	PG	PG	PG	PG	PG
Location	OSU	OSU	OSU	OSU	OSU	UofA	UofA	UofA	UofA	UofA	UofA	UofA	UofA	UofA	UofA	UofA
Occurrence	rim	gm	rim	gm	cor	gm	gm	gm	gm	gm	gm	gm	rim	cor	cor	gm
SiO_2	55.33	50.65	52.76	55.29	49.03	68.16	68.10	68.57	68.03	67.98	68.33	68.13	65.79	65.87	66.42	65.82
Al_2O_3	28.41	31.11	29.95	28.32	32.57	20.06	20.20	20.05	19.95	20.22	20.07	19.97	20.43	21.13	20.42	20.73
FeO^T	0.39	0.48	0.49	0.44	0.45	0.22	0.21	0.07	0.10	0.09	0.19	0.08	0.36	0.33	0.40	0.23
MnO	n.d.	n.d.	n.d.	n.d.	n.d.	b.d.	b.d.	b.d.	0.01	b.d.	0.01	0.01	n.d.	n.d.	n.d.	n.d.
MgO	0.04	0.06	0.02	0.04	0.05	b.d.	b.d.	b.d.	b.d.	0.01	0.01	b.d.	b.d.	b.d.	b.d.	0.01
CaO	10.45	14.06	12.69	10.70	15.69	0.52	0.57	0.06	0.44	0.42	0.50	0.04	1.35	1.77	1.14	1.40
Na_2O	5.44	3.49	4.34	5.36	2.56	10.90	11.07	11.48	11.51	11.06	11.06	11.47	10.63	10.66	11.34	10.84
K_2O	0.12	0.05	0.10	0.15	0.04	0.02	0.09	0.04	0.06	0.04	0.04	0.03	0.02	0.03	0.02	0.07
Total	100.19	99.90	100.35	100.29	100.39	99.88	100.24	100.27	100.10	99.82	100.21	99.73	98.58	99.79	99.74	99.10
Si	9.96	9.25	9.55	9.95	8.94	11.91	11.88	11.93	11.89	11.89	11.91	11.93	11.71	11.61	11.71	11.67
Al	6.02	6.69	6.38	6.00	7.00	4.13	4.15	4.11	4.11	4.16	4.12	4.12	4.28	4.38	4.24	4.33
Fe^{2+}	0.06	0.07	0.08	0.07	0.07	0.03	0.03	0.01	0.02	0.01	0.03	0.01	0.05	0.05	0.06	0.03
Mn	-	-	-	-	-	-	-	-	0.00	-	0.00	0.00	-	-	-	-
Mg	0.01	0.02	0.00	0.01	0.01	-	-	-	-	0.00	0.00	-	-	-	-	0.00
Ca	2.02	2.75	2.46	2.06	3.07	0.10	0.11	0.01	0.08	0.08	0.09	0.01	0.26	0.33	0.22	0.27
Na	1.90	1.24	1.52	1.87	0.91	3.69	3.74	3.87	3.90	3.75	3.74	3.89	3.67	3.64	3.88	3.73
K	0.03	0.01	0.02	0.03	0.01	0.00	0.02	0.01	0.01	0.01	0.01	0.01	0.01	0.01	0.00	0.02
Cations	19.99	20.02	20.02	19.99	20.00	19.87	19.93	19.95	20.01	19.91	19.90	19.96	19.98	20.02	20.11	20.04
An	51.10	68.80	61.40	52.00	77.00	2.60	2.80	0.30	2.10	2.10	2.40	0.20	6.50	8.40	5.20	6.60

Appendix B6. Plagioclase Analyses (continued)

Sample	96-1-3B3	96-1-3B4	96-1-3C1	96-1-5A2	96-1-5A3	96-1-5A4	96-1-5A5	96-1-5A6	96-1-5B1	96-1-5B2	96-1-5B3	96-1-5B4	96-1-5C1	96-1-5C2	96-1-5C3	96-1-5D1
Rock Type	PG	PG	PG	PG	PG	PG	PG	PG	PG	PG	PG	PG	PG	PG	PG	PG
Location	UofA	UofA	UofA	UofA	UofA	UofA	UofA	UofA	UofA	UofA	UofA	UofA	UofA	UofA	UofA	UofA
Occurrence	rim	cor	cor	gm	rim	cor	rim	cor	gm	gm	cor	cor	myr	myr	myr	gm
SiO_2	66.60	65.50	65.72	67.67	67.14	64.85	67.97	67.44	67.65	68.43	67.48	65.63	60.36	59.81	59.71	67.82
Al_2O_3	20.32	21.04	20.58	20.19	20.70	22.09	20.23	20.57	19.91	20.35	20.63	21.08	24.88	25.27	25.29	20.25
FeO^T	0.36	0.34	0.21	0.49	0.47	0.16	0.15	0.13	0.26	0.42	0.20	0.23	0.24	0.25	0.28	0.20
MnO	n.d.	n.d.	n.d.	b.d.	b.d.	b.d.	b.d.	b.d.	b.d.	0.01	b.d.	b.d.	0.04	b.d.	b.d.	b.d.
MgO	0.01	b.d.	b.d.	b.d.	0.01	b.d.	b.d.	b.d.	0.01	0.01	b.d.	b.d.	b.d.	b.d.	0.01	0.01
CaO	1.03	1.85	1.54	1.00	1.32	2.84	0.74	1.09	0.49	0.75	1.34	2.27	6.56	6.78	6.71	0.75
Na_2O	11.28	10.39	11.06	10.66	10.55	9.63	10.98	10.65	10.94	11.08	10.61	9.87	7.72	7.44	7.48	11.11
K_2O	0.12	0.22	0.01	0.06	0.08	0.11	0.07	0.05	0.17	0.12	0.25	0.57	0.13	0.31	0.25	0.06
Total	99.72	99.34	99.12	100.07	100.27	99.68	100.14	99.93	99.43	101.17	100.51	99.65	99.93	99.86	99.73	100.20
Si	11.74	11.60	11.66	11.84	11.74	11.44	11.87	11.80	11.90	11.85	11.77	11.60	10.76	10.68	10.68	11.84
Al	4.22	4.39	4.30	4.16	4.26	4.59	4.16	4.24	4.12	4.15	4.24	4.39	5.22	5.32	5.33	4.17
Fe^{2+}	0.05	0.05	0.03	0.07	0.07	0.02	0.02	0.02	0.04	0.06	0.03	0.03	0.04	0.04	0.04	0.03
Mn	-	-	-	-	-	-	-	-	-	0.00	-	-	0.01	-	-	-
Mg	0.00	-	-	-	0.00	-	-	-	0.00	0.00	-	-	-	-	0.00	0.00
Ca	0.20	0.35	0.29	0.19	0.25	0.54	0.14	0.20	0.09	0.14	0.25	0.43	1.25	1.30	1.29	0.14
Na	3.86	3.57	3.80	3.62	3.58	3.30	3.72	3.61	3.73	3.72	3.59	3.38	2.67	2.58	2.59	3.76
K	0.03	0.05	0.00	0.01	0.02	0.03	0.02	0.01	0.04	0.03	0.06	0.13	0.03	0.07	0.06	0.01
Cations	20.09	20.01	20.09	19.89	19.92	19.92	19.92	19.89	19.92	19.95	19.93	19.96	19.97	19.98	19.98	19.96
An	4.80	8.80	7.10	4.90	6.40	13.90	3.60	5.30	2.40	3.60	6.40	10.90	31.70	32.90	32.70	3.60

Appendix B6. Plagioclase Analyses (continued)

Sample	96-1-5D2	96-1-5D3	96-1-5D4	96-1-10b1	96-1-10b2	96-1-14A3	96-1-14B2	96-1-16B1	96-1-16B2	96-1-16B3	96-1-16B4	96-1-16C1	96-1-16C3	96-1-16C4	96-1-16C5
Rock Type	PG	PG	PG	PG	PG	PG	PG	PG	PG	PG	PG	PG	PG	PG	PG
Location	UofA	UofA	UofA	UofA	UofA	OSU	OSU	UofA	UofA	UofA	UofA	UofA	UofA	UofA	UofA
Occurrence	gm	gm	gm	gm	gm	rim	rim	gm	gm	gm	gm	gm	gm	gm	gm
SiO_2	67.48	68.58	68.79	68.50	68.10	67.99	67.29	58.75	57.61	67.47	67.18	67.75	57.72	62.59	67.00
Al_2O_3	20.52	19.76	19.88	19.86	19.68	19.95	19.66	26.05	26.63	19.69	20.15	19.82	26.94	22.82	20.41
FeO^T	0.26	0.17	0.17	0.48	0.07	0.08	0.05	0.04	0.18	0.02	0.06	b.d.	0.08	0.12	0.02
MnO	0.01	b.d.	b.d.	0.02	0.01	n.d.	n.d.	n.d.	n.d.	n.d.	n.d.	n.d.	n.d.	n.d.	n.d.
MgO	b.d.	b.d.	b.d.	0.02	b.d.	b.d.	b.d.	b.d.	0.01	b.d.	0.01	b.d.	0.01	0.01	b.d.
CaO	1.12	0.23	0.39	0.11	0.10	0.16	0.17	7.44	7.94	0.43	0.78	0.29	8.24	3.77	1.05
Na_2O	10.61	11.47	11.24	11.64	10.98	11.54	11.35	7.50	7.01	11.28	11.17	11.60	6.97	9.24	11.00
K_2O	0.06	0.04	0.03	0.03	0.05	0.04	0.03	0.06	0.06	0.24	0.22	0.24	0.10	0.21	0.25
Total	100.06	100.25	100.50	100.66	98.99	99.77	98.55	99.84	99.44	99.13	99.57	99.70	100.06	98.76	99.73
Si	11.80	11.95	11.95	11.91	11.98	11.91	11.92	10.51	10.37	11.91	11.82	11.90	10.33	11.20	11.78
Al	4.23	4.06	4.07	4.07	4.08	4.12	4.10	5.49	5.64	4.09	4.18	4.10	5.68	4.81	4.23
Fe^{2+}	0.04	0.03	0.03	0.07	0.01	0.01	0.01	0.01	0.03	0.00	0.01	0.00	0.01	0.02	0.00
Mn	0.00	-	-	0.00	0.00	-	-	-	-	-	-	-	-	-	-
Mg	-	-	-	0.01	-	0.00	0.00	-	0.00	-	0.00	-	0.00	0.00	-
Ca	0.21	0.04	0.07	0.02	0.02	0.03	0.03	1.43	1.53	0.08	0.15	0.06	1.58	0.72	0.20
Na	3.60	3.88	3.79	3.93	3.75	3.92	3.90	2.60	2.45	3.86	3.81	3.95	2.42	3.21	3.75
K	0.01	0.01	0.01	0.01	0.01	0.01	0.01	0.01	0.01	0.05	0.05	0.05	0.02	0.05	0.06
Cations	19.89	19.96	19.91	20.01	19.85	19.99	19.97	20.05	20.03	20.00	20.02	20.05	20.05	20.01	20.01
An	5.50	1.10	1.90	0.50	0.50	0.80	0.80	35.30	38.40	2.00	3.70	1.40	39.30	18.20	4.90

Appendix B6. Plagioclase Analyses (continued)

Sample	96-1-16C6	96-1-19B1	96-1-27A1	96-1-27A2	96-1-27B1	96-1-27B2	96-1-27E1	96-1-27E2	96-1-29A1	96-1-29A2	96-2-1C1	96-2-1C2	96-2-1D1	96-2-1D2	96-2-4B1
Rock Type	PG	PG	PG	PG	PG	PG	PG	PG	PG/basalt	PG/basalt	basalt	basalt	basalt	basalt	PG/basalt
Location	UofA	OSU	UofA	UofA	UofA	UofA	UofA	UofA	OSU	OSU	OSU	OSU	OSU	OSU	UofA
Occurrence	gm	gm	cor	rim	cor	rim	rim	rim	gm	gm	gm	gm	gm	gm	cor
SiO_2	66.38	66.63	66.47	66.33	66.54	67.46	66.27	67.18	68.39	67.71	67.88	68.08	66.41	67.83	66.69
Al_2O_3	21.01	20.40	20.74	20.57	20.26	19.86	20.32	20.00	20.18	19.69	20.25	20.44	21.42	19.67	20.42
FeO^T	0.05	b.d.	0.09	0.08	0.05	0.02	0.01	0.10	0.18	0.30	0.23	0.09	0.30	0.23	0.24
MnO	n.d.	n.d.	n.d.	n.d.	n.d.	n.d.	n.d.	n.d.	n.d.	n.d.	n.d.	n.d.	n.d.	n.d.	n.d.
MgO	0.02	0.03	b.d.	0.02	0.01	b.d.	b.d.	0.01	b.d.	0.04	b.d.	b.d.	0.01	b.d.	b.d.
CaO	1.28	0.86	1.10	0.59	0.52	0.32	0.73	0.51	0.32	0.28	0.85	0.61	1.92	0.17	0.42
Na_2O	10.70	10.91	10.79	11.28	11.39	11.86	11.66	11.77	11.41	11.11	10.86	10.69	9.85	11.23	11.69
K_2O	0.35	0.06	0.04	0.31	0.32	0.05	0.07	0.04	0.04	0.05	0.05	0.22	0.06	0.05	0.08
Total	99.79	98.88	99.23	99.18	99.09	99.57	99.06	99.61	100.52	99.19	100.12	100.13	99.98	99.17	99.54
Si	11.67	11.79	11.73	11.73	11.78	11.87	11.74	11.82	11.89	11.93	11.85	11.87	11.64	11.94	11.76
Al	4.35	4.25	4.31	4.29	4.22	4.11	4.24	4.15	4.13	4.09	4.17	4.20	4.42	4.08	4.24
Fe^{2+}	0.01	0.00	0.01	0.01	0.01	0.00	0.00	0.02	0.03	0.05	0.03	0.01	0.04	0.03	0.04
Mn	-	-	-	-	-	-	-	-	-	-	-	-	-	-	-
Mg	0.01	0.01	-	0.01	0.00	-	-	0.00	0.00	0.01	0.00	0.00	0.00	0.00	-
Ca	0.24	0.16	0.21	0.11	0.10	0.06	0.14	0.10	0.06	0.05	0.16	0.11	0.36	0.03	0.08
Na	3.65	3.74	3.69	3.87	3.91	4.05	4.01	4.02	3.85	3.79	3.68	3.62	3.35	3.83	4.00
K	0.08	0.01	0.01	0.07	0.07	0.01	0.02	0.01	0.01	0.01	0.01	0.05	0.01	0.01	0.02
Cations	20.01	19.96	19.96	20.09	20.09	20.10	20.14	20.11	19.97	19.93	19.90	19.86	19.83	19.93	20.12
An	6.10	4.20	5.30	2.80	2.40	1.50	3.30	2.30	1.50	1.40	4.20	3.00	9.70	0.80	1.90

Appendix B6. Plagioclase Analyses (continued)

Sample	96-2-4B2	96-2-4C1	96-2-4C2	96-2-13b1	96-2-13b4	99-1-21A1	99-1-21A2	99-1-21A3	99-1-21B1	99-1-21B2	99-1-21B3	99-1-21C1	99-1-21C2	99-1-21C3	99-1-21D1
Rock Type	PG/basalt	PG/basalt	PG/basalt	PG	PG	gabbro	gabbro	gabbro	gabbro	gabbro	gabbro	gabbro	gabbro	gabbro	gabbro
Location	UofA	UofA	UofA	OSU	OSU	UofA	UofA	UofA	UofA	UofA	UofA	UofA	UofA	UofA	UofA
Occurrence	cor	cor	cor	gm	gm	gm	gm	gm	gm	gm	gm	gm	gm	gm	gm
SiO_2	67.04	67.40	67.87	66.22	67.31	48.93	48.56	48.74	46.41	47.73	47.86	50.18	50.05	49.62	46.87
Al_2O_3	20.52	19.73	19.66	20.93	19.97	32.83	33.24	33.12	34.38	33.81	33.71	31.87	31.99	32.47	34.63
FeO^T	0.14	0.17	0.21	0.21	0.05	0.43	0.40	0.33	0.14	0.46	0.35	0.43	0.26	0.46	0.22
MnO	n.d.	n.d.	n.d.	n.d.	n.d.	0.01	b.d.	b.d.	b.d.	b.d.	b.d.	b.d.	0.01	0.02	b.d.
MgO	b.d.	b.d.	b.d.	b.d.	0.02	0.05	0.02	0.02	b.d.	0.02	0.01	0.03	0.03	0.01	0.05
CaO	0.58	0.16	0.13	1.51	0.20	15.68	16.30	15.83	17.43	16.53	16.56	14.72	14.77	15.38	17.44
Na_2O	11.33	11.94	11.88	10.47	11.29	2.62	2.40	2.55	1.54	2.10	2.11	3.23	3.25	2.80	1.49
K_2O	0.07	0.04	0.05	0.07	0.04	0.01	0.02	0.02	0.03	0.01	0.03	0.04	0.02	0.04	0.02
Total	99.68	99.44	99.80	99.40	98.88	100.56	100.94	100.61	99.93	100.66	100.63	100.50	100.38	100.80	100.72
Si	11.78	11.88	11.91	11.68	11.89	8.91	8.83	8.87	8.54	8.71	8.73	9.12	9.10	9.01	8.55
Al	4.25	4.09	4.06	4.35	4.15	7.04	7.12	7.10	7.45	7.26	7.24	6.82	6.85	6.94	7.44
Fe^{2+}	0.02	0.03	0.03	0.03	0.01	0.07	0.06	0.05	0.02	0.07	0.05	0.07	0.04	0.07	0.03
Mn	-	-	-	-	-	0.00	-	-	-	-	-	-	0.00	0.00	-
Mg	-	-	-	0.00	0.01	0.01	0.01	0.01	-	0.01	0.00	0.01	0.01	0.00	0.01
Ca	0.11	0.03	0.02	0.29	0.04	3.06	3.17	3.09	3.44	3.23	3.24	2.87	2.88	2.99	3.41
Na	3.86	4.08	4.04	3.58	3.87	0.93	0.85	0.90	0.55	0.74	0.75	1.14	1.15	0.99	0.53
K	0.02	0.01	0.01	0.02	0.01	0.00	0.01	0.01	0.01	0.00	0.01	0.01	0.01	0.01	0.01
Cations	20.03	20.11	20.08	19.94	19.97	20.02	20.03	20.02	20.00	20.02	20.02	20.03	20.04	20.01	19.98
An	2.70	0.70	0.60	7.30	1.00	76.70	78.90	77.30	86.10	81.30	81.10	71.40	71.40	75.00	86.50

Appendix B6. Plagioclase Analyses (continued)

Sample	99-1-21D2	99-1-21D3	99-1-21D4	99-1-30A1	99-1-30A2	99-1-30A3	99-1-30A4	99-1-30A5	99-1-30A6	99-1-30B1	99-1-30B2	99-1-30B3	99-1-30B4	99-1-30C1	99-1-30C2
Rock Type	gabbro	gabbro	gabbro	gabbro	gabbro	gabbro	gabbro	gabbro	gabbro	gabbro	gabbro	gabbro	gabbro	gabbro	gabbro
Location	UofA	UofA	UofA	UofA	UofA	UofA	UofA	UofA	UofA	UofA	UofA	UofA	UofA	UofA	UofA
Occurrence	gm	gm	gm	gm	gm	gm	cor	cor	cor	gm	gm	gm	gm	cor	cor
SiO_2	45.57	46.70	47.50	49.47	49.44	48.84	48.95	49.63	49.29	48.89	49.14	49.17	48.43	49.00	49.41
Al_2O_3	36.23	34.94	34.14	32.82	33.08	32.77	33.14	32.65	32.80	33.38	33.27	33.24	33.25	33.05	33.12
FeO^T	0.08	0.08	0.08	0.33	0.30	0.34	0.30	0.34	0.34	0.37	0.33	0.32	0.41	0.41	0.42
MnO	0.01	0.01	b.d.	0.02	b.d.	b.d.	b.d.	b.d.	b.d.	0.01	0.01	b.d.	b.d.	0.01	b.d.
MgO	b.d.	b.d.	0.01	0.03	0.03	0.02	0.01	0.04	0.04	0.08	0.09	0.03	0.05	0.02	0.02
CaO	18.61	17.56	16.87	15.11	15.29	15.45	15.25	14.78	15.37	15.47	15.37	15.39	15.79	15.65	15.05
Na_2O	0.90	1.56	1.99	2.92	2.67	2.65	2.66	2.94	2.62	2.40	2.44	2.42	2.48	2.70	2.74
K_2O	0.01	0.03	0.04	0.02	0.03	0.03	0.04	0.03	0.03	0.03	0.03	0.04	0.03	0.02	0.02
Total	101.41	100.88	100.63	100.72	100.84	100.10	100.35	100.41	100.49	100.63	100.68	100.61	100.44	100.86	100.78
Si	8.28	8.51	8.66	8.98	8.96	8.93	8.92	9.02	8.96	8.88	8.92	8.93	8.84	8.90	8.96
Al	7.75	7.50	7.33	7.01	7.06	7.05	7.11	6.99	7.03	7.14	7.11	7.11	7.14	7.07	7.07
Fe^{2+}	0.01	0.01	0.01	0.05	0.05	0.05	0.05	0.05	0.05	0.06	0.05	0.05	0.06	0.06	0.06
Mn	0.00	0.00	-	0.00	-	-	-	-	-	0.00	0.00	-	-	0.00	-
Mg	-	-	0.00	0.01	0.01	0.01	0.00	0.01	0.01	0.02	0.02	0.01	0.01	0.01	0.01
Ca	3.62	3.43	3.30	2.94	2.97	3.03	2.98	2.88	3.00	3.01	2.99	2.99	3.09	3.05	2.92
Na	0.32	0.55	0.70	1.03	0.94	0.94	0.94	1.04	0.92	0.85	0.86	0.85	0.88	0.95	0.96
K	0.00	0.01	0.01	0.01	0.01	0.01	0.01	0.01	0.01	0.01	0.01	0.01	0.01	0.01	0.01
Cations	19.99	20.01	20.02	20.02	19.98	20.01	20.00	20.00	19.98	19.97	19.95	19.94	20.03	20.04	19.98
An	91.90	86.00	82.20	74.00	75.80	76.20	75.80	73.40	76.30	77.90	77.50	77.70	77.70	76.10	75.10

Appendix B6. Plagioclase Analyses (continued)

Sample	99-1-30C3	99-1-30C4	99-2-1A1	99-2-1A2	99-2-1A3	99-2-1A4	99-2-1B1	99-2-1B2	99-2-1B3	99-2-1B4	99-2-1C5	99-2-1C6	99-2-1C7	101-1-2A1	101-1-2A3	101-1-2A5
Rock Type	gabbro	gabbro	basalt	basalt	basalt	basalt	basalt	basalt	basalt	basalt	basalt	basalt	basalt	basalt	basalt	basalt
Location	UofA	UofA	UofA	UofA	UofA	UofA	UofA	UofA	UofA	UofA	UofA	UofA	UofA	UofA	UofA	UofA
Occurrence	rim	rim	gm	gm	gm	gm	gm	gm	gm	gm	gm	gm	gm	gm	gm	gm
SiO_2	48.58	49.03	47.55	47.43	49.58	49.46	49.18	49.03	51.28	49.41	50.24	49.59	48.77	66.06	68.02	66.55
Al_2O_3	33.61	33.07	33.73	34.27	32.64	32.64	32.95	33.08	31.79	32.81	32.13	32.71	33.02	21.32	20.06	21.20
FeO^T	0.40	0.32	0.48	0.38	0.42	0.46	0.47	0.34	0.44	0.16	0.42	0.41	0.48	0.13	0.19	0.12
MnO	0.02	b.d.	b.d.	b.d.	0.01	0.03	b.d.	0.01	0.04	0.02	b.d.	0.04	b.d.	b.d.	b.d.	0.01
MgO	0.06	0.02	0.04	0.01	0.04	0.04	0.10	0.02	0.08	0.06	0.03	0.02	0.08	0.01	0.03	0.01
CaO	15.82	15.37	16.21	16.44	14.93	14.84	15.47	15.33	13.89	14.90	14.21	14.82	15.53	1.91	0.48	1.53
Na_2O	2.24	2.67	1.97	2.00	2.83	2.96	2.81	2.79	3.53	2.93	3.18	2.96	2.51	10.42	11.32	10.51
K_2O	0.02	0.04	0.02	0.02	0.01	0.03	0.02	0.02	0.02	0.04	b.d.	0.03	0.03	0.07	0.07	0.07
Total	100.75	100.52	100.00	100.55	100.46	100.46	101.00	100.62	101.07	100.33	100.21	100.58	100.42	99.92	100.17	100.00
Si	8.82	8.92	8.72	8.66	9.01	9.00	8.92	8.91	9.24	8.99	9.14	9.01	8.89	11.61	11.88	11.66
Al	7.19	7.08	7.29	7.37	6.99	6.99	7.04	7.08	6.75	7.03	6.88	7.00	7.09	4.41	4.13	4.38
Fe^{2+}	0.06	0.05	0.07	0.06	0.06	0.07	0.07	0.05	0.07	0.02	0.06	0.06	0.07	0.02	0.03	0.02
Mn	0.00	-	-	-	0.00	0.01	-	0.00	0.01	0.00	-	0.01	-	-	-	0.00
Mg	0.02	0.01	0.01	0.00	0.01	0.01	0.03	0.01	0.02	0.02	0.01	0.01	0.02	0.00	0.01	0.00
Ca	3.08	3.00	3.19	3.21	2.91	2.89	3.01	2.99	2.68	2.90	2.77	2.88	3.03	0.36	0.09	0.29
Na	0.79	0.94	0.70	0.71	1.00	1.04	0.99	0.98	1.23	1.03	1.12	1.04	0.89	3.55	3.83	3.57
K	0.01	0.01	0.01	0.01	0.00	0.01	0.01	0.01	0.01	0.01	-	0.01	0.01	0.02	0.02	0.02
Cations	19.97	20.00	19.98	20.01	19.98	20.02	20.05	20.03	20.00	20.01	19.98	20.01	20.00	19.97	19.98	19.94
An	79.50	75.90	81.90	61.80	74.40	73.40	75.20	75.10	68.40	73.60	71.20	73.30	77.20	9.20	2.30	7.40

Appendix B6. Plagioclase Analyses (continued)

Sample	101-1-2B2	101-1-2B4	101-1-24A2	101-1-24A3	101-1-24A6	101-1-24B2	101-1-24B3	101-1-24B4	102-4-1B1	102-4-1B2	102-4-1B3	102-4-1C3	102-4-1C4	105-1-6A1
Rock Type	basalt	basalt	basalt	basalt	basalt	basalt	basalt	basalt	epidosite	epidosite	epidosite	epidosite	epidosite	gabbro
Location	UofA	UofA	UofA	UofA	UofA	UofA	UofA	UofA	UofA	UofA	UofA	UofA	UofA	OSU
Occurrence	gm	gm	gm	gm	gm	gm	gm	gm	gm	gm	gm	gm	gm	inc
SiO_2	67.86	68.21	68.37	64.71	64.34	67.64	57.02	68.06	67.53	67.04	66.50	66.01	66.49	49.23
Al_2O_3	20.33	19.79	20.14	18.53	22.53	20.44	27.17	20.24	19.98	20.12	19.91	20.12	20.24	32.54
FeO^T	0.46	0.15	0.15	0.06	0.15	0.09	0.49	0.07	b.d.	b.d.	0.07	b.d.	0.01	0.33
MnO	0.01	0.01	0.01	0.01	b.d.	b.d.	0.02	b.d.	n.d.	n.d.	n.d.	n.d.	n.d.	n.d.
MgO	b.d.	0.01	0.02	b.d.	0.01	0.01	0.08	0.01	b.d.	b.d.	0.38	0.01	0.01	0.03
CaO	0.64	0.20	0.35	b.d.	3.01	0.89	9.08	0.38	0.23	0.56	0.32	0.60	0.57	14.93
Na_2O	11.16	11.91	11.53	0.09	9.93	11.00	6.12	11.69	11.68	11.58	11.50	11.90	11.26	2.83
K_2O	0.08	0.08	0.20	16.85	0.09	0.09	0.23	0.08	0.07	0.04	0.07	0.07	0.27	0.01
Total	100.54	100.36	100.77	100.25	100.06	100.16	100.21	100.53	99.49	99.34	98.75	98.71	98.85	99.90
Si	11.83	11.90	11.88	11.96	11.34	11.82	10.23	11.85	11.87	11.82	11.80	11.75	11.79	9.00
Al	4.17	4.07	4.12	4.04	4.68	4.21	5.74	4.15	4.14	4.18	4.16	4.22	4.23	7.00
Fe^{2+}	0.07	0.02	0.02	0.01	0.02	0.01	0.07	0.01	0.00	0.00	0.01	0.00	0.00	0.05
Mn	0.00	0.00	0.00	0.00	-	-	0.00	-	-	-	-	-	-	-
Mg	-	0.00	0.01	-	0.00	0.00	0.02	0.00	-	-	0.10	0.00	0.00	0.01
Ca	0.12	0.04	0.07	-	0.57	0.17	1.75	0.07	0.04	0.11	0.06	0.11	0.11	2.92
Na	3.77	4.03	3.88	0.03	3.39	3.73	2.13	3.95	3.98	3.96	3.96	4.11	3.87	1.00
K	0.02	0.02	0.04	3.97	0.02	0.02	0.05	0.02	0.02	0.01	0.02	0.02	0.06	0.00
Cations	19.98	20.08	20.02	20.02	20.02	19.95	19.99	20.05	20.05	20.07	20.10	20.20	20.06	19.99
An	3.10	0.90	1.60	0.00	14.30	4.30	44.40	1.80	1.10	2.60	1.50	2.70	2.70	74.40

Appendix B6. Plagioclase Analyses (continued)

Sample	105-1-6D1	105-1-8(b)A3	105-1-8(b)B1	105-1-8(b)D3	105-1-8(b)E4	105-1-8(b)E5	105-1-8(b)E6	105-1-14B2	105-1-14C1	105-1-21A1	105-1-21A2	105-1-21B1	105-1-21B2
Rock Type	gabbro	gabbro	gabbro	gabbro	gabbro	gabbro	gabbro	gabbro	gabbro	gabbro	gabbro	gabbro	gabbro
Location	OSU	OSU	OSU	OSU	OSU	OSU	OSU	OSU	OSU	UofA	UofA	UofA	UofA
Occurrence	gm	gm	gm	gm	gm	gm	gm	gm	gm	gm	gm	gm	gm
SiO_2	49.42	46.81	46.76	46.35	46.42	46.50	47.47	45.61	46.00	48.65	48.86	48.26	47.30
Al_2O_3	32.67	34.20	34.47	34.65	34.09	34.65	32.68	34.44	33.83	31.85	31.84	32.33	32.82
FeO^T	0.48	0.34	0.35	0.39	0.37	0.30	0.48	0.33	0.31	0.30	0.49	0.43	0.29
MnO	n.d.	n.d.	n.d.	n.d.	n.d.	n.d.	n.d.	n.d.	n.d.	n.d.	n.d.	n.d.	n.d.
MgO	0.01	0.04	0.04	b.d.	0.02	0.01	0.19	b.d.	0.02	b.d.	0.31	0.01	b.d.
CaO	15.32	17.41	17.67	17.38	17.54	17.80	16.03	17.51	18.04	15.50	15.02	15.67	16.28
Na_2O	2.69	1.79	1.65	1.64	1.72	1.63	2.66	1.46	1.65	2.93	2.74	2.82	2.45
K_2O	b.d.	0.01	0.02	b.d.	0.02	b.d.	0.04	b.d.	0.02	0.02	0.04	0.03	0.01
Total	100.60	100.59	100.95	100.41	100.18	100.89	99.54	99.34	99.88	99.25	99.30	99.55	99.15
Si	8.98	8.57	8.53	8.50	8.54	8.49	8.77	8.46	8.51	8.98	9.00	8.90	8.76
Al	6.99	7.37	7.41	7.48	7.39	7.45	7.11	7.52	7.37	6.93	6.91	7.02	7.16
Fe^{2+}	0.07	0.05	0.05	0.06	0.06	0.05	0.07	0.05	0.05	0.05	0.08	0.07	0.05
Mn	-	-	-	-	-	-	-	-	-	-	-	-	-
Mg	0.00	0.01	0.01	-	0.00	0.00	0.05	-	0.01	-	0.09	0.00	-
Ca	2.98	3.41	3.45	3.41	3.46	3.48	3.17	3.48	3.58	3.07	2.97	3.10	3.23
Na	0.95	0.63	0.58	0.58	0.61	0.58	0.95	0.52	0.59	1.05	0.98	1.01	0.88
K	0.00	0.00	0.00	0.00	0.00	-	0.01	-	0.00	0.01	0.01	0.01	0.00
Cations	19.99	20.05	20.05	20.04	20.06	20.06	20.14	20.03	20.10	20.07	20.03	20.09	20.09
An	75.80	84.30	85.50	85.40	84.80	85.80	76.70	86.90	85.70	74.40	75.00	75.30	78.60

Appendix B6. Plagioclase Analyses (continued)

Sample	105-1-21B3	105-1-21C5	105-1-21D3	105-1-21D4	105-1-25A1	105-1-25A1	105-1-25A2	105-1-25A3	105-1-25A4	105-1-25A4	105-1-25C1	105-1-25C1	105-1-25C2
Rock Type	gabbro	gabbro	gabbro	gabbro	gabbro	gabbro	gabbro	gabbro	gabbro	gabbro	gabbro	gabbro	gabbro
Location	UofA	UofA	UofA	UofA	OSU	UofA	UofA	UofA	OSU	UofA	OSU	UofA	UofA
Occurrence	gm	gm	gm	gm	gm	gm	gm	gm	gm	gm	gm	gm	gm
SiO_2	48.60	49.03	48.60	48.98	46.55	45.83	43.52	46.58	46.16	43.64	43.58	43.64	43.74
Al_2O_3	32.17	31.97	31.99	31.75	33.37	34.19	36.27	33.97	34.30	36.18	36.26	36.67	36.60
FeO^T	0.35	0.24	0.33	0.40	0.38	0.41	0.14	0.41	0.34	0.13	0.30	0.23	0.22
MnO	n.d.	n.d.	n.d.	n.d.	n.d.	b.d.	b.d.	0.01	n.d.	b.d.	n.d.	b.d.	0.03
MgO	0.01	0.01	0.01	0.02	b.d.	b.d.	b.d.	0.02	0.01	b.d.	0.01	b.d.	b.d.
CaO	15.18	15.10	15.23	15.23	16.67	17.54	19.49	17.03	17.39	19.53	19.44	19.78	19.52
Na_2O	2.81	3.03	2.92	3.01	2.05	1.63	0.50	1.89	1.70	0.48	0.51	0.36	0.47
K_2O	0.03	0.02	0.03	0.04	b.d.	0.02	0.02	0.01	b.d.	0.01	b.d.	0.02	0.03
Total	99.15	99.40	99.11	99.43	99.01	99.62	99.96	99.91	99.90	99.96	100.10	100.69	100.61
Si	8.97	9.02	8.98	9.02	8.65	8.48	8.07	8.58	8.51	8.08	8.07	8.03	8.05
Al	6.99	6.93	6.96	6.89	7.30	7.45	7.92	7.37	7.45	7.89	7.90	7.95	7.94
Fe^{2+}	0.05	0.04	0.05	0.06	0.06	0.06	0.02	0.06	0.05	0.02	0.05	0.04	0.03
Mn	-	-	-	-	-	-	0.00	0.00	-	-	-	-	0.00
Mg	0.00	0.00	0.00	0.01	-	-	-	0.01	0.00	-	0.00	-	-
Ca	3.00	2.98	3.01	3.01	3.32	3.48	3.87	3.36	3.44	3.88	3.86	3.90	3.85
Na	1.01	1.08	1.05	1.08	0.74	0.59	0.18	0.68	0.61	0.17	0.18	0.13	0.17
K	0.01	0.01	0.01	0.01	0.00	0.01	0.00	0.00	0.00	0.00	0.00	0.01	0.01
Cations	20.03	20.05	20.06	20.07	20.06	20.07	20.06	20.06	20.06	20.05	20.06	20.05	20.05
An	74.80	73.30	74.10	73.50	81.80	85.5	95.4	83.2	84.90	95.7	95.40	96.7	95.7

Appendix B6. Plagioclase Analyses (continued)

Sample	105-1-25C3	105-1-25C4	105-3-6A1	105-3-6A2	105-3-6B5	106-2-5a1	106-2-5c2	106-2-5c4	106-2-10C1	106-2-10C2	106-2-10D1	106-2-10D1	106-2-10D2	106-2-10D2
Rock Type	gabbro	gabbro	basalt	basalt	basalt	gabbro	gabbro	gabbro	gabbro	gabbro	gabbro	gabbro	gabbro	gabbro
Location	UofA	UofA	OSU	OSU	OSU	OSU	OSU	OSU	OSU	OSU	OSU	UofA	OSU	UofA
Occurrence	gm	gm	gm	gm	gm	gm	gm	inc	gm	gm	inc	gm	gm	gm
SiO_2	46.97	46.90	63.14	62.88	63.40	55.32	46.14	43.63	43.73	43.54	45.63	45.14	45.74	46.40
Al_2O_3	33.93	33.90	23.29	23.29	22.43	28.02	33.47	35.09	36.44	36.40	34.47	35.17	34.30	34.09
FeO^T	0.38	0.40	0.10	0.07	0.35	0.44	0.48	0.37	0.14	0.27	0.41	0.20	0.33	0.46
MnO	b.d.	b.d.	n.d.	n.d.	n.d.	n.d.	n.d.	n.d.	n.d.	n.d.	n.d.	b.d.	n.d.	0.01
MgO	0.02	b.d.	0.02	b.d.	0.03	0.02	b.d.	b.d.	b.d.	0.21	0.14	0.02	0.02	0.02
CaO	17.01	16.98	4.24	4.34	3.73	10.10	16.97	18.77	19.90	19.72	17.93	18.30	17.92	17.10
Na_2O	1.84	1.97	8.97	9.02	8.72	5.62	1.90	0.88	0.38	0.30	1.29	1.21	1.32	1.79
K_2O	0.02	0.02	0.04	0.14	0.18	0.09	0.02	0.02	0.03	b.d.	0.02	0.01	b.d.	0.02
Total	100.17	100.17	99.81	99.75	98.84	99.61	98.99	98.76	100.62	100.43	99.90	100.04	99.64	99.89
Si	8.62	8.62	11.17	11.15	11.31	10.01	8.59	8.18	8.06	8.04	8.43	8.33	8.47	8.55
Al	7.34	7.33	4.85	4.86	4.71	5.97	7.34	7.75	7.91	7.91	7.50	7.64	7.48	7.40
Fe^{2+}	0.06	0.06	0.01	0.01	0.05	0.07	0.08	0.06	0.02	0.04	0.06	0.03	0.05	0.07
Mn	-	0.00	-	-	-	-	-	-	-	-	-	-	-	0.00
Mg	0.01	-	0.01	-	0.01	0.01	-	-	-	0.06	0.04	0.01	0.01	0.00
Ca	3.35	3.34	0.81	0.82	0.71	1.96	3.39	3.77	3.93	3.90	3.55	3.62	3.55	3.38
Na	0.66	0.70	3.08	3.10	3.02	1.97	0.69	0.32	0.13	0.11	0.46	0.43	0.48	0.64
K	0.00	0.01	0.01	0.03	0.04	0.02	0.00	0.00	0.01	-	0.00	0.00	-	0.00
Cations	20.03	20.06	19.94	19.98	19.85	20.00	20.08	20.09	20.05	20.05	20.05	20.06	20.03	20.06
An	83.5	82.5	20.70	20.80	18.90	49.60	83.10	92.10	96.50	97.40	88.30	89.3	88.20	84

Appendix B6. Plagioclase Analyses (continued)

Sample	106-2-10D3	106-2-10D3	106-2-10D4	106-2-10D5	106-2-10E2	106-2-11A1	106-2-11A2	106-2-11A3	106-2-11A3	106-2-11A4	106-2-11A4	106-2-11B1	106-2-11B2
Rock Type	gabbro	gabbro	gabbro	gabbro	gabbro	PG	PG	PG	PG	PG	PG	PG	PG
Location	OSU	UofA	UofA	UofA	OSU	UofA	UofA	OSU	UofA	OSU	UofA	UofA	UofA
Occurrence	inc	gm	gm	gm	gm	gm	gm	gm	gm	gm	gm	gm	gm
SiO_2	45.81	44.24	44.50	46.07	45.09	46.73	46.71	47.05	46.43	47.84	58.72	62.55	66.87
Al_2O_3	34.62	35.81	35.59	34.62	35.05	34.19	34.16	33.63	34.17	32.97	26.02	23.41	20.26
FeO^T	0.31	0.30	0.35	0.30	0.49	0.41	0.39	0.40	0.39	0.48	0.11	0.13	0.33
MnO	n.d.	b.d.	b.d.	0.02	n.d.	0.01	b.d.	n.d.	0.02	n.d.	0.01	b.d.	b.d.
MgO	0.03	b.d.	0.01	0.02	0.03	0.01	b.d.	0.01	b.d.	0.02	b.d.	b.d.	b.d.
CaO	17.85	18.84	18.81	17.58	18.41	17.09	17.26	17.04	17.19	16.44	7.16	4.17	0.71
Na_2O	1.24	0.85	0.88	1.64	0.99	1.97	1.90	1.85	1.84	2.22	7.38	9.06	11.14
K_2O	b.d.	0.02	0.03	0.03	b.d.	0.02	0.03	0.04	b.d.	0.01	0.09	0.10	0.04
Total	99.88	100.05	100.17	100.28	100.07	100.44	100.46	100.02	100.04	99.98	99.48	99.41	99.35
Si	8.45	8.18	8.22	8.47	8.33	8.57	8.57	8.65	8.55	8.79	10.53	11.13	11.79
Al	7.52	7.80	7.74	7.49	7.62	7.38	7.38	7.28	7.41	7.13	5.50	4.90	4.21
Fe^{2+}	0.05	0.05	0.05	0.05	0.08	0.06	0.06	0.06	0.06	0.07	0.02	0.02	0.05
Mn	-	-	-	0.00	-	0.00	0.00	-	0.00	-	0.00	-	-
Mg	0.01	-	0.00	0.01	0.01	0.00	-	0.00	-	0.01	-	-	-
Ca	3.53	3.73	3.72	3.46	3.64	3.36	3.39	3.36	3.39	3.24	1.38	0.80	0.13
Na	0.45	0.31	0.31	0.59	0.36	0.70	0.68	0.66	0.66	0.79	2.57	3.12	3.81
K	-	0.01	0.01	0.01	-	0.01	0.01	0.01	-	0.00	0.02	0.02	0.01
Cations	20.00	20.06	20.06	20.07	20.03	20.08	20.08	20.03	20.07	20.03	20.01	19.99	20.01
An	88.80	92.3	92.1	85.4	91.10	82.6	83.3	83.30	83.7	80.30	34.7	20.2	3.4

Appendix B6. Plagioclase Analyses (continued)

Sample	106-2-11B3	106-2-11D2	107-1-14C1	108-1-6A1	108-1-6A2	108-1-6A3	108-1-6A5	108-1-6B1	108-1-6B2	108-1-6C1	108-1-6C3	108-1-6D1	108-1-6D2	108-2-6A1
Rock Type	gabbro	gabbro	basalt	gabbro	gabbro	gabbro	gabbro	gabbro	gabbro	gabbro	gabbro	gabbro	gabbro	gabbro
Location	OSU	OSU	UofA	UofA	UofA	UofA	UofA	UofA	UofA	UofA	UofA	UofA	UofA	UofA
Occurrence	gm	gm	gm	gm	gm	gm	cor	gm	gm	gm	gm	gm	gm	gm
SiO_2	57.09	62.12	50.55	44.23	44.31	44.38	44.39	43.92	44.21	44.24	44.33	44.48	44.29	45.20
Al_2O_3	26.34	23.91	30.66	34.88	34.82	34.68	34.48	35.08	34.72	34.96	34.80	34.57	34.65	34.46
FeO^T	0.20	0.25	0.43	0.28	0.27	0.34	0.27	0.36	0.32	0.28	0.24	0.26	0.31	0.33
MnO	n.d.	n.d.	n.d.	n.d.	n.d.	n.d.	n.d.	n.d.	n.d.	n.d.	n.d.	n.d.	n.d.	n.d.
MgO	b.d.	b.d.	0.09	0.01	0.02	0.01	0.02	0.02	0.03	0.02	0.01	0.01	0.02	0.03
CaO	8.22	5.26	13.72	19.21	18.88	18.97	18.84	18.64	18.83	19.11	18.93	19.04	18.92	17.85
Na_2O	6.65	8.38	4.00	0.82	0.80	0.81	0.83	0.92	0.88	0.75	0.84	0.84	0.84	1.28
K_2O	0.05	0.10	0.03	0.01	0.01	0.03	0.01	0.02	0.03	0.01	0.02	0.02	0.01	0.01
Total	98.56	100.00	99.48	99.44	99.11	99.22	98.84	98.96	99.02	99.37	99.17	99.22	99.04	99.16
Si	10.37	11.01	9.28	8.24	8.27	8.28	8.31	8.22	8.27	8.24	8.27	8.30	8.28	8.41
Al	5.63	4.99	6.63	7.65	7.65	7.62	7.60	7.73	7.64	7.67	7.65	7.59	7.63	7.55
Fe^{2+}	0.03	0.04	0.07	0.04	0.04	0.05	0.04	0.06	0.05	0.04	0.04	0.04	0.05	0.05
Mn	-	-	-	-	-	-	-	-	-	-	-	-	-	-
Mg	-	-	0.03	0.00	0.01	0.00	0.01	0.01	0.01	0.01	0.00	0.00	0.01	0.01
Ca	1.60	1.00	2.70	3.83	3.78	3.79	3.78	3.74	3.77	3.81	3.78	3.81	3.79	3.56
Na	2.34	2.88	1.42	0.30	0.29	0.29	0.30	0.33	0.32	0.27	0.30	0.30	0.30	0.46
K	0.01	0.02	0.01	0.00	0.00	0.01	0.00	0.01	0.01	0.00	0.01	0.01	0.00	0.00
Cations	19.99	19.94	20.12	20.07	20.04	20.05	20.03	20.08	20.07	20.05	20.05	20.05	20.05	20.04
An	40.50	25.60	65.40	92.80	92.80	92.70	92.60	91.70	92.00	93.30	92.50	92.50	92.50	88.50

Appendix B6. Plagioclase Analyses (continued)

Sample	108-2-6A2	108-2-6B1	108-2-6B2	108-2-6B3	108-2-6C1	108-2-6C2	108-2-6C3	108-2-12A1	108-2-12A2	108-2-12A3	108-2-12A4	108-2-12C2	108-2-12C3	108-2-12C4
Rock Type	gabbro	gabbro	gabbro	gabbro	gabbro	gabbro	gabbro	PG	PG	PG	PG	PG	PG	PG
Location	UofA	UofA	UofA	UofA	UofA	UofA	UofA	UofA	UofA	UofA	UofA	UofA	UofA	UofA
Occurrence	gm	gm	gm	gm	inc	inc	cor	gm	gm	gm	gm	gm	gm	gm
SiO_2	44.73	45.56	44.91	44.86	45.08	45.18	44.38	66.91	58.95	64.96	59.15	65.66	67.07	67.97
Al_2O_3	35.17	34.21	34.95	34.88	34.94	34.75	35.85	20.84	26.19	22.26	25.91	21.25	20.21	20.30
FeO^T	0.26	0.40	0.29	0.36	0.45	0.46	0.29	0.04	0.31	0.04	0.40	0.14	0.31	0.35
MnO	n.d.	n.d.	n.d.	n.d.	n.d.	n.d.	n.d.	b.d.	b.d.	b.d.	b.d.	b.d.	0.01	b.d.
MgO	0.02	0.01	0.02	0.04	0.03	0.04	0.03	b.d.	0.01	b.d.	0.02	0.02	b.d.	b.d.
CaO	18.93	17.80	18.19	18.47	17.70	17.70	18.40	1.48	7.95	3.10	7.73	2.03	0.87	0.88
Na_2O	0.96	1.41	1.15	1.08	1.09	1.16	0.62	10.74	6.91	9.98	7.06	10.33	10.82	11.05
K_2O	0.02	0.03	0.01	0.02	0.02	0.03	0.03	0.04	0.05	0.07	0.04	0.04	0.04	0.08
Total	100.09	99.42	99.52	99.71	99.31	99.32	99.60	100.05	100.37	100.41	100.31	99.47	99.33	100.63
Si	8.27	8.46	8.33	8.32	8.37	8.39	8.22	11.72	10.50	11.40	10.54	11.59	11.82	11.83
Al	7.66	7.48	7.64	7.62	7.64	7.60	7.82	4.30	5.49	4.60	5.44	4.42	4.19	4.16
Fe^{2+}	0.04	0.06	0.05	0.06	0.07	0.07	0.05	0.01	0.05	0.01	0.06	0.02	0.05	0.05
Mn	-	-	-	-	-	-	-	-	-	-	-	-	0.00	-
Mg	0.01	0.00	0.01	0.01	0.01	0.01	0.01	-	0.00	-	0.01	0.01	-	-
Ca	3.75	3.54	3.62	3.67	3.52	3.52	3.65	0.28	1.52	0.58	1.48	0.38	0.16	0.16
Na	0.34	0.51	0.41	0.39	0.39	0.42	0.22	3.65	2.39	3.40	2.44	3.54	3.70	3.73
K	0.01	0.01	0.00	0.01	0.01	0.01	0.01	0.01	0.01	0.02	0.01	0.01	0.01	0.02
Cations	20.07	20.05	20.05	20.06	20.00	20.01	19.97	19.96	19.95	20.00	19.96	19.97	19.93	19.96
An	91.50	87.30	89.70	90.30	89.90	89.20	94.10	7.10	38.80	14.60	37.60	9.80	4.20	4.20

Appendix B6. Plagioclase Analyses (continued)

Sample	108-2-12C5	108-2-12E2	108-2-12E3	108-2-12E4	108-3-1E1	108-3-1E2	108-3-1F1	108-3-15A1	108-3-15A2	108-3-15A3	108-3-15B1	108-3-15B2	108-3-15D1	108-3-15D2
Rock Type	PG	PG	PG	PG	basalt	basalt	basalt	PG	PG	PG	PG	PG	PG	PG
Location	UofA	UofA	UofA	UofA	UofA	UofA	UofA	UofA	UofA	UofA	UofA	UofA	UofA	UofA
Occurrence	gm	gm	gm	gm	gm	gm	gm	gm	gm	gm	gm	gm	gm	gm
SiO_2	66.50	60.78	61.07	57.79	65.98	66.09	67.12	60.33	61.86	58.65	55.93	56.26	56.11	53.96
Al_2O_3	20.78	24.85	24.72	26.84	20.56	20.59	20.07	24.61	23.40	25.51	27.74	27.45	27.58	28.78
FeO^T	0.11	0.38	0.33	0.30	0.16	0.24	0.24	0.28	0.35	0.30	0.13	0.21	0.36	0.35
MnO	0.02	0.03	b.d.	b.d.	n.d.	n.d.	n.d.	n.d.	n.d.	n.d.	n.d.	n.d.	n.d.	n.d.
MgO	b.d.	0.02	0.02	b.d.	b.d.	b.d.	0.01	b.d.	b.d.	b.d.	b.d.	0.01	0.02	0.01
CaO	1.60	6.44	6.13	8.54	1.30	1.10	0.75	5.87	4.67	6.70	9.77	9.03	9.19	11.05
Na_2O	10.50	8.01	8.10	6.46	11.28	11.07	11.61	8.19	8.85	7.77	6.14	6.48	6.53	5.38
K_2O	0.06	0.10	0.09	0.08	0.10	0.07	0.06	0.06	0.08	0.11	0.04	0.08	0.09	0.07
Total	99.57	100.61	100.46	100.01	99.38	99.16	99.86	99.34	99.21	99.04	99.75	99.52	99.88	99.60
Si	11.71	10.77	10.82	10.35	11.68	11.70	11.80	10.81	11.06	10.58	10.09	10.16	10.11	9.80
Al	4.31	5.19	5.16	5.66	4.28	4.29	4.16	5.19	4.93	5.42	5.89	5.84	5.85	6.16
Fe^{2+}	0.02	0.06	0.05	0.05	0.02	0.04	0.04	0.04	0.05	0.05	0.02	0.03	0.05	0.05
Mn	0.00	0.01	-	-	-	-	-	-	-	-	-	-	-	-
Mg	-	0.01	0.01	-	-	-	0.00	-	-	-	-	0.00	0.01	0.00
Ca	0.30	1.22	1.16	1.64	0.25	0.21	0.14	1.13	0.89	1.30	1.89	1.75	1.78	2.15
Na	3.58	2.75	2.78	2.24	3.87	3.80	3.96	2.84	3.07	2.72	2.15	2.27	2.28	1.89
K	0.01	0.02	0.02	0.02	0.02	0.02	0.01	0.01	0.02	0.03	0.01	0.02	0.02	0.02
Cations	19.93	20.02	20.00	19.95	20.12	20.06	20.10	20.02	20.01	20.08	20.04	20.06	20.10	20.07
An	7.70	30.60	29.30	42.00	5.90	5.20	3.40	28.30	22.50	32.10	46.70	43.30	43.50	53.00

Appendix B6. Plagioclase Analyses (continued)

Sample	108-3-15D3	108-3-16A1	108-3-16A2	108-3-16D1	108-3-16D2	108-3-16D3	108-3-16D4	108-3-16D5	108-3-16D6	108-3-17A1	108-3-17A3	108-3-17A6	108-3-17A7
Rock Type	PG	epidosite	epidosite	epidosite	epidosite	epidosite	epidosite	epidosite	epidosite	PG	PG	PG	PG
Location	UofA	UofA	UofA	UofA	UofA	UofA	UofA	UofA	UofA	UofA	UofA	UofA	UofA
Occurrence	gm	gm	gm	gm	cor	gm	gm	gm	gm	gm	rim	cor	rim
SiO_2	60.41	67.90	68.22	67.72	67.60	67.72	67.99	68.06	68.10	55.87	66.37	61.81	61.72
Al_2O_3	24.48	20.02	19.71	19.68	19.52	19.69	19.97	19.94	19.84	27.61	21.16	24.18	24.64
FeO^T	0.20	0.15	0.13	0.12	0.25	0.11	0.28	0.30	0.16	0.44	0.26	0.43	0.49
MnO	n.d.	n.d.	n.d.	n.d.	n.d.	n.d.	n.d.	n.d.	n.d.	b.d.	0.02	0.01	b.d.
MgO	b.d.	b.d.	b.d.	0.01	0.01	b.d.	0.01	0.01	0.02	0.04	0.01	0.02	b.d.
CaO	5.86	0.14	0.08	0.08	0.08	0.16	b.d.	0.22	0.19	10.13	1.87	5.50	6.01
Na_2O	8.42	11.90	11.99	11.56	11.85	11.63	11.60	11.90	11.58	5.72	10.77	8.08	8.21
K_2O	0.09	0.04	0.05	0.04	0.04	0.04	0.04	0.03	0.04	0.10	0.07	0.16	0.19
Total	99.46	100.15	100.18	99.21	99.35	99.35	99.89	100.46	99.93	99.91	100.53	100.19	101.26
Si	10.81	11.87	11.92	11.93	11.92	11.92	11.90	11.87	11.92	10.08	11.61	10.95	10.86
Al	5.16	4.12	4.06	4.08	4.05	4.08	4.12	4.10	4.09	5.86	4.36	5.05	5.10
Fe^{2+}	0.03	0.02	0.02	0.02	0.04	0.02	0.04	0.04	0.02	0.07	0.04	0.06	0.07
Mn	-	-	-	-	-	-	-	-	-	-	0.00	0.00	-
Mg	-	-	-	0.00	0.00	-	0.00	0.00	0.01	0.01	0.00	0.01	-
Ca	1.12	0.03	0.02	0.02	0.02	0.03	-	0.04	0.04	1.96	0.35	1.04	1.13
Na	2.92	4.03	4.06	3.95	4.05	3.97	3.94	4.03	3.93	2.00	3.65	2.78	2.80
K	0.02	0.01	0.01	0.01	0.01	0.01	0.01	0.01	0.01	0.02	0.02	0.04	0.04
Cations	20.07	20.08	20.08	20.00	20.08	20.02	20.01	20.09	20.00	20.00	20.04	19.92	20.01
An	27.60	0.60	0.40	0.40	0.40	0.70	0.00	1.00	0.90	49.20	8.70	27.10	28.50

Appendix B6. Plagioclase Analyses (continued)

Sample	108-3-17A8	108-3-17C1	108-3-17C2	108-3-17C3	108-3-17E1	108-3-17E2	110-1-5AB1	110-1-5AB2	110-1-5AB7	110-1-15C3	110-1-15C4	110-1-25A3	110-1-25A4
Rock Type	PG	PG	PG	PG	PG	PG	basalt	basalt	basalt	basalt	basalt	basalt	basalt
Location	UofA	UofA	UofA	UofA	UofA	UofA	UofA	UofA	UofA	UofA	UofA	UofA	UofA
Occurrence	gm	gm	gm	gm	gm	gm	vei	vei	gm	gm	gm	gm	gm
SiO_2	62.44	64.23	62.19	63.17	63.13	56.24	63.54	65.90	63.83	64.73	62.47	66.06	66.80
Al_2O_3	24.24	22.66	23.84	23.33	23.45	27.41	23.15	21.95	23.25	21.32	22.83	21.96	21.56
FeO^T	0.48	0.25	0.38	0.43	0.21	0.39	0.17	0.21	0.17	0.28	0.12	0.11	0.33
MnO	b.d.	0.02	b.d.	b.d.	b.d.	0.01	b.d.	0.02	b.d.	n.d.	n.d.	0.02	b.d.
MgO	0.02	b.d.	0.02	0.02	b.d.	0.05	0.01	0.03	0.03	b.d.	b.d.	0.01	0.04
CaO	5.38	3.66	5.11	4.46	4.57	9.80	4.07	2.43	4.15	2.39	4.26	2.38	1.83
Na_2O	8.67	9.33	8.55	9.16	8.66	5.65	9.10	10.06	9.18	9.76	8.78	10.31	10.56
K_2O	0.09	0.08	0.08	0.11	0.15	0.07	0.17	0.17	0.14	0.12	0.10	0.20	0.10
Total	101.32	100.23	100.17	100.68	100.17	99.62	100.21	100.77	100.75	98.60	98.56	101.05	101.22
Si	10.95	11.31	11.01	11.12	11.14	10.15	11.21	11.50	11.20	11.54	11.20	11.50	11.60
Al	5.01	4.70	4.97	4.84	4.88	5.82	4.81	4.51	4.80	4.48	4.82	4.50	4.41
Fe^{2+}	0.07	0.04	0.06	0.06	0.03	0.06	0.03	0.03	0.03	0.04	0.02	0.02	0.05
Mn	-	0.00	-	-	-	0.00	-	0.00	-	-	-	0.00	-
Mg	0.01	-	0.01	0.01	-	0.01	0.00	0.01	0.01	-	-	0.00	0.01
Ca	1.01	0.69	0.97	0.84	0.86	1.89	0.77	0.45	0.78	0.46	0.82	0.44	0.34
Na	2.95	3.19	2.94	3.13	2.96	1.98	3.11	3.41	3.12	3.37	3.05	3.48	3.56
K	0.02	0.02	0.02	0.03	0.03	0.02	0.04	0.04	0.03	0.03	0.02	0.04	0.02
Cations	20.02	19.94	19.97	20.03	19.91	19.93	19.96	19.96	19.97	19.92	19.93	20.00	19.98
An	25.40	17.70	24.70	21.10	22.40	48.70	19.60	11.60	19.80	11.80	21.00	11.20	8.70

Appendix B6. Plagioclase Analyses (continued)

Sample	110-1-25A4	110-1-25A5	110-1-25A6	110-1-25C1	110-1-25C2	111-1-3D1	111-4-3B1	111-4-3B3	111-4-3C2	111-4-6A1	111-4-6A2	111-4-6A3	111-4-6A4	111-4-6A5
Rock Type	basalt	basalt	basalt	basalt	basalt	basalt	gabbro	gabbro	gabbro	gabbro	gabbo	gabbro	gabbro	gabbro
Location	UofA	UofA	UofA	UofA	UofA	OSU	OSU	OSU	OSU	UofA	UofA	UofA	UofA	UofA
Occurrence	gm?	gm	gm	gm	gm	gm	gm	gm	gm	gm	gm	gm	gm	gm
SiO_2	43.85	65.95	66.34	65.76	66.86	65.73	45.30	46.79	46.40	54.51	53.68	58.20	54.79	55.25
Al_2O_3	36.00	22.07	21.87	21.55	21.03	20.63	35.32	32.78	33.43	29.64	29.77	27.02	29.43	29.03
FeO^T	0.46	0.23	0.18	0.20	0.10	0.33	0.32	0.30	0.32	0.39	0.49	0.28	0.29	0.36
MnO	0.02	0.01	b.d.	0.01	0.01	n.d.	n.d.	n.d.	n.d.	0.02	b.d.	b.d.	b.d.	b.d.
MgO	0.05	0.02	b.d.	0.03	0.01	0.09	b.d.	0.06	0.03	0.03	0.05	b.d.	0.02	0.03
CaO	18.77	2.40	2.35	2.16	1.61	1.33	18.35	16.28	16.15	11.55	12.00	8.61	11.27	10.81
Na_2O	0.45	10.29	10.51	10.57	10.91	10.38	1.05	2.59	2.27	4.95	4.61	6.73	5.06	5.20
K_2O	0.03	0.17	0.13	0.10	0.12	0.07	0.04	0.04	0.04	0.18	0.14	0.31	0.22	0.23
Total	99.63	101.14	101.38	100.38	100.65	98.54	100.39	98.82	98.62	101.27	100.74	101.15	101.08	100.91
Si	8.14	11.48	11.52	11.53	11.67	11.69	8.33	8.71	8.65	9.74	9.66	10.33	9.79	9.88
Al	7.87	4.53	4.47	4.45	4.32	4.32	7.65	7.19	7.34	6.24	6.31	5.65	6.20	6.11
Fe^{2+}	0.07	0.03	0.03	0.03	0.02	0.05	0.05	0.05	0.05	0.06	0.07	0.04	0.04	0.05
Mn	0.00	0.00	-	0.00	0.00	-	-	-	-	0.00	-	-	-	-
Mg	0.01	0.01	-	0.01	0.00	0.02	-	0.02	0.01	0.01	0.01	-	0.01	0.01
Ca	3.73	0.45	0.44	0.41	0.30	0.25	3.62	3.25	3.22	2.21	2.31	1.64	2.16	2.07
Na	0.16	3.47	3.54	3.59	3.69	3.58	0.38	0.93	0.82	1.72	1.61	2.32	1.75	1.80
K	0.01	0.04	0.03	0.02	0.03	0.02	0.01	0.01	0.01	0.04	0.03	0.07	0.05	0.05
Cations	20.00	20.01	20.02	20.04	20.03	19.94	20.03	20.15	20.09	20.01	20.00	20.04	20.00	19.98
An	95.70	11.30	10.90	10.10	7.50	6.60	90.40	77.50	79.50	55.70	58.50	40.70	54.50	52.80

Appendix B6. Plagioclase Analyses (continued)

Sample	111-4-6A6	111-4-6B5	111-4-6B6	111-4-6B7	111-4-6C3	111-4-6C4	113-1-10c1	113-1-10c2	113-1-10c3	113-1-10d1	113-1-10d2	113-1-10d3	113-1-20A2	113-1-20A3
Rock Type	gabbro	gabbro	gabbro	gabbro	gabbro	gabbro	basalt	basalt	basalt	basalt	basalt	basalt	basalt	basalt
Location	UofA	UofA	UofA	UofA	UofA	UofA	OSU	OSU	OSU	OSU	OSU	OSU	UofA	UofA
Occurrence	gm	gm	gm	gm	gm	gm	gm	gm	gm	gm	gm	gm	gm	gm
SiO_2	55.39	54.19	57.20	54.29	53.60	54.20	68.33	67.56	68.18	67.57	67.41	68.04	66.33	66.05
Al_2O_3	29.06	29.81	27.47	29.54	29.92	29.56	19.94	19.82	19.96	20.04	19.91	20.31	20.11	21.22
FeO^T	0.49	0.37	0.42	0.31	0.46	0.47	0.11	0.09	0.18	0.36	0.21	0.19	0.14	0.21
MnO	0.01	b.d.	b.d.	0.02	0.01	0.03	n.d.	n.d.	n.d.	n.d.	n.d.	n.d.	n.d.	n.d.
MgO	0.04	0.01	0.05	0.02	0.04	0.05	b.d.	0.02	0.01	b.d.	0.07	b.d.	b.d.	0.01
CaO	10.79	12.02	9.41	11.81	12.14	11.75	0.14	0.17	0.25	0.25	0.38	0.46	1.15	1.58
Na_2O	5.18	4.56	6.02	4.96	4.56	4.73	10.79	11.59	11.23	11.41	11.08	10.95	10.85	11.24
K_2O	0.22	0.19	0.26	0.19	0.18	0.18	0.03	0.01	0.06	0.03	0.04	0.09	0.08	0.18
Total	101.18	101.15	100.83	101.14	100.91	100.97	99.34	99.27	99.87	99.66	99.10	100.04	98.66	100.49
Si	9.88	9.70	10.20	9.72	9.63	9.72	11.97	11.90	11.92	11.87	11.89	11.88	11.78	11.58
Al	6.11	6.28	5.77	6.23	6.33	6.24	4.11	4.11	4.11	4.14	4.13	4.18	4.21	4.38
Fe^{2+}	0.07	0.06	0.06	0.05	0.07	0.07	0.02	0.01	0.03	0.05	0.03	0.03	0.02	0.03
Mn	0.00	-	-	0.00	0.00	0.01	-	-	-	-	-	-	-	-
Mg	0.01	0.00	0.01	0.01	0.01	0.01	-	0.01	0.00	-	0.02	-	-	0.00
Ca	2.06	2.30	1.80	2.27	2.34	2.26	0.03	0.03	0.05	0.05	0.07	0.09	0.22	0.30
Na	1.79	1.58	2.08	1.72	1.59	1.65	3.67	3.96	3.81	3.88	3.79	3.71	3.74	3.82
K	0.05	0.04	0.06	0.04	0.04	0.04	0.01	0.00	0.01	0.01	0.01	0.02	0.02	0.04
Cations	19.98	19.97	19.98	20.04	20.01	19.99	19.80	20.02	19.93	20.00	19.94	19.89	19.99	20.15
An	52.80	58.60	45.70	56.20	58.90	57.20	0.70	0.80	1.20	1.20	1.90	2.30	5.50	7.10

Appendix B6. Plagioclase Analyses (continued)

Sample	113-2-11A3	113-2-11A4	113-2-11B1	113-2-11B2	113-2-11B3	113-2-11B4	113-2-11C1	113-2-11C2
Rock Type	gabbro	gabbro	gabbro	gabbro	gabbro	gabbro	gabbro	gabbro
Location	UofA	UofA	UofA	UofA	UofA	UofA	UofA	UofA
Occurrence	gm	gm	gm	gm	gm	gm	gm	gm
SiO_2	46.37	46.40	46.50	46.26	46.02	46.48	46.24	46.39
Al_2O_3	34.87	34.70	34.81	34.45	34.96	34.65	34.63	34.64
FeO^T	0.41	0.48	0.48	0.44	0.49	0.45	0.49	0.47
MnO	b.d.	b.d.	0.01	0.01	0.01	b.d.	b.d.	b.d.
MgO	0.12	0.09	0.06	0.11	0.09	0.16	0.08	0.06
CaO	17.90	17.90	17.80	17.86	18.21	17.87	17.94	18.05
Na_2O	1.22	1.17	1.28	1.19	0.97	1.22	1.16	1.15
K_2O	0.02	0.01	b.d.	0.04	0.01	0.01	0.03	0.04
Total	100.91	100.75	100.94	100.36	100.76	100.84	100.57	100.80
Si	8.47	8.48	8.49	8.49	8.42	8.49	8.47	8.48
Al	7.50	7.47	7.48	7.45	7.53	7.45	7.47	7.46
Fe^{2+}	0.06	0.07	0.07	0.07	0.08	0.07	0.08	0.07
Mn	-	-	0.00	0.00	0.00	-	-	-
Mg	0.03	0.03	0.02	0.03	0.03	0.04	0.02	0.02
Ca	3.50	3.51	3.48	3.51	3.57	3.50	3.52	3.54
Na	0.43	0.42	0.45	0.42	0.34	0.43	0.41	0.41
K	0.01	0.00	-	0.01	0.00	0.00	0.01	0.01
Cations	20.00	19.98	19.99	19.99	19.97	19.99	19.99	19.98
An	88.90	89.40	88.50	89.00	91.20	89.00	89.40	89.50

Appendix B7. Amphibole Analyses (recalculated on the basis of 23 anhydrous O)

Sample	90-4-3A1	90-4-3A2	90-4-3A3	90-4-3A4	90-4-3C4	90-4-3C5	90-4-3C6	90-4-7C3	94-1-1A1	94-1-1A2	94-1-1B1	94-1-1B2	94-1-1C1	94-1-1C2	94-1-1D1	94-1-2A1
Occurrence	patchy	patchy	patchy	patchy	patchy	patchy	patchy	patchy	after cpx	after cpx	after cpx	cpx inc	after cpx	after cpx	after cpx	patchy
Rock Type	gabbro	gabbro	gabbro	gabbro	gabbro	gabbro	gabbro	gabbro	gabbro	gabbro	gabbro	gabbro	gabbro	gabbro	gabbro	gabbro
Analysis	ave	ave	ave	ave	ave	ave	ave	ave	15NK	ave	15NK	ave	ave	15NK	ave	15NK
Location	UofA	UofA	UofA	UofA	UofA	UofA	UofA	OSU	OSU	OSU	OSU	OSU	OSU	OSU	OSU	OSU
SiO_2	46.47	45.30	48.00	49.82	44.81	43.94	44.97	52.58	48.54	48.08	50.77	47.03	47.80	50.32	47.91	54.08
TiO_2	0.16	0.15	0.16	0.18	0.03	0.04	0.02	0.22	0.90	0.73	0.28	1.82	0.64	0.08	0.40	0.04
Al_2O_3	10.14	11.41	9.30	7.00	12.51	13.09	11.85	5.03	5.16	7.53	4.10	7.58	7.02	6.03	6.60	1.74
FeO^T	9.81	10.14	9.65	8.49	10.67	10.92	10.60	7.06	14.48	13.63	15.18	13.78	13.37	14.87	14.51	13.88
Cr_2O_3	0.01	b.d.	b.d.	b.d.	b.d.	b.d.	b.d.	0.04	0.09	0.04	b.d.	0.08	b.d.	b.d.	0.03	0.01
MnO	0.18	0.16	0.15	0.13	0.19	0.19	0.17	0.04	0.25	0.15	0.28	0.15	0.19	0.33	0.24	0.32
MgO	15.79	14.91	15.92	17.23	14.87	14.37	14.97	18.65	14.91	14.55	15.64	14.64	15.07	15.38	14.65	15.99
CaO	12.34	12.28	12.44	12.68	12.02	12.12	11.94	12.68	11.33	11.81	10.73	11.66	11.53	10.72	11.28	12.03
Na_2O	1.65	1.92	1.36	0.91	2.06	2.24	1.85	0.36	0.84	1.26	0.69	1.60	1.13	0.83	1.15	0.13
K_2O	0.07	0.08	0.10	0.08	0.09	0.13	0.11	0.03	0.14	0.11	0.06	0.11	0.09	0.05	0.15	b.d.
F	b.d.	b.d.	b.d.	b.d.	b.d.	b.d.	b.d.	0.20	b.d.	0.07	0.04	0.09	0.04	0.05	0.04	0.03
Cl	0.02	0.01	b.d.	b.d.	0.01	0.05	0.04	0.08	0.21	0.40	0.15	0.34	0.22	0.08	0.64	0.02
Total	96.63	96.36	97.08	96.52	97.26	97.09	96.52	96.92	96.76	98.32	97.92	98.80	97.09	98.73	97.55	98.27
Si	6.70	6.59	6.88	7.12	6.45	6.37	6.51	7.42	7.14	6.93	7.35	6.78	6.93	7.22	6.97	7.74
Al^{IV}	1.30	1.41	1.12	0.88	1.55	1.63	1.49	0.58	0.87	1.07	0.65	1.22	1.07	0.78	1.03	0.26
Al^{VI}	0.43	0.54	0.45	0.30	0.57	0.60	0.53	0.25	0.03	0.21	0.05	0.07	0.13	0.23	0.10	0.04
Cr	0.00	-	-	-	-	-	-	0.00	0.01	0.00	-	0.01	-	-	0.00	0.00
Fe^{3+}	0.46	0.38	0.34	0.33	0.54	0.50	0.57	0.27	0.36	0.51	0.33	0.50	0.69	0.29	0.75	0.18
Ti	0.02	0.02	0.02	0.02	0.00	0.00	0.00	0.02	0.10	0.08	0.03	0.20	0.07	0.01	0.04	0.01
Mg	3.40	3.23	3.40	3.67	3.19	3.10	3.23	3.92	3.27	3.13	3.38	3.14	3.26	3.29	3.18	3.41
Fe^{2+}	0.72	0.86	0.82	0.69	0.74	0.83	0.71	0.57	1.42	1.13	1.51	1.16	0.93	1.49	1.01	1.49
Mn	0.02	0.02	0.02	0.02	0.02	0.02	0.02	0.01	0.03	0.02	0.03	0.02	0.02	0.04	0.03	0.04
Ca	1.91	1.91	1.91	1.94	1.85	1.88	1.85	1.92	1.78	1.82	1.67	1.80	1.79	1.65	1.76	1.85
Na	0.462	0.542	0.378	0.253	0.575	0.629	0.52	0.099	0.241	0.351	0.194	0.448	0.319	0.23	0.323	0.037
K	0.01	0.02	0.02	0.02	0.02	0.02	0.02	0.00	0.03	0.02	0.01	0.02	0.02	0.01	0.03	-
Cations	15.43	15.51	15.35	15.24	15.51	15.59	15.46	15.06	15.27	15.28	15.21	15.36	15.22	15.24	15.22	15.04
Cl	0.01	0.00	-	-	0.00	0.01	0.01	0.02	0.05	0.10	0.04	0.08	0.05	0.02	0.16	0.00
F	-	-	-	-	-	-	-	0.09	-	0.03	0.02	0.04	0.02	0.02	0.02	0.01

Notes: Amphibole analyses recalculated using the 15 NK and the average of the 13 CNK and 15 NK methods outlined in Robinson [1982] in order to satisfy crystal-chemical limits; ave = average of 13 CNK and 15 NK methods; b.d. = below detection; cpx = clinopyroxene; vei = vein; inc = inclusion; int = intergranular.

Appendix B7. Amphibole Analyses (continued)

Sample	94-1-2B1	94-1-2B1	94-1-2B2	94-1-2B2	94-1-2B3	94-1-2B5	94-1-2C1	94-1-2C2	94-1-2D1	94-1-2D2	94-1-2E1	94-1-2E2	94-1-3A1	94-1-3B1	94-1-3C1	94-1-3C2
Occurrence	vei	vei	int	vei	vei	vei	after cpx	cpx rim	int	int	cpx inc	after cpx	after cpx	after cpx	cpx rim	after cpx
Rock Type	gabbro	gabbro	gabbro	gabbro	gabbro	gabbro	gabbro	gabbro	gabbro	gabbro	gabbro	gabbro	gabbro	gabbro	gabbro	gabbro
Analysis	ave	ave	ave	ave	15N	ave	15NK	ave	ave	ave	ave	15NK	15NK	15NK	15NK	15NK
Location	OSU	UofA	OSU	UofA	UofA	UofA	OSU	OSU	OSU	OSU	OSU	OSU	OSU	OSU	OSU	OSU
SiO_2	47.91	48.02	47.57	48.34	49.91	47.81	49.73	51.44	46.02	44.10	44.63	48.80	49.46	50.48	49.41	49.44
TiO_2	0.34	0.50	0.65	0.66	0.40	0.56	0.73	0.41	0.50	0.70	2.67	0.35	0.93	0.81	0.97	0.85
Al_2O_3	7.33	7.62	7.58	6.90	6.23	6.03	4.89	5.77	6.96	8.42	9.48	6.68	5.03	4.67	5.84	5.76
FeO^T	13.35	11.82	13.53	11.93	10.98	16.96	11.26	11.09	18.87	18.50	10.99	11.74	12.63	13.15	13.41	13.57
Cr_2O_3	b.d.	0.02	0.03	0.04	0.01	0.02	0.02	b.d.	b.d.	b.d.	0.10	0.03	0.01	b.d.	b.d.	0.02
MnO	0.24	0.20	0.23	0.25	0.27	0.19	0.19	0.25	0.19	0.26	0.13	0.35	0.14	0.17	0.21	0.18
MgO	15.50	15.65	14.58	15.47	16.68	12.36	16.95	17.56	10.82	11.04	15.68	16.89	16.28	15.88	15.81	15.78
CaO	10.97	10.93	11.59	11.30	10.80	11.65	11.76	11.26	11.63	11.71	11.72	10.94	11.44	11.28	11.59	11.33
Na_2O	1.30	1.47	1.29	1.34	1.08	0.74	0.81	0.90	1.15	1.28	1.96	1.29	0.84	0.76	0.99	0.98
K_2O	0.02	0.05	0.03	0.04	0.07	0.29	0.11	0.01	0.05	0.06	b.d.	0.03	0.20	0.18	0.20	0.17
F	0.03	b.d.	b.d.	b.d.	b.d.	b.d.	0.03	b.d.	0.06	0.08	0.34	b.d.	0.05	0.10	0.09	0.12
Cl	0.09	0.09	0.11	0.07	0.05	0.32	0.05	0.08	0.31	0.25	0.10	0.09	0.29	0.31	0.28	0.24
Total	97.08	96.35	97.16	96.30	96.47	96.91	96.50	98.77	96.54	96.39	97.70	97.17	97.28	97.79	98.77	98.43
Si	6.90	6.95	6.90	7.02	7.24	7.09	7.21	7.18	6.93	6.64	6.45	7.04	7.18	7.32	7.10	7.13
Al^{IV}	1.10	1.05	1.10	0.98	0.76	0.91	0.79	0.82	1.07	1.36	1.55	0.96	0.82	0.68	0.90	0.87
Al^{VI}	0.14	0.25	0.20	0.21	0.30	0.14	0.04	0.13	0.17	0.13	0.06	0.18	0.04	0.11	0.09	0.11
Cr	-	0.00	0.00	0.01	0.00	0.00	0.00	-	-	-	0.01	0.00	0.00	-	-	0.00
Fe^{3+}	0.84	0.58	0.60	0.49	0.05	0.53	0.34	0.70	0.57	0.81	0.54	0.34	0.30	0.15	0.29	0.27
Ti	0.04	0.05	0.07	0.07	0.04	0.06	0.08	0.04	0.06	0.08	0.29	0.04	0.10	0.09	0.10	0.09
Mg	3.33	3.38	3.15	3.35	3.61	2.73	3.66	3.66	2.43	2.48	3.38	3.63	3.52	3.43	3.39	3.39
Fe^{2+}	0.76	0.85	1.04	0.96	1.28	1.58	1.02	0.60	1.81	1.52	0.79	1.08	1.24	1.45	1.32	1.36
Mn	0.03	0.02	0.03	0.03	0.03	0.02	0.02	0.03	0.02	0.03	0.02	0.04	0.02	0.02	0.03	0.02
Ca	1.69	1.70	1.80	1.76	1.68	1.85	1.83	1.68	1.88	1.89	1.82	1.69	1.78	1.75	1.78	1.75
Na	0.362	0.41	0.361	0.38	0.30	0.21	0.226	0.244	0.335	0.373	0.549	0.36	0.237	0.214	0.276	0.275
K	0.00	0.01	0.01	0.01	0.01	0.06	0.02	0.00	0.01	0.01	-	0.01	0.04	0.03	0.04	0.03
Cations	15.20	15.26	15.26	15.26	15.32	15.19	15.25	15.08	15.28	15.33	15.45	15.37	15.27	15.25	15.31	15.31
Cl	0.02	0.02	0.03	0.02	0.01	0.08	0.01	0.02	0.08	0.06	0.02	0.02	0.07	0.08	0.07	0.06
F	0.01	-	-	-	-	-	0.01	-	0.03	0.04	0.15	-	0.03	0.05	0.04	0.06

Appendix B7. Amphibole Analyses (continued)

Sample	94-1-3D1	94-1-3E1	94-1-3E2	94-1-3E3	96-1-3A1	96-1-3A2	96-1-3A3	96-1-3B1	96-1-3B2	96-1-3B3	96-1-5A2	96-1-5A4	96-1-5A5	96-1-5B1	96-1-5B3	96-1-5B4
Occurrence	after cpx	after cpx	after cpx	after cpx	patchy	patchy	patchy	after cpx	after cpx	after cpx	after cpx	after cpx	after cpx	after cpx	after cpx	after cpx
Rock Type	gabbro	gabbro	gabbro	gabbro	PG	PG	PG	PG	PG	PG	PG	PG	PG	PG	PG	PG
Analysis	ave	15NK	15NK	15NK	ave	15NK	15NK	15NK	15NK	ave	15NK	15NK	15NK	15NK	15NK	ave
Location	OSU	OSU	OSU	OSU	UofA	UofA	UofA	UofA	UofA	UofA	UofA	UofA	UofA	UofA	UofA	UofA
SiO_2	46.76	48.01	49.50	47.73	41.98	48.81	49.93	44.32	45.33	45.87	46.07	46.47	45.55	45.35	47.55	45.33
TiO_2	1.27	0.45	1.15	1.03	0.12	0.37	0.28	1.32	0.90	0.77	1.17	1.12	0.82	0.69	0.37	0.32
Al_2O_3	7.55	8.33	5.51	6.65	11.94	2.51	1.87	6.08	4.90	4.83	4.48	4.14	4.46	4.31	2.53	7.36
FeO^T	14.10	13.34	13.16	14.56	25.39	28.70	30.10	28.95	29.30	29.57	27.10	26.57	30.91	31.08	33.48	24.41
Cr_2O_3	0.03	b.d.	b.d.	0.03	0.01	b.d.	b.d.	b.d.	0.01	b.d.	0.02	0.02	0.03	b.d.	b.d.	b.d.
MnO	0.25	0.35	0.20	0.20	0.35	0.38	0.42	0.54	0.54	0.50	0.48	0.42	0.42	0.39	0.40	0.20
MgO	14.61	15.39	16.20	14.79	5.15	5.89	5.84	4.92	4.76	4.22	6.70	6.57	3.60	3.39	3.20	7.97
CaO	11.69	10.63	11.80	11.33	10.94	10.28	9.63	9.82	9.93	10.13	9.96	10.05	9.90	10.17	9.34	11.19
Na_2O	1.24	1.45	0.90	1.09	1.24	0.38	0.35	2.04	1.71	1.41	1.39	1.25	0.80	0.73	0.36	1.15
K_2O	0.33	0.06	0.20	0.28	0.14	0.20	0.17	0.73	0.62	0.62	0.55	0.50	0.35	0.37	0.15	0.17
F	0.01	b.d.	0.03	b.d.	0.11	0.14	0.19	0.58	0.50	0.22	b.d.	b.d.	b.d.	b.d.	b.d.	b.d.
Cl	0.41	0.11	0.24	0.36	0.22	0.21	0.19	0.35	0.35	0.52	0.40	0.35	0.57	0.55	0.32	0.33
Total	98.21	98.12	98.88	98.01	97.58	97.87	98.97	99.65	98.84	98.66	98.30	97.44	97.38	97.03	97.70	98.43
Si	6.77	6.93	7.08	6.96	6.44	7.61	7.73	7.00	7.20	7.21	7.20	7.31	7.30	7.30	7.59	6.84
Al^{IV}	1.23	1.07	0.92	1.04	1.56	0.39	0.27	1.00	0.80	0.79	0.80	0.69	0.70	0.70	0.41	1.16
Al^{VI}	0.06	0.34	0.01	0.10	0.60	0.08	0.07	0.13	0.11	0.10	0.03	0.08	0.14	0.11	0.07	0.15
Cr	0.00	-	-	0.00	0.00	-	-	-	0.00	-	0.00	0.00	0.00	-	-	-
Fe^{3+}	0.69	0.21	0.37	0.35	0.75	0.07	0.00	0.00	0.00	0.37	0.00	0.00	0.04	0.12	0.11	0.77
Ti	0.14	0.05	0.12	0.11	0.01	0.04	0.03	0.16	0.11	0.09	0.14	0.13	0.10	0.08	0.04	0.04
Mg	3.15	3.31	3.46	3.21	1.18	1.37	1.35	1.16	1.13	0.99	1.56	1.54	0.86	0.81	0.76	1.79
Fe^{2+}	1.02	1.40	1.20	1.42	2.51	3.67	3.90	3.82	3.89	3.52	3.54	3.50	4.10	4.06	4.37	2.32
Mn	0.03	0.04	0.02	0.02	0.05	0.05	0.06	0.07	0.07	0.07	0.06	0.06	0.06	0.05	0.05	0.03
Ca	1.81	1.64	1.81	1.77	1.80	1.72	1.60	1.66	1.69	1.71	1.67	1.69	1.70	1.75	1.60	1.81
Na	0.349	0.406	0.249	0.307	0.369	0.115	0.105	0.625	0.526	0.43	0.421	0.381	0.249	0.228	0.111	0.336
K	0.06	0.01	0.04	0.05	0.03	0.04	0.03	0.15	0.13	0.12	0.11	0.10	0.07	0.08	0.03	0.03
Cations	15.31	15.42	15.29	15.36	15.29	15.16	15.14	15.77	15.65	15.40	15.53	15.48	15.32	15.30	15.14	15.27
Cl	0.10	0.03	0.06	0.09	0.06	0.06	0.05	0.09	0.09	0.14	0.11	0.09	0.16	0.15	0.09	0.08
F	0.01	-	0.01	-	0.05	0.07	0.09	0.29	0.25	0.11	-	-	-	-	-	-

Appendix B7. Amphibole Analyses (continued)

Sample	96-1-5B5	96-1-5B6	96-1-5D3	96-1-5D4	96-2-13a5	99-1-21A1	99-1-21A2	99-1-21A3	99-1-21B1	99-1-21B2	99-1-21B3	99-1-21B4	99-1-21B5	99-1-21C1	99-1-21C2
Occurrence	after cpx	after cpx	after cpx	after cpx	patchy	cpx rim	cpx rim	cpx rim	vei	vei	vei	patchy	patchy	cpx rim	cpx rim
Rock Type	PG	PG	PG	PG	PG	gabbro	gabbro	gabbro	gabbro	gabbro	gabbro	gabbro	gabbro	gabbro	gabbro
Analysis	15NK	15NK	15NK	15NK	15NK	ave	15NK	ave	ave	ave	ave	15NK	15NK	ave	ave
Location	UofA	UofA	UofA	UofA	OSU	UofA	UofA	UofA	UofA	UofA	UofA	UofA	UofA	UofA	UofA
SiO_2	48.79	44.80	48.98	48.27	52.57	43.68	51.72	49.97	49.07	48.27	48.60	50.78	51.34	43.61	42.72
TiO_2	0.29	1.65	0.47	0.79	0.48	1.72	0.21	0.40	0.25	0.32	0.63	0.26	0.31	2.52	2.60
Al_2O_3	4.35	6.13	1.82	3.09	3.65	11.63	4.84	6.84	7.71	8.11	6.97	5.72	5.15	11.38	11.93
FeO^T	22.54	26.29	27.20	27.91	11.97	10.61	7.74	7.89	9.84	10.23	10.25	8.27	7.64	9.67	10.01
Cr_2O_3	b.d.	b.d.	b.d.	b.d.	0.02	0.04	0.04	0.07	b.d.	b.d.	0.12	0.07	0.06	0.10	0.10
MnO	0.21	0.41	0.34	0.38	0.55	0.13	0.21	0.16	0.23	0.27	0.16	0.19	0.19	0.07	0.09
MgO	9.61	6.73	6.80	6.41	16.39	14.88	19.47	18.28	16.92	16.64	16.58	19.17	19.21	15.41	14.99
CaO	11.27	9.52	9.97	10.54	12.05	11.89	11.56	12.35	11.59	11.26	12.07	10.79	11.59	11.75	11.58
Na_2O	0.54	0.95	0.47	0.44	0.60	2.00	0.80	1.23	1.29	1.55	1.12	0.94	0.88	1.97	2.11
K_2O	0.08	0.60	0.26	0.44	0.02	0.19	0.03	0.05	0.04	0.04	0.06	0.03	0.06	0.13	0.16
F	b.d.	b.d.	b.d.	b.d.	b.d.	b.d.	b.d.	b.d.	b.d.	b.d.	b.d.	b.d.	b.d.	b.d.	b.d.
Cl	0.11	0.38	0.17	0.22	0.01	0.11	0.02	b.d.	0.04	0.03	0.03	0.03	0.02	0.10	0.11
Total	97.79	97.46	96.48	98.49	98.30	96.84	96.60	97.17	96.98	96.72	96.47	96.18	96.39	96.61	96.30
Si	7.35	7.01	7.71	7.46	7.51	6.35	7.34	7.07	6.99	6.91	6.99	7.26	7.31	6.33	6.24
Al^{IV}	0.65	0.99	0.29	0.54	0.50	1.65	0.66	0.93	1.01	1.09	1.01	0.75	0.69	1.67	1.76
Al^{VI}	0.12	0.14	0.04	0.03	0.12	0.34	0.15	0.20	0.29	0.28	0.17	0.22	0.18	0.28	0.29
Cr	-	-	-	-	0.00	0.01	0.00	0.01	-	-	0.01	0.01	0.01	0.01	0.01
Fe^{3+}	0.29	0.05	0.00	0.11	0.10	0.48	0.23	0.43	0.55	0.59	0.51	0.20	0.18	0.44	0.46
Ti	0.03	0.19	0.06	0.09	0.05	0.19	0.02	0.04	0.03	0.03	0.07	0.03	0.03	0.28	0.29
Mg	2.16	1.57	1.60	1.48	3.49	3.23	4.12	3.85	3.59	3.55	3.56	4.08	4.08	3.34	3.26
Fe^{2+}	2.55	3.39	3.58	3.50	1.33	0.81	0.69	0.51	0.62	0.64	0.73	0.79	0.73	0.74	0.77
Mn	0.03	0.05	0.05	0.05	0.07	0.02	0.03	0.02	0.03	0.03	0.02	0.02	0.02	0.01	0.01
Ca	1.82	1.60	1.68	1.75	1.84	1.85	1.76	1.87	1.77	1.73	1.86	1.65	1.77	1.83	1.81
Na	0.158	0.288	0.143	0.132	0.166	0.564	0.22	0.337	0.357	0.43	0.312	0.26	0.243	0.555	0.598
K	0.02	0.12	0.05	0.09	0.00	0.04	0.01	0.01	0.01	0.01	0.01	0.01	0.01	0.02	0.03
Cations	15.17	15.41	15.20	15.22	15.17	15.52	15.23	15.28	15.24	15.29	15.25	15.27	15.25	15.49	15.53
Cl	0.03	0.10	0.05	0.06	0.00	0.03	0.01	-	0.01	0.01	0.01	0.01	0.01	0.03	0.03
F	-	-	-	-	-	-	-	-	-	-	-	-	-	-	-

Appendix B7. Amphibole Analyses (continued)

Sample	99-1-21D1	99-1-21D2	99-1-21D3	99-1-21D4	99-1-30A1	99-1-30A4	99-1-30A5	99-1-30A6	99-1-30B1	99-1-30B2	99-1-30B3	99-1-30B4	99-1-30C1	99-1-30C2	99-1-30C4
Occurrence	vei	vei	vei	vei	patchy	cpx rim	cpx rim	cpx rim	cpx rim	cpx rim	cpx rim	cpx rim	cpx inc	cpx inc	patchy
Rock Type	gabbro	gabbro	gabbro	gabbro	gabbro	gabbro	gabbro	gabbro	gabbro	gabbro	gabbro	gabbro	gabbro	gabbro	gabbro
Analysis	ave	ave	ave	ave	ave	ave	ave	ave	15NK	15NK	ave	ave	15NK	15NK	ave
Location	UofA	UofA	UofA	UofA	UofA	UofA	UofA	UofA	UofA	UofA	UofA	UofA	UofA	UofA	UofA
SiO_2	50.40	49.04	52.93	51.61	50.19	43.65	43.93	44.03	54.93	53.69	43.81	43.50	54.89	54.51	51.45
TiO_2	0.59	0.36	0.25	0.65	0.05	1.98	1.91	1.94	0.16	0.17	1.88	2.30	0.21	0.14	b.d.
Al_2O_3	6.54	6.83	3.23	4.75	6.24	11.65	11.51	11.17	2.07	3.33	11.51	11.10	1.62	1.99	5.43
FeO^T	9.74	9.69	9.25	8.35	9.22	9.06	9.21	9.36	6.69	7.32	9.48	9.54	7.87	5.06	8.79
Cr_2O_3	0.11	0.02	0.19	0.10	b.d.	0.25	0.27	0.27	0.10	0.09	0.17	0.21	0.13	0.14	0.02
MnO	0.21	0.18	0.30	0.20	0.22	0.09	0.09	0.10	0.25	0.23	0.09	0.09	0.34	0.22	0.25
MgO	16.95	16.86	18.00	18.42	17.60	15.80	15.78	15.65	20.14	19.14	15.67	15.70	19.91	21.14	17.94
CaO	12.27	12.31	12.44	12.07	11.95	11.54	11.64	11.73	12.23	12.55	11.71	11.55	11.69	12.49	12.03
Na_2O	1.05	1.08	0.43	0.75	1.11	1.92	2.03	2.13	0.24	0.35	1.93	2.26	0.27	0.33	0.90
K_2O	0.05	0.04	0.04	0.02	0.05	0.17	0.13	0.17	0.02	0.02	0.19	0.17	0.02	0.01	0.02
F	b.d.	b.d.	b.d.	b.d.	b.d.	b.d.	b.d.	b.d.	b.d.	b.d.	b.d.	b.d.	b.d.	b.d.	b.d.
Cl	0.01	0.04	0.01	0.02	b.d.	0.10	0.11	0.11	b.d.	b.d.	0.13	0.13	b.d.	b.d.	0.02
Total	97.81	96.43	96.88	96.84	96.63	95.96	96.34	96.39	96.73	96.80	96.40	96.34	96.82	95.89	96.83
Si	7.14	7.05	7.52	7.31	7.16	6.33	6.36	6.39	7.74	7.59	6.35	6.33	7.76	7.69	7.30
Al^{IV}	0.86	0.95	0.48	0.69	0.84	1.67	1.64	1.61	0.26	0.41	1.65	1.67	0.24	0.31	0.70
Al^{VI}	0.23	0.21	0.06	0.10	0.21	0.32	0.32	0.30	0.08	0.14	0.31	0.24	0.03	0.02	0.21
Cr	0.01	0.00	0.02	0.01	-	0.03	0.03	0.03	0.01	0.01	0.02	0.02	0.02	0.02	0.00
Fe^{3+}	0.34	0.47	0.34	0.42	0.49	0.53	0.49	0.41	0.07	0.12	0.52	0.44	0.08	0.16	0.42
Ti	0.06	0.04	0.03	0.07	0.01	0.22	0.21	0.21	0.02	0.02	0.21	0.25	0.02	0.02	-
Mg	3.58	3.61	3.81	3.89	3.74	3.42	3.41	3.39	4.23	4.03	3.39	3.41	4.20	4.44	3.80
Fe^{2+}	0.81	0.70	0.76	0.57	0.61	0.57	0.63	0.73	0.72	0.75	0.63	0.72	0.85	0.44	0.63
Mn	0.03	0.02	0.04	0.02	0.03	0.01	0.01	0.01	0.03	0.03	0.01	0.01	0.04	0.03	0.03
Ca	1.86	1.90	1.89	1.83	1.83	1.79	1.81	1.83	1.85	1.90	1.82	1.80	1.77	1.89	1.83
Na	0.288	0.301	0.118	0.206	0.307	0.541	0.57	0.599	0.066	0.096	0.543	0.638	0.074	0.09	0.248
K	0.01	0.01	0.01	0.00	0.01	0.03	0.02	0.03	0.00	0.00	0.04	0.03	0.00	0.00	0.00
Cations	15.22	15.25	15.07	15.12	15.22	15.46	15.49	15.54	15.07	15.10	15.48	15.56	15.08	15.09	15.16
Cl	0.00	0.01	0.00	0.01	-	0.03	0.03	0.03	-	-	0.03	0.03	-	-	0.01
F	-	-	-	-	-	-	-	-	-	-	-	-	-	-	-

Appendix B7. Amphibole Analyses (continued)

Sample	99-1-30C5	99-2-12A2	99-2-12A3	99-2-12C1	99-2-12C3	99-2-12C4	99-2-1A1	99-2-1A2	99-2-1A3	99-2-1A4	99-2-1B1	99-2-1B3	99-2-1B5	99-2-1B6	99-2-1C1	99-2-1C2
Occurrence	patchy	patchy	patchy	patchy	patchy	patchy	vei	vei	vei	vei	vei	vei	cpx rim	cpx rim	vei	vei
Rock Type	gabbro	basalt	basalt	basalt	basalt	basalt	basalt	basalt	basalt	basalt	basalt	basalt	basalt	basalt	basalt	basalt
Analysis	ave	15NK	15NK	15NK	15NK	15NK	15NK	15NK	15NK	15NK	15NK	15NK	15NK	15NK	15NK	15NK
Location	UofA	UofA	UofA	UofA	UofA	UofA	UofA	UofA	UofA	UofA	UofA	UofA	UofA	UofA	UofA	UofA
SiO_2	52.04	52.36	52.50	52.19	52.24	52.99	50.97	49.70	51.24	51.50	53.28	53.51	53.70	49.54	50.07	50.90
TiO_2	0.06	0.10	0.05	0.05	0.06	0.04	0.30	0.23	0.24	0.23	0.61	0.31	0.47	0.21	0.35	0.47
Al_2O_3	4.61	2.06	1.55	2.22	1.70	3.16	5.94	6.45	5.92	5.27	2.65	2.79	2.89	7.04	6.48	5.09
FeO^T	8.28	16.29	15.62	18.08	17.38	16.39	10.47	10.84	9.77	9.97	9.77	10.21	9.96	11.47	10.97	10.92
Cr_2O_3	b.d.	0.02	b.d.	0.02	b.d.	b.d.	b.d.	b.d.	0.02	0.01	0.03	0.04	0.03	0.04	0.02	0.06
MnO	0.23	0.78	0.69	0.88	0.93	0.82	0.22	0.22	0.25	0.27	0.23	0.24	0.28	0.25	0.27	0.38
MgO	18.60	13.34	13.48	12.21	12.47	11.61	16.91	16.58	16.73	16.89	17.50	17.68	17.78	15.66	17.03	17.01
CaO	12.20	12.02	12.10	12.15	12.06	11.25	11.69	11.40	11.50	11.88	12.33	12.49	12.09	11.84	10.78	10.66
Na_2O	0.74	0.13	0.17	0.16	0.19	0.71	0.67	0.75	0.58	0.51	0.15	0.18	0.23	0.61	0.84	0.53
K_2O	0.04	0.04	0.06	0.06	0.05	0.06	0.02	0.03	0.03	0.02	0.02	0.02	0.03	0.03	0.01	0.02
F	b.d.	b.d.	b.d.	b.d.	b.d.	b.d.	b.d.	b.d.	b.d.	b.d.	b.d.	b.d.	b.d.	b.d.	b.d.	b.d.
Cl	0.03	0.01	0.02	0.02	b.d.	0.02	0.02	0.02	0.03	0.02	0.01	0.03	0.01	0.02	0.03	0.02
Total	96.83	97.13	96.24	98.02	97.08	97.05	97.21	96.22	96.29	96.56	96.55	97.46	97.44	96.67	96.83	96.00
Si	7.36	7.71	7.79	7.68	7.75	7.91	7.29	7.19	7.39	7.40	7.64	7.61	7.64	7.16	7.20	7.38
Al^{IV}	0.64	0.29	0.21	0.32	0.25	0.09	0.71	0.81	0.61	0.60	0.36	0.40	0.37	0.85	0.80	0.63
Al^{VI}	0.13	0.06	0.06	0.06	0.05	0.46	0.29	0.29	0.39	0.29	0.09	0.07	0.12	0.35	0.30	0.24
Cr	-	0.00	-	0.00	-	-	-	-	0.00	0.00	0.00	0.00	0.00	0.01	0.00	0.01
Fe^{3+}	0.44	0.16	0.07	0.19	0.13	0.00	0.16	0.25	0.00	0.11	0.08	0.20	0.07	0.27	0.19	0.12
Ti	0.01	0.01	0.01	0.01	0.01	0.00	0.03	0.03	0.03	0.03	0.07	0.03	0.05	0.02	0.04	0.05
Mg	3.92	2.93	2.98	2.68	2.76	2.58	3.61	3.58	3.60	3.62	3.74	3.75	3.77	3.37	3.65	3.67
Fe^{2+}	0.54	1.84	1.86	2.04	2.03	2.05	1.09	1.06	1.18	1.09	1.09	1.02	1.11	1.12	1.13	1.20
Mn	0.03	0.10	0.09	0.11	0.12	0.10	0.03	0.03	0.03	0.03	0.03	0.03	0.03	0.03	0.03	0.05
Ca	1.85	1.90	1.92	1.92	1.92	1.80	1.79	1.77	1.78	1.83	1.90	1.90	1.84	1.83	1.66	1.66
Na	0.203	0.037	0.049	0.046	0.055	0.205	0.186	0.21	0.162	0.142	0.042	0.05	0.063	0.171	0.234	0.149
K	0.01	0.01	0.01	0.01	0.01	0.01	0.00	0.01	0.01	0.00	0.00	0.00	0.01	0.01	0.00	0.00
Cations	15.13	15.05	15.06	15.06	15.06	15.22	15.19	15.22	15.17	15.15	15.05	15.05	15.07	15.18	15.24	15.15
Cl	0.01	0.00	0.01	0.01	-	0.01	0.01	0.01	0.01	0.01	0.00	0.01	0.00	0.01	0.01	0.01
F	-	-	-	-	-	-	-	-	-	-	-	-	-	-	-	-

Appendix B7. Amphibole Analyses (continued)

Sample	99-2-1C3	105-1-6A1	105-1-6A2	105-1-6A3	105-1-6B1	105-1-6C2	105-1-6D1	105-1-8(b)B5	105-1-8(b)B6	105-1-8(b)C2	105-1-8(b)C3	105-1-8(b)C5	105-1-8(b)D2
Occurrence	vel	cpx inc	cpx inc	cpx rim	cpx rim	int	after cpx	cpx inc	int	cpx rim	patchy	cpx rim	vel
Rock Type	basalt	gabbro	gabbro	gabbro	gabbro	gabbro	gabbro	gabbro	gabbro	gabbro	gabbro	gabbro	gabbro
Analysis	15NK	ave	ave	ave	ave	ave	ave	ave	ave	ave	ave	ave	15NK
Location	UofA	OSU	OSU	OSU	OSU	OSU	OSU	OSU	OSU	OSU	OSU	OSU	OSU
SiO_2	50.55	43.01	42.71	45.56	43.35	43.34	46.61	43.94	43.53	52.89	55.66	44.14	52.84
TiO_2	0.44	2.74	2.92	1.24	2.43	2.25	0.18	1.60	2.76	0.02	0.02	1.88	0.58
Al_2O_3	5.58	12.28	12.21	11.51	11.57	12.84	10.46	11.64	11.81	4.06	2.50	11.85	3.79
FeO^T	10.27	10.10	9.89	9.45	9.71	8.90	8.75	9.11	9.60	7.67	6.50	9.15	10.64
Cr_2O_3	0.01	0.26	0.27	0.06	0.28	0.14	b.d.	0.35	0.17	b.d.	0.03	0.26	0.10
MnO	0.33	0.13	0.12	0.11	0.20	0.09	0.09	0.10	0.08	0.17	0.16	0.07	0.19
MgO	17.52	15.28	15.47	16.60	16.24	16.46	17.83	16.93	16.28	18.94	20.57	16.82	18.30
CaO	10.80	11.97	11.82	12.16	12.32	11.86	11.91	12.00	12.01	13.04	13.29	12.45	11.87
Na_2O	0.77	2.50	2.58	2.03	2.33	2.56	1.95	2.61	2.08	0.30	0.19	2.15	0.40
K_2O	0.02	0.07	0.07	0.08	0.08	0.08	0.04	0.10	0.11	0.02	b.d.	0.10	0.05
F	b.d.	b.d.	b.d.	b.d.	0.07	0.09	b.d.	b.d.	b.d.	0.02	b.d.	0.06	0.07
Cl	0.01	0.03	0.04	0.06	0.04	0.04	0.04	0.24	0.10	0.02	0.03	0.08	0.12
Total	96.29	98.12	97.84	98.79	98.32	98.51	97.88	98.27	98.36	97.15	98.91	98.75	98.83
Si	7.29	6.17	6.14	6.42	6.19	6.15	6.56	6.24	6.19	7.44	7.64	6.23	7.42
Al^{IV}	0.71	1.83	1.86	1.58	1.82	1.85	1.44	1.76	1.81	0.56	0.36	1.77	0.58
Al^{VI}	0.24	0.25	0.21	0.33	0.13	0.29	0.29	0.19	0.17	0.12	0.04	0.20	0.04
Cr	0.00	0.03	0.03	0.01	0.03	0.02	-	0.04	0.02	-	0.00	0.03	0.01
Fe^{3+}	0.16	0.41	0.44	0.59	0.60	0.56	0.74	0.63	0.63	0.39	0.31	0.66	0.29
Ti	0.05	0.30	0.32	0.13	0.26	0.24	0.02	0.17	0.30	0.00	0.00	0.20	0.06
Mg	3.77	3.27	3.32	3.49	3.45	3.48	3.74	3.59	3.45	3.97	4.21	3.54	3.83
Fe^{2+}	1.08	0.80	0.75	0.52	0.56	0.50	0.29	0.45	0.52	0.52	0.44	0.42	0.96
Mn	0.04	0.02	0.02	0.01	0.02	0.01	0.01	0.01	0.01	0.02	0.02	0.01	0.02
Ca	1.67	1.84	1.82	1.84	1.88	1.80	1.80	1.83	1.83	1.97	1.95	1.88	1.79
Na	0.215	0.697	0.721	0.555	0.644	0.703	0.534	0.719	0.573	0.082	0.05	0.588	0.109
K	0.00	0.01	0.01	0.01	0.01	0.02	0.01	0.02	0.02	0.00	-	0.02	0.01
Cations	15.22	15.63	15.64	15.48	15.60	15.61	15.43	15.65	15.50	15.07	15.03	15.54	15.12
Cl	0.00	0.01	0.01	0.02	0.01	0.01	0.01	0.06	0.02	0.01	0.01	0.02	0.03
F	-	-	-	-	0.03	0.04	-	-	-	0.01	-	0.03	0.03

Appendix B7. Amphibole Analyses (continued)

Sample	105-1-14A2	105-1-14A3	105-1-14B3	105-1-14B4	105-1-14C2	105-1-14C3	105-1-21A1	105-1-21A2	105-1-21B1	105-1-21B2	105-1-21B3	105-1-21C1	105-1-21C2
Occurrence	int	int	int	int	int	int	cpx rim	cpx rim	cpx rim	cpx rim	cpx rim	cpx rim	cpx rim
Rock Type	gabbro	gabbro	gabbro	gabbro	gabbro	gabbro	gabbro	gabbro	gabbro	gabbro	gabbro	gabbro	gabbro
Analysis	ave	ave	ave	ave	ave	ave	ave	ave	ave	ave	ave	ave	ave
Location	OSU	OSU	OSU	OSU	OSU	OSU	UofA	UofA	UofA	UofA	UofA	UofA	UofA
SiO_2	42.41	44.21	43.39	42.61	44.13	43.45	42.99	43.00	42.87	43.81	42.98	42.77	42.86
TiO_2	2.80	2.54	2.81	2.75	2.28	1.99	2.65	2.42	2.32	1.30	2.35	2.58	2.42
Al_2O_3	11.64	10.13	11.91	11.44	11.47	11.71	12.14	12.24	12.07	11.82	12.17	12.05	12.17
FeO^T	10.56	10.79	9.91	10.53	10.59	10.69	9.04	9.23	8.82	8.82	8.84	8.94	9.12
Cr_2O_3	0.06	0.01	0.04	b.d.	0.25	0.18	0.42	0.36	0.28	0.40	0.28	0.29	0.31
MnO	0.15	0.10	0.10	0.13	0.10	0.17	0.11	0.11	0.09	0.10	0.12	0.12	0.11
MgO	15.58	15.99	15.95	15.62	16.09	15.40	15.48	15.44	15.68	16.48	16.00	15.85	15.61
CaO	11.78	12.07	11.97	11.49	11.74	12.13	11.62	11.75	11.71	11.69	11.66	11.54	11.51
Na_2O	2.58	2.17	2.47	2.34	2.36	1.89	2.70	2.71	2.65	2.55	2.75	2.78	2.68
K_2O	0.04	0.06	0.08	0.08	0.07	0.10	0.10	0.10	0.10	0.10	0.11	0.13	0.10
F	0.02	0.06	0.02	0.01	0.11	b.d.	b.d.	b.d.	b.d.	b.d.	b.d.	b.d.	b.d.
Cl	0.06	0.04	0.05	0.05	0.06	0.06	0.04	0.05	0.03	0.03	0.04	0.04	0.04
Total	97.60	98.15	98.66	97.05	99.00	97.59	96.87	97.05	96.34	96.70	97.02	96.80	96.62
Si	6.13	6.35	6.19	6.18	6.25	6.24	6.23	6.23	6.24	6.30	6.21	6.20	6.22
Al^{IV}	1.87	1.65	1.81	1.82	1.75	1.76	1.77	1.77	1.76	1.70	1.79	1.80	1.78
Al^{VI}	0.12	0.06	0.19	0.13	0.17	0.22	0.30	0.31	0.31	0.30	0.28	0.26	0.30
Cr	0.01	0.00	0.00	-	0.03	0.02	0.05	0.04	0.03	0.05	0.03	0.03	0.04
Fe^{3+}	0.59	0.58	0.50	0.65	0.64	0.68	0.30	0.30	0.33	0.56	0.39	0.36	0.37
Ti	0.31	0.27	0.30	0.30	0.24	0.22	0.29	0.26	0.25	0.14	0.26	0.28	0.26
Mg	3.36	3.42	3.39	3.38	3.40	3.30	3.34	3.33	3.40	3.53	3.45	3.43	3.38
Fe^{2+}	0.69	0.72	0.68	0.63	0.62	0.61	0.80	0.82	0.74	0.51	0.68	0.72	0.74
Mn	0.02	0.01	0.01	0.02	0.01	0.02	0.01	0.01	0.01	0.01	0.01	0.01	0.01
Ca	1.83	1.86	1.83	1.79	1.78	1.87	1.80	1.82	1.83	1.80	1.80	1.79	1.79
Na	0.722	0.603	0.684	0.658	0.648	0.528	0.758	0.761	0.748	0.711	0.77	0.781	0.754
K	0.01	0.01	0.01	0.01	0.01	0.02	0.02	0.02	0.02	0.02	0.02	0.02	0.02
Cations	15.64	15.54	15.61	15.56	15.54	15.48	15.67	15.69	15.67	15.62	15.69	15.70	15.66
Cl	0.01	0.01	0.01	0.01	0.01	0.02	0.01	0.01	0.01	0.01	0.01	0.01	0.01
F	0.01	0.03	0.01	0.01	0.05	-	-	-	-	-	-	-	-

Appendix B7. Amphibole Analyses (continued)

Sample	105-1-21C3	105-1-25A1	105-1-25A1	105-1-25A2	105-1-25A2	105-1-25A3	105-1-25A4	105-1-25A4	105-1-25B1	105-1-25B4	105-1-25B6	105-1-25C1	105-1-25C1
Occurrence	cpx rim	vei	vei	vei	vei	vei	cpx rim	vei	vei	vei	int	vei	vei
Rock Type	gabbro	gabbro	gabbro	gabbro	gabbro	gabbro	gabbro	gabbro	gabbro	gabbro	gabbro	gabbro	gabbro
Analysis	ave	ave	ave	ave	ave	ave	ave	ave	15NK	15NK	ave	ave	ave
Location	UofA	OSU	UofA	OSU	UofA	UofA	OSU	UofA	OSU	OSU	OSU	OSU	UofA
SiO_2	42.97	46.29	46.19	47.49	46.39	46.60	43.50	44.41	55.68	52.08	41.87	48.96	45.99
TiO_2	2.61	0.23	0.22	0.37	0.27	0.22	3.10	0.38	0.10	b.d.	3.21	0.05	0.22
Al_2O_3	12.07	10.06	10.79	9.46	9.67	9.66	11.96	10.92	2.88	4.16	12.06	9.82	10.49
FeO^T	9.24	12.59	11.88	13.01	11.02	12.20	10.63	12.32	7.70	9.92	10.01	11.30	11.88
Cr_2O_3	0.40	0.01	b.d.	b.d.	0.02	0.02	0.22	0.03	0.03	0.02	0.16	0.01	0.03
MnO	0.11	0.16	0.20	0.29	0.22	0.19	0.11	0.26	0.21	0.22	0.12	0.26	0.21
MgO	15.36	14.91	13.81	14.52	14.98	14.39	14.77	13.84	18.78	19.37	15.45	15.10	14.93
CaO	11.67	12.29	12.01	11.86	11.61	11.85	11.99	11.61	12.85	11.43	11.76	11.28	11.46
Na_2O	2.78	1.23	1.17	1.07	1.08	1.02	2.34	1.31	0.15	0.12	2.47	1.20	1.43
K_2O	0.12	0.02	0.03	b.d.	0.01	0.02	0.09	0.03	b.d.	0.01	0.08	0.02	0.04
F	b.d.	0.08	b.d.	0.05	b.d.	b.d.	0.04	b.d.	b.d.	0.10	0.14	0.10	b.d.
Cl	0.03	0.07	0.07	0.06	0.05	0.04	0.04	0.05	0.03	0.01	0.06	0.06	0.03
Total	96.96	97.91	96.37	98.19	95.30	96.19	98.56	95.13	98.38	97.42	97.25	98.15	96.68
Si	6.24	6.63	6.72	6.78	6.77	6.77	6.24	6.55	7.77	7.33	6.08	6.93	6.63
Al^{IV}	1.76	1.37	1.28	1.22	1.23	1.23	1.76	1.46	0.24	0.67	1.92	1.07	1.37
Al^{VI}	0.30	0.32	0.57	0.37	0.43	0.42	0.27	0.44	0.24	0.02	0.14	0.57	0.41
Cr	0.05	0.00	-	-	0.00	0.00	0.02	0.00	0.00	0.00	0.02	0.00	0.00
Fe^{3+}	0.27	0.78	0.46	0.68	0.64	0.63	0.30	0.72	0.00	0.62	0.54	0.46	0.74
Ti	0.29	0.03	0.02	0.04	0.03	0.02	0.33	0.04	0.01	-	0.35	0.01	0.02
Mg	3.32	3.18	3.00	3.09	3.26	3.12	3.16	3.04	3.91	4.06	3.34	3.19	3.21
Fe^{2+}	0.85	0.72	0.98	0.88	0.71	0.85	0.98	0.80	0.90	0.55	0.68	0.88	0.69
Mn	0.01	0.02	0.02	0.04	0.03	0.02	0.01	0.03	0.02	0.03	0.01	0.03	0.03
Ca	1.81	1.88	1.87	1.81	1.81	1.85	1.84	1.83	1.92	1.72	1.83	1.71	1.77
Na	0.782	0.341	0.33	0.295	0.31	0.29	0.65	0.38	0.042	0.033	0.695	0.33	0.40
K	0.02	0.00	0.01	-	0.00	0.00	0.02	0.01	-	0.00	0.02	0.00	0.01
Cations	15.71	15.28	15.27	15.20	15.21	15.21	15.58	15.29	15.04	15.04	15.62	15.18	15.29
Cl	0.01	0.02	0.02	0.01	0.01	0.01	0.01	0.01	0.01	0.00	0.01	0.02	0.01
F	-	0.03	-	0.02	-	-	0.02	-	-	0.04	0.07	0.05	-

Appendix B7. Amphibole Analyses (continued)

Sample	105-1-25C2	105-1-25C2	105-1-25C3	105-1-25C5	105-1-25D1	105-1-25D3	105-1-25D4	105-1-25D5	105-1-25D6	105-1-25D7	105-3-6C2	105-3-6C3	105-3-6C4	105-3-6D5
Occurrence	vei	vel	patchy	cpx rim	vei	vel	vei	vei	cpx rim	cpx rim	patchy	patchy	after cpx	after cpx
Rock Type	gabbro	gabbro	gabbro	gabbro	gabbro	gabbro	gabbro	gabbro	gabbro	gabbro	basalt	basalt	basalt	basalt
Analysis	ave	ave	15NK	15NK	ave	ave	ave	ave	15NK	15NK	15NK	15NK	15NK	15NK
Location	OSU	UofA	OSU	OSU	OSU	OSU	OSU	OSU	OSU	OSU	OSU	OSU	OSU	OSU
SiO_2	49.69	45.77	54.38	55.58	47.47	47.53	46.90	49.10	53.96	53.26	50.97	49.46	49.66	41.96
TiO_2	0.06	0.01	0.08	0.09	0.43	0.99	0.87	0.23	0.03	0.38	0.19	0.19	0.33	0.11
Al_2O_3	7.82	11.19	3.21	4.10	7.92	8.34	9.39	8.08	3.14	6.79	2.95	3.87	4.07	9.19
FeO^T	10.74	9.94	5.60	9.44	15.40	10.18	10.16	9.58	10.74	5.78	21.25	22.83	24.94	25.12
Cr_2O_3	0.03	b.d.	0.02	0.03	0.02	0.14	0.12	0.02	b.d.	0.07	b.d.	b.d.	0.04	b.d.
MnO	0.20	0.21	0.18	0.15	0.24	0.14	0.12	0.15	0.26	0.04	0.33	0.32	0.82	0.46
MgO	17.19	15.62	21.56	17.17	12.94	17.07	16.61	17.22	16.96	18.54	10.53	10.27	7.86	11.01
CaO	12.08	11.96	12.44	11.41	12.46	12.20	12.20	12.35	12.88	11.11	11.51	11.32	9.90	7.59
Na_2O	0.94	1.47	0.42	0.20	1.01	1.72	1.74	1.41	0.18	1.18	0.25	0.32	0.54	0.20
K_2O	0.02	0.02	b.d.	0.01	0.05	0.09	0.10	0.13	b.d.	0.05	0.09	0.08	0.06	0.11
F	0.03	b.d.	0.02	b.d.	0.05	0.02	b.d.	0.04	0.05	b.d.	0.10	0.05	0.47	0.20
Cl	0.07	0.04	0.02	0.05	0.13	0.16	0.13	0.24	0.02	0.07	0.04	0.03	0.06	0.13
Total	98.84	96.23	97.91	98.21	98.09	98.44	98.23	98.53	98.22	97.20	98.20	98.73	98.71	96.08
Si	6.94	6.59	7.52	7.84	6.91	6.73	6.66	6.93	7.64	7.54	7.59	7.35	7.55	6.37
Al^{IV}	1.06	1.41	0.49	0.16	1.09	1.27	1.34	1.08	0.36	0.46	0.41	0.65	0.45	1.63
Al^{VI}	0.23	0.49	0.04	0.52	0.27	0.12	0.23	0.27	0.16	0.67	0.11	0.03	0.28	0.01
Cr	0.00	-	0.00	0.00	0.00	0.02	0.01	0.00	-	0.01	-	-	0.00	-
Fe^{3+}	0.77	0.66	0.32	0.00	0.50	0.59	0.58	0.49	0.14	0.00	0.16	0.48	0.00	1.51
Ti	0.01	0.00	0.01	0.01	0.05	0.11	0.09	0.03	0.00	0.04	0.02	0.02	0.04	0.01
Mg	3.58	3.36	4.44	3.61	2.81	3.60	3.52	3.62	3.58	3.91	2.34	2.28	1.78	2.49
Fe^{2+}	0.49	0.54	0.33	1.11	1.38	0.62	0.63	0.64	1.13	0.68	2.49	2.36	3.17	1.68
Mn	0.02	0.03	0.02	0.02	0.03	0.02	0.01	0.02	0.03	0.01	0.04	0.04	0.11	0.06
Ca	1.81	1.85	1.84	1.73	1.94	1.85	1.86	1.87	1.95	1.69	1.84	1.80	1.61	1.23
Na	0.256	0.41	0.112	0.054	0.284	0.472	0.48	0.386	0.049	0.324	0.072	0.093	0.16	0.06
K	0.00	0.00	-	0.00	0.01	0.02	0.02	0.02	-	0.01	0.02	0.02	0.01	0.02
Cations	15.16	15.33	15.11	15.06	15.26	15.41	15.42	15.34	15.05	15.33	15.09	15.11	15.17	15.08
Cl	0.02	0.01	0.01	0.01	0.03	0.04	0.03	0.06	0.00	0.02	0.01	0.01	0.02	0.03
F	0.01	-	0.01	-	0.02	0.01	-	0.02	0.02	-	0.05	0.02	0.23	0.10

Appendix B7. Amphibole Analyses (continued)

Sample	106-2-5a1	106-2-5a2	106-2-5b1	106-2-5b3	106-2-5c1	106-2-5c2	106-2-5c3	106-2-5c4	106-2-5d4	106-2-10A1	106-2-10A2	106-2-10A3	106-2-10B1	106-2-10B2
Occurrence	after cpx	after cpx	int	int	cpx rim	cpx rim	cpx inc	cpx inc	cpx rim	cpx rim	cpx inc	cpx inc	patchy	patchy
Rock Type	gabbro	gabbro	gabbro	gabbro	gabbro	gabbro	gabbro	gabbro	gabbro	gabbro	gabbro	gabbro	gabbro	gabbro
Analysis	ave	15NK	ave	15NK	ave	ave	ave	ave	15NK	15NK	ave	ave	ave	ave
Location	OSU	OSU	OSU	OSU	OSU	OSU	OSU	OSU	OSU	OSU	OSU	OSU	OSU	OSU
SiO_2	45.90	48.76	44.13	45.30	45.96	46.65	47.80	44.38	47.60	54.97	43.47	44.76	44.31	46.08
TiO_2	0.96	1.02	0.54	1.32	1.42	0.82	1.02	1.75	0.09	0.04	1.96	1.31	0.26	0.03
Al_2O_3	7.79	7.04	11.84	9.83	8.83	6.13	6.25	9.65	7.52	2.91	11.12	9.85	12.52	12.85
FeO^T	21.34	13.61	15.61	15.43	16.51	20.05	13.36	14.27	20.74	6.60	10.28	9.83	9.22	9.20
Cr_2O_3	b.d.	0.02	0.02	0.03	b.d.	0.01	b.d.	b.d.	b.d.	b.d.	0.09	0.12	b.d.	b.d.
MnO	0.29	0.28	0.31	0.42	0.35	0.29	0.28	0.29	0.63	0.15	0.12	0.11	0.18	0.17
MgO	9.05	14.88	12.67	13.55	12.29	10.67	14.96	13.76	12.15	21.92	16.07	16.39	17.33	17.31
CaO	11.56	11.31	11.21	10.21	11.66	11.84	12.07	11.47	8.80	11.44	11.98	12.06	11.24	11.04
Na_2O	0.80	0.92	1.66	1.34	1.02	0.79	0.72	1.60	0.44	0.48	1.50	1.43	1.93	1.88
K_2O	0.30	0.10	0.18	0.03	0.15	0.34	0.15	0.11	0.16	b.d.	0.25	0.18	0.09	0.12
F	0.09	0.03	0.08	b.d.	b.d.	b.d.	b.d.	0.04	0.05	0.04	0.04	0.02	0.02	0.07
Cl	0.40	0.07	0.26	0.07	0.09	0.25	0.12	0.05	0.08	0.03	0.05	0.05	0.12	0.11
Total	98.47	98.02	98.49	97.51	98.27	97.84	96.74	97.35	98.26	98.56	96.83	95.98	97.21	98.85
Si	6.87	7.05	6.39	6.64	6.69	6.97	6.96	6.48	7.00	7.57	6.26	6.48	6.26	6.40
Al^{IV}	1.14	0.95	1.62	1.36	1.31	1.04	1.04	1.52	1.00	0.44	1.74	1.52	1.74	1.61
Al^{VI}	0.24	0.25	0.40	0.34	0.21	0.04	0.03	0.13	0.31	0.04	0.15	0.16	0.35	0.50
Cr	-	0.00	0.00	0.00	-	0.00	-	-	-	-	0.01	0.01	-	-
Fe^{3+}	0.55	0.20	0.87	0.34	0.67	0.63	0.67	0.75	0.52	0.26	0.86	0.76	0.85	0.72
Ti	0.11	0.11	0.06	0.15	0.16	0.09	0.11	0.19	0.01	0.00	0.21	0.14	0.03	0.00
Mg	2.02	3.21	2.73	2.96	2.67	2.37	3.25	2.99	2.67	4.50	3.45	3.54	3.65	3.58
Fe^{2+}	2.12	1.44	1.02	1.56	1.35	1.88	0.95	0.99	2.04	0.50	0.38	0.43	0.24	0.35
Mn	0.04	0.04	0.04	0.05	0.04	0.04	0.03	0.04	0.08	0.02	0.01	0.01	0.02	0.02
Ca	1.85	1.75	1.74	1.60	1.82	1.89	1.88	1.79	1.39	1.69	1.85	1.87	1.70	1.64
Na	0.233	0.258	0.467	0.381	0.288	0.23	0.204	0.453	0.125	0.128	0.42	0.4	0.53	0.507
K	0.06	0.02	0.03	0.01	0.03	0.07	0.03	0.02	0.03	-	0.05	0.03	0.02	0.02
Cations	15.21	15.28	15.36	15.39	15.22	15.24	15.17	15.36	15.16	15.13	15.39	15.37	15.39	15.34
Cl	0.10	0.02	0.06	0.02	0.02	0.06	0.03	0.01	0.02	0.01	0.01	0.01	0.03	0.03
F	0.04	0.01	0.04	-	-	-	-	0.02	0.02	0.02	0.02	0.01	0.01	0.03

Appendix B7. Amphibole Analyses (continued)

Sample	106-2-10C1	106-2-10D1	106-2-10D1	106-2-10D2	106-2-10D2	106-2-10D3	106-2-10D3	106-2-10D4	106-2-10D4	106-2-10D5	106-2-10E8	106-2-10E9	106-2-10E10
Occurrence	int	int	int	int	int	int	int	int	int	int	cpx inc	cpx inc	cpx inc
Rock Type	gabbro	gabbro	gabbro	gabbro	gabbro	gabbro	gabbro	gabbro	gabbro	gabbro	gabbro	gabbro	gabbro
Analysis	15NK	ave	15N	ave	15N	15NK	15N	ave	15N	15N	15NK	ave	ave
Location	OSU	OSU	UofA	OSU	UofA	OSU	UofA	OSU	UofA	UofA	OSU	OSU	OSU
SiO_2	49.57	44.43	50.87	45.31	51.53	44.88	48.66	45.05	50.70	47.33	46.39	43.45	47.91
TiO_2	0.20	1.96	0.25	1.79	0.24	1.97	0.39	1.89	0.48	0.98	1.64	2.58	0.71
Al_2O_3	8.34	9.28	4.14	8.93	3.94	9.12	6.16	9.36	5.39	8.06	9.49	10.80	8.66
FeO^T	12.70	13.25	13.23	13.27	12.59	12.88	13.79	12.79	10.00	13.88	11.06	11.46	10.51
Cr_2O_3	b.d.	0.05	0.02	b.d.	0.02	0.01	0.01	0.03	b.d.	0.04	0.08	0.05	b.d.
MnO	0.37	0.20	0.26	0.18	0.21	0.18	0.22	0.16	0.23	0.23	0.15	0.14	0.06
MgO	19.64	14.62	15.87	14.57	16.10	15.43	15.02	15.04	18.16	14.24	15.35	15.32	16.66
CaO	7.43	11.14	10.87	11.22	11.49	11.14	10.83	11.20	10.82	10.97	10.47	11.94	12.57
Na_2O	1.01	1.55	0.53	1.34	0.40	1.46	0.83	1.38	0.71	1.06	1.34	1.64	1.19
K_2O	0.08	0.13	0.07	0.13	0.05	0.12	0.13	0.12	0.04	0.17	0.15	0.23	0.11
F	0.04	b.d.	b.d.	0.02	b.d.	b.d.	b.d.	0.02	b.d.	b.d.	b.d.	0.05	b.d.
Cl	0.15	0.07	0.08	0.08	0.06	0.06	0.11	0.08	0.06	0.16	0.14	0.06	0.10
Total	99.52	96.61	96.17	96.83	96.61	97.24	96.14	97.09	96.59	97.08	96.17	97.68	98.50
Si	6.90	6.48	7.44	6.59	7.48	6.54	7.16	6.51	7.27	6.94	6.80	6.26	6.77
Al^{IV}	1.10	1.52	0.56	1.41	0.52	1.46	0.84	1.49	0.73	1.07	1.20	1.74	1.23
Al^{VI}	0.27	0.08	0.16	0.12	0.15	0.10	0.23	0.11	0.18	0.33	0.44	0.10	0.21
Cr	-	0.01	0.00	-	0.00	0.00	0.00	0.00	-	0.01	0.01	0.01	-
Fe^{3+}	0.50	0.82	0.18	0.76	0.20	0.49	0.26	0.84	0.25	0.19	0.00	0.74	0.63
Ti	0.02	0.22	0.03	0.20	0.03	0.22	0.04	0.21	0.05	0.11	0.18	0.28	0.08
Mg	4.08	3.18	3.46	3.16	3.48	3.35	3.30	3.24	3.88	3.11	3.35	3.29	3.51
Fe^{2+}	0.98	0.80	1.44	0.86	1.33	1.08	1.44	0.71	0.95	1.51	1.36	0.64	0.62
Mn	0.04	0.02	0.03	0.02	0.03	0.02	0.03	0.02	0.03	0.03	0.02	0.02	0.01
Ca	1.11	1.74	1.70	1.75	1.79	1.74	1.71	1.74	1.66	1.72	1.64	1.84	1.90
Na	0.272	0.437	0.15	0.377	0.11	0.414	0.24	0.387	0.20	0.30	0.381	0.459	0.327
K	0.01	0.02	0.01	0.03	0.01	0.02	0.02	0.02	0.01	0.03	0.03	0.04	0.02
Cations	15.29	15.32	15.16	15.27	15.12	15.44	15.26	15.27	15.21	15.33	15.41	15.42	15.30
Cl	0.03	0.02	0.02	0.02	0.02	0.01	0.03	0.02	0.02	0.04	0.03	0.02	0.03
F	0.02	-	-	0.01	-	-	-	0.01	-	-	-	0.03	-

Appendix B7. Amphibole Analyses (continued)

Sample	106-2-11A1	106-2-11A2	106-2-11A3	106-2-11A3	106-2-11A4	106-2-11A4	106-2-11A5	106-2-11B1	106-2-11B2	106-2-11B3	106-2-11B4	106-2-11D4	106-2-11D5
Occurrence	int	int	vei	int	int	int	int	int	int	int	int	int	int
Rock Type	PG	PG	PG	PG	PG	PG	PG	PG	PG	PG	PG	PG	PG
Analysis	ave	ave	ave	ave	ave	15N	ave	15N	15N	ave	15NK	15NK	15NK
Location	UofA	UofA	OSU	UofA	OSU	UofA	OSU	UofA	UofA	OSU	OSU	OSU	OSU
SiO_2	42.94	44.19	47.58	44.08	44.53	51.23	45.34	51.80	51.37	43.72	43.03	48.97	47.88
TiO_2	2.29	2.37	0.31	2.28	2.50	0.20	2.19	0.07	0.07	2.34	2.56	1.00	1.44
Al_2O_3	10.75	10.25	6.79	10.34	10.40	3.60	9.31	1.97	1.92	10.31	10.43	5.31	6.88
FeO^T	15.46	13.03	19.12	13.08	14.05	15.90	13.77	18.72	18.49	13.31	13.18	17.12	15.89
Cr_2O_3	0.03	b.d.	0.03	b.d.	0.02	b.d.	0.01	b.d.	b.d.	0.01	0.02	b.d.	b.d.
MnO	0.41	0.26	0.47	0.30	0.27	0.38	0.27	0.64	0.61	0.27	0.26	0.42	0.41
MgO	12.25	14.17	10.86	13.87	13.94	12.94	14.60	11.59	11.51	14.46	14.40	13.33	14.23
CaO	10.80	10.96	11.76	10.78	11.10	11.90	10.93	11.81	11.70	11.09	11.03	10.90	10.93
Na_2O	1.72	1.76	0.64	1.48	1.94	0.26	1.60	0.14	0.13	1.43	1.79	0.65	0.97
K_2O	0.14	0.17	0.09	0.11	0.10	0.05	0.10	0.05	0.03	0.13	0.11	0.08	0.09
F	b.d.	b.d.	0.09	b.d.	0.09	b.d.	0.17	b.d.	b.d.	b.d.	0.02	b.d.	b.d.
Cl	0.04	0.05	0.02	0.04	0.06	0.01	0.07	b.d.	0.01	0.05	0.04	0.08	0.07
Total	96.80	97.21	97.72	96.36	98.98	96.47	98.34	96.79	95.84	97.12	96.85	97.86	98.79
Si	6.35	6.43	7.03	6.45	6.40	7.59	6.52	7.75	7.76	6.34	6.34	7.19	6.93
Al^{IV}	1.65	1.57	0.97	1.55	1.60	0.41	1.48	0.25	0.25	1.66	1.66	0.81	1.07
Al^{VI}	0.22	0.19	0.21	0.23	0.16	0.22	0.09	0.09	0.10	0.10	0.15	0.10	0.10
Cr	0.00	-	0.00	-	0.00	-	0.00	-	-	0.00	0.00	-	-
Fe^{3+}	0.71	0.65	0.63	0.71	0.65	0.07	0.79	0.09	0.09	0.92	0.41	0.29	0.36
Ti	0.26	0.26	0.04	0.25	0.27	0.02	0.24	0.01	0.01	0.26	0.28	0.11	0.16
Mg	2.70	3.07	2.39	3.03	2.99	2.86	3.13	2.58	2.59	3.13	3.16	2.92	3.07
Fe^{2+}	1.20	0.94	1.73	0.90	1.04	1.90	0.87	2.25	2.25	0.70	1.22	1.82	1.56
Mn	0.05	0.03	0.06	0.04	0.03	0.05	0.03	0.08	0.08	0.03	0.03	0.05	0.05
Ca	1.71	1.71	1.86	1.69	1.71	1.89	1.68	1.89	1.89	1.72	1.74	1.71	1.70
Na	0.49	0.50	0.184	0.42	0.54	0.08	0.445	0.04	0.04	0.402	0.512	0.186	0.273
K	0.03	0.03	0.02	0.02	0.02	0.01	0.02	0.01	0.01	0.02	0.02	0.02	0.02
Cations	15.37	15.37	15.13	15.28	15.41	15.08	15.30	15.05	15.04	15.28	15.53	15.20	15.29
Cl	0.01	0.01	0.00	0.01	0.01	0.00	0.02	-	0.00	0.01	0.01	0.02	0.02
F	-	-	0.04	-	0.04	-	0.08	-	-	-	0.01	-	-

Appendix B7. Amphibole Analyses (continued)

Sample	106-2-11D6	106-2-11D7	106-2-11D8	106-2-11D9	106-2-11D10	107-1-14A1	107-1-14A2	107-1-14A3	107-1-14B1	107-1-14B2	107-1-14B3	107-1-14B4	107-1-14B5
Occurrence	int	int	int	int	int	after cpx	after cpx	after cpx	after cpx	after cpx	after cpx	after cpx	after cpx
Rock Type	PG	PG	PG	PG	PG	basalt	basalt	basalt	basalt	basalt	basalt	basalt	basalt
Analysis	15NK	15NK	15NK	15NK	15NK	15NK	15NK	15NK	15NK	15NK	15NK	15NK	15NK
Location	OSU	OSU	OSU	OSU	OSU	UofA	UofA	UofA	UofA	UofA	UofA	UofA	UofA
SiO_2	47.26	46.22	47.12	49.22	48.19	51.40	51.60	51.69	50.36	52.09	51.19	51.48	51.72
TiO_2	1.29	1.89	1.54	0.60	1.40	0.28	0.25	0.24	0.23	0.28	0.25	0.23	0.25
Al_2O_3	6.51	8.22	6.98	5.17	7.12	4.38	4.11	4.10	5.04	3.50	4.61	4.20	4.23
FeO^T	16.57	15.04	15.04	15.56	15.04	14.71	14.68	14.50	15.20	14.42	14.66	14.62	14.16
Cr_2O_3	b.d.	b.d.	0.01	b.d.	b.d.	0.02	0.04	0.05	b.d.	b.d.	b.d.	0.01	0.01
MnO	0.33	0.31	0.39	0.28	0.42	0.29	0.26	0.29	0.28	0.26	0.27	0.27	0.29
MgO	13.26	14.06	14.48	13.93	14.34	14.56	14.65	14.80	13.67	14.87	14.56	14.78	15.00
CaO	11.85	10.90	11.00	11.90	10.93	11.57	11.70	11.71	11.52	11.72	11.74	11.70	11.60
Na_2O	0.68	1.50	1.21	0.50	1.14	0.30	0.29	0.28	0.36	0.23	0.35	0.29	0.34
K_2O	0.16	0.09	0.07	0.16	0.07	0.07	0.07	0.06	0.07	0.08	0.06	0.07	0.07
F	0.13	0.11	0.09	0.06	0.14	b.d.	b.d.	b.d.	0.01	b.d.	b.d.	b.d.	b.d.
Cl	0.14	0.05	0.05	0.18	0.07	0.05	0.03	0.02	0.05	0.02	0.04	0.03	0.01
Total	98.20	98.37	97.97	97.54	98.86	97.61	97.64	97.69	96.79	97.47	97.73	97.67	97.67
Si	6.92	6.74	6.88	7.20	6.97	7.45	7.48	7.48	7.40	7.56	7.41	7.45	7.48
Al^{IV}	1.08	1.26	1.12	0.80	1.03	0.55	0.52	0.53	0.60	0.45	0.59	0.55	0.52
Al^{VI}	0.04	0.16	0.08	0.09	0.19	0.20	0.18	0.17	0.27	0.15	0.20	0.17	0.20
Cr	-	-	0.00	-	-	0.00	0.01	0.01	-	-	-	0.00	0.00
Fe^{3+}	0.54	0.25	0.35	0.41	0.20	0.18	0.19	0.20	0.17	0.15	0.22	0.24	0.17
Ti	0.14	0.21	0.17	0.07	0.15	0.03	0.03	0.03	0.03	0.03	0.03	0.03	0.03
Mg	2.89	3.06	3.15	3.04	3.09	3.15	3.16	3.19	2.99	3.22	3.14	3.19	3.23
Fe^{2+}	1.49	1.59	1.48	1.50	1.62	1.60	1.59	1.55	1.70	1.60	1.55	1.53	1.55
Mn	0.04	0.04	0.05	0.03	0.05	0.04	0.03	0.04	0.04	0.03	0.03	0.03	0.04
Ca	1.86	1.70	1.72	1.87	1.70	1.80	1.82	1.81	1.81	1.82	1.82	1.81	1.80
Na	0.193	0.424	0.341	0.14	0.32	0.084	0.081	0.079	0.103	0.065	0.098	0.081	0.095
K	0.03	0.02	0.01	0.03	0.01	0.01	0.01	0.01	0.01	0.02	0.01	0.01	0.01
Cations	15.22	15.44	15.36	15.17	15.33	15.10	15.09	15.09	15.12	15.08	15.11	15.09	15.11
Cl	0.04	0.01	0.01	0.04	0.02	0.01	0.01	0.01	0.01	0.01	0.01	0.01	0.00
F	0.06	0.05	0.04	0.03	0.06	-	-	-	0.01	-	-	-	-

Appendix B7. Amphibole Analyses (continued)

Sample	107-1-14C1	107-1-14C2	107-1-14C3	108-1-6A1	108-1-6A2	108-1-6A3	108-1-6A4	108-1-6A5	108-1-6B1	108-1-6B2	108-1-6B3	108-1-6C1	108-1-6C2	108-1-6D1
Occurrence	after cpx	after cpx	after cpx	cpx rim	cpx rim	cpx rim	cpx inc	cpx inc	cpx rim	cpx rim	cpx inc	cpx rim	cpx inc	cpx rim
Rock Type	basalt	basalt	basalt	gabbro	gabbro	gabbro	gabbro	gabbro	gabbro	gabbro	gabbro	gabbro	gabbro	gabbro
Analysis	15NK	15NK	15NK	ave	15NK	ave	ave	ave	15NK	15NK	15NK	ave	ave	15NK
Location	UofA	UofA	UofA	UofA	UofA	UofA	UofA	UofA	UofA	UofA	UofA	UofA	UofA	UofA
SiO_2	52.17	50.98	51.12	52.02	53.32	51.10	48.78	49.40	55.59	54.33	52.65	51.91	48.13	56.26
TiO_2	0.36	0.22	0.21	0.18	0.22	0.24	0.61	0.68	0.08	0.21	0.28	0.23	0.59	0.10
Al_2O_3	3.82	4.64	4.37	5.31	3.85	6.03	8.57	7.89	1.79	3.26	4.88	5.57	8.93	1.17
FeO^T	14.76	14.93	14.82	7.37	6.71	7.56	7.49	7.38	6.02	6.75	5.86	6.97	7.25	6.31
Cr_2O_3	b.d.	b.d.	0.01	0.05	0.11	0.08	0.06	0.23	0.09	0.06	0.05	0.09	0.11	0.03
MnO	0.26	0.27	0.27	0.08	0.08	0.11	0.08	0.08	0.11	0.10	0.08	0.08	0.05	0.16
MgO	14.76	14.35	14.44	18.90	20.10	18.66	18.25	18.43	21.10	19.95	20.31	19.31	18.15	21.33
CaO	11.72	11.73	11.64	12.57	12.54	12.32	12.22	12.33	12.24	12.67	12.48	12.38	12.18	12.22
Na_2O	0.26	0.38	0.31	0.70	0.49	0.88	1.25	1.22	0.21	0.39	0.72	0.78	1.30	0.11
K_2O	0.09	0.06	0.07	0.06	0.06	0.07	0.14	0.02	0.05	0.07	0.04	0.08	0.11	0.03
F	b.d.	b.d.	b.d.	b.d.	b.d.	b.d.	b.d.	b.d.	b.d.	b.d.	b.d.	b.d.	b.d.	b.d.
Cl	0.03	0.03	0.02	b.d.	b.d.	0.02	0.02	b.d.	b.d.	b.d.	b.d.	0.01	b.d.	b.d.
Total	98.23	97.59	97.27	97.19	97.37	96.99	97.41	97.43	97.19	97.73	97.30	97.32	96.69	97.69
Si	7.52	7.40	7.44	7.31	7.46	7.20	6.86	6.93	7.76	7.59	7.36	7.26	6.81	7.81
Al^{IV}	0.48	0.60	0.56	0.69	0.54	0.80	1.14	1.07	0.25	0.41	0.64	0.74	1.19	0.19
Al^{VI}	0.17	0.20	0.19	0.19	0.10	0.21	0.28	0.24	0.05	0.12	0.17	0.18	0.30	0.00
Cr	-	-	0.00	0.01	0.01	0.01	0.01	0.03	0.01	0.01	0.01	0.01	0.01	0.00
Fe^{3+}	0.15	0.23	0.22	0.37	0.24	0.43	0.52	0.48	0.10	0.12	0.20	0.43	0.53	0.13
Ti	0.04	0.02	0.02	0.02	0.02	0.03	0.07	0.07	0.01	0.02	0.03	0.02	0.06	0.01
Mg	3.17	3.11	3.13	3.96	4.19	3.92	3.83	3.86	4.39	4.15	4.23	4.03	3.83	4.42
Fe^{2+}	1.63	1.58	1.58	0.50	0.55	0.46	0.36	0.39	0.60	0.67	0.48	0.39	0.33	0.61
Mn	0.03	0.03	0.03	0.01	0.01	0.01	0.01	0.01	0.01	0.01	0.01	0.01	0.01	0.02
Ca	1.81	1.83	1.82	1.89	1.88	1.86	1.84	1.85	1.83	1.90	1.87	1.86	1.85	1.82
Na	0.073	0.107	0.087	0.191	0.133	0.24	0.341	0.332	0.057	0.106	0.195	0.212	0.356	0.03
K	0.02	0.01	0.01	0.01	0.01	0.01	0.03	0.00	0.01	0.01	0.01	0.01	0.02	0.01
Cations	15.09	15.12	15.10	15.14	15.14	15.18	15.28	15.26	15.07	15.12	15.20	15.15	15.30	15.04
Cl	0.01	0.01	0.01	-	-	0.01	0.01	-	-	-	-	0.00	-	-
F	-	-	-	-	-	-	-	-	-	-	-	-	-	-

Appendix B7. Amphibole Analyses (continued)

Sample	108-1-6D2	108-1-6D3	108-2-6A1	108-2-6B1	108-2-6B2	108-2-6C1	108-3-1E1	108-3-1E2	108-3-1F1	108-2-12E1	108-2-12E2	108-2-12E3	108-2-12E4	108-3-15A1
Occurrence	after cpx	after cpx	patchy	cpx rim	cpx rim	cpx rim	after cpx	after cpx	after cpx	after cpx	after cpx	after cpx	after cpx	after cpx
Rock Type	gabbro	gabbro	gabbro	gabbro	gabbro	gabbro	basalt	basalt	basalt	PG	PG	PG	PG	basalt
Analysis	ave	ave	ave	ave	ave	ave	15NK	15NK	15NK	15NK	15NK	15NK	ave	15NK
Location	UofA	UofA	UofA	UofA	UofA	UofA	UofA	UofA	UofA	UofA	UofA	UofA	UofA	UofA
SiO_2	51.26	51.71	46.18	49.09	52.12	46.13	50.70	50.35	51.79	45.57	44.35	49.07	43.50	51.82
TiO_2	0.30	0.26	0.13	0.39	0.21	0.68	0.29	0.35	0.39	0.99	0.97	1.14	0.34	0.42
Al_2O_3	6.45	5.83	12.94	8.43	4.99	10.89	3.14	3.61	3.27	4.96	5.41	3.11	10.53	3.98
FeO^T	8.13	7.56	6.61	7.45	5.87	7.46	20.34	23.29	20.75	29.10	28.58	26.02	23.91	14.82
Cr_2O_3	0.07	0.09	0.03	0.34	0.30	0.34	0.05	0.01	0.05	0.02	b.d.	b.d.	0.01	b.d.
MnO	0.11	0.13	0.09	0.11	0.06	0.10	0.37	0.56	0.46	0.45	0.46	0.48	0.27	0.32
MgO	18.15	18.68	17.40	18.43	20.02	17.18	11.09	8.77	12.33	4.86	4.69	8.22	6.50	14.84
CaO	12.15	12.27	11.83	12.29	12.45	12.32	11.32	11.37	9.24	9.92	9.92	9.54	11.10	11.59
Na_2O	0.78	0.64	1.81	1.32	0.82	1.88	0.35	0.34	0.58	0.52	0.61	0.23	1.06	0.40
K_2O	0.08	0.06	0.12	0.06	0.06	0.11	0.06	0.08	0.05	0.60	0.73	0.37	0.34	0.10
F	b.d.	b.d.	b.d.	b.d.	b.d.	b.d.	0.08	0.08	0.08	b.d.	b.d.	b.d.	b.d.	0.05
Cl	0.02	0.01	0.19	b.d.	0.02	0.01	0.02	0.01	0.13	0.56	0.55	0.22	0.50	0.06
Total	97.43	97.15	97.30	97.57	96.62	96.76	97.76	98.81	99.07	97.53	96.27	98.40	98.05	98.40
Si	7.20	7.26	6.50	6.87	7.30	6.57	7.56	7.55	7.62	7.21	7.13	7.49	6.62	7.47
Al^{IV}	0.80	0.74	1.50	1.13	0.70	1.43	0.44	0.45	0.38	0.79	0.88	0.51	1.39	0.53
Al^{VI}	0.27	0.22	0.64	0.26	0.13	0.40	0.11	0.18	0.18	0.14	0.15	0.05	0.50	0.15
Cr	0.01	0.01	0.00	0.04	0.03	0.04	0.01	0.00	0.01	0.00	-	-	0.00	-
Fe^{3+}	0.41	0.43	0.48	0.54	0.40	0.44	0.15	0.08	0.00	0.13	0.15	0.05	0.63	0.16
Ti	0.03	0.03	0.01	0.04	0.02	0.07	0.03	0.04	0.04	0.12	0.12	0.13	0.04	0.05
Mg	3.80	3.91	3.65	3.85	4.18	3.65	2.46	1.96	2.70	1.15	1.12	1.87	1.47	3.19
Fe^{2+}	0.54	0.45	0.30	0.33	0.29	0.45	2.38	2.84	2.55	3.72	3.69	3.27	2.41	1.63
Mn	0.01	0.02	0.01	0.01	0.01	0.01	0.05	0.07	0.06	0.06	0.06	0.06	0.04	0.04
Ca	1.83	1.85	1.78	1.84	1.87	1.88	1.81	1.83	1.46	1.68	1.71	1.56	1.81	1.79
Na	0.213	0.174	0.494	0.358	0.223	0.519	0.101	0.099	0.165	0.16	0.19	0.068	0.313	0.112
K	0.01	0.01	0.02	0.01	0.01	0.02	0.01	0.02	0.01	0.12	0.15	0.07	0.07	0.02
Cations	15.14	15.10	15.40	15.29	15.16	15.48	15.11	15.11	15.18	15.28	15.34	15.14	15.28	15.13
Cl	0.01	0.00	0.05	-	0.01	0.00	0.01	0.00	0.03	0.15	0.15	0.06	0.13	0.02
F	-	-	-	-	-	-	0.04	0.04	0.04	-	-	-	-	0.02

Appendix B7. Amphibole Analyses (continued)

Sample	108-3-15A2	108-3-15A3	108-3-15B1	108-3-15B2	108-3-15B3	108-3-15B4	108-3-15D1	108-3-15D2	108-3-15D3	108-3-16A1	108-3-16A2	108-3-16A3	108-3-16A4
Occurrence	after cpx	after cpx	after cpx	after cpx	after cpx	after cpx	after cpx	after cpx	after cpx	patchy	patchy	patchy	patchy
Rock Type	basalt	basalt	basalt	basalt	basalt	basalt	basalt	basalt	basalt	epidosite	epidosite	epidosite	epidosite
Analysis	15NK	15NK	15NK	15NK	15NK	15NK	15NK	15NK	15NK	15NK	15NK	15NK	15NK
Location	UofA	UofA	UofA	UofA	UofA	UofA	UofA	UofA	UofA	UofA	UofA	UofA	UofA
SiO_2	51.11	51.20	50.56	50.55	49.74	49.80	50.95	52.26	50.81	50.39	51.07	51.84	49.97
TiO_2	0.47	0.52	0.61	0.54	0.59	0.57	0.63	0.58	0.63	0.59	0.72	0.61	1.02
Al_2O_3	4.15	4.36	4.69	4.78	5.52	5.13	4.57	3.34	4.46	3.17	3.36	2.24	3.02
FeO^T	14.81	14.63	15.21	15.41	15.63	15.51	15.10	14.61	15.00	19.34	18.11	17.64	18.65
Cr_2O_3	0.02	0.01	0.06	0.01	0.04	0.06	0.02	b.d.	b.d.	0.02	b.d.	b.d.	b.d.
MnO	0.31	0.30	0.35	0.33	0.35	0.33	0.30	0.38	0.32	0.32	0.31	0.37	0.28
MgO	14.71	15.02	14.34	14.24	13.76	14.02	14.48	15.27	14.51	13.40	13.68	14.65	13.20
CaO	11.44	10.88	11.22	11.32	11.26	11.29	11.29	11.06	11.15	8.52	9.25	8.20	9.19
Na_2O	0.44	0.41	0.69	0.69	0.81	0.81	0.62	0.44	0.58	1.32	1.14	2.06	2.02
K_2O	0.11	0.10	0.15	0.14	0.15	0.14	0.13	0.12	0.11	0.25	0.28	0.32	0.39
F	0.04	0.05	b.d.	0.03	0.03	0.08	0.02	0.02	0.02	0.23	0.16	1.06	0.91
Cl	0.07	0.07	0.11	0.09	0.09	0.13	0.11	0.11	0.12	0.17	0.15	0.08	0.08
Total	97.66	97.54	97.93	98.12	97.93	97.81	98.20	98.19	97.71	97.70	98.23	99.07	98.73
Si	7.43	7.44	7.36	7.35	7.27	7.28	7.39	7.55	7.41	7.55	7.56	7.73	7.52
Al^{IV}	0.57	0.56	0.64	0.65	0.73	0.72	0.61	0.45	0.60	0.45	0.44	0.27	0.48
Al^{VI}	0.14	0.18	0.17	0.17	0.22	0.17	0.17	0.12	0.17	0.11	0.15	0.12	0.06
Cr	0.00	0.00	0.01	0.00	0.01	0.01	0.00	-	-	0.00	-	-	-
Fe^{3+}	0.18	0.13	0.11	0.14	0.12	0.16	0.10	0.05	0.10	0.00	0.00	0.00	0.00
Ti	0.05	0.06	0.07	0.06	0.07	0.06	0.07	0.06	0.07	0.07	0.08	0.07	0.12
Mg	3.19	3.25	3.11	3.09	3.00	3.06	3.13	3.29	3.15	2.99	3.02	3.26	2.96
Fe^{2+}	1.62	1.65	1.75	1.74	1.79	1.74	1.74	1.71	1.73	2.42	2.24	2.20	2.35
Mn	0.04	0.04	0.04	0.04	0.04	0.04	0.04	0.05	0.04	0.04	0.04	0.05	0.04
Ca	1.78	1.69	1.75	1.76	1.76	1.77	1.76	1.71	1.74	1.37	1.47	1.31	1.48
Na	0.124	0.115	0.195	0.195	0.229	0.23	0.174	0.123	0.164	0.383	0.327	0.595	0.59
K	0.02	0.02	0.03	0.03	0.03	0.03	0.02	0.02	0.02	0.05	0.05	0.06	0.08
Cations	15.14	15.13	15.22	15.22	15.26	15.26	15.20	15.15	15.18	15.43	15.38	15.66	15.66
Cl	0.02	0.02	0.03	0.02	0.02	0.03	0.03	0.03	0.03	0.04	0.04	0.02	0.02
F	0.02	0.02	-	0.01	0.01	0.04	0.01	0.01	0.01	0.11	0.08	0.50	0.43

Appendix B7. Amphibole Analyses (continued)

Sample	108-3-16A5	108-3-16C1	108-3-16D1	108-3-16D2	108-3-16D3	108-3-16D5	108-3-16D6	108-3-16D7	108-3-17A1	108-3-17A3	108-3-17A4	108-3-17A5	108-3-17A6
Occurrence	patchy	patchy	patchy	patchy	patchy	patchy	patchy	patchy	after cpx	after cpx	after cpx	after cpx	after cpx
Rock Type	epidosite	epidosite	epidosite	epidosite	epidosite	epidosite	epidosite	epidosite	PG	PG	PG	PG	PG
Analysis	15NK	15NK	15NK	15NK	15NK	15NK	15NK	15NK	15NK	15NK	15NK	15NK	15NK
Location	UofA	UofA	UofA	UofA	UofA	UofA	UofA	UofA	UofA	UofA	UofA	UofA	UofA
SiO_2	50.51	51.25	50.81	51.27	51.07	52.27	51.07	51.99	49.62	45.27	48.72	48.40	48.71
TiO_2	0.63	0.82	0.73	0.83	0.66	0.83	0.97	0.62	0.64	1.46	0.46	0.42	0.45
Al_2O_3	3.37	2.54	2.39	2.70	2.78	2.66	3.20	2.35	3.83	7.86	5.19	5.47	5.15
FeO^T	20.08	16.77	17.33	17.05	17.91	17.27	17.15	16.86	19.29	20.15	18.76	19.09	18.99
Cr_2O_3	b.d.	b.d.	b.d.	b.d.	0.01	0.01	b.d.	0.01	0.03	0.01	b.d.	b.d.	0.04
MnO	0.32	0.27	0.30	0.28	0.33	0.28	0.27	0.33	0.40	0.33	0.30	0.31	0.34
MgO	13.22	14.67	13.71	14.25	14.09	14.23	13.94	14.99	12.75	10.17	11.81	11.63	11.95
CaO	8.70	8.73	9.47	8.78	8.61	9.71	9.68	8.24	9.58	10.98	11.10	11.06	11.00
Na_2O	1.17	2.22	0.94	2.45	2.16	1.01	1.57	2.39	0.55	0.77	0.58	0.87	0.77
K_2O	0.27	0.36	0.24	0.39	0.37	0.22	0.34	0.36	0.17	0.26	0.19	0.20	0.18
F	0.13	1.11	0.03	1.21	1.00	0.10	0.48	1.24	b.d.	b.d.	b.d.	b.d.	b.d.
Cl	0.22	0.07	0.09	0.03	0.08	0.08	0.06	0.07	0.16	0.31	0.24	0.36	0.28
Total	98.62	98.81	96.04	99.24	99.06	98.66	98.73	99.44	96.99	97.56	97.35	97.81	97.82
Si	7.50	7.66	7.66	7.67	7.64	7.66	7.56	7.74	7.42	6.81	7.26	7.22	7.24
Al^{IV}	0.50	0.34	0.34	0.33	0.37	0.34	0.44	0.26	0.59	1.19	0.74	0.78	0.76
Al^{VI}	0.09	0.11	0.08	0.15	0.12	0.12	0.12	0.15	0.09	0.20	0.17	0.18	0.14
Cr	-	-	-	-	0.00	0.00	-	0.00	0.00	0.00	-	-	0.01
Fe^{3+}	0.00	0.00	0.00	0.00	0.00	0.00	0.00	0.00	0.16	0.38	0.26	0.22	0.26
Ti	0.07	0.09	0.08	0.09	0.07	0.09	0.11	0.07	0.07	0.17	0.05	0.05	0.05
Mg	2.93	3.27	3.08	3.18	3.14	3.11	3.08	3.33	2.84	2.28	2.63	2.59	2.65
Fe^{2+}	2.49	2.10	2.19	2.14	2.24	2.12	2.12	2.10	2.25	2.16	2.08	2.16	2.10
Mn	0.04	0.03	0.04	0.04	0.04	0.04	0.03	0.04	0.05	0.04	0.04	0.04	0.04
Ca	1.38	1.40	1.53	1.41	1.38	1.53	1.54	1.31	1.53	1.77	1.77	1.77	1.75
Na	0.337	0.644	0.275	0.711	0.626	0.287	0.451	0.69	0.159	0.225	0.168	0.252	0.222
K	0.05	0.07	0.05	0.07	0.07	0.04	0.06	0.07	0.03	0.05	0.04	0.04	0.03
Cations	15.39	15.71	15.32	15.79	15.70	15.33	15.52	15.76	15.19	15.28	15.20	15.29	15.26
Cl	0.06	0.02	0.02	0.01	0.02	0.02	0.02	0.02	0.04	0.08	0.06	0.09	0.07
F	0.06	0.53	0.01	0.57	0.47	0.05	0.23	0.58	-	-	-	-	-

Appendix B7. Amphibole Analyses (continued)

Sample	108-3-17A7	108-3-17C1	108-3-17C2	108-3-17C3	108-3-17E1	108-3-17E2	110-1-15B1	110-1-15B2	110-1-15C1	110-1-15C2	110-1-15C3	110-1-15C4	110-1-15D1	110-1-15E1
Occurrence	after cpx	after cpx	after cpx	after cpx	after cpx	after cpx	vei	vei	after cpx	after cpx	vei	after cpx	patchy	patchy
Rock Type	PG	PG	PG	PG	PG	PG	basalt	basalt	basalt	basalt	basalt	basalt	basalt	basalt
Analysis	15NK	15NK	ave	15NK	15NK	15NK	15NK	15NK	ave	15NK	15NK	15NK	15NK	15NK
Location	UofA	UofA	UofA	UofA	UofA	UofA	UofA	UofA	UofA	UofA	UofA	UofA	UofA	UofA
SiO_2	48.62	48.26	47.11	48.88	49.25	48.39	51.92	52.18	48.25	45.56	49.37	49.04	52.10	50.45
TiO_2	0.48	0.38	0.71	0.38	0.79	0.46	0.05	0.02	1.39	2.09	1.17	0.91	0.09	0.09
Al_2O_3	5.23	5.10	5.87	4.59	3.86	5.60	0.96	0.97	6.22	8.23	5.01	5.32	2.06	3.99
FeO^T	18.89	18.62	19.78	18.83	18.35	19.92	22.55	22.15	17.17	17.08	15.45	16.88	21.94	18.20
Cr_2O_3	b.d.	b.d.	b.d.	0.01	0.03	b.d.	0.01	0.01	0.03	0.02	0.04	0.25	0.01	0.04
MnO	0.34	0.25	0.34	0.34	0.44	0.34	0.64	0.58	0.20	0.21	0.19	0.25	0.39	0.25
MgO	11.90	11.57	10.82	11.97	12.70	11.26	9.11	9.16	12.66	12.77	14.08	13.37	9.61	12.12
CaO	11.01	11.11	11.28	11.22	10.52	11.26	12.28	12.12	10.33	9.73	10.57	10.42	11.93	12.00
Na_2O	0.77	0.74	0.79	0.63	0.62	0.81	0.04	0.03	1.46	2.66	1.41	1.12	0.16	0.39
K_2O	0.15	0.17	0.25	0.19	0.15	0.22	0.05	0.05	0.23	0.21	0.16	0.19	0.11	0.13
F	b.d.	b.d.	b.d.	b.d.	b.d.	b.d.	b.d.	b.d.	b.d.	0.36	b.d.	0.03	b.d.	0.05
Cl	0.29	0.28	0.31	0.20	0.17	0.25	0.02	0.01	0.13	0.21	0.10	0.09	0.01	b.d.
Total	97.68	96.48	97.26	97.23	96.85	98.51	97.62	97.27	98.04	99.11	97.51	97.62	98.40	97.67
Si	7.24	7.28	7.05	7.30	7.36	7.18	7.85	7.91	7.06	6.78	7.29	7.24	7.79	7.45
Al^{IV}	0.76	0.72	0.95	0.70	0.64	0.82	0.15	0.09	0.94	1.22	0.71	0.76	0.22	0.55
Al^{VI}	0.16	0.18	0.08	0.10	0.04	0.16	0.02	0.08	0.13	0.23	0.16	0.16	0.15	0.14
Cr	-	-	-	0.00	0.00	-	0.00	0.00	0.00	0.00	0.01	0.03	0.00	0.01
Fe^{3+}	0.25	0.21	0.64	0.29	0.21	0.29	0.10	0.00	0.53	0.00	0.00	0.01	0.00	0.25
Ti	0.05	0.04	0.08	0.04	0.09	0.05	0.01	0.00	0.15	0.23	0.13	0.10	0.01	0.01
Mg	2.64	2.60	2.41	2.66	2.83	2.49	2.05	2.07	2.76	2.83	3.10	2.94	2.14	2.67
Fe^{2+}	2.10	2.14	1.83	2.06	2.09	2.18	2.75	2.81	1.57	2.13	1.91	2.08	2.74	2.00
Mn	0.04	0.03	0.04	0.04	0.06	0.04	0.08	0.08	0.03	0.03	0.02	0.03	0.05	0.03
Ca	1.76	1.80	1.81	1.80	1.69	1.79	1.99	1.97	1.62	1.55	1.67	1.65	1.91	1.90
Na	0.222	0.216	0.229	0.182	0.18	0.233	0.012	0.009	0.414	0.768	0.404	0.321	0.046	0.112
K	0.03	0.03	0.05	0.04	0.03	0.04	0.01	0.01	0.04	0.04	0.03	0.04	0.02	0.02
Cations	15.25	15.25	15.17	15.22	15.21	15.28	15.02	15.02	15.26	15.81	15.43	15.36	15.07	15.14
Cl	0.07	0.07	0.08	0.05	0.04	0.06	0.01	0.00	0.03	0.05	0.03	0.02	0.00	-
F	-	-	-	-	-	-	-	-	-	0.17	-	0.01	-	0.02

Appendix B7. Amphibole Analyses (continued)

Sample	110-1-15E2	110-1-15F1	110-1-25A1	110-1-25A2	110-1-25A5	110-1-25C1	110-1-25C2	111-4-3A3	111-4-3B3	111-4-3C1	111-4-6A1	111-4-6A3	111-4-6A4	111-4-6B1
Occurrence	patchy	patchy	patchy	patchy	patchy	patchy	patchy	after cpx	patchy	cpx inc	after cpx	after cpx	after cpx	after cpx
Rock Type	basalt	basalt	basalt	basalt	basalt	basalt	basalt	gabbro	gabbro	gabbro	gabbro	gabbro	gabbro	gabbro
Analysis	15NK	ave	ave	15NK	15NK	15NK	15NK	15NK	15NK	15NK	15NK	15NK	15NK	ave
Location	UofA	UofA	UofA	UofA	UofA	UofA	UofA	OSU	OSU	OSU	UofA	UofA	UofA	UofA
SiO_2	52.16	50.02	48.53	50.20	50.43	51.80	47.72	52.93	51.78	52.42	51.98	48.68	52.94	47.12
TiO_2	0.09	0.07	1.12	0.86	0.64	0.15	0.59	0.06	0.08	0.17	0.39	0.74	0.10	1.25
Al_2O_3	2.60	4.45	7.32	3.55	2.83	1.68	4.17	3.97	4.19	5.26	3.45	6.41	3.01	7.24
FeO^T	18.14	18.05	11.16	18.79	21.27	21.56	25.69	9.09	11.50	9.89	12.46	14.15	12.23	14.80
Cr_2O_3	0.02	0.03	0.08	0.01	b.d.	b.d.	0.25	0.02	0.03	0.02	0.02	b.d.	0.01	0.05
MnO	0.22	0.20	0.16	0.24	0.39	0.16	0.29	0.28	0.38	0.30	0.23	0.27	0.27	0.22
MgO	12.13	11.96	16.46	13.40	13.62	9.75	8.87	20.50	17.05	18.13	17.21	15.11	17.43	13.50
CaO	11.99	12.11	10.99	9.09	7.20	11.62	8.19	9.85	12.34	11.98	11.08	11.16	11.22	11.57
Na_2O	0.25	0.42	1.36	0.97	0.89	0.17	1.04	0.32	0.32	0.47	0.41	1.00	0.34	0.94
K_2O	0.07	0.11	0.25	0.25	0.11	0.11	0.27	0.05	0.04	0.07	0.14	0.45	0.13	0.52
F	b.d.	b.d.	b.d.	b.d.	b.d.	b.d.	b.d.	0.04	b.d.	b.d.	b.d.	b.d.	b.d.	b.d.
Cl	0.01	0.02	0.09	0.13	0.14	0.01	0.22	0.03	0.05	0.04	0.09	0.22	0.09	0.22
Total	97.66	97.41	97.44	97.48	97.52	97.01	97.05	97.12	97.73	98.71	97.44	98.19	97.76	97.38
Si	7.70	7.38	6.93	7.48	7.54	7.85	7.38	7.45	7.37	7.34	7.46	7.07	7.56	6.90
Al^{IV}	0.30	0.62	1.07	0.52	0.46	0.16	0.62	0.55	0.63	0.66	0.54	0.93	0.44	1.10
Al^{VI}	0.15	0.15	0.16	0.10	0.03	0.15	0.14	0.10	0.07	0.21	0.05	0.16	0.07	0.15
Cr	0.00	0.00	0.01	0.00	-	-	0.03	0.00	0.00	0.00	0.00	-	0.00	0.01
Fe^{3+}	0.04	0.41	0.57	0.00	0.01	0.00	0.00	0.34	0.44	0.28	0.27	0.24	0.23	0.49
Ti	0.01	0.01	0.12	0.10	0.07	0.02	0.07	0.01	0.01	0.02	0.04	0.08	0.01	0.14
Mg	2.67	2.63	3.51	2.98	3.03	2.20	2.05	4.30	3.62	3.78	3.68	3.27	3.71	2.95
Fe^{2+}	2.20	1.82	0.76	2.34	2.65	2.73	3.32	0.73	0.93	0.88	1.23	1.47	1.23	1.32
Mn	0.03	0.03	0.02	0.03	0.05	0.02	0.04	0.03	0.05	0.04	0.03	0.03	0.03	0.03
Ca	1.90	1.91	1.68	1.45	1.15	1.89	1.36	1.49	1.88	1.80	1.70	1.74	1.72	1.82
Na	0.072	0.12	0.377	0.28	0.258	0.05	0.312	0.087	0.088	0.126	0.114	0.281	0.094	0.267
K	0.01	0.02	0.05	0.05	0.02	0.02	0.05	0.01	0.01	0.01	0.03	0.08	0.02	0.10
Cations	15.09	15.09	15.25	15.33	15.28	15.07	15.37	15.10	15.10	15.14	15.14	15.37	15.12	15.27
Cl	0.00	0.01	0.02	0.03	0.04	0.00	0.06	0.01	0.01	0.01	0.02	0.05	0.02	0.06
F	-	-	-	-	-	-	-	0.02	-	-	-	-	-	-

Appendix B7. Amphibole Analyses (continued)

Sample	111-4-6B2	111-4-6C2	111-4-6C3	111-4-6C4	112-2-1A1	112-2-1A2	112-2-1A3	112-2-1A4	112-2-1B1	112-2-1B2	112-2-1B3	112-2-1B4	112-2-1B5	112-2-1B6
Occurrence	after cpx	after cpx	after cpx	after cpx	cpx inc	cpx inc	cpx inc	cpx inc	patchy	patchy	patchy	patchy	patchy	patchy
Rock Type	gabbro	gabbro	gabbro	gabbro	gabbro	gabbro	gabbro	gabbro	gabbro	gabbro	gabbro	gabbro	gabbro	gabbro
Analysis	ave	15NK	ave	15NK	ave	ave	ave	ave	ave	ave	ave	ave	ave	ave
Location	UofA	UofA	UofA	UofA	UofA	UofA	UofA	UofA	UofA	UofA	UofA	UofA	UofA	UofA
SiO_2	48.40	48.26	47.31	48.27	46.27	44.17	45.54	44.07	42.63	50.59	42.63	50.87	47.76	49.37
TiO_2	0.95	1.25	1.52	1.29	1.04	1.46	1.30	1.54	b.d.	0.20	0.03	0.02	b.d.	0.03
Al_2O_3	6.06	6.36	6.99	6.26	10.57	12.02	11.35	12.10	16.07	5.80	15.35	4.54	10.56	5.25
FeO^T	14.82	14.16	14.63	13.94	5.60	5.73	5.70	5.70	7.49	9.29	8.18	14.12	5.88	15.70
Cr_2O_3	0.03	0.03	b.d.	0.01	1.20	1.43	1.19	1.23	b.d.	b.d.	b.d.	0.01	b.d.	0.03
MnO	0.23	0.25	0.22	0.25	0.08	0.05	0.09	0.07	0.08	0.13	0.11	0.31	0.11	0.31
MgO	13.77	14.83	14.03	14.87	18.00	17.35	17.63	17.44	15.61	17.11	15.38	13.71	18.00	12.66
CaO	11.77	10.89	11.11	10.85	11.86	11.81	11.80	11.80	12.39	12.55	12.53	12.53	12.38	12.31
Na_2O	0.65	1.07	1.02	0.94	2.11	2.42	2.23	2.40	2.65	0.84	2.55	0.52	1.85	0.81
K_2O	0.41	0.33	0.50	0.40	b.d.	0.08	0.05	0.20	0.07	0.05	0.06	0.05	0.04	0.04
F	b.d.	b.d.	b.d.	b.d.	b.d.	b.d.	b.d.	b.d.	b.d.	b.d.	b.d.	b.d.	b.d.	b.d.
Cl	0.17	0.18	0.23	0.17	b.d.	b.d.	b.d.	0.01	0.10	0.04	0.07	b.d.	0.04	0.01
Total	97.23	97.58	97.56	97.24	95.53	95.09	95.69	95.33	97.09	96.60	96.89	96.67	96.62	96.49
Si	7.08	7.06	6.90	7.08	6.58	6.34	6.49	6.32	6.10	7.25	6.13	7.46	6.77	7.32
Al^{IV}	0.92	0.94	1.10	0.92	1.42	1.67	1.52	1.68	1.90	0.75	1.87	0.54	1.23	0.68
Al^{VI}	0.12	0.16	0.10	0.16	0.35	0.37	0.39	0.36	0.81	0.23	0.73	0.24	0.54	0.23
Cr	0.00	0.00	-	0.00	0.14	0.16	0.13	0.14	-	-	-	0.00	-	0.00
Fe^{3+}	0.49	0.14	0.57	0.13	0.33	0.33	0.31	0.34	0.45	0.32	0.48	0.17	0.30	0.25
Ti	0.11	0.14	0.17	0.14	0.11	0.16	0.14	0.17	-	0.02	0.00	0.00	-	0.00
Mg	3.00	3.23	3.05	3.25	3.82	3.71	3.74	3.73	3.33	3.66	3.30	3.00	3.81	2.80
Fe^{2+}	1.32	1.59	1.21	1.58	0.33	0.35	0.37	0.34	0.45	0.80	0.51	1.57	0.40	1.70
Mn	0.03	0.03	0.03	0.03	0.01	0.01	0.01	0.01	0.01	0.02	0.01	0.04	0.01	0.04
Ca	1.84	1.71	1.74	1.71	1.81	1.82	1.80	1.81	1.90	1.93	1.93	1.97	1.88	1.96
Na	0.184	0.303	0.289	0.267	0.582	0.673	0.615	0.668	0.735	0.233	0.712	0.148	0.509	0.232
K	0.08	0.06	0.09	0.08	-	0.02	0.01	0.04	0.01	0.01	0.01	0.01	0.01	0.01
Cations	15.18	15.37	15.24	15.34	15.48	15.59	15.52	15.60	15.70	15.20	15.69	15.14	15.45	15.22
Cl	0.04	0.05	0.06	0.04	-	-	-	0.00	0.02	0.01	0.02	-	0.01	0.00
F	-	-	-	-	-	-	-	-	-	-	-	-	-	-

Appendix B7. Amphibole Analyses (continued)

Sample	112-2-1C1	112-2-1C2	112-2-1C3	113-1-10a1	113-2-4A1	113-2-4A2	113-2-4A3	113-2-4A5	113-2-4A6	113-2-4B1	113-2-4B2	113-2-4B3	113-2-4B4	113-2-4C1
Occurrence	cpx rim	cpx rim	cpx rim	patchy	cpx rim	cpx rim	cpx rim	cpx rim	cpx rim	after cpx	after cpx	after cpx	after cpx	cpx inc
Rock Type	gabbro	gabbro	gabbro	basalt	gabbro	gabbro	gabbro	gabbro	gabbro	gabbro	gabbro	gabbro	gabbro	gabbro
Analysis	ave	ave	ave	15NK	ave	ave	ave	ave	ave	ave	ave	ave	ave	ave
Location	UofA	UofA	UofA	OSU	UofA	UofA	UofA	UofA	UofA	UofA	UofA	UofA	UofA	UofA
SiO_2	52.66	53.55	51.55	52.22	48.52	48.09	44.03	47.75	44.70	46.01	47.84	45.90	43.96	44.06
TiO_2	0.21	0.13	0.22	0.18	0.06	0.12	1.80	0.11	1.40	0.08	0.07	0.09	1.82	0.68
Al_2O_3	3.59	3.16	4.66	2.51	8.59	8.54	10.51	9.03	10.65	10.44	9.10	10.83	10.87	11.42
FeO^T	6.47	6.64	6.94	18.78	6.96	7.29	7.76	6.70	7.29	10.58	6.80	7.43	7.55	5.94
Cr_2O_3	0.24	0.32	0.46	0.01	0.12	0.11	0.87	0.14	0.58	0.01	0.08	0.11	1.18	1.93
MnO	0.12	0.11	0.11	0.40	0.10	0.09	0.08	0.08	0.05	0.06	0.04	0.08	0.08	0.05
MgO	19.73	19.95	19.00	12.28	19.43	19.32	17.05	19.13	17.77	16.34	19.05	18.52	17.03	17.95
CaO	12.72	12.66	12.73	11.96	11.31	11.43	11.45	11.71	11.65	11.54	11.69	11.32	11.53	11.84
Na_2O	0.72	0.59	0.91	0.21	2.23	2.15	2.64	2.07	2.51	1.89	2.02	2.32	2.68	2.53
K_2O	0.04	0.03	0.04	0.03	0.10	0.10	0.25	0.14	0.25	0.12	0.16	0.15	0.24	0.16
F	b.d.	b.d.	b.d.	0.04	b.d.	b.d.	b.d.	b.d.	b.d.	b.d.	b.d.	b.d.	b.d.	b.d.
Cl	b.d.	0.01	0.01	0.01	0.18	0.20	0.24	0.17	0.23	0.20	0.14	0.24	0.23	0.25
Total	96.26	96.83	96.17	98.61	97.48	97.33	95.81	96.89	96.50	97.26	96.91	96.88	95.99	94.88
Si	7.45	7.51	7.32	7.64	6.81	6.77	6.38	6.75	6.41	6.58	6.76	6.50	6.34	6.31
Al^{IV}	0.55	0.49	0.68	0.36	1.19	1.23	1.62	1.25	1.59	1.42	1.24	1.50	1.66	1.69
Al^{VI}	0.05	0.03	0.10	0.08	0.23	0.18	0.17	0.25	0.21	0.34	0.27	0.31	0.19	0.24
Cr	0.03	0.04	0.05	0.00	0.01	0.01	0.10	0.02	0.07	0.00	0.01	0.01	0.13	0.22
Fe^{3+}	0.31	0.33	0.30	0.17	0.48	0.55	0.40	0.52	0.50	0.76	0.52	0.60	0.38	0.48
Ti	0.02	0.01	0.02	0.02	0.01	0.01	0.20	0.01	0.15	0.01	0.01	0.01	0.20	0.07
Mg	4.16	4.17	4.02	2.68	4.07	4.05	3.68	4.03	3.80	3.49	4.01	3.91	3.66	3.84
Fe^{2+}	0.46	0.45	0.53	2.12	0.34	0.31	0.54	0.28	0.37	0.51	0.29	0.28	0.53	0.24
Mn	0.01	0.01	0.01	0.05	0.01	0.01	0.01	0.01	0.01	0.01	0.00	0.01	0.01	0.01
Ca	1.93	1.90	1.94	1.88	1.70	1.72	1.78	1.77	1.79	1.77	1.77	1.72	1.78	1.82
Na	0.198	0.16	0.25	0.058	0.607	0.587	0.742	0.567	0.697	0.524	0.554	0.638	0.75	0.703
K	0.01	0.01	0.01	0.01	0.02	0.02	0.05	0.03	0.05	0.02	0.03	0.03	0.04	0.03
Cations	15.17	15.11	15.22	15.07	15.47	15.46	15.67	15.47	15.63	15.42	15.46	15.52	15.68	15.64
Cl	-	0.00	0.00	0.00	0.04	0.05	0.06	0.04	0.06	0.05	0.03	0.06	0.06	0.06
F	-	-	-	0.02	-	-	-	-	-	-	-	-	-	-

Appendix B7. Amphibole Analyses (continued)

Sample	113-2-4C2	113-2-4C4	113-2-11A3	113-2-11A4	113-2-11A5	113-2-11A6	113-2-11B1	113-2-11B2	113-2-11B3	113-2-11B4	113-2-11C1	113-2-11C2	113-2-11C3	113-2-11C4
Occurrence	cpx inc	cpx inc	patchy	patchy	patchy	patchy	cpx rim	cpx rim	cpx inc	cpx inc	patchy	patchy	patchy	patchy
Rock Type	gabbro	gabbro	gabbro	gabbro	gabbro	gabbro	gabbro	gabbro	gabbro	gabbro	gabbro	gabbro	gabbro	gabbro
Analysis	ave	ave	ave	ave	ave	ave	ave	ave	ave	ave	ave	ave	15NK	ave
Location	UofA	UofA	UofA	UofA	UofA	UofA	UofA	UofA	UofA	UofA	UofA	UofA	UofA	UofA
SiO_2	47.67	44.53	46.49	46.20	45.23	44.32	46.58	45.32	46.91	48.42	45.63	49.81	55.46	48.11
TiO_2	0.49	0.86	0.13	0.13	b.d.	0.01	0.70	1.78	0.74	0.50	0.07	0.14	0.01	0.07
Al_2O_3	8.33	10.60	11.17	11.66	12.35	12.50	9.90	10.17	9.66	8.01	9.81	3.66	3.43	6.60
FeO^T	4.90	6.96	6.62	6.52	9.46	9.57	7.25	7.00	7.36	7.33	10.40	19.64	3.32	14.75
Cr_2O_3	1.63	1.82	0.03	0.03	b.d.	b.d.	0.55	0.52	0.65	0.51	b.d.	b.d.	0.02	b.d.
MnO	0.07	0.07	0.10	0.12	0.06	0.08	0.07	0.07	0.07	0.11	0.16	0.85	0.09	0.19
MgO	19.34	17.70	18.87	18.75	16.67	16.52	18.78	18.17	18.50	19.46	16.84	10.47	21.65	13.96
CaO	11.88	11.52	11.45	11.24	11.63	11.66	11.32	11.33	11.37	10.91	11.95	11.84	12.95	12.15
Na_2O	1.91	2.53	2.36	2.31	2.05	2.32	2.19	2.69	2.26	1.95	2.24	0.70	0.29	1.29
K_2O	0.11	0.20	0.12	0.07	0.10	0.14	0.10	0.11	0.12	0.08	0.12	0.06	0.02	0.04
F	b.d.	b.d.	b.d.	b.d.	b.d.	b.d.	b.d.	b.d.	b.d.	b.d.	b.d.	b.d.	b.d.	b.d.
Cl	0.13	0.21	0.14	0.10	0.11	0.06	0.11	0.19	0.13	0.18	0.18	b.d.	b.d.	0.01
Total	94.83	95.18	97.45	97.10	97.66	97.18	97.00	96.83	97.12	96.95	97.40	97.17	97.22	97.17
Si	6.77	6.39	6.53	6.49	6.41	6.33	6.56	6.46	6.61	6.79	6.54	7.47	7.67	7.03
Al^{IV}	1.23	1.61	1.47	1.51	1.60	1.67	1.44	1.54	1.39	1.21	1.46	0.53	0.34	0.97
Al^{VI}	0.17	0.18	0.37	0.42	0.46	0.43	0.20	0.17	0.22	0.12	0.20	0.12	0.22	0.17
Cr	0.18	0.21	0.00	0.00	-	-	0.06	0.06	0.07	0.06	-	-	0.00	-
Fe^{3+}	0.35	0.50	0.51	0.50	0.77	0.79	0.55	0.42	0.50	0.52	0.77	0.27	0.03	0.51
Ti	0.05	0.09	0.01	0.01	-	0.00	0.07	0.19	0.08	0.05	0.01	0.02	0.00	0.01
Mg	4.10	3.79	3.95	3.93	3.52	3.52	3.94	3.86	3.89	4.07	3.60	2.34	4.46	3.04
Fe^{2+}	0.23	0.34	0.27	0.26	0.36	0.35	0.30	0.42	0.37	0.35	0.48	2.19	0.36	1.29
Mn	0.01	0.01	0.01	0.01	0.01	0.01	0.01	0.01	0.01	0.01	0.02	0.11	0.01	0.02
Ca	1.81	1.77	1.72	1.69	1.76	1.78	1.71	1.73	1.72	1.64	1.84	1.90	1.92	1.90
Na	0.526	0.704	0.642	0.629	0.563	0.642	0.598	0.744	0.618	0.531	0.623	0.204	0.078	0.366
K	0.02	0.04	0.02	0.01	0.02	0.03	0.02	0.02	0.02	0.01	0.02	0.01	0.00	0.01
Cations	15.44	15.62	15.52	15.48	15.46	15.55	15.46	15.62	15.49	15.35	15.56	15.16	15.08	15.32
Cl	0.03	0.05	0.03	0.02	0.03	0.02	0.03	0.05	0.03	0.04	0.04	-	-	0.00
F	-	-	-	-	-	-	-	-	-	-	-	-	-	-

Appendix B7. Amphibole Analyses (continued)

Sample	113-2-11C5	113-2-11C6	113-2-11C7	113-2-11C8	113-2-11C9	13-2-11C10	113-2-11D1	113-2-11D2	113-2-11D3	113-2-11D4	113-2-11E1	113-2-11E2	113-2-11E3	113-2-11E4
Occurrence	patchy	patchy	patchy	patchy	patchy	patchy	patchy	patchy	patchy	patchy	after cpx	after cpx	after cpx	after cpx
Rock Type	gabbro	gabbro	gabbro	gabbro	gabbro	gabbro	gabbro	gabbro	gabbro	gabbro	gabbro	gabbro	gabbro	gabbro
Analysis	ave	ave	ave	ave	ave	ave	ave	ave	ave	ave	ave	ave	ave	ave
Location	UofA	UofA	UofA	UofA	UofA	UofA	UofA	UofA	UofA	UofA	UofA	UofA	UofA	UofA
SiO_2	50.45	45.87	47.73	44.80	49.42	48.16	47.15	44.20	44.94	43.74	49.09	48.46	45.72	47.29
TiO_2	0.01	0.04	0.27	0.05	0.04	0.13	0.32	0.92	0.04	0.12	0.45	0.25	0.33	0.33
Al_2O_3	3.43	10.75	9.45	10.46	5.97	6.69	10.28	13.11	10.38	11.40	8.30	9.35	11.81	10.08
FeO^T	18.94	8.78	6.56	10.86	12.69	14.66	6.52	6.71	8.68	9.32	6.34	5.70	5.66	5.97
Cr_2O_3	0.01	b.d.	0.22	0.01	b.d.	0.01	0.04	0.06	0.03	0.01	0.15	0.07	0.22	b.d.
MnO	0.74	0.15	0.08	0.10	0.11	0.17	0.10	0.08	0.13	0.17	0.10	0.10	0.03	0.10
MgO	11.02	17.19	19.17	15.92	15.49	13.84	19.29	17.57	18.24	17.54	19.19	19.32	18.50	19.08
CaO	11.99	12.03	11.37	11.83	12.20	12.22	11.47	11.63	12.06	11.96	11.28	11.60	11.68	11.63
Na_2O	0.64	2.30	1.85	2.32	1.16	1.35	2.09	2.66	2.62	2.74	1.72	2.07	2.69	2.14
K_2O	0.05	0.14	0.07	0.13	0.06	0.06	0.10	0.11	0.22	0.17	0.08	0.09	0.09	0.10
F	b.d.	b.d.	b.d.	b.d.	b.d.	b.d.	b.d.	b.d.	b.d.	b.d.	b.d.	b.d.	b.d.	b.d.
Cl	b.d.	0.10	0.11	0.22	0.01	0.02	0.11	0.23	0.05	0.06	0.12	0.10	0.17	0.14
Total	97.27	97.35	96.66	96.69	97.15	97.30	97.43	97.22	97.36	97.22	96.67	97.04	96.68	96.86
Si	7.53	6.54	6.71	6.50	7.15	7.04	6.60	6.28	6.40	6.26	6.91	6.81	6.49	6.67
Al^{IV}	0.47	1.46	1.29	1.50	0.86	0.96	1.40	1.72	1.60	1.74	1.09	1.19	1.52	1.33
Al^{VI}	0.13	0.35	0.28	0.29	0.16	0.19	0.29	0.47	0.14	0.18	0.29	0.36	0.46	0.35
Cr	0.00	-	0.02	0.00	-	0.00	0.00	0.01	0.00	0.00	0.02	0.01	0.03	-
Fe^{3+}	0.24	0.61	0.51	0.69	0.47	0.43	0.53	0.48	0.81	0.88	0.39	0.36	0.37	0.43
Ti	0.00	0.00	0.03	0.01	0.00	0.01	0.03	0.10	0.00	0.01	0.05	0.03	0.04	0.04
Mg	2.45	3.66	4.02	3.45	3.34	3.02	4.03	3.72	3.87	3.74	4.03	4.05	3.91	4.01
Fe^{2+}	2.13	0.44	0.27	0.63	1.07	1.36	0.24	0.32	0.23	0.24	0.36	0.31	0.30	0.27
Mn	0.09	0.02	0.01	0.01	0.01	0.02	0.01	0.01	0.02	0.02	0.01	0.01	0.00	0.01
Ca	1.92	1.84	1.71	1.84	1.89	1.91	1.72	1.77	1.84	1.83	1.70	1.75	1.78	1.76
Na	0.186	0.636	0.505	0.653	0.325	0.383	0.568	0.733	0.724	0.76	0.469	0.564	0.74	0.585
K	0.01	0.03	0.01	0.02	0.01	0.01	0.02	0.02	0.04	0.03	0.01	0.02	0.02	0.02
Cations	15.15	15.58	15.37	15.59	15.28	15.35	15.44	15.63	15.68	15.70	15.33	15.45	15.64	15.48
Cl	-	0.02	0.03	0.05	0.00	0.01	0.03	0.06	0.01	0.02	0.03	0.02	0.04	0.03
F	-	-	-	-	-	-	-	-	-	-	-	-	-	-

Appendix C

EPIDOSITE AND PLAGIOGRANITE TRACE ELEMENT GEOCHEMISTRY

Whole rock trace element analyses of the epidosite samples were collected by solution ICP-MS at the University of Victoria. Epidosite samples were digested using a modified sodium-peroxide sinter technique [*Longerich et al.*, 1990], in which 0.5 ml of 30% H_2O_2 was added before final dilution with water to 90g to aid in the dissolution of the sinter cake. Preliminary plagiogranite analyses were performed on samples digested using an HF-HNO_3 technique [*Jenner et al.*, 1990].

Appendix C1. Epidosite Trace Element Analyses (ppm)

Sample	KG99004	KG99005	KG99006	96-1-14	99-2-8	102-4-1	106-3-16	113-1-26
Ba	6.3	5.6	4.5	2.1	3.7	60.4	3.4	3.3
Th	0.2	0.4	0.2	0.3	0.2	1.4	0.1	0.1
La	1.4	1.7	2.3	4.5	3.5	7.8	2.3	1.5
Ce	4.3	5.0	7.1	14.5	11.8	18.3	8.1	3.4
Pr	0.8	1.0	1.2	2.6	2.1	2.4	1.4	0.6
Sr	222.4	149.0	155.6	140.1	339.5	142.4	138.7	421.7
Nd	4.3	5.1	6.8	14.8	11.2	10.1	7.7	3.0
Zr	36.3	41.6	56.4	79.7	110.9	73.2	69.6	27.0
Hf	1.2	1.5	1.7	2.5	3.0	2.2	2.0	0.7
Sm	1.7	2.1	2.4	5.1	3.8	2.6	2.6	0.9
Eu	0.6	0.8	0.8	2.0	1.3	0.6	1.1	1.0
Gd	2.6	3.1	3.5	7.2	5.4	3.1	3.7	1.3
Tb	0.5	0.6	0.7	1.3	0.9	0.5	0.7	0.2
Dy	3.4	4.0	4.5	8.5	6.3	3.7	4.5	1.8
Y	18.5	20.9	24.6	43.4	33.7	21.1	22.8	11.5
Ho	0.7	0.9	0.9	1.8	1.3	0.8	0.9	0.4
Er	2.4	2.8	3.0	5.4	4.1	2.7	2.8	1.3
Tm	0.4	0.5	0.4	0.8	0.6	0.5	0.4	0.2
Yb	2.3	2.6	2.8	5.0	3.8	2.8	2.7	1.2
Lu	0.3	0.4	0.4	0.7	0.5	0.4	0.4	0.1

Appendix C2. Preliminary Plagiogranite Trace Element Analyses (ppm)

Sample	96-1-3 (a)	96-1-3 (b)	96-1-16L (a)	96-1-16L (b)	96-1-16D	96-1-19	96-1-27
Ce	20.2	20.3	12.1	12.8	20.9	34.6	20.9
Dy	9.2	9.3	6.0	6.0	6.9	19.7	10.2
Er	5.9	5.9	3.8	3.8	4.2	13.0	6.2
Eu	1.7	1.7	1.0	1.0	1.3	1.7	1.7
Gd	6.8	6.8	4.1	4.1	6.0	14.3	7.6
Ho	2.1	2.1	1.4	1.3	1.5	4.4	2.2
La	7.2	7.1	3.7	3.8	6.5	8.5	6.2
Lu	0.8	0.8	0.6	0.5	0.6	1.5	0.8
Nd	18.2	18.1	11.8	12.8	20.2	37.1	21.1
Pr	3.2	3.2	2.0	2.2	3.6	6.6	3.8
Sm	6.0	6.0	4.1	4.1	6.3	12.6	7.1
Tb	1.4	1.4	0.9	0.9	1.1	2.8	1.5
Tm	0.9	0.9	0.6	0.6	0.6	1.9	0.9
Yb	5.6	5.5	3.7	3.6	3.9	11.6	5.7

Appendix D

GEOTHERMOMETRY

Metamorphic temperatures were calculated using the geothermometers of Holland and Blundy [1994] on element abundances determined by electron microprobe from amphibole-plagioclase pairs. Both thermometers require recaculation of the amphibole analyses using the method outlined in Holland and Blundy [1994]. Care was taken to analyze mineral grains which did not display fine scale zoning in backscattered electron images. The edenite-tremolite (ed-tr) exchange thermometer was used for samples that contain quartz and the edenite-richterite (ed-ri) thermometer was used for samples that do not. Forty-two pairs (of 173) failed one or more of the compositional criteria imposed by Holland and Blundy's [1994] data set. The stated uncertainty in the thermometers is ±40°C in the range 400° to 900°C (edenite-tremolite) and 500° to 900°C (edentite-richterite) [*Holland and Blundy*, 1994]. Type refers to the amphibole mode of occurrence described in Chapter 3. X (ab) refers to the mole fraction of albite in coexisting plagioclase. The presence or absence of quartz is indicated in the table to help justify which thermometer was used. Average (Ave.) temperatures for grains displaying the same texture in the same sample were used to construct Figure 3.6. N = number of analyses used in the average.

Appendix D. Geothermometry Data

Sample	Lab	Rock Type	Type	X (ab)	T (ed-tr)	T (ed-ri)	Quartz	Temp.	Ave.	N
94-1-1C1	OSU	gabbro	after cpx	0.44	827	811	N	811	790	3
94-1-1C2	OSU	gabbro	after cpx	0.44	735	744	N	744		
94-1-1D1	OSU	gabbro	after cpx	0.44	826	814	N	814		
94-1-2B1	OSU	gabbro	vein	0.22	884	868	N	868	815	5
94-1-2B1	UofA	gabbro	vein	0.33	813	805	N	805		
94-1-2B2	OSU	gabbro	cpx rim	0.27	863	826	N	826	801	4
94-1-2B2	UofA	gabbro	vein	0.29	825	817	N	817		
94-1-2B3	UofA	gabbro	vein	0.33	748	761	N	761		
94-1-2B4	UofA	gabbro	vein	0.26	776	775	N	775		
94-1-2C2	OSU	gabbro	cpx rim	0.36	747	760	N	760		
94-1-2D1	OSU	gabbro	after cpx	0.47	832	778	N	778		
94-1-2D2	OSU	gabbro	cpx rim	0.44	919	823	N	823		
94-1-2E2	OSU	gabbro	cpx rim	0.31	860	847	N	847		
94-1-3B1	OSU	gabbro	after cpx	0.40	743	772	N	772	792	4
94-1-3C1	OSU	gabbro	after cpx	0.38	834	782	N	782		
94-1-3D1	OSU	gabbro	after cpx	0.39	904	822	N	822		
94-1-3E1	OSU	gabbro	after cpx	0.48	807	792	N	792		
96-1-3A1	UofA	PG	patchy	0.93	666	-	Y	666	618	2
96-1-3A2	UofA	PG	patchy	0.93	569	-	Y	569		
96-1-3B1	UofA	PG	after cpx	0.89	770	678	Y	678	698	3
96-1-3B2	UofA	PG	after cpx	0.93	723	-	Y	723		
96-1-3B3	UofA	PG	after cpx	0.95	692	-	Y	692		
96-1-5A4	UofA	PG	after cpx	0.96	699	-	Y	699	646	5
96-1-5A5	UofA	PG	after cpx	0.95	667	-	Y	667		
96-1-5B1	UofA	PG	after cpx	0.97	664	-	Y	664		
96-1-5D3	UofA	PG	after cpx	0.99	571	-	Y	571		
96-1-5D4	UofA	PG	after cpx	0.98	629	-	Y	629		
96-2-13a2	OSU	PG	patchy	0.92	675	-	Y	675	625	2
96-2-13b1	OSU	PG	patchy	0.92	575	-	Y	575		
99-2-1A1	UofA	basalt	vein	0.18	762	760	N	760	710	5
99-2-1A2	UofA	basalt	vein	0.18	660	670	N	670		
99-2-1A3	UofA	basalt	vein	0.26	655	669	N	669		
99-2-1C1	UofA	basalt	vein	0.29	679	693	N	693		
99-2-1C2	UofA	basalt	vein	0.26	738	756	N	756		
99-1-21A1	UofA	gabbro	cpx rim	0.23	765	791	N	791	810	4
99-1-21A2	UofA	gabbro	cpx rim	0.21	849	795	N	795		
99-1-21A3	UofA	gabbro	cpx rim	0.23	815	793	N	793		
99-1-21B1	UofA	gabbro	vein	0.14	909	861	N	861	862	4
99-1-21B2	UofA	gabbro	vein	0.19	878	820	N	820		
99-1-21B3	UofA	gabbro	vein	0.19	1055	891	N	891		
99-1-21C1	UofA	gabbro	cpx rim	0.28	1011	874	N	874		
99-1-21D1	UofA	gabbro	vein	0.13	901	830	N	830		
99-1-30A4	UofA	gabbro	magmatic	0.26	965	840	N	840	861	4
99-1-30A5	UofA	gabbro	magmatic	0.24	980	845	N	845		

Appendix D. Geothermometry Data (continued)

Sample	Lab	Rock Type	Type	X (ab)	T (ed-tr)	T (ed-ri)	Quartz	Temp.	Ave.	N
99-1-30B2	UofA	gabbro	magmatic	0.22	997	858	N	858		
99-1-30B3	UofA	gabbro	magmatic	0.22	1057	901	N	901		
99-1-30B4	UofA	gabbro	cpx rim	0.22	714	721	N	721		
105-1-6A1	OSU	gabbro	magmatic	0.26	1080	887	N	887	859	3
105-1-6C2	OSU	gabbro	magmatic	0.26	1061	889	N	889		
105-1-6D1	OSU	gabbro	magmatic	0.24	924	802	N	802		
105-1-21A1	UofA	gabbro	magmatic	0.25	1051	894	N	894	885	7
105-1-21A2	UofA	gabbro	magmatic	0.25	1046	880	N	880		
105-1-21B1	UofA	gabbro	magmatic	0.25	1042	878	N	878		
105-1-21B2	UofA	gabbro	magmatic	0.21	1044	873	N	873		
105-1-21B3	UofA	gabbro	magmatic	0.25	1077	899	N	899		
105-1-21C3	UofA	gabbro	magmatic	0.33	1010	877	N	877		
105-1-21C3	UofA	gabbro	magmatic	0.27	1046	891	N	891		
105-1-25A1	OSU	gabbro	vein	0.18	926	811	N	811	803	5
105-1-25A1	UofA	gabbro	vein	0.14	822	723	N	723		
105-1-25A2	OSU	gabbro	vein	0.16	848	794	N	794		
105-1-25A4	OSU	gabbro	magmatic	0.15	1170	925	N	925		
105-1-25A4	UofA	gabbro	vein	0.17	823	763	N	763		
105-1-25D4	OSU	gabbro	vein	0.10	1109	917	N	917		
106-2-5a1	OSU	gabbro	after cpx	0.50	761	738	N	738	734	2
106-2-5a2	OSU	gabbro	after cpx	0.56	751	729	N	729		
106-2-5c1	OSU	gabbro	cpx rim	0.20	895	848	N	848	835	2
106-2-5c2	OSU	gabbro	cpx rim	0.17	911	821	N	821		
106-2-10D1	OSU	gabbro	magmatic	0.12	1160	981	N	981	921	3
106-2-10D1	UofA	gabbro	vein	0.11	755	805	N	805	891	2
106-2-10D2	OSU	gabbro	magmatic	0.12	1067	977	N	977		
106-2-10D4	OSU	gabbro	magmatic	0.11	1121	995	N	995		
106-2-10D5	UofA	gabbro	vein	0.14	876	841	N	841		
106-2-11A1	UofA	PG	magmatic	0.17	1071	954	Y	954		
106-2-11A2	UofA	PG	magmatic	0.17	1064	975	Y	975		
106-2-11A3	UofA	PG	magmatic	0.16	1012	952	Y	952		
106-2-11A5	OSU	PG	magmatic	0.16	1074	962	Y	962	815	4
106-2-11D9	OSU	PG	after cpx	0.52	716	717	Y	716		
106-2-11D10	OSU	PG	after cpx	0.74	768	715	Y	768	716	2
107-1-14A1	UofA	basalt	after cpx	0.28	620	-	Y	620	617	8
107-1-14A2	UofA	basalt	after cpx	0.28	622	-	Y	622		
107-1-14A3	UofA	basalt	after cpx	0.31	619	-	Y	619		
107-1-14B1	UofA	basalt	after cpx	0.27	628	-	Y	628		
107-1-14B2	UofA	basalt	after cpx	0.34	580	-	Y	580		
107-1-14B3	UofA	basalt	after cpx	0.33	634	-	Y	634		
107-1-14C1	UofA	basalt	after cpx	0.34	593	-	Y	593		
107-1-14C2	UofA	basalt	after cpx	0.35	642	-	Y	642		
108-2-6B1	UofA	gabbro	cpx rim	0.13	932	790	N	790	817	3
108-2-6B2	UofA	gabbro	cpx rim	0.10	858	803	N	803		

Appendix D. Geothermometry Data (continued)

Sample	Lab	Rock Type	Type	X (ab)	T (ed-tr)	T (ed-ri)	Quartz	Temp.	Ave.	N
108-2-6C1	UofA	gabbro	cpx rim	0.10	1045	817	N	817		
108-2-12E2	UofA	PG	after cpx	0.69	689	683	Y	689	661	3
108-2-12E3	UofA	PG	after cpx	0.7	577	-	Y	577		
108-2-12E4	UofA	PG	after cpx	0.58	717	674	Y	717		
108-3-1E1	UofA	basalt	after cpx	0.94	573	-	Y	573	564	3
108-3-1E2	UofA	basalt	after cpx	0.94	550	-	Y	550		
108-3-1F1	UofA	basalt	after cpx	0.96	568	-	Y	568		
108-3-15A1	UofA	basalt	after cpx	0.71	604	-	Y	604	646	8
108-3-15A2	UofA	basalt	after cpx	0.77	617	-	Y	617		
108-3-15A3	UofA	basalt	after cpx	0.67	611	-	Y	611		
108-3-15B1	UofA	basalt	after cpx	0.53	698	711	Y	698		
108-3-15B2	UofA	basalt	after cpx	0.56	690	703	Y	690		
108-3-15D1	UofA	basalt	after cpx	0.56	674	689	Y	674		
108-3-15D2	UofA	basalt	after cpx	0.47	635	697	Y	635		
108-3-15D3	UofA	basalt	after cpx	0.72	640	629	Y	640		
108-3-16A3	UofA	epidosite	patchy	0.99	617	-	Y	617	625	7
108-3-16A3	UofA	epidosite	patchy	0.99	617	-	Y	617		
108-3-16D1	UofA	epidosite	patchy	0.99	615	-	Y	615		
108-3-16D2	UofA	epidosite	patchy	1.00	631	-	Y	631		
108-3-16D2	UofA	epidosite	patchy	0.99	632	-	Y	632		
108-3-16D5	UofA	epidosite	patchy	0.99	608	-	Y	608		
108-3-16D6	UofA	epidosite	patchy	0.99	655	-	Y	655		
108-3-17A1	UofA	PG	after cpx	0.91	635	-	Y	635	701	8
108-3-17A3	UofA	PG	after cpx	0.7	753	702	Y	753		
108-3-17A5	UofA	PG	after cpx	0.74	702	669	Y	702		
108-3-17C1	UofA	PG	after cpx	0.82	668	614	Y	668		
108-3-17C2	UofA	PG	after cpx	0.75	724	679	Y	724		
108-3-17C3	UofA	PG	after cpx	0.78	676	640	Y	676		
108-3-17E1	UofA	PG	after cpx	0.77	698	-	Y	698		
108-3-17E2	UofA	PG	after cpx	0.51	753	758	Y	753		
110-1-15C1	UofA	basalt	patchy	0.85	723	665	N	665	719	2
110-1-15C2	UofA	basalt	after cpx	0.81	826	773	N	773	710	2
110-1-15C3	UofA	basalt	after cpx	0.87	717	646	N	646		
110-1-15C4	UofA	basalt	patchy	0.78	720	677	N	677		
110-1-25C1	UofA	basalt	patchy	0.89	681	625	N	615		
111-4-6A3	UofA	gabbro	after cpx	0.58	767	762	N	762	784	6
111-4-6A4	UofA	gabbro	after cpx	0.46	792	778	N	778		
111-4-6B1	UofA	gabbro	after cpx	0.4	743	742	N	742		
111-4-6C2	UofA	gabbro	after cpx	0.42	813	812	N	812		
111-4-6C3	UofA	gabbro	after cpx	0.4	792	801	N	801		
111-4-6C4	UofA	gabbro	after cpx	0.42	909	808	N	808		
113-1-10a1	OSU	basalt	patchy	0.98	521	-	Y	521		
113-2-11B1	UofA	gabbro	magmatic	0.12	1221	977	N	977		

Appendix E

WHOLE ROCK MAJOR ELEMENT AND OXYGEN ISOTOPE ANALYSES

OXYGEN ISOTOPES

Whole rock powders were either prepared from rock chips in a tungsten carbide mill at the University of Victoria or obtained from colleagues at the University of Tasmania. Mineral separates were prepared from epidotized plagiogranite samples crushed with a steel mortar. The samples were sieved then quartz and epidote were separated using both magnetic and hand picking techniques. The final purity of the mineral separates was checked under a binocular microscope. Oxygen isotopic compositions of whole rock powders and quartz and epidote mineral separates were determined using the BrF_5 method of Clayton and Mayeda [1963] at the University of Alberta. Reaction temperatures were between 600° and 650°C. All samples were dried at ~100°C, loaded into Ni reaction vessels, and then outgassed at ~150°C under vacuum to remove any remaining adsorbed water prior to reaction with BrF_5. Oxygen from the silicate phases was recovered quantitatively and converted to CO_2 by passing it over a carbon rod suspended from a platinum wire in the vacuum line. The carbon rod was heated by two incandescent light sources. The converted CO_2 was condensed in the sample tube with liquid nitrogen. The isotopic compositions are reported with respect to SMOW (standard mean ocean water) in the usual δ notation where:

$$\delta_{sample} = \left[\frac{(^{18}O/^{16}O)_{\text{sample}}}{(^{18}O/^{16}O)_{\text{standard}}} - 1 \right] \times 1000$$

The fractionation factor between CO_2 and water was taken to be 1.0407 [see discussion in *O'Neil et al.*, 1975]. Reproducibility of replicate analyses of samples and standards is better than ± 0.2 ‰, except for a few samples with high water contents that have higher reproducibilities of ±0.3‰ due to less predictable oxygen yields.

MAJOR ELEMENT ANALYSES

Samples from our collection were analyzed for major elements by X-ray fluorescence (XRF) at Cominco Ltd. Exploration Research Laboratory. Samples from Dr. T. Falloon were analyzed by XRF at the University of Tasmania.

Appendix E. Whole rock major element and oxygen isotope analyses.

Sample	Rock Type	SiO_2	TiO_2	Al_2O_3	FeO^T	MnO	MgO	CaO	Na_2O	K_2O	P_2O_5	LOI	$\delta^{18}O$
89-3-1	Basalt	49.51	0.75	18.95	10.79	0.19	5.22	11.24	2.58	0.59	0.18	2.50	9.3
91-3-1	Basalt	51.31	0.88	15.80	12.97	0.20	5.95	9.63	2.70	0.53	0.04	3.05	10.6
100-1-19	Basalt	50.47	0.71	16.40	8.34	0.20	8.59	12.32	2.67	0.26	0.04	2.14	9.2
101-1-6	Basalt	56.73	1.66	15.97	8.29	0.20	5.68	4.68	6.54	0.11	0.14	3.21	8.6
110-1-1	Basalt	49.20	1.33	15.80	10.73	0.18	8.51	11.74	2.33	0.09	0.09	2.41	5.4
110-1-17	Basalt	49.92	1.64	14.91	12.11	0.19	7.27	10.93	2.57	0.32	0.14	1.60	7.0
88-1-8	Boninite	54.69	0.27	12.58	7.56	0.17	13.47	8.18	2.23	0.82	0.03	5.49	12.9
102-1-4	Boninite	52.50	0.17	12.42	7.89	0.17	14.47	9.71	2.05	0.63	b.d.	5.45	12.0
102-1-20	Boninite	53.40	0.18	13.89	8.57	0.13	10.55	9.56	2.00	1.70	0.02	4.99	13.4
111-1-8	Diabase	49.78	1.77	14.35	12.07	0.21	7.21	11.57	2.67	0.20	0.15	0.50	6.8
87-1-1	Diabase	55.33	0.85	14.92	11.90	0.18	4.56	8.92	2.43	0.84	0.09	1.60	6.6
90-1-16	Diabase	52.50	0.98	14.62	10.76	0.19	7.48	10.83	2.47	0.08	0.08	0.97	7.2
90-1-19	Diabase	52.77	1.31	13.84	12.80	0.21	6.47	9.63	2.75	0.10	0.12	1.60	7.5
99-2-10	Diabase	51.95	1.90	14.91	12.24	0.41	6.67	7.50	4.06	0.22	0.15	3.09	5.8
100-1-39	Diabase	50.01	1.49	14.31	10.49	0.19	9.98	10.28	2.94	0.16	0.16	2.30	8.6
101-1-2	Diabase	53.65	1.65	14.92	11.36	0.21	5.94	6.49	5.32	0.33	0.14	2.34	8.9
110-1-24	Diabase	50.30	1.43	15.30	11.23	0.24	7.01	11.48	2.60	0.29	0.12	1.58	7.0
111-1-3	Diabase	58.06	0.89	15.85	11.79	0.21	6.70	2.27	3.75	0.39	0.07	4.73	6.6
111-1-20	Diabase	54.51	1.18	16.62	13.21	0.16	5.49	2.44	5.91	0.36	0.12	3.63	8.7
90-4-1	Gabbro	49.37	0.10	21.59	3.14	0.07	7.64	16.65	1.36	0.05	0.01	2.04	5.6
90-4-2	Gabbro	49.44	0.14	19.26	3.88	0.07	9.07	16.82	1.25	0.05	0.01	2.42	6.5
90-4-3	Gabbro	50.37	0.10	17.97	5.21	0.08	11.82	11.85	2.05	0.54	0.01	6.69	8.0
99-2-1	Gabbro	50.31	0.23	20.10	5.05	0.10	8.40	13.39	2.28	0.16	b.d.	3.75	6.6
99-1-26	Gabbro	50.91	0.35	17.79	4.13	0.09	8.26	16.64	1.80	0.03	0.01	0.99	4.7
99-1-33	Gabbro	51.38	0.25	16.35	6.54	0.12	9.98	13.64	1.71	0.02	0.01	0.40	5.5
111-4-3	Gabbro	47.12	0.10	18.94	5.04	0.11	12.90	14.32	1.45	0.02	0.01	4.40	6.3
111-4-6	Gabbro	52.57	0.53	17.88	8.30	0.15	6.77	10.49	2.98	0.28	0.05	1.52	7.6
112-2-1	Gabbro	45.98	0.11	19.35	2.77	0.05	10.33	21.04	0.24	0.10	0.02	5.03	5.9
98-2-1	Peridotite	44.46	0.01	0.10	8.40	0.10	46.15	0.74	0.01	0.01	0.01	b.d.	5.8
112-1-7	Peridotite	46.10	0.01	0.27	8.39	0.08	45.02	0.06	0.04	0.01	0.01	14.06	4.8
96-1-3	Plagiogranite	n.d.	n.d.	n.d.	n.d.	n.d.	n.d.	n.d.	n.d.	n.d.	n.d.	n.d.	7.4
96-1-10	Plagiogranite	67.70	0.65	14.26	6.35	0.02	1.06	4.74	4.99	0.01	0.20	1.37	8.1
96-1-15	Plagiogranite	67.37	0.70	13.96	7.55	0.03	1.12	3.44	5.56	0.02	0.26	1.29	8.4
96-1-16L	Plagiogranite	n.d.	n.d.	n.d.	n.d.	n.d.	n.d.	n.d.	n.d.	n.d.	n.d.	n.d.	6.5
96-1-16D	Plagiogranite	n.d.	n.d.	n.d.	n.d.	n.d.	n.d.	n.d.	n.d.	n.d.	n.d.	n.d.	5.5
96-1-19	Plagiogranite	n.d.	n.d.	n.d.	n.d.	n.d.	n.d.	n.d.	n.d.	n.d.	n.d.	n.d.	10.6
96-1-27	Plagiogranite	n.d.	n.d.	n.d.	n.d.	n.d.	n.d.	n.d.	n.d.	n.d.	n.d.	n.d.	7.3
96-1-29	Plagiogranite	71.51	0.35	12.79	4.51	0.05	0.29	7.42	3.02	0.01	0.05	1.16	6.6
96-1-30	Plagiogranite	63.33	0.52	15.17	7.25	0.05	0.66	12.28	0.58	0.05	0.10	2.00	6.3
96-1-35	Plagiogranite	74.79	0.35	11.93	3.20	0.07	0.20	5.80	3.61	0.01	0.05	0.81	6.3

Note: Major element analyses (wt %) were recalculated to 100 percent on an anhydrous basis. All Fe as FeO. Isotope values are quoted in ‰ relative to the SMOW standard. b.d. = below detection; n.d. = not determined.